frontiers | Research Topics

Pain and pain-related neuropsychiatric disorders: from mechanistic insights to innovative therapeutic strategies

Edited by
Álvaro Llorente-Berzal, Francesca Guida and Fabio Turco

Coordinated by
Rosmara Infantino

Published in
Frontiers in Pharmacology
Frontiers in Molecular Neuroscience
Frontiers in Neurology
Frontiers in Neuroscience

ISSN 1664-8714
ISBN 978-2-8325-6215-4
DOI 10.3389/978-2-8325-6215-4

About Frontiers

Frontiers is more than just an open access publisher of scholarly articles: it is a pioneering approach to the world of academia, radically improving the way scholarly research is managed. The grand vision of Frontiers is a world where all people have an equal opportunity to seek, share and generate knowledge. Frontiers provides immediate and permanent online open access to all its publications, but this alone is not enough to realize our grand goals.

Frontiers journal series

The Frontiers journal series is a multi-tier and interdisciplinary set of open-access, online journals, promising a paradigm shift from the current review, selection and dissemination processes in academic publishing. All Frontiers journals are driven by researchers for researchers; therefore, they constitute a service to the scholarly community. At the same time, the *Frontiers journal series* operates on a revolutionary invention, the tiered publishing system, initially addressing specific communities of scholars, and gradually climbing up to broader public understanding, thus serving the interests of the lay society, too.

Dedication to quality

Each Frontiers article is a landmark of the highest quality, thanks to genuinely collaborative interactions between authors and review editors, who include some of the world's best academicians. Research must be certified by peers before entering a stream of knowledge that may eventually reach the public - and shape society; therefore, Frontiers only applies the most rigorous and unbiased reviews. Frontiers revolutionizes research publishing by freely delivering the most outstanding research, evaluated with no bias from both the academic and social point of view. By applying the most advanced information technologies, Frontiers is catapulting scholarly publishing into a new generation.

What are Frontiers Research Topics?

Frontiers Research Topics are very popular trademarks of the *Frontiers journals series*: they are collections of at least ten articles, all centered on a particular subject. With their unique mix of varied contributions from Original Research to Review Articles, Frontiers Research Topics unify the most influential researchers, the latest key findings and historical advances in a hot research area.

Find out more on how to host your own Frontiers Research Topic or contribute to one as an author by contacting the Frontiers editorial office: frontiersin.org/about/contact

Pain and pain-related neuropsychiatric disorders: from mechanistic insights to innovative therapeutic strategies

Topic editors
Álvaro Llorente-Berzal — Autonomous University of Madrid, Spain
Francesca Guida — University of Campania Luigi Vanvitelli, Italy
Fabio Turco — Cannabiscientia SA, Switzerland

Topic coordinator
Rosmara Infantino — University of Galway, Ireland

Citation
Llorente-Berzal, Á., Guida, F., Turco, F., Infantino, R., eds. (2025). *Pain and pain-related neuropsychiatric disorders: from mechanistic insights to innovative therapeutic strategies*. Lausanne: Frontiers Media SA. doi: 10.3389/978-2-8325-6215-4

Table of contents

frontiers | Frontiers in Pharmacology

TYPE Editorial
PUBLISHED 25 March 2025
DOI 10.3389/fphar.2025.1593890

OPEN ACCESS

EDITED AND REVIEWED BY
Nicholas M. Barnes,
University of Birmingham, United Kingdom

*CORRESPONDENCE
Rosmara Infantino,
rosmara.infantino@universityofgalway.ie

RECEIVED 14 March 2025
ACCEPTED 19 March 2025
PUBLISHED 25 March 2025

CITATION
Infantino R, Turco F, Guida F and Llorente-Berzal Á (2025) Editorial: Pain and pain-related neuropsychiatric disorders: from mechanistic insights to innovative therapeutic strategies.
Front. Pharmacol. 16:1593890.
doi: 10.3389/fphar.2025.1593890

Editorial: Pain and pain-related neuropsychiatric disorders: from mechanistic insights to innovative therapeutic strategies

Rosmara Infantino[1,2,3]*, Fabio Turco[4], Francesca Guida[5] and Álvaro Llorente-Berzal[6]

[1]Pharmacology and Therapeutics, School of Medicine, University of Galway, Galway, Ireland, [2]Centre for Pain Research, University of Galway, Galway, Ireland, [3]Galway Neuroscience Centre, University of Galway, Galway, Ireland, [4]Cannabiscientia SA, Zurich, Switzerland, [5]Section of Pharmacology L. Donatelli, Department of Experimental Medicine, University of Campania Luigi Vanvitelli, Naples, Campania, Italy, [6]Department of Physiology, Faculty of Medicine, Autonomous University of Madrid, Madrid, Madrid, Spain

KEYWORDS

chronic pain, pain mechanisms, pain models, pain therapies, neuropsychiatric disorders

Editorial on the Research Topic
Pain and pain-related neuropsychiatric disorders: from mechanistic insights to innovative therapeutic strategies

Introduction

Chronic pain is a pervasive health challenge, affecting approximately 30 per cent of the world's population and imposing a significant personal and socio-economic burden. In addition to its sensory components, chronic pain has important affective and cognitive dimensions and is closely linked to neuropsychiatric complications, including anxiety, depression and cognitive dysfunction. Despite significant advances in basic and clinical research, the management of chronic pain remains inadequate, as translation from mechanistic findings to clinical applications faces persistent barriers. Similarly, clinical observations often lack mechanistic context by not being adequately integrated with basic research. The aim of this special Research Topic was to fill this gap by promoting a synergistic integration of preclinical and clinical trends towards new pharmacological approaches or strategies to improve pain management. Particular attention has been given to sex and gender differences in pain perception. In addition, with a view to sustainability, special emphasis was placed on mechanistic and clinical studies on substances of natural origin.

Mechanistic insights charting a path for translational impact

A fundamental step toward improving chronic pain treatment lies in deciphering its underlying neurobiological mechanisms with the use of well-characterised animal models. In this regard, the preclinical study by Di Marino et al. extends behavioural characterisation of the paclitaxel model of chemotherapy-induced neuropathic pain in rats of both sexes, and sheds light on the status of the endocannabinoid system in this model. Their work lays a solid foundation for potential targeting of endocannabinoid signalling as a novel therapeutic strategy. The endocannabinoid system is explored also in the work by Yuan et al. They explore novel pathways, including the role of VD-hemopressin (α) and RVD-hemopressin (α) in electroacupuncture-mediated pain relief, highlighting a role for the cannabinoid type 1 (CB_1) receptor. Qu et al. further elaborate on neuropathic pain mechanisms, demonstrating the efficacy of the plant Dahuang Fuzi, whose decoction has been used for millennia in traditional Chinese medicine, in inhibiting TNF-α and PI3K-AKT signalling in the chronic constriction injury model (CCI) of neuropathic pain. Novel insight on thermal nociception is offered by Engel et al. Their work investigates the interplay between sodium-activated potassium channel Slick (Kcnt2) and the transient receptor potential melastatin (TRPM3), which is highly co-expressed in specialised heat-sensitive neurons, highlighting possible new pharmacological targets.

Clinical studies and systematic reviews: toward personalised medicine

Clinical studies included in this Research Topic represent a significant contribution to developing patient-centered interventions.

Baeumler et al. contribute to the ongoing debate on predicting acupuncture analgesic response in relation to high temporal summation (TS), reporting that acupuncture effectively reduces pain in patients with chronic non-specific low back pain (LBP) regardless of TS levels, supporting its use as a viable treatment for a broader population. The clinical trial by Scuteri et al. presents compelling evidence on the efficacy of a nanoparticle formulation of bergamot essential oil (NanoBEO) in managing both pain and agitation in patients with severe dementia, highlighting a natural-derived alternative to conventional analgesics in these complex patients already undergoing polypharmacotherapy. Takahashi et al. further explore the neuropsychiatric component in ADHD-comorbid nociplastic pain, highlighting the functional hyperactivity of the praecuneus, a key brain region involved in self-referential thinking, attention, and pain processing. A focus on the affective component, including the pain catastrophizing, of menstrual pain is given by Hsu et al. They investigate how catechol-O-methyltransferase (COMT) Val158Met polymorphisms influence the top-down pain modulation within the reward system, significantly contributing to individual differences in pain regulation. Papa et al. provide crucial long-term data on buprenorphine transdermal patches, demonstrating its sustained analgesic effects with reduced side effects and reduced risk of addiction compared to other opioids, reinforcing its role as a viable option for chronic pain management. Finally, the metabolomic profile of the novel anti-NGF antibody DS002 is reported by Jin et al. This phase I study shows how cartilage and bone metabolism are not significantly affected by treatment with the antibody, suggesting that DS002 may offer a safer alternative to existing anti-NGF analgesics with fewer joint-related adverse effects.

Systematic reviews also play a pivotal role in consolidating knowledge and guiding future research.

The meta-analysis by Peng et al. on levetiracetam for paediatric migraine prophylaxis offers valuable insights into its efficacy and underscores the need for further exploration on its safety profile. Starting from a case report, the scoping review by Peraire et al. on ziconotide-related psychosis raises awareness of the neuropsychiatric implications of this treatment. A mechanism related to the blockade of N-type voltage-gated calcium channels in glutamatergic and GABAergic neurons is hypothesised, highlighting the critical need to balance pain relief and patient safety.

Reviews and future directions

As the field evolves, reviews provide a comprehensive synthesis of emerging trends and future perspectives. The discussion by Yang et al. on mirogabalin as a novel calcium channel α2δ ligand underscores its promising role in the treatment of neuropathic pain and related comorbidities. Finally, Kasahara et al. explore the potential of ADHD medications for chronic pain management, opening new interdisciplinary avenues.

Looking ahead, advancing personalised medicine, exploring sex-specific differences, and targeting novel pharmacological pathways will refine pain treatment. Integrating mechanistic insights with clinical applications is essential for addressing pain and its neuropsychiatric complexities. This Research Topic highlights the crucial link between basic and clinical research, pushing us closer to effective solutions for chronic pain and associated disorders.

Author contributions

RI: Writing–original draft, Conceptualization, Writing–review and editing. FT: Writing–review and editing, Conceptualization. FG: Writing–review and editing, Conceptualization. ÁL-B: Writing–review and editing, Conceptualization.

Funding

The author(s) declare that no financial support was received for the research and/or publication of this article.

Conflict of interest

Author FT is employed by Cannabiscientia SA (scientific and educational company).

The remaining authors declare that the research was conducted in the absence of any commercial or financial

relationships that could be construed as a potential conflict of interest.

Generative AI statement

The author(s) declare that no Generative AI was used in the creation of this manuscript.

Publisher's note

frontiers | Frontiers in Pharmacology

TYPE Clinical Trial
PUBLISHED 01 August 2024
DOI 10.3389/fphar.2024.1417851

OPEN ACCESS

EDITED BY
Fabio Turco,
Cannabiscientia SA, Switzerland

REVIEWED BY
Alberto Chiarugi,
University of Florence, Italy
Chiara Resnati,
University of Milan, Italy

*CORRESPONDENCE
Damiana Scuteri,
damiana.scuteri@unicz.it

‡A complete list of Pilot BRAINAID Trial investigators and sites is given in the supplementary material

†These authors share last authorship

RECEIVED 15 April 2024
ACCEPTED 27 June 2024
PUBLISHED 01 August 2024

CITATION
Scuteri D, Pagliaro M, Mantia I, Contrada M, Pignolo L, Tonin P, Nicotera P, Bagetta G, Corasaniti MT and the Pilot BRAINAID Trial investigators (2024), Efficacy of therapeutic intervention with NanoBEO to manage agitation and pain in patients suffering from severe dementia: a pilot clinical trial.
Front. Pharmacol. 15:1417851.
doi: 10.3389/fphar.2024.1417851

Efficacy of therapeutic intervention with NanoBEO to manage agitation and pain in patients suffering from severe dementia: a pilot clinical trial

Damiana Scuteri[1]*, Martina Pagliaro[2], Isabel Mantia[3], Marianna Contrada[3], Loris Pignolo[3], Paolo Tonin[3], Pierluigi Nicotera[4], Giacinto Bagetta[2†], Maria Tiziana Corasaniti[1†] and the Pilot BRAINAID Trial investigators[‡]

[1]Department of Health Sciences, University "Magna Graecia" of Catanzaro, Catanzaro, Italy, [2]Preclinical and Translational Pharmacology, Department of Pharmacy, Health Science and Nutrition, University of Calabria, Cosenza, Italy, [3]Regional Center for Serious Brain Injuries, S. Anna Institute, Crotone, Italy, [4]The German center for Neurodegenerative Diseases (DZNE), Bonn, Germany

Background: An estimated 57.4 million people live with dementia worldwide, with the social burden of the disease steadily growing. Despite the approval of lecanemab and ongoing trials, there is still a lack of effective and safe treatments for behavioral and psychological symptoms of dementia (BPSD), which affect 99% of patients. Agitation is one of the most disabling BPSD, with a cross-sectional prevalence of ≥50% in nursing homes, and refers to help-seeking behavior in response to various sources of discomfort, among which pain is a crucial component.

Methods: This pilot phase of the BRAINAID (NCT04321889) trial aimed to assess the effectiveness of the patented nanotechnological device NanoBEO in older (≥65 years) people with severe dementia. This randomized placebo-controlled trial, with quadruple masking that involved all operators and participants, followed the SPIRIT and CONSORT statements. A total of 29 patients completed the trial. The patients were randomly allocated in a 1:1 ratio to the NanoBEO or placebo group, and the corresponding product was applied on both arms once daily for 4 weeks, with a 4-week follow-up period. The primary endpoint was efficacy against agitation. The secondary endpoints were efficacy against agitation at follow-up and efficacy against pain. Any adverse events were reported, and biochemical analyses were performed.

Results: The NanoBEO intervention reduced the frequency (28%) and level of disruptiveness of agitated behaviors. The effect on frequency was statistically significant after 2 weeks of treatment. The efficacy of NanoBEO on agitated behaviors lasted for the entire 4-week treatment period. No additional psychotropic drugs were prescribed throughout the study duration. The results after 1 week of treatment demonstrated that NanoBEO had statistically significant analgesic efficacy (45.46% improvement in pain intensity). The treatment was well tolerated.

Discussion: This trial investigated the efficacy of NanoBEO therapy in managing agitation and pain in dementia. No need for rescue medications was recorded,

strengthening the efficacy of NanoBEO in prolonged therapy for advanced-stage dementia and the usefulness of the intervention in the deprescription of potentially harmful drugs. This study provided a robust rationale for the application of NanoBEO in a subsequent large-scale pivotal trial to allow clinical translation of the product.

Clinical Trial Registration: ClinicalTrials.gov, identifier NCT04321889.

KEYWORDS

NanoBEO, agitation, dementia, behavioural and psychological symptoms of dementia, pain, pilot clinical trial, BRAINAID, NCT04321889

1 Introduction

The medical and social burden of dementia is steadily growing. The disease affects approximately 57.4 million people worldwide, with the number estimated to triple by 2050, and more women are living with dementia than men (women:men ratio of 1.67) (GBD, 2022). The recent approval by the Food and Drug Administration (FDA) of lecanemab for early Alzheimer's disease (AD) (Doggrell, 2024) renewed interest in the β-amyloid (Aβ) theory. The lack of disease-modifying drugs may lead to inappropriate treatment of the behavioral and psychological symptoms of dementia (BPSD), without much supporting evidence for the efficacy or safety of interventions (Scuteri et al., 2021b). Ongoing clinical trials are investigating pathophysiology-based disease-modifying medications, from small molecules such as simufilam (Wang et al., 2023) (NCT05575076; NCT04994483) to passive immunotherapies such as the novel remternetug directed against a pyroglutamated form of Aβ (NCT05463731). Despite progress, the main target remains the stage of amnestic mild cognitive impairment (aMCI) and prodromal AD (Huang et al., 2023). Potential therapeutic mechanisms involve neuroprotection, anti-inflammation, cognitive enhancement, neuropsychiatric control and, in the frame of the latter actions, drugs that can induce autophagy are promising candidates to reduce neurodegeneration (Chu, 2006; Metaxakis et al., 2018). However, clinically useful autophagy inducers with measurable effect on autophagy that are safe and can cross the blood–brain barrier deserve further investigation (Corasaniti et al., 2024).

With almost all patients (99%) experiencing at least one symptom (Pinyopornpanish et al., 2022), management of BPSD is challenging, mainly in the advanced stages of the disease. BPSD are presented differently across individuals and with various degrees of severity, and are associated with poor outcomes (Cerejeira et al., 2012). Moreover, it is important to point out the need for consideration and inclusion in clinical trials of several, less frequently occurring, phenotypes such as posterior cortical atrophy (Bejanin and Villain, 2024). BPSD usually occur chronically in a fluctuating pattern, and patients present at least one symptom at subsequent assessments; thus, BPSD are associated with longitudinal cognitive decline (Burhanullah et al., 2020). Recently, the presence of BPSD was linked to gray and white matter lesions, with multiple correlations observed in patients with hyperactivity using single-photon emission computed tomography (SPECT) and T1-weighted magnetic resonance imaging (MRI) (Nakase et al., 2023). BPSD are often under-recognized and early depression and mild behavioral impairment (MBI) can be prodromal to cognitive impairment (Ismail et al., 2017); however, this knowledge did not spur effective and safe pharmacological therapies (Scuteri et al., 2021b). The prospective, population-based, longitudinal Cardiovascular Health Study-Cognition Study demonstrated a high risk of developing MCI in up to 19.7% of the people who experience moderate-to-high depressive symptoms (Barnes et al., 2006). In particular, the results by the European Alzheimer's Disease Consortium in 2,808 patients with dementia demonstrate a consistent occurrence of hyperactivity, affective symptoms, psychosis, and apathy, with the latter two symptoms correlated with the use of cholinesterase inhibitors and dementia severity, respectively (Aalten et al., 2008). The prevalence of some BPSD was estimated in people with dementia (PwD; n = 587) and non-affected counterparts (n = 2,050) in a population-based longitudinal study of ageing; the study highlighted that all BPSD (except sleep disorders) occurred more often in PwD and that certain symptoms—psychosis/apathy, depression/anxiety, irritability/persecution, and wandering/sleep problems—co-occurred (Savva et al., 2018). All these findings point to the burden of BPSD.

Agitation is one the most common and disabling BPSD that mainly affects PwD at moderate to severe stages. A cross-sectional prevalence of over 50% in nursing homes has been reported, with at least one item of the Cohen-Mansfield Agitation Inventory (CMAI) presented weekly in 75.4% of the cases (Testad et al., 2007). Moreover, a high correlation has been found between the CMAI score and stage of dementia (Spearman rho = 0.421, p = 0.000); patients who received psychoactive medication had a higher mean CMAI score (39.9, SD 13.1), and the use of psychotropic drugs correlated with the stage of dementia (Testad et al., 2007). Dementia is often underdiagnosed and co-occurring with agitation and inappropriate treatment (Scuteri et al., 2021e), as evidenced in data collected from a sample of 1,163 patients, of whom 81% presented with dementia, 72% experienced clinically relevant BPSD, and 75% received psychotropic medications (Selbæk et al., 2007).

Agitation can be defined as help-seeking behavior in response to various sources of discomfort, among which pain is a crucial component (Husebo et al., 2014). PwD are usually affected by age-related comorbidities that cause chronic pain, which remains underdiagnosed because of the lack of self-report measures

(Sampson et al., 2015); in fact, approximately 80% of the patients with dementia in nursing homes experience pain (Achterberg et al., 2013). Agitation treatment relies on atypical antipsychotics, among which risperidone has received approval and, on 11 May 2023, the FDA announced the supplemental approval of brexpiprazole for the treatment of agitation associated with dementia (Cummings et al., 2024); notably, these drugs potentially increase the risk of death due to cardio-cerebrovascular accidents (Schneider et al., 2005; Cummings et al., 2024). In people with moderate-to-severe, but not mild, AD, memantine exerts a small clinical effect (McShane et al., 2019), while other, off-label, drugs, such as antidepressants and benzodiazepines, worsen cognitive decline and enhance the risk of harmful falls (Harris and Lykina, 2022).

In view of the possible role of non-pharmacological therapies in BPSD (Davison et al., 2024), the correlation between pain and agitation, and the confirmed priority of analgesia in BPSD management, appropriate and integrated measures to target pain (Corbett et al., 2014) are needed to safely treat agitation. Although aromatherapy with *Melissa officinalis* essential oil improves the CMAI score (Ballard et al., 2002), its superiority to placebo or donepezil has not been demonstrated (Burns et al., 2011). Likewise, the efficacy of aromatherapy with *Lavandula angustifolia* essential oil is controversial (Holmes et al., 2002; Lin et al., 2007; O'Connor et al., 2013; Moorman Li et al., 2017; Zalomonson et al., 2019). Managing the robust scent of essential oils poses considerable challenges when designing real-world double-blinded clinical trials; this and other methodological biases have hindered any definite conclusions regarding the efficacy of aromatherapy in dementia (Forrester et al., 2014), similar to the situation regarding the application of nutraceuticals in other neurodegenerative diseases such as glaucoma (Scuteri et al., 2020). Strong preclinical evidence of efficacy has been reported for the essential oil of bergamot (BEO; *Citrus bergamia* Risso et Poiteau) in models of pain relevant to clinical conditions (Scuteri et al., 2021c). Efficacy has been shown after continuous administration (Hamamura et al., 2020) and via inhalation (Scuteri et al., 2018; Scuteri et al., 2022d) and transdermal application (Scuteri et al., 2022c), useful for aromatherapy. Furthermore, BEO exerts anxiolytic activity devoid of the sedative effects typical of benzodiazepines (Rombolà et al., 2020). The nonvolatile fraction of BEO, representing the 4%–7% of total, contains furocoumarins, e.g., bergapten (Mondello et al., 1993; Dugo et al., 2000), that can induce phototoxic reactions of the skin caused by the photoactivation of bergapten due to ultraviolet light (Zaynoun et al., 1977). BEO was delivered in a bergapten-free form to avoid phototoxicity, the only documented side effect according to the assessment report of the European Medicine Agency (EMA) (13 September 2011 EMA/HMPC/56155/2011 Committee on Herbal Medicinal Products [HMPC]). In fact, furocoumarin-free BEO was engineered in a nano-size delivery system, based on solid lipid nanoparticles, and formulated as an odorless cream known as NanoBEO (Scuteri et al., 2021a).

In the frame of the pilot phase of the BRAINAID trial (NCT04321889) (Scuteri et al., 2021d), the aim of the present clinical study was to assess the effectiveness of NanoBEO on agitation as primary endpoint and pain as secondary endpoint in PwD at the severe stage. To the best of our knowledge, this is the first trial allowing double-blindness, and also quadruple masking, due to the entrapment of BEO aroma, to investigate the effects of the formulation on agitation in severe dementia.

2 Materials and methods

The aim of the present pilot clinical study was to assess the effect of NanoBEO on agitation in older people with severe dementia. NanoBEO was prepared as an odorless cream, indistinguishable from the placebo cream, using nanotechnology to load BEO. This pilot trial was designed as a randomized, quadruple-blind placebo-controlled trial (NCT04321889) and was registered in ClinicalTrials.gov on 23 March 2020, to assess the efficacy of furocoumarin-free BEO loaded in a nanocarrier delivery system in the treatment of agitation in older individuals with severe dementia. This study was approved by the Calabria Region Ethics Committee (protocol No. 352, first version; 21 November 2019). The protocol and trial followed the Standard Protocol Items: Recommendations for Interventional Trials (SPIRIT) (An-Wen et al., 2013) and the Consolidated Standards of Reporting Trials (CONSORT) (Kenneth et al., 2010) guidelines.

This trial was designed as a prospective, single-center, exploratory interventional study without a drug. The coordination center was Sant'Anna Institute, the regional center of care and research for severe brain injuries, which specializes in motor and cognitive treatment and rehabilitation of patients with neurological diseases. The data were collected from nursing homes in Southern Italy, which were recruited for this study. This clinical trial was intended as a pilot study before a subsequent large-scale, adequately powered, pivotal study.

The primary endpoint was the clinical effectiveness of NanoBEO in a 4-week treatment of agitation in patients with severe dementia. The secondary endpoints were changes in agitation in a follow-up period after the end of the intervention and the clinical efficacy of NanoBEO against pain in patients with severe dementia.

2.1 Eligibility criteria

Consecutive patients with a diagnosis of dementia were enrolled according to the following inclusion criteria: 1) mini-mental state examination (MMSE) score ≤12 and 2) provision of informed consent by a legal representative.

Patients were reported to receive quetiapine and promazine for psychotic, aggressive disorders and mirtazapine, paroxetine, trazodone and alprazolam, bromazepam, delorazepam or clonazepam for depressive and anxious manifestations (also concurrently in some cases) and, occasionally, acetaminophen. One case of use of haloperidol, one of zolpidem and one of gabapentin were recorded at baseline. The patients were allowed to receive authorized concurrent therapies for the treatment of agitation (risperidone for aggressive behavior). Therapies for the treatment of other chronic comorbidities—such as drugs for the

treatment of hypertension or diabetes, for gastric protection, anti-inflammatories, and antibiotics—were allowed. A legal representative of the patient was informed about the study and provided a consent form, which was collected by healthcare operators.

Patients with a clinical history of disabling neurological or psychiatric diseases (including Parkinson's disease, stroke, cerebral hemorrhage, delirium, and psychosis) were excluded.

2.2 Treatments and chemicals

For the production of NanoBEO according to the patent specifications (request and concession number 102019000013353) (Scuteri et al., 2021a), BEO was kindly supplied by Capua 1880 S.r.l. (Campo Calabro, Reggio Calabria, Italy). The chemical composition of BEO and the percentage ranges of its most abundant components are presented in Table 1.

TABLE 1 Percentage ranges of the main components of the essential oil of bergamot (BEO).

Chemical substance	Ranges (%)
α-Pinene	0.7–2.0
Sabinene	0.5–2.0
β-Pinene	5.0–10.0
Limonene	30.0–50.0
γ-Terpinene	6.0–18.5
Linalool	6.0–15.0
Linalyl acetate	23.0–35.0
Geranial	< 0.5
Geranyl acetate	0.1–0.7
Cariophyllene	0.2–0.5

2.3 Collection of biological specimens

Biological specimens for biochemical analyses (azotemia and serum creatinine, creatine phosphokinase [CPK], and transaminase levels) were collected before treatment and weekly during treatment and follow-up, in accordance with standard care practices.

2.4 Treatment schedule and procedure

The patients who met all the inclusion criteria and none of the exclusion criteria were enrolled in the study and randomized in a 1:1 allocation ratio to the active intervention (NanoBEO) or the placebo group. To avoid any bias associated with sequence generation, the design involved no blocking (e.g., incomplete randomization). The allocation randomization codes were obtained using the random number generator in Microsoft Office Excel 2010 (Milan, Italy). No member of the trial who administered the treatments or analyzed the data had access to the codes until the end of the trial, to ensure adequate allocation concealment and prevent performance and detection biases. The operators who independently recruited patients were different from those who generated the allocation sequence and those who assigned participants to the two arms. Healthcare personnel, patients, outcome assessors, and data analysts were blinded to the assignment to interventions, allowing quadruple masking. To guarantee security and data quality, two operators performed double data entry and the collection and maintenance of patient information was only handled by the administration staff of the clinical trial unit at the coordinating center; this strategy was selected to protect confidentiality before, during, and after the trial. After randomization (T0), all patients in both groups were administered one application containing a dose of 1 g of active cream or placebo cream on each arm once daily for 4 weeks between 8:00 and 10:00 a.m. A single dispenser covered the entire 4-week treatment. The procedure was completed in approximately 2 min. The packaging was identical for NanoBEO and the placebo and the two products were indistinguishable in terms of appearance, texture, and scent. After signing the informed consent form to participate in the study, the patients at T0 were assessed for baseline clinimetric variables using MMSE, CMAI, and the Italian Mobilization–Observation–Behavior–Intensity–Dementia (I-MOBID2) pain scale. We also collected anamnestic data, which included significant medical events in the last 30 days, administered drugs or changes in therapies, and any complementary therapies. Administration of CMAI and MOBID-2 was repeated weekly for 4 weeks (T1A first week, T1B, second week, T1C third week, T1D last week of treatment) and again weekly for another 4 weeks (T2A first week, T2B, second week, T2C third week, T2D last week of follow-up). A schematic representation of the study procedure is shown in Figure 1. Adverse events were recorded on a specific form to assess the following aspects: symptom severity (mild, moderate, or severe); correlation with treatment administration (suspected/not suspected); duration (start and end or if present at the time of the final evaluation); and serious adverse events.

This trial recruited patients with difficulties in communication, who resided in nursing homes; NanoBEO and the placebo cream were topically administered by healthcare operators to ensure that the specified interventions were adhered to. The healthcare operators were asked to retain each empty dispenser. To avoid attrition bias due to deviations from the protocol by excluding patients from the analysis who failed to follow to the protocol, we used an intention-to-treat approach, declaring drop-outs and including patients up to trial discontinuation.

2.5 Outcome measures

The outcome measures were the CMAI scores for agitation and I-MOBID2 scores for pain. All the raters and responders (as the CMAI is assessed by a researcher/operator who interviews a caregiver) underwent training, in which descriptions of the tools used were provided to guarantee correct execution of the assessment and inter-rater reliability. As per the a priori-set protocol of the study, the same rater performed the baseline

	STUDY PERIOD									
	Enrolment	Allocation	Post-allocation:Interventions				Follow-up			
TIMEPOINT	-within 2 weeks	baseline	week 1	week 2	week 3	week 4	week 5	week 6	week 7	week 8
ENROLMENT:	X									
Eligibility screen	X									
Informed consent	X									
Physical examination	X									
Allocation		X								
INTERVENTIONS:										
BEO cream			←	—	—	→				
Placebo			←	—	—	→				
ASSESSMENTS:										
CMAI		X	X	X	X	X	X	X	X	X
MOBID-2		X	X	X	X	X	X	X	X	X
Routine clinical and neurophysiological assessments and hemato-biochemical parameters		X				X				

FIGURE 1
Schedule for patient enrollment, treatment administration, follow-up, and related outcome measures. CMAI, Cohen-Mansfield Agitation Inventory; MOBID-2, Mobilization–Observation–Behavior–Intensity–Dementia test.

assessment and the evaluations during treatment administration and follow-up. As reported above, pain assessment in PwD with communicative difficulties is complex and observational pain scales have been devised for patients with severe dementia and compromised communicative abilities. The CMAI assessment was completed in 20 min, while the I-MOBID2 assessment required approximately 5–6 min. A template of the data collection form, which was then copied into Excel format, is shown in Figure 2.

2.6 Statistical analysis

The patients were considered in pain when the I-MOBID2 items or overall pain intensity were scored ≥3 and with a CMAI score for agitation ≥39. No sample power calculation was performed because this study was not interventional with new drugs; however, the pilot phase of the BRAINAID clinical trial for which a statistical analysis plan (SAP) with sample power calculation has been provided (Scuteri et al., 2021d). The statistical differences between the two groups for baseline patient characteristics were assessed using the Student's t-test and Mann–Whitney *U* test (MWU). The results are presented as the median, with 95% confidence intervals (CI) and interquartile range (IQR). The statistical differences in individual medians were assessed using two-way ANOVA for repeated measures, followed by Tukey's multiple comparison test. All analyses were performed using Microsoft Office Excel 10 and GraphPad Prism 6.0 (GraphPad Software by Dotmatics, CA). Values of $p \leq 0.05$ were considered statistically significant.

3 Results

3.1 Characteristics of the patients

Thirty-one patients were screened for eligibility. One patient was transferred to another nursing home and was excluded. Thus, the study included 30 participants from eight nursing homes. Of these

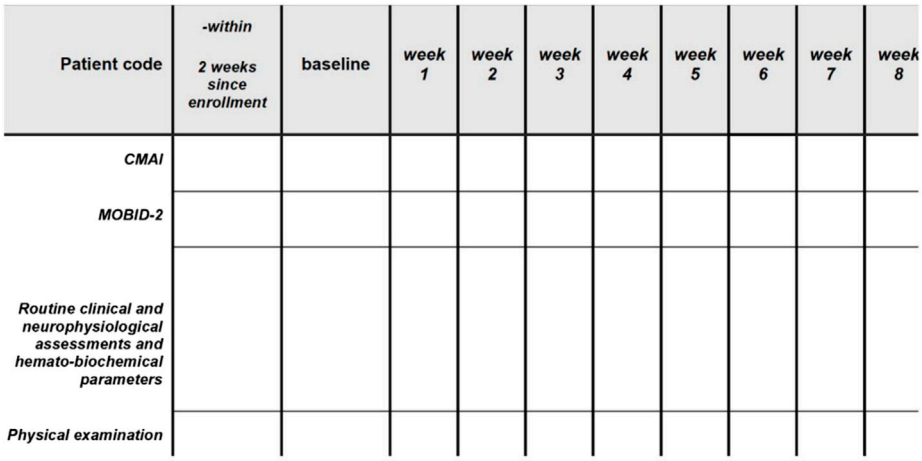

FIGURE 2
Data collection form.

TABLE 2 Age and baseline assessment of agitation and pain in the patients enrolled in the trial and subsequently allocated to the NanoBEO and placebo groups.

Baseline characteristics	NanoBEO group (n = 14)	Placebo group (n = 16)	Statistical analysis: *p*-Value and 95% CI
Age (mean ± SD)	86.07 ± 7.26	87.50 ± 6.68	0.58 *t*-test
CMAI-frequency (F; median)	50.50	50.50	0.64 (−21.00; −11.00) MWU test
CMAI-disruptiveness (D; median)	43.00	43.00	0.43 (−14.00; −6.00) MWU test
I-MOBID2 (median)	5.5	3.00	0.17 (−3.00; 1.00) MWU test

SD, standard deviation; CI, confidence intervals; I-MOBID2, Italian Mobilization–Observation–Behavior–Intensity–Dementia; MWU, Mann–Whitney *U* test.

patients, 14 were allocated to the NanoBEO arm and 16 to the placebo arm. The baseline characteristics of the two groups were similar, except for a trend for higher, but not significantly different, baseline I-MOBID2 scores in the NanoBEO group. The mean age of all participants was 86.83 ± 6.87 (standard deviation [SD]) years, with a mean age of 87.50 ± 6.68 and 86.07 ± 7.26 for the patients allocated to the placebo and NanoBEO arms, respectively. Most patients were women, with one male patient per group, in agreement with descriptions of the sex distribution and prevalence of the disease and considering the small sample size. Apart from one patient who was subsequently allocated to the placebo group, all the patients were prescribed at least one psychotropic medication, with one patient receiving only dihydrocodeine with psychotropic action. The baseline characteristics of the patients are presented in Table 2.

Twenty-nine patients (96.67%) completed the intervention phase and follow-up. One participant (age, 92 years) in the placebo group died after having completed the first week of treatment; his death was attributed to cardiac and respiratory illness and was unrelated to the study treatment. Over the course of the study, no additional psychotropic drugs were prescribed as rescue medications for increased agitation. The analysis includes data from 16 patients in the placebo group for the first week and from 15 patients after the death of one patient. The processes related to enrollment, group allocation, follow-up, and analysis are reported in the CONSORT flow diagram in Figure 3.

3.2 Efficacy of treatment on agitation

A reduction in both the frequency (Figures 4A–C) and level of disruptiveness (Figures 5A–C) of agitated behaviors, as assessed by the CMAI scores, were observed in the patients allocated to the NanoBEO group in comparison to those in the placebo group. The CMAI is a caregiver-rated questionnaire that consists of 29 items that examine behaviors associated with agitation; the scores range from 29 to 203, with significant agitation indicated at scores ≥39. The frequency of presentation of each behavior is rated on a seven-point scale based on assessments in the preceding 2 weeks. The frequency of occurrence of behaviors was rated as follows: never; less than once a week; once or twice a week; several times a week; once or twice per d; several times per d; and several times per h. Each behavior can be represented by a wide spectrum of impairments; thus, the raters and respondents were provided with a detailed description of behaviors. Correct execution of the test was

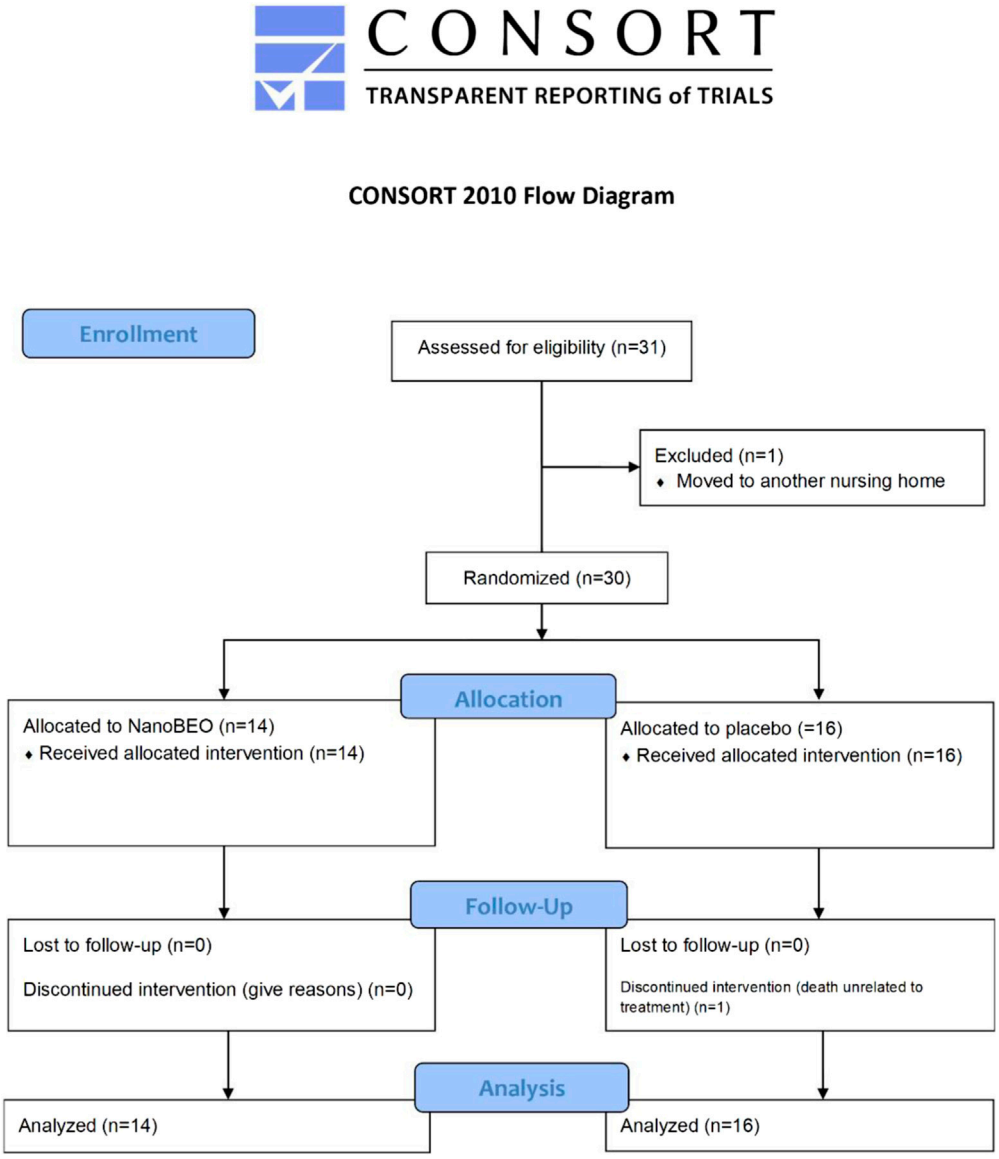

FIGURE 3
Consolidated Standards of Reporting Trials (CONSORT) flow diagram of progress through the various stages—enrollment, allocation, intervention, follow-up, drop-out, and analysis—of the pilot trial on the effectiveness and safety of NanoBEO in dementia.

explained, emphasizing that the closest related item and similar behavioral indicators should be included, even when these were not exactly reported in the behavioral descriptors. To assess the level of agitation, the assessor/interviewer conducted an interview with the caregiver/respondent familiar with the patients, who was provided with a copy of the scale several days before. On the day of assessment, the interviewer explained the importance of the scale and the procedure, read aloud each item, and performed a face-to-face interview without influencing the answers, in a quiet room and without interruptions. Apart from rating frequency, ratings of the disruptiveness of the observed behaviors were included, with questions examining the level of disruptiveness of each item to the staff according to the following grading: not at all; a little; moderately; very much; extremely. The corresponding numeric rating scale was as follows: 1 = never; 2 = less than once a week but still occurring; 3 = once or twice a week; 4 = several times a week; 5 = once or twice per d; 6 = several times per d; 7 = several times per h. The obtained scores reflected the average frequency of occurrence in the previous 2 weeks. NanoBEO was most effective at improving the frequency of occurrence of agitated behaviors at the first time point (Figure 4B), which corresponds to 2 weeks of treatment. Statistically significant differences were noted for all time points *versus* baseline for frequency (Figure 4C; time factor $^{****}p < 0.0001$; participant matching $^{****}p < 0.0001$; NanoBEO: 2, 4, and 6 weeks $^{**}p < 0.01$; 8 weeks $^{***}p < 0.001$) and for disruptiveness (Figure 5C; time factor $^{****}p < 0.0001$; participant matching $^{****}p < 0.0001$; NanoBEO: 2 weeks $^{**}p < 0.01$; 4, 6, and 8 weeks $^{***}p < 0.001$). A 28% improvement in the frequency of agitated behaviors was

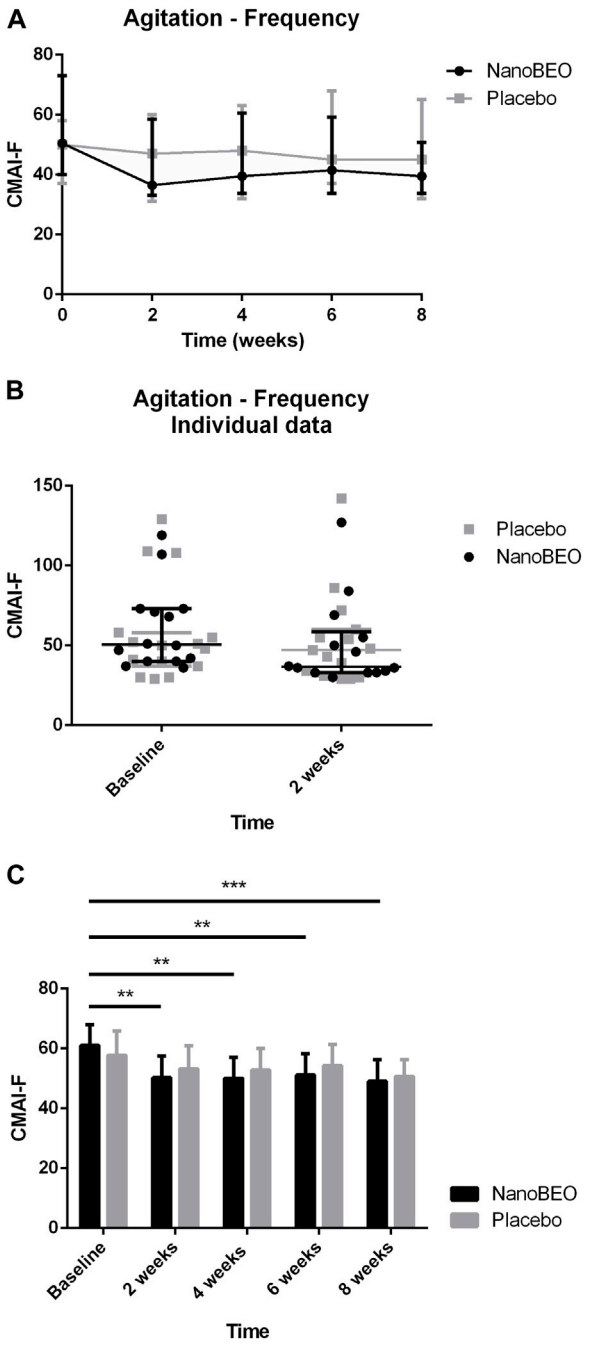

FIGURE 4
Efficacy of NanoBEO on the frequency of agitation based on the CMAI-F scores during treatment and follow-up **(A)** and as individual data at baseline and after 2 weeks of treatment **(B)**; data are expressed as the median + interquartile range (IQR). Patients allocated to the NanoBEO group experienced a reduction in CMAI-F scores than did patients allocated to the placebo group. **(C)** Statistically significant differences regarding NanoBEO efficacy were observed for all time points *versus* baseline (data are expressed as the mean ± SEM; time factor ****$p < 0.0001$; participant matching ****$p < 0.0001$; NanoBEO: 2, 4, and 6 weeks **$p < 0.05$, 8 weeks ***$p < 0.001$). *p values <0.05 are considered to indicate statistical significance. n: NanoBEO = 14, placebo = 16. SEM, standard error of the mean.

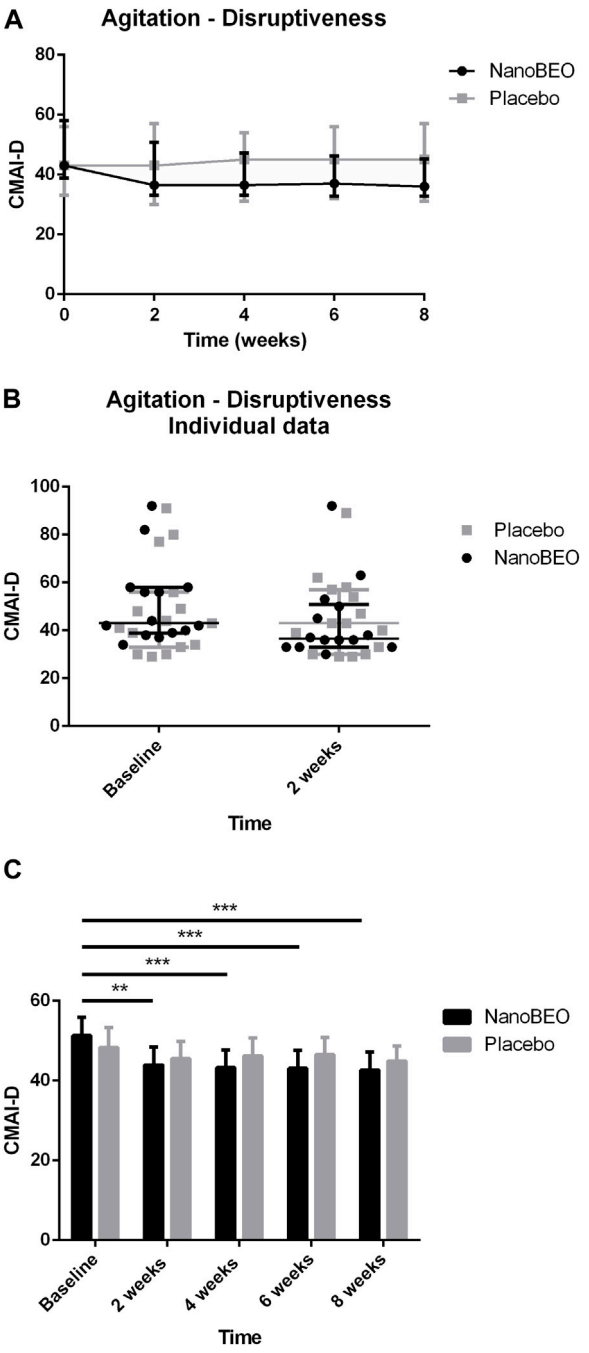

FIGURE 5
Efficacy of NanoBEO on disruptiveness of agitation based on the CMAI-D scores during treatment and follow-up **(A)** and as individual data at baseline and after 2 weeks of treatment **(B)**; data are expressed as the median + IQR. Patients allocated to the NanoBEO group experienced a reduction in CMAI-D scores than did patients allocated to the placebo group. **(C)** Statistically significant differences regarding NanoBEO efficacy were observed for all time points *versus* baseline (data are expressed as the mean ± SEM; time factor ****$p < 0.0001$; participant matching ****$p < 0.0001$; NanoBEO: 2 weeks **$p < 0.01$; 4, 6 and 8 weeks ***$p < 0.001$). *p values <0.05 indicate statistical significance. n: NanoBEO = 14, placebo = 16.

observed in the NanoBEO group in comparison with 6.93% in the placebo group. The observed rate was nearly as high as the threshold rate of 30% for improvement, which is generally regarded as significant in clinical trials that investigate the efficacy of interventions for the management of BPSD (Ballard et al., 2002); this is an important result, despite the

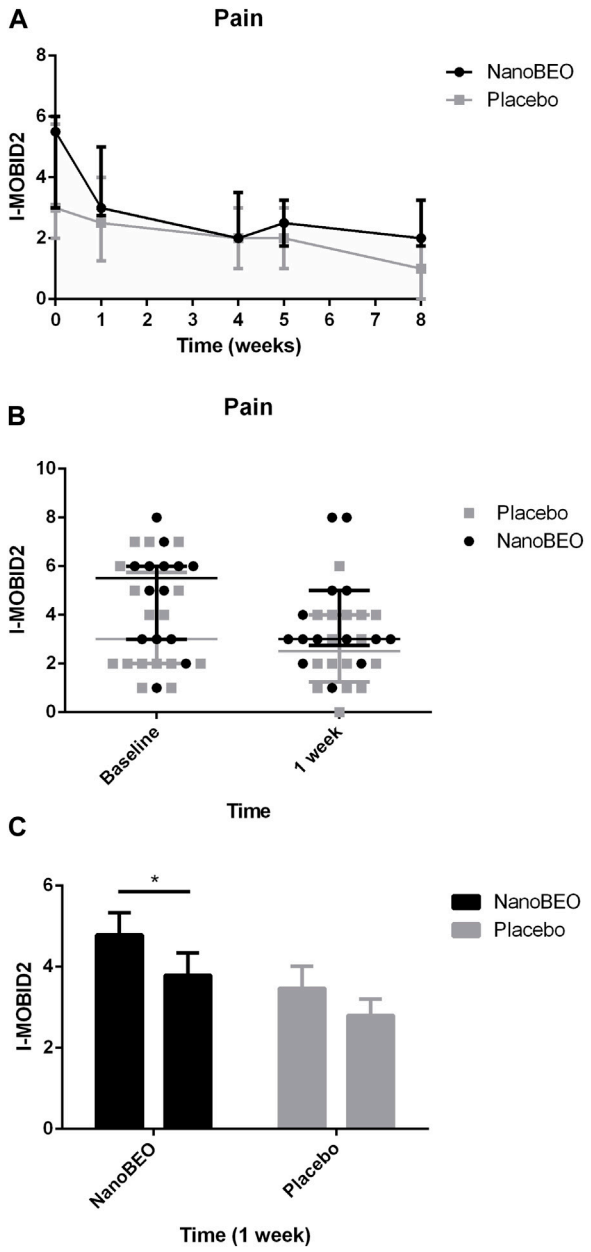

FIGURE 6
Efficacy of NanoBEO on pain based on the I-MOBID2 scores during treatment and follow-up **(A)** and as individual data at baseline and after 1 week of treatment **(B)**; data are expressed as the median + IQR. Patients allocated to the NanoBEO group exhibited decreased I-MOBID2 scores than did patients in the placebo group after 1 week; the scores decreased until the end of treatment and increased during the follow-up period but without reaching the baseline value. **(C)** Statistically significant differences in the effectiveness of NanoBEO (data are expressed as the mean ± SEM; time factor $^{**}p = 0.0031$; participant matching $^{****}p < 0.0001$; NanoBEO baseline vs 1 week $^{*}p < 0.05$). $^{*}p$ values <0.05 indicate statistical significance. n: NanoBEO = 14, placebo = 16.

underpowered study due to the pilot nature of the clinical trial. Individual data showed a homogeneous distribution, confirming the effectiveness of NanoBEO against agitation in most patients regarding the frequency and disruptiveness of behaviors. The effects were present in the entire 4-week treatment period for both factors. The effect on frequency gradually decreased during follow-up, while that on disruptiveness was maintained after the end of treatment and for the entire 4 weeks of follow-up.

3.3 Efficacy on pain

The patients allocated to the NanoBEO group presented with higher pain intensity at baseline than the patients in the placebo group, as assessed by the I-MOBID2 scores, although this trend did not reach statistical significance (Figures 6A–C). These differences in the baseline values influenced the differences between the two arms throughout the study period. The I-MOBID2 pain scale was

TABLE 3 Assessment of biochemical parameters—azotemia (a), and levels of serum creatinine (b), creatine phosphokinase (CPK; c), and transaminases (d, e)—at baseline, after 4-week treatment with NanoBEO and at the end of the follow-up period. The reference values, depending on the laboratory, are reported in brackets.

Azotemia (mg/dL)			
Patient ID	Baseline	Treatment (week 4)	Follow-up (week 8)
D02	42.00 (17.00–43.00)	53.00 (17.00–43.00)	46.7 (17.00–43.00)
D04	74.00 (17.00–43.00)	111.00 (17.00–43.00)	82.9 (17.00–43.00)
D06	77.00 (17.00–43.00)	54.00 (17.00–43.00)	74.00 (17.00–43.00)
D08	39.00 (17.00–43.00)	46.00 (17.00–43.00)	32.00 (17.00–43.00)
D13	____	95.00 (17.00–43.00)	79.00 (17.00–43.00)
D14	29.00 (17.00–43.00)	41.00 (17.00–43.00)	66.00 (17.00–43.00)
D16	48.00 (10.00–55.00)	41.00 (10.00–55.00)	50.00 (10.00–55.00)
D19	61.00 (10.00–55.00)	45.00 (10.00–55.00)	46.00 (10.00–55.00)
D20	78.00 (10.00–55.00)	95.00 (10.00–55.00)	110.00 (10.00–55.00)
D22	35.00 (17.00–43,00)	33.00 (17.00–43.00)	34,3 (17.00–43.00)
D23	55.00 (17.00–43.00)	31.00 (17.00–43.00)	49.1 (17.00–43.00)
D27	41.00 (20.00–50.00)	29.00 (10.00–50.00)	35.00 (10.00–50.00)
D28	49.00 (10.00–50.00)	53.00 (10.00–50.00)	58.00 (10.00–50.00)
D31	37.00 (10.00–50.00)	44.00 (10.00–50.00)	37.00 (10.00–50.00)
Serum creatinine (mg/dL)			
Patient ID	Baseline	Treatment (week 4)	Follow-up (week 8)
D02	0.83 (0.66–1.09)	0.92 (0.66–1.09)	0.87 (0.66–1.09)
D04	1.4 (0.66–1.09)	1.62 (0.66–1.09)	1.48 (0.66–1.09)
D06	1.23 (0.66–1.09)	1.15 (0.66–1.09)	1.14 (0.66–1.09)
D08	0.93 (0.66–1.09)	1.09 (0.66–1.09)	0.81 (0.66–1.09)
D13	____	1.7 (0.66–1.09)	1.77 (0.66–1.09)
D14	0.78 (0.66–1.09)	0.9 (0.66–1.09)	0.9 (0.66–1.09)
D16	0.88 (0.60–1.30)	0.84 (0.50–0.90)	0.84 (0.50–0.90)
D19	0.95 (0.60–1.30)	0.82 (0.50–0.90)	0.89 (0.50–0.90)
D20	1.42 (0.60–1.30)	1.40 (0.50–0.90)	1.63 (0.50–0.90)
D22	0.64 (0.66–1.09)	0.68 (0.66–1.09)	0.77 (0.66–1.09)
D23	0.84 (0.66–1.09)	0.74 (0.66–1.09)	0.95 (0.66–1.09)
D27	1.19 (0.50–0.90)	0.99 (0.60–1.30)	1.14 (0.60–1.30)
D28	0.59 (0.70–1.40)	0.68 (0.70–1.40)	0.57 (0.70–1.40)
D31	0.73 (0.60–1.30)	0.77 (0.60–1.30)	0.67 (0.60–1.30)
Creatine phosphokinase (CPK; IU)			
Patient ID	Baseline	Treatment (week 4)	Follow-up (week 8)
D02	42 (0–145)	59 (0–145)	66 (0–145)
D04	28 (0–145)	20 (0–145)	19 (0–145)
D06	58 (0–145)	27 (0–145)	31 (0–145)

(Continued on following page)

TABLE 3 (*Continued*) Assessment of biochemical parameters—azotemia (a), and levels of serum creatinine (b), creatine phosphokinase (CPK; c), and transaminases (d, e)—at baseline, after 4-week treatment with NanoBEO and at the end of the follow-up period. The reference values, depending on the laboratory, are reported in brackets.

Creatine phosphokinase (CPK; IU)			
Patient ID	Baseline	Treatment (week 4)	Follow-up (week 8)
D08	19 (0–145)	25 (0–145)	20 (0–145)
D13	93 (0–145)	88 (0–145)	100 (0–145)
D14	30 (0–145)	35 (0–145)	73 (0–145)
D16	____	____	____
D19	77 (26–192)	57 (26–192)	49 (26–192)
D20	42 (26–192)	34 (26–192)	44 (26–192)
D22	30 (0–145)	40 (0–145)	25 (0–145)
D23	46 (0–145)	50 (0–145)	53 (0–145)
D27	____	16 (34–145)	15 (34–145)
D28	47 (46–171)	46 (46–171)	39 (46–171)
D31	36 (34–145)	15 (34–145)	15 (34–145)
Serum GOT transaminase (IU)			
Patient ID	Baseline	Treatment (week 4)	Follow-up (week 8)
D02	20 (11–34)	23 (11–34)	17 (11–34)
D04	15 (11–34)	16 (11–34)	11 (11–34)
D06	16 (11–34)	17 (11–34)	18 (11–34)
D08	16 (11–34)	17 (11–34)	15 (11–34)
D13	____	39 (11–34)	40 (11–34)
D14	10 (11–34)	16 (11–34)	65 (11–34)
D16	21 (0–33)	14 (0–33)	15 (0–33)
D19	16 (0–33)	12 (0–33)	11 (0–33)
D20	41 (0–33)	31 (0–33)	28 (0–33)
D22	12 (11–34)	13 (11–34)	11 (11–34)
D23	19 (11–34)	30 (11–34)	20 (11–34)
D27	16 (0–31)	22 (5–38)	12 (5–38)
D28	13 (5–38)	21 (5–38)	12 (5–38)
D31	28 (5–38)	40 (5–38)	18 (5–38)
Serum GPT transaminase (IU)			
Patient ID	Baseline	Treatment (week 4)	Follow-up (week 8)
D02	11 (7–41)	14 (7–41)	9 (7–41)
D04	4 (7–41)	4 (7–41)	3 (7–41)
D06	9 (7–41)	12 (7–41)	10 (7–41)
D08	13 (7–41)	9 (7–41)	7 (7–41)
D13	____	21 (7–41)	24 (7–41)
D14	9 (7–41)	15 (7–41)	14 (7–41)

(Continued on following page)

TABLE 3 (*Continued*) Assessment of biochemical parameters—azotemia (a), and levels of serum creatinine (b), creatine phosphokinase (CPK; c), and transaminases (d, e)—at baseline, after 4-week treatment with NanoBEO and at the end of the follow-up period. The reference values, depending on the laboratory, are reported in brackets.

Serum GPT transaminase (IU)			
Patient ID	Baseline	Treatment (week 4)	Follow-up (week 8)
D16	7 (0–32)	8 (0–32)	16 (0–32)
D19	9 (0–32)	11 (0–32)	10 (0–32)
D20	19 (0–32)	14 (0–32)	10 (0–32)
D22	7 (7–41)	10 (7–41)	7 (7–41)
D23	7 (7–41)	23 (7–41)	8 (7–41)
D27	10 (0–31)	____	15 (0–49)
D28	12 (0–49)	23 (0–49)	14 (0–49)
D31	34 (0–49)	45 (0–49)	19 (0–49)

GPT: glutamic-pyruvic transaminase (also known as alanine aminotransferase [ALT]).
GOT: glutamic-oxaloacetic transaminase (also known as aspartate aminotransferase [AST]).

recently made available for the Italian nursing homes, after validation in a cohort of patients with AD with communication issues, aged 65 years and older and with an MMSE score ≤12 (Scuteri et al., 2022a). We selected I-MOBID2 because it is the only pain scale to consider co-occurrence of musculoskeletal and visceral pain (Hadjistavropoulos et al., 2007) and to allow examination of even hidden pain conditions through active, guided movements (Husebo et al., 2010). The I-MOBID2 has demonstrated good face and content validity (0.89), high construct validity (Spearman rank-order correlation Rho = 0.748), reliable internal consistency (Cronbach's α coefficient = 0.751), good-to-excellent inter-rater (intraclass correlation coefficient [ICC] = 0.778) and test–retest (ICC = 0.902) reliability, and good inter-rater and test–retest agreement (Cohen's K = 0.744) with short training and average execution time of 5.8 min (Scuteri et al., 2022a). Hence, we obtained all relevant data using a tool that allowed assessment in the absence of confounding bias attributed to the influence of stressors on the patients. For pain as secondary endpoint, the results after 1 week of treatment demonstrated that NanoBEO had a statistically significant analgesic efficacy in comparison with the placebo (Figure 6C), even in our heterogeneous sample of patients regarding pain intensity. The data after the entire 4-week treatment with NanoBEO demonstrated increased effectiveness, with the reported intensity reduced up to half of that at baseline (Figures 6A–C). In particular, the improvement in pain intensity after the first week of treatment reached 45.46% compared with 16.67% of the placebo. The observed rate exceeded the threshold rate of 30% for improvement; this value generally reflects clinically important changes in clinical trials that investigate the efficacy of interventions for pain management, according to the recommendations of the Initiative on Methods, Measurement, and Pain Assessment in Clinical Trials (IMMPACT) (Dworkin et al., 2008). After 1 week of follow-up (week 5) and at the end of the entire observational period (week 8), pain intensity in the NanoBEO group progressively returned to the level after 1 week of treatment, although differences were not statistically significant (Figure 6A).

3.4 Safety

Treatment with NanoBEO was well tolerated and no patient discontinued the trial because of adverse reactions related to the application. No side effects were reported at any of the 4-week assessments and during the follow-up period. The biochemical analyses were not affected by the NanoBEO treatment, as presented in Tables 3A–E for the main parameters.

4 Discussion

Although BPSD were initially considered in relation to cognitive decline, their high prevalence suggests that they are important markers for the prognosis of dementia and determinants of quality of life (Cerejeira et al., 2012). In the complex framework of lack of disease-modifying therapies for all disease stages and universally efficacious, recent pharmacological approaches have focused on cannabinoids. However, these should be reserved for PwD who do not present with significant cardiovascular disease, which is common in this population because of age-related comorbidities (Scuteri et al., 2022b). The lack of effective and safe treatments for the management of agitation, one of the most challenging BPSD for clinicians and caregivers, prompted the identification of symptom-specific, patient-centered, non-pharmacological interventions, which target the needs that may trigger the behavioral disorder (Eunhee et al., 2023). This aspect is of utmost importance, particularly for the steadily growing population of older PwD who are subjected to polydrug therapies for chronic medical conditions other than dementia (at rates higher than those for cognitively intact counterparts) (Nørgaard et al., 2017; Growdon

et al., 2021); a non-pharmacological approach may be a safe option to avoid drug interactions (Letinier et al., 2022) and increased adverse effects due to inappropriate prescriptions (Rodrigues and Oliveira, 2016) or disrupted metabolism and elimination processes (Mangoni and Jackson, 2004; McLachlan et al., 2009). Furthermore, deprescribing is fundamental, considering that these patients are excluded from clinical trials for pain conditions unrelated to dementia, thus leading to unpredictable adverse reactions (Scuteri et al., 2022e; Scuteri et al., 2022f). PwD in advanced stages and older than 65 years are reported to receive five or more medications of which, in 39% of cases, at least one is potentially inappropriate according to the Beers Criteria (Riedl et al., 2022).

As the available pharmacological treatments have limited efficacy and considerable side effects, the present pilot clinical trial investigated the efficacy and safety of a non-pharmacological device based on an essential oil with anxiolytic-like activity and, different from benzodiazepines, devoid of sedative properties. Furthermore, according to the preclinical evidence generated on BEO, its combination with morphine enhanced the anti-allodynic effect (Kuwahata et al., 2013) and, in the formalin test, pretreatment with the opioid receptor antagonist naloxone methiodide, not able to cross blood brain barrier, attenuated the effect of BEO, thus suggesting potential involvement of peripheral opioid mechanisms (Katsuyama et al., 2015). Low concentrations of BEO can induce the exocytosis of glutamate that modulates pain through mGluRs, involved in the release of endogenous opioid peptides and endocannabinoids with analgesic activity (Scuteri et al., 2019). Twenty-nine patients (96.67%) completed the trial (treatment period and follow-up). A decrease in the frequency and disruptiveness of agitated behaviors was demonstrated in the NanoBEO group compared with that of the placebo group. NanoBEO was most effective after 2 weeks of treatment, and improvement in the frequency of agitated behaviors reached 28% compared with 6.93% in the placebo group; the rate is nearly up to the threshold rate of 30% improvement that is generally regarded as clinically significant in trials on the efficacy of interventions for the management of BPSD (Ballard et al., 2002). This result is noteworthy, even more so when considering that this was an underpowered pilot clinical trial. Additionally, our finding is important in view of the high placebo response rates registered in this context (Ballard and O'Brien, 1999; Ballard et al., 2002) and of the modest effectiveness of neuroleptics in reducing symptoms (Schneider et al., 1990). The individual data displayed a homogeneous distribution that supports the effectiveness of the treatment on agitation in most patients regarding the frequency and disruptiveness of agitated behavior, as measured using CMAI. The efficacy of NanoBEO on agitated behaviors was observed for the entire 4-week treatment period for both variables. The effect on frequency gradually decreased during the follow-up period, while that on disruptiveness was retained after the end of the treatment and for the entire 4-week follow-up period. Interestingly, no additional psychotropic drugs were prescribed as rescue medication for agitation during the study, strengthening the efficacy of NanoBEO in prolonged therapy of advanced dementia.

The Describe–Investigate–Create–Evaluate (DICE) model suggests that BPSD is caused by disruptions in brain circuitries that predispose to enhanced vulnerability to triggers such as pain; accordingly, assessment and treatment are fundamental to handling symptoms such as agitation (Kales et al., 2014; 2015; 2019a; Kales et al., 2019b). Supporting evidence demonstrates that older adults require treatment for at least 6 months to alleviate chronic pain (Blyth et al., 2001), with unsuccessful outcomes in approximately 80% of the cases (American Geriatrics Society Panel on the Pharmacological Management of Persistent Pain in Older, 2009). Undertreated pain remarkably affects the Italian population. This was demonstrated by the Italian Silver Network Home Care project, according to which, of the approximately 49% of the patients who experience daily pain, only 25% receive a World Health Organization (WHO) I level analgesic (Landi et al., 2001). In this context, the purpose of the present clinical trial was to shed light on the possible increased efficacy of NanoBEO in PwD attributed to its double effect on both the primary endpoint of agitation and the secondary endpoint of pain. The results after 1 week of treatment confirmed the significant analgesic efficacy of NanoBEO compared with that of the placebo. The data after completion of the entire intervention with NanoBEO demonstrated increased effectiveness, with decreased levels of pain intensity up to approximately half of that at baseline. After 1 week of follow-up (week 5) and at the end of the observation period (week 8), the level of pain intensity in the NanoBEO group progressively returned to the level recorded after 1 week of treatment. The improvement in pain intensity, as measured by I-MOBID2, after the first week of treatment was 45.46% compared to 16.67% of the placebo. The recorded rate exceeded the threshold of 30% for clinically important rates in clinical trials on the efficacy of interventions for pain management according to IMMPACT recommendations (Dworkin et al., 2008).

The limitations of this study include the small sample size because of the pilot nature of the trial, the difference in pain intensity at baseline in the two groups, and flaws in two dispensers (one each in the NanoBEO and placebo groups), which were replaced. The treatment with NanoBEO was well tolerated and no patient discontinued the trial because of adverse reactions related to the treatment. No side effects were reported at any of the 4-week assessments and during follow-up. Additionally, the biochemical analyses (azotemia, and serum creatinine, CPK, and transaminase levels) were not influenced by the treatment with NanoBEO, demonstrating the safety of the product.

This pilot study supplied substantial evidence for the subsequent large-scale pivotal trial that will address all present limitations; we expect to confirm these promising results and will investigate the efficacy and safety of aromatherapy using a rigorous blinded design adequately powered to allow the clinical translation of NanoBEO.

Data availability statement

The original contributions presented in the study are included in the article/Supplementary Material, further inquiries can be directed to the corresponding author.

Ethics statement

The studies involving humans were approved by Calabria Region Ethics Committee protocol No. 352 first version (21 November 2019). The studies were conducted in accordance with the local legislation and institutional requirements. Written informed consent for participation in this study was provided by the participants' legal guardians/next of kin.

Author contributions

DS: Conceptualization, Formal Analysis, Methodology, Project administration, Writing–original draft, Writing–review and editing. MP: Data curation, Methodology, Writing–original draft. IM: Data curation, Methodology, Writing–original draft. MC: Data curation, Methodology, Writing–original draft. LP: Data curation, Project administration, Writing–original draft. PT: Data curation, Project administration, Writing–original draft. PN: Conceptualization, Formal Analysis, Project administration, Writing–review and editing. GB: Conceptualization, Formal Analysis, Project administration, Writing–review and editing. MTC: Conceptualization, Formal Analysis, Project administration, Writing–review and editing. Pilot BRAINAID Trial investigators: Writing–original draft.

Funding

The author(s) declare that financial support was received for the research, authorship, and/or publication of this article. This research is coordinated by DS and received partial financial support from: 1) Phase 2 RIABEO Funding (Executive Decree n.6790 of 22 June 2022) Progetto Ingegno POR Calabria FESR 2014/2020—Azione 1 1 5—Sostegno all'Avanzamento tecnologico delle Imprese Attraverso il Finanziamento di Linee Pilota e Azioni di Validazione Precoce di Prodotti e di Dimostrazione su Larga Scala (DDG N. 12814 DEL 17 October 2019); 2) the Italian Ministry of Health: NET-2016-02361805 (WP 5); 3) PRIN 2022 PNRR (Project code P2022 CJNW). Financial support to M.T.C. has been provided by #NEXTGENERATIONEU (NGEU) and funded by the Ministry of University and Research (MUR), National Recovery and Resilience Plan (NRRP), project MNESYS (PE0000006)—A Multiscale integrated approach to the study of the nervous system in health and disease (DN. 1553 11.10.2022). We acknowledge co-funding from Next Generation EU, in the context of the National Recovery and Resilience Plan, Investment PE8 – Project Age-It: "Ageing Well in an Ageing Society". G.B. was co-financed by the Next Generation EU [DM 1557 11.10.2022].

Conflict of interest

The authors declare that the research was conducted in the absence of any commercial or financial relationships that could be construed as a potential conflict of interest.

The author(s) declared that they were an editorial board member of Frontiers, at the time of submission. This had no impact on the peer review process and the final decision.

Publisher's note

Supplementary material

The Supplementary Material for this article can be found online at: https://www.frontiersin.org/articles/10.3389/fphar.2024.1417851/full#supplementary-material

References

Aalten, P., Verhey, F. R. J., Boziki, M., Brugnolo, A., Bullock, R., Byrne, E. J., et al. (2008). Consistency of neuropsychiatric syndromes across dementias: results from the European alzheimer disease Consortium: Part II. *Dementia Geriatric Cognitive Disord.* 25 (1), 1–8. doi:10.1159/000111082

Achterberg, W. P., Pieper, M. J., van Dalen-Kok, A. H., de Waal, M. W., Husebo, B. S., Lautenbacher, S., et al. (2013). Pain management in patients with dementia. *Clin. Interv. Aging* 8, 1471–1482. doi:10.2147/cia.s36739

American Geriatrics Society Panel on the Pharmacological Management of Persistent Pain in Older (2009). Pharmacological management of persistent pain in older persons. *J. Am. Geriatrics Soc.* 57 (8), 1331–1346. doi:10.1111/j.1532-5415.2009.02376.x

An-Wen, C., Jennifer, M. T., Peter, C. G., Douglas, G. A., Howard, M., Jesse, A. B., et al. (2013). SPIRIT 2013 explanation and elaboration: guidance for protocols of clinical trials. *BMJ Br. Med. J.* 346, e7586. doi:10.1136/bmj.e7586

Ballard, C., and O'Brien, J. (1999). Treating behavioural and psychological signs in Alzheimer's disease. *Bmj* 319 (7203), 138–139. doi:10.1136/bmj.319.7203.138

Ballard, C. G., O'Brien, J. T., Reichelt, K., and Perry, E. K. (2002). Aromatherapy as a safe and effective treatment for the management of agitation in severe dementia: the results of a double-blind, placebo-controlled trial with Melissa. *J. Clin. Psychiatry* 63 (7), 553–558. doi:10.4088/jcp.v63n0703

Barnes, D. E., Alexopoulos, G. S., Lopez, O. L., Williamson, J. D., and Yaffe, K. (2006). Depressive symptoms, vascular disease, and mild cognitive impairment: findings from the cardiovascular health study. *Archives General Psychiatry* 63 (3), 273–279. doi:10.1001/archpsyc.63.3.273

Bejanin, A., and Villain, N. (2024). Posterior cortical atrophy: new insights into treatments and biomarkers for Alzheimer's disease. *Lancet Neurology* 23 (2), 127–128. doi:10.1016/S1474-4422(23)00501-X

Blyth, F. M., March, L. M., Brnabic, A. J. M., Jorm, L. R., Williamson, M., and Cousins, M. J. (2001). Chronic pain in Australia: a prevalence study. *PAIN* 89 (2), 127–134. doi:10.1016/s0304-3959(00)00355-9

Burhanullah, M. H., Tschanz, J. T., Peters, M. E., Leoutsakos, J. M., Matyi, J., Lyketsos, C. G., et al. (2020). Neuropsychiatric symptoms as risk factors for cognitive decline in clinically normal older adults: the cache county study. *Am. J. Geriatr. Psychiatry* 28 (1), 64–71. doi:10.1016/j.jagp.2019.03.023

Burns, A., Perry, E., Holmes, C., Francis, P., Morris, J., Howes, M. J., et al. (2011). A double-blind placebo-controlled randomized trial of Melissa officinalis oil and donepezil for the treatment of agitation in Alzheimer's disease. *Dement. Geriatr. Cogn. Disord.* 31 (2), 158–164. doi:10.1159/000324438

Cerejeira, J., Lagarto, L., and Mukaetova-Ladinska, E. (2012). Behavioral and psychological symptoms of dementia. *Front. Neurology* 3, 73. doi:10.3389/fneur.2012.00073

Chu, C. T. (2006). Autophagic stress in neuronal injury and disease. *J. Neuropathology Exp. Neurology* 65 (5), 423–432. doi:10.1097/01.jnen.0000229233.75253.be

Corasaniti, M. T., Bagetta, G., Nicotera, P., Maione, S., Tonin, P., Guida, F., et al. (2024). Exploitation of autophagy inducers in the management of dementia: a systematic review. *Int. J. Mol. Sci.* 25 (2), 1264. doi:10.3390/ijms25021264

Corbett, A., Husebo, B. S., Achterberg, W. P., Aarsland, D., Erdal, A., and Flo, E. (2014). The importance of pain management in older people with dementia. *Br. Med. Bull.* 111 (1), 139–148. doi:10.1093/bmb/ldu023

Cummings, J., Lanctot, K., Grossberg, G., and Ballard, C. (2024). Progress in pharmacologic management of neuropsychiatric syndromes in neurodegenerative disorders: a review. *JAMA Neurol.* 81, 645–653. doi:10.1001/jamaneurol.2024.0586

Davison, T. E., Bhar, S., Wells, Y., Owen, P. J., You, E., Doyle, C., et al. (2024). Psychological therapies for depression in older adults residing in long-term care settings. *Cochrane Database Syst. Rev.* 3 (3). doi:10.1002/14651858.CD013059.pub2

Doggrell, S. A. (2024). More failure with solanezumab - this time in preclinical Alzheimer's disease. *Expert Opin. Biol. Ther.* 24, 119–123. doi:10.1080/14712598.2024.2325551

Dugo, P., Mondello, L., Dugo, L., Stancanelli, R., and Dugo, G. (2000). LC-MS for the identification of oxygen heterocyclic compounds in citrus essential oils. *J. Pharm. Biomed. Anal.* 24 (1), 147–154. doi:10.1016/s0731-7085(00)00400-3

Dworkin, R. H., Turk, D. C., Wyrwich, K. W., Beaton, D., Cleeland, C. S., Farrar, J. T., et al. (2008). Interpreting the clinical importance of treatment outcomes in chronic pain clinical trials: IMMPACT recommendations. *J. Pain* 9 (2), 105–121. doi:10.1016/j.jpain.2007.09.005

Eunhee, C., Min Jung, K., Minhee, Y., Jiyoon, J., Jungwon, C., and Ji Yeon, L. (2023). Symptom-specific non-pharmacological interventions for behavioural and psychological symptoms of dementia: protocol of an umbrella review of systematic reviews of randomised controlled trials. *BMJ Open* 13 (2), e070317. doi:10.1136/bmjopen-2022-070317

Forrester, L. T., Maayan, N., Orrell, M., Spector, A. E., Buchan, L. D., and Soares-Weiser, K. (2014). Aromatherapy for dementia. *Cochrane Database Syst. Rev.* 2, Cd003150. doi:10.1002/14651858.CD003150.pub2

GBD (2022). Estimation of the global prevalence of dementia in 2019 and forecasted prevalence in 2050: an analysis for the Global Burden of Disease Study 2019. *Lancet Public Health* 7 (2), e105–e125. doi:10.1016/s2468-2667(21)00249-8

Growdon, M. E., Gan, S., Yaffe, K., and Steinman, M. A. (2021). Polypharmacy among older adults with dementia compared with those without dementia in the United States. *J. Am. Geriatrics Soc.* 69 (9), 2464–2475. doi:10.1111/jgs.17291

Hadjistavropoulos, T., Herr, K., Turk, D. C., Fine, P. G., Dworkin, R. H., Helme, R., et al. (2007). An interdisciplinary expert consensus statement on assessment of pain in older persons. *Clin. J. Pain* 23, S1–S43. doi:10.1097/AJP.0b013e31802be869

Hamamura, K., Katsuyama, S., Komatsu, T., Scuteri, D., Bagetta, G., Aritake, K., et al. (2020). Behavioral effects of continuously administered bergamot essential oil on mice with partial sciatic nerve ligation. *Front. Pharmacol.* 11, 1310. doi:10.3389/fphar.2020.01310

Harris, C. M., and Lykina, T. (2022). Fall-risk-increasing drugs in people with dementia who live in a residential aged care facility: a pilot study. *Cureus* 14 (4), e24559. doi:10.7759/cureus.24559

Holmes, C., Hopkins, V., Hensford, C., MacLaughlin, V., Wilkinson, D., and Rosenvinge, H. (2002). Lavender oil as a treatment for agitated behaviour in severe dementia: a placebo controlled study. *Int. J. Geriatr. Psychiatry* 17 (4), 305–308. doi:10.1002/gps.593

Huang, L. K., Kuan, Y. C., Lin, H. W., and Hu, C. J. (2023). Clinical trials of new drugs for Alzheimer disease: a 2020-2023 update. *J. Biomed. Sci.* 30 (1), 83. doi:10.1186/s12929-023-00976-6

Husebo, B. S., Ballard, C., Cohen-Mansfield, J., Seifert, R., and Aarsland, D. (2014). The response of agitated behavior to pain management in persons with dementia. *Am. J. Geriatr. Psychiatry* 22 (7), 708–717. doi:10.1016/j.jagp.2012.12.006

Husebo, B. S., Strand, L. I., Moe-Nilssen, R., Husebo, S. B., and Ljunggren, A. E. (2010). Pain in older persons with severe dementia. Psychometric properties of the mobilization–observation–behaviour–intensity–dementia (MOBID-2) pain scale in a clinical setting. *Scand. J. Caring Sci.* 24 (2), 380–391. doi:10.1111/j.1471-6712.2009.00710.x

Ismail, Z., Agüera-Ortiz, L., Brodaty, H., Cieslak, A., Cummings, J., Fischer, C. E., et al. (2017). The mild behavioral impairment checklist (MBI-C): a rating scale for neuropsychiatric symptoms in pre-dementia populations. *J. Alzheimer's Dis.* 56, 929–938. doi:10.3233/JAD-160979

Kales, H. C., Gitlin, L. N., Lyketsos, C. G., and Detroit Expert Panel on Assessment and Management of Neuropsychiatric Symptoms of Dementia (2014). Management of neuropsychiatric symptoms of dementia in clinical settings: recommendations from a multidisciplinary expert panel. *J. Am. Geriatr. Soc.* 62 (4), 762–769. doi:10.1111/jgs.12730

Kales, H. C., Gitlin, L. N., and Lyketsos, C. G. (2015). Assessment and management of behavioral and psychological symptoms of dementia. *Bmj* 350, h369. doi:10.1136/bmj.h369

Kales, H. C., Gitlin, L. N., and Lyketsos, C. G. (2019a). When less is more, but still not enough: why focusing on limiting antipsychotics in people with dementia is the wrong policy imperative. *J. Am. Med. Dir. Assoc.* 20 (9), 1074–1079. doi:10.1016/j.jamda.2019.05.022

Kales, H. C., Lyketsos, C. G., Miller, E. M., and Ballard, C. (2019b). Management of behavioral and psychological symptoms in people with Alzheimer's disease: an international Delphi consensus. *Int. Psychogeriatr.* 31 (1), 83–90. doi:10.1017/s1041610218000534

Kenneth, F. S., Douglas, G. A., David, M., and CONSORT Group (2010). CONSORT 2010 Statement: updated guidelines for reporting parallel group randomised trials. *BMJ* 340, c332. doi:10.1136/bmj.c332

Landi, F., Onder, G., Cesari, M., Gambassi, G., Steel, K., Russo, A., et al. (2001). Pain management in frail, community-living elderly patients. *Archives Intern. Med.* 161 (22), 2721–2724. doi:10.1001/archinte.161.22.2721

Letinier, L., Pujade, I., Duthoit, P., Evrard, G., Salvo, F., Gil-Jardine, C., et al. (2022). Emergency department admissions induced by drug–drug interactions in the elderly: a cross-sectional study. *Clin. Transl. Sci.* 15 (6), 1472–1481. doi:10.1111/cts.13262

Lin, P. W., Chan, W. C., Ng, B. F., and Lam, L. C. (2007). Efficacy of aromatherapy (Lavandula angustifolia) as an intervention for agitated behaviours in Chinese older persons with dementia: a cross-over randomized trial. *Int. J. Geriatr. Psychiatry* 22 (5), 405–410. doi:10.1002/gps.1688

Mangoni, A. A., and Jackson, S. H. (2004). Age-related changes in pharmacokinetics and pharmacodynamics: basic principles and practical applications. *Br. J. Clin. Pharmacol.* 57 (1), 6–14. doi:10.1046/j.1365-2125.2003.02007.x

McLachlan, A. J., Hilmer, S. N., and Le Couteur, D. G. (2009). Variability in response to medicines in older people: phenotypic and genotypic factors. *Clin. Pharmacol. Ther.* 85 (4), 431–433. doi:10.1038/clpt.2009.1

McShane, R., Westby, M. J., Roberts, E., Minakaran, N., Schneider, L., Farrimond, L. E., et al. (2019). Memantine for dementia. *Cochrane Database Syst. Rev.* 3 (3), CD003154. doi:10.1002/14651858.CD003154.pub6

Metaxakis, A., Ploumi, C., and Tavernarakis, N. (2018). Autophagy in age-associated neurodegeneration. *Cells* 7 (5), 37. doi:10.3390/cells7050037

Mondello, L., Stagno d'Alcontres, I., Del Duce, R., and Crispo, F. (1993). On the genuineness of citrus essential oils. Part XL. The composition of the coumarins and psoralens of calabrian bergamot essential oil (Citrus bergamia Risso). *Flavour Fragr. J.* 8 (1), 17–24. doi:10.1002/ffj.2730080105

Moorman Li, R., Gilbert, B., Orman, A., Aldridge, P., Leger-Krall, S., Anderson, C., et al. (2017). Evaluating the effects of diffused lavender in an adult day care center for patients with dementia in an effort to decrease behavioral issues: a pilot study. *J. Drug Assess.* 6 (1), 1–5. doi:10.1080/21556660.2016.1278545

Nakase, T., Thyreau, B., Tatewaki, Y., Tomita, N., Takano, Y., Muranaka, M., et al. (2023). Association between gray and white matter lesions and its involvement in clinical symptoms of alzheimer's-type dementia. *J. Clin. Med.* 12 (24), 7642. doi:10.3390/jcm12247642

Nørgaard, A., Jensen-Dahm, C., Gasse, C., Hansen, E. S., and Waldemar, G. (2017). Psychotropic polypharmacy in patients with dementia: prevalence and predictors. *J. Alzheimer's Dis.* 56, 707–716. doi:10.3233/JAD-160828

O'Connor, D. W., Eppingstall, B., Taffe, J., and van der Ploeg, E. S. (2013). A randomized, controlled cross-over trial of dermally-applied lavender (Lavandula angustifolia) oil as a treatment of agitated behaviour in dementia. *BMC Complement. Altern. Med.* 13, 315. doi:10.1186/1472-6882-13-315

Pinyopornpanish, K., Soontornpun, A., Wongpakaran, T., Wongpakaran, N., Tanprawate, S., Pinyopornpanish, K., et al. (2022). Impact of behavioral and psychological symptoms of Alzheimer's disease on caregiver outcomes. *Sci. Rep.* 12 (1), 14138. doi:10.1038/s41598-022-18470-8

Riedl, L., Kiesel, E., Hartmann, J., Fischer, J., Roßmeier, C., Haller, B., et al. (2022). A bitter pill to swallow - polypharmacy and psychotropic treatment in people with advanced dementia. *BMC Geriatr.* 22 (1), 214. doi:10.1186/s12877-022-02914-x

Rodrigues, M. C. S., and Oliveira, C. d. (2016). Drug-drug interactions and adverse drug reactions in polypharmacy among older adults: an integrative review. *Rev. Latino-Americana Enferm.* 24, e2800. doi:10.1590/1518-8345.1316.2800

Rombolà, L., Scuteri, D., Watanabe, C., Sakurada, S., Hamamura, K., Sakurada, T., et al. (2020). Role of 5-ht1a receptor in the anxiolytic-relaxant effects of bergamot essential oil in rodent. *Int. J. Mol. Sci.* 21 (7), 2597. doi:10.3390/ijms21072597

Sampson, E. L., White, N., Lord, K., Leurent, B., Vickerstaff, V., Scott, S., et al. (2015). Pain, agitation, and behavioural problems in people with dementia admitted to general hospital wards: a longitudinal cohort study. *PAIN* 156 (4), 675–683. doi:10.1097/j.pain.0000000000000095

Savva, G. M., Zaccai, J., Matthews, F. E., Davidson, J. E., McKeith, I., Brayne, C., et al. (2018). Prevalence, correlates and course of behavioural and psychological symptoms of dementia in the population. *Br. J. Psychiatry* 194 (3), 212–219. doi:10.1192/bjp.bp.108.049619

Schneider, L. S., Dagerman, K. S., and Insel, P. (2005). Risk of death with atypical antipsychotic drug treatment for dementia: meta-analysis of randomized placebo-controlled trials. *Jama* 294 (15), 1934–1943. doi:10.1001/jama.294.15.1934

Schneider, L. S., Pollock, V. E., and Lyness, S. A. (1990). A metaanalysis of controlled trials of neuroleptic treatment in dementia. *J. Am. Geriatr. Soc.* 38 (5), 553–563. doi:10.1111/j.1532-5415.1990.tb02407.x

Scuteri, D., Cassano, R., Trombino, S., Russo, R., Mizoguchi, H., Watanabe, C., et al. (2021a). Development and translation of NanoBEO, a nanotechnology-based delivery system of bergamot essential oil deprived of furocumarins, in the control of agitation in severe dementia. *Pharmaceutics* 13 (3), 379. doi:10.3390/pharmaceutics13030379

Scuteri, D., Contrada, M., Loria, T., Sturino, D., Cerasa, A., Tonin, P., et al. (2022a). Pain and agitation treatment in severe dementia patients: the need for Italian Mobilization-Observation-Behavior-Intensity-Dementia (I-MOBID2) pain scale translation, adaptation and validation with psychometric testing. *Biomed. Pharmacother.* 150, 113013. doi:10.1016/j.biopha.2022.113013

Scuteri, D., Corasaniti, M. T., Tonin, P., Nicotera, P., and Bagetta, G. (2021b). New trends in pharmacological control of neuropsychiatric symptoms of dementia. *Curr. Opin. Pharmacol.* 61, 69–76. doi:10.1016/j.coph.2021.09.002

Scuteri, D., Crudo, M., Rombolà, L., Watanabe, C., Mizoguchi, H., Sakurada, S., et al. (2018). Antinociceptive effect of inhalation of the essential oil of bergamot in mice. *Fitoterapia* 129, 20–24. doi:10.1016/j.fitote.2018.06.007

Scuteri, D., Guida, F., Boccella, S., Luongo, L., Maione, S., Tonin, P., et al. (2022b). NAbiximols clinical translation to the treatment of pain and agitation in severe dementia (NACTOPAISD): clinical trial protocol. *Biomed. Pharmacother.* 153, 113488. doi:10.1016/j.biopha.2022.113488

Scuteri, D., Sakurada, T., Tonin, P., Corasaniti, M. T., and Bagetta, G. (2021c). Editorial: "Novel pain therapeutics: from basic research to clinical translation and rehabilitation". *Front. Pharmacol.* 12, 681422. doi:10.3389/fphar.2021.681422

Scuteri, D., Rombolà, L., Crudo, M., Watanabe, C., Mizoguchi, H., Sakurada, S., et al. (2022c). Translational value of the transdermal administration of bergamot essential oil and of its fractions. *Pharmaceutics* 14 (5), 1006. doi:10.3390/pharmaceutics14051006

Scuteri, D., Rombolà, L., Crudo, M., Watanabe, C., Mizoguchi, H., Sakurada, S., et al. (2022d). Preclinical characterization of antinociceptive effect of bergamot essential oil and of its fractions for rational translation in complementary therapy. *Pharmaceutics* 14 (2), 312. doi:10.3390/pharmaceutics14020312

Scuteri, D., Rombolà, L., Watanabe, C., Sakurada, S., Corasaniti, M. T., Bagetta, G., et al. (2020). Impact of nutraceuticals on glaucoma: a systematic review. *Prog. Brain Res.* 257, 141–154. doi:10.1016/bs.pbr.2020.07.014

Scuteri, D., Sandrini, G., Tamburin, S., Corasaniti, M. T., Nicotera, P., Tonin, P., et al. (2021d). Bergamot rehabilitation AgaINst agitation in dementia (BRAINAID): study protocol for a randomized, double-blind, placebo-controlled trial to assess the efficacy of furocoumarin-free bergamot loaded in a nanotechnology-based delivery system of the essential oil in the treatment of agitation in elderly affected by severe dementia. *Phytother. Res.* 35 (10), 5333–5338. doi:10.1002/ptr.7223

Scuteri, D., Tonin, P., Nicotera, P., Bagetta, G., and Corasaniti, M. T. (2022e). Real world considerations for newly approved CGRP receptor antagonists in migraine care. *Expert Rev. Neurother.* 22 (3), 221–230. doi:10.1080/14737175.2022.2049758

Scuteri, D., Tonin, P., Nicotera, P., Vulnera, M., Altieri, G. C., Tarsitano, A., et al. (2022f). Pooled analysis of real-world evidence supports anti-CGRP mAbs and OnabotulinumtoxinA combined trial in chronic migraine. *Toxins (Basel)* 14 (8), 529. doi:10.3390/toxins14080529

Scuteri, D., Vulnera, M., Piro, B., Bossio, R. B., Morrone, L. A., Sandrini, G., et al. (2021e). Pattern of treatment of behavioural and psychological symptoms of dementia and pain: evidence on pharmacoutilization from a large real-world sample and from a centre for cognitive disturbances and dementia. *Eur. J. Clin. Pharmacol.* 77 (2), 241–249. doi:10.1007/s00228-020-02995-w

Selbæk, G., Kirkevold, Ø., and Engedal, K. (2007). The prevalence of psychiatric symptoms and behavioural disturbances and the use of psychotropic drugs in Norwegian nursing homes. *Int. J. Geriatric Psychiatry* 22 (9), 843–849. doi:10.1002/gps.1749

Testad, I., Aasland, A. M., and Aarsland, D. (2007). Prevalence and correlates of disruptive behavior in patients in Norwegian nursing homes. *Int. J. Geriatric Psychiatry* 22 (9), 916–921. doi:10.1002/gps.1766

Wang, H. Y., Cecon, E., Dam, J., Pei, Z., Jockers, R., and Burns, L. H. (2023). Simufilam reverses aberrant receptor interactions of filamin A in alzheimer's disease. *Int. J. Mol. Sci.* 24 (18), 13927. doi:10.3390/ijms241813927

Zalomonson, S., Freud, T., Punchik, B., Samson, T., Lebedinsky, S., and Press, Y. (2019). The results of a crossover placebo-controlled study of the effect of lavender oil on behavioral and psychological symptoms of dementia. *Rejuvenation Res.* 22 (3), 246–253. doi:10.1089/rej.2018.2123

Zaynoun, S. T., Johnson, B. E., and Frain-Bell, W. (1977). A study of oil of bergamot and its importance as a phototoxic agent. I. Characterization and quantification of the photoactive component. *Br. J. Dermatol* 96 (5), 475–482. doi:10.1111/j.1365-2133.1977.tb07149.x

Glossary

AD	Alzheimer's disease
ALT	alanine aminotransferase
aMCI	amnestic mild cognitive impairment
AST	aspartate aminotransferase
Aβ	β-amyloid
BEO	bergamot essential oil
BPSD	behavioral and psychological symptoms of dementia
CI	confidence intervals
CMAI	Cohen-Mansfield Agitation Inventory
CONSORT	Consolidated Standards of Reporting Trials
CPK	creatine phosphokinase
DICE	Describe–Investigate–Create–Evaluate
EMA	European Medicine Agency
FDA	Food and Drug Administration
GOT	glutamic-oxaloacetic transaminase
GPT	glutamic-pyruvic transaminase
HMPC	Committee on Herbal Medicinal Products
ICC	intraclass correlation coefficient
IMMPACT	Initiative on Methods, Measurement, and Pain Assessment in Clinical Trials
I-MOBID2	Italian Mobilization–Observation–Behavior–Intensity–Dementia
IQR	interquartile range
MBI	mild behavioral impairment
MMSE	mini-mental state examination
MRI	magnetic resonance imaging
MWU	Mann–Whitney *U* test
PwD	people with dementia
SAP	statistical analysis plan
SD	standard deviation
SEM	standard error of the mean
SPECT	single-photon emission computed tomography
SPIRIT	Standard Protocol Items: Recommendations for Interventional Trials
WHO	World Health Organization

frontiers | Frontiers in Pharmacology

TYPE Original Research
PUBLISHED 06 August 2024
DOI 10.3389/fphar.2024.1407897

OPEN ACCESS

EDITED BY
Francesca Guida,
University of Campania Luigi Vanvitelli, Italy

REVIEWED BY
Damiana Scuteri,
University of Calabria, Italy
Álvaro Llorente-Berzal,
Autonomous University of Madrid, Spain

*CORRESPONDENCE
Zhisheng Liu,
liuzhisheng@hust.edu.cn

RECEIVED 27 March 2024
ACCEPTED 04 June 2024
PUBLISHED 06 August 2024

CITATION
Peng J, Liu L, Li Q, Liu M, Zhou R, Chen L and Liu Z (2024), Efficacy and safety of levetiracetam for migraine prophylaxis in children: a systematic review and meta-analysis.
Front. Pharmacol. 15:1407897.
doi: 10.3389/fphar.2024.1407897

Efficacy and safety of levetiracetam for migraine prophylaxis in children: a systematic review and meta-analysis

Jing Peng[1], Linhui Liu[1], Qiaoling Li[1], Maochang Liu[1], Rong Zhou[1], Li Chen[1] and Zhisheng Liu[2]*

[1]Department of Pharmacy, Wuhan Children's Hospital, Tongji Medical College, Huazhong University of Science and Technology, Wuhan, China, [2]Department of Neurology, Wuhan Children's Hospital, Tongji Medical College, Huazhong University of Science and Technology, Wuhan, China

Background: Levetiracetam (LEV), an antiepileptic drug, has been effective in adult migraine prevention but lacks extensive research in children. This study evaluates LEV's efficacy and safety for pediatric migraine prophylaxis.

Methods: We reviewed randomized controlled trials (RCTs) and non-RCTs in major databases through 8 January 2024, focusing on four efficacy endpoints and adverse drug reactions (ADRs). Data synthesis involved pooled relative risks or odds ratios for dichotomous outcomes and mean differences for continuous outcomes, using fixed- or random-effects models as appropriate.

Results: Eight studies with 190 participants showed that after taking LEV, the mean headache frequency decreased 5.19 per month (MD: −5.19, 95% CI: −7.11 to −3.27, $p < 0.00001$) and improved headache-free rates to 28% (95% CI: 0.17–0.41). More than 83% experienced a >50% reduction in monthly headache frequency. The migraine disability score decreased by 33.51 points (MD: −33.51, 95% CI: −38.46 to −28.55, $p < 0.00001$). ADR incidence did not significantly differ between LEV and control groups (RR: 1.06, 95% CI: 0.39 to 2.85, $p = 0.91$), with an overall ADR rate of 18% (95% CI: 0.13–0.24). The most common ADR was irritability (12%), leading to treatment discontinuation in 13% of cases (95% CI: 0.05–0.30).

Conclusion: LEV has shown good efficacy in preventing pediatric migraines. However, its safety requires further confirmation through more extensive and well-designed RCTs.

Systematic Review Registration: Identifier PROSPERO CRD42024497643.

KEYWORDS

migraine, prophylaxis, meta-analysis, levetiracetam, children

Abbreviations: LEV, levetiracetam; RCT, randomized controlled trial; ADR, adverse drug reaction; RR, relative risk; OR, odd ratio; MD, mean difference; PedMIDAS, pediatric migraine disability assessment score; AED, antiepileptic drugs; CNKI, China National Knowledge Infrastructure; VIP, China Science and Technology Journal Database; PRISMA, Preferred Reporting Items for Systematic Reviews and Meta-Analysis CHARMS, Critical Appraisal and Data Extraction for Systematic Reviews of Prediction Modelling Studies; RoB2, risk of bias tool; ROBINS-I, Risk of Bias In Non-randomized Studies-of Interventions.

1 Introduction

Migraine is a prevalent condition among children, significantly impacting their daily functioning and overall wellbeing. Approximately 10% of children aged between 5 and 15 years experience migraines (Ozge et al., 2013). In pediatric emergency departments, up to 18% of children present with migraine-related symptoms (Mirzaei, 2004). Approximately 25% of children with migraines have a frequency of one attack per month or less, while approximately 61% of them require prophylaxis treatment due to experiencing more than four severe headache attacks per month (Moaiedi and Boroomand, 2004). Migraines in children differ from those in adults as they often occur without aura and affect both sides of the head. The duration of headaches is shorter compared to that in adults. During migraine attacks, children commonly experience severe pain that can significantly impair their daily functioning. Students with migraines frequently miss school, face academic difficulties, and withdraw from sports due to recurrent headaches (Khazaie et al., 2014). Recurrent migraine episodes also impact communication abilities and overall quality of life for affected individuals by interfering with daily activities (Gunner et al., 2008). The impact on academic achievement, memory retention, personality development, interpersonal relationships, and school attendance varies depending on the causes behind the headaches as well as their frequency and severity among children (Bahrami, 2006). Furthermore, childhood migraines can persist into adulthood with recurring episodes (Montazerlotfelahi et al., 2019), and children and adolescents with migraine are at a higher risk of attention-deficit hyperactivity disorder (ADHD) (Arruda et al., 2020), sleep disorders (Pavkovic and Kothare, 2020), anxiety, and depression (Falla et al., 2022), which lead to significant burdens on personal and societal levels due to associated disorders and psychological stressors. Early diagnosis and intervention play a crucial role in improving long-term outcomes for childhood migraines (Ayatollahi and Khosravi, 2005; Zamani and Ghofrani, 2006).

Two primary strategies are employed in the treatment of migraine headaches: acute intervention and prophylactic therapy. Patients who suffer from frequent or prolonged migraine attacks have difficulty tolerating the mental impact of migraines, or for whom standard therapies are infeasible, may benefit from prophylactic therapy (Fallah et al., 2013). There are both non-pharmacological and pharmacological treatments for migraine prophylaxis (Fallahzade et al., 2010). Non-pharmacological therapies include sleep patterns, diet, physical activity, stress management, and avoiding stimulants (Solomon, 1992). On the pharmacological front, a range of compounds are utilized, including beta blockers, antidepressants, calcium channel blockers, antiepileptic drugs (AEDs), and antihistamines, all aimed at preventing migraine onset (Taghdiri and Razavi, 2004; Hershey and Winner, 2005; Ayatollahi and Khosravi, 2006; Magis and Schoenen, 2011). Specifically, AEDs such as topiramate and valproate are known to suppress cortical hyperexcitability and mitigate cortical spreading depression (Costa et al., 2013; Aurora and Brin, 2017). However, the long-term use of these medications can be concerning due to potential teratogenic effects and possible adverse drug reactions (ADRs) (Marmura, 2014; Stadelmaier et al., 2017). Other AEDs, such as levetiracetam (LEV), lamotrigine, and gabapentin, had also been explored for their prophylactic potential in adult and pediatric migraine populations (Krymchantowski et al., 2002; Eiland et al., 2007; Bakola et al., 2009; Verma et al., 2013).

Pediatric drug research faces several challenges, including the high costs and relatively low profits associated with developing medications for a smaller patient population, along with the complexities inherent in conducting clinical research on children. Concerns regarding the safety and efficacy of medications in this demographic, coupled with a lack of robust policy support, further complicate matters (Cheng et al., 2023). Nonetheless, there is considerable potential in repurposing drugs with established safety profiles for new indications. The appeal of drug repositioning lies in the extensive knowledge base regarding the safety, pharmacokinetics, and pharmacodynamics of these medications, which have been widely used in clinical practice. This approach typically carries lower risks and costs compared to the development of novel drugs. However, despite the proven safety and efficacy of these drugs in their original contexts, thorough research and additional clinical trials are essential to ensure their safety and effectiveness when used for new indications.

Levetiracetam is rapidly and almost completely absorbed following oral administration. Compared to other antiepileptic drugs, it exhibits minimal protein binding and does not involve the hepatic cytochrome P450 system. (Fayyazi et al., 2023). Currently, there are limited reports on the use of levetiracetam for the treatment of headaches. Some evidence from open-label trials and retrospective reviews points to the efficacy of levetiracetam in adult patients (Tsaousi et al., 2020; Evers et al., 2022). Although preliminary data from a few reviews and open-label studies with small sample sizes (Pakalnis et al., 2007; Sadeghian and Motiei-Langroudi, 2015; Yen et al., 2021) suggest potential benefits of levetiracetam in preventing migraines in children and adolescents, there is a current scarcity of robust evidence, largely due to the limited number of published cases. In light of this, the present study aims to conduct a systematic review and meta-analysis to quantitatively synthesize emerging evidence and to evaluate the efficacy and safety of levetiracetam in preventing migraine attacks in the pediatric population.

2 Data and methods

2.1 Protocol and registration

Our meta-analysis adhered to the guidelines of the declaration Preferred Reporting Items for Systematic Reviews and Meta-Analysis (PRISMA) (Page et al., 2021) and the recommendations of the Cochrane Handbook for Systematic Reviews of Interventions. This review was registered on the International Prospective Register of Systematic Reviews—PROSPERO (CRD42024497643) and no protocol changes occurred.

2.2 Literature search

Chinese and English databases were systematically searched, considering the large population size and language universality. The databases searched including China National Knowledge

Infrastructure (CNKI), Wanfang, China Science and Technology Journal Database (VIP), Embase, PubMed, Web of Science, and Cochrane databases (up to 8 January 2024), following terms and Boolean operators were used in MeSH and free-text searches: Levetiracetam AND (Migraine OR Headache) AND (prophylaxis OR prevention). The detailed strategies used for the search can be found in the Supplementarty Table S1. Additional studies were identified through reference reviews.

2.3 Selection criteria

The PICOTS system recommended by the Critical Appraisal and Data Extraction for Systematic Reviews of Prediction Modelling Studies (CHARMS) checklist (Moons et al., 2014) was utilized. This system helps frame the review's aim, search strategy, and study inclusion and exclusion criteria (Debray et al., 2017).

The inclusion criteria for studies were as follows:

P (Population): Patients under 18 years of age with a history of migraine.

I (Intervention model): Prophylaxis with LEV.

C (Comparator): Prophylactic use of placebo or other drugs.

O (Outcome): According to the guidelines of the Clinical Trials Standing Committee and the Child and Adolescent Standing Committee of the International Headache Society (Abu-Arafeh et al., 2019), we chose the efficacy outcomes: 1) headache frequency per month, as measured by headache days or migraine days; 2) headache-free; 3) ≥50% reduction in monthly headache frequency. The safety of LEV as the types and number of drug ADRs. Other outcomes included the degree of disability—the pediatric migraine disability assessment score (PedMIDAS).

T (Timing): Without limiting the duration of treatment and patient-related follow-up cycles.

S (Setting): Peer-reviewed original research articles of any study design (randomized, controlled trials and non-randomized, controlled trials) involving prospective or retrospective data collection comparing LEV administration to other AEDs, no exposed control group, or single-arm clinical trial.

The exclusion criteria were as follows: (1) studies that had unclear clinical outcomes or duplicated reporting of patient cohorts; (2) not written in English or Chinese; (3) the full text could not be retrieved despite contacting the authors via email.

2.4 Literature screening and data extraction

Two researchers (Jing P and Linhui L) independently screened titles, abstracts, and full texts, then extracted data from eligible original articles, and resolved disagreements through discussion with a third author (Qiaolin L). Microsoft Excel 2013 was used to extract data. The four RCT studies selected different control drugs, so it is not meaningful to use them in combination to evaluate efficacy. Therefore, we extracted data using the same method as the four single-arm studies. Data extraction included author, year, country, study type, inclusion criteria, patient details, headache frequency per month, PedMIDAS, intervention, follow-up, outcome, and control group details. We contacted the trial authors for missing and questionable data if needed.

2.5 Risk of bias assessment

Two authors independently appraised risk of bias of each study using the Cochrane risk of bias tool (RoB2) for RCTs and Risk of Bias In Non-randomized Studies-of Interventions (ROBINS-I) for non-RCTs (Morgan et al., 2018; Minozzi et al., 2022). Discrepancies were resolved through discussion or consultation with a third author.

2.6 Statistical analysis

Data analysis was conducted using RevMan 5.3.5 software. For dichotomous data, we utilized the pooled relative risk (RR) or odds ratio (OR) with a 95% confidence interval (95% CI). Continuous data were analyzed using the mean difference (MD) and 95% CI.

When conducting a meta-analysis on binary data without a control group, using data such as efficacy rates and the incidence rates of ADRs, it is important to recognize the unique characteristics of this type of data. These data include only a single group with the number of events (X) and the total sample size (n), without a control group. When calculating the event rate (P) and its standard error (SE), if the conditions for n*P and n*(1-P) being greater than 5 are not satisfied, or if the number of events is zero—indicating a non-normal distribution of the incidence rate (Yue-hong et al., 2014)—the method for analyzing ratio-type data should be applied. This method is detailed as follows:

$$P = \ln(\text{odds}) = \ln\left(X/(n-X)\right).$$

$$SE = SE(\ln(\text{odds})) = \sqrt{\frac{1}{X} + \frac{1}{(n-X)}}.$$

As with any ratio type data, the following conversion calculations must be performed in order to obtain the rate and its 95% CI based on RevMan's odd ratio (OR) value.

Conversion of effect indicators:

$$Pf = OR/(1 + OR).$$

95% CI Lower bound conversion:

$$LL = LLOR/(1 + LLOR).$$

95% CI Upper limit conversion:

$$UL = ULOR/(1 + ULOR)$$

Note: In order to distinguish the above occurrence rate from the conversion calculated rate, the conversion calculated rate is expressed as Pf.

We used Cochrane Q and I^2 tests to evaluate the heterogeneity across the studies. If the heterogeneity among the studies was not statistically significant ($I^2 < 50\%$), a fixed-effects model was used, and in case of significant heterogeneity ($I^2 \geq 50\%$), a random-effects model was used. Subgroup analysis was not performed due to the small sample size and strict inclusion and exclusion criteria. Potential publication bias was examined graphically using a funnel plot. In order to investigate the impact of each study on the overall effect size, we conducted a leave-one-out sensitivity analysis. This analysis involved excluding one study at a time

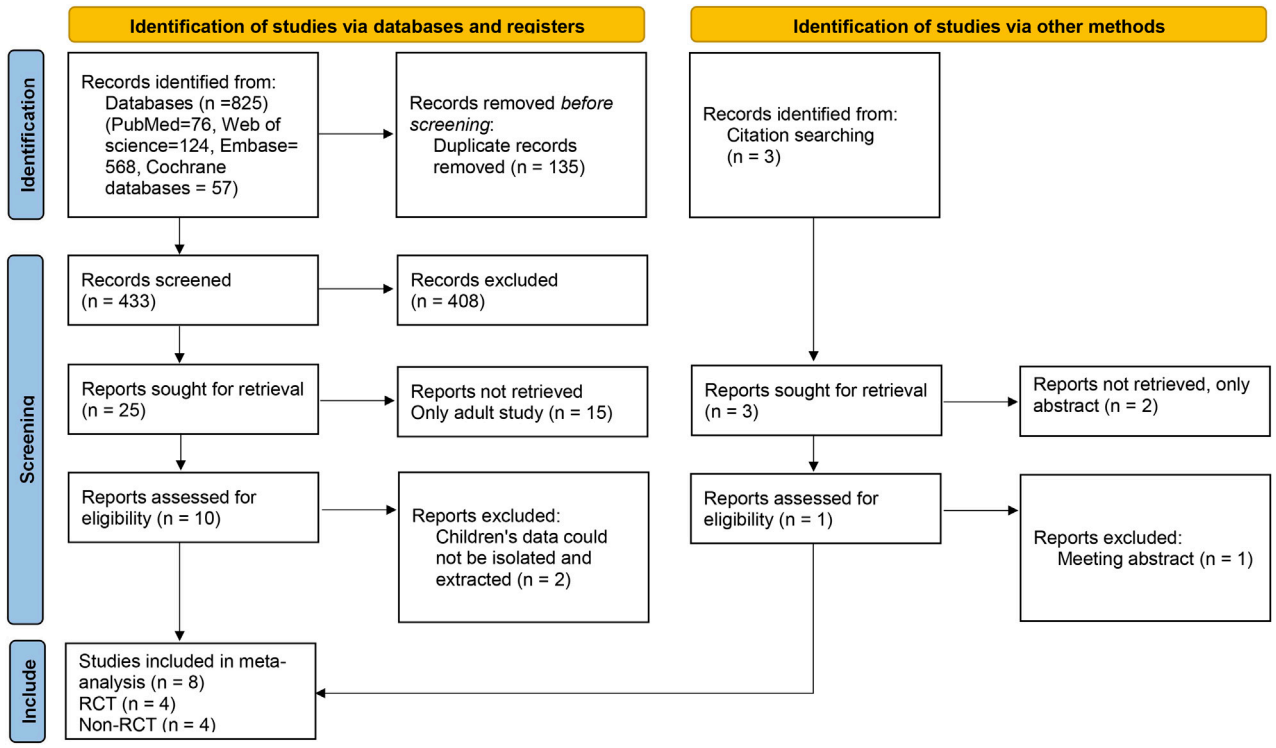

FIGURE 1
Flow chart of literature screening.

and calculating the pooled effect estimates for the remaining studies. The statistical tests were all conducted using a two-tailed significance level set at $p < 0.05$.

3 Results

3.1 Literature search results

A total of 825 relevant articles were obtained after a preliminary search, and 433 remained after duplicate articles were excluded. After the preliminary screening of titles and abstracts, a total of 25 articles met the requirements after excluding reviews, letters, abstracts, guidelines, and articles not belonging to the research field. After reading the full texts, eight articles (four RCTs and four non-RCTs) were included in the meta-analysis (Miller, 2004; Pakalnis et al., 2007; Awaad and Rizk, 2014; Sediqi et al., 2017; Rahman et al., 2018; Ghazavi et al., 2019; Montazerlotfelahi et al., 2019; Fayyazi et al., 2023). The literature selection flow chart is shown in Figure 1.

3.2 Basic characteristics of included studies

Of the eight included studies, the total number of participants was 190. The basic characteristics of all the studies are shown in Table 1. Four RCTs compared LEV to propranolol and sodium valproate (Fayyazi et al., 2023), amitriptyline (Ghazavi et al., 2019), placebo (Montazerlotfelahi et al., 2019), and flunarizine (Rahman et al., 2018). Four non-RCTs were single-arm studies. LEV was administered at the minimum dose of 20 mg/kg, which is recommended in pediatric textbooks (Sediqi et al., 2017). During the studies, the minimum starting dose of levetiracetam was 10 mg/kg/day, and if necessary, the dosage of levetiracetam was increased. According to the guidelines, a minimum treatment period of 84 days (12 weeks) is recommended. Treatment periods longer than 84 days can be used to evaluate cumulative benefits or persistence of efficacy and to collect additional safety and tolerability data. In all eight studies, the treatment duration exceeded 12 weeks, and we analyzed outcome data from the maximum duration of follow-up in each study.

3.3 Risk of bias

The outcomes of all studies indicated moderate to low risk of bias (Figures 2, 3). Most of the RCTs showed a low risk of bias. However, one study (Fayyazi et al., 2023) had a moderate risk due to several factors: the lack of blinding for participants, personnel, and outcome assessors, as well as changes in the type of treatment administered due to inefficacy and ADRs. Considering the ethical factors, such deviations are sometimes unavoidable, but this study did not conduct a comparative study between the intervention group and the control group, its impact on the overall risk of bias is minimal. All of the non-RCT studies were rated as having a moderate risk using the ROBINS-I tool (the studies were sound for a non-randomized study with regard to this domain but cannot

TABLE 1 The characteristics of included studies.

Author (Year)	Country	Study type	Inclusion criteria	No. of patients (female)	Age, y, mean ± SD	Headache frequency per month, mean ± SD	PedMIDAS tool, mean ± SD	Intervention	Follow-up period	Outcome assessment (index)	Control group drugs (dose)
Fayyazi et al. (2023)	Iran	RCT	ICHD-3 criteria; aged 5 to 15; at least one of the following criteria: a) more than one headache attack per week; b) more than three headache attacks per month; c) more than 1-day school absenteeism per month due to headache; d) PedMIDAS>20	13 (NA)	NA	1.8 ± 4.1	4.35 ± 19.17	50 mg/kg/day	1, 4, 6 m	①②④⑤	Propranolol (1 mg/kg/day); Sodium Valproate (15 mg/kg/day)
Ghazavi et al. (2019)	Iran	RCT	Aged 5 to 15; ICHD-3 criteria; at least four attacks of headache per month that either lasted at least 2 hours or had moderate to severe intensity; had headaches >6 months before enrolment and had not been administered a migraine prophylactic agent	30 (14)	10.6 ± 2.6	12 (4–30) median (range)	66 (12–102) median (range)	10 or 20 mg/kg/day twice a day	1, 3 m	③⑤	Amitriptyline (1 mg/kg/day)
Montazerlotfelahi et al. (2019)	Iran	RCT	Aged 4 to17; IHS criteria; have at least four migrainous episodes per month or to have severe disabling or intolerable headache	34 (19)	10.4 ± 2.4	11.6 ± 4.8	NA	20 or 40 mg/kg/day twice a day	4, 8, and 12w	②③⑤	Placebo
Rahman et al. (2018)	Bangladesh	RCT	Aged 6 to 15; ICHD-3 criteria; attack frequency >4 per month; suffering from migraine attacks for at least 1 year before study entry	36 (22)	10.77 ± 2.35	9.41 ± 3.12	64.25 ± 19.63	20 mg/kg/day twice a day	1, 3 m	①④⑤	Flunarizine (5 mg/day)
Sediqi et al. (2017)	Iran	non-RCT	Aged 4 to 14; ICHD-3 criteria; PedMIDAS>20; headache attacks of more than once per week	30 (16)	9.3 ± 2.5	37.63 ± 24.05	34.77 ± 16.63	20 mg/kg/d	3, 6 m	①②④⑤	_

(Continued on following page)

10.3389/fphar.2024.1407897

10.3389/fphar.2024.1407897

TABLE 1 (*Continued*) The characteristics of included studies.

Author (Year)	Country	Study type	Inclusion criteria	No. of patients (female)	Age, y, mean ± SD	Headache frequency per month, mean ± SD	PedMIDAS tool, mean ± SD	Intervention	Follow-up period	Outcome assessment (index)	Control group drugs (dose)
Awaad and Rizk (2014)	Kingdom of Saudi Arabia	retrospective	Aged 12 to 18; IHS criteria; non-responsiveness (or failure) to traditional headache management	8 (2)	10.6 ± 2.6	8–30	NA	20–60 mg/kg/day twice a day	6 m	⑤	–
Pakalnis et al. (2007)	United States of America	An Open-Label Study	Aged 6 to 17; with 4–8 migraine attacks a month; ICHD-2 criteria	20 (5)	10.65 ± 2.60	5.95 ± 1.76	47.55 ± 32.24	20 or 40 mg/kg/day twice a day	2–3 m	①②③④⑤	–
Miller (2004)	United States of America	retrospective	age≤17; IHS criteria	19 (9)	11.9 (3–17)	6.3 ± 3.8	NA	125–750 mg twice a day	4.1 (1.25–7)m	①②⑤	–

ICHD, international classification of headache disorders; HIS, international headache society; -, no exposed control group; ① headache frequency per month; ② headache-free; ③ more than 50% reduction in headache frequency; ④ PedMIDAS, tool; ⑤ adverse drug reaction.

considered comparable to a well performed randomized trial). Funnel plots indicated some publication bias (Supplementary Figures S1–S8). We observed some heterogeneity among studies included in the meta-analysis.

3.4 Meta-analysis results

3.4.1 Headache frequency

Headache frequency was standardized to number of headaches per month. Whenever possible, we pooled frequency as the number of headaches per a month. In the 2017 study by Sediqi et al., patients were asked to write down the days when they experience headache, duration of headache, migraine-associated symptoms, and duration of migraine-associated symptoms in a headache diary. Then, the patients were contacted monthly by phone call, or if needed, they were visited in person. However, the baseline headache frequency reported in Table 1 of the results was 37.63 ± 24.05 per month, a number that exceeds the theoretical upper limit of 31 days within a single month. We attempted to contact the corresponding author of the study by email and did not receive any recovery. As a result, we have unanimously decided to exclude the data from this study from our research. After excluding this study, we found that the heterogeneity of our research has decreased, with the I^2 value dropping from 90% to 75%. A significant reduction in monthly headache frequency was observed in the post-LEV group compared to the pre-LEV group in the meta-analysis of the four studies (Figure 4A). After taking LEV, the mean headache frequency decreased 5.19 per month (overall MD: −5.19, 95% CI: −7.11 to −3.27, I^2 = 75%, $p < 0.00001$).

3.4.2 Headache free

The patient was identified as a headache-free case if the number of headaches became zero (Sediqi et al., 2017), or patients were migraine-free (Pakalnis et al., 2007), or elimination of migraine (Miller, 2004), or complete elimination of headaches (Montazerlotfelahi et al., 2019), or PedMIDAS < 10, headache score < 2, and 1 < headache frequency (per week) < 2 after 3 months (Fayyazi et al., 2023). Headache free was calculated as the incidence rate and standard error (overall Odd: 0.38, 95% CI: 0.20 to 0.70, I^2 = 50%), according to formula conversion, headache-free incidence after LEV was 28% (95% CI: 0.17–0.41) (Figure 4B).

3.4.3 People with migraine had a greater than 50% reduction in headache frequency

The number of cases reporting a reduction in monthly headache frequency of more than 50% was reported in three articles (Pakalnis et al., 2007; Ghazavi et al., 2019; Montazerlotfelahi et al., 2019). The incidence rate and standard error were calculated as a percentage in people whose headache frequency was reduced greater than 50% in monthly (overall Odd: 4.93, 95% CI: 1.66 to 14.60, I^2 = 65%). According to formula conversion, the incidence of headache frequency reduction >50% in monthly after LEV was 83% (95% CI: 0.62–0.94) (Figure 4C).

3.4.4 PedMIDAS

As a secondary endpoint, PedMIDAS can be used to evaluate the impact of treatment on participants' disability and functioning. Four

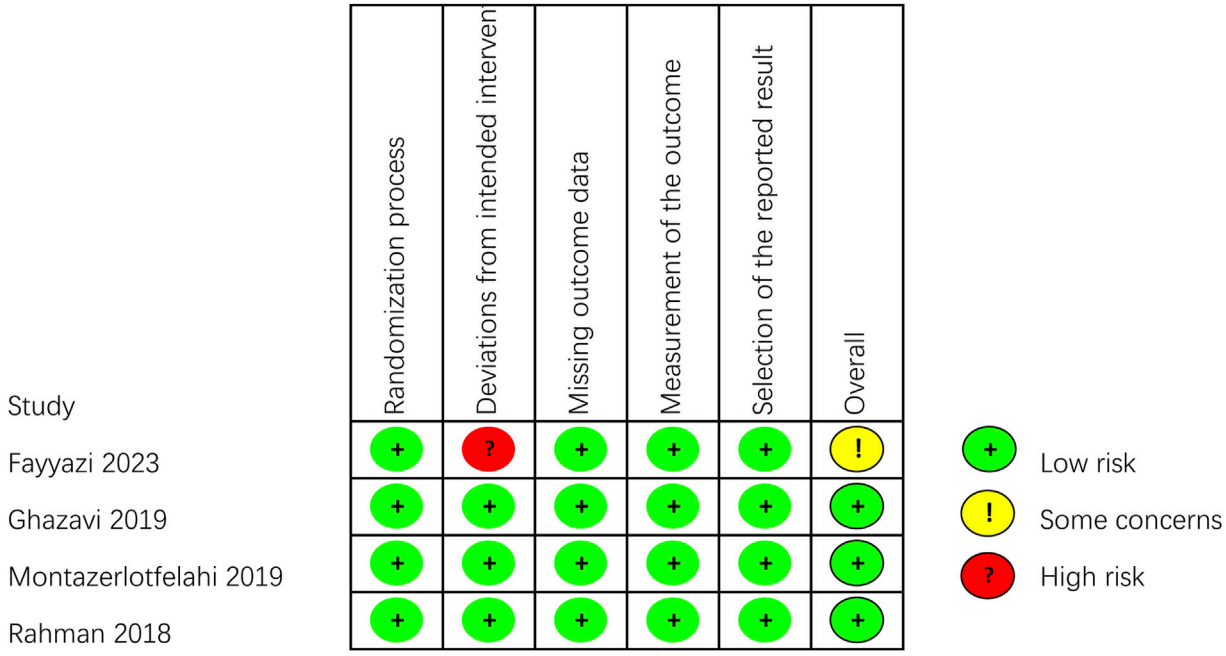

FIGURE 2
Critical appraisal of RCTs according to the Cochrane Collaboration's tool for assessing risk of bias in RCTs (Rob2).

studies reported the results of PedMIDAS in patients before and after the use of LEV. The results indicated a significant decrease in PedMIDAS following LEV treatment (Figure 4D). Through sensitivity analysis, we discovered that the Fayyazi et al. (2023) study had substantial heterogeneity. In sensitivity analysis, after excluding the Fayyazi et al. (2023) study, the heterogeneity of the studies was significantly decreased (I^2 decreased from 91% to 6%). Their actual PedMIDAS was only approximately 4, which was not consistent with the inclusion criteria with a score higher than 20 score in PedMIDAS described in their research article. After we sent emails to the author and did not receive any recovery, we unanimously decided to exclude the data of this study. The results of the meta-analysis with three studies demonstrated that PedMIDAS could decrease by 33.51 points after taking LEV (overall MD: −33.51, 95% CI: −38.46 to −28.55, I^2 = 6%, p < 0.00001).

3.4.5 Adverse drug reactions

ADRs were reported in all eight studies following LEV treatment, involving a total of 23 patients. No serious side effects were reported in these studies. The incidence rate and standard error of ADRs were calculated in the meta-analysis (overall Odd: 0.22, 95% CI: 0.15 to 0.32, I^2 = 0%) (Figure 5A). Using the formula conversion, ADR incidence after LEV was 18% (95% CI: 0.13–0.24). No significant difference in the incidence rate of ADR was found between LEV and placebo or other drugs (RR: 1.06, 95% CI: 0.39 to 2.85, I^2 = 52%, p = 0.91) (Figure 5B).

The main ADRs reported in the eight studies were as follows: nagging, negotiating, agitation, aggression, irritability, bad temperament, exhibited hostile behavior, moodiness, mild tic, hyperactive, mild memory problems, dizziness, vertigo, severe drowsiness, asthenia/somnolence, poor sleep, day-time sedation, acne, lack of appetite, increased appetite, and weight gain, in which behavioral changes were the most common ADRs. Seven studies (Miller, 2004; Pakalnis et al., 2007; Awaad and Rizk, 2014; Rahman et al., 2018; Ghazavi et al., 2019; Montazerlotfelahi et al., 2019; Fayyazi et al., 2023) reported a total of 17 patients experiencing irritability/agitation as the ADR after using LEV (Odd: 0.14, 95% CI: 0.08 to 0.23, I^2 = 0%) (Figure 5C). Using the formula conversion, the incidence of irritability/agitation was 12% (95% CI: 0.07–0.19). Interestingly, some parents reported that irritability and bad temperament disappeared during the trial (Miller, 2004; Ghazavi et al., 2019; Montazerlotfelahi et al., 2019).

A total of four cases discontinued treatment due to ADRs (overall Odd: 0.15, 95% CI: 0.05 to 0.42, I^2 = 0%) (Figure 5D), three of which were due to agitation, aggression, irritability, and severe drowsiness (Miller, 2004; Fayyazi et al., 2023) and one patient due to asthenia/somnolence and dizziness (Miller, 2004). Using the formula conversion, the discontinued treatment incidence was 13% (95% CI: 0.05–0.30).

4 Discussion

4.1 Summary of results

Levetiracetam has been extensively used in pediatric patients, primarily for epilepsy management. To the best of our knowledge, this study represents the first meta-analysis focused solely on children, assessing the efficacy and safety of levetiracetam for migraine prophylaxis. In this meta-analysis, we evaluated the efficacy and safety of levetiracetam for migraine prophylaxis in pediatric patients. As a result, there is a significant amount of data available regarding its safety and

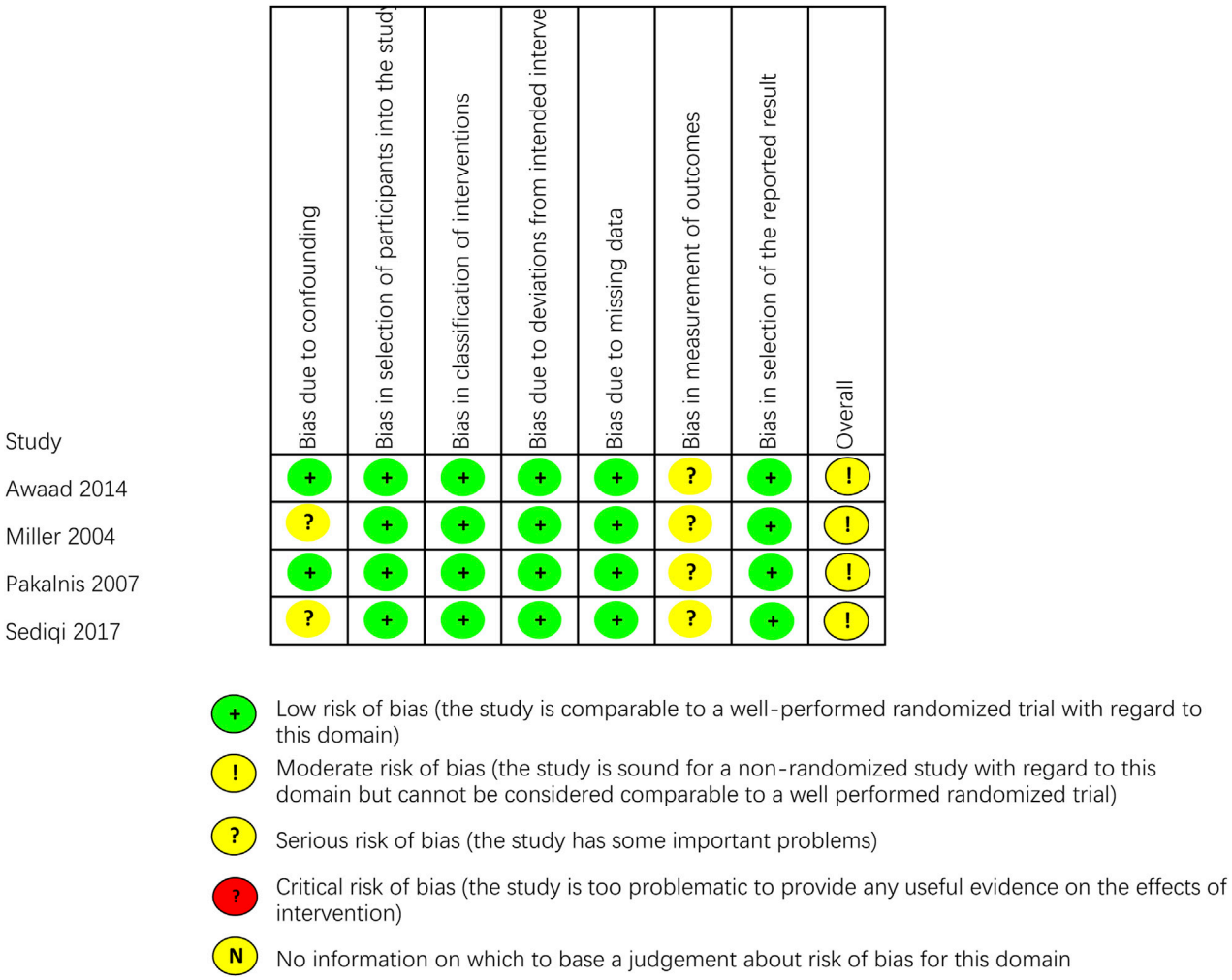

FIGURE 3
Critical appraisal of non-RCTs according to the Cochrane Collaboration's tool for assessing risk of bias in non-RCTs (ROBINS-I).

tolerability. However, it is important to note that these data may not be applicable to other conditions with a higher risk-to-benefit ratio. Based on the findings of this meta-analysis, the dosages used for migraine prevention were similar to those used for epilepsy. The ADRs reported were generally mild to moderate. It is important to highlight that most of the included studies had a limited sample size, which could affect the interpretation of the ADRs. These findings collectively highlight the substantial potential of levetiracetam in preventing migraines in children.

4.2 Certainty in the evidence

High placebo responses in pediatric migraine trials present a significant challenge (Abu-Arafeh et al., 2023). The scarcity of RCTs for levetiracetam in children and adolescents may be attributed to this challenge, which impacts the identification of effective treatments (Balottin and Termine, 2007). In the absence of randomized parallel controls, single-arm studies can introduce bias, leading to uncertainties in benefit–risk assessments. Open-label trials, where both investigators and participants are aware of the treatment allocation, may also introduce biases into patient-reported outcomes. Furthermore, patient-reported outcomes may be influenced by factors such as treatment switching and subjectivity. To minimize bias in patient-reported outcomes, various study design elements and analysis methods have been employed. These include the incorporation of washout periods (Pakalnis et al., 2007; Awaad and Rizk, 2014; Rahman et al., 2018; Ghazavi et al., 2019; Montazerlotfelahi et al., 2019), utilization of multilevel outcome measures and endpoints (Miller, 2004; Pakalnis et al., 2007; Awaad and Rizk, 2014; Sediqi et al., 2017; Rahman et al., 2018; Ghazavi et al., 2019; Montazerlotfelahi et al., 2019; Fayyazi et al., 2023), ensuring uniformity in tablet shape and color (Ghazavi et al., 2019; Montazerlotfelahi et al., 2019), maintaining headache diaries or questionnaires (Miller, 2004; Pakalnis et al., 2007; Sediqi et al., 2017; Rahman et al., 2018; Ghazavi et al., 2019; Montazerlotfelahi et al., 2019; Fayyazi et al., 2023), and the application of intention-to-treat analysis (Sediqi et al., 2017; Rahman et al., 2018; Ghazavi et al., 2019; Fayyazi et al., 2023).

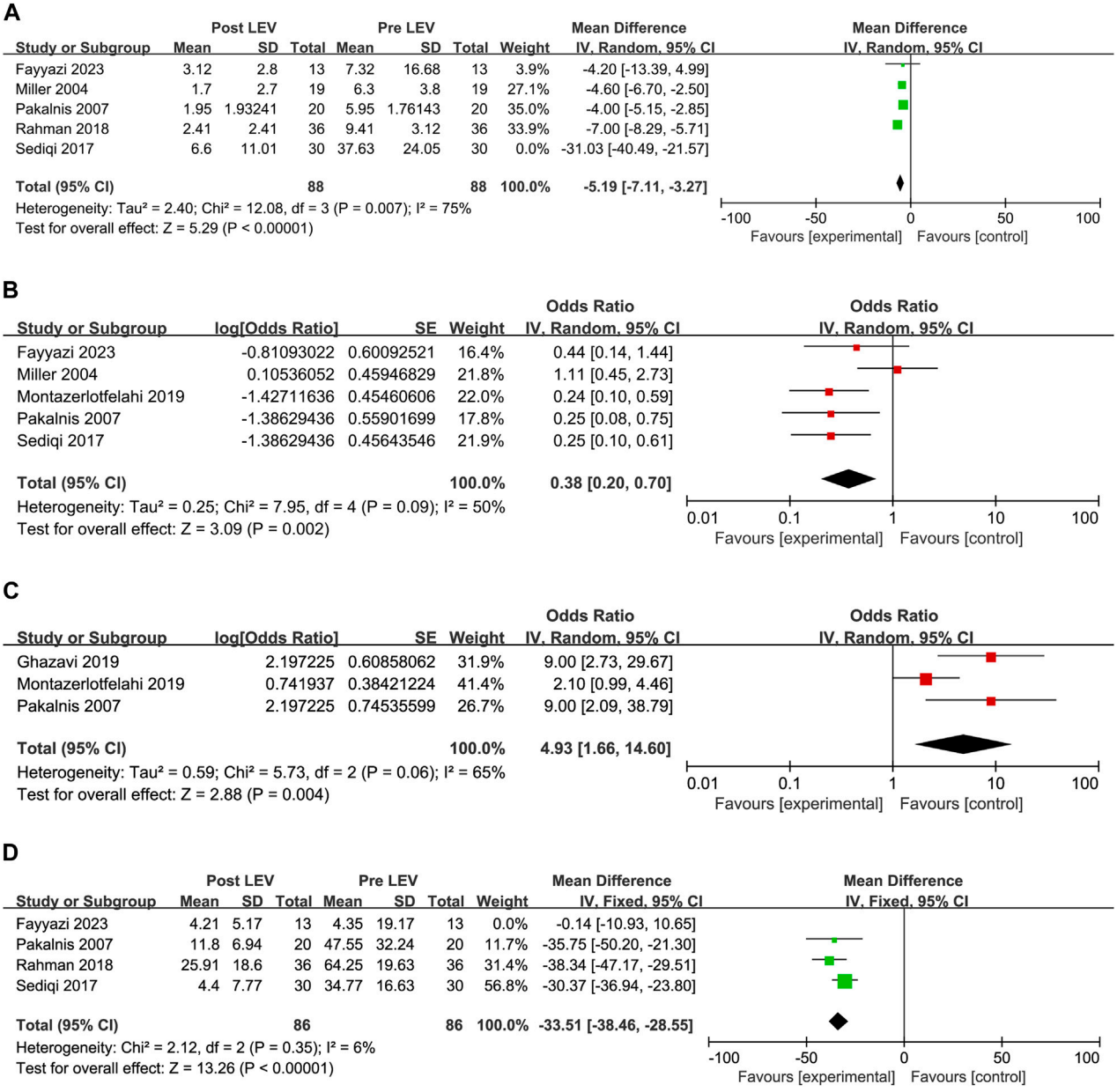

FIGURE 4
Forest plots. **(A)** Results of monthly headache frequency. **(B)** Results of the incidence rate of headache free. **(C)** Results of the incidence rate of headache frequency reduction greater than 50% monthly. **(D)** Results of PedMIDAS.

4.3 Comparison to other reviews

In recent years, antiepileptic drugs (AEDs) have garnered increased attention for their potential in preventing migraines, particularly in adults. A review has indicated that current evidence does not yield strong conclusions regarding the effectiveness of AEDs for this purpose, with the exception of gabapentin, pregabalin, topiramate, and valproate in adults with episodic migraines. However, it is noteworthy that in certain trials, levetiracetam demonstrated significantly greater efficacy than the placebo in reducing headache frequency (Linde et al., 2013). This observation is further supported by two additional studies (Capuano et al., 2004; Bakola et al., 2009). On the other hand, findings regarding the treatment of migraines in children are less consistent. To date, no medications have been approved by the U.S. Food and Drug Administration for migraine prophylaxis in children. Among the drugs with available data, topiramate and valproic acid have been most extensively studied for their use in pediatric migraine prophylaxis, showing efficacy in reducing migraine frequency and duration in children. In contrast, there are limited data on the use of levetiracetam in this demographic (Balottin and Termine, 2007; Eiland et al., 2007). Some randomized controlled trials (RCTs) and open-label, uncontrolled studies have shown levetiracetam to be effective in reducing migraine frequency

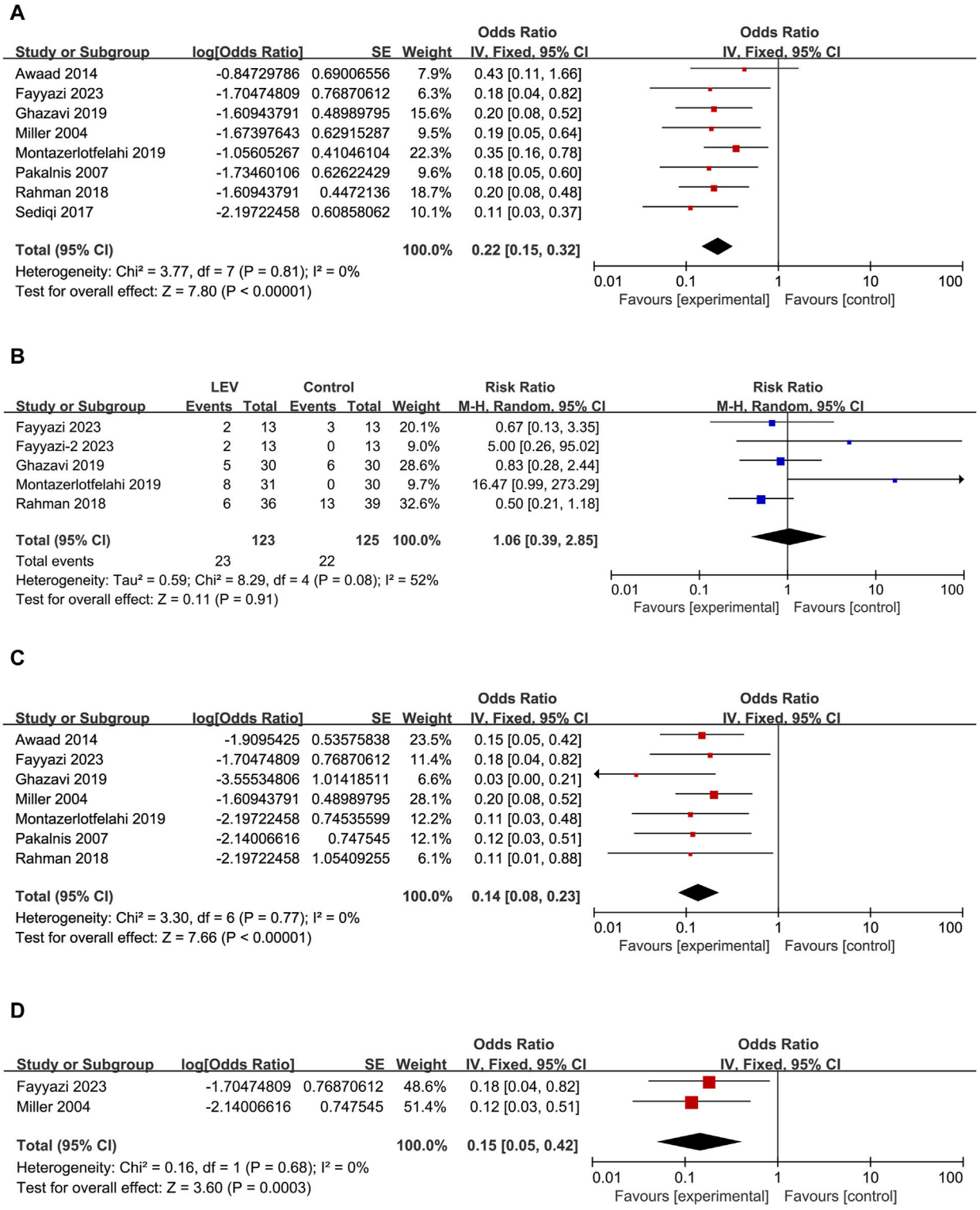

FIGURE 5
Forest plots. **(A)** Results of the incidence rate of ADRs. **(B)** Results of the risk ratio of ADRs between LEV and placebo or other drugs. Note: the control group for Fayyazi et al. (2023) was sodium valproate. The control group for Fayyazi-2 2023 was propranolol. **(C)** Results of the incidence rate of irritability/agitation. **(D)** Results of the incidence rate of discontinued treatment.

and disability in children (Sediqi et al., 2017; Fayyazi et al., 2023). However, a common limitation of these studies is their small sample size. A systematic review assessing the efficacy and safety of levetiracetam for migraine prophylaxis, which included pediatric, adult, and elderly patients, noted that more significant side effects leading to treatment discontinuation were observed in pediatric

studies compared to those in adults aged 18–60 years (Watkins et al., 2018). Nonetheless, when compared to other AEDs, the side effects associated with levetiracetam in pediatric patients appear to be less severe, suggesting that it may still be a viable option for this population. A previous meta-analysis, which included patients aged 4–72 years, provided limited specific insights into the efficacy of levetiracetam for pediatric migraines (Yen et al., 2021). However, only two trials (Pakalnis et al., 2007; Montazerlotfelahi et al., 2019) discussed the efficacy of levetiracetam in pediatric migraines, limiting the scope for specific conclusions for this age group. Although a subgroup analysis was performed to differentiate between adult and pediatric populations, only one RCT study was included in the forest plot analysis (Montazerlotfelahi et al., 2019). Individual study results are often insufficient to provide definitive answers, especially when they cannot be consistently replicated. A meta-analysis, which combines the results of multiple studies on a single topic, can help reconcile discrepancies among studies. One significant advantage of meta-analysis is its ability to provide a more precise estimate of the effect size with substantially increased statistical power, which is particularly valuable when primary studies are underpowered due to small sample sizes. A meta-analysis can yield conclusive results where individual studies are inconclusive (Lee, 2018). Therefore, in this study, we conducted a meta-analysis to synthesize previously published, albeit limited, quantitative research relevant to a broad spectrum of clinical questions. Our analysis included four RCT studies, each with different control groups. Rather than simply comparing the intervention group to the control groups, we consolidated the data from the levetiracetam intervention groups across studies and combined this with data from four single-arm trials.

4.4 Implications for this research

ADRs, especially those leading to discontinuation, are crucial measures of preventive migraine treatment tolerability (Abu-Arafeh et al., 2019). In this study, the 13% discontinuation rate due to ADRs, characterized by symptoms such as irritability, agitation, and aggression, emphasizes the importance of safety considerations in pediatric patients. Side effects including irritability, somnolence, dizziness, hyperactive behavior, moodiness, and hostility were also reported in adults (Sadeghian and Motiei-Langroudi, 2015). Among the reported side effects, behavioral changes and psychotic reactions are notably more common in younger patients, particularly those under 4 years of age (Verrotti et al., 2010). This is particularly significant for considering ADRs in children, potentially leading to behavioral changes. In the future, well-designed RCTs with larger sample sizes are essential to thoroughly assess levetiracetam's safety in pediatric migraine prevention.

4.5 Strengths and limitations

The strengths of this study include, first, to the best of our knowledge, this is the first meta-analysis focusing exclusively on the efficacy and safety of levetiracetam for migraine prophylaxis in children. Second, we conducted rigorous statistical analyses, adhering to the PRISMA guidelines and the Cochrane Handbook for Systematic Reviews of Interventions, with the review registered in PROSPERO, to ensure the stability and reliability of our results. Lastly, data extraction and methodological quality assessment were independently conducted by two authors, while two authors independently evaluated the risk of bias in each study using the Cochrane's RoB2 tool for RCTs and the ROBINS-I tool for non-RCTs.

Limitations of this study include, first, that the eight included studies ranged from 2004 to 2023, resulting in significant heterogeneity. This is due to considerable temporal and geographical heterogeneity among the single-arm trials. Despite rigorous attempts, we were unable to accurately identify the source of heterogeneity using subgroup analysis. Second, our focus on pediatric migraine prophylaxis resulted in a limited pool of relevant studies for inclusion, thus limiting our analysis to the assessment of efficacy and adverse reactions, without conclusively determining whether levetiracetam is the preferred treatment option. Third, our inability to conduct an in-depth analysis of the ADRs, highlighting the need for larger RCTs to provide conclusive evidence.

5 Conclusion

This study highlights the significant potential of levetiracetam in the prophylaxis of migraines among the pediatric population. Despite evident efficacy, a 13% discontinuation rate due to ADRs, with irritability being a notable concern, raises safety concerns. Future research should prioritize well-designed, large-sample RCTs to fully understand the efficacy and safety profile of levetiracetam in preventing pediatric migraines.

Data availability statement

The original contributions presented in the study are included in the article/Supplementary Material; further inquiries can be directed to the corresponding author.

Author contributions

JP: writing–original draft, visualization, project administration, methodology, formal analysis, data curation, and conceptualization. LL: writing–review and editing, methodology, investigation, formal analysis, and data curation. QL: writing–review and editing, methodology, investigation, formal analysis, and data curation. ML: writing–review and editing and validation. RZ: writing–review and editing and validation. LC: writing–review and editing and validation. ZL: writing–review and editing, supervision, funding acquisition, and conceptualization.

Funding

The author(s) declare that financial support was received for the research, authorship, and/or publication of this article from Hubei Province Science and Technology Plan Project - Clinical Medical Research Center for Children's Neurodevelopment (No. 2022DCC020).

Conflict of interest

The authors declare that the research was conducted in the absence of any commercial or financial relationships that could be construed as a potential conflict of interest.

Publisher's note

All claims expressed in this article are solely those of the authors and do not necessarily represent those of their affiliated organizations, or those of the publisher, the editors, and the reviewers. Any product that may be evaluated in this article, or claim that may be made by its manufacturer, is not guaranteed or endorsed by the publisher.

Supplementary material

The Supplementary Material for this article can be found online at: https://www.frontiersin.org/articles/10.3389/fphar.2024.1407897/full#supplementary-material

References

Abu-Arafeh, I., Hershey, A. D., Diener, H. C., Tassorelli, C., and Clinical Trials Standing Committee and the Child and Adolescent Standing Committee of the International Headache Society (2019). Guidelines of the International Headache Society for controlled trials of preventive treatment of migraine in children and adolescents, 1st edition. *Cephalalgia* 39 (7), 803–816. doi:10.1177/0333102419842188

Abu-Arafeh, I., Hershey, A. D., Diener, H. C., and Tassorelli, C. (2023). Guidelines Update: guidelines of the International Headache Society for controlled trials of preventive treatment of migraine in children and adolescents, 1st edition - an experience-based update. *Cephalalgia* 43 (5), 3331024231178239. doi:10.1177/03331024231178239

Arruda, M. A., Arruda, R., Guidetti, V., and Bigal, M. E. (2020). ADHD is comorbid to migraine in childhood: a population-based study. *J. Atten. Disord.* 24 (7), 990–1001. doi:10.1177/1087054717710767

Aurora, S. K., and Brin, M. F. (2017). Chronic migraine: an update on Physiology, imaging, and the mechanism of action of two available pharmacologic therapies. *Headache* 57 (1), 109–125. doi:10.1111/head.12999

Awaad, Y., and Rizk, T. (2014). Levetiracetam in the treatment of pediatric headache. *J. Taibah Univ. Med. Sci.* 9 (1), 74–77. doi:10.1016/j.jtumed.2013.05.004

Ayatollahi, S., and Khosravi, A. (2005). A case-control study of migraine and tension-type headache's risk factors among Shiraz schoolchildren. *Sci. J. Hamadan Univ. Med. Sci.* 11 (4), 37–42.

Ayatollahi, S. M., and Khosravi, A. (2006). Prevalence of migraine and tension-type headache in primary-school children in Shiraz. *East Mediterr. Health J.* 12 (6), 809–817.

Bahrami, P. (2006). Incidence of Migraine in high school students in Khorramabad. *Yafteh* 7, 55–60.

Bakola, E., Skapinakis, P., Tzoufi, M., Damigos, D., and Mavreas, V. (2009). Anticonvulsant drugs for pediatric migraine prevention: an evidence-based review. *Eur. J. Pain* 13 (9), 893–901. doi:10.1016/j.ejpain.2008.11.004

Balottin, U., and Termine, C. (2007). Recommendations for the management of migraine in paediatric patients. *Expert Opin. Pharmacother.* 8 (6), 731–744. doi:10.1517/14656566.8.6.731

Capuano, A., Vollono, C., Mei, D., Pierguidi, L., Ferraro, D., and Di Trapani, G. (2004). Antiepileptic drugs in migraine prophylaxis: state of the art. *Clin. Ter.* 155 (2-3), 79–87.

Cheng, K., Mahler, F., Lutsar, I., Nafria Escalera, B., Breitenstein, S., Vassal, G., et al. (2023). Clinical, methodology, and patient/carer expert advice in pediatric drug development by conect4children. *Clin. Transl. Sci.* 16 (3), 478–488. doi:10.1111/cts.13459

Costa, C., Tozzi, A., Rainero, I., Cupini, L. M., Calabresi, P., Ayata, C., et al. (2013). Cortical spreading depression as a target for anti-migraine agents. *J. Headache Pain* 14 (1), 62. doi:10.1186/1129-2377-14-62

Debray, T. P., Damen, J. A., Snell, K. I., Ensor, J., Hooft, L., Reitsma, J. B., et al. (2017). A guide to systematic review and meta-analysis of prediction model performance. *BMJ* 356, i6460. doi:10.1136/bmj.i6460

Eiland, L. S., Jenkins, L. S., and Durham, S. H. (2007). Pediatric migraine: pharmacologic agents for prophylaxis. *Ann. Pharmacother.* 41 (7), 1181–1190. doi:10.1345/aph.1K049

Evers, S., Frese, A., Summ, O., Husstedt, I. W., and Marziniak, M. (2022). Levetiracetam in the prophylactic treatment of episodic migraine: a prospective open label study. *Cephalalgia* 42 (11-12), 1218–1224. doi:10.1177/03331024221103815

Falla, K., Kuziek, J., Mahnaz, S. R., Noel, M., Ronksley, P. E., and Orr, S. L. (2022). Anxiety and depressive symptoms and disorders in children and adolescents with migraine: a systematic review and meta-analysis. *JAMA Pediatr.* 176 (12), 1176–1187. doi:10.1001/jamapediatrics.2022.3940

Fallah, R., Divanizadeh, M., Karimi, M., and Ordooei, M. (2013). Evaluation of efficacy and safety of propranolol for pediatric migraine prophylaxis. *J. Shahid Sadoughi Univ. Med. Sci.* 21 (1), 94–100.

Fallahzade, H., Alihaydari, A., and Hoseini, H. (2010). Prevalence of migraine and tension headache in students of guidance schools in Yazd city, 2008. *Razi J. Med. Sci.* 17 (76), 52–61.

Fayyazi, A., Pezeshki, N., Mansuri, H., and Khajeh, A. (2023). Comparing prophylactic effect of levetiracetam, sodium valproate, and propranolol in pediatric migraine: a randomized clinical trial. *Iran. J. Child. Neurol.* 17 (4), 105–115. doi:10.22037/ijcn.v17i1.21330

Ghazavi, M. R., Jelodar, G., Yaghini, O., Nasiri, J., Sadeghian, S., and Malamiri, R. A. (2019). The efficacy and safety of levetiracetam in the prophylaxis of migraine headaches in children-a randomised trial. *Pediatr. Pol.* 94 (3), 145–150. doi:10.5114/POLP.2019.86434

Gunner, K. B., Smith, H. D., and Ferguson, L. E. (2008). Practice guideline for diagnosis and management of migraine headaches in children and adolescents: Part two. *J. Pediatr. Health Care* 22 (1), 52–59. doi:10.1016/j.pedhc.2007.10.009

Hershey, A. D., and Winner, P. K. (2005). Pediatric migraine: recognition and treatment. *J. Am. Osteopath. Assoc.* 105 (4_ Suppl), 2S–8S.

Khazaie, T., Dehghany, M., Sharifzadeh, G., Reyasie, H., Phani, J., and Usefi, H. (2014). Evaluation of the factors associated with overweight and obesity in 30-to 50-year-old women of sabzevar. *Iran. J. Epidemiol.* 10 (1), 73–80.

Krymchantowski, A. V., Bigal, M. E., and Moreira, P. F. (2002). New and emerging prophylactic agents for migraine. *CNS Drugs* 16 (9), 611–634. doi:10.2165/00023210-200216090-00003

Lee, Y. H. (2018). An overview of meta-analysis for clinicians. *Korean J. Intern Med.* 33 (2), 277–283. doi:10.3904/kjim.2016.195

Linde, M., Mulleners, W. M., Chronicle, E. P., and McCrory, D. C. (2013). Antiepileptics other than gabapentin, pregabalin, topiramate, and valproate for the prophylaxis of episodic migraine in adults. *Cochrane Database Syst. Rev.* 2013 (6), CD010608. doi:10.1002/14651858.CD010608

Magis, D., and Schoenen, J. (2011). Treatment of migraine: update on new therapies. *Curr. Opin. neurology* 24 (3), 203–210. doi:10.1097/WCO.0b013e3283462c3f

Marmura, M. J. (2014). Safety of topiramate for treating migraines. *Expert Opin. Drug Saf.* 3 (9), 1241–1247. doi:10.1517/14740338.2014.934669

Miller, G. S. (2004). Efficacy and safety of levetiracetam in pediatric migraine. *Headache* 44 (3), 238–243. doi:10.1111/j.1526-4610.2004.04053.x

Minozzi, S., Dwan, K., Borrelli, F., and Filippini, G. (2022). Reliability of the revised Cochrane risk-of-bias tool for randomised trials (RoB2) improved with the use of implementation instruction. *J. Clin. Epidemiol.* 141, 99–105. doi:10.1016/j.jclinepi.2021.09.021

Mirzaei, G.-r. (2004). A review of cammon migraine in girls high school and related fall in education in Shahrekord region. *J. Shahrekord Univ. Med. Sci.* 5 (4), 55–62.

Moaiedi, A., and Boroomand, S. (2004). Causes of headache in patients referring to Bandar Abbas pediatric hospital. *Bimon. J. Hormozgan Univ. Med. Sci.* 8 (2), 73–76.

Montazerlotfelahi, H., Amanat, M., Tavasoli, A. R., Agah, E., Zamani, G. R., Sander, J. W., et al. (2019). Levetiracetam for prophylactic treatment of pediatric migraine: a randomized double-blind placebo-controlled trial. *Cephalalgia* 39 (12), 1509–1517. doi:10.1177/0333102419851814

Moons, K. G., de Groot, J. A., Bouwmeester, W., Vergouwe, Y., Mallett, S., Altman, D. G., et al. (2014). Critical appraisal and data extraction for systematic reviews of prediction modelling studies: the CHARMS checklist. *PLoS Med.* 11 (10), e1001744. doi:10.1371/journal.pmed.1001744

Morgan, R. L., Thayer, K. A., Santesso, N., Holloway, A. C., Blain, R., Eftim, S. E., et al. (2018). Evaluation of the risk of bias in non-randomized studies of interventions (ROBINS-I) and the 'target experiment' concept in studies of exposures: rationale and preliminary instrument development. *Environ. Int.* 120, 382–387. doi:10.1016/j.envint.2018.08.018

Ozge, A., Saşmaz, T., Buğdaycı, R., Cakmak, S. E., Kurt, A. Ö., Kaleağası, S. H., et al. (2013). The prevalence of chronic and episodic migraine in children and adolescents. *Eur. J. Neurol.* 20 (1), 95–101. doi:10.1111/j.1468-1331.2012.03795.x

Page, M. J., McKenzie, J. E., Bossuyt, P. M., Boutron, I., Hoffmann, T. C., Mulrow, C. D., et al. (2021). The PRISMA 2020 statement: an updated guideline for reporting systematic reviews. *BMJ* 372, n71. doi:10.1136/bmj.n71

Pakalnis, A., Kring, D., and Meier, L. (2007). Levetiracetam prophylaxis in pediatric migraine--an open-label study. *Headache* 47 (3), 427–430. doi:10.1111/j.1526-4610.2007.00728.x

Pavkovic, I. M., and Kothare, S. V. (2020). Migraine and sleep in children: a bidirectional relationship. *Pediatr. Neurol.* 109, 20–27. doi:10.1016/j.pediatrneurol.2019.12.013

Rahman, S. M., Kundu, G. K., Fatema, K., Akhter, S., and Rahman, M. (2018). Comparison between flunarizine and levetiracetam in paediatric migraine prophylaxis. *Bangladesh Med. J. Khulna* 51 (1-2), 35–39. doi:10.3329/bmjk.v51i1-2.40472

Sadeghian, H., and Motiei-Langroudi, R. (2015). Comparison of Levetiracetam and sodium Valproate in migraine prophylaxis: a randomized placebo-controlled study. *Ann. Indian Acad. Neurol.* 18 (1), 45–48. doi:10.4103/0972-2327.144290

Sediqi, M., Yavari, B., and Almasi, A. (2017). Prophylactic efficacy of levetiracetam on migraine headaches in children aged 4-14-year-old. *Ann. Trop. Med. Public Health* 10, 1547–1551. doi:10.4103/ATMPH.ATMPH_499_17

Solomon, G. D. (1992). The practicing physicians approach to headache. *Clin. J. Pain* 8 (4), 370. doi:10.1097/00002508-199212000-00015

Stadelmaier, R., Nasri, H., Deutsch, C. K., Bauman, M., Hunt, A., Stodgell, C. J., et al. (2017). Exposure to sodium valproate during pregnancy: facial features and signs of autism. *Birth Defects Res.* 109 (14), 1134–1143. doi:10.1002/bdr2.1052

Taghdiri, M., and Razavi, Z. (2004). Comparison of the therapeutic effects and side effects of sodium valproate and propranolol in preventing migraine headaches in children. *Sci. J. Hamadan Univ. Med. Sci.* 11 (2), 38–42.

Tsaousi, G., Pourzitaki, C., Siafis, S., Kyrgidis, A., Grosomanidis, V., Kouvelas, D., et al. (2020). Levetiracetam as preventive treatment in adults with migraine: an up-to-date systematic review and quantitative meta-analysis. *Eur. J. Clin. Pharmacol.* 76 (2), 161–174. doi:10.1007/s00228-019-02790-2

Verma, A., Srivastava, D., Kumar, A., and Singh, V. (2013). Levetiracetam in migraine prophylaxis: a randomized placebo-controlled study in a rural medical institute in northern India. *Clin. Neuropharmacol.* 36 (6), 193–197. doi:10.1097/WNF.0000000000000005

Verrotti, A., D'Adamo, E., Parisi, P., Chiarelli, F., and Curatolo, P. (2010). Levetiracetam in childhood epilepsy. *Paediatr. Drugs* 12 (3), 177–186. doi:10.2165/11316250-000000000-00000

Watkins, A. K., Gee, M. E., and Brown, J. N. (2018). Efficacy and safety of levetiracetam for migraine prophylaxis: a systematic review. *J. Clin. Pharm. Ther.* 43 (4), 467–475. doi:10.1111/jcpt.12715

Yen, P. H., Kuan, Y. C., Tam, K. W., Chung, C. C., Hong, C. T., and Huang, Y. H. (2021). Efficacy of levetiracetam for migraine prophylaxis: a systematic review and meta-analysis. *J. Formos. Med. Assoc.* 120 (1 Pt 3), 755–764. doi:10.1016/j.jfma.2020.08.020

Yue-hong, C., Liang, D. U., Xing-yuan, G., and Guan-jian, L. I. U. (2014). Implement meta-analysis with non-comparative binary data in RevMan software. *Chin. J. Evidence-Based Med.* 14 (7), 889–896. doi:10.7507/1672-2531.20140147

Zamani, G., and Ghofrani, M. (2006). Prophylactic sodium valproate and propranolol in childhood migraine: a randomized clinical trial. *Tehran Univ. Med. J. TUMS Publ.* 64 (4), 69–77.

frontiers | Frontiers in Pharmacology

TYPE Original Research
PUBLISHED 08 August 2024
DOI 10.3389/fphar.2024.1454601

OPEN ACCESS

EDITED BY
Álvaro Llorente-Berzal,
Autonomous University of Madrid, Spain

REVIEWED BY
Silvia Mazzoleni,
IRCCS Fondazione Salvatore Maugeri, Italy
Mellar Pilgrim Davis,
Geisinger Health System, United States

*CORRESPONDENCE
Alfonso Papa,
alfonsopapa@libero.it

†These authors have contributed equally to this work and share last authorship

RECEIVED 25 June 2024
ACCEPTED 26 July 2024
PUBLISHED 08 August 2024

CITATION
Papa A, Salzano AM, Di Dato MT, Desiderio V, Buonavolontà P, Mango P, Saracco E, Tammaro D, Luongo L and Maione S (2024) Long-term efficacy and reduced side-effects of buprenorphine in patients with moderate and severe chronic pain.
Front. Pharmacol. 15:1454601.
doi: 10.3389/fphar.2024.1454601

Long-term efficacy and reduced side-effects of buprenorphine in patients with moderate and severe chronic pain

Alfonso Papa[1]*, Anna Maria Salzano[1], Maria Teresa Di Dato[1], Vincenzo Desiderio[2], Pietro Buonavolontà[1], Pietro Mango[1], Elisabetta Saracco[1], Dario Tammaro[1], Livio Luongo[3†] and Sabatino Maione[3†]

[1]Department of Pain Management—AO "Ospedale dei Colli"–Monaldi Hospital, Napoli, Italy, [2]Department of Experimental Medicine, University of Campania "Luigi Vanvitelli", Naples, Italy, [3]Department of Experimental Medicine, Division of Pharmacology, University of Campania "Luigi Vanvitelli", Naples, Italy

Background: Chronic pain significantly impacts quality of life and poses substantial public health challenges. Buprenorphine, a synthetic analog of thebaine, is recognized for its potential in managing moderate to severe chronic pain with fewer side effects and a lower incidence of tolerance compared to traditional opioids.

Objective: This retrospective study aimed to assess the long-term efficacy and safety of buprenorphine transdermal patches in patients with moderate and severe chronic pain, with a focus on pain relief sustainability and tolerance development.

Methods: This retrospective observational study involved 246 patients prescribed buprenorphine transdermal patches. We evaluated changes in pain intensity using the Numeric Rating Scale (NRS), assessed opioid tolerance based on FDA guidelines for morphine-equivalent doses, and measured patient-reported outcomes through the Patients' Global Impression of Change (PGIC). Any adverse events were also recorded.

Results: Over the 36-month period, there was a significant reduction in NRS scores for both moderate and severe pain patients, demonstrating buprenorphine's sustained analgesic effect. Tolerance measurement indicated that no patients required increases in morphine-equivalent doses that would meet or exceed the FDA's threshold for opioid tolerance (60 mg/day of morphine or equivalent). Additionally, patient satisfaction was high, with the PGIC reflecting significant improvements in pain management and overall wellbeing. The side effects were minimal, with skin reactions and nausea being the most commonly reported but manageable adverse events.

Conclusion: The study findings validate the long-term use of buprenorphine transdermal patches as an effective and safe option for chronic pain management, maintaining efficacy without significant tolerance development. These results support the continued and expanded use of buprenorphine in clinical settings, emphasizing its role in reducing the burdens of chronic pain and

opioid-related side effects. Further research is encouraged to refine pain management protocols and explore buprenorphine's full potential in diverse patient populations.

KEYWORDS

chronic pain, opioids, tolerance, transdermal patches, pain relief, opioid crisis

1 Introduction

Chronic pain represents a significant challenge in clinical management, often leading to compromised quality of life for patients. Recent estimates from the World Health Organization (WHO) indicate that chronic pain impacts approximately 20% of the world's population, significantly impairing daily functionality, interpersonal relationships, and emotional wellbeing (Mills et al., 2019). In the United States, the economic burden of chronic pain, encompassing medical expenses and productivity losses, ranges between US$560 and US$635 billion annually (Nahin et al., 2023). Furthermore, chronic pain is associated with various comorbidities, including depression, anxiety, physical disability, hypo cognition and sleep disturbances, further contributing to the overall burden of the disease (Cohen et al., 2021).

Opioids still represent a cornerstone in the pharmacological armamentarium for treating moderate and severe chronic pain (Alorfi, 2023). Nevertheless, chronic opioid therapy with potent (schedule II) opioids like morphine, oxycodone, fentanyl, hydrocodone, and hydromorphone poses numerous challenges, including severe side effects such as hypogonadism, infections, immunosuppression, respiratory depression, and mortality (Holtman and Jellish, 2012; Poon et al., 2021). Additionally, gastrointestinal issues such as opioid-induced constipation (are highly prevalent, often emerging as a primary reason for discontinuing opioid therapy (Sizar et al., 2023).

Tolerance, along with the potential for abuse and dependence, represents another significant challenge in opioid therapy (Mercadante et al., 2019). Tolerance occurs when the efficacy of a drug diminishes over time, leading to the need for higher doses to achieve the same therapeutic effect. Mechanisms underlying opioid tolerance involve drug-induced adaptations or allostatic changes at various levels, including cellular, circuitry, and systemic levels (Aston-Jones and Harris, 2004; Christie, 2008). The development of tolerance presents a significant issue, as it demands higher opioid doses to achieve the same therapeutic effect. This phenomenon not only reduces the effectiveness of opioids but also raises the likelihood of experiencing withdrawal symptoms and developing addiction. Additionally, long-term opioid therapy may lead to dose escalation, potentially inducing opioid-induced hyperalgesia, characterized by increased sensitivity to painful stimuli, exacerbating rather than alleviating pain perception (Mercadante et al., 2019) The addictive nature of opioids has contributed to the opioid crisis, posing a substantial challenge to various sectors including social, economic, and public health not only in the United States but also in other countries (Jalali et al., 2020). Millions of prescription opioids are misused annually, resulting in significant financial costs and high overdose death rates. To address this crisis, the US Department of Health and Human Services established a task force promoting better pain management practices (Gudin and Fudin, 2020).

One recommended approach is the preferential use of buprenorphine, not only for opioid use disorder but also for pain management, suggesting it as a primary option when clinically indicated rather than a secondary choice after other opioids failure (Pergolizzi et al., 2008; Breivik, 2013; Ehrlich and Darcq, 2018).

Buprenorphine, a lipophilic opioid analgesic derived from thebaine, has emerged as a promising option due to its unique pharmacodynamics (Webster et al., 2020). Buprenorphine binds to mu (MOR), kappa (KOR), and delta (DOR) opioid receptors, exhibiting a sort of biased agonism towards MOR and antagonism towards KOR and DOR (Pergolizzi et al., 2010; Webster et al., 2020; Infantino et al., 2021). Additionally, it binds to opioid-like receptor 1 (OLR-1), the receptor for orphanin FQ/nociception (Pergolizzi et al., 2010; Infantino et al., 2021). The biased agonism of buprenorphine at MOR, coupled with its distinct pharmacokinetic properties, contributes to its efficacy and safety profile.

Buprenorphine exhibits unique binding characteristics, primarily binding to acidic glycoproteins like α1-acid glycoprotein (AGP) rather than extensively to plasma proteins such as albumin (Pergolizzi et al., 2010). This differential binding minimizes drug-drug interactions in the distribution phase and enhances bioavailability, making buprenorphine a preferred option in elderly patients, in which the levels of albumin are decreased without changes in the AGP (Pergolizzi et al., 2010; Infantino et al., 2021). The pharmacological advantages of buprenorphine extend to its metabolism and excretion, which are favorable in clinical practice. Being metabolized primarily by cytochrome (CYP) 3A4 to its metabolite norbuprenorphine, buprenorphine is associated with fewer drug interactions, in the metabolism phase, compared to other opioids (Zhang et al., 2003). This is due to the possibility to directly conjugate buprenorphine by skipping the CYP activity. Importantly, its minimal renal excretion renders it suitable for use in patients with renal failure without necessitating dosage adjustments (Owsiany et al., 2019; Zhuo et al., 2021).

Finally, in response to the opioid epidemic and the need for enhanced chronic pain management, new methods of drug administration have been developed, including tamper-resistant formulations. Among these innovations, the transdermal drug delivery system stands out as a notable advancement, offering distinct benefits compared to conventional routes like parenteral and oral administration (Alkilaniet al., 2015). Transdermal delivery avoids discomfort associated with injections and multiple oral doses, provides constant plasma drug concentrations, bypasses hepatic metabolism and poor absorption from the gastrointestinal tract,

and enhances patient compliance by reducing the frequency of administration. Additionally, the risk of local adverse events is minimized as the site of drug delivery can be regularly changed (Evans and Easthope, 2003).

Considering these characteristics, buprenorphine transdermal patches emerge as a preferred option for managing chronic pain, particularly in populations such as the elderly and those with renal and hepatic impairments (Plosker, 2011). However, despite its potential benefits, there remains a need for further research to elucidate its full mechanisms of action and optimize its clinical use.

According to NIH guidelines, buprenorphine is mainly used to treat moderate to severe pain, as it exhibits only partial analgesic activity at the mu-opioid receptor and exhibits a ceiling effect (Kumar et al., 2023). However, buprenorphine shows a ceiling effect on those MORs involved in respiratory depression but not on the MORs active at the pain axis that drive the analgesia. Intriguingly, unlike traditional opioids, buprenorphine demonstrates biased agonism towards MOR, preferentially activating G protein-mediated signaling over β-arrestin-mediated signaling (Neto et al., 2020; Infantino et al., 2021). This selective activation results in analgesia with reduced side effects such as respiratory depression and constipation (Neto et al., 2020; Webster et al., 2020; Infantino et al., 2021). Hence, buprenorphine could be considered a frontline treatment option for individuals suffering from severe pain, particularly if it exhibits lower tolerance induction compared to alternative opioids.

By analyzing buprenorphine's efficacy, tolerance induction, and side effects over a 3-year follow-up period in patients with moderate and severe chronic pain, this retrospective study aims to offer insights into the effectiveness of buprenorphine in managing long-term pain. These findings will provide valuable information to clinical practice, facilitating the optimization of patient care in this challenging population.

2 Materials and methods

2.1 Study design

This study is an investigator-initiated, monocentric, retrospective, observational study designed to assess the long-term efficacy and safety of buprenorphine in the management of moderate and severe chronic pain. The retrospective analysis focused on patients who were administered buprenorphine's transdermal patches as part of their treatment regimen between January 2021 and January 2024 at the Pain Department of the Azienda Ospedaliera Specialistica dei Colli–Ospedale Monaldi Napoli, Italy.

The study received ethical approval from the Campania SUD Ethics Committee, approval number AOC/0011976/2024. Prior to participation, all patients provided informed consent. This study strictly adhered to the ethical standards of the committee responsible for human experimentation (institutional and national) and the Helsinki Declaration of 1975, as updated in 2008, ensuring the highest ethical considerations and patient safety throughout the study period.

2.2 Data source

Data were gathered from the electronic health records of patients who were prescribed buprenorphine as part of their chronic pain management strategy. The treatment regimen consisted of administering buprenorphine's transdermal patches according to individual patient needs, as determined by their managing healthcare professionals at the Azienda Ospedaliera Specialistica dei Colli–Ospedale Monaldi, Napoli, Italy. The specific dosage and frequency of buprenorphine administration were tailored to the severity of the pain and the patient's overall response to the treatment, adhering to standard clinical practices for pain management.

In addition to the investigational treatment data, all concurrent treatments provided alongside buprenorphine, as well as any treatments received within 7 days prior to the initiation of buprenorphine therapy, were documented. This included the type of medication, dosage, and administration dates and times. Demographic details, medical history, weight measurements, adverse events, and clinical outcomes were also systematically recorded.

Patients were followed for a period of 3 years. Comprehensive physical examinations and complete pain evaluations were conducted at the start of buprenorphine treatment and at 6, 12, 24 and 36 months, including assessments of pain symptoms, physical function, and overall wellbeing.

2.3 Inclusion and exclusion criteria

2.3.1 Inclusion criteria

- Patients aged 18 years and above.
- Patients naïve to opioid.
- Diagnosis of moderate or severe chronic pain, originating from various etiologies, including but not limited to musculoskeletal, myofascial, rheumatic conditions, and neuropathic pain; the pain should have persisted for more than 3 months, aligning with the chronic pain definition.
- A baseline Numeric Rating Scale (NRS) score for pain greater than 5, indicating moderate to severe pain intensity.
- Treatment with buprenorphine for a minimum duration of 6 months.

2.3.2 Exclusion criteria

- Oncological patients
- Patients receiving concurrent treatments that could influence the assessment of buprenorphine's efficacy, such as other major opioids, or invasive therapies.
- Pregnant or breastfeeding women.
- Patients with a history of past opioid abuse.
- A known allergy or hypersensitivity to buprenorphine or any of its components.

2.4 Clinical investigation endpoints

The study meticulously tracked and analyzed patient outcomes and complications from medical records to assess the efficacy and safety of buprenorphine in chronic pain management.

2.4.1 Primary efficacy endpoint

The reduction of pain in patients with moderate and severe chronic pain as quantified by changes in the Numeric Rating Scale (NRS) scores at each follow-up period compared to baseline, with a specific focus on the sustained efficacy over 36 months.

2.4.2 Secondary efficacy endpoints

- The percentage of responders at each follow-up interval (6, 12, 24, and 36 months), where responders are defined by significant reductions in NRS scores (as defined in the statistical analysis section) and positive evaluations on the Patients' Global Impression of Change (PGIC).
- Patient satisfaction and quality of life improvements, measured by PGIC and supplemented by detailed patient interviews and quality of life assessments to provide a comprehensive view of the treatment impact over time.
- Evaluation of opioid tolerance development, specifically assessing if patients required increasing doses of buprenorphine to achieve the same level of pain relief initially provided by the treatment over the 36-month period. Tolerance, as defined by the US Food and Drug Administration (FDA), is quantified by the rate of dosage increase required to maintain effective pain management, with a significant increase indicating the development of tolerance.

2.4.3 Safety endpoint

Safety assessments focused on the documentation and analysis of adverse events (AEs). These events were coded using the Medical Dictionary for Regulatory Activities (MedDRA) version 16.0 and categorized by system organ class and preferred terminology (Harrison and Mozzicato, 2009). The analysis included a detailed summary of adverse drug effects (ADEs) directly attributable to buprenorphine, serious adverse events (SAEs), and any adverse events prompting discontinuation of the therapy, thereby offering a thorough evaluation of buprenorphine's safety profile in the treatment regimen for moderate to severe chronic pain.

2.5 Buprenorphine's transdermal patches

The study utilized buprenorphine transdermal patches, marketed under the commercial name Busette (Sandoz, Basel, Switzerland), for the management of moderate to severe chronic pain in adults. These patches are specifically designed for long-term pain that requires the use of a strong painkiller. Busette transdermal patches contains buprenorphine as the active ingredient, and the patches are designed for transdermal use. The patches have been applied to clean, intact, non-irritated skin on the upper torso, upper arm, or the upper back. Patients have been advised to change the patch every 7 days, preferably at the same time to maintain consistent pain relief. These patches have been chosen because they provide a controlled, steady release of buprenorphine, offering a manageable option for adults dealing with chronic pain.

2.6 Measurement of pain

The Numeric Rating Scale (NRS) is a widely utilized tool for pain assessment, renowned for its simplicity in administration. It is a unidimensional scale, designed exclusively to measure pain intensity without considering other factors. The NRS is a numeric scale ranging from 0 to 10, where each number represents a level of pain experienced by the patient: a score of 0 indicates no pain; a score of 10 represents the maximum imaginable pain; scores between 1 and 9 signify increasing levels of pain intensity. According to literature data, this study classifies patients with moderate pain as those with a NRS score ranging from 5 to 6. Patients experiencing severe pain are classified as those with an NRS score equal to or greater than 6 (McCormack et al., 1988; Hawker et al., 2011; Alschuler et al., 2012).

2.7 Measurement of patients' degree of satisfaction

The Patients' Global Impression of Change (PGIC) scale is specifically designed to assess patients' perceptions of change following treatment, that is, whether they feel "better" or "worse." (Eremenco et al., 2022) It is a 7-point verbal scale offering options ranging from "very much improved" to "very much worsened," including "much improved," "minimally improved," "no change," "minimally worsened," and "much worsened." The PGIC is widely used in clinical studies that assess pain relief following treatment due to its ease of administration, scoring simplicity, and because it is a generic scale applicable across a wide range of conditions and treatments.

2.8 Measurement of buprenorphine tolerance

The measurement of buprenorphine tolerance, administered via transdermal patches (Busette), was a crucial aspect of assessing long-term treatment efficacy for patients with moderate and severe chronic pain. The FDA defines opioid tolerance as the need for increasing doses of an opioid to maintain the same level of analgesia that could previously be achieved at lower doses, without the progression of the underlying cause of pain.According to the FDA, opioid tolerance is considered to have developed when a patient requires at least 60 mg/day of morphine or an equianalgesic dose of another opioid for at least 1 week (Dowell et al., 2022; Rx only, 2024). In contrast, analgesic tolerance refers to the general reduction in the effectiveness of any analgesic medication over time, necessitating higher doses to achieve the same level of pain relief. In this study, we focused on opioid tolerance, as defined by FDA (Dowell et al., 2022). To determine the development of tolerance to buprenorphine, we translated the dosages of buprenorphine administered to patients into morphine-equivalent doses using an equianalgesic conversion factor. According to the conversion factor provided by the FDA and other governmental organizations, 5 μg per hour of transdermal buprenorphine is equivalent to 12 mg per 24 h of morphine, and, thus, the threshold dose of 60 mg/day of morphine correspond to 25mcg/h of transdermal buprnorphine (Cancer et al., 2012, Care Network; Opioid conversion ratios Guidance document 2, 2021).

Therefore, we used the following formula to calculate the morphine-equivalent doses from the administered buprenorphine doses:

TABLE 1 Patient's demographic data. The table shows the distribution of patients by severity of pain and gender, along with average age.

	Total number of patients	Male	Female	Mean age
Moderate pain	75	14	61	70.8
Severe pain	171	60	111	69.5

$$\text{Morphine Equivalent Dose (mg)} = \text{Buprenorphine Dosage (mcg)} \times (12/5)$$

For each patient, buprenorphine dosages at baseline, 6, 12, 24, and 36 months were recorded. These dosages were then converted to their morphine-equivalent using the above formula to assess if they reached or exceeded the 60 mg/day morphine threshold (or the 25mcg/h of transdermal buprenorphine threshold) indicative of opioid tolerance. The development of tolerance was evaluated by analyzing the trends in morphine-equivalent doses over time. An increasing trend in these doses approaching or surpassing the tolerance threshold would indicate the development of tolerance. Statistical methods used included linear regression to analyze the rate of increase in morphine-equivalent doses over time, with a focus on the slope of the regression line. A steeper slope would suggest a higher rate of tolerance development.

2.9 Statistical analysis

All analyses were conducted on an intent-to-treat basis, with missing data addressed using multiple imputation techniques to maintain the robustness of our findings. The promoter center's database includes approximately 280 potentially selectable patients. Given the retrospective nature of the study, it was deemed appropriate to analyze the data from as many patients as possible.

The treatment effect is represented as follows: Prog = NRS outcome at 36 months of treatment; BAS = NRS outcome at baseline. The null hypothesis is represented by Prog = BAS, and the alternative hypothesis by Prog ≠ BAS. Statistical tests (paired samples Student's t-test, two-tailed) have been conducted at a significance level of 0.05 to demonstrate improvement in scores after the treatment period. The paired Samples *t*-test (two tailed) was employed to compare the mean NRS scores at baseline and subsequent follow-up intervals (6, 12, 24, and 36 months). Prior to applying the paired samples *t*-test, data normality was assessed using the Shapiro-Wilk test, and homogeneity of variances was checked via Levene's test. Where assumptions were not met, non-parametric alternatives were employed. The Sídák's Multiple Comparisons Test was specifically used to adjust for multiple comparisons in scenarios where pain scores were compared across more than two time points. This approach helped to maintain the overall Type I error rate, providing a more stringent criterion for statistical significance, especially relevant in the assessments from baseline to subsequent follow-ups. The Chi-square Test for contingency tables was applied to evaluate the distribution of categorical data derived from the PGIC. The Mann-Whitney *U* Test was used to compare the distributions of PGIC scores between patients with moderate and severe pain. A linear regression analysis was employed to assess the rate of increase in morphine-equivalent doses over time, which is indicative of potential tolerance development. The slope of the regression line provided a quantifiable measure of how dosage requirements changed over the study period, offering insights into whether patients were developing tolerance to buprenorphine.

3 Results

3.1 Patients demographic

The study analyzed a cohort of 246 patients, consisting of 74 males and 172 females. The mean age was 70.13 years (SD = 8.45) for individuals experiencing moderate pain and 69.45 years (SD = 9.72) for those with severe pain, with ages ranging from a minimum of 55 to a maximum of 85 years across the participant group (Table 1). For the sake of clarity and to minimize potential confounding variables, only patients diagnosed with arthritis and arthritis-related pain were included in the study.

In addition to buprenorphine, patients were often prescribed a variety of concomitant treatments to address their chronic pain and related conditions. Out of the 248 enrolled patients, 118 starting with severe pain and 34 with moderate pain were prescribed with adjuvant therapies. These included anticonvulsants, topical agents for localized pain relief, antidepressants, sedatives, and NSAIDs/corticosteroids (Figure 1).

3.2 NRS score in patients with moderate pain

Patients with moderate pain are defined those with a NRS score ranging from 5 to 6. Data are presented in Figure 2. Initially, patients exhibited a significant reduction in pain from baseline (mean NRS = 5.76) to 6 months (mean NRS = 3.932), with a mean difference of 1.828 (95% CI: 1.521–2.135). This change was statistically significant ($p < 0.00001$), as indicated by Šídák's multiple comparisons test, highlighting the immediate impact of the treatment regimen.

From 6 to 12 months, the pain scores further decreased, moving from a mean of 3.932 to 3.197, and achieving a mean difference of 0.7348 (95% CI: 0.4771–0.9926). This reduction was also significant ($p < 0.00001$), demonstrating continued effectiveness of the intervention over the medium term. The period from 12 to 24 months showed a slight, non-significant increase in pain scores (mean difference = −0.06494, 95% CI: −0.2663 to 0.1365), with a *p*-value of 0.8746. This stabilization suggests a plateau in the treatment effect or adaptation of the pain perception among patients. Between 24 and 36 months, the analysis indicated a non-significant change in pain levels with a mean difference of 1.190 (95% CI: −1.103–3.484) and a *p*-value of 0.1682. Despite this, the general trend from initial to final assessment shows a substantial overall decrease in pain levels.

Comparing NRS score between baseline and 36 months, we found a substantial reduction in pain levels over the 36-month period ($p < 0.00001$). The statistical analysis confirms that the decrease in pain scores is not only statistically significant but also clinically relevant, indicating the potential benefits of continued and consistent pain management strategies over extended periods.

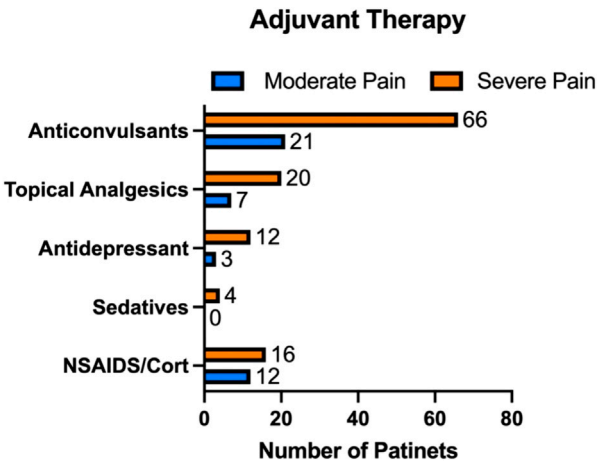

FIGURE 1
Additional therapies prescribed alongside buprenorphine for chronic pain management. Among the 248 patients enrolled, 118 with severe pain and 34 with moderate pain were prescribed adjuvant treatments, including anticonvulsants, topical agents, antidepressants, sedatives, and NSAIDs/corticosteroids.

3.3 NRS score in patients with severe pain

Patients with severe pain are those with a NRS score equal to or greater than 6. Data are presented in Figure 3. Initially, patients reported a high average NRS score of 7.503 (±1.507 SE) at baseline, reflecting severe pain. By the 6-month mark, this score significantly decreased to 4.810, with a mean difference of 2.693 (95% CI: 2.445–2.940), and a p-value <0.00001. This substantial decrease indicates a strong initial response to the treatment. Further decreases were observed at subsequent intervals. From 6 to 12 months, the NRS score reduced to 4.132, showing a mean difference of 0.6784 (95% CI: 0.5309 to 0.8259, $p < 0.00001$). Between 12 and 24 months, a smaller yet significant reduction occurred, lowering the NRS to 3.902 (mean difference = 0.2302, 95% CI: 0.09596 to 0.3644, $p = 0.00001$). The most notable continued improvement was between 24 and 36 months. The NRS score further declined to 2.956, with a mean difference of 0.9459 (95% CI: 0.6724 to 1.219, $p < 0.00001$). This persistent decrease underscores the treatment's sustained effectiveness over the long term.

By comparing NRS scores at baseline and 36 months, we observed a significant decline in pain intensity over the 36-month timeframe ($p < 0.00001$). As with patients with moderate pain, this reduction in pain scores is not just statistically noteworthy but also clinically meaningful, underscoring the potential advantages of maintaining consistent pain management strategies over prolonged durations.

3.4 Patients' satisfaction (PGIC test)

The PGIC results from this clinical retrospective study (Figure 4) reflect patient-reported outcomes, providing insights into their satisfaction with the treatment. In the study, patients with moderate pain showed significant improvements, with many reporting being "much improved" or "very much improved." Specifically, out of the total respondents, 44 reported being "much improved" and 8 "very much improved." Conversely, patients with severe pain, while also showing a significant number of positive responses, had a more varied spectrum of improvement. A substantial 113 patients reported feeling "much improved," and 31 felt "very much improved."

A contingency analysis of the PGIC data, evaluated through a chi-square test, confirmed the statistical significance of these observations with a p-value of 0.00002, indicating a strong association between the degree of pain relief and the initial severity of pain. This result underscores the effectiveness of buprenorphine in significantly improving patient outcomes across different pain intensities.

Additionally, a Mann-Whitney test comparing the distribution of PGIC scores between moderate and severe pain groups did not show a statistically significant difference (p-value = 0.6871), suggesting that buprenorphine's effectiveness in improving patient satisfaction is consistent across these groups despite the severity of pain. Overall, the data from the PGIC scale indicates high levels of patient satisfaction with buprenorphine treatment for pain.

3.5 Longitudinal responder rates in pain management over 36 months

The secondary endpoint of our study was the evaluation of responder rates at 6, 12, 24, and 36 months, where responders were classified based on significant reductions in pain intensity as quantified by the NRS score (Figures 2, 3) and positive evaluations on the of PGIC (Figure 4). The data provided detailed changes in NRS scores and corresponding PGIC outcomes for patients with moderate and severe pain, which enabled a comprehensive assessment of treatment efficacy over the specified periods.

For patients with moderate pain, substantial improvements were consistently observed across all intervals. At 6 months, the mean NRS score significantly reduced from baseline, which continued to decrease through the 12-, and 24-month assessments. The largest reduction was noted from baseline to

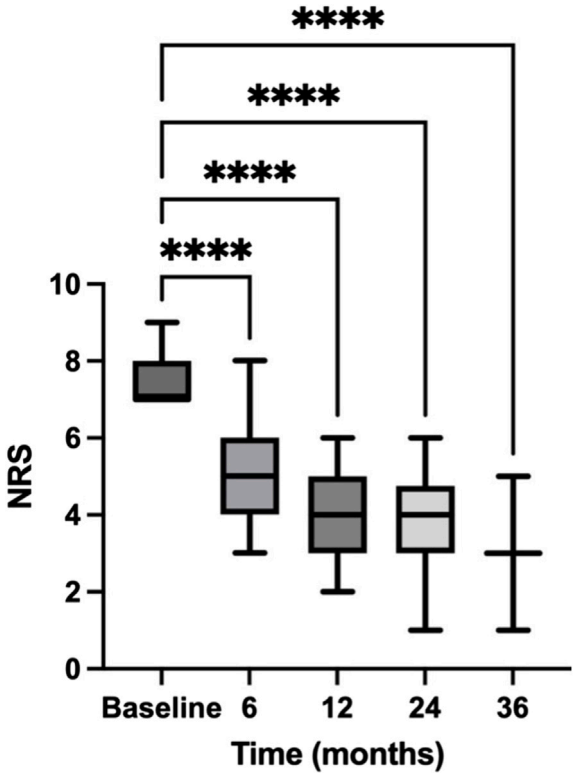

FIGURE 2
Temporal reduction in NRS scores for patients with moderate pain. This figure charts the trajectory of Numeric Rating Scale (NRS) scores for patients with moderate pain over a 36-month period. The NRS scores indicate patient-reported pain levels at baseline and subsequent intervals of 6, 12, 24, and 36 months, documenting the progression of pain relief in patients with moderate pain over the study period. Data are presented as mean ± standard error (SE). **** = $p < 0.0001$.

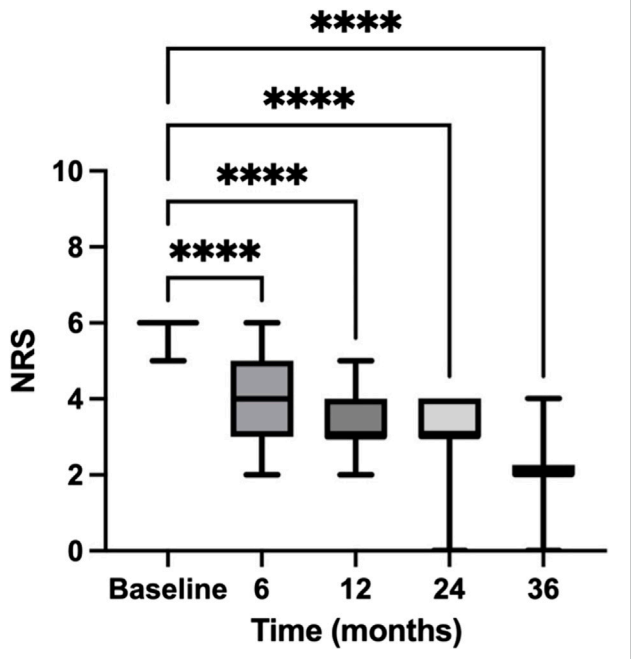

FIGURE 3
Temporal reduction in NRS scores for patients with severe pain. This figure charts the trajectory of Numeric Rating Scale (NRS) scores for patients with severe pain over a 36-month period. The NRS scores indicate patient-reported pain levels at baseline and subsequent intervals of 6, 12, 24, and 36 months, documenting the progression of pain relief in patients with severe pain over the study period. Data are presented as mean ± standard error (SE). **** = $p < 0.0001$.

6 months, with continuous albeit smaller improvements thereafter. At 36 months, despite the non-significant *p*-value, the overall trend indicated a marked improvement from the initial state. According to the PGIC, a majority of these patients reported improvements ranging from "minimally improved" to "very much improved," with the peak improvement noted at 6 and 12 months.

In severe pain patients, the responder rate was even more pronounced. Starting with a higher baseline NRS score, the decrease by the 6-month mark was significant, continuing through to 36 months. The NRS scores indicated a steady and significant decrease in pain levels, with the most notable improvement between baseline and the final assessment. PGIC results mirrored these findings, with a significant number of patients reporting "much improved" to "very much improved" statuses, particularly notable in the later stages of the study period.

Overall, the percentage of responders, classified by significant NRS reductions and positive PGIC scores, consistently increased over time in both moderate and severe pain groups. The chi-square test confirmed the statistical significance of these observations across different intervals, illustrating the effectiveness of the treatment in managing pain and improving patient perceptions over the long term. This sustained improvement over 36 months highlights the potential of consistent pain management strategies to enhance patient outcomes significantly.

3.6 Buprenorphine's efficacy in preventing opioid tolerance among moderate pain patients

To determine if tolerance developed in our study, we calculated the morphine-equivalent dose for each patient (as specified in the *Materials and Methods* section) at various time points—baseline, 6, 12, 24, and 36 months.

The dosages administered were as follows: at baseline, 5 mcg; at 6 months, 5.11 mcg; at 12 months, 9.32 mcg; at 24 months, 9.29 mcg; and at 36 months, 11.07 mcg. These dosages, when converted to morphine equivalents, resulted in: 12 mg at baseline, 12.246 mg at 6 months, 22.368 mg at 12 months, 22.296 mg at 24 months, and 26.568 mg at 36 months.

None of the calculated morphine-equivalent doses approached the FDA threshold of 60 mg/day (or the 25mcg/h of transdermal buprenorphine threshold), suggesting that none of the patients reached the opioid tolerance level under buprenorphine treatment throughout the 36-month study period.

Statistical analysis, particularly linear regression, was employed to trace the trajectory of doses over time (Figure 5). The findings indicated a gradual increase in the morphine-equivalent doses, reflected by a slope of 0.4117 mg/month. However, even at 36 months, the projected average dose remained substantially

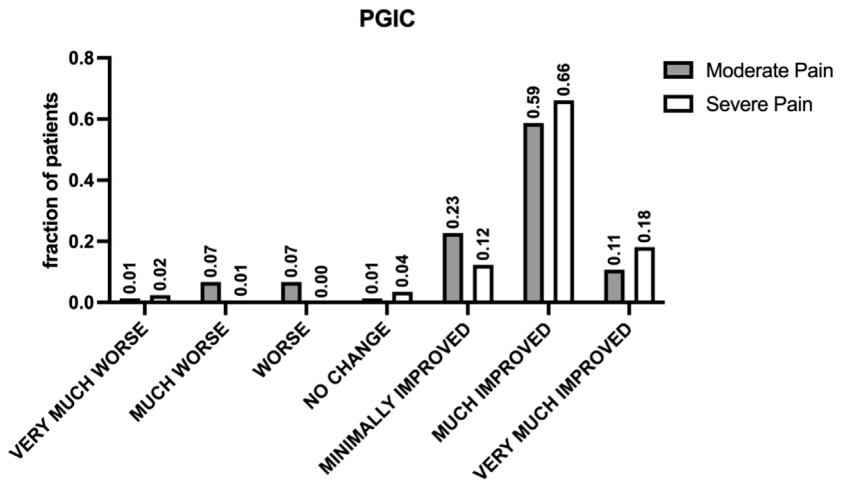

FIGURE 4
Patient-reported outcomes assessed by PGIC. The figure shows the results of the Patients' Global Impression of Change (PGIC) scale, specifically designed to assess patients' perceptions of change following treatment. This seven-point verbal scale offers options ranging from "very much improved" to "very much worsened," including "much improved," "minimally improved," "no change," "minimally worsened," and "much worsened." indicating high levels of patient satisfaction and perceived improvement in pain management across different pain intensities.

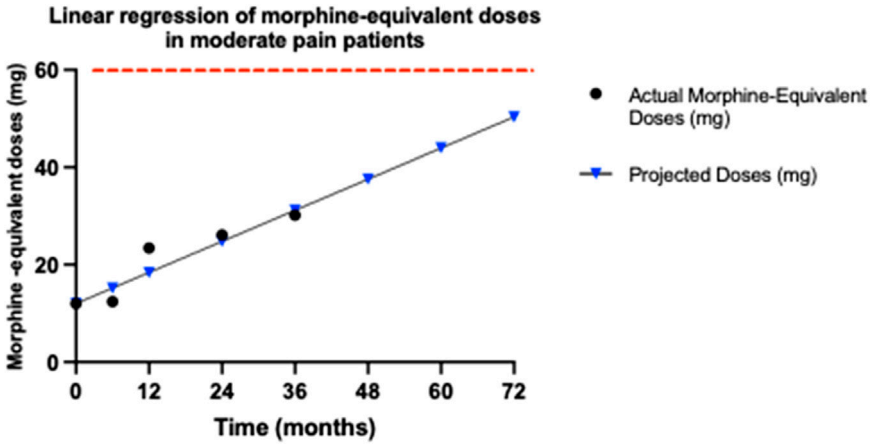

FIGURE 5
Trends in morphine-equivalent doses for moderate pain patients. This graph illustrates the morphine-equivalent doses, calculated from buprenorphine dosages over 36 months for patients with moderate pain, using an equianalgesic conversion factor, where 5 μg per hour of transdermal buprenorphine equates to 12 mg of morphine per day. The doses at each time point (baseline, 6, 12, 24, and 36 months) are plotted to assess any increase that might indicate opioid tolerance. The graph displays both the actual recorded doses until 36 months (black dots) and the projected morphine-equivalent doses (blue triangles) up to 72 months, in patients with moderate pain. The red dashed line indicates the opioid tolerance threshold of 60 mg/day, as defined by FDA. Linear regression analysis was employed to determine the slope of the dose trend, represented as mg/month, which quantifies the rate of increase in dosage requirements. The slope of 0.4117 mg/month suggests a very gradual increase in required dosage, remaining significantly below the 60 mg/day threshold associated with opioid tolerance, even at a projected period of 72 months.

below the tolerance threshold, suggesting that the moderate pain patients did not develop significant opioid tolerance within the study period. This is particularly highlighted by the minimal increase observed between 12 and 36 months. To further analyze the trend of developing tolerance in patients with moderate pain, we projected the increase in buprenorphine dosage over 72 months. Even with this extended projection, the anticipated doses at 72 months remain below the 60 mg/day of morphine (or the 25mcg/h transdermal buprenorphine) tolerance threshold.

This indicates that buprenorphine is effective in managing moderate pain without leading to the development of opioid tolerance. This outcome highlights buprenorphine's potential to provide sustained pain relief in patients with moderate pain, while minimizing the risk of tolerance, a significant advantage over other opioids where tolerance development is more common.

3.7 Buprenorphine's efficacy in preventing opioid tolerance among severe pain patients

We also assessed the potential development of opioid tolerance in the long-term treatment of severe pain with buprenorphine. We

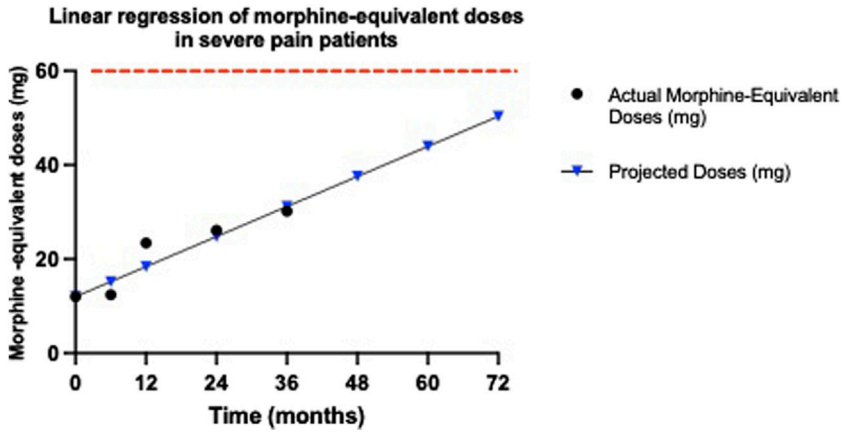

FIGURE 6
Morphine-equivalent dose trends for severe pain patients. This graph illustrates the morphine-equivalent doses derived from buprenorphine dosages for patients with severe pain, calculated using an equianalgesic conversion, where 5 μg per hour of transdermal buprenorphine corresponds to 12 mg of morphine per day. Dose trends are presented from baseline through 36 months to monitor for signs of opioid tolerance. The graph displays both the actual recorded doses until 36 months (black dots) and the projected morphine-equivalent doses (blue triangles) up to 72 months, in patients with moderate pain. The red dashed line indicates the opioid tolerance threshold of 60 mg/day, as defined by FDA. Linear regression analysis provides the slope of these trends, measured in mg/month, to evaluate the rate of increase in dosage requirements. The obtained slope of 0.5325 mg/month indicates a modest upward trend in required dosages. Despite this increase, the doses remain well below the FDA's 60 mg/day threshold for opioid tolerance.

performed the same analyses and calculations as in patients with moderate pain.

For severe pain patients, the dosages administered were as follows: at baseline, 5 mcg; at 6 months, 5.17 mcg; at 12 months, 9.71 mcg; at 24 months, 10.89 mcg; and at 36 months, 12.57 mcg. These dosages, when converted to morphine equivalents, resulted in: 12 mg at baseline, 12.408 mg at 6 months, 23.304 mg at 12 months, 26.136 mg at 24 months, and 30.168 mg at 36 months. Each of these morphine-equivalent doses remains well below the 60 mg threshold defined by the FDA for opioid tolerance. These findings indicate that none of the severe pain patients treated with buprenorphine developed opioid tolerance over the 36-month period.

Moreover, despite a consistent uptrend in doses, depicted by a regression slope of 0.5325 mg/month, the results revealed that even after 36 months, the morphine-equivalent doses remained significantly below the critical threshold of 60 mg/day of morphine (or the 25 mcg/h of transdermal buprenorphine) (Figure 6). Even among patients with severe pain, the dosage increase observed between 12 and 36 months was minimal, further underscoring underscores the sustained efficacy of buprenorphine in providing long-term pain relief without significant tolerance development. Specifically, the projected dose at 36 months approached only 31.6629 mg, well under the threshold required for the development of opioid tolerance. To further investigate the trend of developing tolerance, we projected the increase in buprenorphine dosage over a 72-month period. Even with this projection, the anticipated doses at 72 months remain below the 60 mg/day tolerance threshold.

These results underscores buprenorphine's efficacy not only in effectively managing severe pain but also in maintaining its effectiveness without escalating to tolerance. Such data affirm the suitability of buprenorphine for long-term management of severe pain, highlighting its potential as a key therapeutic in opioid stewardship initiatives aimed at reducing the risk of tolerance and dependence.

3.8 Safety

The following adverse events were reported (Table 2): constipation, reported by 1 patient (0.41% of the total cohort); skin reactions, reported by 6 patients, (2.44%); pruritus, experienced by 3 patients (1.22%); headache, reported by 3 patients (1.22%); nausea, reported by 2 patients (0.81%). No patients in this study reported issues as opioid use disorder or opioid abuse. These findings suggest that despite buprenorphine transdermal patches are generally well-tolerated, some patients may experience mild to moderate side effects, the most common of which are skin reactions.

4 Discussion

The findings from this retrospective study emphasize the sustained efficacy and reduced side effects of buprenorphine in managing moderate and severe chronic pain, reinforcing its role as a pivotal tool in the pain management spectrum. Notably, the study revealed a significant reduction in pain scores over a 36-month period, demonstrating buprenorphine's potential for long-term use, without the significant risk of side effects and with a reduced tolerance development that is often associated with other opioids.

This is consistent with the body of research that highlights buprenorphine's distinct advantages in pain management. For example, a multicenter, randomized, double-blind, placebo-controlled trial demonstrated that buprenorphine provides

TABLE 2 Adverse events reported in the study cohort. The table presents the adverse events reported during the study, including constipation, skin reactions, pruritus, headache, and nausea, along with the number of patients affected and the percentage relative to the total cohort.

Adverse event	Number of patients	Percentage of total cohort (%)
Constipation	1	0.41
Skin reactions	6	2.44
Pruritus	3	1.22
Headache	3	1.22
Nausea	2	0.81

effective pain relief with stable dosing over time in patients with chronic non-cancer pain (Sittl et al., 2003). This stability in dosing is particularly important in the context of chronic pain management, as it reduces the risks associated with dose escalation, such as increased side effects and the potential for tolerance development. Davis and colleagues further highlight buprenorphine's clinical benefits, noting its stable pharmacokinetic profile which is less influenced by patient-specific factors such as renal function (Davis et al., 2018). This aspect is particularly advantageous in elderly chronic pain populations, where such comorbidities are common. Additionally, buprenorphine's unique receptor binding properties may be able to provide an analgesic effect without the high risk of abuse and tolerance seen with other opioids (Davis et al., 2018) Similarly, Infantino et al. elaborate on buprenorphine's distinct pharmacological actions, such as its biased agonism at mu-opioid receptors and high affinity for opioid-like receptor 1, which contribute to its effectiveness in neuropathic pain, a condition often resistant to traditional opioids (Infantino et al., 2021). This is in line with the low incidence of side effects, such as constipation and skin reactions, noted in our study, supporting buprenorphine's favorable safety profile, which is crucial for enhancing patient compliance and quality of life. The concept of biased or even protean agonism at opioid receptors may explain how certain receptor ligands might preferentially activate beneficial signaling pathways while avoiding those leading to adverse effects (Neto et al., 2020; Infantino et al., 2021). Particularly, the low incidence of gastrointestinal symptoms such as constipation and nausea is noteworthy, as these are often more prevalent with traditional opioid therapies. A possible explanation comes from a study by Neto et al. (2020), which detailed the genetic and pharmacological characteristics of opioid receptor interactions, According to these authors, the biased agonism of buprenorphine preferentially activates G-protein pathways over beta-arrestin pathways. This selective activation is crucial because beta-arrestin pathway activation is often linked to adverse gastrointestinal effects, including opioid-induced constipation. By minimizing beta-arrestin pathway activation, buprenorphine significantly reduces the likelihood of these side effects, such as nausea and costipation. Moreover, buprenorphine's antagonistic action at KOR may also play a role in mitigating gastrointestinal side effects. KOR activation has been associated with dysphoria and diuresis, but its antagonism by buprenorphine could contribute to a more favorable side effect profile. Moreover, in this study, no patients reported issues as opioid use disorder and abuse, further highlighting buprenorphine's favorable profile. Overall, our data indicate that the safety profile of buprenorphine transdermal patches appears favorable, with the majority of adverse events being minor and manageable.

Further examination of patient satisfaction, as measured by the PGIC, shows that most patients reported significant improvements in their pain and overall wellbeing. This aligns with previous findings, which highlight the patient-centered benefits of buprenorphine, particularly its ability to provide stable pain control with minimal side effects (Pergolizzi et al., 2010; Ehrlich and Darcq, 2018; Webster et al., 2020).

A pivotal finding from our study indicates that buprenorphine does not lead to significant tolerance development, both in patients with moderate and severe pain. According to FDA guidelines (as defined in the fentanyl official labeling), opioid tolerance is defined as needing 60 mg/day of morphine or an equivalent dose of another opioid for a week or more. (Dowell et al., 2022; "Rx only -Fentanyl Full Prescribing Information") In our study, even after 36 months, the morphine-equivalent doses of buprenorphine remained well below this threshold, with only a minor increase in dosage observed between 12 and 36 months. This stability in dosing highlights the sustained efficacy of buprenorphine, minimizing the risk of tolerance development. This outcome contrasts sharply with typical results seen in patients treated with other long-term opioids, where tolerance development often necessitates progressively larger doses to achieve the same pain relief effect (Volkow and Blanco, 2021). Our findings suggest that buprenorphine maintains its efficacy over long periods without the need for significant dose escalations. The gentle upward trajectory of the dosage increase, even at 36 months, suggests that the increases were minimal and remained well below the threshold that would indicate significant tolerance. This slow rate of increase, especially between 12 and 36 months, further underscores the drug's resilience against the typical rapid tolerance development seen with other opioids. Furthermore, when extrapolated to a 72-month period, the dosages delivered via buprenorphine transdermal patches remain significantly below the 60 mg/day morphine-equivalent threshold, both in patients with moderate and severe pain, which would suggest the development of opioid tolerance.

From our data it appears that the choice of transdermal patches for opioid delivery offers a winning strategy in pain management, due to several key pharmacological and patient compliance factors. Transdermal buprenorphine provides a controlled, continuous delivery of the medication over a 7-day period, ensuring stable plasma drug concentrations and minimizing fluctuations that can lead to breakthrough pain or side effects associated with peak levels (Plosker, 2011). This consistent delivery helps in managing pain effectively without the peaks and troughs associated with oral or sublingual forms, which can enhance patient compliance and overall pain management. The pharmacokinetics of transdermal buprenorphine minimize drug-drug interactions and reduce the incidence of central nervous system side effects such as cognitive impairment and sedation, which are often seen with other opioids. This is especially beneficial in elderly patients or those with renal and hepatic impairments, where managing side effects and interactions becomes crucial (Owsiany et al., 2019; Zhuo et al., 2021).

Additionally, there is a ceiling effect for respiratory depression, enhancing the safety profile of buprenorphine, especially in a population at risk of opioid overdosage (Plosker, 2011; Owsiany et al., 2019; Neto et al., 2020; Infantino et al., 2021).

Our retrospective study offers valuable real-world insights on buprenorphine's long-term efficacy in managing chronic pain in both moderate and severe pain patients, but come with inherent limitations. Selection bias can occur since data are limited to existing medical records, potentially overlooking pertinent information. Issues like recall bias from inconsistent records, uncontrolled confounding variables, and variability in data quality can affect the study's reliability. Additionally, the lack of randomization means our data can suggest associations but not establish causality. Despite these limitations, our study benefits from a large sample size and longitudinal data spanning 3 years, which enhances the reliability of the findings and their applicability in clinical settings. The specificity of data on morphine-equivalent doses and the comprehensive measures of both efficacy and safety provide a comprehensive view of buprenorphine's role in pain management. These strengths underscore the usefulness of buprenorphine in clinical practice while highlighting the necessity of cautious interpretation of results due to the study's retrospective nature. For these reasons, while our retrospective design inherently limits the ability to draw causal inferences, the use of advanced statistical controls and long-term follow-up contribute to a robust dataset from which meaningful conclusions can be drawn about buprenorphine's efficacy and safety.

In conclusion, our findings support recent guidelines by health authorities advocating for the expanded use of buprenorphine in chronic pain management. This study provides empirical support for such policies, emphasizing buprenorphine's lower risk profile compared to traditional opioids. These findings advocate for broader clinical use and potential policy shifts to favor buprenorphine as a frontline treatment in chronic pain management strategies, thereby improving patient outcomes and addressing critical aspects of the worldwide opioid crisis.

Data availability statement

The original contributions presented in the study are included in the article/supplementary material, further inquiries can be directed to the corresponding author.

Ethics statement

The studies involving humans were approved by the Campania SUD Ethics Committee, approval number AOC/0011976/2024. The studies were conducted in accordance with the local legislation and institutional requirements. Written informed consent for participation was obtained from the participants or the participants' legal guardians/next of kin in accordance with the national legislation and institutional requirements.

Author contributions

AP: Conceptualization, Methodology, Project administration, Resources, Supervision, Validation, Writing–original draft, Writing–review and editing. AS: Investigation, Writing–original draft, Writing–review and editing. MD: Investigation, Writing–original draft, Writing–review and editing. VD: Data curation, Formal Analysis, Methodology, Writing–original draft, Writing–review and editing. PB: Investigation, Writing–original draft, Writing–review and editing. PM: Investigation, Writing–original draft, Writing–review and editing. ES: Investigation, Writing–original draft, Writing–review and editing. DT: Investigation, Writing–original draft, Writing–review and editing. LL: Conceptualization, Data curation, Methodology, Supervision, Writing–original draft, Writing–review and editing. SM: Data curation, Writing–original draft, Writing–review and editing.

Funding

The author(s) declare that no financial support was received for the research, authorship, and/or publication of this article.

Conflict of interest

The authors declare that the research was conducted in the absence of any commercial or financial relationships that could be construed as a potential conflict of interest.

The author(s) declared that they were an editorial board member of Frontiers, at the time of submission. This had no impact on the peer review process and the final decision.

Publisher's note

References

Alkilani, A. Z., McCrudden, M. T. C., and Donnelly, R. F. (2015). Transdermal drug delivery: innovative pharmaceutical developments based on disruption of the barrier properties of the stratum corneum. *Pharmaceutics* 7 (4), 438–470. doi:10.3390/PHARMACEUTICS7040438

Alorfi, N. M. (2023). Pharmacological methods of pain management: narrative review of medication used. *Int. J. General Med.* 16, 3247–3256. doi:10.2147/IJGM.S419239

Alschuler, K. N., Jensen, M. P., and Ehde, D. M. (2012). Defining mild, moderate, and severe pain in persons with multiple sclerosis. *Pain Med. (United States)* 13 (10), 1358–1365. doi:10.1111/j.1526-4637.2012.01471.x

Aston-Jones, G., and Harris, G. C. (2004). Brain substrates for increased drug seeking during protracted withdrawal. *Neuropharmacology* 47 (Suppl. 1), 167–179. doi:10.1016/J.NEUROPHARM.2004.06.020

Breivik, H. (2013). Buprenorphine - the ideal drug for most clinical indications for an opioid? *Scand. J. Pain* 4 (3), 146–147. doi:10.1016/J.SJPAIN.2013.05.005

Cancer, W., Care Network, P., and Health, W. (2016). *Opioid conversion guide How to use the conversion guide*.

Christie, M. J. (2008). Cellular neuroadaptations to chronic opioids: tolerance, withdrawal and addiction. *Br. J. Pharmacol.* 154 (2), 384–396. doi:10.1038/BJP.2008.100

Cohen, S. P., Vase, L., and Hooten, W. M. (2021). Chronic pain: an update on burden, best practices, and new advances. *Lancet* 397 (10289), 2082–2097. doi:10.1016/S0140-6736(21)00393-7

Davis, M. P., Pasternak, G., and Behm, B. (2018). Treating chronic pain: an overview of clinical studies centered on the buprenorphine option. *Drugs* 78 (12), 1211–1228. doi:10.1007/S40265-018-0953-Z

Dowell, D., Ragan, K. R., Jones, C. M., Baldwin, G. T., and Chou, R. (2022). CDC clinical practice guideline for prescribing opioids for pain — United States, 2022. *MMWR Recomm. Rep.* 71 (RR-3), 1–95. doi:10.15585/mmwr.rr7103a1

Ehrlich, A. T., and Darcq, E. (2018). Recommending buprenorphine for pain management. *Pain Manag.* 9 (1), 13–16. doi:10.2217/PMT-2018-0069

Eremenco, S., Chen, W. H., Blum, S. I., Bush, E. N., Bushnell, D. M., DeBusk, K., et al. (2022). Comparing patient global impression of severity and patient global impression of change to evaluate test–retest reliability of depression, non-small cell lung cancer, and asthma measures. *Qual. Life Res.* 31 (12), 3501–3512. doi:10.1007/S11136-022-03180-5

Evans, H. C., and Easthope, S. E. (2003). Transdermal buprenorphine. *Drugs* 63 (19), 1999–2012. doi:10.2165/00003495-200363190-00003

Gudin, J., and Fudin, J. (2020). A narrative pharmacological review of buprenorphine: a unique opioid for the treatment of chronic pain. *Pain Ther.* 9 (1), 41–54. doi:10.1007/S40122-019-00143-6

Harrison, J., and Mozzicato, P. (2009). MedDRA®: the tale of a terminology: side effects of drugs essay. *Side Eff. Drugs Annu.* 31 (C), xii. doi:10.1016/S0378-6080(09)03160-2

Hawker, G. A., Mian, S., Kendzerska, T., and French, M. (2011). Measures of adult pain: visual analog scale for pain (VAS pain), numeric rating scale for pain (NRS pain), McGill pain questionnaire (MPQ), short-form McGill pain questionnaire (SF-MPQ), chronic pain grade scale (CPGS), short form-36 bodily pain scale (SF-36 BPS), and measure of intermittent and constant osteoarthritis pain (ICOAP). *Arthritis Care Res.* 63 (Suppl. 11), S240–S252. doi:10.1002/ACR.20543

Holtman, J. R., and Jellish, W. S. (2012). Opioid-induced hyperalgesia and burn pain. *J. Burn Care Res.* 33 (6), 692–701. doi:10.1097/BCR.0b013e31825adcb0

Infantino, R., Mattia, C., Locarini, P., Pastore, A. L., Maione, S., and Luongo, L. (2021). Buprenorphine: far beyond the "ceiling". *Biomolecules* 11 (6), 816. doi:10.3390/BIOM11060816

Jalali, M. S., Botticelli, M., Hwang, R. C., Koh, H. K., and McHugh, R. K. (2020). The opioid crisis: a contextual, social-ecological framework. *Health Res. Policy Syst.* 18 (1), 87–89. doi:10.1186/s12961-020-00596-8

Kumar, R., Viswanath, O., and Saadabadi, A. (2023). Buprenorphine. *StatPearls*. Available at: https://www.ncbi.nlm.nih.gov/books/NBK459126/(Accessed May 13, 2024).

McCormack, H. M., Horne, D.J. de L., and Sheather, S. (1988). Clinical applications of visual analogue scales: a critical review. *Psychol. Med.* 18 (4), 1007–1019. doi:10.1017/S0033291700009934

Mercadante, S., Arcuri, E., and Santoni, A. (2019). Opioid-induced tolerance and hyperalgesia. *CNS drugs* 33 (10), 943–955. doi:10.1007/S40263-019-00660-0

Mills, S. E. E., Nicolson, K. P., and Smith, B. H. (2019). Chronic pain: a review of its epidemiology and associated factors in population-based studies. *BJA Br. J. Anaesth.* 123 (2), e273–e283. doi:10.1016/J.BJA.2019.03.023

Nahin, R. L., Feinberg, T., Kapos, F. P., and Terman, G. W. (2023). Estimated rates of incident and persistent chronic pain among US adults, 2019-2020. *JAMA Netw. open* 6 (5), e2313563. doi:10.1001/JAMANETWORKOPEN.2023.13563

Neto, J. A., Costanzini, A., De Giorgio, R., Lambert, D. G., Ruzza, C., and Calò, G. (2020). Biased versus partial agonism in the search for safer opioid analgesics. *Molecules* 25 (17), 3870. doi:10.3390/MOLECULES25173870

Opioid conversion ratios Guidance document 2 Safer Care Victoria Opioid conversion guidance (2021). Available at: www.safercare.vic.gov.au (Accessed May 13, 2024).

Owsiany, M. T., Hawley, C. E., Triantafylidis, L. K., and Paik, J. M. (2019). Opioid management in older adults with chronic kidney disease: a review. *Am. J. Med.* 132 (12), 1386–1393. doi:10.1016/J.AMJMED.2019.06.014

Pergolizzi, J., Aloisi, A. M., Dahan, A., Filitz, J., Langford, R., Likar, R., et al. (2010). Current knowledge of buprenorphine and its unique pharmacological profile. *Pain Pract. official J. World Inst. Pain* 10 (5), 428–450. doi:10.1111/J.1533-2500.2010.00378.X

Pergolizzi, J., Böger, R. H., Budd, K., Dahan, A., Erdine, S., Hans, G., et al. (2008). Opioids and the management of chronic severe pain in the elderly: consensus statement of an international expert panel with focus on the six clinically most often used world health organization step III opioids (Buprenorphine, Fentanyl, Hydromorphone, Methadone, Morphine, Oxycodone). *Pain Pract.* 8 (4), 287–313. doi:10.1111/J.1533-2500.2008.00204.X

Plosker, G. L. (2011). Buprenorphine 5, 10 and 20 μg/h transdermal patch: a review of its use in the management of chronic non-malignant pain. *Drugs* 71 (18), 2491–2509. doi:10.2165/11208250-000000000-00000

Poon, A., Ing, J., and Hsu, E. (2021). Opioid-related side effects and management. *Cancer Treat. Res.* 182, 97–105. doi:10.1007/978-3-030-81526-4_7

Rx only (2024). Fentanyl full prescribing information. Available at: https://www.accessdata.fda.gov/drugsatfda_docs/label/2008/019813s033lbl.pdf (Accessed May 13, 2024).

Sittl, R., Griessinger, N., and Likar, R. (2003). Analgesic efficacy and tolerability of transdermal buprenorphine in patients with inadequately controlled chronic pain related to cancer and other disorders: a multicenter, randomized, double-blind, placebo-controlled trial. *Clin. Ther.* 25, 150–168. doi:10.1016/s0149-2918(03)90019-1

Sizar, O., Genova, R., and Gupta, M. (2023). Opioid-induced constipation. *StatPearls*. Available at: https://www.ncbi.nlm.nih.gov/books/NBK493184/(Accessed May 13, 2024).

Volkow, N. D., and Blanco, C. (2021). The changing opioid crisis: development, challenges and opportunities. *Mol. psychiatry* 26 (1), 218–233. doi:10.1038/S41380-020-0661-4

Webster, L., Gudin, J., Raffa, R. B., Kuchera, J., Rauck, R., Fudin, J., et al. (2020). Understanding buprenorphine for use in chronic pain: expert opinion. *Off. J. Am. Acad. Pain Med.* 21 (4), 714–723. doi:10.1093/PM/PNZ356

Zhang, W., Ramamoorthy, Y., Tyndale, R. F., and Sellers, E. M. (2003). Interaction of buprenorphine and its metabolite norbuprenorphine with cytochromes p450 *in vitro*. *Drug metab. Dispos. Biol. fate Chem.* 31 (6), 768–772. doi:10.1124/DMD.31.6.768

Zhuo, M., Triantafylidis, L. K., Li, J., and Paik, J. M. (2021). Opioid use in the nondialysis chronic kidney disease population. *Semin. Nephrol.* 41 (1), 33–41. doi:10.1016/J.SEMNEPHROL.2021.02.004

frontiers | Frontiers in Pharmacology

TYPE Correction
PUBLISHED 30 September 2024
DOI 10.3389/fphar.2024.1491886

OPEN ACCESS

EDITED AND REVIEWED BY
Álvaro Llorente-Berzal,
Autonomous University of Madrid, Spain

*CORRESPONDENCE
Alfonso Papa,
alfonsopapa@libero.it

†These authors have contributed equally to this work and share last authorship

RECEIVED 05 September 2024
ACCEPTED 10 September 2024
PUBLISHED 30 September 2024

CITATION
Papa A, Salzano AM, Di Dato MT, Desiderio V, Buonavolontà P, Mango P, Saracco E, Tammaro D, Luongo L and Maione S (2024) Corrigendum: Long-term efficacy and reduced side-effects of buprenorphine in patients with moderate and severe chronic pain. *Front. Pharmacol.* 15:1491886. doi: 10.3389/fphar.2024.1491886

Corrigendum: Long-term efficacy and reduced side-effects of buprenorphine in patients with moderate and severe chronic pain

Alfonso Papa[1]*, Anna Maria Salzano[1], Maria Teresa Di Dato[1], Vincenzo Desiderio[2], Pietro Buonavolontà[1], Pietro Mango[1], Elisabetta Saracco[1], Dario Tammaro[1], Livio Luongo[3†] and Sabatino Maione[3†]

[1]Department of Pain Management—AO "Ospedale dei Colli"–Monaldi Hospital, Napoli, Italy, [2]Department of Experimental Medicine, University of Campania "Luigi Vanvitelli", Naples, Italy, [3]Department of Experimental Medicine, Division of Pharmacology, University of Campania "Luigi Vanvitelli", Naples, Italy

KEYWORDS

chronic pain, opioids, tolerance, ransdermal patches, pain relief, opioid crisis

A Corrigendum on
Long-term efficacy and reduced side-effects of buprenorphine in patients with moderate and severe chronic pain

by Papa A, Salzano AM, Di Dato MT, Desiderio V, Buonavolontà P, Mango P, Saracco E, Tammaro D, Luongo L and Maione S (2024). Front. Pharmacol. 15:1454601. doi: 10.3389/fphar.2024.1454601

In the published article, there was an error in Figures 1, 4, 5 as published. The figures were mismatched with their respective images.

Figure 1 should display the image originally intended for Figure 5; the caption remains correct. The corrected Figure 1 and its caption appear below.

Figure 4 should display the image originally intended for Figure 1; the caption remains correct. The corrected Figure 4 and its caption appear below.

Figure 5 should display the image originally intended for Figure 4; the caption remains correct. The corrected Figure 5 and its caption appear below.

The authors apologize for this error and state that this does not change the scientific conclusions of the article in any way. The original article has been updated.

Publisher's note

All claims expressed in this article are solely those of the authors and do not necessarily represent those of their affiliated organizations, or those of the publisher, the editors and the reviewers. Any product that may be evaluated in this article, or claim that may be made by its manufacturer, is not guaranteed or endorsed by the publisher.

10.3389/fphar.2024.1491886

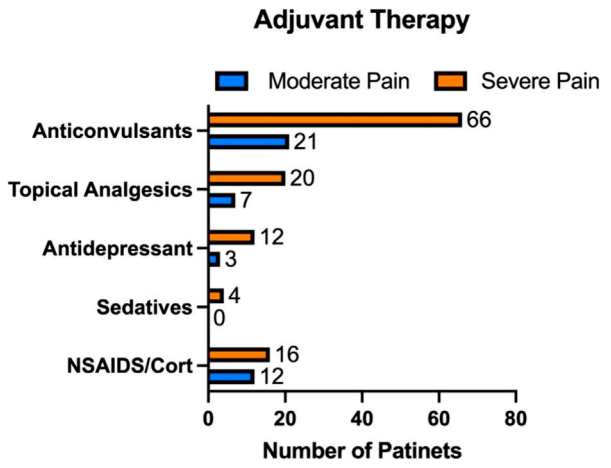

FIGURE 1
Additional therapies prescribed alongside buprenorphine for chronic pain management. Among the 248 patients enrolled, 118 with severe pain and 34 with moderate pain were prescribed adjuvant treatments, including anticonvulsants, topical agents, antidepressants, sedatives, and NSAIDs/corticosteroids.

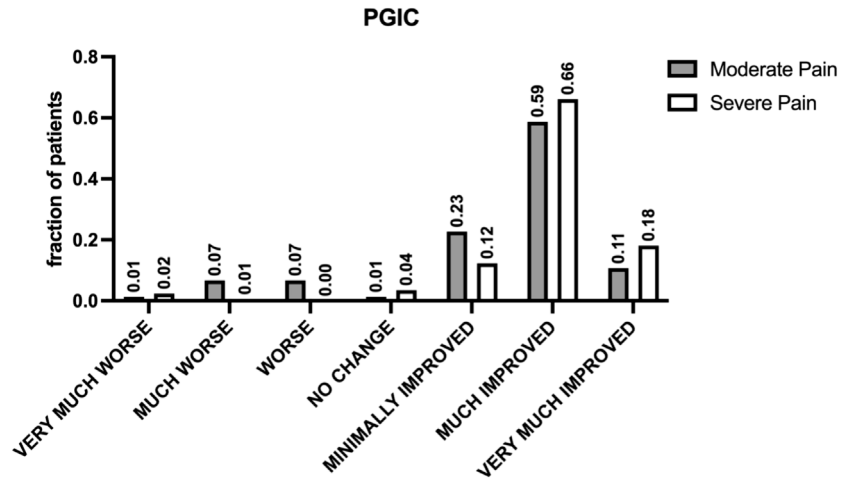

FIGURE 4
Patient-reported outcomes assessed by PGIC. The figure shows the results of the Patients' Global Impression of Change (PGIC) scale, specifically designed to assess patients' perceptions of change following treatment. This seven-point verbal scale offers options ranging from "very much improved" to "very much worsened," including "much improved," "minimally improved," "no change," "minimally worsened," and "much worsened." indicating high levels of patient satisfaction and perceived improvement in pain management across different pain intensities.

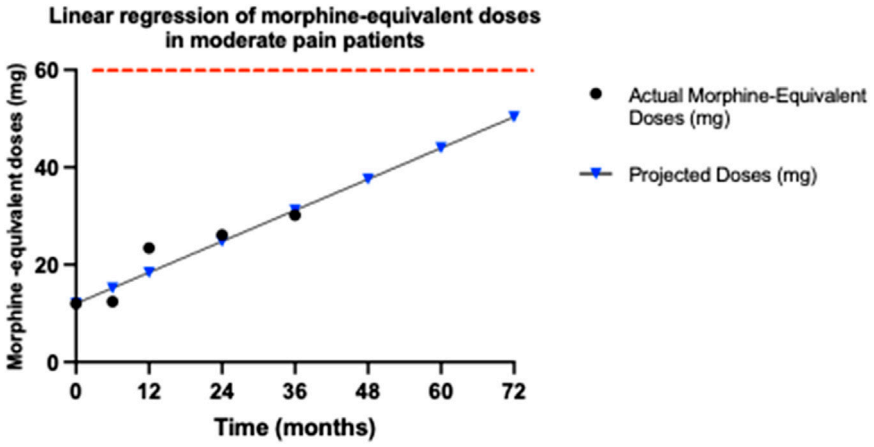

FIGURE 5
Trends in morphine-equivalent doses for moderate pain patients. This graph illustrates the morphine-equivalent doses, calculated from buprenorphine dosages over 36 months for patients with moderate pain, using an equianalgesic conversion factor, where 5 μg per hour of transdermal buprenorphine equates to 12 mg of morphine per day. The doses at each time point (baseline, 6, 12, 24, and 36 months) are plotted to assess any increase that might indicate opioid tolerance. The graph displays both the actual recorded doses until 36 months (black dots) and the projected morphine-equivalent doses (blue triangles) up to 72 months, in patients with moderate pain. The red dashed line indicates the opioid tolerance threshold of 60 mg/day, as defined by FDA. Linear regression analysis was employed to determine the slope of the dose trend, represented as mg/month, which quantifies the rate of increase in dosage requirements. The slope of 0.4117 mg/month suggests a very gradual increase in required dosage, remaining significantly below the 60 mg/day threshold associated with opioid tolerance, even at a projected period of 72 months.

frontiers | Frontiers in Pharmacology

TYPE Original Research
PUBLISHED 12 August 2024
DOI 10.3389/fphar.2024.1396790

OPEN ACCESS

EDITED BY
Álvaro Llorente-Berzal,
Autonomous University of Madrid, Spain

REVIEWED BY
Rosmara Infantino,
Centre for Pain Research, University of Galway, Ireland
Carmela Belardo,
Second University of Naples, Italy

*CORRESPONDENCE
Juan Li,
juanli2003@njglyy.com
Chunhe Wang,
wangc@dartsbio.com
Runbin Sun,
runbinsun@gmail.com

RECEIVED 06 March 2024
ACCEPTED 29 July 2024
PUBLISHED 12 August 2024

CITATION
Jin D, Yang H, Chen Z, Hong Y, Ma H, Xu Z, Cao B, Fei F, Zhang Y, Wu W, Tang L, Sun R, Wang C and Li J (2024) Effect of the novel anti-NGF monoclonal antibody DS002 on the metabolomics of pain mediators, cartilage and bone.
Front. Pharmacol. 15:1396790.
doi: 10.3389/fphar.2024.1396790

Effect of the novel anti-NGF monoclonal antibody DS002 on the metabolomics of pain mediators, cartilage and bone

Dandan Jin[1], Haoyi Yang[1], Zhiyou Chen[1], Yuxin Hong[1], Hehua Ma[2], Zhenzhen Xu[2], Bei Cao[2], Fei Fei[2], Yuwen Zhang[3], Weitao Wu[4], Lei Tang[4], Runbin Sun[1,2,3]*, Chunhe Wang[4]* and Juan Li[1,2,3]*

[1]Department of Phase I Clinical Trials Unit, Nanjing Drum Tower Hospital Affiliated to Nanjing University of Chinese Medicine, Nanjing, China, [2]Department of Phase I Clinical Trials Unit, Nanjing Drum Tower Hospital, Affiliated Hospital of Medical School, Nanjing University, Nanjing, China, [3]Department of Phase I Clinical Trials Unit, China Pharmaceutical University Nanjing Drum Tower Hospital, Nanjing, China, [4]Dartsbio Pharmaceuticals Ltd., Zhongshan, Guangdong, China

The anti-nerve growth factor antibody class of drugs interrupts signaling by blocking NGF binding to TrkA receptors for the treatment of pain; however, this target class of drugs has been associated with serious adverse effects in the joints during clinical trials. DS002 is a novel anti-nerve growth factor antibody drug independently developed by Guangdong Dashi Pharmaceuticals. The main purpose of this study is to explore the correlation between DS002 and pain as well as cartilage and bone metabolism with the help of metabolomics technology and the principle of enzyme-linked reaction, and to examine whether DS002 will produce serious adverse effects in joints caused by its same target class of drugs, in order to provide more scientific basis for the safety and efficacy of DS002. Our results showed that DS002 mainly affected the metabolism of aromatic amino acids and other metabolites, of which six metabolites, l -phenylalanine, 5-hydroxytryptophan, 5-hydroxytryptamine hydrochloride, 3-indolepropionic acid, kynuric acid, and kynurenine, were significantly altered, which may be related to the effectiveness of DS002 in treating pain. In addition, there were no significant changes in biological indicators related to cartilage and bone metabolism *in vivo*, suggesting that DS002 would not have a significant effect on cartilage and bone metabolism, so we hypothesize that DS002 may not produce the serious adverse effects in joints caused by its fellow target analogs. Therefore, the Anti-NGF analgesic drug DS002 has the potential to become a promising drug in the field of analgesia, providing pain patients with an efficient treatment option without adverse effects.

KEYWORDS

metabolomics, pain, aromatic amino acids, biomarkers, anti-ngf drugs

1 Introduction

Chronic pain is an unsolved global healthcare problem that remains a major cause of suffering, disability, and substantial economic burden worldwide (Cohen et al., 2021). It is estimated that the rate of chronic pain in humans is as high as 20% each year (Dahlhamer et al., 2018). The International Association for the Study of Pain (IASP) defines pain as

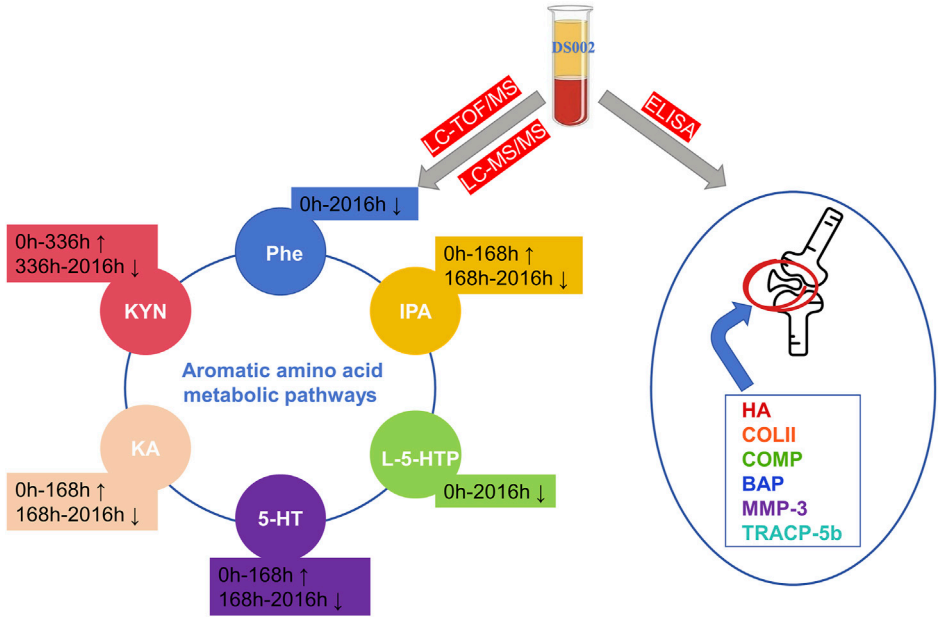

GRAPHICAL ABSTRACT

unpleasant sensory and emotional experiences related to or similar to actual or potential tissue damage (Raja et al., 20220). Pain can be categorized as acute or chronic based on the duration and nature of its occurrence. Modern medical research has proven that acute pain is a symptom that goes away as the disease gets better; However, chronic pain usually lasts for more than 1 month or even 3 months, and this pain is no longer a symptom, but should be treated as a disease. The occurrence of pain is caused by many factors. In addition to the impact of injury or disease, there are physical perception, psychological and emotional changes, genetic factors, etc. Due to the complexity of pain, the results of the current treatment of chronic pain are unsatisfactory (The, 2021). Currently available analgesics do not meet treatment goals. For example, opioids and non-steroidal anti-inflammatory drugs (nsaids), two commonly used analgesics in clinical practice, have different side effects in chronic pain. The main adverse reactions induced by opioids include analgesic tolerance, addiction and physical tolerance, nausea and vomiting, constipation, and respiratory depression (Paul et al., 2021). The long-term use of NSAIDs can produce gastric bleeding and cardiovascular-related adverse reactions (Trelle et al., 2011). The different side effects greatly limit the widespread use of these two classes of drugs. Therefore, there is an unmet need for effective analgesic drugs that are safer and more tolerable than currently available treatments.

Nerve growth factor (NGF) was first discovered by Rita Levi-Montalcini (Levi-Montalcini, 1952). NGF in the body is both an essential protein and an important pain-producing substance (Hirose et al., 2016). It has been found that NGF binding can be two types of receptors (Landreth and Shooter, 1980), the protomyosin receptor kinase a (TrkA), which has a high affinity for NGF, and the p75 neurotrophic factor receptor (p75NTR), which has a low affinity for NGF. NGF is secreted by inflammatory cells in damaged tissues and by Schwann cells in damaged nerves (Thacker et al., 2007; Basbaum et al., 2009). When tissue injury occurs, NGFs are abundantly expressed at the site of injury and bind to TrkA receptors on the cell membranes of sensory nerve endings, which in turn transmits pain signals, ultimately leading to the onset of pain. Therefore, in cases where an inflammatory response persists with damaging pain, such as low back pain, back pain, autoimmune diseases - rheumatism, etc., or in cases of neuropathic pain, NGF induces sensitization of the peripheral and central systems, which can lead to nociceptive hypersensitivity and anisocoria, and analgesics that block NGF/TrKA signaling can be very effective in these pathologies (Hirose et al., 2016). In recent years, researchers have also identified it as one of the key targets for drugs to treat chronic pain. Currently, the main NGF/TrkA inhibitor drugs are anti-NGF antibodies and TrkA activity inhibitors (Hirose et al., 2016). This study will focus on a new anti-NGF antibody, which have shown promising results in clinical studies and are expected to provide new clinical treatment strategies for chronic pain in the future.

Metabolomics is the quantitative and qualitative analysis of all small molecules in a biological sample at a certain time and under certain conditions. It is a accredited methodology with more than 20 years of practical experience. At present, metabolomics has been extended to many disciplines (Jeyarajah et al., 2006; Wishart, 2016; González-Domínguez et al., 2020). Metabolomics technologies have improved the mechanistic understanding, diagnosis, and treatment of various diseases by utilizing biological samples from humans and animal and cellular models of human diseases. Although the relationship between metabolomics and pain may be complex because the occurrence of pain is accompanied by multiple physiological symptoms, these issues have the potential to manifest through the level of metabolomics (Miettinen et al., 2021), which will facilitate the development of mechanism-based pain diagnostics to support mechanism-based therapeutic approaches. Metabolomics research has the potential to advance these goals because it can discover pain biomarkers to improve pain

treatment options, facilitate drug development progress, and ultimately reduce the burden of chronic pain.

DS002 is an anti-NGF monoclonal antibody developed by Tashi Pharmaceutical (Guangdong) Co. Ltd. It interrupts the signal transmission by blocking the binding of NGF to the TrkA receptor, making it unable to stimulate the corresponding sensory neurons, and finally achieving an analgesic effect. Currently, a phase I clinical trial of DS002 has been completed and published in our laboratory (Ma et al., 2022). This study aims to explore the effects of DS002 on pain, cartilage and bone metabolism-related markers, and the changes in metabolic profile *in vivo*, to provide more evaluation basis for the drug development of DS002.

2 Methods

2.1 Sample collection

The study samples were obtained from the Phase I clinical Trial Center of Nanjing Drum Tower Hospital. Blood samples from 48 healthy subjects were enrolled in this study and divided into seven different DS002 dose groups (0.5, 1, 2, 4, 7, 12, 20 mg), and 432 blood samples were collected. The samples used in this study were PK blood samples at 0 h and D4 (72 h), D8 (168 h), D15 (336 h), D29 (672 h), D43 (1008 h), D57 (1344 h), D85 (2016 h), D113 (2688 h) after administration. The collected blood samples were used to determine the changes in serum metabonomics before and at different time points after administration, and the changes of cartilage and bone metabolism-related indexes before and at different time points after administration were determined by enzyme-linked immunosorbent assay (ELISA). This study (CTR20210155) was approved by the Ethics Committee of Drum Tower Hospital, the Affiliated Hospital of Nanjing University Medical School.

2.2 Subjects

The project included healthy male and female subjects aged 18–45 years, with female subjects not pregnant or breastfeeding. Enrolled subjects have a body mass index (BMI) of 19.0–26.0 kg/m^2 and weigh ≥50 kg for males and ≥45 kg for females. Subjects agree to have no fertility or sperm/egg donation plans and to voluntarily use a medically recognised and effective form of contraception for the duration of the trial up to 6 months after dosing. Subjects are sufficiently aware of the content, objectives and characteristics of the study to be able to complete the study as planned and are willing to serve as subjects and are able to sign an informed consent form.

Subjects were excluded if they met any one of the following exclusion criteria: previous history of allergy or hypersensitivity; subjects with a history of osteoarthritic disease, a history of peripheral or autonomic neuropathy, a history of sensory abnormalities and hypoesthesia, a disease or history of unexplained spontaneous bleeding and/or post-traumatic hemorrhage with more than one bleed, a history of thyroid dysfunction or thyroid hormone abnormality, a history of a malignant neoplasm or a history of malignant neoplasms, an individual with an inherited immunodeficiency, or a family history of inherited immunodeficiencies; smokers, alcoholics or drug users; subjects should not take any prescription drugs, over-the-counter medications, or natural health supplements for 14 days prior to screening.

2.3 Sample preparation, instrument conditions and data analysis of metabolomics

The specific steps of sample processing were as follows: take 100 μL serum and add 400 μL methanol solution containing isotope internal standard. The samples were shaken for 3 min at 18,000 rpm*10 min and centrifuged at 4°C. 400 μL of the supernatant was transferred to an EP tube and centrifuged again in the same way. 100 μL of the supernatant was taken and 10 μL of the sample was injected. An equal volume of all samples was mixed to prepare quality control samples (QC). QC samples are part of the system regulation and quality control process. The processing and testing of QC samples are similar to those of the analyzed samples, which helps to obtain reliable and high-quality metabolomics data.

LC-TOF/MS instrument conditions:the chromatographic column was Waters HSS T3 (2.1 mm × 100 mm, 1.8 um), the flow rate was 0.3 mL/min, the column temperature was 40°C, and the mobile phase was A: water phase (0.1% formic acid-water). B: organic phase (acetonitrile), MS scanning range: 50 to 1,200 Da. LC-MS/MS instrument conditions: the chromatographic column was Waters HSS T3 (2.1 mm × 100 mm, 1.8 um), the flow rate was 3 mL/min, the column temperature was 40°C, the mobile phase A was 0.1% formic acid water, and the mobile phase B was 0.1% formic acid acetonitrile. Gradient elution: mobile phase B was 10% (0.00–1.00 min), 10%–90% (1.00–9.00 min), 90% (9.00–12.00 min), 90%–10% (12.00–12.10 min), 10% (12.10–15.00 min), the injection volume was 5 uL per injection.

Based on the metabolomics data obtained by LC-TOF/MS, the raw data were converted into mzXML format by MSconvert software. Subsequent analyses were performed using the tidymass package installed in the R project (version >4.2.2). GraphPad Prism 9.0.0 software was used for statistical analysis based on the metabolomics data obtained by LC-MS/MS. Data were expressed as mean and standard deviation, and differences between groups were analyzed by one-way analysis of variance (ANOVA). Differences between all groups were compared first, and then between two pairs. $p < 0.05$ was considered significant in all statistical tests.

2.4 ELISA method and data analysis

The three kits of hyaluronic acid (HA), cartilage oligomeric matrix protein (COMP), and collagen type II (COL2α1) used in this study were purchased from Signalway Antibody (SAB, United States). The three kits of matrix metalloproteinase-3 (MMP-3), human bone-derived alkaline phosphatase (BAP), and tartrate-resistant acid phosphatase (TRACP-5) were purchased from Shanghai Jining Industrial Co., LTD. Sample testing procedures were performed exactly according to the instructions included with each kit. The data were analyzed by GraphPad Prism 9.0.0 software.

3 Results

3.1 Non-targeted metabolomics to screen small molecule metabolites related to pain

PLS-DA and OPLS-DA are supervised multivariate data analysis and belong to model methods. They use partial least squares regression to establish the relationship model between metabolite expression and sample type to reduce the data dimension. This supervised mode can better establish the relationship between samples and better obtain the different information between groups. In this study, PLS-DA and OPLS-DA results of each dose group showed that the pre-administration and the post-administration could be significantly separated in Electrospray ionization positive ion mode (ESI+) and Electrospray ionization negative ion mode (ESI-) (Figures 1A–G, 2A–G, 3A–G, 4A–G), suggesting that DS002 had A significant effect on the metabolism of the body. There was no over-fitting in the models of each group, and the prediction performance was good, indicating that the results were more accurate. Multivariate analysis was used to analyze the control and administration groups of different dose groups, and the differential metabolites between the control and administration groups were screened by setting the range of change fold and significance. We found that the levels of metabolites *in vivo* increased or decreased after administration of DS002. KEGG database was used to perform metabolic pathway enrichment analysis of differential metabolites in each dose group, and the pathways involved in each dose group were: 0.5 mg: Phenylalanine, tyrosine and tryptophan biosynthesis, Phenylalanine metabolism, Histidine metabolism, Primary bile acid biosynthesis, Aminoacyl-trna biosynthesis; 1 mg: Caffeine metabolism, Linoleic acid metabolism, α-linoleic acid metabolism, Arachidonic acid metabolism, Glycerophospholipid metabolism; 2 mg: Phenylalanine metabolism, Phenylalanine, tyrosine and tryptophan biosynthesis, Aminoacyl-tRNA biosynthesis, Primary bile acid biosynthesis, Ubiquinone and other terpene quinone biosynthesis, Sphingolipid metabolism, Arginine and proline metabolism, Tyrosine metabolism; 4 mg: Phenylalanine metabolism, Phenylalanine, tyrosine and tryptophan biosynthesis, Ubiquinone and other terpene quinone biosynthesis, Caffeine metabolism, Sphingolipid metabolism, Primary bile acid biosynthesis, Tyrosine metabolism, Purine metabolism; 7 mg: Phenylalanine metabolism, Phenylalanine, tyrosine and tryptophan biosynthesis, Linoleic acid metabolism, Caffeine metabolism, Aminoacyl-tRNA biosynthesis, Ubiquinone and other terpene quinone biosynthesis, Pyrimidine metabolism, Tyrosine metabolism; 12 mg: Unsaturated fatty acid biosynthesis, Linoleic acid metabolism, Phenylalanine, tyrosine and tryptophan biosynthesis, Phenylalanine metabolism, Citrate cycle (TCA), Alanine, aspartate and glutamate metabolism, Glyoxylate and dicarboxylic acid metabolism, Glycerophospholipid metabolism; 20 mg: Aminoacyl-tRNA biosynthesis, Phenylalanine, tyrosine and tryptophan biosynthesis, Arginine biosynthesis, Arginine and proline metabolism, Glutathione and glutamate metabolism, Glutathione metabolism, Ubiquinone and other terpene quinone biosynthesis, Phenylalanine metabolism, Alanine, aspartate and glutamate metabolism, Tyrosine metabolism (Figure 5). It is worth noting that aromatic amino acid metabolic pathways were found in the differential metabolic pathways of the six dose groups, and aromatic amino acids mainly included tyrosine, phenylalanine and tryptophan. Finally, the differential metabolites were summarized in the form of Venn diagram through the website Bioinformatics. Tryptophan was found in the differential metabolites of the five dose groups under ESI+ and ESI- modes (Figure 6). The compounds contained in each color region are listed in Supplementary Tables S1, S2. Therefore, aromatic amino acids were selected for the next targeted metabolomics analysis.

3.2 Targeted metabolomics for accurate quantification of aromatic amino acids and their metabolites

Based on the results of non-targeted metabolomics experiments, we first established a targeted determination method for aromatic amino acids by liquid chromatography-tandem mass spectrometry. We used targeted metabolomics to accurately quantify aromatic amino acids and their metabolites. Statistical analysis of the targeted metabolomics data revealed that changes in important metabolites were statistically significant only in the highest administered dose group. The results showed that after administration of 20 mg, the concentrations of L-phenylalanine and 5-hydroxytryptophan decreased after administration; the concentrations of 3-indolepropionic acid, tryptamine hydrochloride, Kynurenic acid, and kynurenine increased first and then decreased (Figures 7A–F). The levels of these metabolites were then quantified in the placebo group and showed different trends between the placebo group and the treated group (Supplementary Figure S1). Therefore, we hypothesise that changes in these metabolites may be related to the effects of DS002 on pain, and that changes in these metabolites may stimulate the antisensory potential of the organism.

3.3 Changes in cartilage and bone metabolism-related indicators

Identifying the blood levels and distribution of different markers related to cartilage and bone metabolism can help to assess the risk of osteoarthritis. In our study, the concentrations of serum-related markers of cartilage and bone metabolism were determined before and after DS002 administration. The results showed that the serum concentrations of the six indicators related to cartilage and bone did not differ significantly with the changes in dose and time of administration (Figures 8A–F), indicating that DS002 had no significant effect on the markers related to cartilage and bone metabolism. So, we hypothesized that DS002 might not cause the serious adverse effects of joint necrosis and rapidly worsening osteoarthritis caused by the same target drug class.

4 Discussion

Pain is a common problem and is the main reason people seek medical care. But satisfactory clinical protocols for the treatment of pain remain elusive. Anti-NGF monoclonal antibody is a new class of analgesic drugs. In the studies that have been done on the

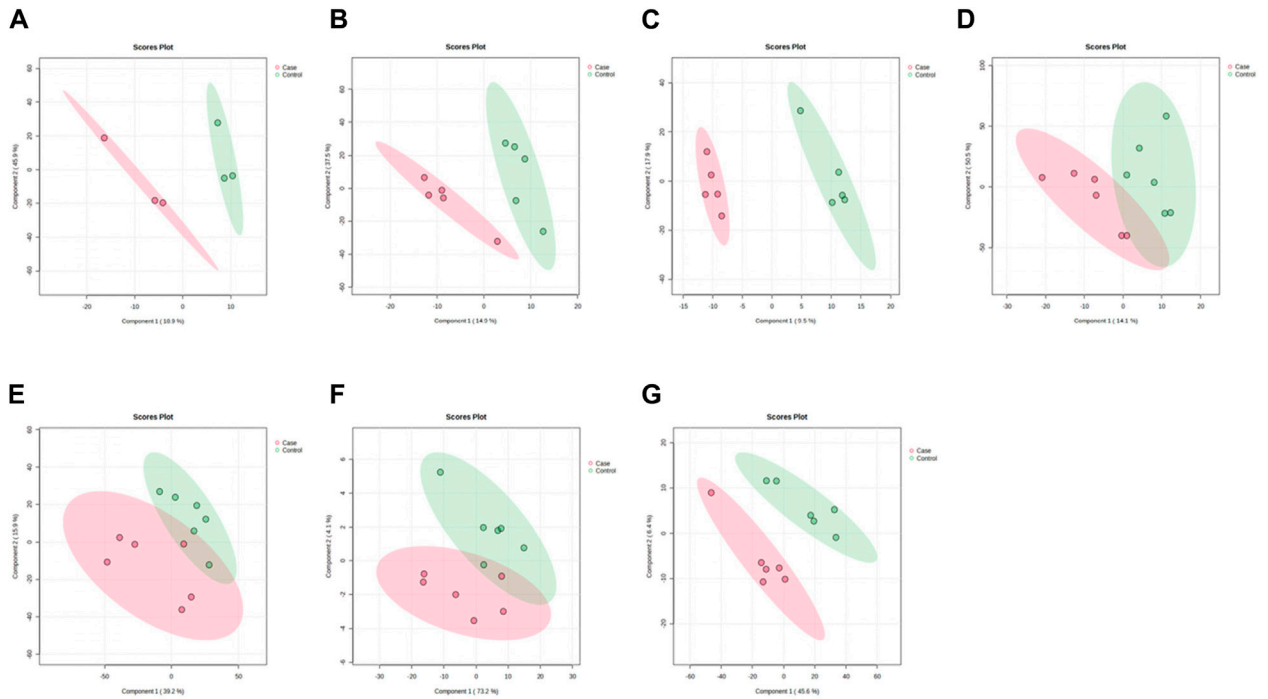

FIGURE 1
PLSDA plots of samples in ESI + mode before and after administration in different dose groups. The doses were 0.5 mg panel **(A)**, 1 mg panel **(B)**, 2 mg panel **(C)**, 4 mg panel **(D)**, 7 mg panel **(E)**, 12 mg panel **(F)**, and 20 mg panel **(G)**.The red color represents the serum sample collected at 168 h after administration, which is the post-administration. The green represents the serum sample collected at 0 h before administration, which is the pre-administration.

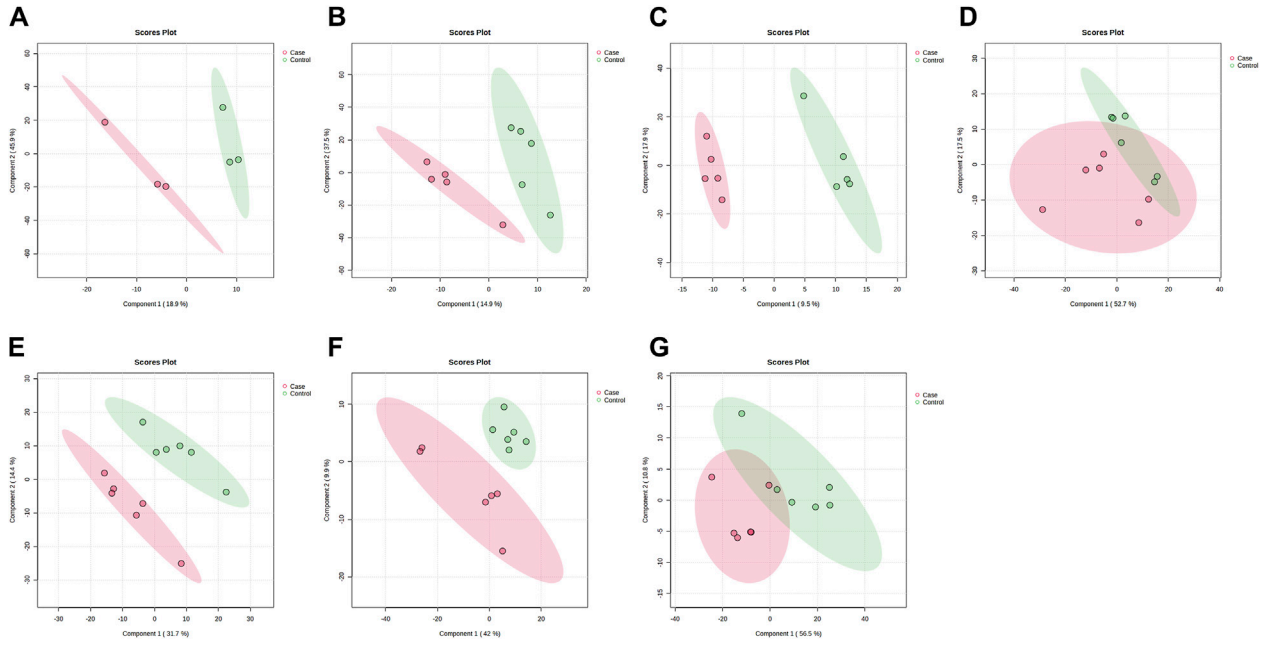

FIGURE 2
PLSDA plots of samples in ESI-mode before and after administration in different dose groups. The doses were 0.5 mg panel **(A)**, 1 mg panel **(B)**, 2 mg panel **(C)**, 4 mg panel **(D)**, 7 mg panel **(E)**, 12 mg panel **(F)**, and 20 mg panel **(G)**. The red dots represent the serum samples collected at 168 h after administration, which is the post-administration. The green dots represent the serum samples collected at 0 h before administration and are the pre-administration.

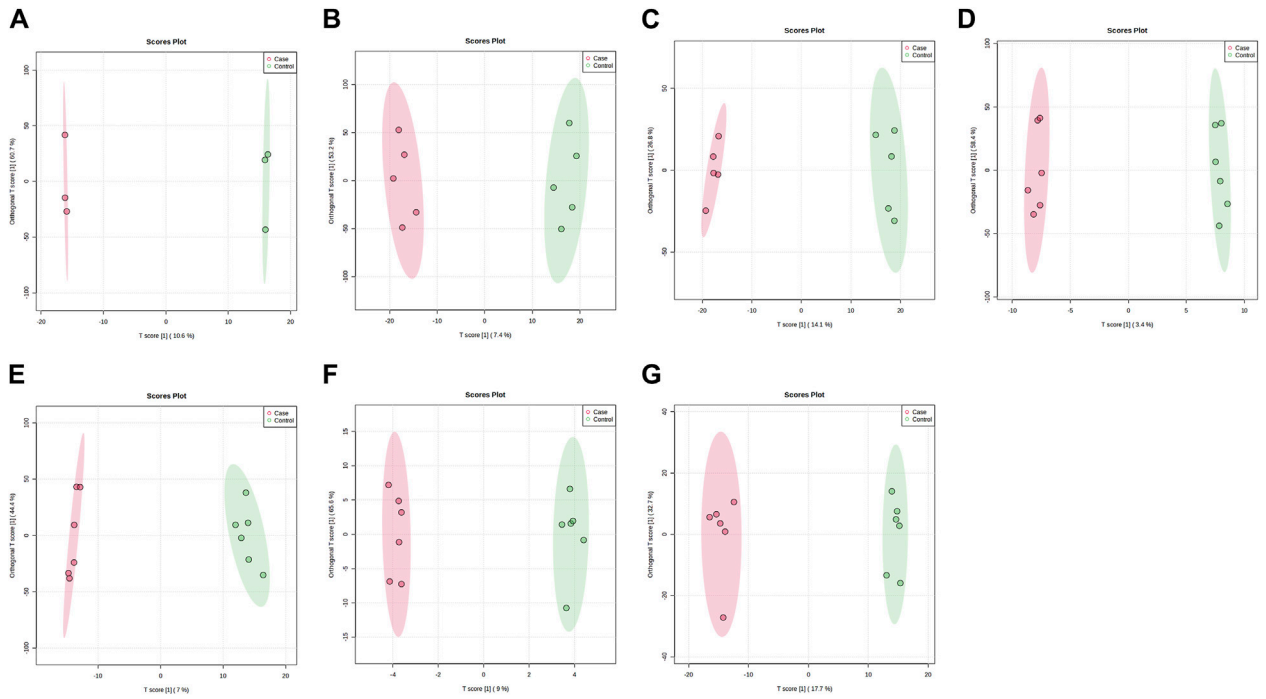

FIGURE 3
OPLS-DA plots of samples in ESI + mode before and after administration in different dose groups. The doses were 0.5 mg panel **(A)**, 1 mg panel **(B)**, 2 mg panel **(C)**, 4 mg panel **(D)**, 7 mg panel **(E)**, 12 mg panel **(F)**, and 20 mg panel **(G)**. The red dots represent the serum samples collected at 168 h after administration, which is the post-administration. The green dots represent the serum samples collected at 0 h before administration and are the pre-administration.

treatment of pain with this class of drugs, it has shown high efficacy in the treatment of pain, far exceeding the efficacy of existing drugs, and is non-addictive. *In vitro* studies showed that DS002 successfully blocked the binding of NGF and TrkA receptors, thereby blocking the transmission of pain signals. DS002, as a novel analgesic drug targeting NGF, has the potential to become a new generation of drugs for treating chronic pain, nevertheless, previous studies have shown that co-targeted drugs of DS002 cause serious adverse effects on joints. In addition, the results of our Phase I clinical trial demonstrated that DS002 did not experience dose-limiting toxicity in terms of safety and did not meet dose-escalation termination criteria in the range of 0.5–20 mg administered (Ma et al., 2022). Five subjects developed arthralgia during the course of the trial, four subjects treated with DS002 (one in the 4.0 dose group, one in the 12.0 dose group, and two in the 20.0 mg dose group) and one in the placebo group, although the symptoms that developed were medically diagnosed to be mild, and all eventually resolved without intervention. No serious bone and joint events or peripheral neuropathy/sensory abnormalities were noted throughout the trial. Rapidly progressive arthritis (RPOA) was not observed even when the drug was administered at high doses. As this was the most prominent concern when the FDA shelved the development programme for similar anti-NGF drugs. Therefore, in the present study, we continued to investigate the effects of DS002 on cartilage and bone metabolism-related markers to better clarify whether it produces the same target drug-induced adverse effects in the joints and to discuss its safety in healthy subjects. Meanwhile, this study also explores the changes in metabolite levels in healthy subjects after taking DS002 from the perspective of blood metabolomics, and links the changes in metabolites to the mechanism of pain occurrence, to explore the reasons for the therapeutic effect of DS002, and to provide more scientific basis for advancing the marketing of DS002.

Previous Tanezumab clinical trial data showed joint adverse effects, including osteonecrosis and rapidly worsening osteoarthritis, in the same class as DS002 (Jayabalan and Schnitzer, 2017). Hyaluronic acid (HA) is the main component of the cartilage matrix, which can bind to CD44 receptors, thereby inhibiting the expression of interleukin (IL) 1β and reducing the production of matrix metalloproteinase 3 (MMP-3) (Karna et al., 2008). HA can enter the peripheral blood circulation through lymphatic circulation, and the expression level of HA is positively correlated with the severity of arthritis. Matrix metalloproteinases (MMPs) have been reported to play an essential role in the pathogenesis of osteoarthritis, as they are involved in the degradation of all matrices outside the cell except polysaccharides (Grillet et al., 2023; Murphy et al., 2002). Among them, MMP-3 is the most important protease involved in cartilage degradation, which can be regulated by IL-1 and TNF-α cytokines (Shi et al., 2022), followed by activation of other interstitial collagenases to degrade type II collagen (COL II), accelerates cartilage destruction. COL II is the main extracellular matrix protein in cartilage, and its degraded fragments will further accelerate the progression of osteoarthritis, promote the degradation of COL II, and accelerate the destruction of cartilage (Poole et al., 2002). Cartilage oligomeric matrix protein (COMP) is secreted by osteoblasts and synovium

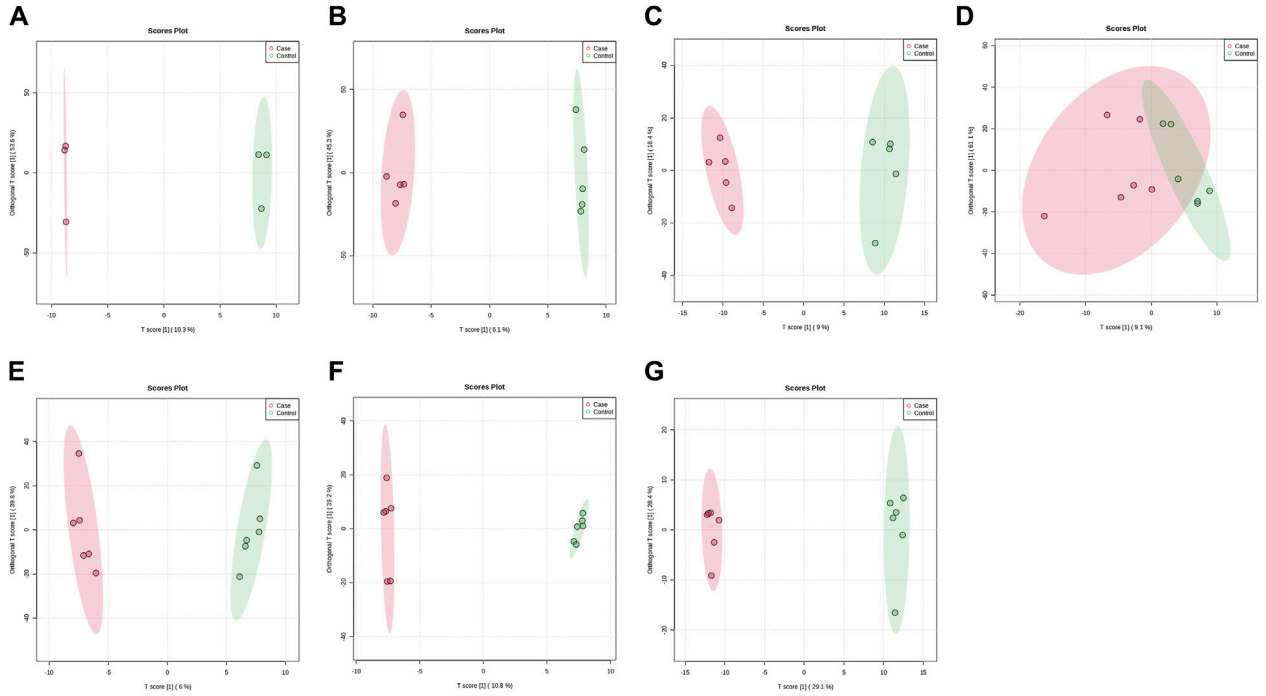

FIGURE 4
OPLS-DA plots of samples in ESI-mode before and after administration in different dose groups. The doses were 0.5 mg panel **(A)**, 1 mg panel **(B)**, 2 mg panel **(C)**, 4 mg panel **(D)**, 7 mg panel **(E)**, 12 mg panel **(F)**, and 20 mg panel **(G)**. The red dots represent the serum samples collected at 168 h after administration, which is the post-administration. The green dots represent the serum samples collected at 0 h before administration and are the pre-administration.

cells and is related to cartilage metabolism. After articular cartilage injury, cartilage matrix degradation produces COMP, which can be released into the blood (Maly et al., 2021). Bone alkaline phosphatase (BAP) is secreted by osteoblasts during the maturation stage and binds to bone matrix after being secreted to the extracellular space. It is a special sensitive index reflecting bone formation. In osteoporosis, bone calcification is insufficient. Osteoblasts proliferate actively and cannot transform into osteocytes. Osteoblasts proliferate actively and secrete a large amount of BAP into the blood. Tartrate resistant acid phosphatase 5b (TRACP-5b) is an enzyme secreted by activated bone calpain and is a good marker of bone resorption and osteoclast activity. Its concentration can be measured to understand bone metabolism status (Terpos et al., 2005). In this study, the concentrations of HA, MMP-3, COLII, COMP, BAP, TRACP-5b, which are related to cartilage and bone metabolism, did not change significantly over time in healthy subjects after treatment of different doses of DS002. These results indicated that the administration of monoclonal antibody DS002 did not cause fluctuations in the content of metabolites related to cartilage and bone metabolism, indicating that DS002 had no significant effect on the relevant parameters of cartilage and bone metabolism.

When pain occurs, a series of changes are reflected in the body's metabolites. Specific blood, urine, and saliva biomarkers can be used to determine the degree of risk of chronic pain and can be used as prognostic markers of pain progression and treatment response (Hagedorn et al., 2021). In the present study, we measured the therapeutic effect of DS002 by investigating the blood metabolic profile. After DS002 administration, the body's metabolism was significantly affected. The changes in metabolites involved in different metabolic pathways. According to previous studies, the metabolites in these metabolic pathways have been shown to be related to the occurrence and development of different pain. For example, researchers have found a link between amino acid metabolism and pain (Alexander et al., 2013; Teckchandani et al., 2021), the ratio of tryptophan to kynurenine is increased during back pain (Staats Pires et al., 2020), glutamate levels increase with the onset of fibromyalgia (Clos-Garcia et al., 2019), phosphocholine, alanine, and taurine are elevated in neuropathic pain (Finco et al., 2016). As the occurrence of pain is accompanied by a series of symptoms, different metabolic pathways can also indirectly affect pain. Studies have shown that the methionine metabolism pathway is related to sleep problems, and the glutathione metabolism pathway is related to obesity, and pain, sleep and obesity affect each other (Suzuki et al., 2015; Miettinen et al., 2019), so the imbalance of these two pathways will also affect pain. So we propose that the treatment of pain with DS002 may have a relationship to changes in these pathways. In our results, aromatic amino acid metabolic pathways account for the most significant proportion, such as the biosynthesis of phenylalanine, tyrosine, and tryptophan, as well as phenylalanine and tyrosine metabolism. These results may be relevant to the treatment of pain with DS002, because the amino acid metabolic pathway is related to the basal metabolic recovery of the body, and correct regulation reduces inflammatory response and affects nerve conduction. In addition, amino acids are the main substrate for producing

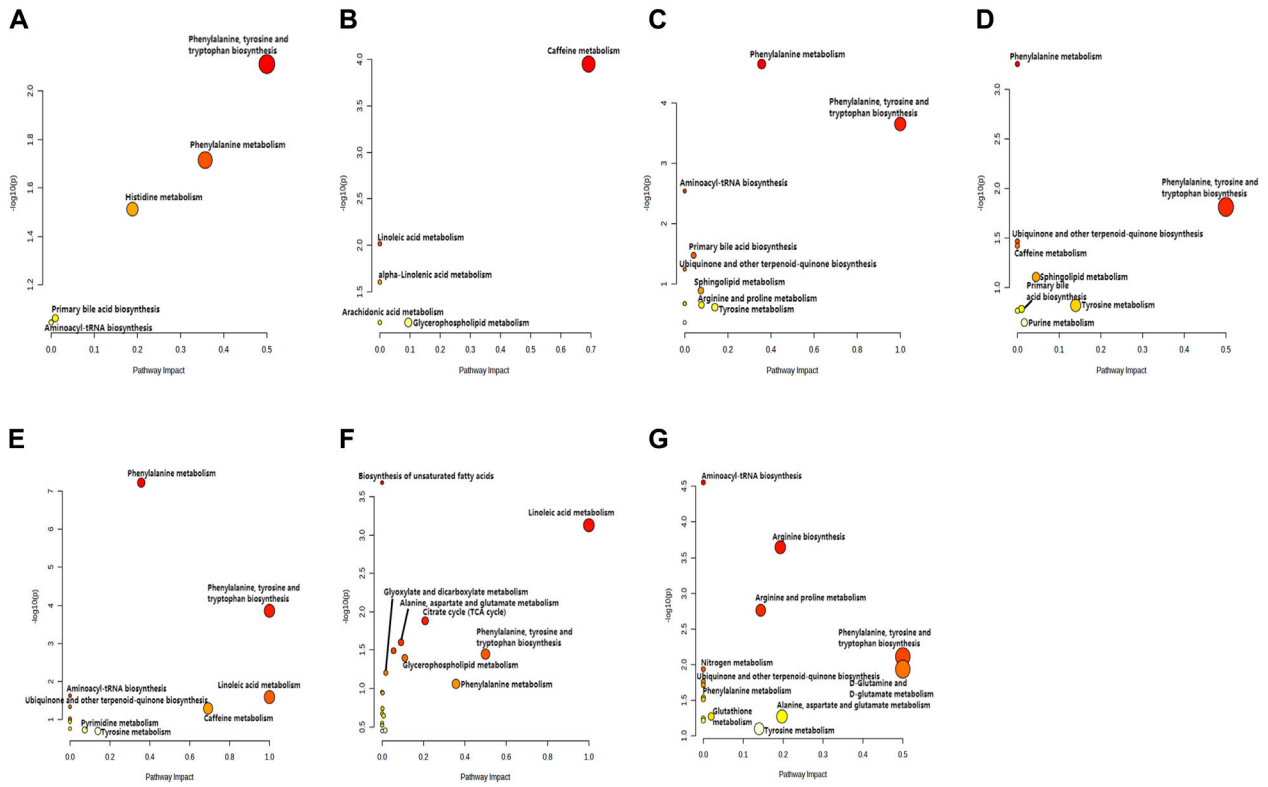

FIGURE 5
KEGG enrichment analysis of relevant pathways in different administration dose groups. Scatter plot of pathways enriched by important differential metabolites. The *X*-axis and size of a node indicate the influence of that path in the topological analysis pathway, and the *Y*-axis and color of a node indicate statistical significance. The doses were 0.5 mg panel **(A)**, 1 mg panel **(B)**, 2 mg panel **(C)**, 4 mg panel **(D)**, 7 mg panel **(E)**, 12 mg panel **(F)**, and 20 mg panel **(G)**.

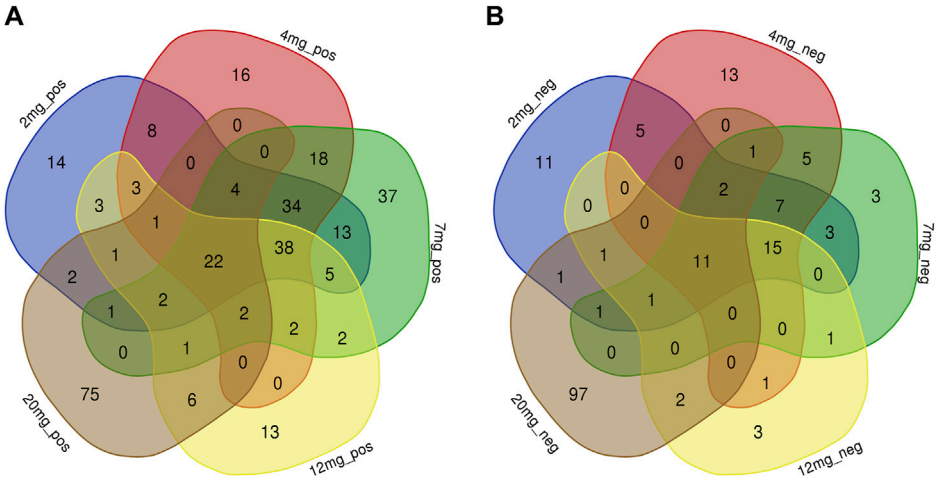

FIGURE 6
Common differential metabolites of five drug dose groups (2, 4, 7, 12, and 20 mg) in ESI+ and ESI-mode were screened by Venn diagram. Each colour area represents a dose group, numbers in individual colour areas indicate the number of different metabolites in that dose group, and numbers in overlapping colour areas indicate the number of metabolites that are common to two or more dose groups. The numbers in the centre of the graph indicate the number of metabolites shared among the five groups, and the Supplementary Table S1 lists the metabolites for each dose group.
(A): ESI + mode; **(B)** ESI-mode.

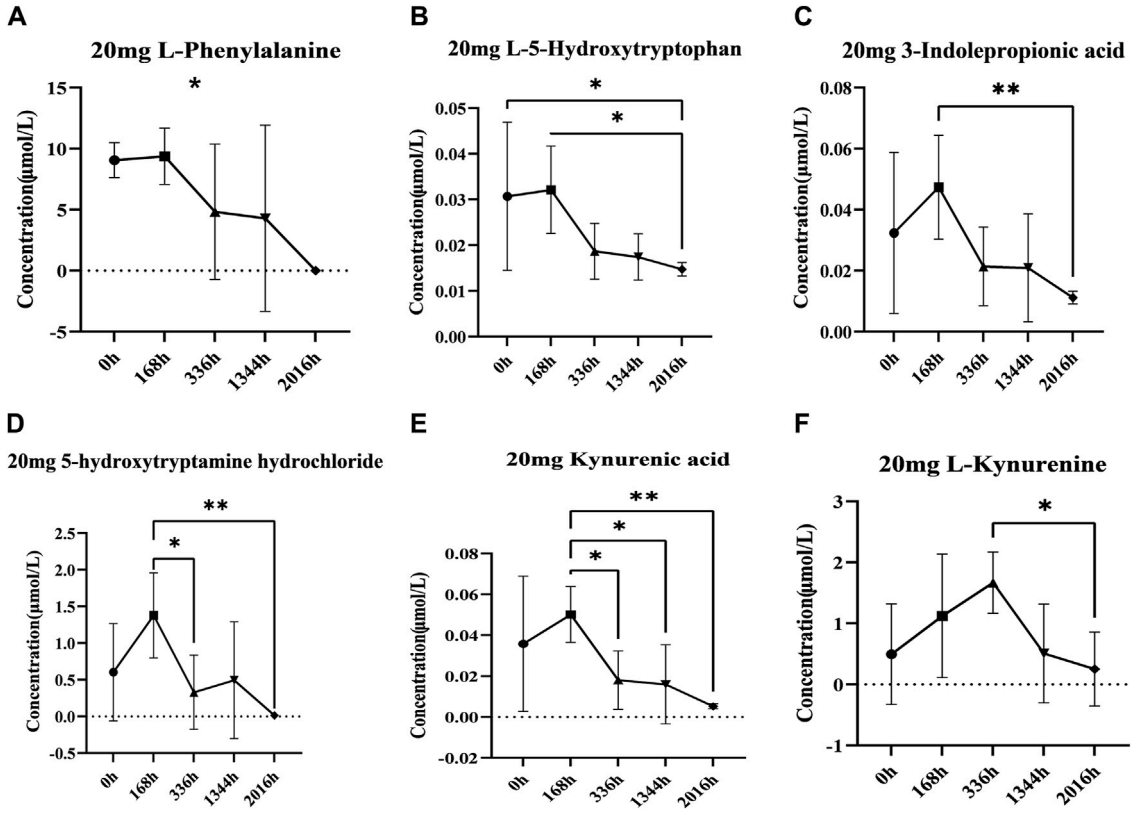

FIGURE 7
Analysis of concentration trends of important metabolites *in vivo*. Line graphs **(A)** L-phenylalanine, **(B)** L-5-hydroxytryptophan, **(C)** Indole-3-propionic acid, **(D)** 5-Hydroxytryptamine hydrochloride, **(E)** Kynurenic acid and **(F)** L-kynurenine describe the changing trend of each differential metabolite with administration time. * indicates $p < 0.05$.

neurotransmitters, and neurotransmitter-mediated pain regulation is the primary way.

Phenylalanine and tryptophan are essential amino acids for the human body and belong to the aromatic amino acids. Most phenylalanine in the body is oxidized to tyrosine, an amino acid associated with analgesic neurotransmitters, through the catalytic action of phenylalanine hydrogenase. The pathophysiological mechanisms underlying the onset and resolution of pain are intricate, and many different neurotransmitter systems are involved in the transmission, processing, and control of pain (Millan, 2002). In previous studies, Amino acid metabolites, including L-tryptophan, L-histidine, and L-tyrosine, were significantly decreased in the brain of pain model mice, suggesting that neuropathic pain may be promoted by the reduction of amino acids related to analgesic neurotransmitters. Therefore, we infer that the *in vivo* metabolic conversion of PHE to amino acids related to analgesic neurotransmitters would be involved in the therapeutic effect of DS002. Tryptophan is an essential amino acid for generating and maintaining proteins, muscles, enzymes, and neurotransmitters in the human body (Kértési et al., 2022). The tryptophan metabolism pathway includes the kynurenine, serotonin, and indole pathways. Changes in tryptophan levels can lead to imbalances in the synthesis and metabolism of downstream metabolites, which may be related to the pathological and physiological mechanisms of neurological and psychiatric diseases (Comai et al., 2020). Recent studies have shown that the dysregulation of the kynurenine pathway and the changes of metabolites in its pathway are associated with neurotoxicity and inflammation, and many metabolites are associated with chronic pain (Tanaka et al., 2021). Tryptophan enters the kynurenine metabolic pathway through indoleamine 2, 3-dioxygenase (IDO) and tryptophan 2, 3-dioxygenase (TDO) and generates kynurenine, which is irreversibly converted to kynurenic acid (KA) by kynurenine aminotransferase (KATs) (Schwarcz et al., 2012). KA is a neuroactive metabolite which belongs to the antiexcitotoxin and has neuroprotective effects (Fehér et al., 2019). The activity of KA at different targets is the primary mechanism by which it achieves specific functions. KA exerts its neuroprotective effect by antagonizing NMDA receptors (Birch et al., 1988), and previous studies have shown that marked reductions in neuroprotective metabolites occur in patients with psychiatric disorders (Athnaiel et al., 2022). KA interacts with g protein-coupled receptor 35 (GPR35) to indirectly reduce inflammation (Wirthgen et al., 2017), which is highly correlated with chronic pain. Thus, the neuroprotective and inflammatory response effects of KA suggest elevated levels of KA and other metabolites with similar properties when treating chronic pain symptoms.

In recent years, a great deal of research has been conducted on the role of 5-HT in chronic pain states.5-HT is metabolised in the

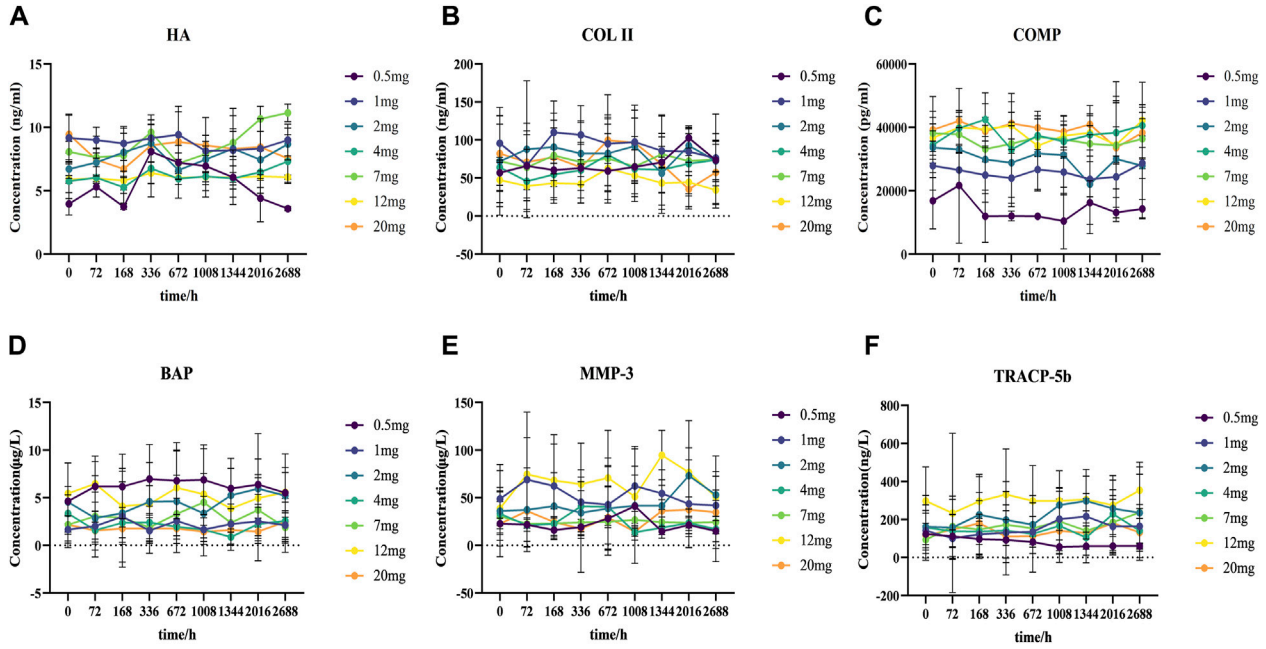

FIGURE 8
Analysis of the trend changes of markers related to cartilage and bone metabolism over time and dosing increments.Scatter plot **(A)** Hyaluronic acid (HA), **(B)** TypeIIcollagen (COLII), **(C)** Cartilage oligomeric matrix protein (COMP), **(D)** Bone-specific alkaline phosphatase (BAP), **(E)** Matrix metalloproteinase 3 (MMP-3), and **(F)** tartrate-resistant acid phosphatase 5b (TRACP-5b) depict the trends of each marker as a function of administration time and dose.

body by: the small amount of tryptophan in the body is catalyzed by tryptophan hydroxylase (TPH) to generate 5-hydroxytryptophan (5-HTP). The aromatic L-amino acid decarboxylase interacts with the cofactor Pyridoxal 5-phosphate to convert 5-HTP to 5-hydroxytryptamine (5-HT) (Daubert and Condron, 2010). 5-HT, also known as serotonin, is an excitatory neurotransmitter in the human central nervous system, which causes the contraction of vascular smooth muscle, thereby potentially regulating pain (Taylor and Basbaum, 1995; Xue et al., 2023). Endogenous 5-HT was released in response to tissue injury in mast cells, platelets and endothelial cells, while multiple neuronal 5-HT receptors were detected in the periphery, suggesting that 5-HT can interfere with injurious transmission at peripheral sites (Bardin, 2011). Previous studies have also pointed to the complex relationship between 5-HT and pain, for example: intradermal administration of 5-HT to rats causes dose-dependent nociceptive hypersensitivity (Taiwo and Levine, 1992); plantar injections of 5-HT result in plantar oedema and intense flinching and licking behaviour (Sufka et al., 1992); In healthy volunteers, intradermal injections of low concentrations of 5-HT produced burning pain (Lischetzki et al., 2001), while injections into the mandibular occlusal muscle produced nociceptive hypersensitivity (Ernberg et al., 2000); Furthermore, In a carrageenan inflammatory pain model, administration of the 5-HT3 antagonist ICS-205930 by plantar administration at different times resulted in complete suppression of nociceptive hypersensitivity to foot inflammation, a process accompanied by 5-HT release (Eschalier et al., 1989). Taken together, these studies suggest that 5-HT release sensitises sensory nerve fibres in response to inflammation or tissue damage and promotes peripheral sensitisation through direct or indirect mechanisms. It has been shown that patients with chronic pain exhibit weaker endogenous pain inhibitory processes compared to pain-free individuals, and that the involvement of downward inhibition may represent an endogenous mechanism to prevent the chronicisation of pain (Ossipov et al., 2014). *In vivo*, the periaqueductal grey matter (PAG) is a brain region capable of activating endogenous pain inhibitory systems, and the PAG influences downstream pain modulation primarily through its interconnections with the rostral ventromedial medulla (RVM) (Ossipov et al., 2014), whereas the activation of downstream projections from the RVM induces the release of serotonin (Foo and Mason, 2003; Wei et al., 2010; Hossaini et al., 2012). 5-HT can exhibit both pro- and antinociception throughout, depending on the subtype of 5-HT receptor it activates, with activation of 5-HT1A, 5-HT1B, 5-HT1D, and 5-HT7 receptors tending to be antinociceptive, and 5-HT2A and 5-HT3 receptors tending to be proinjury sensory (Suzuki et al., 2004; Sasaki et al., 2006; Bannister et al., 2009; Dogrul et al., 2009); there is also a large body of research pointing to the inhibitory and facilitatory effects of the downstream 5-HT pathway on spinal neuronal excitability and pain-related behaviours, depending on the acute or persistent pain state (Bardin, 2011). In conclusion, these results suggest that 5-TH and the downstream 5-TH pathway play an important role in pain transmission in a complex pathological manner.

A minimal amount of tryptophan in the body can also be converted into indole and its derivatives, such as indole-3-acetic acid, indole-3-propionic acid, etc. under the action of the gut microbiota (Wei et al., 2021). Indole and its derivatives can contribute to the regulation of inflammatory responses (Venkatesh et al., 2014), which are highly correlated with the occurrence of pain. Therefore, indole and its

derivatives can also affect the progression of pain. In addition, the gut microbiota is also an important regulator of visceral pain. In recent years, it has been found that the gut microbiota also plays a crucial role in chronic pain (Guo et al., 2019). In summary, these associations potentially suggest a correlation between changes in metabolite levels and the efficacy of DS002 in treating pain.

From the above, our findings suggest that DS002 has greater advantages in the treatment of pain compared with the existing drugs and the drugs in the same target class as DS002. Of course, the study has limitations. Our method of administration is a single dose in healthy people, which is different from clinical drug administration. Therefore, the application of DS002 in the clinical treatment of pain needs to be further explored.

5 Conclusion

Our results showed that DS002 caused the changes in the aromatic amino acid metabolic pathway in subjects treated with it. Among them, the changes in the concentration of L-phenylalanine, 5-hydroxytryptophan, 5-hydroxytryptamine, kynurenic acid, kynurenine, and indole-3-propionic acid may be related to the therapeutic effect of DS002 for treating pain. After administration, there were no significant changes in cartilage and bone metabolism indicators, and we preliminarily speculate that DS002 will not produce severe adverse reactions as the same target class of drugs. Our research provides a specific basis for DS002, and aromatic amino acids and their metabolites may serve as biomarkers for treating pain. Combined with the clinical results of the previous study of DS002 in our laboratory, it can more strongly demonstrate the enormous potential of anti-NGF drugs represented by DS002 in treating pain.

Data availability statement

The original contributions presented in the study are included in the article/Supplementary Material, further inquiries can be directed to the corresponding authors.

Ethics statement

The studies involving humans were approved by Ethics Committee of Nanjing Drum Tower Hospital. The studies were conducted in accordance with the local legislation and institutional requirements. The participants provided their written informed consent to participate in this study.

Author contributions

DJ: Data curation, Formal Analysis, Methodology, Resources, Software, Writing–original draft, Writing–review and editing. HY: Data curation, Resources, Software, Writing–original draft. ZC: Data curation, Formal Analysis, Methodology, Resources, Software, Writing–original draft. YH: Data curation, Formal Analysis, Resources, Software, Validation, Writing–original draft. HM: Data curation, Formal Analysis, Methodology, Resources, Writing–original draft. ZX: Data curation, Formal Analysis, Methodology, Resources, Software, Writing–original draft. BC: Conceptualization, Investigation, Supervision, Validation, Visualization, Writing–original draft. FF: Conceptualization, Data curation, Formal Analysis, Investigation, Methodology, Resources, Supervision, Validation, Writing–original draft. YZ: Data curation, Formal Analysis, Resources, Software, Writing–original draft. WW: Conceptualization, Formal Analysis, Investigation, Project administration, Resources, Visualization, Writing–original draft. LT: Formal Analysis, Investigation, Project administration, Resources, Software, Visualization, Writing–original draft. RS: Data curation, Formal Analysis, Investigation, Methodology, Resources, Software, Supervision, Validation, Visualization, Writing–review and editing, Writing–original draft. CW: Funding acquisition, Project administration, Supervision, Validation, Visualization, Writing–original draft, Writing–review and editing. JL: Data curation, Formal Analysis, Funding acquisition, Investigation, Methodology, Resources, Software, Supervision, Writing–original draft, Writing–review and editing.

Funding

The author(s) declare that financial support was received for the research, authorship, and/or publication of this article. The project was funded by the National Natural Science Foundation of China (31371399).

Acknowledgments

The authors would like to thank the following people for their contributions: All volunteers who participated in this study and all the investigators.

Conflict of interest

Authors WW, LT and CW were employed by Dartsbio Pharmaceuticals, Ltd.

The remaining authors declare that the research was conducted in the absence of any commercial or financial relationships that could be construed as a potential conflict of interest.

Publisher's note

Supplementary material

The Supplementary Material for this article can be found online at: https://www.frontiersin.org/articles/10.3389/fphar.2024.1396790/full#supplementary-material

References

Alexander, G. M., Reichenberger, E., Peterlin, B. L., Perreault, M. J., Grothusen, J. R., and Schwartzman, R. J. (2013). Plasma amino acids changes in complex regional pain syndrome. *Pain Res. Treat.* 2013, 742407. doi:10.1155/2013/742407

Athnaiel, O., Ong, C., and Knezevic, N. N. (2022). The role of kynurenine and its metabolites in comorbid chronic pain and depression. *Metabolites* 12 (10), 950. doi:10.3390/metabo12100950

Bannister, K., Bee, L. A., and Dickenson, A. H. (2009). Preclinical and early clinical investigations related to monoaminergic pain modulation. *Neurotherapeutics* 6 (4), 703–712. doi:10.1016/j.nurt.2009.07.009

Bardin, L. (2011). The complex role of serotonin and 5-HT receptors in chronic pain. *Behav. Pharmacol.* 22 (5-6), 390–404. doi:10.1097/FBP.0b013e328349aae4

Basbaum, A. I., Bautista, D. M., Scherrer, G., and Julius, D. (2009). Cellular and molecular mechanisms of pain. *Cell* 139 (2), 267–284. doi:10.1016/j.cell.2009.09.028

Birch, P. J., Grossman, C. J., and Hayes, A. G. (1988). Kynurenic acid antagonises responses to NMDA via an action at the strychnine-insensitive glycine receptor. *Eur. J. Pharmacol.* 154 (1), 85–87. doi:10.1016/0014-2999(88)90367-6

Clos-Garcia, M., Andrés-Marin, N., Fernández-Eulate, G., Abecia, L., Lavín, J. L., van Liempd, S., et al. (2019). Gut microbiome and serum metabolome analyses identify molecular biomarkers and altered glutamate metabolism in fibromyalgia. *EBioMedicine* 46, 499–511. doi:10.1016/j.ebiom.2019.07.031

Cohen, S. P., Vase, L., and Hooten, W. M. (2021). Chronic pain: an update on burden, best practices, and new advances. *Lancet* 397 (10289), 2082–2097. doi:10.1016/S0140-6736(21)00393-7

Comai, S., Bertazzo, A., Brughera, M., and Crotti, S. (2020). Tryptophan in health and disease. *Adv. Clin. Chem.* 95, 165–218. doi:10.1016/bs.acc.2019.08.005

Dahlhamer, J., Lucas, J., Zelaya, C., Nahin, R., Mackey, S., DeBar, L., et al. (2018). Prevalence of chronic pain and high-impact chronic pain among adults - United States, 2016. *MMWR Morb. Mortal. Wkly. Rep.* 67 (36), 1001–1006. doi:10.15585/mmwr.mm6736a2

Daubert, E. A., and Condron, B. G. (2010). Serotonin: a regulator of neuronal morphology and circuitry. *Trends Neurosci.* 33 (9), 424–434. doi:10.1016/j.tins.2010.05.005

Dogrul, A., Ossipov, M. H., and Porreca, F. (2009). Differential mediation of descending pain facilitation and inhibition by spinal 5HT-3 and 5HT-7 receptors. *Brain Res.* 1280, 52–59. doi:10.1016/j.brainres.2009.05.001

Ernberg, M., Lundeberg, T., and Kopp, S. (2000). Pain and allodynia/hyperalgesia induced by intramuscular injection of serotonin in patients with fibromyalgia and healthy individuals. *Pain* 85 (1-2), 31–39. doi:10.1016/s0304-3959(99)00233-x

Eschalier, A., Kayser, V., and Guilbaud, G. (1989). Influence of a specific 5-HT3 antagonist on carrageenan-induced hyperalgesia in rats. *Pain* 36 (2), 249–255. doi:10.1016/0304-3959(89)90030-4

Fehér, E., Szatmári, I., Dudás, T., Zalatnai, A., Farkas, T., Lőrinczi, B., et al. (2019). Structural evaluation and electrophysiological effects of some kynurenic acid analogs. *Molecules* 24 (19), 3502. doi:10.3390/molecules24193502

Finco, G., Locci, E., Mura, P., Massa, R., Noto, A., Musu, M., et al. (2016). Can urine metabolomics Be helpful in differentiating neuropathic and nociceptive pain? A proof-of-concept study. *PLoS One* 11 (3), e0150476. doi:10.1371/journal.pone.0150476

Foo, H., and Mason, P. (2003). Brainstem modulation of pain during sleep and waking. *Sleep. Med. Rev.* 7 (2), 145–154. doi:10.1053/smrv.2002.0224

González-Domínguez, R., Jáuregui, O., Mena, P., Hanhineva, K., Tinahones, F. J., Angelino, D., et al. (2020). Quantifying the human diet in the crosstalk between nutrition and health by multi-targeted metabolomics of food and microbiota-derived metabolites. *Int. J. Obes. (Lond)* 44 (12), 2372–2381. doi:10.1038/s41366-020-0628-1

Grillet, B., Pereira, R. V. S., Van Damme, J., Abu El-Asrar, A., Proost, P., and Opdenakker, G. (2023). Matrix metalloproteinases in arthritis: towards precision medicine. *Nat. Rev. Rheumatol.* 19 (6), 363–377. doi:10.1038/s41584-023-00966-w

Guo, R., Chen, L.-H., Xing, C., and Liu, T. (2019). Pain regulation by gut microbiota: molecular mechanisms and therapeutic potential. *Br. J. Anaesth.* 123 (5), 637–654. doi:10.1016/j.bja.2019.07.026

Hagedorn, J. M., Gunn, J., Budwany, R., D'Souza, R. S., Chakravarthy, K., and Deer, T. R. (2021). How well do current laboratory biomarkers inform clinical decision-making in chronic pain management? *J. Pain Res.* 14, 3695–3710. doi:10.2147/JPR.S311974

Hirose, M., Kuroda, Y., and Murata, E. (2016). NGF/TrkA signaling as a therapeutic target for pain. *Pain Pract.* 16 (2), 175–182. doi:10.1111/papr.12342

Hossaini, M., Goos, J. A. C., Kohli, S. K., and Holstege, J. C. (2012). Distribution of glycine/GABA neurons in the ventromedial medulla with descending spinal projections and evidence for an ascending glycine/GABA projection. *PLoS One* 7 (4), e35293. doi:10.1371/journal.pone.0035293

Jayabalan, P., and Schnitzer, T. J. (2017). Tanezumab in the treatment of chronic musculoskeletal conditions. *Expert Opin. Biol. Ther.* 17 (2), 245–254. doi:10.1080/14712598.2017.1271873

Jeyarajah, E. J., Cromwell, W. C., and Otvos, J. D. (2006). Lipoprotein particle analysis by nuclear magnetic resonance spectroscopy. *Clin. Lab. Med.* 26 (4), 847–870. doi:10.1016/j.cll.2006.07.006

Karna, E., Miltyk, W., Surazyński, A., and Pałka, J. A. (2008). Protective effect of hyaluronic acid on interleukin-1-induced deregulation of beta1-integrin and insulin-like growth factor-I receptor signaling and collagen biosynthesis in cultured human chondrocytes. *Mol. Cell Biochem.* 308 (1-2), 57–64. doi:10.1007/s11010-007-9612-5

Körtési, T., Spekker, E., and Vécsei, L. (2022). Exploring the tryptophan metabolic pathways in migraine-related mechanisms. *Cells* 11 (23), 3795. doi:10.3390/cells11233795

Landreth, G. E., and Shooter, E. M. (1980). Nerve growth factor receptors on PC12 cells: ligand-induced conversion from low-to high-affinity states. *Proc. Natl. Acad. Sci. U. S. A.* 77 (8), 4751–4755. doi:10.1073/pnas.77.8.4751

Levi-Montalcini, R. (1952). Effects of mouse tumor transplantation on the nervous system. *Ann. N. Y. Acad. Sci.* 55 (2), 330–344. doi:10.1111/j.1749-6632.1952.tb26548.x

Lischetzki, G., Rukwied, R., Handwerker, H. O., and Schmelz, M. (2001). Nociceptor activation and protein extravasation induced by inflammatory mediators in human skin. *Eur. J. Pain* 5 (1), 49–57. doi:10.1053/eujp.2000.0214

Ma, T., Cao, B., Huang, L., Yang, Y., Geng, Y., Xie, P., et al. (2022). First-in-human study to assess the safety, tolerability, pharmacokinetics and immunogenicity of DS002, an anti-nerve growth factor monoclonal antibody. *Front. Pharmacol.* 13, 1075309. doi:10.3389/fphar.2022.1075309

Maly, K., Andres Sastre, E., Farrell, E., Meurer, A., and Zaucke, F. (2021). COMP and TSP-4: functional roles in articular cartilage and relevance in osteoarthritis. *Int. J. Mol. Sci.* 22 (5), 2242. doi:10.3390/ijms22052242

Miettinen, T., Kautiainen, H., Mäntyselkä, P., Linton, S. J., and Kalso, E. (2019). Pain interference type and level guide the assessment process in chronic pain: categorizing pain patients entering tertiary pain treatment with the Brief Pain Inventory. *PLoS One* 14 (8), e0221437. doi:10.1371/journal.pone.0221437

Miettinen, T., Mäntyselkä, P., Hagelberg, N., Mustola, S., Kalso, E., and Lötsch, J. (2021). Machine learning suggests sleep as a core factor in chronic pain. *Pain* 162 (1), 109–123. doi:10.1097/j.pain.0000000000002002

Millan, M. J. (2002). Descending control of pain. *Prog. Neurobiol.* 66 (6), 355–474. doi:10.1016/s0301-0082(02)00009-6

Murphy, G., Knauper, V., Atkinson, S., Butler, G., English, W., Hutton, M., et al. (2002). Matrix metalloproteinases in arthritic disease. *Arthritis Res.* 4 (3), S39–S49. doi:10.1186/ar572

Ossipov, M. H., Morimura, K., and Porreca, F. (2014). Descending pain modulation and chronification of pain. *Curr. Opin. Support Palliat. Care* 8 (2), 143–151. doi:10.1097/SPC.0000000000000055

Paul, A. K., Smith, C. M., Rahmatullah, M., Nissapatorn, V., Wilairatana, P., Spetea, M., et al. (2021). Opioid analgesia and opioid-induced adverse effects: a review. *Pharm. (Basel)* 14 (11), 1091. doi:10.3390/ph14111091

Poole, A. R., Kobayashi, M., Yasuda, T., Laverty, S., Mwale, F., Kojima, T., et al. (2002). Type II collagen degradation and its regulation in articular cartilage in osteoarthritis. *Ann. Rheum. Dis.* 61 (2), ii78–ii81. doi:10.1136/ard.61.suppl_2.ii78

Raja, S. N., Carr, D. B., Cohen, M., Finnerup, N. B., Flor, H., Gibson, S., et al. (2020). The revised International Association for the Study of Pain definition of pain: concepts, challenges, and compromises. *Pain* 161 (9), 1976–1982. doi:10.1097/j.pain.0000000000001939

Sasaki, M., Obata, H., Kawahara, K., Saito, S., and Goto, F. (2006). Peripheral 5-HT2A receptor antagonism attenuates primary thermal hyperalgesia and secondary mechanical allodynia after thermal injury in rats. *Pain* 122 (1-2), 130–136. doi:10.1016/j.pain.2006.01.021

Schwarcz, R., Bruno, J. P., Muchowski, P. J., and Wu, H.-Q. (2012). Kynurenines in the mammalian brain: when physiology meets pathology. *Nat. Rev. Neurosci.* 13 (7), 465–477. doi:10.1038/nrn3257

Shi, B., Guo, X., Iv, A., Zhang, Z., and Shi, X. (2022). Polymorphism of MMP-3 gene and imbalance expression of MMP-3/TIMP-1 in articular cartilage are associated with an endemic osteochondropathy, Kashin- Beck disease. *BMC Musculoskelet. Disord.* 23 (1), 3. doi:10.1186/s12891-021-04952-9

Staats Pires, A., Tan, V. X., Heng, B., Guillemin, G. J., and Latini, A. (2020). Kynurenine and tetrahydrobiopterin pathways crosstalk in pain hypersensitivity. *Front. Neurosci.* 14, 620. doi:10.3389/fnins.2020.00620

Sufka, K. J., Schomburg, F. M., and Giordano, J. (1992). Receptor mediation of 5-HT-induced inflammation and nociception in rats. *Pharmacol. Biochem. Behav.* 41 (1), 53–56. doi:10.1016/0091-3057(92)90058-n

Suzuki, K., Miyamoto, M., Miyamoto, T., Numao, A., Suzuki, S., Sakuta, H., et al. (2015). Sleep apnoea headache in obstructive sleep apnoea syndrome patients presenting with morning headache: comparison of the ICHD-2 and ICHD-3 beta criteria. *J. Headache Pain* 16, 56. doi:10.1186/s10194-015-0540-6

Suzuki, R., Rygh, L. J., and Dickenson, A. H. (2004). Bad news from the brain: descending 5-HT pathways that control spinal pain processing. *Trends Pharmacol. Sci.* 25 (12), 613–617. doi:10.1016/j.tips.2004.10.002

Taiwo, Y. O., and Levine, J. D. (1992). Serotonin is a directly-acting hyperalgesic agent in the rat. *Neuroscience* 48 (2), 485–490. doi:10.1016/0306-4522(92)90508-y

Tanaka, M., Török, N., Tóth, F., Szabó, Á., and Vécsei, L. (2021). Co-players in chronic pain: neuroinflammation and the tryptophan-kynurenine metabolic pathway. *Biomedicines* 9 (8), 897. doi:10.3390/biomedicines9080897

Taylor, B. K., and Basbaum, A. I. (1995). Neurochemical characterization of extracellular serotonin in the rostral ventromedial medulla and its modulation by noxious stimuli. *J. Neurochem.* 65 (2), 578–589. doi:10.1046/j.1471-4159.1995.65020578.x

Teckchandani, S., Nagana Gowda, G. A., Raftery, D., and Curatolo, M. (2021). Metabolomics in chronic pain research. *Eur. J. Pain* 25 (2), 313–326. doi:10.1002/ejp.1677

Terpos, E., Politou, M., and Rahemtulla, A. (2005). The role of markers of bone remodeling in multiple myeloma. *Blood Rev.* 19 (3), 125–142. doi:10.1016/j.blre.2004.06.001

Thacker, M. A., Clark, A. K., Marchand, F., and McMahon, S. B. (2007). Pathophysiology of peripheral neuropathic pain: immune cells and molecules. *Anesth. Analg.* 105 (3), 838–847. doi:10.1213/01.ane.0000275190.42912.37

The, L. (2021). Rethinking chronic pain. *Lancet* 397 (10289), 2023. doi:10.1016/s0140-6736(21)01194-6

Trelle, S., Reichenbach, S., Wandel, S., Hildebrand, P., Tschannen, B., Villiger, P. M., et al. (2011). Cardiovascular safety of non-steroidal anti-inflammatory drugs: network meta-analysis. *BMJ* 342, c7086. doi:10.1136/bmj.c7086

Venkatesh, M., Mukherjee, S., Wang, H., Li, H., Sun, K., Benechet, A. P., et al. (2014). Symbiotic bacterial metabolites regulate gastrointestinal barrier function via the xenobiotic sensor PXR and Toll-like receptor 4. *Immunity* 41 (2), 296–310. doi:10.1016/j.immuni.2014.06.014

Wei, F., Dubner, R., Zou, S., Ren, K., Bai, G., Wei, D., et al. (2010). Molecular depletion of descending serotonin unmasks its novel facilitatory role in the development of persistent pain. *J. Neurosci.* 30 (25), 8624–8636. doi:10.1523/JNEUROSCI.5389-09.2010

Wei, G. Z., Martin, K. A., Xing, P. Y., Agrawal, R., Whiley, L., Wood, T. K., et al. (2021). Tryptophan-metabolizing gut microbes regulate adult neurogenesis via the aryl hydrocarbon receptor. *Proc. Natl. Acad. Sci. U. S. A.* 118 (27), e2021091118. doi:10.1073/pnas.2021091118

Wirthgen, E., Hoeflich, A., Rebl, A., and Günther, J. (2017). Kynurenic acid: the janus-faced role of an immunomodulatory tryptophan metabolite and its link to pathological conditions. *Front. Immunol.* 8, 1957. doi:10.3389/fimmu.2017.01957

Wishart, D. S. (2016). Emerging applications of metabolomics in drug discovery and precision medicine. *Nat. Rev. Drug Discov.* 15 (7), 473–484. doi:10.1038/nrd.2016.32

Xue, C., Li, G., Zheng, Q., Gu, X., Shi, Q., Su, Y., et al. (2023). Tryptophan metabolism in health and disease. *Cell Metab.* 35 (8), 1304–1326. doi:10.1016/j.cmet.2023.06.004

frontiers | Frontiers in Neurology

TYPE Original Research
PUBLISHED 23 August 2024
DOI 10.3389/fneur.2024.1335356

OPEN ACCESS

EDITED BY
Francesca Guida,
University of Campania Luigi Vanvitelli, Italy

REVIEWED BY
Joanna Dietzel,
Charité University Medicine Berlin, Germany
Frauke Musial,
UiT The Arctic University of Norway, Norway
MingCheng Huang,
China Medical University Hospital, Taiwan
Geng-Hao Liu,
Chang Gung University, Taiwan

*CORRESPONDENCE
Petra Baeumler
petra.baeumler@med.uni-muenchen.de

RECEIVED 01 December 2023
ACCEPTED 05 August 2024
PUBLISHED 23 August 2024

CITATION
Baeumler P, Schäfer M, Möhring L and Irnich D (2024) Temporal summation does not predict the acupuncture response in patients with chronic non-specific low back pain.
Front. Neurol. 15:1335356.
doi: 10.3389/fneur.2024.1335356

Temporal summation does not predict the acupuncture response in patients with chronic non-specific low back pain

Petra Baeumler*, Margherita Schäfer, Luise Möhring and Dominik Irnich

Multidisciplinary Pain Center, Department of Anaesthesiology, LMU University Hospital, LMU Munich, Munich, Germany

Introduction: Previously, we had observed that immediate pain reduction after one acupuncture treatment was associated with high temporal summation of pain (TS) at a pain free control site and younger age in a mixed population of chronic pain patients. The aim of the present study was to verify these results in chronic non-specific low back pain (LBP) and to collect pilot data on the association between TS and the response to an acupuncture series.

Methods: TS at a pain free control site (back of dominant hand) and at the pain site was quantified by the pin-prick induced wind-up ratio (WUR) in 60 LBP patients aged 50 years or younger. Response to one acupuncture treatment was assessed by change in pain intensity and pressure pain threshold (PPT) at the pain site. The primary hypothesis was that a high TS (WUR > 2.5) would be associated with a clinically relevant reduction in pain intensity of at least 30%. In study part two, 26 patients received nine additional treatments. Response to the acupuncture series was assessed by the pain intensity during the last week, the PPT and the Hannover functional ability questionnaire (FFbH-R).

Results: An immediate reduction in pain intensity of at least 30% was frequent irrespective of TS at the control site (low vs. high TS 58% vs. 72%, $p = 0.266$). High TS at the pain site was also not significantly associated with a clinically relevant immediate reduction in pain intensity (low vs. high TS 46% vs. 73%, $p = 0.064$). The PPT was not changed after one acupuncture treatment. Study part two did not reveal a consistent association between TS at the control site and any of the outcome measures but also a trend toward a higher chance for a clinically relevant response along with low TS at the pain site.

Conclusion: Our results do not suggest an important role of TS for predicting a clinically important acupuncture effect or the response to a series of 10 acupuncture treatments in patients with chronic non-specific LBP. Overall high response rates imply that acupuncture is a suitable treatment option for LBP patients irrespective of their TS.

KEYWORDS

quantitative sensory testing, responder, central sensitization, wind-up ratio, cohort study, predictor, chronic pain

1 Introduction

Acupuncture is used worldwide (1), with growing popularity (2–4). High quality randomized controlled trials support its effectiveness in the treatment of chronic pain (5). However, as for pharmacological pain management, just around half of chronic pain patients treated with acupuncture experience a clinically relevant improvement (6). In order to minimize adverse outcomes through ineffective pain treatment, the identification of patient characteristics that predict the effectiveness of acupuncture appears crucial. In the past, sociodemographic characteristics, disease severity and expectations of treatment outcomes have been studied the most, but revealed no substantial predictive value (7–11). Thus, the question arises whether response to acupuncture can be predicted on the basis of neurophysiological considerations. The analgesic effects of acupuncture involve local, segmental and central mechanisms (12–14). When it comes to treating chronic pain, the potential of acupuncture to modulate central sensitization processes seems to play an eminent role (15, 16). Consequently, we hypothesized that chronic pain patients with particularly pronounced signs of central sensitization might profit the most from acupuncture.

Elevated temporal summation of pain (TS) is a characteristic sensory sign in various chronic pain conditions that indicates facilitation of the ascending pain pathway (17–20). TS describes the increase of the perceived pain intensity during repetitive application of uniform pain stimuli. This usual physiological phenomenon arises from rapid facilitation of spinal synaptic transmission (also termed wind-up), and permanent augmentation of synaptic strength between nociceptive afferents and spinal projection neurons in chronic pain states can result in elevated TS (21). Various types of noxious stimuli can be used to elicit TS. In their validated and standardized protocol for quantitative sensory testing the German Research Network on Neuropathic Pain implemented the so called wind-up ratio (WUR) – the ratio of the pain intensity elicited by ten uniform pin-prick stimuli over the pain intensity elicited by one pin-prick stimulus (22).

Indeed, one of our previous studies showed a positive association between the pin-prick induced TS at a pain free control site and the immediate analgesic response to acupuncture in a mixed patient population suffering from different chronic pain conditions (23). Furthermore, we observed an independent impact of age. Conversely, results of this study did not support a robust relationship between the immediate response to acupuncture and the TS at the most painful body site.

The aim of the present study was to verify the association between high TS at a pain free control site and the immediate response to acupuncture in a patient population with a specific pain condition, namely chronic non-specific low back pain (LBP). A secondary aim of this study was to collect pilot data about potential associations between the TS at a pain free control site and the pain site at the lower back with the response to a series of ten acupuncture treatments.

LBP was chosen for the following reasons: First, LBP is one of the most frequent chronic pain conditions (24–27), and a large part of LBP is non-specific with central sensitization processes constituting an important component of chronic LBP (28, 29). Second, acupuncture is recommended for its treatment (30, 31) while not negating limitations of the existing evidence (32). Third, as for other chronic pain conditions responder rates among chronic LBP patients after acupuncture have been estimated to be around 50% (33).

In addition to pain intensity, the pressure pain threshold (PPT) at the lower back and LBP related functional disability were chosen as additional outcome measures in the present study to further objectify our findings. The PPT at the lower back of LBP patients has been shown to be reduced in comparison to healthy controls (34, 35). Furthermore, the PPT has been shown to be reliably increased by acupuncture in healthy subjects and pain patients (36, 37); particularly in LBP patients either through dry needling of myofascial trigger points or through needling at traditional acupuncture points (38–42).

2 Methods

2.1 Study design

Aim of this prospective cohort study was to evaluate whether the previously identified association between high TS and the immediate pain relief through acupuncture in a mixed population of patients suffering from different chronic pain conditions (23) can be confirmed in a more narrowly defined population of patients with chronic non-specific LBP. Due to the impact of age on this association observed in the previous study, patients age in this trial was restricted to 50 years or younger. The acupuncture treatments followed a semi-standardized regimen used in the large German acupuncture trials on LBP (43). The immediate acupuncture effect was evaluated by assessing the current pain intensity and the PPT at the pain site before and directly after treatment. An immediate reduction of the pain intensity of at least 30% was defined as the primary outcome measure. Before acupuncture treatment, an independent examiner assessed TS as the pin-prick induced WUR at the pain site and at the dorsum of the dominant hand which served as a control site. Examiners assessing the outcome measures were blinded for the patients' TS.

Additionally, the second part of this study was designed to collect data about whether TS might also predict the treatment effect of a whole acupuncture series. Therefore, the study protocol foresaw that two subgroups of patients with high TS (WUR $\geq$ 3.5) and low TS (WUR $\leq$ 2.0) at the control site would receive nine additional acupuncture treatments (ten treatments in total over four weeks with a maximum of three treatments per week). Against the protocol, four patients with a WUR between 2.6 and 3.0 were accidently also included in this second study part. The treatment effect of the whole acupuncture series was evaluated by assessing the pain intensity and back pain-related disability (Hannover functional ability questionnaire, FFbHR) during the last week before inclusion and in the week after the last acupuncture treatment. Additionally, the PPT was again assessed at the last study visit 1 week after treatment termination. As in study part one, examiners performing the outcome assessments were blinded against the patients' TS.

2.2 Patients

General inclusion criteria were age between 18 and 50 years, good command of the German language and written informed consent. The restriction to adult patients aged 50 years or younger was based on our previous observation, that the association between TS and the acupuncture response was most pronounced in this age group (23).

Specific inclusion criteria were the diagnosis of chronic non-specific LBP as defined by the German National Disease Management Guideline [*Nationale Versorgungsleitline nicht-spezifischer Kreuzschmerz* (44)] with the main pain site being located in the segments L1 to L5, a pain duration of more than three months and an average pain intensity during the week prior to inclusion of over 40 on a 100 mm visual analog scale (VAS). Exclusion criteria were specific LBP, acute necessity of further diagnostic or therapeutic procedures, previous back/spine surgery, malignant rheumatoid or chronic inflammatory diseases, severe psychiatric disorders, previous major depression, pregnancy, regular intake of opioids, antidepressants or anticonvulsants, acute or chronic complaints at the hands and acupuncture within the last 6 months.

Patients were recruited through information sheets displayed in pharmacies and primary care facilities (private medical and physiotherapist practices), posters displayed at the Munich railway station and in employee facilities of the University Hospital LMU Munich. In addition, notifications about the study were sent twice to an LMU e-mail distribution list of voluntary recipients. Interested patients were first screened per telephone. Remaining patients were invited to the study center. After written informed consent was obtained, patients were subjected to an initial medical examination during which the diagnosis of specific or non-specific LBP was established through evaluation of red flags, and the necessity of immediate further diagnostic or therapeutic procedures was determined.

2.3 Intervention

Acupuncture treatments were performed by experienced acupuncturists, who were medical doctors with at least 300 hours of acupuncture training and at least ten years of acupuncture practice. Treatments followed a semi-standardized protocol corresponding to the acupuncture regimen applied in the large health insurance sponsored German acupuncture trials (43). This regimen combines obligatory and facultative points. Out of 27 local/segmental points (BL 20 to BL 34, BL50 to BL 54, GB 30, GV 3, GV 4, GV 5, GV 6, EX-B 2, EX-B 9) at the lower back, at least four had to be chosen and needled bilaterally (except for governor vessel points). In case of pseudoradicular symptomatology two further local points were supposed to be selected. Furthermore, out of twelve distal points (SI 3, BL 40, BL 60, BL 62, KI 3, KI 7, GB 31, GB 34, GB 41, LR 3, GV 14, GV 20) at least two were to be selected and needled bilaterally; except for governor vessel (GV) points. Thus, depending on the presence of a pseudoradicular symptomatology the minimum number of obligatory needles was twelve or 16, respectively. Acupuncturists were free to choose further body or microsystem points, but the total number of needles was not supposed to exceed 20. Acupuncture points were selected according to a thorough TCM anamneses performed before the first treatment and adjusted according to the patients' reactions during the subsequent treatments. Acupuncturists were free to choose needle size and to stimulate the needles either manually by rotation or up and down movement or electrically with Han-frequency. Needle stimulation was adjusted to be intense but not painful. At each needle insertion elicitation of deqi was intended but not forced. Resting time with needles in place was 25 minutes at minimum. Acupuncture treatment was initiated at the day of inclusion in all but one case who received the first acupuncture treatment on the day subsequent to inclusion. In case of participation in the second study part patients received ten acupuncture treatments in total within four weeks with a maximum of three treatments per week. Adverse events were documented by the acupuncturists and examiners. Patients were queried before each treatment about eventual adverse events related to the previous acupuncture and after each treatment about adverse events of the recent acupuncture.

2.4 Outcome measures and predictor variables

2.4.1 Pain intensity

The primary outcome was the occurrence of a reduction in current pain intensity of at least 30% immediately after one acupuncture treatment which was shown to represent a clinically meaningful pain relief (45). According to recommendations of the US Initiative on Methods, Measurement, and Pain Assessment in Clinical Trials [IMMPACT (46, 47)] the occurrence of a reduction in current pain intensity of at least 50% was also reported. Pain intensity was evaluated by means of a 100 mm VAS (0 = no pain, 100 = maximum imaginable pain). The current pain intensity was determined directly before and after the first acupuncture treatment always prior to the assessment of the PPT and the TS.

The average pain intensity during the week prior to inclusion was determined in the course of the verification of in- and exclusion criteria on the day of inclusion. In case of participation in the second study part the average pain intensity during the week after treatment termination was assessed on a separate study visit. For the reduction in the average pain intensity during the last week, it was also documented whether it attained at least 30% or 50%, respectively.

Percent changes in pain intensity were calculated as follows with negative percent changes indicating an improvement.

$$\%\Delta VAS = \frac{\left(VAS_{post} - VAS_{baseline}\right)}{VAS_{baseline}} * 100$$

2.4.2 Pressure pain threshold

The pressure pain threshold (PPT) was determined at the most painful segment at the lower back (two finger breadths lateral to the spinous process). PPT assessments adhered to the protocol of quantitative sensory testing established by the German Research Network on Neuropathic Pain (22). Pressure was applied by a Fisher-algometer (FDK20, 2–10 kg/cm2, Wagner Instruments, Greenwich, CT, United States). The force was increased by 0.5 kg/cm^2 per second until the patients indicated the onset of pressure pain. The arithmetic mean of three measurements were calculated to represent the final PPT score. Time points of PPT assessments were before and after the first acupuncture treatment as well as one week after the tenth acupuncture treatment in patients taking part in the second study part. In accordance with the definition of a clinically relevant pain relief, we also documented whether the PPT had increased by at least 30% at the two time points in comparison to baseline. A 30%

elevation of the PPT appears clinically relevant according to following consideration: The PPT at paravertebral measure sites at the lower back in LBP patients has been estimated to lie around 3 kg/cm^2 (35). Thus, a 30% elevation would correspond to 1.05 kg/cm^2. Changes of this magnitude were observed after dry needling at similar measure sites in LBP patients (42) as well as in one of our own previous trials after segmental needling at the leg in healthy volunteers (36).

Percent changes in the PPT were calculated as follows:

$$\%\Delta PPT = \frac{\left(PPT_{post} - PPT_{baseline}\right)}{PPT_{baseline}} * 100 .$$

As higher thresholds indicate that higher pressure is required to elicit pain, positive percent changes indicate an improvement.

2.4.3 Hannover functional ability questionnaire

The FFbH-R is a twelve-item questionnaire quantifying the functional ability in activities of daily living among patients with LBP with satisfactory internal consistency, high test–retest reliability and sensitivity to change (48, 49). Items are scored on a three-point scale (2 = performance of task without difficulties; 1 = performance of task with difficulties; 0 = performance of task only with help from others). The final FFbH-R score is calculated according to Kohlmann and Raspe (48) by rescaling the mean of all valid items to a score between 0% (worst functional ability) and 100% (best functional ability). Patients filled out the FFbHR before the first acupuncture treatment and in study part two at the follow-up visit one week after termination of the tenth acupuncture treatment.

As for the other outcomes, cases were categorized in those with a 30% or larger improvement and those with less than 30% improvement. Percent changes in the FFbHR score were calculated as follows:

$$\%\Delta \mathrm{FFbHR} = \frac{\left(\mathrm{FFbHR}_{post} - \mathrm{FFbHR}_{baseline}\right)}{\mathrm{FFbHR}_{baseline}} * 100 .$$

As higher scores indicate better functioning, positive percent changes indicate an improvement.

2.4.4 Temporal summation

Temporal summation (TS) was quantified by the pin-prick induced wind-up ratio (WUR) according to the protocol of quantitative sensory testing established by the German Research Network on Neuropathic Pain (22). The WUR is calculated as the ratio of the pain rating evoked by ten pin-prick stimuli over the pain rating evoked by one pin-prick stimulus. The pin-prick evoked pain is rated on a verbal rating scale (0–100). We calculated the mean of three WUR assessments conducted at an interval of five minutes each at the control site (dorsum of the dominant hand) and at the pain site (two finger breadths lateral to the spinous process). To avoid an impact of the TS assessments on the subsequent PPT assessments at the pain site, patients were asked to wait and relax for 15 min between the two tests. Pin-pricks (MRC Systems GmbH-Medizintechnische Systeme, Heidelberg, Germany) of either 128, 256, or 512 mN were used according to the patient's sensitivity in the respective measurement area. Floor and ceiling effects were thereby omitted.

2.4.5 Patient characteristics

On the day of inclusion the patients' age, sex, pain duration and current medication were documented.

2.5 Biometry

2.5.1 Sample size calculation

The sample size estimation was based on the results of our previous study among patients below the age of 53 years (23). We anticipated a percentage of patients with high TS of 40%, an average responder rate of 44% and an odds ratio (OR) of 4.5 for the association between clinically relevant acupuncture response and high TS. A sample size calculation based on these parameters, a power of 80% and an alpha error of 5% resulted in 56 required patients which we rounded to 60 in order to account for drop-outs.

2.5.2 Data analysis

Due to the skewed distributions of some continuous variables, descriptive statistics are presented in this manuscript as medians and interquartile ranges. Categorical variables are presented as absolute and relative frequencies. Differences between outcomes at baseline and at follow-up time points were evaluated by the Wilcoxon rank sum test.

As described above, outcomes were dichotomized at a cut-off of ≥30% improvement reflecting a clinically relevant change. The percent change of the current pain intensity was also dichotomized at a cut-off of ≥50%. According to the primary study hypothesis based on our previous study, TS at the control and the pain site was categorized into high WUR (>2.5) and low WUR (≤2.5). Logistic regression models were used to assess whether high TS at the control or pain site predicted the likelihood to experience a clinically relevant immediate response to one acupuncture treatment as indicated by the dichotomized outcomes. In order to assess potential confounding the following patient characteristics were included as covariates: age and sex, use of analgesics, pain duration, baseline pain intensity (current and during last week before inclusion), baseline PPT and baseline FFbHR scores. Separate models were used in order to avoid multicollinearity. Adjusted analyses were omitted for mutually exclusive categories.

The Mann–Whitney-U test was used to compare percentage changes in outcomes between patients with high and low TS. Comparisons of baseline values and patient characteristics between patients with and without a clinically relevant pain relief after one or ten acupuncture treatments, respectively, were conducted by Mann–Whitney-U test for continuous variables and by Fisher's test for dichotomous variables.

The relationship between percent changes in outcome variables and TS at the control and pain site in their uncategorized, continuous form were explored graphically in scatter plots and by generalized linear models implementing maximum likelihood estimation and an identity link function. The WUR and the PPT approached a log-normal distribution and were thus log-transformed before inclusion in GLM-models.

The pilot data collected in the second study part on the relationship between the responses to a series of ten acupuncture treatments and TS at the control and the pain site were only descriptively analyzed. These data were used to calculate the sample sizes that would be required in eventual confirmatory trials on the predictive value of TS for the response to acupuncture.

2.6 Ethics

The present investigation was approved by the Ethics Committee of the Medical Faculty of the Ludwig-Maximilians University (LMU),

Munich, Germany and was performed in accordance with the declaration of Helsinki (50). Data management and storage adhered to the German data-protection act. Study data were pseudonymized and are kept separate from personal information in the research facilities of the Multidisciplinary Pain Center, Department of Anaesthesiology, LMU University Hospital, LMU Munich, Germany for ten years. All participating patients gave voluntary written informed consent and were free to withdraw from the study at any point. Patients were remunerated with 40 Euro for completion of study part one and with 85 Euro for completion of study part two. Patients who visited the study center for the screening visit, but did not meet in- or exclusion criteria were compensated with ten Euro.

3 Results

3.1 Patient characteristics

In total 433 patients were screened. Reasons for non-inclusion are displayed in Figure 1. Sixty-three patients provided written informed

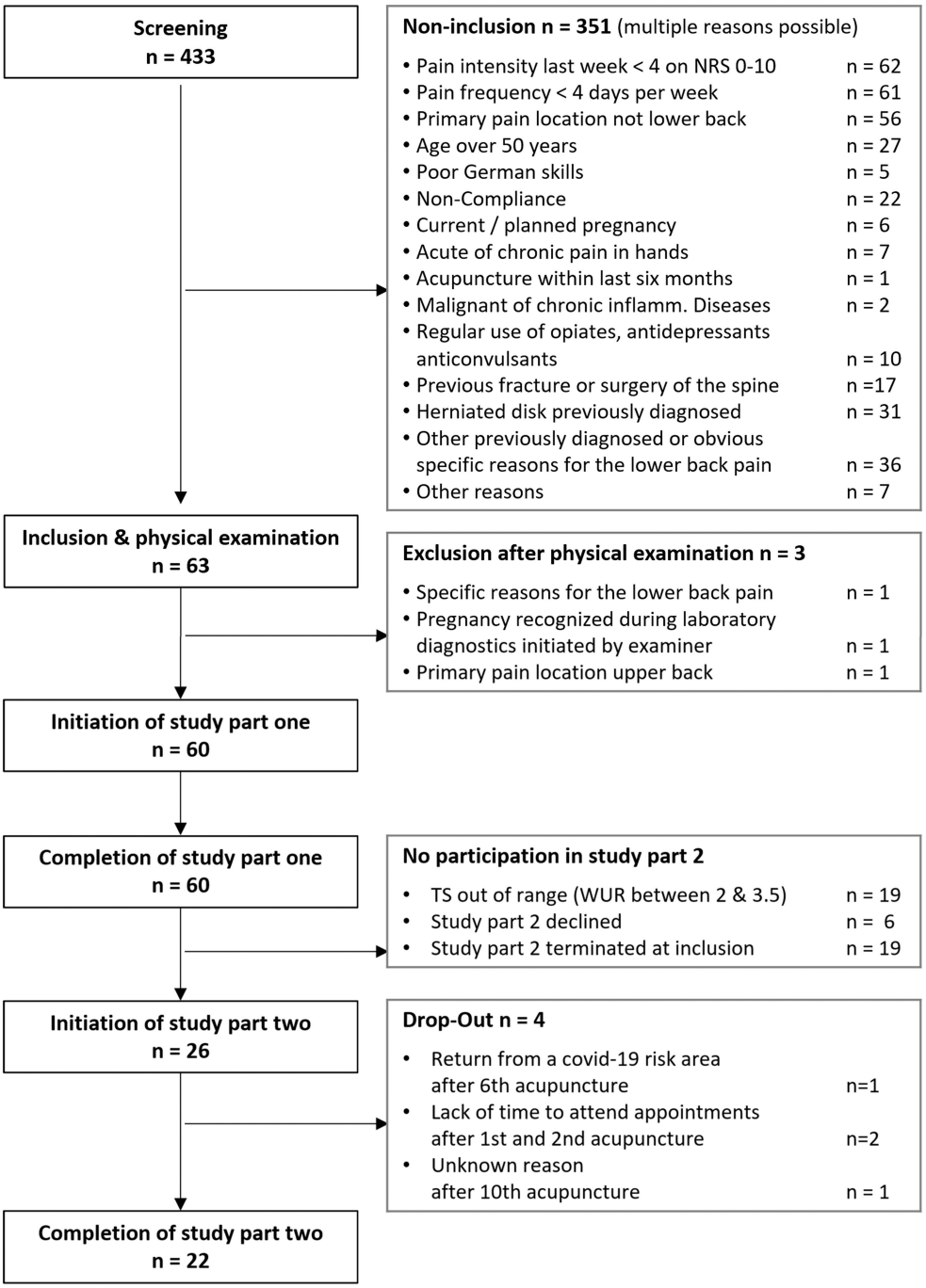

FIGURE 1
Study flow diagram.

consent to participate in the study. Three of those were excluded again after the physical examination. Thus, 60 patients were finally subjected to study part one which was completed on the day of inclusion by 59 patients and on the subsequent day by one patient. Twenty-six patients were allocated to study part two, but four dropped out before the final visit, resulting in 22 complete data sets (Figure 1).

The majority of patients were female (75%), and the median age was 26.0 years (IQR [21.0; 38.8]). Pain duration varied between four months and 32 years with a median of 45.5 months [14.3; 91.5]. Main pain was most prevalent in the segments L4 and L5 (78%) and at the right body side (69%). About a third of patients used analgesics on demand. Among those 21 patients, 17 used oral non-steroidal anti-inflammatory drugs (NSAID), three paracetamol, two metamizole and one a topical NSAID. In addition, five patients (8%) were on vitamin D or vitamin B12 supplementation and eight (13%) on thyroxine supplementation. In all but one patient, the dominant hand was the right hand that served as the control site for the determination of the TS. 1.5 cun, used to define the measure site at the back, varied between three and four centimeters with a median of 3.4 cm [3.2; 3.7]. In around half of the cases, a pin-prick of 256 mN strength was used for TS determination, in one third a pin-prick of 512 mN. Median TS as evaluated by the WUR varied between 1.1 and 13.8 at the control site and between 1.0 and 7.5 at the pain site with similar medians (1.9 [1.5; 3.3] and 1.6 [1.4; 2.5]). 40% of patients exhibited a WUR of over 2.5 at the control site and 25% showed a WUR over 2.5 at the pain site. Characteristics of patients participating in study part two resembled the total population (Table 1).

TABLE 1 Patient characteristics.

		Study part 1	Study part 2
		n = 60	*n* = 22
Age (years), median [IQR]		26.0 [21.0; 38.8]	30.5 [22.8; 43.3]
Female, *n* (%)		45 (75)	18 (82)
Pain duration (months), median [IQR]		45.5 [14.3; 91.5]	48.5 [14.5; 96.3]
Segment of main pain, *n* (%)	L1	6 (10)	2 (9)
	L2	3 (5)	0
	L3	4 (7)	2 (9)
	L4	23 (38)	8 (36)
	L5	24 (40)	10 (45)
Body side of main pain, *n* (%)	Left	18 (31)	7 (32)
	Right	40 (69)	15 (68)
Analgesic medication, *n* (%)		21 (35)	5 (23)
Vitamin D or B12, *n* (%)		5 (8)	2 (9)
Thyroxine, *n* (%)		8 (13)	5 (23)
Dominant hand, *n* (%)	Left	1 (2)	0
	Right	59 (98)	22 (100)
2 finger breadths (cm), median [IQR]		3.4 [3.2; 3.7]	3.4 [3.2; 3.7]
Pin-prick for TS assessment control site, *n* (%)	128 mN	8 (13)	2 (9)
	256 mN	32 (53)	10 (45)
	512 mN	20 (33)	10 (45)
Pin-prick for TS assessment pain site, *n* (%)	128 mN	11 (18)	4 (18)
	256 mN	31 (52)	12 (55)
	512 mN	18 (30)	6 (27)
TS as WUR (NRS-ratio), median [IQR]	Control site	1.9 [1.5; 3.3]	1.9 [1.6; 3.5]
	Pain site	1.6 [1.4; 2.5]	1.6 [1.4; 2.6]
High TS (WUR > 2.5), *n* (%)	Control site	24 (40)	10 (45)
	Pain site	15 (25)	5 (23)

IQR, interquartile range; cm, centimeters; mN, millinewton; TS, pin-prick induced temporal summation of pain as evaluated by the wind-up ratio (WUR) with WUR calculated as pain intensity on the numeric rating scale (NRS 0–100) evoked by 10 stimuli divided by pain intensity evoked by one stimulus (high TS (WUR > 2.5) indicates central sensitization).

3.2 Treatment characteristics

Of the 273 acupuncture treatments conducted, 264 (97%) were in accordance with the semi-standardized protocol. At the discretion of the acupuncturist, the number of needles was reduced in six treatments and increased in three treatments. The number of needles per acupuncture session varied between 13 and 22. The median number of needles was 19 (IQR [18; 20], min-max [13–22]). Points most commonly used in the first treatment resembled those most commonly used in the subsequent treatments (Supplementary Table 1). Most common points out of the set for obligatory points were BL 23, BL 25, BL 40, GB 34, and KID 3. These were used in over 50% of the initial acupuncture treatments; BL 23 and BL25 even in 90% of treatments. Obligatory points needled in at least 30% to 50% of all initial treatments were BL 27, LR 3, GV 4, BL 26, and BL 24. Most commonly treated facultative points (30% to 63% of treatments) were microsystem points at the ear, namely the ear zone for the lumbar spine as well as the ear points Shenmen and Jerome. Most commonly used needles had a diameter of 0.2 mm (63% of all needles), followed by 0.3 mm diameter needles (29%) and 0.16 mm diameter needles (8%). In single cases also smaller needles (diameter 0.15 or 0.12 mm) were used. In all treatments acupuncturists decided not to use electrical needle stimulation.

Twenty six patients reported a total of 42 adverse events during or following 35 treatments. All adverse events resolved latest within the next days. None of the patients discontinued treatment or withdrew from the study because of adverse events. Most frequently reported events were small haematoma ($n=6$) and bleeding ($n=4$) at the needling site, pain after needle insertion ($n=5$) or after needle withdrawal ($n=8$), transient paraesthesia after needle withdrawal ($n=6$) and vertigo directly after treatment ($n=5$). Adverse events that occurred once during or following one of the acupuncture treatments were an emotional reaction with crying, a cramp in the plantar part of the foot, muscular tension in the area of the sacroiliac joint, flatulence with diarrhea, nausea, transient aggravation of symptoms and vertigo on the first post-treatment day. None of the adverse events were serious or required treatment.

3.3 Change in outcome measures over time

Change in outcome measures over time are depicted in Table 2. Current pain was significantly reduced immediately after the first acupuncture treatment, as was the average pain intensity during the last week evaluated one week after the tenth treatment. Two thirds of patients

10.3389/fneur.2024.1335356

TABLE 2 Change in outcome measures over time.

Time point	Current pain VAS (0–100) median [IQR]	Pain last week VAS (0–100) median [IQR]	PPT kg/cm² median [IQR]	FFbHR (0–100) Median [IQR]
Study part 1 *n* = 60				
Baseline (t0)	45.0 [33.0; 55.0]	58.5 [50.0; 62.8]	3.4 [2.3; 4.4]	83.3 [75.0; 91.7]
Post 1st acu (t1)	25.5 [9.3; 34.8]	-	3.3 [2.2; 4.8]	-
p-value	<0.001*	-	0.466	-
Crude change Δt0–t1	−17.5 [−32.8; −5.5]	-	−0.2 [−0.5; 0.5]	-
Percent change %Δt0–t1	−47.2 [−75.3; −17.8]	-	−5.8 [−15.6; 14.3]	-
Study part 2 *n* = 22				
Baseline (t0)	44.5 [33.8; 55.5]	60.5 [49.8; 65.8]	3.5 [2.1; 4.3]	81.3 [72.9; 87.5]
1w after 10th acu (t2)	-	19.5 [11.5; 39.5]	4.0 [2.5; 5.7]	89.6 [83.3; 100.0]
p-value	-	< 0.001*	0.006*	0.014*
Crude change Δt0–t2	-	−35.5 [−43.3; −22.3]	0.7 [−0.3; 1.8]	4.2 [−1.0; 20.8]
Percent change %Δ t0–t2	-	−65.9 [−80.2; −35.5]	17.9 [−11.9; 39.4]	4.7 [−1.1; 26.7]

Acu, acupuncture; VAS, visual analog scale; PPT, pressure pain threshold; FFbHR, Hannover functional ability questionnaire; IQR, interquartile range; *Statistically significant change from baseline on an α-level of 5% as evaluated by the Wilcoxon rank sum test.

(67%, *n* = 40) experienced an immediate pain reduction of 30% or more and half of the patients (*n* = 30) an immediate pain reduction of 50% or more after the first acupuncture treatment. Among patients in study part two, a reduction in average pain during the last week of at least 30% or 50% was reported by 82% (*n* = 18) and 68% (*n* = 15) of patients, respectively, one week after the tenth treatment.

The PPT at the pain site remained unchanged immediately after the first acupuncture treatment, but was significantly elevated one week after the tenth treatment among patients participating in study part two. Only 13% (*n* = 8) of patients experienced an elevation of the PPT of at least 30% after the first acupuncture treatment. One week after the tenth acupuncture treatment, the PPT was elevated by at least 30% in 36% (*n* = 8) of the patients in study part two.

FFbHR scores significantly improved between baseline and one week after the tenth treatment. At baseline, 5% of the patients (*n* = 3) showed clinically relevant impairments in physical functioning (FFbHR < 60), 42% (*n* = 25) showed moderate impairments (FFbHR < 80/≥60) and 53% showed normal physical functioning (FFbHR ≥ 80) [categorization according to Kohlmann & Raspe (48)]. A similar distribution of FFbHR baseline scores was found in patients participating in study part two. One week after ten acupuncture sessions the proportion of patients with normal physical functioning had increased to 82, and 18% (*n* = 4) had experienced an increase of the FFbHR score of at least 30%.

3.4 Association between temporal summation and the immediate acupuncture response (study part one)

3.4.1 Primary endpoint: association between temporal summation at the dorsum of the hand with a clinically relevant pain relief immediately after one acupuncture treatment

In contrast to the primary study hypothesis, immediate analgesic response to one acupuncture treatment was not positively associated with high TS at the dorsum of the hand (control site). The chance to experience a reduction of the current pain intensity of at least 30% or 50% did not differ significantly between patients with a high TS (WUR > 2.5) and low TS (WUR ≤ 2.5) at the control site (Table 3). A 30% reduction in current pain was experienced by 72% of patients with a low TS and by 58% of patients with a high TS at the control site (OR [95%-CI] 0.54 [0.18; 1.60], $p = 0.266$). The proportions of patients with a 50% reduction in current pain were 53% among patient with low TS and 46% among patients with high TS, respectively (OR [95%-CI] of 0.76 [0.27; 2.13], $p = 0.598$). Adjusted logistic regression analyses did not indicate any change in OR estimates neither through age, sex, pain duration, use of analgesics, baseline current pain, pain during the week before inclusion, baseline PPT nor through the baseline FFbHR score (Supplementary Table 2).

The cumulative response function illustrates that, irrespective of the responder definition, responder rates after one acupuncture treatment of patients with high and low TS at the control site did not differ importantly (Figure 2A). Likewise, the median percentage change in current pain intensity did not differ between patients with low and high TS at the control site (−50.0% [−74.2%; −23.6%] vs. −36.2% [−77.2%; −1.1%], MW-test $p = 0.478$).

3.4.2 Secondary endpoints for associations between temporal summation and immediate effects of one acupuncture treatment

High TS at the pain site was also not significantly associated with a clinically relevant immediate reduction of current pain intensity after the first acupuncture treatment. There was only a non-significant trend toward a higher chance for a reduction of the current pain intensity of at least 30% in patients with a low TS at the pain site (WUR ≤ 2.5) than in patients with a high TS at the pain site (WUR > 2.5); 73% vs. 46% (Table 3). This trend also remained in the adjusted logistic regression analyses (Supplementary Table 2). The cumulative response function also illustrates that higher responder rates among patients with a low TS at the pain site occurred largely

TABLE 3 Differences of response to first acupuncture between patients with a high and low temporal summation.

After 1st acupuncture		WUR ≤ 2.5	WUR > 2.5	OR [95%-CI]	*p*-value
		TS at control site		**Log regression**	
%Δ VAS	No	10	10	0.54 [0.18; 1.60]	0.266
≥30%	Yes	26	14		
%Δ VAS	No	17	13	0.76 [0.27; 2.13]	0.598
≥50%	Yes	19	11		
%Δ PPT	No	31	21	0.89 [0.19; 4.11]	0.877
≥30%	Yes	5	3		
		TS at pain site		**Log regression**	
%Δ VAS	No	12	8	0.32 [0.09; 1.07]	0.064
≥30%	Yes	33	7		
%Δ VAS	No	20	10	0.40 [0.12; 1.36]	0.142
≥50%	Yes	25	5		
%Δ PPT	No	37	15	Fisher's test	0.182
≥30%	Yes	8	0		

TS, temporal summation as evaluated by the wind-up ratio (WUR with high TS (WUR > 2.5) indicating central sensitization); Log regression, logistic regression; OR, odds ratio; 95%-CI, 95% confidence interval; %Δ VAS, percent reduction in current pain intensity as evaluated by the visual analog scale; %Δ PPT, percent elevation in pressure pain threshold; More detailed model characteristics and covariate adjusted models are depicted in Supplementary Table 2.

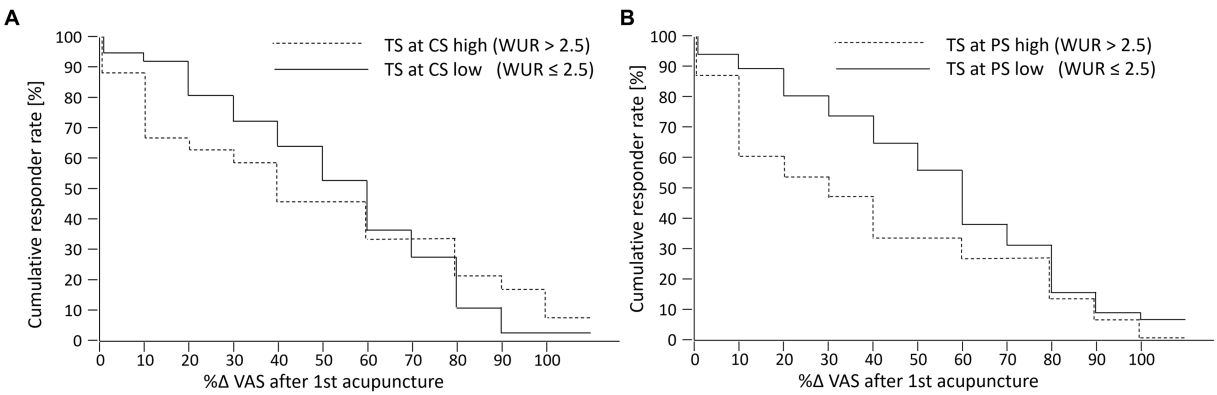

FIGURE 2
(A, B) Cumulative response function of percent change in current pain intensity after first acupuncture. TS, temporal summation as evaluated by the wind-up ratio (WUR with high TS (WUR > 2,5) indicating central sensitization); CS, control site at the dorsum of the dominant hand; PS, pain site at the lower back; %Δ; VAS, percent change in current pain intensity as evaluated by the visual analog scale (0–100).

independent from the responder definition (Figure 2B). Accordingly, the median percentage change in current pain intensity tended to be larger in patients with a low TS than patients with high TS at the pain site (−50.9% [−75.6%; −25.1%] vs. −29.3% [−70.2%; 0.0%], MW-test $p = 0.077$).

The chance for an increase of the PPT of at least 30% did not differ between patients with a high and those with a low TS at the control site (13% vs. 14%, Table 3). Logistic regression with adjustment for covariates did also not indicate that TS at the control site was associated with the likelihood for an increase in the PPT of at least 30% (Supplementary Table 2). In contrast, none of the patients with a high TS at the pain site experienced an elevation of the PPT of at least 30%, while 18% of the patients with a low TS at the pain site showed such immediate response (Table 3). The median PPT percent change did neither differ between patients with low and high TS at the control site (−12.6% [−20.3%; 6.0%] vs. 0.6% [−11.9%; 25.0%], MW-test $p = 0.083$) nor between patients with low and high TS at the pain site (−7.8% [−16.9%; 13.5%] vs. −3.4% [−13.5; 20.5], MW-test $p = 0.739$).

In Figure 3 the log-transformed WUR at the control and the pain site are plotted against the percent change in current pain intensity and PPT, respectively. Regression analysis of the total sample and the two strata with high and low TS did not reveal any significant linear relationship. Again, there was a trend toward larger reductions in the current pain intensity along with lower TS at the pain site (β [95%-CI] WUR_{log} 40.5 [−1.5; 82.5], $p = 0.059$, Figure 3C).

Patient characteristics and baseline values of outcomes did not differ between patients with a reduction in pain intensity of at least 30% or 50% and those without such response after the first acupuncture treatment (Supplementary Table 3).

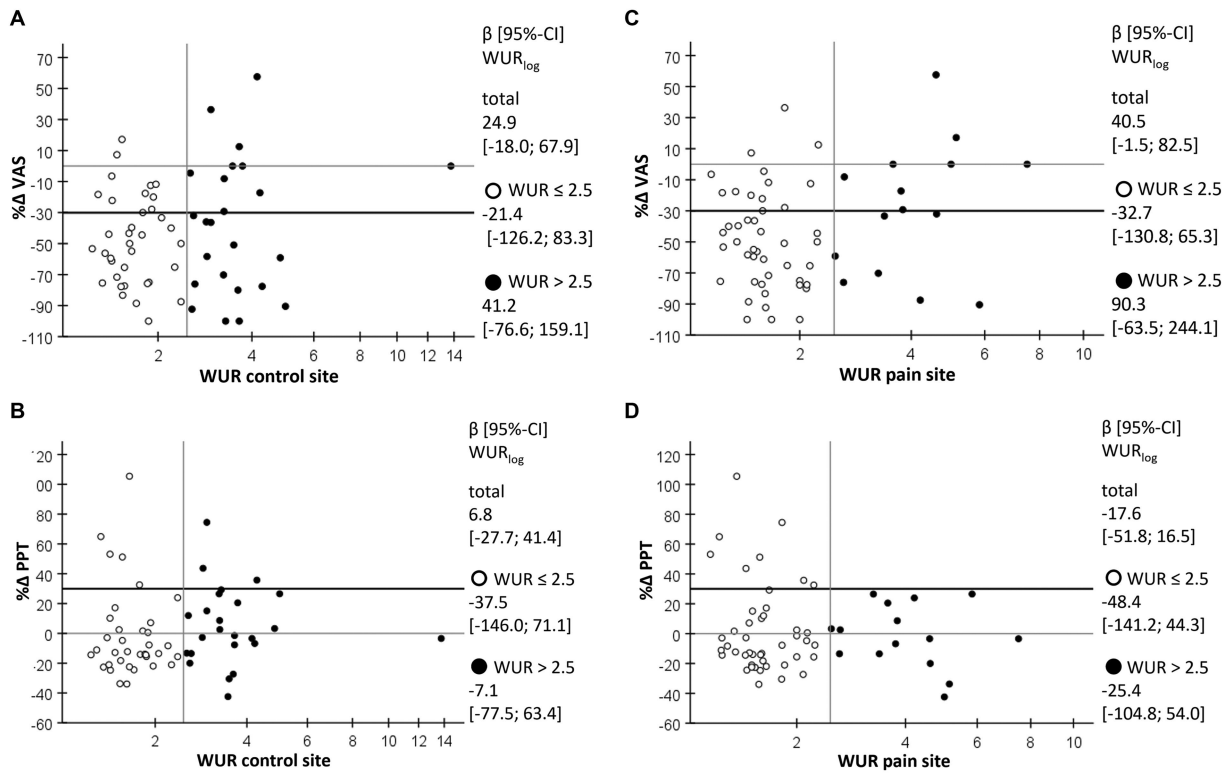

FIGURE 3
Scatterplot of percent change in outcomes after the first acupuncture against TS at the control and the pain site. **(A)** Percent change in current pain intensity (%Δ VAS) as evaluated by the visual analog scale against the wind-up ratio (WUR) as a measure for temporal summation of pain at the control site with high TS (WUR > 2.5) indicating central sensitization. **(B)** Percent change in pressure pain threshold (%Δ PPT) against the WUR at the control site. **(C)** Percent change in current pain intensity (%Δ VAS) as evaluated by the visual analog scale against the WUR at the pain site. **(D)** Percent change in pressure pain threshold (%Δ PPT) against the WUR at the pain site; empty circles, cases with WUR ≤ 2.5; filled circles, cases with WUR > 2.5; β [95%-CI] WURlog, regression coefficient of logarithmized WUR as estimated by generalized linear model.

3.5 Association between temporal summation and the response to a series of acupuncture treatments (study part two)

The second study part foresaw the inclusion of patients with a substantially low TS (WUR ≤ 2.0) and high TS (WUR ≥ 3.5) at the control site. A protocol violation caused an additional inclusion of four patients with a TS between 2.6 and 3.0 at the control site. In the following, we describe both, the per protocol (PP)-data and all patient data obtained in study part two (intention to treat (ITT)-data). Descriptive statistics of both, the ITT- and the PP-data, indicate that, patients with a low TS at the pain site showed a reduction in the pain intensity within the last week of at least 30% or 50% as well as an increase in the PPT and the FFbHR score of at least 30% more frequently than those with a high TS. Association between TS at the control site and outcomes were less clear, but all OR were also below one (Table 4).

Sample size calculations based on these pilot data (per protocol data, alpha level 0.05 and 80% power) resulted in 78 patients for the association between the likelihood of a pain reduction of at least 30% after ten acupuncture treatments with a low TS at the pain site at the lower back and in 240 patients for the association between the likelihood of a pain reduction of at least 30% after ten acupuncture treatments with a low TS at the dorsum of the hand.

The ITT-data revealed linear associations between TS a the control site and the reduction of the pain intensity (β [95%-CI] WUR_{log} 294.4 [185.8; 402.9], $p < 0.001$) as well as with the improvement in physical functioning (β [95%-CI] WUR_{log} −184.7 [−267.7; −101.7], $p < 0.000$) after ten acupuncture treatments only within the subgroup characterized by a TS at the control site of WUR > 2.5 ($n = 10$). In contrast, within patients with a WUR ≤ 2.0 ($n = 12$), response to a series of acupuncture treatments and TS was not associated. There were also no linear relationships between TS at the pain site and any of the outcomes, neither in the total sample nor in the two strata with low and high TS (Figure 4).

There were no important differences in patient characteristics and baseline values of outcomes between patients with a reduction in pain intensity of at least 30% or 50% and those without such response after a series of ten acupuncture treatments (Supplementary Table 3).

4 Discussion

The results presented here suggest, that the previously observed prediction of a clinically relevant immediate acupuncture response in young and middle aged chronic pain patients by an elevated TS (23) cannot be transferred to chronic LBP patients. Our primary hypothesis was not confirmed. We had hypothesized, that chronic LBP patients

TABLE 4 Differences of response to ten acupuncture treatment between patients with a high and low temporal summation.

		Intention to treat analysis			Per protocol analysis		
		WUR ≤ 2	WUR > 2.5	OR [95%-CI]	WUR ≤ 2	WUR ≥ 3.5	OR [95%-CI]
		TS at control site			**TS at control site**		
%Δ VAS	No	2	2	0.80 [0.09; 7.00]	2	2	0.40 [0.04; 3.90]
≥30%	Yes	10	8		10	4	
%Δ VAS	No	3	4	0.50 [0.08; 3.08]	3	4	0.17 [0.02; 1.42]
≥50%	Yes	9	6		9	2	
%Δ PPT	No	7	7	0.60 [0.10; 3.54]	7	5	0.28 [0.02; 3.19]
≥30%	Yes	5	3		5	1	
%Δ FFbHR	No	9	9	0.33 [0.03; 3.84]	9	6	
≥30%	Yes	3	1		3	0	
		TS at pain site			**TS at pain site**		
%Δ VAS	No	2	2	0.20 [0.02; 2.03]	2	2	0.17 [0.01; 1.96]
≥ 30%	Yes	15	3		12	2	
%Δ VAS	No	4	3	0.21 [0.02; 1.69]	4	3	0.13 [0.01; 1.70]
≥50%	Yes	13	2		10	1	
%Δ PPT	No	10	4	0.36 [0.03; 3.92]	8	4	
≥30%	Yes	7	1		6	0	
%Δ FFbHR	No	13	5		11	4	
≥30%	Yes	4	0		3	0	

TS, temporal summation as evaluated by the wind-up ratio (WUR with high TS (WUR > 2.5) indicating central sensitization); OR, odds ratio; 95%-CI, 95% confidence interval; %Δ VAS, percent reduction in current pain intensity as evaluated by the visual analog scale; %Δ PPT, percent elevation in pressure pain threshold; %Δ FFbHR, percent elevation in the sum score of the Hannover Functional Ability Questionnaire.

aged 50 years or younger with a high TS (WUR > 2.5) at a pain-free control site (dorsum of the dominant hand) would be more likely to show a clinically relevant reduction in pain intensity (≥30%) immediately after a single acupuncture treatment than patients with a low TS. Responder rates and overall immediate pain reduction was similar among chronic LBP with high and low TS at the pain free control site. Furthermore, high TS at the pain site at the lower back area was not significantly associated with the immediate response to acupuncture. The percentage of patients with a higher immediate reduction in pain intensity was descriptively even higher among those with low TS at the pain site. A single acupuncture treatment did not affect the PPT at the pain site irrespective of TS at the control and the pain site.

Study part two did not reveal a consistent association between TS at the pain free control site and any of the outcome measures. There was a close negative association between TS and the reduction in pain intensity and the improvement in physical functioning among patients with a WUR > 2.5 at the control site. However, this finding pertains to ten cases only of which four were included unintendedly due to a protocol violation and should thus not be overstated. Still venturing an interpretation, one might hypothesize that a polynomial or spline function would best describe the relationship between the response to a series of acupuncture treatments and TS (with a minimum around WUR 2.5). A recent study by another research group did not find a linear relationship between heat induced TS at the thenar eminence and the reduction in pain intensity after a series of acupuncture treatments in LBP patients (51). The authors however did not explore non-linear associations and did not provide an informative graph of their data. In line with study part one, a low TS at the pain site also tended to be associated with the response to a series of ten acupuncture treatments.

Overall, patients in this study responded well to acupuncture with a median absolute reduction of 17.5 VAS-points of the current pain intensity after one treatment (47.2% median percentage change) and a median absolute reduction of 35.5 VAS-points of last week's pain after ten treatments (65.9% median percentage change). This effect is in the upper range of acupuncture effects on non-specific LBP-pain observed in large clinical trials (52–54). Furthermore, the proportion of patients with normal physical functioning increased from 53 to 82% after ten acupuncture treatments. The PPT at the pain site did not yet change after one acupuncture treatment, but was significantly elevated by 0.7 kg/cm^2 (17.9% median percent change) after a series of ten acupuncture treatments. This is still in the lower range of effects on the PPT that have been observed in studies on body acupuncture or dry needling (41, 42, 55), but for example Leite et al. did not observe any change of the PPT after ten electroacupuncture treatments with a similar point regimen as in our study (56). Additionally, post treatment PPT of 4 kg/cm^2 was still markedly below the PPT at paravertebral measure sites at the lumbar spine in healthy persons [around 5 kg/cm^2 (35)].

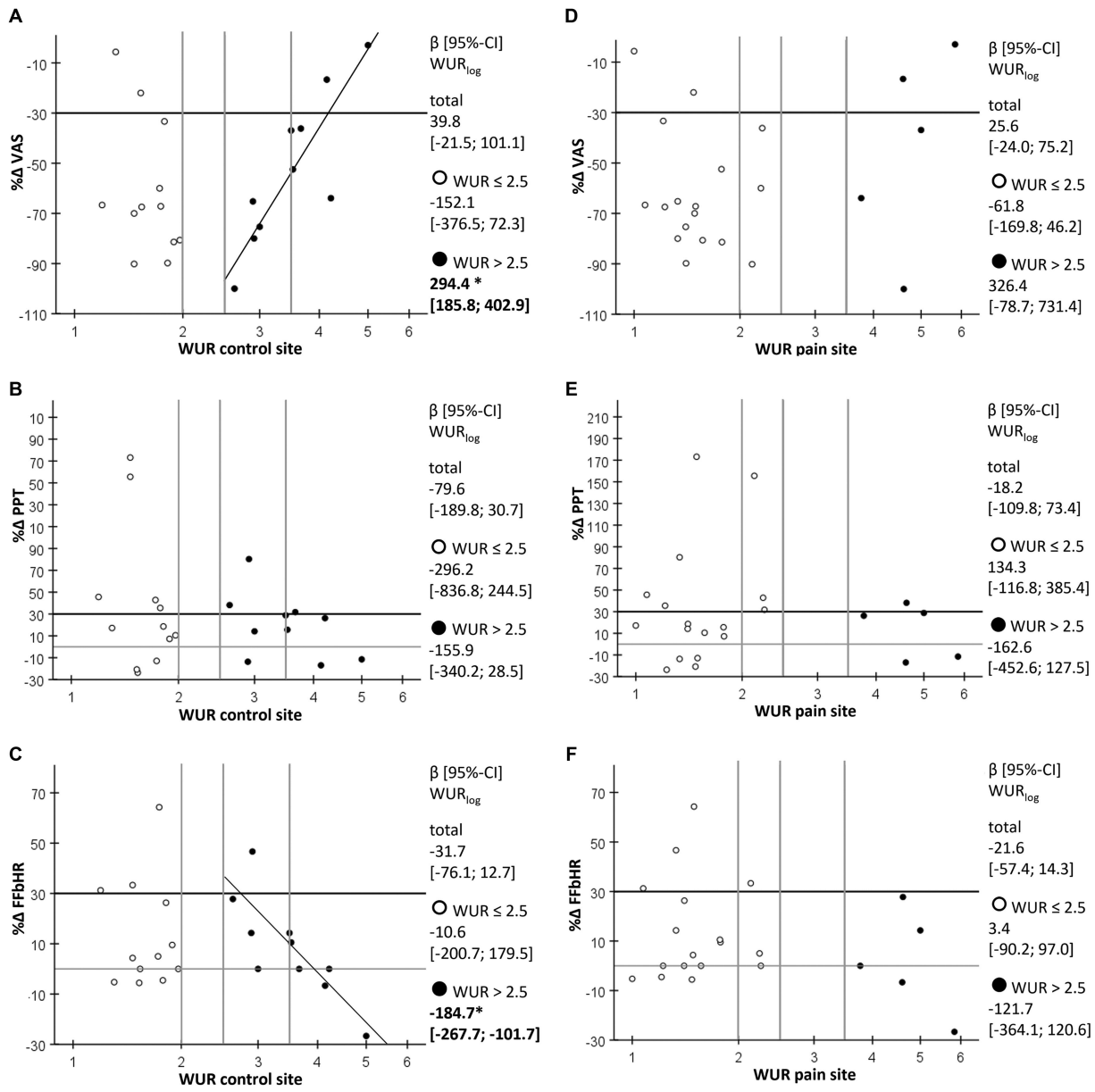

FIGURE 4
Scatterplot of percent change in pain intensity, PPT and FFbHR-scores after ten acupuncture treatments against TS at the control and the pain site. **(A)** Percent change in current pain intensity (%Δ VAS) as evaluated by the visual analog scale against the wind-up ratio (WUR) as a measure for temporal summation of pain (TS) at the control site with high TS (WUR > 2.5) indicating central sensitization. **(B)** Percent change in pressure pain threshold (%Δ PPT) against the WUR at the control site. **(C)** Percent change in the sum score of the Hannover functional ability questionnaire (%Δ FFbHR) against the WUR at the control site. **(D)** Percent change in current pain intensity (%Δ VAS) as evaluated by the visual analog scale against the WUR at the pain site. **(E)** Percent change in pressure pain threshold (%Δ PPT) against the WUR at the pain site. **(F)** Percent change in the sum score of the Hannover functional ability questionnaire (%Δ FFbHR) against the WUR at the pain site; empty circles, cases with WUR ≤ 2.5; filled circles, cases with WUR > 2.5; β [95%-CI] WURlog, regression coefficient of logarithmized WUR as estimated by generalized linear model; *, significant with p-value < 0.001 (other associations were not significant with p-values > 0.05).

The main difference between the results of our previous and our present study is a much higher responder rate (≥30% immediate pain reduction after one treatment) among patients with a low TS. Responder rates were substantially larger among patients with a low TS at the control site in the present study than among similarly aged patients with low TS at the control site in the previous study (72% vs. 18%). Conversely, responder rates among patients with a high TS at the control site were similar in the present and in the previous study (58% vs. 50%). The same accounts for the comparison of responder rates between the two studies in patients with a low TS at the pain site (73% vs. 23%) and high TS at the pain site (47% vs. 41%). This implies that treatment of chronic non-specific LBP patients with acupuncture can be recommended irrespective of their TS.

The relationship between TS and the response to acupuncture may differ between pain conditions. Future research needs to explore

in which chronic pain conditions TS may predict the response to acupuncture; e.g., chronic widespread pain vs. localized pain conditions or nociceptive vs. nociplastic vs. neuropathic pain. Patients in the present study suffered exclusively from non-specific LBP, while the mixed population of chronic pain patients in the previous study included also cases with multiple pain sites and diagnoses as well as specific pain conditions. Specific causes of pain (trauma, degeneration, inflammation or nerve damage) and stage of chronicity may affect the relationship between TS and the acupuncture response. The diverging results of the present and our previous study can be discussed in the light of further patient and treatment specific aspects.

First, one might argue that patients in the present study were less advanced in their pain disorder which could have contributed to their overall high acupuncture response. Patients in the previous study were all taking part in a multimodal pain program in a university outpatient pain clinic (tertiary care), and over half of the patients showed a high degree of chronicity. In the present study, only 5% of patients showed clinically relevant impairments in physical functioning as evaluated by the FFbHR despite similar pain intensities as the population in our previous study (median [IQR] on VAS/VRS (0–100) of current pain 45 [33; 55] vs. 45 [30; 60] and average pain 59 [50.0; 63] vs. 50 [40; 60]). Thus, patients in the present study might have had good pain coping abilities, which has been identified to be at least positively associated with the response to an acupuncture series in LBP patients (51, 57). Furthermore, it appears possible that a more functional endogenous pain control, whose activation is one of the primary mechanisms of acupuncture analgesia, could have contributed to a better immediate acupuncture response among patients of the present study. Therefore, investigating the relationship between CPM and immediate acupuncture effects on pain seems of particular interest. One recent trial in LBP patients showed no linear relationship between the CPM and the change in pain of chronic LBP patients after a series of acupuncture treatments (51). However, restauration of impaired CPM (58) over a series of acupuncture treatments might decouple the baseline CPM from effects of an acupuncture series despite its potential relationship with the immediate acupuncture effects.

Second, the more intense acupuncture regimen in the present study (13 to 22 needles) might have been more optimal for chronic LBP patients without prominent sensitization (normal/low TS) than the rather reticent needling regimen in the previous study (five to ten needles). This might explain in particular the high response rates in this subgroup. More needles seem to be associated with larger effect sizes (59). At the same time the treatment did not seem to be overly intense for highly sensitized patients. Other researchers had proposed that intensity of acupuncture treatments should be adapted according to their level of sensitization, as they had observed an association between poor acupuncture responses and low electrical and pressure pain thresholds in fibromyalgia and scar pain patients (60, 61). This cannot be conjectured for the population of chronic non-specific LBP patients aged 50 years or younger in our study. Responder rates were high irrespective of TS and also irrespective of the PPT. An additional explanation for this result could be that non-specific LBP can generally be targeted well by the semi-standardized acupuncture regimen applied here. It was designed during the planning of the large health insurance sponsored German acupuncture trials by several renown acupuncture experts. The combination of local and distal points chosen according to TCM theory and segmental organization might indeed be best suited for the homogeneous patient population included in our study. In other less locally circumscribed or more complex pain conditions, that characterized the population of our previous study, a more individual acupuncture approach might be needed. Such approach might even be developed during the course of a treatment series which might explain, why effects of the first acupuncture treatment varied more in our previous study.

The external validity of our results extends only to patients with non-specific chronic LBP aged 50 years or younger without other pain conditions and general good physical function. The acupuncture regimen applied here followed the protocol of the large German acupuncture trials (43) which had been designed also in consultation with the senior author of this article. This semi-standardized regimen combines distant acupuncture points (at non-pain-sites), segmental and local acupuncture points as well as facultative points chosen according to the patients' constitution and current situation. The overall beneficial treatment effects observed in our study confirm its suitability. We neither identified TS nor any other patient characteristic to be predictive for the overall good acupuncture response. Thus, our results do not suggest any restrictions to the application of acupuncture to such patients in routine care. Previous studies also do not give rise to the presumption that acupuncture response in chronic LBP would be associated with the patients' age (9, 51) or pain duration (9, 11). The role of potential interactions between the use of analgesics and acupuncture treatments might require further exploration. We are only aware of one study that identified lower responses to acupuncture in chronic LBP patients using narcotics (without further specification) (9) but not in those using other medications. Comparison to our results is limited as patients in our study only used non-opioid analgesics.

4.1 Limitations

Despite the fact that this study clearly answers its primary research question, there are some limitations to be discussed. First, the proportion of patients with a pain reduction of at least 30%, both immediately after one and also after ten acupuncture treatments, was extremely high, and the proportion of patients with an elevation of the PPT and the FFbHR score of at least 30% was very low. This lowered the power of our responder analysis. Nevertheless, our results clearly contrast our primary hypothesis that high TS at the control site would be associated with a higher chance for a clinically relevant acupuncture response. The respective OR were below one for all outcomes. Therefore, our conclusion that the finding of our previous study cannot be generalized is fully supported by the results of the present study. Second, unmeasured confounders could have impacted our results. However, the most important confounders suggested in the scientific literature [age, sex, pain duration, baseline pain, baseline PPT and use of analgesics (9, 10)] were addressed. We did not explore the impact of expectation on our results. However, previous studies suggest that patient expectations do not seem to explain an important part of the variance in acupuncture effects on LBP (7, 9, 62–64). Furthermore, risk factors for non-specific LBP such as lifestyle, obesity, physical workload and depressive mood were not taken into

account (65–69). Their potential impact on the acupuncture treatment response remains unexplored.

4.2 Implications for future research

As many factors, especially the risk factors for pain chronification just mentioned, can affect peripheral nerve fiber function and drive central sensitization, they should be considered in future research addressing sensory signs as predictors for the acupuncture treatment response. Generally, the discrepancies between our two studies and the fact that also previous research did not identify eminent predictors for the acupuncture response suggest a rather complex prediction network. When continuing this research, it appears advisable to promote large multicenter trials that allow a standardized collection of multifaceted data in much larger and diverse patient populations. Only such data would allow for the development of multifactor prediction models that are needed as a basis for informed treatment decisions.

The importance of approaches to precision medicine cannot be overrated. Applying ineffective treatments contributes to the risk of further pain chronification not least due to the deterioration of the patients' confidence in a possible improvement. Furthermore, despite the fact that acupuncture can be considered fairly safe, it still bears the risk also for significant adverse events (70). For proper risk benefit considerations, more precise estimations of the expected benefits through acupuncture are crucial. In addition, human and financial resources need to be allocated efficiently in order to provide the best possible care to a maximum number of patients. Given the high prevalence of chronic pain, especially low-back pain, it is a moral obligation of the research community to continue building the path toward an individualized treatment.

5 Conclusion

Our results do not suggest an important role of TS for predicting a clinically important acupuncture effect or the response to a series of ten acupuncture treatments in patients with chronic non-specific LBP. Overall high response rates imply that acupuncture is a suitable treatment option for LBP patients irrespective of their TS.

Data availability statement

The raw data supporting the conclusions of this article will be made available by the authors, without undue reservation.

Ethics statement

The studies involving humans were approved by the Ethics Committee of the Medical Faculty of the Ludwig-Maximilians University (LMU), Munich, Germany. The studies were conducted in accordance with the local legislation and institutional requirements. The participants provided their written informed consent to participate in this study.

Author contributions

PB: Writing – review & editing, Writing – original draft, Visualization, Supervision, Project administration, Methodology, Investigation, Funding acquisition, Formal analysis, Data curation, Conceptualization. MS: Writing – review & editing, Writing – original draft, Project administration, Methodology, Investigation, Formal analysis, Data curation. LM: Writing – review & editing, Writing – original draft, Project administration, Methodology, Investigation, Formal analysis, Data curation. DI: Writing – review & editing, Writing – original draft, Supervision, Project administration, Methodology, Investigation, Funding acquisition, Conceptualization.

Funding

The author(s) declare that financial support was received for the research, authorship, and/or publication of this article. Conduct of the study was funded by the Funding Program for Research and Teaching (*Förderprogramm für Forschung und Lehre,* FöFoLe) of the Medical Faculty of the LMU Munich (grant number 1006).

Acknowledgments

The authors thank Peter Conzen for his advice on the study design and Erika Weber as well as Christina Deisenrieder for their support in organizing the study. Furthermore, we thank Sarah Feldmeier for her support in producing Figures 3, 4.

Conflict of interest

PB and DI receive honoraria and travel costs from non-profit academic organizations, physician chambers and universities for teaching and lecturing on pain research, pain medicine, integrative medicine and acupuncture.

The remaining authors declare that the research was conducted in the absence of any commercial or financial relationships that could be construed as a potential conflict of interest.

Publisher's note

Supplementary material

The Supplementary material for this article can be found online at: https://www.frontiersin.org/articles/10.3389/fneur.2024.1335356/full#supplementary-material

References

1. World Health Organization. WHO global report on traditional and complementary medicine 2019. (2019). World Health Organization: Geneva. Available online at: https://apps.who.int/iris/bitstream/handle/10665/312342/9789241515436-eng.pdf (Accessed August 12, 2022).

2. Bundesärztekammer. Ärztestatistik—Deutschland. (2021). Available online at: https://www.bundesaerztekammer.de/baek/ueber-uns/aerztestatistik/aerztestatistik-2021 (Accessed August 12, 2022).

3. Chinese Medicine Board of Australia. Registrant data. (2022). Available online at: https://www.chinesemedicineboard.gov.au/About/Statistics.aspx (Accessed August 12, 2022).

4. Clarke TC, Black LI, Stussman BJ, Barnes PM, Nahin RL. Trends in the use of complementary health approaches among adults: United States, 2002-2012. *Natl Health Stat Rep*. (2015) 79:1–16.

5. Vickers AJ, Vertosick EA, Lewith G, MacPherson H, Foster NE, Sherman KJ, et al. Acupuncture for chronic pain: update of an individual patient data Meta-analysis. *J Pain*. (2018) 19:455–74. doi: 10.1016/j.jpain.2017.11.005

6. Vickers AJ, Linde K. Acupuncture for chronic pain. *JAMA*. (2014) 311:955–6. doi: 10.1001/jama.2013.285478

7. Barth J, Muff S, Kern A, Zieger A, Keiser S, Zoller M, et al. Effect of briefing on acupuncture treatment outcome expectations, pain, and adverse side effects among patients with chronic low Back pain: a randomized clinical trial. *JAMA Netw Open*. (2021) 4:e2121418. doi: 10.1001/jamanetworkopen.2021.21418

8. Colagiuri B, Smith CA. A systematic review of the effect of expectancy on treatment responses to acupuncture. *Evid Based Complement Alternat Med*. (2012) 2012:857804:1–12. doi: 10.1155/2012/857804

9. Sherman KJ, Cherkin DC, Ichikawa L, Avins AL, Barlow WE, Khalsa PS, et al. Characteristics of patients with chronic back pain who benefit from acupuncture. *BMC Musculoskelet Disord*. (2009) 10:114. doi: 10.1186/1471-2474-10-114

10. Witt CM, Schützler L, Lüdtke R, Wegscheider K, Willich SN. Patient characteristics and variation in treatment outcomes: which patients benefit most from acupuncture for chronic pain? *Clin J Pain*. (2011) 27:550–5. doi: 10.1097/AJP.0b013e31820dfbf5

11. Witt CM, Vertosick EA, Foster NE, Lewith G, Linde K, MacPherson H, et al. The effect of patient characteristics on acupuncture treatment outcomes: an individual patient data Meta-analysis of 20,827 chronic pain patients in randomized controlled trials. *Clin J Pain*. (2019) 35:428–34. doi: 10.1097/ajp.0000000000000691

12. Dou B, Li Y, Ma J, Xu Z, Fan W, Tian L, et al. Role of Neuroimmune crosstalk in mediating the anti-inflammatory and analgesic effects of acupuncture on inflammatory pain. *Front Neurosci*. (2021) 15:695670. doi: 10.3389/fnins.2021.695670

13. Filshie J, White A, Cummings M. An introduction to western medical acupuncture. Edinburgh: Elsevier (2016).

14. Zhang R, Lao L, Ren K, Berman BM. Mechanisms of acupuncture-electroacupuncture on persistent pain. *Anesthesiology*. (2014) 120:482–503. doi: 10.1097/ALN.0000000000000101

15. Lai HC, Lin YW, Hsieh CL. Acupuncture-analgesia-mediated alleviation of central sensitization. *Evid Based Complement Alternat Med*. (2019) 2019:1–13. doi: 10.1155/2019/6173412

16. Lyu Z, Guo Y, Gong Y, Fan W, Dou B, Li N, et al. The role of neuroglial crosstalk and synaptic plasticity-mediated central sensitization in acupuncture analgesia. *Neural Plast*. (2021) 2021:1–18. doi: 10.1155/2021/8881557

17. Gerhardt A, Eich W, Janke S, Leisner S, Treede RD, Tesarz J. Chronic widespread Back pain is distinct from chronic local Back pain: evidence from quantitative sensory testing, pain drawings, and psychometrics. *Clin J Pain*. (2015) 32:568–79. doi: 10.1097/AJP.0000000000000300

18. Rabey M, Slater H, O'Sullivan P, Beales D, Smith A. Somatosensory nociceptive characteristics differentiate subgroups in people with chronic low back pain: a cluster analysis. *Pain*. (2015) 156:1874–84. doi: 10.1097/j.pain.0000000000000244

19. Staud R, Vierck CJ, Cannon RL, Mauderli AP, Price DD. Abnormal sensitization and temporal summation of second pain (wind-up) in patients with fibromyalgia syndrome. *Pain*. (2001) 91:165–75. doi: 10.1016/S0304-3959(00)00432-2

20. Vaegter HB, Graven-Nielsen T. Pain modulatory phenotypes differentiate subgroups with different clinical and experimental pain sensitivity. *Pain*. (2016) 157:1480–8. doi: 10.1097/j.pain.0000000000000543

21. Herrero JF, Laird JM, López-García JA. Wind-up of spinal cord neurones and pain sensation: much ado about something? *Prog Neurobiol*. (2000) 61:169–203. doi: 10.1016/s0301-0082(99)00051-9

22. Rolke R, Baron R, Maier C, Tolle TR, Treede RD, Beyer A, et al. Quantitative sensory testing in the German research network on neuropathic pain (DFNS): standardized protocol and reference values. *Pain*. (2006) 123:231–43. doi: 10.1016/j.pain.2006.01.041

23. Baeumler PI, Conzen P, Irnich D. High temporal summation of pain predicts immediate analgesic effect of acupuncture in chronic pain patients-a prospective cohort study. *Front Neurosci*. (2019) 13:498. doi: 10.3389/fnins.2019.00498

24. Breivik H, Collett B, Ventafridda V, Cohen R, Gallacher D. Survey of chronic pain in Europe: prevalence, impact on daily life, and treatment. *Eur J Pain*. (2006) 10:287–333. doi: 10.1016/j.ejpain.2005.06.009

25. El-Metwally A, Shaikh Q, Aldiab A, Al-Zahrani J, Al-Ghamdi S, Alrasheed AA, et al. The prevalence of chronic pain and its associated factors among Saudi Al-Kharj population; a cross sectional study. *BMC Musculoskelet Disord*. (2019) 20:177. doi: 10.1186/s12891-019-2555-7

26. Elliott AM, Smith BH, Penny KI, Smith WC, Chambers WA. The epidemiology of chronic pain in the community. *Lancet*. (1999) 354:1248–52. doi: 10.1016/s0140-6736(99)03057-3

27. Ohayon MM, Schatzberg AF. Chronic pain and major depressive disorder in the general population. *J Psychiatr Res*. (2010) 44:454–61. doi: 10.1016/j.jpsychires.2009.10.013

28. Balague F, Mannion AF, Pellise F, Cedraschi C. Non-specific low back pain. *Lancet*. (2012) 379:482–91. doi: 10.1016/S0140-6736(11)60610-7

29. Deyo RA, Weinstein JN. Low back pain. *N Engl J Med*. (2001) 344:363–70. doi: 10.1056/nejm200102013440508

30. Lemmon R, Hampton A. Nonpharmacologic treatment of chronic pain: what works? *J Fam Pract*. (2018) 67:474–83.

31. Qaseem A, Wilt TJ, McLean RM, Forciea MA, Denberg TD, Barry MJ, et al. Noninvasive treatments for acute, subacute, and chronic low Back pain: a clinical practice guideline from the American College of Physicians. *Ann Intern Med*. (2017) 166:514–30. doi: 10.7326/m16-2367

32. Mu J, Furlan AD, Lam WY, Hsu MY, Ning Z, Lao L. Acupuncture for chronic nonspecific low back pain. *Cochrane Database Syst Rev*. (2020) 2020:Cd013814. doi: 10.1002/14651858.cd013814

33. Haake M, Müller HH, Schade-Brittinger C, Basler HD, Schäfer H, Maier C, et al. German acupuncture trials (GERAC) for chronic low back pain: randomized, multicenter, blinded, parallel-group trial with 3 groups. *Arch Intern Med*. (2007) 167:1892–8. doi: 10.1001/archinte.167.17.1892

34. Imamura M, Chen J, Matsubayashi SR, Targino RA, Alfieri FM, Bueno DK, et al. Changes in pressure pain threshold in patients with chronic nonspecific low back pain. *Spine (Phila Pa 1976)*. (2013) 38:2098–107. doi: 10.1097/01.brs.0000435027.50317.d7

35. Tan H, Tumilty S, Chapple C, Liu L, Othman R, Baxter GD. Acupoints sensitization in people with and without chronic low back pain:a matched-sample cross-sectional study. *J Back Musculoskelet Rehabil*. (2022) 36:137. doi: 10.3233/bmr-210297

36. Baeumler PI, Fleckenstein J, Benedikt F, Bader J, Irnich D. Acupuncture-induced changes of pressure pain threshold are mediated by segmental inhibition--a randomized controlled trial. *Pain*. (2015) 156:2245–55. doi: 10.1097/j.pain.0000000000000283

37. Baeumler PI, Fleckenstein J, Takayama S, Simang M, Seki T, Irnich D. Effects of acupuncture on sensory perception: a systematic review and meta-analysis. *PLoS One*. (2014) 9:e113731. doi: 10.1371/journal.pone.0113731

38. de Carvalho RC, Parisi JR, Prado WA, de Araújo JE, Silva AM, Silva JRT, et al. Single or multiple Electroacupuncture sessions in nonspecific low Back pain: are we low-responders to Electroacupuncture? *J Acupunct Meridian Stud*. (2018) 11:54–61. doi: 10.1016/j.jams.2018.02.002

39. Kumnerddee W. Effectiveness comparison between Thai traditional massage and Chinese acupuncture for myofascial back pain in Thai military personnel: a preliminary report. *J Med Assoc Thail*. (2009) 92:S117–23.

40. Perez-Palomares S, Olivan-Blazquez B, Magallon-Botaya R, De-La-Torre-Beldarrain MML, Gaspar-Calvo E, Romo-Calvo L, et al. Percutaneous electrical nerve stimulation versus dry needling: effectiveness in the treatment of chronic low back pain. *J Musculoskelet Pain*. (2010) 18:23–30. doi: 10.3109/10582450903496047

41. Téllez-García M, De-la-Llave-Rincón AI, Salom-Moreno J, Palacios-Ceña M, Ortega-Santiago R, Fernández-de-Las-Peñas C. Neuroscience education in addition to trigger point dry needling for the management of patients with mechanical chronic low back pain: a preliminary clinical trial. *J Bodyw Mov Ther*. (2015) 19:464–72. doi: 10.1016/j.jbmt.2014.11.012

42. Wang-Price S, Zafereo J, Couch Z, Brizzolara K, Heins T, Smith L. Short-term effects of two deep dry needling techniques on pressure pain thresholds and electromyographic amplitude of the lumbosacral multifidus in patients with low back pain—a randomized clinical trial. *J Man Manip Ther*. (2020) 28:254–65. doi: 10.1080/10669817.2020.1714165

43. Brinkhaus B, Becker-Witt C, Jena S, Linde K, Streng A, Wagenpfeil S, et al. Acupuncture randomized trials (ART) in patients with chronic low back pain and osteoarthritis of the knee—design and protocols. *Forsch Komplementarmed Klass Naturheilkd*. (2003) 10:185–91. doi: 10.1159/000073474

44. Bundesärztekammer, Kassenärztliche Bundesvereinigung, and Arbeitsgemeinschaft der Wissenschaftlichen Medizinischen Fachgesellschaften. Nationale Versorgungsleitlinie Kreuzschmerz. (2017). Available online at: https://www.leitlinien.de/themen/kreuzschmerz/2-auflage (Accessed March 2, 2017).

45. Farrar JT, Young JP Jr, LaMoreaux L, Werth JL, Poole MR. Clinical importance of changes in chronic pain intensity measured on an 11-point numerical pain rating scale. *Pain*. (2001) 94:149–58. doi: 10.1016/S0304-3959(01)00349-9

46. Dworkin RH, Turk DC, Farrar JT, Haythornthwaite JA, Jensen MP, Katz NP, et al. Core outcome measures for chronic pain clinical trials: IMMPACT recommendations. *Pain*. (2005) 113:9–19. doi: 10.1016/j.pain.2004.09.012

47. Dworkin RH, Turk DC, Wyrwich KW, Beaton D, Cleeland CS, Farrar JT, et al. Interpreting the clinical importance of treatment outcomes in chronic pain clinical trials: IMMPACT recommendations. *J Pain*. (2008) 9:105–21. doi: 10.1016/j.jpain.2007.09.005

48. Kohlmann T, Raspe H. Die patientennahe Diagnostik von Funktionseinschränkungen im Alltag. *Psychom Theory*. (1994) 6:21–7.

49. Roese I, Kohlmann T, Raspe H. Measuring functional capacity in backache patients in rehabilitation: a comparison of standardized questionnaires. *Rehabilitation*. (1996) 35:103–8.

50. The World Medical Association. Declaration of Helsinki—updated version Seoul, Korea 2008. (2008). Available online at: https://www.wma.net/what-we-do/medical-ethics/declaration-of-helsinki/doh-oct2008/ (Accessed August 12, 2022).

51. Kong JT, Puetz C, Tian L, Haynes I, Lee E, Stafford RS, et al. Effect of Electroacupuncture vs sham treatment on change in pain severity among adults with chronic low Back pain: a randomized clinical trial. *JAMA Netw Open*. (2020) 3:e2022787. doi: 10.1001/jamanetworkopen.2020.22787

52. Brinkhaus B, Witt CM, Jena S, Linde K, Streng A, Wagenpfeil S, et al. Acupuncture in patients with chronic low back pain: a randomized controlled trial. *Arch Intern Med*. (2006) 166:450–7. doi: 10.1001/archinte.166.4.450

53. Cho YJ, Song YK, Cha YY, Shin BC, Shin IH, Park HJ, et al. Acupuncture for chronic low back pain: a multicenter, randomized, patient-assessor blind, sham-controlled clinical trial. *Spine*. (2013) 38:549–57. doi: 10.1097/BRS.0b013e318275e601

54. Molsberger AF, Mau J, Pawelec DB, Winkler J. Does acupuncture improve the orthopedic management of chronic low back pain--a randomized, blinded, controlled trial with 3 months follow up. *Pain*. (2002) 99:579–87. doi: 10.1016/s0304-3959(02)00269-5

55. Koppenhaver SL, Walker MJ, Su J, McGowen JM, Umlauf L, Harris KD, et al. Changes in lumbar multifidus muscle function and nociceptive sensitivity in low back pain patient responders versus non-responders after dry needling treatment. *Man Ther*. (2015) 20:769–76. doi: 10.1016/j.math.2015.03.003

56. Leite PMS, Mendonça ARC, Maciel LYS, Poderoso-Neto ML, Araujo CCA, Góis HCJ, et al. Does Electroacupuncture treatment reduce pain and change quantitative sensory testing responses in patients with chronic nonspecific low Back pain? A randomized controlled clinical trial. *Evid Based Complement Alternat Med*. (2018) 2018:8586746. doi: 10.1155/2018/8586746

57. Bishop FL, Yardley L, Prescott P, Cooper C, Little P, Lewith GT. Psychological covariates of longitudinal changes in back-related disability in patients undergoing acupuncture. *Clin J Pain*. (2015) 31:254–64. doi: 10.1097/ajp.0000000000000108

58. Lv ZT, Shen LL, Zhu B, Zhang ZQ, Ma CY, Huang GF, et al. Effects of intensity of electroacupuncture on chronic pain in patients with knee osteoarthritis: a randomized controlled trial. *Arthritis Res Ther*. (2019) 21:120. doi: 10.1186/s13075-019-1899-6

59. MacPherson H, Maschino AC, Lewith G, Foster NE, Witt CM, Vickers AJ. Characteristics of acupuncture treatment associated with outcome: an individual patient meta-analysis of 17,922 patients with chronic pain in randomised controlled trials. *PLoS One*. (2013) 8:e77438. doi: 10.1371/journal.pone.0077438

60. Cuignet O, Pirlot A, Ortiz S, Rose T. The effects of electroacupuncture on analgesia and peripheral sensory thresholds in patients with burn scar pain. *Burns*. (2015) 41:1298–305. doi: 10.1016/j.burns.2015.03.002

61. Zucker NA, Tsodikov A, Mist SD, Cina S, Napadow V, Harris RE. Evoked pressure pain sensitivity is associated with differential analgesic response to Verum and sham acupuncture in fibromyalgia. *Pain Med*. (2017) 18:1582–92. doi: 10.1093/pm/pnx001

62. Bishop F, Al-Abbadey M, Roberts L, MacPherson H, Stuart B, Carnes D, et al. Direct and mediated effects of treatment context on low back pain outcome: a prospective cohort study. *BMJ Open*. (2021) 11:e044831. doi: 10.1136/bmjopen-2020-044831

63. Sherman KJ, Cherkin DC, Ichikawa L, Avins AL, Delaney K, Barlow WE, et al. Treatment expectations and preferences as predictors of outcome of acupuncture for chronic back pain. *Spine*. (2010) 35:1471–7. doi: 10.1097/BRS.0b013e3181c2a8d3

64. Zieger A, Kern A, Barth J, Witt CM. Do patients' pre-treatment expectations about acupuncture effectiveness predict treatment outcome in patients with chronic low back pain? A secondary analysis of data from a randomised controlled clinical trial. *PLoS One*. (2022) 17:e0268646. doi: 10.1371/journal.pone.0268646

65. Coenen P, Gouttebarge V, van der Burght AS, van Dieën JH, Frings-Dresen MH, van der Beek AJ, et al. The effect of lifting during work on low back pain: a health impact assessment based on a meta-analysis. *Occup Environ Med*. (2014) 71:871–7. doi: 10.1136/oemed-2014-102346

66. Pincus T, Burton AK, Vogel S, Field AP. A systematic review of psychological factors as predictors of chronicity/disability in prospective cohorts of low back pain. *Spine*. (2002) 27:E109–20. doi: 10.1097/00007632-200203010-00017

67. Shiri R, Karppinen J, Leino-Arjas P, Solovieva S, Viikari-Juntura E. The association between obesity and low back pain: a meta-analysis. *Am J Epidemiol*. (2010a) 171:135–54. doi: 10.1093/aje/kwp356

68. Shiri R, Karppinen J, Leino-Arjas P, Solovieva S, Viikari-Juntura E. The association between smoking and low back pain: a meta-analysis. *Am J Med*. (2010b) 123:87.e7–87.e35. doi: 10.1016/j.amjmed.2009.05.028

69. Stevans JM, Delitto A, Khoja SS, Patterson CG, Smith CN, Schneider MJ, et al. Risk factors associated with transition from acute to chronic low Back pain in US patients seeking primary care. *JAMA Netw Open*. (2021) 4:e2037371. doi: 10.1001/jamanetworkopen.2020.37371

70. Bäumler P, Zhang W, Stübinger T, Irnich D. Acupuncture-related adverse events: systematic review and meta-analyses of prospective clinical studies. *BMJ Open*. (2021) 11:e045961. doi: 10.1136/bmjopen-2020-045961

frontiers | Frontiers in Molecular Neuroscience

TYPE Original Research
PUBLISHED 03 September 2024
DOI 10.3389/fnmol.2024.1457602

OPEN ACCESS

EDITED BY
Álvaro Llorente-Berzal,
Autonomous University of Madrid, Spain

REVIEWED BY
Yuncong Ma,
University of Pennsylvania, United States
Dafa Shi,
Second Affiliated Hospital of Shantou University Medical College, China
R. V. Belfin,
Karunya Institute of Technology and Sciences, India

*CORRESPONDENCE
Jen-Chuen Hsieh
✉ jchsiehibru@nycu.edu.tw

RECEIVED 01 July 2024
ACCEPTED 12 August 2024
PUBLISHED 03 September 2024

CITATION
Hsu P-S, Liu C-H, Yang C-J, Lee L-C, Li W-C, Chao H-T, Lin M-W, Chen L-F and Hsieh J-C (2024) Reward system neurodynamics during menstrual pain modulated by *COMT* Val158Met polymorphisms.
Front. Mol. Neurosci. 17:1457602.
doi: 10.3389/fnmol.2024.1457602

Reward system neurodynamics during menstrual pain modulated by *COMT* Val158Met polymorphisms

Pei-Shan Hsu[1,2,3], Ching-Hsiung Liu[2,4], Ching-Ju Yang[1,2,5,6], Lin-Chien Lee[2,7], Wei-Chi Li[1,2,5], Hsiang-Tai Chao[8], Ming-Wei Lin[9], Li-Fen Chen[1,2,10,11] and Jen-Chuen Hsieh[2,5,6,10]*

[1]Institute of Brain Science, College of Medicine, National Yang Ming Chiao Tung University, Taipei, Taiwan, [2]Integrated Brain Research Unit, Division of Clinical Research, Department of Medical Research, Taipei Veterans General Hospital, Taipei, Taiwan, [3]Department of Chinese Medicine, Taipei Tzu Chi Hospital, Buddhist Tzu Chi Medical Foundation, New Taipei City, Taiwan, [4]Department of Neurology, Lotung Poh-Ai Hospital, Yilan, Taiwan, [5]Department of Biological Science and Technology, College of Engineering Bioscience, National Yang Ming Chiao Tung University, Hsinchu, Taiwan, [6]Center for Intelligent Drug Systems and Smart Bio-devices, National Yang Ming Chiao Tung University, Hsinchu, Taiwan, [7]Department of Physical Medicine and Rehabilitation, Cheng Hsin General Hospital, Taipei, Taiwan, [8]Department of Obstetrics and Gynecology, Taipei Veterans General Hospital, Taipei, Taiwan, [9]Institute of Public Health, National Yang Ming Chiao Tung University, Taipei, Taiwan, [10]Brain Research Center, National Yang Ming Chiao Tung University, Taipei, Taiwan, [11]Institute of Biomedical Informatics, College of Medicine, National Yang Ming Chiao Tung University, Taipei, Taiwan

Introduction: Primary dysmenorrhea (PDM), characterized by cyclic pain, may involve pain modulation within the reward system (RS). The Catechol-O-methyltransferase (*COMT*) Val158Met polymorphism, which significantly influences dopamine activity, is linked to the regulation of both acute and chronic pain. This study examines the differential neurodynamic modulation in the RS associated with *COMT* Val158Met polymorphisms during menstrual pain among PDM subjects.

Method: Ninety-one PDM subjects underwent resting-state fMRI during menstruation and were genotyped for *COMT* Val158Met polymorphisms. The amplitude of low-frequency fluctuation (ALFF) and functional connectivity (FC) analyses were used to assess the RS response. Psychological evaluations included the McGill Pain Questionnaire, Pain Catastrophizing Scale, Beck Anxiety Inventory, and Beck Depression Inventory.

Result: Val/Val homozygotes (n = 50) and Met carriers (n = 41) showed no significant differences in McGill Pain Questionnaire, Beck Anxiety Inventory, and Beck Depression Inventory. However, Met carriers exhibited lower scores on the Pain Catastrophizing Scale. Distinct FC patterns was observed between Val/Val homozygotes and Met carriers, specifically between the nucleus accumbens (NAc) and prefrontal cortex, NAc and inferior parietal lobe, ventral tegmental area (VTA) and prefrontal cortex, VTA and precentral gyrus, and VTA and superior parietal lobe. Only Met carriers showed significant correlations between ALFF and FC values of the NAc and VTA with pain-related metrics (McGill Pain Questionnaire and Pain Catastrophizing Scale scores). NAc ALFF and NAc-prefrontal cortex FC values positively correlated with pain-related metrics, while VTA ALFF and VTA-prefrontal cortex and VTA-superior parietal lobe FC values negatively correlated with pain-related metrics.

Discussion: This study reveals that the *COMT* Val158Met polymorphism results in genotype-specific functional changes in the brain's RS during menstrual pain.

In Met carriers, engagement of these regions is potentially linked to motivational reward-seeking and top-down modulation. This polymorphism likely influences the RS's responses, significantly contributing to individual differences in pain regulation.

KEYWORDS

primary dysmenorrhea, *COMT* Val158Met polymorphism, functional magnetic resonance imaging, amplitude of low-frequency fluctuation, functional connectivity, reward system

1 Introduction

Primary dysmenorrhea (PDM) is a common gynecological pain issue among young women, causing lower abdominal pain for 1–2 days each month (Itani et al., 2022). Its main mechanism may involve myometrial hypercontractility and vasoconstriction contributed by increasing inflammatory factors such as prostaglandins, cytokines, and vasopressin, but there are no observable pelvic abnormalities (Berkley, 2013). Current neuroimaging studies have found adaptive or maladaptive functional or structural changes in the brain's pain processing network associated with this cyclical menstrual pain (Tu et al., 2010; Tu et al., 2013; Wei et al., 2016a; Lee et al., 2023), which is related to individual differences in gene polymorphism such as *BDNF* and *OPRM1* (Wei et al., 2016b; Wei et al., 2017; Hsu et al., 2023), suggesting individual differences in pain modulation may linked to genetics.

The mesolimbic dopamine pathway, often referred to as the reward pathway, links the ventral tegmental area (VTA) and nucleus accumbens (NAc) while interacting with the prefrontal cortex (PFC) (Goeders and Smith, 1983), together constituting part of the overall reward system (RS). The RS plays a crucial role in the sensory, affective-motivational, and cognitive aspects of both acute and chronic pain (Elman and Borsook, 2016; Serafini et al., 2020). Acute pain stimuli can activate the RS to modulate pain in a multidimensional manner (Becerra et al., 2001), whereas chronic pain can disrupt the brain's RS, impairing the ability to cope with pain (Baliki et al., 2012). Studies on PDM have also noted changes in the RS, featuring both adaptive and maladaptive alterations (Zhang et al., 2019; Liu et al., 2023b).

Catechol-O-methyltransferase (COMT), a key enzyme in dopamine catabolism, is predominantly found in brain regions associated with the RS, such as the frontal cortex, striatum, amygdala, and midbrain, with particularly high levels in the frontal cortex (Matsumoto et al., 2003). In animal studies, COMT deficiency has been shown to significantly increase dopamine concentration (Gogos et al., 1998; Käenmäki et al., 2010). A common functional polymorphism in the *COMT* gene results in the substitution of valine (Val) with methionine (Met) at codon 158 (Val158Met). The Met allele homozygosity leads to a three- to four-fold reduction in COMT enzyme activity compared to Val homozygotes (Weinshilboum et al., 1999). The Met allele, associated with reduced enzyme activity, results in elevated tonic dopamine levels and decreased phasic dopamine release. This adjustment stabilizes networks involved in sustained cognitive functions, such as working memory, but may reduce the flexibility to adapt active networks (Bilder et al., 2004).

The *COMT* Val158Met polymorphism influences both acute and chronic pain modulation by altering dopamine levels in pain-related regions (Andersen and Skorpen, 2009). In acute pain scenarios, individuals who are Met homozygotes often exhibit heightened responses to experimental pain, increased mu-opioid receptor binding, but a diminished mu-opioid system response (Zubieta et al., 2003). Additionally, due to their increased pain sensitivity, the Met homozygotes often show greater reward responsiveness and engage more in reward-seeking behavior during decision-making tasks (Lancaster et al., 2012). In chronic pain conditions, the Met allele is frequently associated with increased pain sensitization and enhanced opioid efficacy (Rakvåg et al., 2008; Cohen et al., 2009; Gerra et al., 2022). The heightened pain sensitivity in Met allele homozygotes with chronic pain is thought to be related to compromised D2 receptor-mediated descending pain inhibition (Andersen and Skorpen, 2009). However, the impact of this polymorphism varies, showing less consistent results across various chronic pain syndromes (Ding et al., 2010; Patanwala et al., 2017).

This article investigates the impact of the *COMT* Val158Met polymorphism on RS neurodynamics using resting-state functional magnetic resonance imaging (rs-fMRI) and its association with menstrual pain in young females with PDM. The study focuses on key RS regions, specifically the NAc and the VTA. To measure spontaneous brain activity, an amplitude of low-frequency fluctuations (ALFF) analysis is conducted. This analysis assesses the variance of low-frequency BOLD signal fluctuations, with higher values indicating increased spontaneous brain activity (Zang et al., 2007). Additionally, functional connectivity (FC) analysis is performed using the NAc and VTA as seed regions to observe their interactions with other brain regions.

2 Materials and methods

2.1 Baseline information

2.1.1 Subjects

PDM participants were included based on the following criteria: (1) having a regular menstrual cycle of approximately 27–32 days, (2) being right-handedness as determined by the Edinburgh Handedness Inventory, and (3) having a history of menstrual pain lasting more than 6 months, with an average pain score greater than 4 on a 0–10 verbal numerical scale (VNS) for the past 6 months under routine management for those with PDM. Exclusion criteria included: (1) use of any medications, contraceptives, or hormone supplements in the

6 months prior to the study, (2) pituitary gland disease, (3) organic pelvic disease, (4) psychiatric or neurological disorders, (5) head injury with loss of consciousness, (6) pregnancy or plans to conceive, (7) history of childbirth, and (8) presence of metal implants, pacemakers, claustrophobia, or any contraindications to MRI. Participants were prohibited from taking analgesics 24 h before the experiment. All PDM subjects underwent diagnosis by a gynecologist and pelvic ultrasound to rule out organic pelvic diseases.

Participants with PDM were recruited through internet advertisements, initially enrolling 201 subjects. Nine were excluded due to secondary dysmenorrhea identified by pelvic ultrasound, 18 were excluded for incidental brain anomalies or abnormalities found on MRI scans, and 68 declined to participate. The final sample comprised 106 PDM subjects who completed both behavioral assessments and neuroimaging scans. Among these, 15 were further excluded due to failed genotyping or excessive head motion (>2 mm or 2 degrees) during scans. Ultimately, the study included 91 PDM patients, consisting of 4 with the Met/Met genotype, 37 with the Val/Met genotype, and 50 with the Val/Val genotype (Figure 1).

2.1.2 Experimental design

MRI scans comprising T1-weighted structural images and T2-weighted gradient echo planar images (EPI) were conducted within the first 1–3 days of menstruation. The short-form McGill Pain Questionnaire (MPQ) (Melzack, 1987), the Pain Catastrophizing Scale (PCS) (Sullivan et al., 1995), Beck Anxiety Inventory (BAI) (Beck and Steer, 1993) and Beck Depression Inventory (BDI) (Beck et al., 1996) were employed to assess participants' pain experience and psychological status during this menstrual phase. Blood samples were collected for genotyping before gonadal hormone assay. Detailed genotyping and hormone measurement methods were provided in the Supplementary material.

2.1.3 Demographic and psychological measurement

Data analysis was performed using GraphPad Prism 9 (version 9.1.1). The Hardy–Weinberg equilibrium of the *COMT* Val158Met genotype distribution was assessed using the chi-square test. Demographic information, pain-related metrics, and psychological measurements of Met carrier and Val/Val homozygotes in *COMT* Val158Met polymorphism were compared. The normalcy of data distribution was assessed using the Anderson-Darling normality test. For normal distribution data, a two-sample t-test was employed. Alternatively, for non-normally distributed data, the Mann–Whitney U test was used. Results were reported as mean ± standard deviation (SD), with statistical significance defined as $p < 0.05$.

2.2 Image analysis

2.2.1 Image acquisition

rsfMRI images were acquired using a 3.0 T MRI scanner (Magnetom Trio Tim, Siemens, Erlangen, Germany) at the National Yang Ming Chiao Tung University, with 12-channel head coil. T2*-weighted gradient echo planar imaging (EPI) sequences were used, with parameters: repetition time (TR) = 2,500 ms, echo time (TE) = 30 ms, flip angle = 90°, field of view (FOV) = 220 mm × 220 mm, matrix size = 64 × 64, slice thickness = 3.4 mm, and 200 volumes per run. High-resolution T1-weighted structural images were obtained using the magnetization-prepared rapid gradient-echo (MPRAGE)

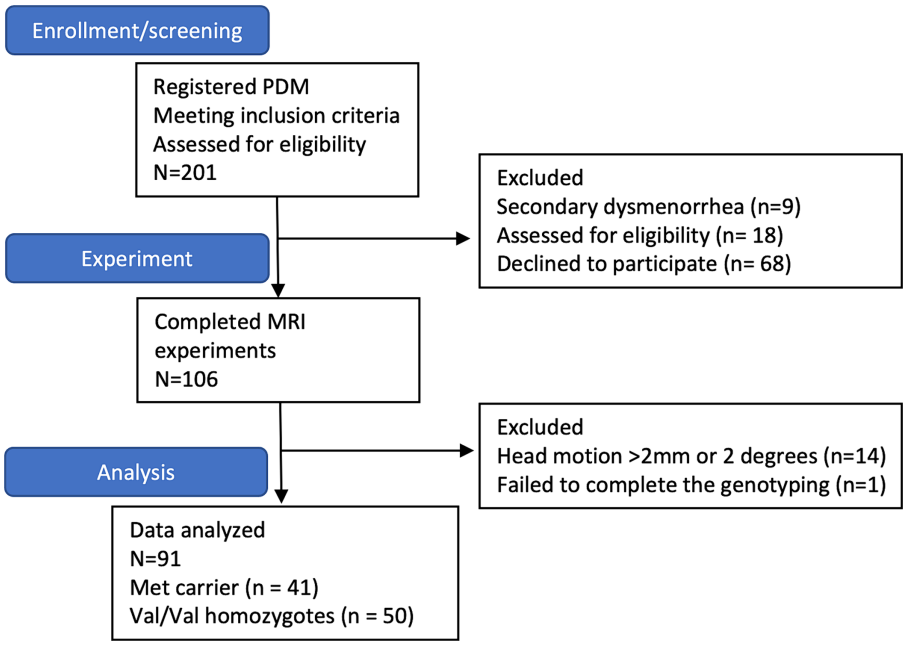

FIGURE 1
The subject flow chart. The flowchart indicates that 201 subjects with primary dysmenorrhea are initially enrolled. However, nine are excluded due to secondary dysmenorrhea; 18 are excluded due to abnormal brain findings, and eight decline participation. Ultimately, 106 subjects complete the MRI study. Among them, 14 subjects are excluded due to excessive head motion (>2 mm or 2 degrees) during scanning, and one does not successfully complete genotyping. Consequently, the final sample size comprises 91 subjects (41 Met carriers and 50 Val/Val homozygotes).

sequence (TR/TE = 2,530 ms/3.03 ms, flip angle = 7°, FOV = 224 mm × 256 mm, matrix size = 224 × 256, slice thickness = 1 mm). The initial 3 EPI scans were discarded for signal stabilization. Participants were instructed to stay awake with eyes open and heads still using head cushions and earplugs to minimize movement and noise.

2.2.2 Image preprocessing

The fMRI were preprocessed using (DPARSF) V5.2 advanced edition, built on the Data Processing and Analysis of Brain Imaging (DPABI) toolbox V6.0 (Yan et al., 2016) and Statistical Parametrical Mapping 12 (SPM12[1]) in MATLAB R2018b (The MathWorks, Inc., Natick, MA, USA). The preprocessing steps included: (1) slice timing correction, (2) realignment for head motion correction, excluding participants with head motion >2 mm displacement or > 2° rotation, (3) co-registration of T1-weighted images with mean functional image, (4) segmentation into gray matter, white matter, and cerebrospinal fluid according, (5) nuisance regression was performed using the Friston 24-parameter model (Friston et al., 1996) and SPM default masks to remove head motion parameters, as well as signals from white matter and cerebrospinal fluid. (6) spatial normalization to study-specific Diffeomorphic Anatomical Registration Through Exponentiated Lie Algebra (DARTEL) template (Ashburner, 2007) transformed to the Montreal Neurological Institute (MNI-152) space, with 3 mm isotropic voxels, (7) temporal band-pass filtering (0.01 to 0.1 Hz) and (8) smoothed with a 6 mm full-width at half-maximum (FWHM). Global signal regression (GSR) was not performed to avoid exaggerating negative correlation (Murphy et al., 2009) and distorting between-group differences (Saad et al., 2012).

2.2.3 Definition of NAc and VTA (seed region of interest)

Given the pivotal roles of the NAc and the VTA in pain modulation and reward processing within the brain's RS (DosSantos et al., 2017), we created masks for these regions to conduct region of interest (ROI)-based analyses. The NAc mask was derived from the Harvard-Oxford Subcortical Atlas (Frazier et al., 2005), while the VTA mask was delineated based on the 7 T MRI atlas (Trutti et al., 2021), using manually delineation in FSLeyes[2] (Mowinckel and Vidal-Piñeiro, 2020; Supplementary Figure 1).

2.2.4 ROI-based ALFF analysis of NAc and VTA

For ALFF analysis, each voxel's power spectrum within 0.01–0.1 Hz was calculated using a Fast Fourier Transform (FFT) (Zuo et al., 2010) and normalized to z-score maps by dividing the voxel's power by the global mean. Averaged ALFF *z*-values were extracted from the NAc and VTA ROIs using the DPABI ROI signal extractor for between-group contrasts, with statistical significance set at $p < 0.05$.

2.2.5 ROI-seed FC analysis

The image analyses in our study were performed utilizing a pre-defined RS mask created from a probabilistic map associated with "reward" from meta-analyses accessible on Neurosyn.org (Yarkoni et al., 2011).[3] This mask encompasses VTA, NAc, amygdala, basal ganglion, insula, hippocampus, PFC, sensory/motor cortex, and superior/inferior parietal lobe (Supplementary Figure 1).

Individual FC maps were generated by calculating Pearson's correlation coefficients (r) between the ROI located in the NAc and VTA, and other brain regions. The reference time course was obtained by averaging the time course of all voxels within each seed ROI. Correlation coefficients between the reference time course and the time course of each voxel were then computed to generate the FC map. To normalize the distribution, Fisher's r-to-z transformation was applied to convert *r*-values to *z*-values. Between-group differences were assessed using a two-sample t-test on the FC maps derived from NAc and VTA seed, with significance set at uncorrected voxel levels of $p < 0.001$ and $p < 0.005$, followed by the family-wise error (FWE)-corrected cluster level of $p < 0.05$ in DPABI software framework. Gonadal hormones were controlled for by regressing them out as non-interest covariates in the statistical model.

2.2.6 Correlation

To understand how the brain's RS responds to menstrual pain across various *COMT* Val158Met genotypes, we correlate pain-related metrics with ALFF *z*-values from the NAc and VTA, and *z*-value FC values from regions with significant genotype differences in NAc or VTA FC for each genotype. Specifically, we examine correlations between present pain intensity (PPI) and pain rating index (PRI) sensory scores from the MPQ to assess the pain's impact on the RS. Additionally, we explore correlations with the PCS helplessness score due to significant genotype differences observed during the menstrual phase. Pearson correlation analysis was applied, and statistical significance was defined as $p < 0.05$. To account for multiple comparisons, a Bonferroni's correction was applied by adjusting the *p*-value to 0.0167 (0.05 divided by 3), considering that three measures (PRI sensory, PPI, PCS helpless) were analyzed.

3 Results

3.1 Demographics and clinical characteristics

As shown in Table 1, 50 Val/Val homozygotes and 41 Met carriers were included in the final analysis. The subjects in the study had a long history of menstrual pain, lasting an average of 8.38 ± 3.04 years, with pain lasting approximately 2 days per menstrual cycle (1.83 ± 0.84). More than half of the subjects with PDM (56%) reported absenteeism from school or work due to their menstrual pain, and 54.9% required analgesics. There were no significant differences in scores on the MPQ (Met carrier = 30.00 ± 15.59, Val/Val = 31.91 ± 12.91), PPI (Met carrier = 2.65 ± 1.14, Val/Val = 2.60 ± 0.99), BAI (Met carrier = 11.3 ± 7.10, Val/Val = 12.08 ± 8.85), and BDI (Met carrier = 10.20 ± 6.77, Val/Val = 11.12 ± 7.78) among the different genotypes. However, the Met carrier exhibited lower PCS scores compared to Val/Val (Met carrier = 17.25 ± 11. 10, Val/Val = 22.28 ± 10.90, $p = 0.02$), particularly in the sub-scale of Pain helplessness (Met carrier = 7.58 ± 5.57, Val/Val = 10.34 ± 5.17, $p = 0.01$) (Table 1). There were no significant differences in demographic variables such as age (Met carrier = 23.15 ± 2.32, Val/Val = 23.04 ± 2.34), education (Met carrier = 15.94 ± 1.09, Val/Val = 16.00 ± 1.09), body mass index (BMI) (Met carrier = 21.11 ± 3.70, Val/Val = 20.70 ± 2.65), Edinburgh

1 http://www.fil.ion.ucl.ac.uk/spm
2 https://git.fmrib.ox.ac.uk/fsl/fsleyes/fsleyes/
3 https://neurosynth.org

TABLE 1 Demographic data and baseline information.

	Met (A) carrier ($n = 41$)	Val/Val (G) ($n = 50$)	p-value
Age (years)	23.15 ± 2.32	23.04 ± 2.34	0.82
Education (years)	15.94 ± 1.09	16.00 ± 1.09	0.68
BMI (kg/m2)	21.11 ± 3.70	20.70 ± 2.65	0.79
Edinburgh Handedness Inventory (%)	77.76 ± 21.39	85.06 ± 17.31	0.14
Years of menstruating (year)	11.00 ± 2.71	10.90 ± 2.43	0.96
Menarche age (years old)	12.15 ± 1.18	12.20 ± 1.18	0.87
Menstrual cycle (in days)	29.53 ± 1.37	29.11 ± 1.59	0.05
PCS total scores (range, 0–52)	17.25 ± 11. 10	22.28 ± 10.90	0.02
Pain rumination (range, 0–16)	6.65 ± 3.84	8.14 ± 4.24	0.09
Pain helplessness (range, 0–24)	7.58 ± 5.57	10.34 ± 5.17	0.01
Pain magnification (range, 0–12)	3.03 ± 2.36	3.80 ± 2.42	0.10
MPQ			
PRI scores (range, 0–78)	30.00 ± 15.59	31.91 ± 12.91	0.56
Sensory (range, 0–42)	16.70 ± 7.95	17.62 ± 6.48	0.57
Affective (range, 0–14)	3.78 ± 3.16	3.96 ± 2.57	0.47
Evaluation (range, 0–5)	2.27 ± 1.91	2.75 ± 2.12	0.34
Miscellaneous (range, 0–17)	7.24 ± 4.73	7.58 ± 3.85	0.72
PPI scores (range, 0–5)	2.65 ± 1.14	2.60 ± 0.99	0.69
BAI	11.3 ± 7.10	12.08 ± 8.85	0.98
BDI	10.20 ± 6.77	11.12 ± 7.78	0.56

Data are presented as the mean ± SD. BMI, body mass index; PCS, pain catastrophizing scale; MPQ, McGill pain questionnaire; PRI, pain rating index; PPI, present pain intensity; BAI, Beck Anxiety Inventory; BDI, Beck Depression Inventory BDI.

Handedness Inventory scores (Met carrier = 77.76 ± 21.39, Val/Val = 85.06 ± 17.31), years of menstruating (Met carrier = 11.00 ± 2.71, Val/Val = 10.90 ± 2.43), menarche age (Met carrier = 12.15 ± 1.18, Val/Val = 12.20 ± 1.18), and days of menstrual cycle (Met carrier = 29.53 ± 1.37, Val/Val = 29.11 ± 1.59) among the different genotypes (Table 1).

3.2 Genetic data

The distribution of the *COMT* Val158Met gene in the PDM subjects ($p = 0.97$) was consistent with the Hardy–Weinberg equilibrium. Due to the limited number of Met/Met homozygotes, the Val/Met heterozygotes and Met/Met homozygotes were combined and analyzed together as Met allele carriers.

3.3 Differences in ALFF analysis in ROI

There were no significant differences in the extracted mean z-values of ALFF between the genotypes for either the left or right NAc and VTA (Supplementary Figure 2).

3.4 Differences in ROI-seed FC

In NAc-seeded FC, Met-carriers showed decreased connectivity between the NAc and the orbital part of the inferior frontal gyrus (IFG) [ventrolateral prefrontal cortex (vlPFC)], rectus [ventromedial prefrontal cortex (vmPFC)], middle frontal gyrus (MFC) [dorsolateral prefrontal cortex (dlPFC)], and inferior parietal lobule (IPL) compared to Val/Val homozygotes (Table 2 and Figure 2A). In VTA- seeded FC, Met-carriers exhibited decreased connectivity between the VTA and the MFC (dlPFC), precentral gyrus, and superior parietal lobule (SPL) compared to Val/Val homozygotes (Table 2 and Figure 2B).

3.5 Correlation

In Met carriers of PDM during the menstrual phase, NAc showed a positive correlation between ALFF values and PCS helplessness scores ($p = 0.15$, $r = 0.39$) (Table 3 and Figure 3A). The VTA exhibited negative correlations between ALFF values and PRI sensory scores (left: $p = 0.02$, $r = -0.39$; right: $p = 0.02$, $r = -0.39$), PPI (left: $p < 0.01$, $r = -0.50$; right: $p < 0.01$, $r = -0.53$), and PCS helplessness scores (left: $p = 0.01$, $r = -0.40$; right: $p = 0.02$, $r = -0.39$) (Table 3 and Figure 3C). Additionally, NAc FC to the Rectus (vmPFC) was positively correlated with PPI ($p = 0.05$, $r = 0.33$) (Table 3 and Figure 3B), while VTA FC to the medial frontal cortex (dlPFC) ($p = 0.03$, $r = -0.35$) and bilateral SPL were negatively correlated with PRI sensory scores (right: $p = 0.03$, $r = -0.35$; left: $p = 0.03$, $r = -0.36$) (Table 3 and Figures 3D,E). No significant correlations were found between ALFF or FC values and pain-related metrics in Val/Val homozygotes (Table 3).

TABLE 2 FC differences in the RS between genotypes.

Seed	Contrast of genotype	Region, laterality	BA	Cluster	*t* score	Peak coordinate		
						x	*y*	*z*
NAc	Met carrier < Val/Val	NS						
	Met carrier < Val/Val	R Orbital IFG (vlPFC)*	47	170	4.35	34	32	−18
		L Rectus (vmPFC)*	11	305	4.00	−4	46	−16
		R MFC (dlPFC)	46	182	3.73	44	40	18
		L IPL	40	85	3.27	−36	−48	46
VTA	Met carrier > Val/Val	NS						
	Met carrier < Val/Val	R MFC (dlPFC)*	46	158	3.98	48	40	16
		L Precentral		75	3.02	−48	2	28
		R SPL		359	3.93	32	−60	56
		L SPL*	7	389	4.34	−26	−60	48

Peak coordinates refer to the MNI space. Significance was set at the uncorrected voxel level $p < 0.005$ followed by the family-wise error corrected cluster level $p < 0.05$; FC, functional connectivity; RS, reward system; NAc, nucleus accumbens; VTA, ventral tegmental area; BA, Brodmann area; NS, non-significant; R, right; L, left; IFG, inferior frontal gyrus; vlPFC, ventrolateral prefrontal cortex; vmPFC, ventromedial prefrontal cortex; MFC, middle frontal gyrus; dlPFC, dorsolateral prefrontal cortex; IPL, inferior parietal lobule; SPL, superior parietal lobule. *Denotes significant results thresholded at an uncorrected voxel threshold of $p < 0.001$.

TABLE 3 Correlation between RS neurodynamic metrics and psychological pain metrics.

Genotype	Region	Method	Psychological pain metrics	*p*-value	*r*
Region of interest					
Met carrier	L. NAc	ALFF	PCS helplessness score	0.0151*	0.3818
	R. NAc	ALFF	NS		
	L. VTA	ALFF	MPQ_PRI sensory score	0.0183	−0.3858
			PPI	0.0017*	−0.4985
			PCS helplessness score	0.0103*	−0.4013
	R. VTA	ALFF	MPQ_PRI sensory score	0.0186	−0.3852
			PPI	0.0007*	−0.5314
			PCS helplessness score	0.0195	−0.3680
Val/Val	NS				
Significant regions of FC analysis					
Met carrier	L Rectus (vmPFC)	NAc FC	PPI	0.0490	0.3260
	R MFC (dlPFC)	VTA FC	MPQ_PRI_Sensory score	0.0330	−0.3513
	R SPL	VTA FC	MPQ_PRI_Sensory score	0.0345	−0.3485
	L SPL	VTA FC	MPQ_PRI_Sensory score	0.0264	−0.3649
Val/Val	NS				

RS, reward system; R, right; L, left; NAc, Nucleus accumbens; VTA, ventral tegmental area; ALFF, amplitude of low frequency fluctuations; PCS, pain catastrophizing scale; MPQ, McGill pain questionnaire; PRI, pain rating index; PPI, present pain intensity; NS, non-significant; FC, functional connectivity; vmPFC, ventromedial prefrontal cortex; MFC, middle frontal gyrus; dlPFC, dorsolateral prefrontal cortex; SPL, superior parietal lobule. *Signifies significant results after Bonferroni correction ($p < 0.016$).

4 Discussion

This study demonstrates that the *COMT* Val158Met polymorphism leads to genotype-specific differences in the FC (Val > Met) and distinct correlation patterns between neurodynamic metrics and pain metrics within key RS areas, specifically the NAc and VTA, during menstrual pain. Met carriers exhibit dynamic changes that correlate with pain metrics, suggesting an active role of their RS in driving motivation and top-down regulation. In contrast, the Val genotype, which shows greater individual variations and lacks a clear correlation with the pain metrics, aligning with the proposition of a higher functionality.

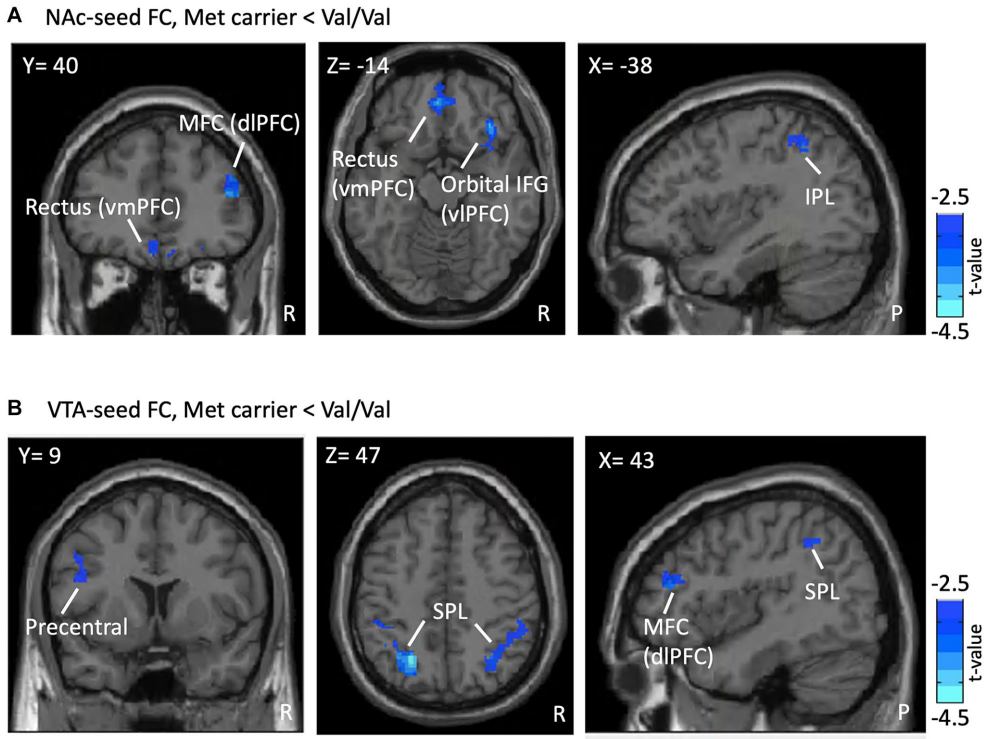

FIGURE 2
FC differences in the RS between genotypes. Presented are the outcomes of FC analyses, illustrating differences associated with the *COMT* Val158Met polymorphism within a reward-oriented mask defined on Neurosyn.org. **(A)** Shows lower NAc-seeded FC in Met carriers between the NAc and regions including the MFC (dlPFC), rectus (vmPFC), orbital IFG (vlPFC), and IPL compared to Val/Val homozygotes (blue region). **(B)** Reveals lower VTA-seeded FC in Met carriers between the VTA and the MFC (dlPFC), precentral gyrus, and SPL. Results are thresholded at the uncorrected voxel level $p = 0.005$, followed by the FWE-corrected cluster level $p = 0.05$. The color bar denotes the t-score. ROI, region of interest; FC, functional connectivity; RS, reward system; NAc, nucleus accumbens; MFC, middle frontal gyrus; dlPFC, dorsolateral prefrontal cortex; vmPFC, ventromedial prefrontal cortex; IFG, inferior frontal gyrus; vlPFC, ventrolateral prefrontal cortex; IPL, inferior parietal lobule; VTA, ventral tegmental area; SPL, superior parietal lobule; R, right; P, posterior.

4.1 The RS psychoneurodynamics of Met carriers implicating pain-avoidance motivation

Although there were no differences in NAc ALFF values between genotypes (Supplementary Figure 2), Met carriers showed a positive correlation between NAc ALFF values and PCS helplessness scores (Table 3 and Figure 3A). Additionally, the FC between the NAc and vmPFC positively correlated with PPI (Table 3 and Figure 3B). These suggest that Met carriers may be associated with a stronger motivation to alleviate menstrual pain as a reward (Leknes et al., 2011), aligning with increased reward-seeking and more expressed pleasant responses in Met genotype individuals (Frank et al., 2009; Lancaster et al., 2012). Reward seeking and motivation are primarily driven by dopaminergic signals from the VTA to the NA (Navratilova and Porreca, 2014). The vmPFC plays a crucial role in processing rewards and regulating emotions, while dopaminergic projections from the PFC to the NAc modulate these functions (Huang et al., 2019). Given that COMT is primarily found in the PFC (Matsumoto et al., 2003), the *COMT* Val158Met polymorphism may modulate pain-relief motivation during menstrual pain.

4.2 Enhanced pain modulation in Met carrier

Despite no differences in VTA ALFF values between genotypes (Supplementary Figure 2), Met carriers exhibited negative correlations between VTA ALFF values and PRI sensory scores (Table 3 and Figure 3C), PCS helplessness scores, and PPI. Additionally, FC between the VTA and dlPFC/SPL negatively correlated with PRI sensory scores (Table 3 and Figures 3D,E). Higher VTA ALFF and FC values are associated with lower PCS, PRI, and PPI, suggesting that VTA activity may modulate the pain experience in Met carriers. The VTA, a dopaminergic center of the motivational circuit (Navratilova and Porreca, 2014), interacts with the SPL, which processes and integrates sensory information (Teixeira et al., 2014; Passarelli et al., 2021). The VTA also interacts with the dlPFC, which is involved in emotional regulation (Buhle et al., 2014; Frank et al., 2014) and top-down pain suppression (Lorenz et al., 2003; Seminowicz and Moayedi, 2017).

The VTA interacts with the NAc (Navratilova and Porreca, 2014) and possibly projects to the periaqueductal gray (PAG) (Omelchenko and Sesack, 2010; Ntamati et al., 2018; Cappon et al., 2019), a core

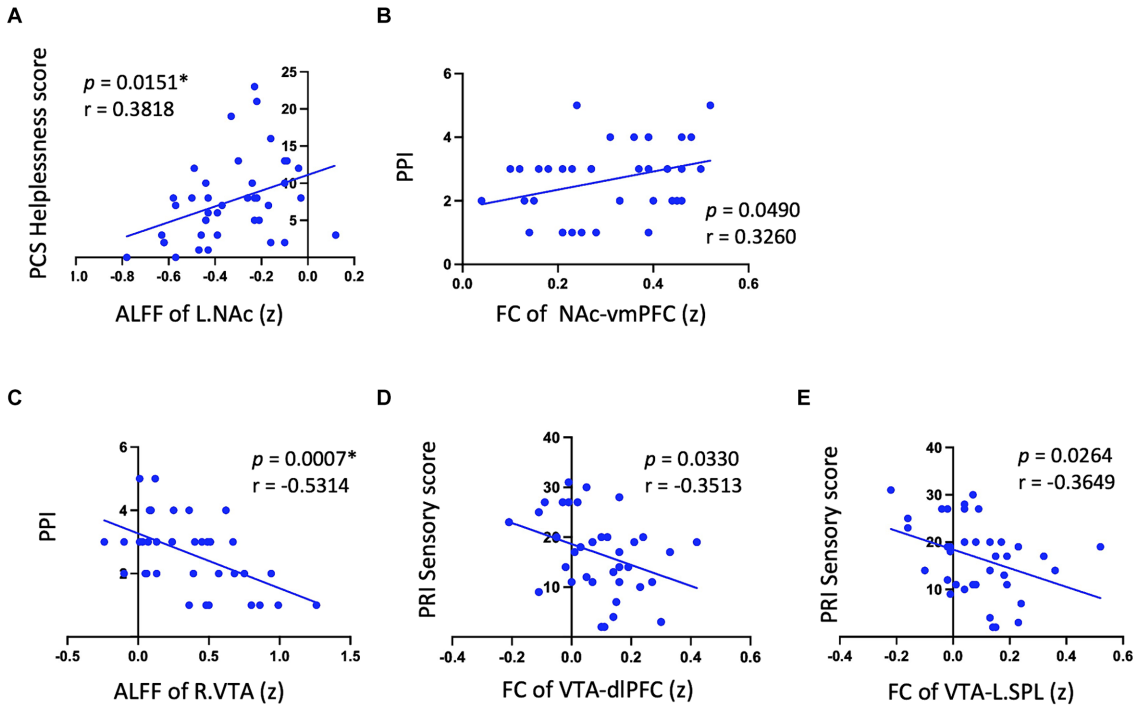

FIGURE 3
Significant correlation between psychological pain metrics and RS neurodynamic metrics in met carriers. Significant results are observed only in Met carriers. **(A)** Shows a positive correlation between NAc ALFF values and PCS helplessness scores. **(B)** Indicates that NAc FC to the Rectus (vmPFC) is positively correlated with PPI. **(C)** Displays a negative correlation between VTA ALFF values and PPI. **(D,E)** Reveal that VTA FC to the medial frontal cortex (dlPFC) and bilateral SPL are negatively correlated with PRI sensory scores. This figure displays only a significant subset of the correlation data to illustrate the positive and negative correlation trends between neurodynamic metrics and pain metrics in the NAc and VTA. Detailed data are provided in Table 3. RS, reward system; L, left; NAc, nucleus accumbens; ALFF, amplitude of low-frequency fluctuations; PCS, pain catastrophizing scale; FC, functional connectivity; vmPFC, ventromedial prefrontal cortex; PPI, present pain intensity; R, right; VTA, ventral tegmental area; dlPFC, dorsolateral prefrontal cortex; SPL, superior parietal lobule; PRI, pain rating index. (z) indicates z-transformed mean values for ALFF and FC. *Signifies significant results after Bonferroni correction ($p < 0.016$).

region of the descending pain modulation and opioid modulation systems (Linnman et al., 2012). The negative correlations between VTA neurodynamic metrics and pain psychological metrics in Met carriers may be mediated by the interaction between the dopamine system and the mu-opioid system (Zubieta et al., 2003; Rakvåg et al., 2008). This is supported by findings that the Met allele, associated with lower COMT enzyme activity, shows higher mu-opioid receptor binding in striatal regions, which potentially regulates the motivational circuit by integrating sensory information and motor response with affective and cognitive influences (Zubieta et al., 2003).

While both the VTA and NAc are involved in motivation and reward (Navratilova and Porreca, 2014), they may have different modulation mechanisms through their synergy with various brain areas (Haber and Knutson, 2010; Mitsi and Zachariou, 2016). The differing responses of the VTA and NAc to menstrual pain may reflect the RS's multi-dimensional adaptation in PDM subjects. However, the stronger coupling between neurodynamic expressions and psychological manifestations in Met carriers may implicate reduced flexibility in their RS. The Met allele of the *COMT* gene is associated with lower COMT activity, which is hypothesized to increase tonic dopamine levels while decreasing phasic dopamine release. This alteration enhances brain network stability but reduces flexibility (Bilder et al., 2004). Such a reduction in flexibility may increase the risk of developing chronic pain (Bilder et al., 2004; Andersen and Skorpen, 2009). Given that functional pain disorders and chronic pain conditions such as irritable bowel syndrome, fibromyalgia, chronic fatigue syndrome, and lower back pain may co-occur with PDM later in life (Altman et al., 2006; Berkley, 2013; Chung et al., 2014; Tu et al., 2020), further longitudinal exploration of the potential association between Met carriers and chronic pain can be both heuristic and significant.

4.3 Lower helplessness score in Met carriers

In our study, there were no significant differences in MPQ and PPI scores between genotypes (Table 1), suggesting that the *COMT* Val158Met polymorphism does not impact pain intensity in young PDM subjects. However, Met carriers had significantly lower total PCS scores, particularly in the helplessness domain (Table 1). The PCS assesses cognitive-affective responses to pain, emphasizing negative aspects such as helplessness (Sullivan et al., 1995). These responses may be underpinned by the brain's attention network (Rischer et al., 2020) and limbic system (Bushnell et al., 2013; Galambos et al., 2019), which can interfere with the descending pain inhibitory system (Toledo et al., 2020). An active RS can enhance positive affect and motivation (Navratilova and Porreca, 2014), potentially counteracting

negative emotional states like helplessness (Kuhl, 1981; Butler and Roediger, 2008). Therefore, the lower PCS helplessness scores in Met carriers may be ascribed to stronger motivation and enhanced pain modulation.

4.4 Val homozygotes with diverse responses

Val homozygotes exhibit higher NAc/VTA-seed FC without a clear correlation to pain metrics, potentially indicating diversity in brain-behavior relationship. The enhanced FC regions in Val homozygotes are related to pain modulation, such as the SPL and IPL for sensory processing (Teixeira et al., 2014; Berlucchi and Vallar, 2018), dlPFC and mPFC for emotional and cognitive top-down pain modulation (Lorenz et al., 2003; Ong et al., 2019), and the precentral gyrus for descending pain modulation in PDM subjects (Wei et al., 2016a; Hsu et al., 2023; Figures 2A,B). Val allele carriers may engage dlPFC and insula as compared to Met allele carriers during pain (Schmahl et al., 2012). Additionally, a previous study reported that the rs4680 Val allele, when combined with different rs4818 and rs6269 sequences, leads to varying levels of pain sensitivity (Diatchenko et al., 2005). This variability in sensitivities may account for the lack of a direct correlation between RS neurodynamics and psychological pain metrics. Thus, Val homozygotes demonstrate greater flexibility, potentially adaptive, in the RS, consistent with the tonic-phasic dopamine hypothesis (Bilder et al., 2004).

4.5 Limitations and further consideration

This study has several limitations. First, due to the lower prevalence of Met/Met homozygotes in East Asians for the *COMT* Val158Met polymorphism (Wang et al., 2016), our study lacked a sufficient number of Met/Met individuals, requiring us to group genotypes into Met carriers and Val groups. The predominance of Val/Met genotypes among Met carriers suggests that their RS regulation may primarily reflect Val/Met characteristics. Second, using pain metrics to infer the RS's motivational response requires further behavioral testing to confirm elevated motivation (Leknes et al., 2011). Third, considering that PDM is not classified as a neuropsychiatric disease with prominent functional and structural changes, we aimed to capture subtle yet potentially significant information to provide valuable insight for future research (Marek et al., 2022). Therefore, we presented two levels of statistical information in the results: a relatively permissive uncorrected voxel level of $p < 0.005$ and more stringent uncorrected voxel level of $p < 0.001$, both followed by a family-wise error (FWE) corrected cluster level of $p < 0.05$. This approach has been adopted by many authors in the field of neuroimaging (e.g., Roiser et al., 2016; Wei et al., 2016b; Liu et al., 2023a). However, the risk of false positives should be carefully considered in data interpretation (Marek et al., 2022). Fourth, considering that *COMT* polymorphisms' influence on pain sensitivity may extend beyond single SNP variations and affect opioid consumption (Zubieta et al., 2003; Diatchenko et al., 2005), future studies should analyze additional haplotype sequences and explore gene–gene interactions within *COMT*.

5 Conclusion

This study provides novel insight into the neurodynamic impact of the *COMT* Val158Met polymorphism on VTA and NAc-based RS's FC. During the menstrual cycle, the functional dynamics of the RS exhibit varying modulation flexibility associated with the individual's *COMT* Val158Met genotype. These genetic factors influencing brain resilience may contribute to individual pain experience and coping mechanisms in PDM, potentially affecting future vulnerability to other chronic pain disorders. Further research is required to determine if the *COMT*-genotype-specific modulation of RSs correlates with other chronic pain conditions later in life.

Data availability statement

The raw data supporting the conclusions of this article will be made available by the authors, without undue reservation.

Ethics statement

The studies involving humans were approved by Institutional Review Board of Taipei Veterans General Hospital. The studies were conducted in accordance with the local legislation and institutional requirements. The participants provided their written informed consent to participate in this study.

Author contributions

P-SH: Conceptualization, Data curation, Formal analysis, Investigation, Methodology, Validation, Visualization, Writing – original draft. C-HL: Investigation, Validation, Writing – review & editing. C-JY: Formal analysis, Validation, Writing – review & editing. L-CL: Investigation, Validation, Writing – review & editing. W-CL: Data curation, Investigation, Writing – review & editing. H-TC: Investigation, Resources, Writing – review & editing. M-WL: Methodology, Resources, Writing – review & editing. L-FC: Conceptualization, Funding acquisition, Methodology, Resources, Writing – review & editing. J-CH: Conceptualization, Methodology, Project administration, Resources, Supervision, Writing – review & editing.

Funding

The author(s) declare that financial support was received for the research, authorship, and/or publication of this article. This work was supported by the Taipei Veterans General Hospital (V100D-001, V100D-001-1, V100D-001-2, and V101C-152), National Science and Technology Council (NSC 100-2314-B010-006-MY3, NSC 100-2629-B-010-001, NSC 102-2629-B-010-001, MOST 103-2321-B-010-020, MOST 106-2629-B-010-001-MY3, MOST 108-2314-B-010-001, MOST 109-2314-B-101-001-MY3, and MOST 109-2314-B-350-001), TVGH-NTUH joint research program (VN103-4, VN104-03, and VN105-03), and the Aim for the Top University Plan of the Ministry of Education of National Yang-Ming University. The funders had no

role in study design, data collection and analysis, the decision to publish, or manuscript preparation.

Acknowledgments

The authors thank all participants in this study and appreciate Intan Low, Tzu-Yi Hong, and Tzu-Ling Tzeng for their technical and experimental help.

Conflict of interest

The authors declare that the research was conducted in the absence of any commercial or financial relationships that could be construed as a potential conflict of interest.

Publisher's note

Supplementary material

The Supplementary material for this article can be found online at: https://www.frontiersin.org/articles/10.3389/fnmol.2024.1457602/full#supplementary-material

References

Altman, G., Cain, K. C., Motzer, S., Jarrett, M., Burr, R., and Heitkemper, M. (2006). Increased symptoms in female IBS patients with dysmenorrhea and PMS. *Gastroenterol. Nurs.* 29, 4–11. doi: 10.1097/00001610-200601000-00002

Andersen, S., and Skorpen, F. (2009). Variation in the *COMT* gene: implications for pain perception and pain treatment. *Pharmacogenomics* 10, 669–684. doi: 10.2217/pgs.09.13

Ashburner, J. (2007). A fast diffeomorphic image registration algorithm. *Neuroimage* 38, 95–113. doi: 10.1016/j.neuroimage.2007.07.007

Baliki, M. N., Petre, B., Torbey, S., Herrmann, K. M., Huang, L., Schnitzer, T. J., et al. (2012). Corticostriatal functional connectivity predicts transition to chronic back pain. *Nat. Neurosci.* 15, 1117–1119. doi: 10.1038/nn.3153

Becerra, L., Breiter, H. C., Wise, R., Gonzalez, R. G., and Borsook, D. (2001). Reward circuitry activation by noxious thermal stimuli. *Neuron* 32, 927–946. doi: 10.1016/S0896-6273(01)00533-5

Beck, A. T., and Steer, R. (1993). Manual for the back anxiety inventrory. San Antonio: Psychological Corporation.

Beck, A. T., Steer, R., and Brown, G. (1996). Manual for beck depression inventory-II. San Antonio: Psychological Corporation.

Berkley, K. J. (2013). Primary dysmenorrhea: an urgent mandate. *Pain* 1:8.

Berlucchi, G., and Vallar, G. (2018). The history of the neurophysiology and neurology of the parietal lobe. *Handb. Clin. Neurol.* 151, 3–30. doi: 10.1016/B978-0-444-63622-5.00001-2

Bilder, R. M., Volavka, J., Lachman, H. M., and Grace, A. A. (2004). The catechol-O-methyltransferase polymorphism: relations to the tonic–phasic dopamine hypothesis and neuropsychiatric phenotypes. *Neuropsychopharmacology* 29, 1943–1961. doi: 10.1038/sj.npp.1300542

Buhle, J. T., Silvers, J. A., Wager, T. D., Lopez, R., Onyemekwu, C., Kober, H., et al. (2014). Cognitive reappraisal of emotion: a meta-analysis of human neuroimaging studies. *Cereb. Cortex* 24, 2981–2990. doi: 10.1093/cercor/bht154

Bushnell, M. C., Čeko, M., and Low, L. A. (2013). Cognitive and emotional control of pain and its disruption in chronic pain. *Nat. Rev. Neurosci.* 14, 502–511. doi: 10.1038/nrn3516

Butler, A. C., and Roediger, H. L. (2008). Feedback enhances the positive effects and reduces the negative effects of multiple-choice testing. *Mem. Cogn.* 36, 604–616. doi: 10.3758/MC.36.3.604

Cappon, D., Ryterska, A., Lagrata, S., Miller, S., Akram, H., Hyam, J., et al. (2019). Ventral tegmental area deep brain stimulation for chronic cluster headache: effects on cognition, mood, pain report behaviour and quality of life. *Cephalalgia* 39, 1099–1110. doi: 10.1177/0333102419839957

Chung, S. D., Liu, S. P., Lin, H. C., and Kang, J. H. (2014). Association of dysmenorrhea with interstitial cystitis/bladder pain syndrome: a case–control study. *Acta Obstet. Gynecol. Scand.* 93, 921–925. doi: 10.1111/aogs.12437

Cohen, H., Neumann, L., Glazer, Y., Ebstein, R., and Buskila, D. (2009). The relationship between a common catechol-O-methyltransferase (*COMT*) polymorphism val158met and fibromyalgia. *Clin. Exp. Rheumatol.* 27, S51–S56.

Diatchenko, L., Slade, G. D., Nackley, A. G., Bhalang, K., Sigurdsson, A., Belfer, I., et al. (2005). Genetic basis for individual variations in pain perception and the development of a chronic pain condition. *Hum. Mol. Genet.* 14, 135–143. doi: 10.1093/hmg/ddi013

Ding, J., Xu, X., Rana, N., and Dmowski, W. (2010). *COMT* Val-158-met gene polymorphism is not associated with endometriosis-related pain. *Fertil. Steril.* 94:S207. doi: 10.1016/j.fertnstert.2010.07.801

DosSantos, M. F., Moura, B. D. S., and And Dasilva, A. F. (2017). Reward circuitry plasticity in pain perception and modulation. *Front. Pharmacol.* 8:790. doi: 10.3389/fphar.2017.00790

Elman, I., and Borsook, D. (2016). Common brain mechanisms of chronic pain and addiction. *Neuron* 89, 11–36. doi: 10.1016/j.neuron.2015.11.027

Frank, D., Dewitt, M., Hudgens-Haney, M., Schaeffer, D., Ball, B., Schwarz, N., et al. (2014). Emotion regulation: quantitative meta-analysis of functional activation and deactivation. *Neurosci. Biobehav. Rev.* 45, 202–211. doi: 10.1016/j.neubiorev.2014.06.010

Frank, M. J., Doll, B. B., Oas-Terpstra, J., and Moreno, F. (2009). Prefrontal and striatal dopaminergic genes predict individual differences in exploration and exploitation. *Nat. Neurosci.* 12, 1062–1068. doi: 10.1038/nn.2342

Frazier, J. A., Chiu, S., Breeze, J. L., Makris, N., Lange, N., Kennedy, D. N., et al. (2005). Structural brain magnetic resonance imaging of limbic and thalamic volumes in pediatric bipolar disorder. *Am. J. Psychiatry* 162, 1256–1265. doi: 10.1176/appi.ajp.162.7.1256

Friston, K. J., Williams, S., Howard, R., Frackowiak, R. S., and Turner, R. (1996). Movement-related effects in fMRI time-series. *Magn. Reson. Med.* 35, 346–355. doi: 10.1002/mrm.1910350312

Galambos, A., Szabó, E., Nagy, Z., Édes, A. E., Kocsel, N., Juhász, G., et al. (2019). A systematic review of structural and functional MRI studies on pain catastrophizing. *J. Pain Res.* 12, 1155–1178. doi: 10.2147/JPR.S192246

Gerra, M. C., Dallabona, C., Manfredini, M., Giordano, R., Capriotti, C., González-Villar, A., et al. (2022). The polymorphism Val158Met in the *COMT* gene: disrupted dopamine system in fibromyalgia patients? *Pain* 10:3313. doi: 10.1097/j.pain.0000000000003313

Goeders, N. E., and Smith, J. E. (1983). Cortical dopaminergic involvement in cocaine reinforcement. *Science* 221, 773–775. doi: 10.1126/science.6879176

Gogos, J. A., Morgan, M., Luine, V., Santha, M., Ogawa, S., Pfaff, D., et al. (1998). Catechol-O-methyltransferase-deficient mice exhibit sexually dimorphic changes in catecholamine levels and behavior. *Proc. Natl. Acad. Sci.* 95, 9991–9996. doi: 10.1073/pnas.95.17.9991

Haber, S. N., and Knutson, B. (2010). The reward circuit: linking primate anatomy and human imaging. *Neuropsychopharmacology* 35, 4–26. doi: 10.1038/npp.2009.129

Hsu, P.-S., Cheng, C.-M., Chao, H.-T., Lin, M.-W., Li, W.-C., Lee, L.-C., et al. (2023). OPRM1 A118G polymorphism modulating motor pathway for pain adaptability in women with primary dysmenorrhea. *Front. Neurosci.* 17:1179851. doi: 10.3389/fnins.2023.1179851

Huang, S., Borgland, S. L., and Zamponi, G. W. (2019). Dopaminergic modulation of pain signals in the medial prefrontal cortex: challenges and perspectives. *Neurosci. Lett.* 702, 71–76. doi: 10.1016/j.neulet.2018.11.043

Itani, R., Soubra, L., Karout, S., Rahme, D., Karout, L., and Khojah, H. M. (2022). Primary dysmenorrhea: pathophysiology, diagnosis, and treatment updates. *Korean J. Fam. Med.* 43, 101–108. doi: 10.4082/kjfm.21.0103

Käenmäki, M., Tammimäki, A., Myöhänen, T., Pakarinen, K., Amberg, C., Karayiorgou, M., et al. (2010). Quantitative role of *COMT* in dopamine clearance in the prefrontal cortex of freely moving mice. *J. Neurochem.* 114, 1745–1755. doi: 10.1111/j.1471-4159.2010.06889.x

Kuhl, J. (1981). Motivational and functional helplessness: the moderating effect of state versus action orientation. *J. Pers. Soc. Psychol.* 40, 155–170. doi: 10.1037/0022-3514.40.1.155

Lancaster, T., Linden, D., and Heerey, E. (2012). *COMT* val158met predicts reward responsiveness in humans. *Genes Brain Behav.* 11, 986–992. doi: 10.1111/j.1601-183X.2012.00838.x

Lee, L.-C., Chen, Y.-Y., Li, W.-C., Yang, C.-J., Liu, C.-H., Low, I., et al. (2023). Adaptive neuroplasticity in the default mode network contributing to absence of central sensitization in primary dysmenorrhea. *Front. Neurosci.* 17:144. doi: 10.3389/fnins.2023.1094988

Leknes, S., Lee, M., Berna, C., Andersson, J., and Tracey, I. (2011). Relief as a reward: hedonic and neural responses to safety from pain. *PLoS One* 6:e17870. doi: 10.1371/journal.pone.0017870

Linnman, C., Moulton, E. A., Barmettler, G., Becerra, L., and Borsook, D. (2012). Neuroimaging of the periaqueductal gray: state of the field. *Neuroimage* 60, 505–522. doi: 10.1016/j.neuroimage.2011.11.095

Liu, N., Huo, J., Li, Y., Hao, Y., Dai, N., Wu, J., et al. (2023a). Changes in brain structure and related functional connectivity during menstruation in women with primary dysmenorrhea. *Quant. Imaging Med. Surg.* 13, 1071–1082. doi: 10.21037/qims-22-683

Liu, N., Li, Y., Hong, Y., Huo, J., Chang, T., Wang, H., et al. (2023b). Altered brain activities in mesocorticolimbic pathway in primary dysmenorrhea patients of long-term menstrual pain. *Front. Neurosci.* 17:1098573. doi: 10.3389/fnins.2023.1098573

Lorenz, J., Minoshima, S., and Casey, K. (2003). Keeping pain out of mind: the role of the dorsolateral prefrontal cortex in pain modulation. *Brain* 126, 1079–1091. doi: 10.1093/brain/awg102

Marek, S., Tervo-Clemmens, B., Calabro, F. J., Montez, D. F., Kay, B. P., Hatoum, A. S., et al. (2022). Reproducible brain-wide association studies require thousands of individuals. *Nature* 603, 654–660. doi: 10.1038/s41586-022-04492-9

Matsumoto, M., Weickert, C. S., Akil, M., Lipska, B., Hyde, T., Herman, M., et al. (2003). Catechol O-methyltransferase mRNA expression in human and rat brain: evidence for a role in cortical neuronal function. *Neuroscience* 116, 127–137. doi: 10.1016/S0306-4522(02)00556-0

Melzack, R. (1987). The short-form McGill pain questionnaire. *Pain* 30, 191–197. doi: 10.1016/0304-3959(87)91074-8

Mitsi, V., and Zachariou, V. (2016). Modulation of pain, nociception, and analgesia by the brain reward center. *Neuroscience* 338, 81–92. doi: 10.1016/j.neuroscience.2016.05.017

Mowinckel, A. M., and Vidal-Piñeiro, D. (2020). Visualization of brain statistics with R packages ggseg and ggseg3d. *Adv. Methods Pract. Psychol. Sci.* 3, 466–483. doi: 10.1177/2515245920928009

Murphy, K., Birn, R. M., Handwerker, D. A., Jones, T. B., and Bandettini, P. A. (2009). The impact of global signal regression on resting state correlations: are anti-correlated networks introduced? *Neuroimage* 44, 893–905. doi: 10.1016/j.neuroimage.2008.09.036

Navratilova, E., and Porreca, F. (2014). Reward and motivation in pain and pain relief. *Nat. Neurosci.* 17, 1304–1312. doi: 10.1038/nn.3811

Ntamati, N. R., Creed, M., Achargui, R., and Lüscher, C. (2018). Periaqueductal efferents to dopamine and GABA neurons of the VTA. *PLoS One* 13:e0190297. doi: 10.1371/journal.pone.0190297

Omelchenko, N., and Sesack, S. R. (2010). Periaqueductal gray afferents synapse onto dopamine and GABA neurons in the rat ventral tegmental area. *J. Neurosci. Res.* 88, 981–991. doi: 10.1002/jnr.22265

Ong, W.-Y., Stohler, C. S., and Herr, D. R. (2019). Role of the prefrontal cortex in pain processing. *Mol. Neurobiol.* 56, 1137–1166. doi: 10.1007/s12035-018-1130-9

Passarelli, L., Gamberini, M., and Fattori, P. (2021). The superior parietal lobule of primates: a sensory-motor hub for interaction with the environment. *J. Integr. Neurosci.* 20, 157–171. doi: 10.31083/j.jin.2021.01.334

Patanwala, I. Y., Lamvu, G., Ledger, W. J., Witzeman, K., Marvel, R., Rapkin, A., et al. (2017). Catechol-O-methyltransferase gene polymorphism and vulvar pain in women with vulvodynia. *Am. J. Obstet. Gynecol.* 216, 395.e1–e396. doi: 10.1016/j.ajog.2016.10.020

Rakvåg, T. T., Ross, J. R., Sato, H., Skorpen, F., Kaasa, S., and Klepstad, P. (2008). Genetic variation in the catechol-O-methyltransferase (*COMT*) gene and morphine requirements in cancer patients with pain. *Mol. Pain* 4:64. doi: 10.1186/1744-8069-4-64

Rischer, K. M., González-Roldán, A. M., Montoya, P., Gigl, S., Anton, F., and van der Meulen, M. (2020). Distraction from pain: the role of selective attention and pain catastrophizing. *Eur. J. Pain* 24, 1880–1891. doi: 10.1002/ejp.1634

Roiser, J., Linden, D., Gorno-Tempinin, M., Moran, R., Dickerson, B., and Grafton, S. (2016). Minimum statistical standards for submissions to Neuroimage: clinical. *Neuroimage Clin.* 12, 1045–1047. doi: 10.1016/j.nicl.2016.08.002

Saad, Z. S., Gotts, S. J., Murphy, K., Chen, G., Jo, H. J., Martin, A., et al. (2012). Trouble at rest: how correlation patterns and group differences become distorted after global signal regression. *Brain Connect.* 2, 25–32. doi: 10.1089/brain.2012.0080

Schmahl, C., Ludäscher, P., Greffrath, W., Kraus, A., Valerius, G., Schulze, T. G., et al. (2012). *COMT* val158met polymorphism and neural pain processing. *PLoS One* 7:e23658. doi: 10.1371/journal.pone.0023658

Seminowicz, D. A., and Moayedi, M. (2017). The dorsolateral prefrontal cortex in acute and chronic pain. *J. Pain* 18, 1027–1035. doi: 10.1016/j.jpain.2017.03.008

Serafini, R. A., Pryce, K. D., and Zachariou, V. (2020). The mesolimbic dopamine system in chronic pain and associated affective comorbidities. *Biol. Psychiatry* 87, 64–73. doi: 10.1016/j.biopsych.2019.10.018

Sullivan, M. J., Bishop, S. R., and Pivik, J. (1995). The pain catastrophizing scale: development and validation. *Psychol. Assess.* 7, 524–532. doi: 10.1037/1040-3590.7.4.524

Teixeira, S., Machado, S., Velasques, B., Sanfim, A., Minc, D., Peressutti, C., et al. (2014). Integrative parietal cortex processes: neurological and psychiatric aspects. *J. Neurol. Sci.* 338, 12–22. doi: 10.1016/j.jns.2013.12.025

Toledo, T. A., Kuhn, B. L., Payne, M. F., Lannon, E. W., Palit, S., Sturycz, C. A., et al. (2020). The effect of pain catastrophizing on endogenous inhibition of pain and spinal nociception in native Americans: results from the Oklahoma study of native American pain risk. *Ann. Behav. Med.* 54, 575–594. doi: 10.1093/abm/kaaa004

Trutti, A. C., Fontanesi, L., Mulder, M. J., Bazin, P.-L., Hommel, B., and Forstmann, B. U. (2021). A probabilistic atlas of the human ventral tegmental area (VTA) based on 7 tesla MRI data. *Brain Struct. Funct.* 226, 1155–1167. doi: 10.1007/s00429-021-02231-w

Tu, C.-H., Lin, C.-L., Yang, S.-T., Shen, W.-C., and Chen, Y.-H. (2020). Hormonal contraceptive treatment may reduce the risk of fibromyalgia in women with dysmenorrhea: a cohort study. *J. Pers. Med.* 10:280. doi: 10.3390/jpm10040280

Tu, C.-H., Niddam, D. M., Chao, H.-T., Chen, L.-F., Chen, Y.-S., Wu, Y.-T., et al. (2010). Brain morphological changes associated with cyclic menstrual pain. *Pain* 150, 462–468. doi: 10.1016/j.pain.2010.05.026

Tu, C.-H., Niddam, D. M., Yeh, T.-C., Lirng, J.-F., Cheng, C.-M., Chou, C.-C., et al. (2013). Menstrual pain is associated with rapid structural alterations in the brain. *Pain* 154, 1718–1724. doi: 10.1016/j.pain.2013.05.022

Wang, M., Ma, Y., Yuan, W., Su, K., and Li, M. D. (2016). Meta-analysis of the *COMT* Val158Met polymorphism in major depressive disorder: effect of ethnicity. *J. Neuroimmune Pharmacol.* 11, 434–445. doi: 10.1007/s11481-016-9651-3

Wei, S.-Y., Chao, H.-T., Tu, C.-H., Li, W.-C., Low, I., Chuang, C.-Y., et al. (2016a). Changes in functional connectivity of pain modulatory systems in women with primary dysmenorrhea. *Pain* 157, 92–102. doi: 10.1097/j.pain.0000000000000340

Wei, S.-Y., Chao, H.-T., Tu, C.-H., Lin, M.-W., Li, W.-C., Low, I., et al. (2016b). The *BDNF* Val66Met polymorphism is associated with the functional connectivity dynamics of pain modulatory systems in primary dysmenorrhea. *Sci. Rep.* 6:23639. doi: 10.1038/srep23639

Wei, S.-Y., Chen, L.-F., Lin, M.-W., Li, W.-C., Low, I., Yang, C.-J., et al. (2017). The *OPRM1* A118G polymorphism modulates the descending pain modulatory system for individual pain experience in young women with primary dysmenorrhea. *Sci. Rep.* 7, 1–11. doi: 10.1038/srep39906

Weinshilboum, R. M., Otterness, D. M., and Szumlanski, C. L. (1999). Methylation pharmacogenetics: catechol O-methyltransferase, thiopurine methyltransferase, and histamine N-methyltransferase. *Annu. Rev. Pharmacol. Toxicol.* 39, 19–52. doi: 10.1146/annurev.pharmtox.39.1.19

Yan, C.-G., Wang, X.-D., Zuo, X.-N., and Zang, Y.-F. (2016). DPABI: data processing & analysis for (resting-state) brain imaging. *Neuroinformatics* 14, 339–351. doi: 10.1007/s12021-016-9299-4

Yarkoni, T., Poldrack, R. A., Nichols, T. E., Van Essen, D. C., and Wager, T. D. (2011). Large-scale automated synthesis of human functional neuroimaging data. *Nat. Methods* 8, 665–670. doi: 10.1038/nmeth.1635

Zang, Y.-F., He, Y., Zhu, C.-Z., Cao, Q.-J., Sui, M.-Q., Liang, M., et al. (2007). Altered baseline brain activity in children with ADHD revealed by resting-state functional MRI. *Brain Dev.* 29, 83–91. doi: 10.1016/j.braindev.2006.07.002

Zhang, Q., Yu, S., Wang, Y., Wang, M., Yang, Y., Wei, W., et al. (2019). Abnormal reward system network in primary dysmenorrhea. *Mol. Pain* 15:174480691986209. doi: 10.1177/1744806919862096

Zubieta, J.-K., Heitzeg, M. M., Smith, Y. R., Bueller, J. A., Xu, K., Xu, Y., et al. (2003). *COMT* val158met genotype affects μ-opioid neurotransmitter responses to a pain stressor. *Science* 299, 1240–1243. doi: 10.1126/science.1078546

Zuo, X.-N., Di Martino, A., Kelly, C., Shehzad, Z. E., Gee, D. G., Klein, D. F., et al. (2010). The oscillating brain: complex and reliable. *Neuroimage* 49, 1432–1445. doi: 10.1016/j.neuroimage.2009.09.037

frontiers | Frontiers in Pharmacology

TYPE Original Research
PUBLISHED 01 October 2024
DOI 10.3389/fphar.2024.1439448

OPEN ACCESS

EDITED BY
Fabio Turco,
Cannabiscientia SA, Switzerland

REVIEWED BY
Milena Melake Teweldemedhin,
University of Campania Luigi Vanvitelli, Italy
Salvador Sierra,
University of Michigan, United States
Damiana Scuteri,
University Magna Graecia of Catanzaro, Italy

*CORRESPONDENCE
Fuquan Huo,
huofq@xjtu.edu.cn
Man Li,
liman73@mails.tjmu.edu.cn

RECEIVED 28 May 2024
ACCEPTED 16 August 2024
PUBLISHED 01 October 2024

CITATION
Yuan X, Guo Y, Yi H, Hou X, Zhao Y, Wang Y, Jia H, Baba SS, Li M and Huo F (2024) Hemoglobin α-derived peptides VD-hemopressin (α) and RVD-hemopressin (α) are involved in electroacupuncture inhibition of chronic pain.
Front. Pharmacol. 15:1439448.
doi: 10.3389/fphar.2024.1439448

Hemoglobin α-derived peptides VD-hemopressin (α) and RVD-hemopressin (α) are involved in electroacupuncture inhibition of chronic pain

Xiaocui Yuan[1,2], Yixiao Guo[1,2], Huiyuan Yi[1,2], Xuemei Hou[1,2], Yulong Zhao[1,2], Yuying Wang[1,2], Hong Jia[1,2], Sani Sa'idu Baba[1,3], Man Li[4]* and Fuquan Huo[1,2]*

[1]Department of Physiology and Pathophysiology, School of Basic Medical Sciences, Institute of Neuroscience, Translational Medicine Institute, Xi'an Jiaotong University Health Science Center, Xi'an, China, [2]Key Laboratory of Environment and Genes Related to Diseases (Xi'an Jiaotong University), Ministry of Education, Xi'an, China, [3]Neuroscience and pathophysiology unit, Department of Human physiology, Faculty of Basic Medical Sciences, College of Health Sciences, Bayero University Kano, Kano, Nigeria, [4]Department of Neurobiology and Key Laboratory of Neurological Diseases of Ministry of Education, The Institute of Brain Research, School of Basic Medicine, Tongji Medical College, Huazhong University of Science and Technology, Wuhan, China

Introduction: Knee osteoarthritis (KOA) is a chronic degenerative bone metabolic disease that primarily affects older adults, leading to chronic pain and disability that affect patients' daily activities. Electroacupuncture (EA) is a commonly used method for the treatment of chronic pain in clinical practice. Previous studies indicate that the endocannabinoid system is involved in EA analgesia, but whether endocannabinopeptide VD-hemopressin (α) and RVD-hemopressin (α) derived from hemoglobin chains are involved in EA analgesia is unclear.

Methods: RNA-seq technology was used to screen which genes involved in EA analgesia. The expression of hemoglobin α chain and 26S proteasome were determined by Western blotting. The level of VD-hemopressin (α) and RVD-hemopressin (α) were measured by UPLC-MS/MS. Microinjection VD-Hemopressin (α), RVD-Hemopressin (α) and 26S proteasome inhibitor MG-132 into vlPAG, then observe mechanical and thermal pain thresholds.

Results: Therefore, we used RNA-seq to obtain differentially expressed genes *Hba-a1* and *Hba-a2* involved in EA analgesia in the periaqueductal gray (PAG), which were translated into the hemoglobin α chain. EA significantly increased the expression of the hemoglobin α chain and the level of hemopressin (α) and RVD-hemopressin (α). Microinjection of VD-hemopressin (α) and RVD-hemopressin (α) into the ventrolateral periaqueductal gray (vlPAG) mimicked the analgesic effect of EA, while CB1 receptor antagonist AM251 reversed this effect. EA significantly increased the expression of 26S proteasome in KOA mice. Microinjection of 26S

Abbreviations: 2-AG, 2-araehidonoyl glycerol; AEA, arachidonic ethanolamine anandamide; EA, electroacupuncture; KOA, knee osteoarthritis; MIA, monosodium iodoacetate; PAG, periaqueductal gray; vlPAG, ventrolateral pariaqueducta gray.

proteasome inhibitor MG132 before EA prevented both the anti-allodynic effect and upregulation of the concentration of RVD-hemopressin (α) by EA treatment and upregulated the expression of the hemoglobin α chain.

Discussion: Our data suggest that EA upregulated the concentration of VD-hemopressin (α) and RVD-hemopressin (α) through enhancement of the hemoglobin α chain degradation by 26S proteasome in the PAG, then activated the CB1 receptor, thereby exerting inhibition of chronic pain in a mouse model of KOA. These results provide new insights into the EA analgesic mechanisms and reveal possible targets for EA treatment of chronic pain.

KEYWORDS

Knee osteoarthritis (KOA), Electroacupuncture analgesia, VD-hemopressin (α), RVD-hemopressin (α), 26S proteasome, Chronic pain

1 Introduction

Knee osteoarthritis (KOA) is a chronic condition characterized by knee joint degeneration that usually occurs from middle to older ages. In clinical practice, patients with KOA may experience joint pain, stiffness, and functional limitation associated with inflammation and effusion in the knee, which may affect their quality of life (Luan et al., 2021). Previous studies proved that electroacupuncture (EA) is effective in relieving chronic pain in KOA patients and animal models of KOA (Lv et al., 2019; Yuan T. et al., 2018). Accumulating evidence indicates that the classical lipophilic endocannabinoid arachidonic ethanolamine anandamide (AEA) and 2-arachidonoyl glycerol (2-AG) are involved in EA analgesia (Chen et al., 2009; Jiang et al., 2022; Yuan et al., 2018b). In addition, recent studies have shown that apart from the classical lipophilic endocannabinoid AEA and 2-AG, a class of cannabinopeptide ligands derived from hemoglobin α and β chains were isolated and identified from rodent brains and were found to have different affinity and selectivity for CB1 and CB2 receptors. Moreover, they have also been found to play certain regulatory roles in pain, feeding, learning, and memory (Leone et al., 2018; Zhang et al., 2016; Zheng et al., 2018). However, it is unclear whether cannabinopeptide ligands derived from hemoglobin chains are involved in EA analgesia.

Gomes et al. identified VD-hemopressin (α) and RVD-hemopressin (α) peptides derived from the hemoglobin α chain in the mouse brain using a peptide omics strategy, and *in vitro* functional experiments have shown that VD-hemopressin (α) and RVD-hemopressin (α) act as selective agonists for CB1 receptor, sustain the increase the release of intracellular Ca^{2+}, and lead to increase ERK phosphorylation levels, suggesting that VD-hemopressin (α) and RVD-hemopressin (α) are cannabinopeptide ligands (Gomes et al., 2009). Previous studies have shown that both lateral ventricle and intrathecal injection of VD-hemopressin (α) can induce CB1 receptor-mediated analgesia in a test of acute pain caused by photothermal tail flick (Han et al., 2014; Zheng et al., 2017). In one study, VD-hemopressin (α) was injected into the lateral ventricle in pathological models of postoperative pain, formalin-induced inflammatory pain phase Ⅰ, and visceral pain, and a dose-dependent analgesic effect was observed (Zheng et al., 2017). These results indicate that VD-hemopressin (α) has an analgesic effect in the lateral ventricle and the intrathecal space. The ventrolateral periaqueductal gray (vlPAG) is a key structure in the modulation of pain, and our previous studies have also found that the vlPAG is involved in EA analgesia (Yuan et al., 2018c). However, whether VD-hemopressin (α) and RVD-hemopressin (α) are involved in EA analgesia in the vlPAG needs to be further explored.

VD-hemopressin (α) and RVD-hemopressin (α) are considered non-classical neuropeptides. Unlike classical neuropeptides, they are produced in the brain as neuropeptides derived from cytosolic proteins (Gelman and Fricker, 2010), but how they are produced is still unclear. In erythrocytes, hemoglobin is degraded by the proteasome after its ubiquitination or oxidation (Pacifici, Kono, and Davies, 1993; Wenzel and Baumeister, 1993). The proteasome is a large proteolytic complex ubiquitously distributed among mammalian cells, including neuronal cells (Tai and Schuman, 2008). Furthermore, the 26S proteasome is known to generate peptides ranging in length from 3 to 22 amino acids (Kisselev et al., 1999), consistent with the size of VD-hemopressin (α) and RVD-hemopressin (α). Therefore, one possible mechanism is that VD-hemopressin (α) and RVD-hemopressin (α) may be produced through 26S proteasome degradation of the hemoglobin α chain in neurons of the mouse brain.

In the present study, we determined whether the hemoglobin α chain is involved in the EA-mediated inhibition of chronic pain in a mouse model of KOA. Then, we examined whether VD-hemopressin (α) and RVD-hemopressin (α) are involved in the mechanism of EA-mediated inhibition of chronic pain. We also explored whether EA inhibited chronic pain by promoting 26S proteasome degradation of the hemoglobin α chain to produce VD-hemopressin (α) and RVD-hemopressin (α).

2 Methods and materials

2.1 Animals

Experiments were performed on 8-week-old male C57BL/6 J mice weighing 22–25 g (Medical Experimental Animal Center of Xi'an Jiaotong University). Male mice are preferred in our studies to eliminate variability introduced by hormonal cycles in female mice. Mice were housed in groups of 6 per home cage (32 cm × 21.5 cm × 17 cm) and had free access to food and water. All mice were maintained under controlled temperature (25 ± 2°C), humidity (50% ± 10%), and with a 12:12 h light/dark cycle (lights on at

8:00 a.m.). The study was conducted in compliance with the ethical guidelines of the International Association for the Study of Pain (Zimmermann, 1983) and approved by the Biomedical Ethics Committee of the Xi'an Jiaotong University Health Science Center (Animal committee number: 2019–841). Based on previous experience and pre-experiments, we estimated the sample size based on at least 80% power and α = 0.05. Each group used in the RNA-seq and quantitative polymerase chain reaction experiments contained three mice. In the Western blotting experiments, the number of mice in each group was 3–4. In experiments that analyzed the level of VD-hemopressin (α) and RVD-hemopressin (α), the number of mice in each group was 4–6. In the nociceptive behavioral tests, the number of mice in each group was 5–11.

2.2 Induction of knee osteoarthritis (KOA)

The mouse model of KOA was established following previously described procedures (La Porta et al., 2013). After mice were briefly anesthetized with isoflurane, 5 μL of monosodium iodoacetate (5 mg/mL; MIA; Sigma, UK) was injected into the left knee joint cavity. The concentration of MIA selected in this study can cause histological (Yuan T. et al., 2018) and pain behavioral changes (Harvey and Dickenson, 2009) in mice. MIA was dissolved in sterile saline. The control group animals were given 5 μL of sterile saline.

2.3 EA treatment

In the EA group, EA stimulation was performed on the left hindlimb of the mice, "Neixiyan" (Ex-LE4) and "Dubi" (ST35), from the second day of establishing the KOA model. The EA frequency was 2 Hz, the intensity was 1 mA, and the wave width was 0.1 m. EA was performed once every other day for 4 weeks, and each treatment lasted for 30 min. The present study opted for the parameter selection of EA according to our previous research (Yuan et al., 2018b).

The needles were inserted into the Ex-LE4 and ST35 points, respectively, 2–3 mm deep, corresponding to how humans would be treated. Ex-LE4 and ST35 are below the knee joint, located at the depression on the left and right sides of the patella. Ex-LE4 and ST35 were chosen because their use frequency is the highest in KOA, and they are specific acupoints for treating knee problems (Ng, Leung, and Poon, 2003; Selfe and Taylor, 2008).

2.4 RNA-seq analysis

Differential expression genes in the PAG of mice were determined by RNA-seq. By virtue of no difference in nociceptive threshold between the KOA group and the sham EA group (needling without electricity) in previous studies (Yuan et al., 2022; Yuan et al., 2018c), the mice that were used for the differential gene expression analysis were assigned to the CON, KOA, and EA groups. Nine mice were deeply anesthetized with 3%–5% isoflurane; the mice were then decapitated, and the PAG was dissected. The brain was removed from the skull and placed on a plate with the ventral surface up. The midbrain was taken and evenly cut into three subsections. The PAG was obtained with a 20G needle solution from the middle subsection of the midbrain and then placed into All Protect™ Nucleic Acid and Protein Stabilization Reagent for Animal Tissue (Beyotime Biotechnology, Shanghai, China).

Total RNA was isolated from the PAG specimens using a TRIzol reagent (Invitrogen, United States) according to the manufacturer's protocol. Half of the RNA was used for sequencing analysis, and half was used for RT-qPCR validation. The RNA purity, concentration, and integrity were assessed by an RNA6000 Nano Reagents Port 1 Assay Kit of the Agilent Bioanalyzer 2100 system (Agilent Technologies). The final cDNA was sent for library preparation, and sequencing was performed by Wuhan BGI Technology Co., LTD., Wuhan, China (www.bgitechsolutions.com). We estimated the expression levels for all transcripts using the RSEM tool and calculated the expression levels for mRNAs in terms of fragments per kilobase of transcript per million mapped reads (FPKM). The differentially expressed genes (DEGs) were selected by the Noiseq method (comparison between every two groups) with fold change ≥2 and diverge probability ≥0.8. Clustering analysis of DEGs was performed with cluster (de Hoon et al., 2004; Eisen et al., 1998) and Java Treeview (Saldanha, 2004) software according to the CON-VS-KOA.KOA-VS-EA cluster plans for DEGs.

2.5 Quantitative polymerase chain reaction

The RNA-seq data were confirmed through RT-qPCR. cDNA was synthesized using the ReverTra Ace-a-TM (Toyobo, Japan) according to the manufacturer's protocol. RT-qPCR analyses for mRNA were performed in a CFX96 system (Bio-Rad, UK) using the SYBR Green PCR amplification reagent (Toyobo, Japan), and the relative expression levels were quantified using CFX Manager software. β-Actin was used as the reference gene for normalization. The relative differences were expressed as the fold-matched control values calculated using the comparative cycle method ($2^{-\triangle\triangle CT}$). A list of primers of selected genes is shown in Supplementary Table S1.

2.6 Nociceptive behavioral tests

Mechanical allodynia and heat hyperalgesia were also demonstrated in the hind paw of animals with KOA (Fernihough et al., 2004; La Porta et al., 2013). Mice were habituated to the testing environment for 30 min at least 3 days before testing. The baseline nociceptive thresholds were tested for 3 days before the MIA injection, and the average thresholds of 3 days were calculated as the baseline. After KOA induction, the nociceptive thresholds were tested once every other day, starting from the 18th day to 4 weeks.

The up-down method was implemented for the mechanical allodynia test (Chaplan et al., 1994). Mice were placed into a customized cage individually, and mechanical allodynia was determined with a series of von Frey filaments (Stoelting, Kiel, WI, United States). The area tested was the central plantar surface of the left hind paw, and von Frey filaments were applied perpendicularly to the plantar surface and maintained for 6 s until an S-shape formed. Sharp withdrawal, immediate flinching, or the raising, removal, shaking, or licking of the hind paw was considered a positive response. The test was repeated twice with a 5-min interval, and the average value was calculated.

The thermal test was performed by observing the paw withdrawal latency (PWL) to noxious heat with a model 336 analgesia meter (IITC, Inc., Life Science Instruments, Woodland Hills, CA, United States). A cut-off time of 20 s was used to avoid tissue damage to the animals' paws. The test was repeated five times, and the mean value was calculated.

2.7 Analysis of VD-hemopressin (α) and RVD-hemopressin (α) by ultra-high performance liquid chromatography–tandem mass spectrometry (UPLC-MS/MS)

The PAG tissues were removed 4 weeks after vehicle or MIA injection. The PAG tissues were weighed, and eight times that weight of acetonitrile (ACN) was added and homogenized, after which ultrasonic treatment was performed for 20 min. After centrifugation at 13,000 rpm for 10 min, the supernatant was removed and filtered with a 0.22 μm filter membrane, followed by quantification with LC-MS/MS. Analyses were conducted on UPLC (I-Class)-MS (XEXO TQ-MS) and MassLynx V4.1 workstation. The parameters of mass spectrum detection of components to be measured were source voltages 3.00 KV; source temperature: 450°C; gas flow: 800 L/Hr; cone: 50 L/Hr. Analytical LC separations were performed on a Waters ACQUITY UPLC BEH-C18 (2.1*50 mm, 1.7 μm) with a flow rate of 0.3 mL/min and column temperature of 35°C using a gradient of ACN (eluent B) and water (eluent A), both containing 0.1% formic acid. The gradient was as follows: 2% eluent B for 1.0 min; 2%–100% B from 1.0 to 2.0 min and held at 100% from 2.0 to 3.5 min. From 3.5 to 4.0 min, the column was re-equilibrated to 2% B and conditioned from 4.0 to 6.0 min at 2% B (Bauer et al., 2012).

2.8 Western blotting

The PAG was removed as described above and put immediately into Allprotect™ Nucleic Acid and Protein Stabilization Reagent for Animal Tissue (Beyotime Biotechnology, Shanghai, China). The PAG tissues were then processed for protein extraction and Western blotting using the procedure described in detail in our previous study (Yuan et al., 2022; Yuan et al., 2021). After measuring protein concentrations using the BCA Protein Assay Kit (Beyotime Biotechnology, Shanghai, China), the samples were separated with 10% or 12% denaturing SDS-PAGE and transferred to a polyvinylidene fluoride (PVDF) membrane. PVDF membranes were blocked in TBST (pH 7.6, containing 0.1% Tween 20% and 5% non-fat milk) for 1 h at room temperature. Subsequently, the PVDF membranes were incubated with rabbit monoclonal anti-hemoglobin α antibody (1:1000, Abcam, UK), rabbit polyclonal anti-proteasome 26S S2 antibody (1:2000, Abcam, UK), or mouse monoclonal anti-β-actin antibody (1:5000; Proteintech, USA) at 4°C overnight. After washing with TBST, the blots were then incubated with the horseradish peroxidase-conjugated anti-rabbit or anti-mouse secondary antibodies (1:5000; EMD Millipore, Darmstadt, Germany). Protein bands were detected using an ECL kit (ECL-plus, EMD Millipore, Darmstadt, Germany) and captured using the Champchemi system with the SageCapture software (Sagecreation Service for Life Science, Beijing, China). The band intensity was quantified and analyzed using ImageJ software. The protein levels were quantitated relative to β-actin. Finally, the relative protein expression was normalized to the respective control group.

2.9 Intracerebral guide cannula placement

Mice were anesthetized with 2% sodium pentobarbital (50 mg/kg, intraperitoneal) and implanted with a guide cannula (RWD, China) 0.5 mm above the right vlPAG (AP: −4.8 mm, LM: +0.5 mm from midline, DV: −2.8 mm, from the skull surface) according to a mouse atlas. Once the animals recovered from anesthesia, sodium penicillin was administered (0.2 million units/day for 3 days, intraperitoneally) to prevent wounds and intracerebral infections. The animals were carefully nursed and fed in clean cages for at least 7 days to recover from the surgery.

2.10 Drug administration

On the 18th day after KOA induction, an injection cannula, connected to a 1 μL microsyringe, was extended 0.5 mm beyond the tip of the guide cannula for drug microinjection into the vlPAG. The drugs were dissolved in saline or 10% DMSO and then slowly infused through the microsyringe at a constant speed over a 1 min period. The injection cannula was left at the injection site for an additional 1 min to allow for complete diffusion of the injected drug. Drugs used in this study include the m-RVD-hemopressin (α) and m-VD-hemopressin (α), synthesized by Nanjing Synpeptide Biological Co., Ltd., which were dissolved in the 0.9% saline. MG132 (Z-Leu-Leu-Leu-al), a 26S proteasome inhibitor (Merck Millipore, United States) and AM251, a CB1 receptor selective antagonist (MCE, United States) were dissolved in the 10% dimethyl sulfoxide (10% DMSO; Sigma-Aldrich).

Drug doses were chosen according to previous studies (Han et al., 2014; Zheng et al., 2018) and our preliminary experiments. We used VD-hemopressin (α) at a concentration of 10 nmol in our study because it had been reported that intracerebroventricular administration of VD-hemopressin (α) produced a dose-dependent antinociception, and 10 nmol VD-hemopressin (α) also has an analgesic effect (Han et al., 2014; Zheng et al., 2018). RVD-hemopressin (α) was administered in various doses (1 nmol, 2 nmol, 5 nmol). MG132 (0.4 μg) was administered for 30 min before EA treatment (Yang et al., 2008). AM251 (20 nmol) was administered for 10 min prior to VD-hemopressin (α) and RVD-hemopressin (α) injections (Han et al., 2014). Equal volumes of 0.9% saline or 10% DMSO were injected into the vlPAG as vehicle controls.

2.11 Statistical analysis

All data were expressed as the means ± standard error (SEM). Behavioral data were analyzed using two-way repeated-measures ANOVA, followed by a Bonferroni *post hoc* analysis of multiple

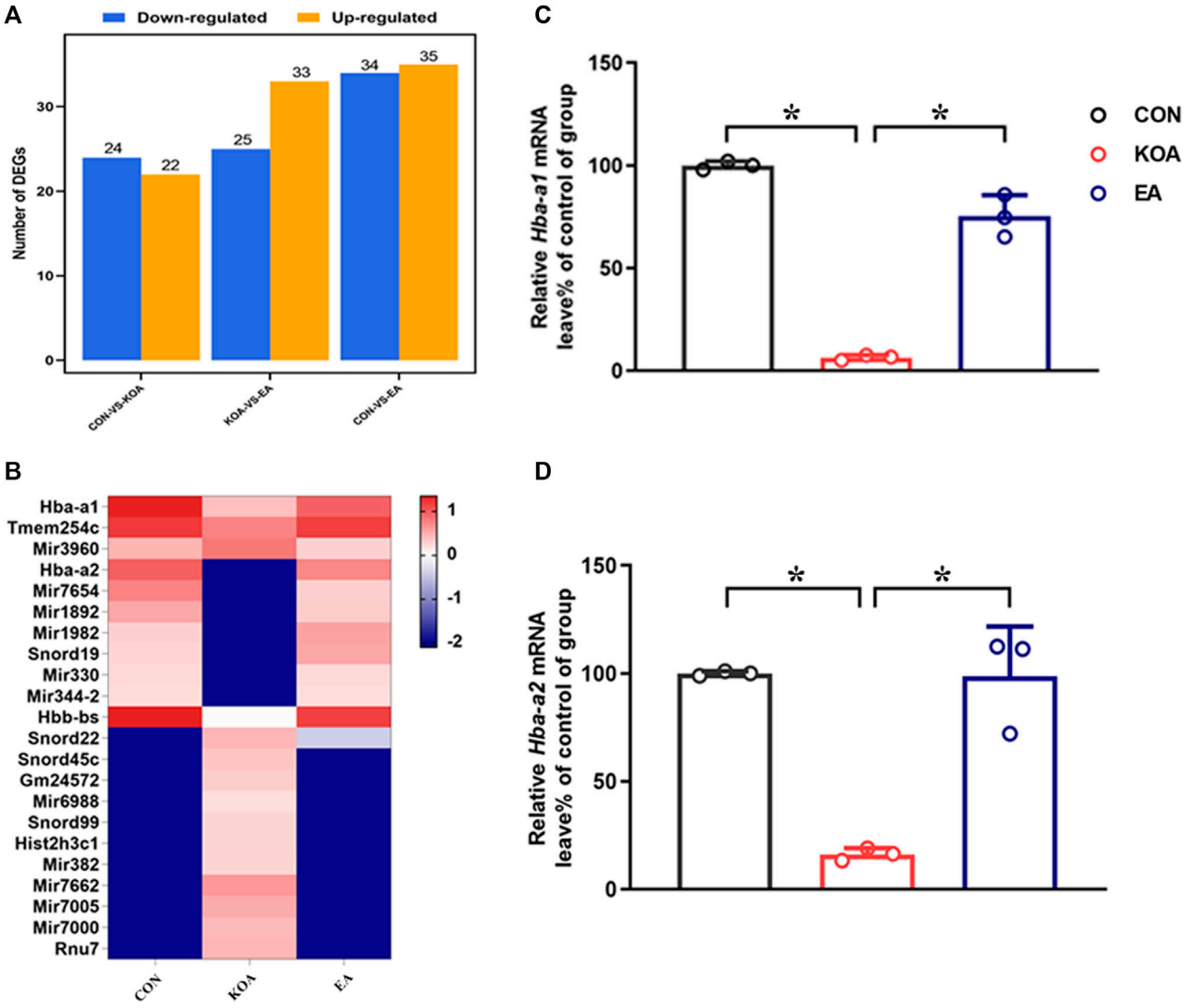

FIGURE 1
Screening differentially expressed genes (DEGs) *Hba-a1* and *Hba-a2* involved in EA analgesia in the periaqueductal gray. **(A)** DEG statistics. The *X*-axis represents pairwise comparisons, and the *Y*-axis shows the number of screened DEGs. The blue bars denote downregulated genes, and the orange bars denote the upregulated ones. **(B)** Heatmap of DEGs in the KOA, EA, and control groups. **(C)** Summary data show the effect of KOA and EA on the level of the *Hba-a1* in PAG tissues. **(D)** Summary data show the effect of KOA and EA on the level of the *Hba-a2* in PAG tissues. Data are expressed as means ± SEM (n = 3 mice in each group). *$p < 0.05$.

comparisons. Other data were analyzed by one-way ANOVA followed by a Newman–Keuls *post hoc* test with a two-tailed hypothesis or t-tests with a two-tailed hypothesis. All analyses were performed using the GraphPad Prism 9.0 software. The criterion for statistical significance was set as $p < 0.05$.

3 Results

3.1 RNA-seq screened differentially expressed genes *Hba-a1* and *Hba-a2* involved in EA analgesia

We used RNA-sequencing (RNA-seq) to compare gene alternations in the EA, KOA, and control groups. As shown in Figure 1A, compared with the control group, 24 genes were downregulated, and 22 genes were upregulated in the KOA group, and 34 genes were downregulated, and 35 genes were upregulated in the EA group. Moreover, compared with the KOA group, 25 genes were downregulated, and 33 genes were upregulated in the EA group. Genes with similar expression patterns usually have the same functional correlation. Cluster analysis showed that 22 genes were significantly altered, including 10 genes that were downregulated in the KOA group while upregulated in the EA group and 12 genes that were upregulated in the KOA group while downregulated in the EA group (Figure 1B).

Among these DEGs, the gene *Hba-a2*, which encoded the hemoglobin α chain, has the largest fold change. Interestingly, recent studies have shown that a class of cannabinopeptide

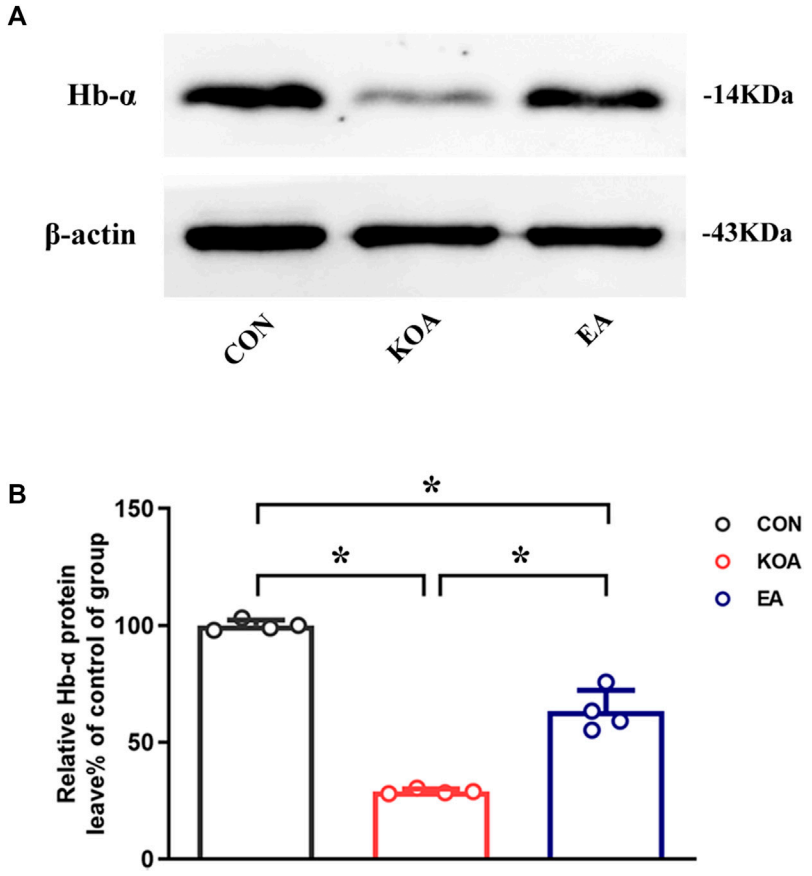

FIGURE 2
Quantitative analysis of the protein level of hemoglobin α-chain in the PAG tissues. **(A)** The representative gel image shows the protein level of the hemoglobin α-chain in PAG tissues obtained from the control (CON), KOA, and KOA treated with EA groups. β-actin was used as a loading control. The protein band at 14 kDa corresponds to the hemoglobin α-chain. **(B)** Summary data show the effect of KOA and EA on the protein level of the hemoglobin α-chain in PAG tissues. Data are expressed as means ± SEM (n = 4 mice in each group). *$p < 0.05$.

ligands derived from hemoglobin α play certain regulatory roles in pain, feeding, learning, and memory (Leone et al., 2018; Zhang et al., 2016; Zheng et al., 2018). In addition, the gene *Hba-a1,* which also encoded the hemoglobin α chain, was found to have changed by more than threefold compared with the control group. Therefore, we chose *Hba-a1* and *Hba-a2* to further explore in this study. RT-qPCR was used to verify that observation, and it was found that the expressions of *Hba-a1* and *Hba-a2* in the PAG of KOA mice were significantly downregulated compared with the control group, and EA significantly increased the expression of both *Hba-a1* and *Hba-a2*, which was consistent with the results of RNA-seq ($p < 0.05$; Figures 1C, D).

3.2 EA reversed the reduction of hemoglobin α-chain expression in the PAG of KOA mice

Because *Hba-a1* and *Hba-a2* encode the hemoglobin α chain, we used the Western blotting technique to observe the protein level of the hemoglobin α chain in the PAG. The hemoglobin α chain protein bands were present in the PAG tissues (Figure 2A). The hemoglobin α chain protein level in the PAG was significantly lower than that in the control group 4 weeks after KOA induction ($p < 0.05$; Figure 2B). EA treatment at 2Hz + 1 mA significantly increased the hemoglobin α chain level in the PAG compared with that in the KOA group ($p < 0.05$; Figure 2B), indicating that the hemoglobin α chain is involved in EA analgesia.

3.3 EA reversed the reduction of VD-hemopressin (α) and RVD-hemopressin (α) concentration in the PAG of KOA mice

Several studies have identified that VD-hemopressin (α) and RVD-hemopressin (α) peptides derived from the hemoglobin α chain in mouse brain and produced analgesic effects mediated by CB1 receptor (Gomes et al., 2009; Han et al., 2014; Zheng et al., 2017). Therefore, we determined whether EA increases the concentration of VD-hemopressin (α) and RVD-hemopressin (α) in the PAG.

The VD-hemopressin (α) and RVD-hemopressin (α) were detected in the PAG in all three groups 4 weeks after KOA induction. Compared with the control group, the VD-hemopressin (α) and RVD-hemopressin (α) levels in the PAG were significantly reduced in KOA mice ($p < 0.05$; Figures 3A, B). EA significantly increased the VD-hemopressin (α) and RVD-

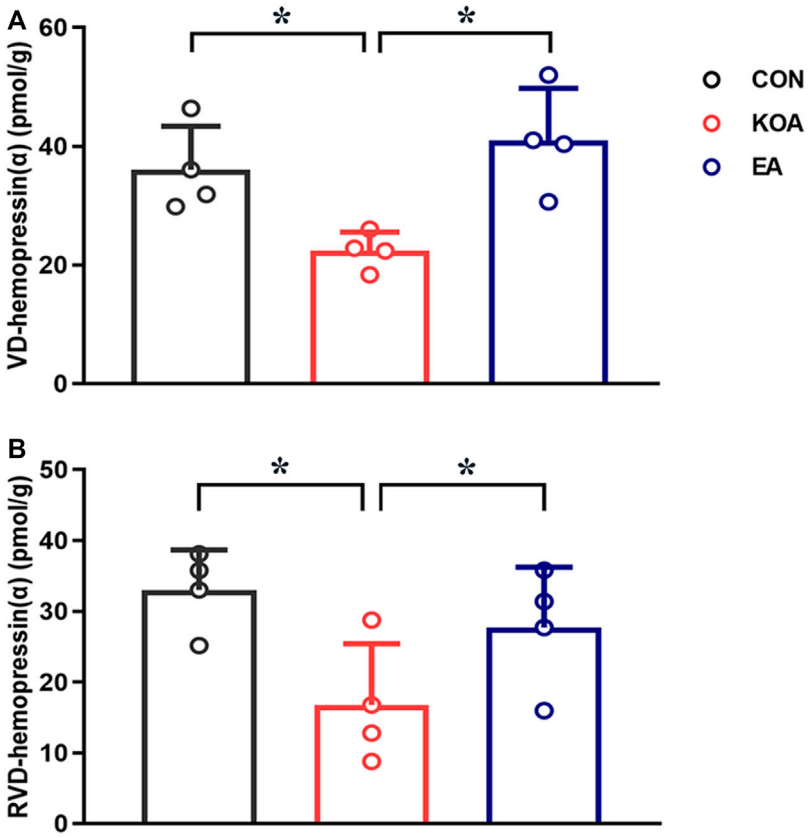

FIGURE 3
Quantitative analysis of the VD-hemopressin (α) and RVD-hemopressin (α) concentrations in the PAG. **(A)** Summary data show the effect of KOA and EA on the concentration of VD-hemopressin (α) in the PAG. **(B)** Summary data show the effect of KOA and EA on the concentration of RVD-hemopressin (α) in the PAG. Data are expressed as means ± SEM (n = 4 mice in each group). *$p < 0.05$.

hemopressin (α) levels in the PAG of KOA mice ($p < 0.05$; Figures 3A, B).

3.4 Microinjection of VD-hemopressin (α) into the vlPAG mimicked the EA effect on pain hypersensitivity

Chronic pain was found to be established on the 17th day after KOA surgery, according to our previous research (Yuan. et al., 2018). In line with this, we microinjected VD-hemopressin (α) and RVD-hemopressin (α) into the right vlPAG on the 18th day after KOA induction, once every other day for five times. There was no difference in the baseline mechanical withdrawal threshold and thermal withdrawal latency between different groups before MIA injection. Microinjection of saline into the vlPAG did not influence the mechanical withdrawal threshold and thermal withdrawal latency induced by MIA ($p > 0.05$; Figure 4).

Microinjection of VD-hemopressin (α) (10 nmol/0.5 μL) into the vlPAG, contralateral to the affected knee, markedly increased the mechanical withdrawal thresholds of KOA mice ($p < 0.05$), as well as the EA group ($p < 0.05$). As shown in Figure 4A, the time course curves (i.e., CON, KOA + Saline, EA, and 10 nmol VD-hemopressin (α) groups) were significantly different between treatments ($F_{(3, 280)} = 1489.06$; $p < 0.0001$), across times ($F_{(6, 280)} = 392.57$; $p < 0.0001$), and for their interactions ($F_{(18, 280)} = 54.7$; $p < 0.0001$). Further analyses showed that the mechanical thresholds in the VD-hemopressin (α) group were significantly higher than those in the KOA + Saline group from the 23rd to the 27th day after KOA induction ($p < 0.05$), as well as those in the EA group ($p < 0.05$). No significant difference was observed between the VD-hemopressin (α) group and the EA group from the 23rd to the 27th day after KOA induction ($p > 0.05$; Figure 4A).

Microinjection of 10 nmol VD-hemopressin (α) into the vlPAG also significantly increased the thermal withdrawal latency of KOA mice, as well as the EA group ($p < 0.05$). As shown in Figure 4B, the time course curves (i.e., CON, KOA + Saline, EA, and 10 nmol VD-hemopressin (α) groups) were significantly different between treatments ($F_{(3, 196)} = 1259.61$; $p < 0.0001$), across times ($F_{(6, 196)} = 358.24$; $p < 0.0001$), and for their interactions ($F_{(18, 196)} = 49.49$; $p < 0.0001$). Further analyses showed that the mechanical thresholds in the 10 nmol VD-hemopressin (α) group were significantly higher than those in the KOA + Saline group from the 21st to the 27th day after KOA induction, as well as those in the EA group ($p < 0.05$). No significant difference was measured between the 10 nmol VD-hemopressin (α) group and EA group from the 21st to the 27th day after KOA induction ($p > 0.05$; Figure 4B), indicating clearly the mimicking capacity of VD-hemopressin (α) for EA.

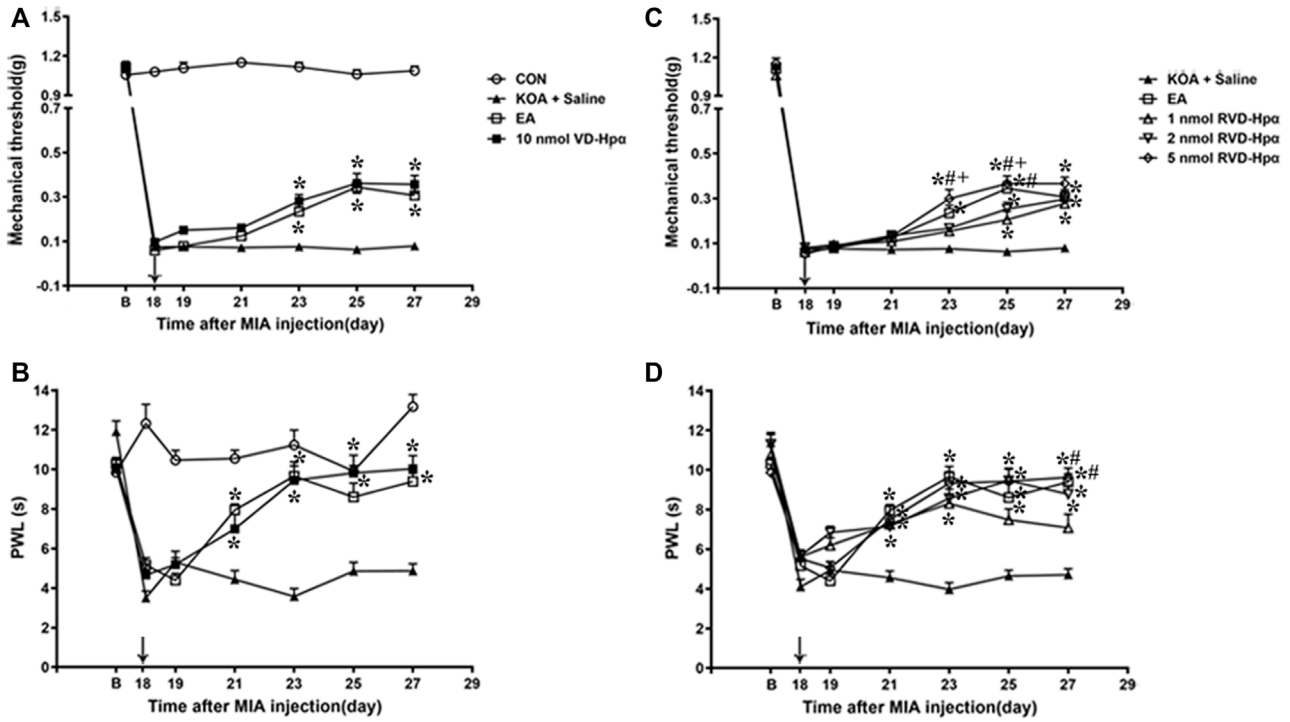

FIGURE 4
Time course of the effect of VD-hemopressin (α) and RVD-hemopressin (α) on pain hypersensitivity in KOA mice. **(A, B)** Time course of tactile threshold in response to von Frey filaments or a noxious heat stimulus in CON, KOA + saline, EA, and 10 nmol VD-hemopressin (α) mice. **(C, D)** Time course of the effect of different concentrations of RVD-hemopressin (α) on tactile and thermal withdrawal thresholds of KOA mice. VD-hemopressin (α) or RVD-hemopressin (α) was microinjected into the vlPAG, or the mice received EA stimulation starting from 18 days after MIA injection, once every other day for five times, as indicated by the black arrow. Data are expressed as means ± SEM (n = 8–11 mice in each group). *$p < 0.05$, compared with the KOA + Saline group; #$p < 0.05$, compared with the 1 nmol RVD-hemopressin (α) group; + $p < 0.05$, compared with the 2 nmol RVD-hemopressin (α) group.

3.5 Microinjection of RVD-hemopressin (α) into the vlPAG mimicked the EA effect on pain hypersensitivity

A microinjection of RVD-hemopressin (α) (1 nmol, 2 nmol, 5 nmol; 0.5 μL) into the vlPAG markedly increased the mechanical withdrawal thresholds of the KOA mice ($p < 0.05$), as well as the EA group ($p < 0.05$). As shown in Figure 4C, the time course curves (i.e., KOA + Saline, EA, and RVD-hemopressin (α) groups) were significantly different between treatments ($F_{(4, 343)} = 28.59$; $p < 0.0001$), across times ($F_{(6, 343)} = 1249.47$; $p < 0.0001$), and for their interactions ($F_{(24, 343)} = 6.22$; $p < 0.0001$). Further analyses showed that the mechanical thresholds in the 1 nmol and 2 nmol RVD-hemopressin (α) groups were significantly higher than those in the KOA + Saline group from the 25th to the 27th day after KOA induction ($p < 0.05$). The mechanical thresholds in the 5 nmol RVD-hemopressin (α) group were significantly higher than those in the KOA + Saline group from the 23rd to the 27th day after KOA induction, as well as those in the EA group ($p < 0.05$). In addition, the analgesic effects induced by 5 nmol RVD-hemopressin (α) on the mechanical thresholds were significantly higher than those in the 1 nmol RVD-hemopressin (α) and the 2 nmol RVD-hemopressin (α) ($p < 0.05$) groups from the 23rd to 25th day after KOA induction. The mechanical thresholds in the 1 nmol RVD-hemopressin (α) group were significantly lower than those in the EA group on the 25th day after KOA induction ($p < 0.05$). No significant difference was observed between the 5 nmol RVD-hemopressin (α) group and the EA group from the 23rd to the 27th day after KOA induction ($p > 0.05$; Figure 4C), signifying the occurrence of similar roles of RVD-hemopressin at 5 nmol concentration and EA.

Microinjection of RVD-hemopressin (α) (1 nmol, 2 nmol, 5 nmol; 0.5 μL) into the vlPAG also increased the thermal withdrawal latency ($p < 0.05$). As shown in Figure 4D, the time course curves (i.e., KOA + Saline, EA, and RVD-hemopressin (α) groups) were significantly different between treatments ($F_{(4, 280)} = 39.73$; $p < 0.0001$), across times ($F_{(6, 280)} = 75.55$; $p < 0.0001$), and for their interactions ($F_{(24, 280} = 6.03$; $p < 0.0001$). Further analyses showed that the withdrawal latency in the 1 nmol, 2 nmol, and 5 nmol RVD-hemopressin (α) groups was significantly higher than the KOA + Saline group from the 21st to the 27th day after KOA induction, as well as the EA group ($p < 0.05$). In addition, the analgesic effects induced by EA and 5 nmol RVD-hemopressin (α) on the withdrawal latency were significantly higher than the 1 nmol RVD-hemopressin (α) group on the 27th day after KOA induction ($p < 0.05$). No significant difference was detected between the 2 nmol and 5 nmol RVD-hemopressin (α)

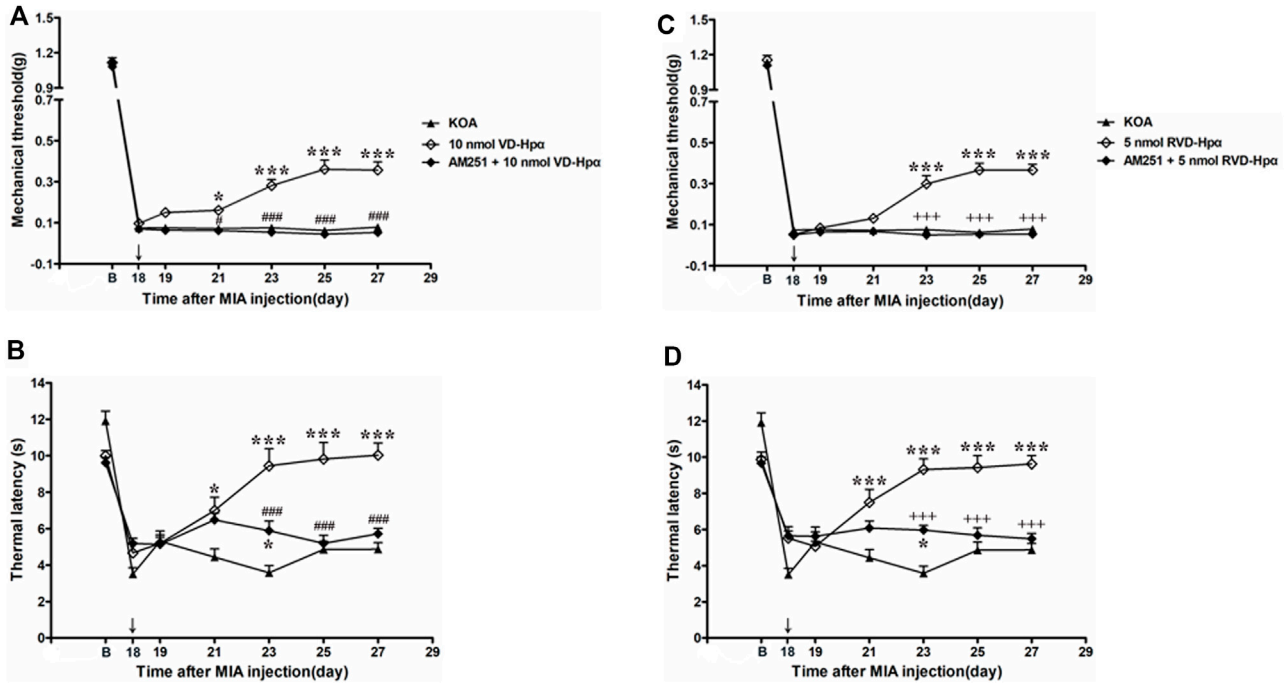

FIGURE 5
Effects of the CB1 receptor antagonist AM251 on VD-hemopressin (α) and RVD-hemopressin (α) analgesia. **(A, B)** Time course of the effect of the CB1 receptor antagonist AM251 on tactile and thermal withdrawal thresholds of VD-hemopressin (α) mice. **(C, D)** Time course of the effect of the CB1 receptor antagonist AM251 on tactile and thermal withdrawal thresholds of RVD-hemopressin (α) mice. The CB1 receptor antagonist AM251 was microinjected into the vlPAG 10 min before VD-hemopressin (α) or RVD-hemopressin (α) starting from 18 days after MIA injection, once every other day for five times, as indicated by the black arrow. *$p < 0.05$; ***$p < 0.001$, compared with KOA group; ###$p < 0.001$, compared with the 10 nmol VD-hemopressin (α) group; +++ $p < 0.001$, compared with the 5-nmol RVD-hemopressin (α) group. Data are expressed as means ± SEM (n = 5–11 mice in each group).

groups and the EA group from the 21st to the 27th day after KOA induction ($p > 0.05$; Figure 4D).

3.6 Microinjection of the CB1 receptor antagonist AM251 into the vlPAG reversed the VD-hemopressin (α) effect on pain hypersensitivity

To identify whether the CB1 receptor was involved in the analgesic effect of VD-hemopressin (α), the CB1 receptor selective antagonist AM251 (20 nmol/0.5 μL) was administered 10 min before injection of 10 nmol VD-hemopressin (α). The AM251 was found to reverse the VD-hemopressin (α) effect on the tactile withdrawal thresholds ($p < 0.001$). As shown in Figure 5A, the time course curves (i.e., KOA, 10 nmol VD-hemopressin (α), and AM251 + 10 nmol VD-hemopressin (α) groups) were significantly different between treatments ($F_{(2, 189)} = 93.34$; $p < 0.0001$), across times ($F_{(6, 189)} = 750.8$; $p < 0.0001$), and for their interactions ($F_{(12, 189)} = 9.961$; $p < 0.0001$). Further analyses showed that the mechanical thresholds in the AM251 + 10 nmol VD-hemopressin (α) group were significantly less than those in the AM251 group from the 21st to the 27th day after KOA induction ($p < 0.05$; Figure 5A). No significant difference was measured between the AM251 + 10 nmol VD-hemopressin (α) group and the KOA group ($p > 0.05$; Figure 5A).

Similarly, the AM251 also reversed the 10 nmol VD-hemopressin (α) effect on the thermal withdrawal latency ($p < 0.001$). As shown in Figure 5B, the time course curves (i.e., KOA, 10 nmol VD-hemopressin (α), and AM251 + 10 nmol VD-hemopressin (α) groups) were significantly different between treatments ($F_{(2, 126)} = 44.66$; $p < 0.0001$), across times ($F_{(6, 126)} = 43.67$; $p < 0.0001$), and for their interactions ($F_{(12, 126)} = 10.12$; $p < 0.0001$). Further analyses showed that the withdrawal latency in the AM251 + 10 nmol VD-hemopressin (α) group was significantly less than the AM251 group from the 23rd to the 27th day after KOA induction ($p < 0.05$; Figure 5B). The withdrawal latency in the AM251 + 10 nmol VD-hemopressin (α) group was also significantly higher than in the KOA group on the 23rd day after KOA induction ($p < 0.05$; Figure 5B).

3.7 Microinjection of the CB1 receptor antagonist AM251 into the vlPAG reversed the RVD-hemopressin (α) effect on pain hypersensitivity

We microinjected the CB1 receptor antagonist AM251 (20 nmol) into the vlPAG to determine whether the

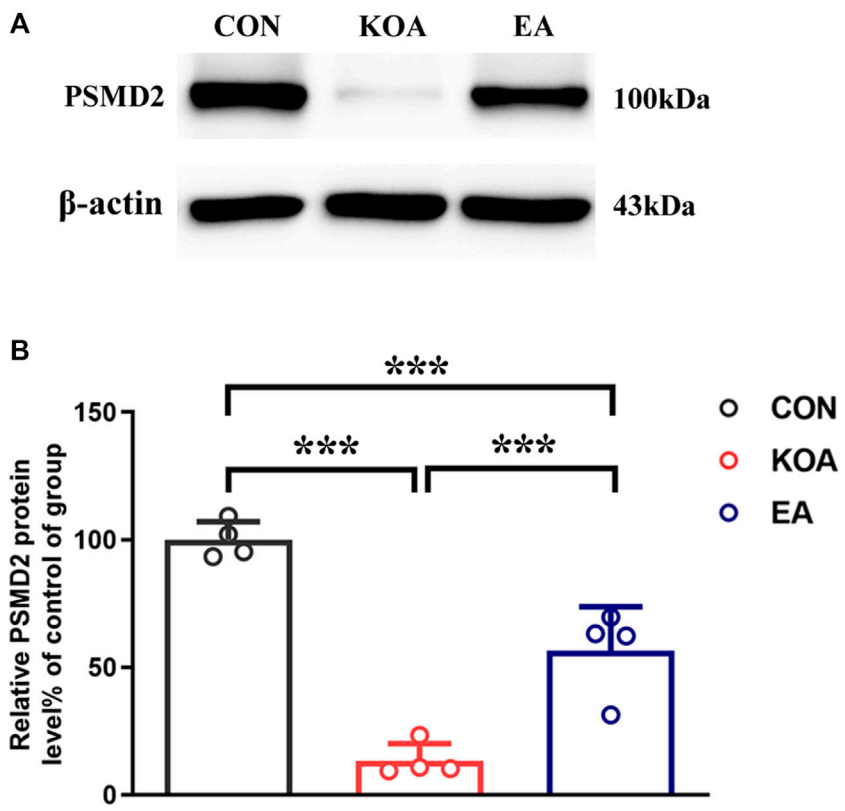

FIGURE 6
Quantitative analysis of the protein level of 26S proteasome (PSMD2) in the PAG tissues. **(A)** The representative gel image shows the protein level of the PSMD2 in PAG tissues obtained from control (CON), KOA, and KOA treated with EA. β-actin was used as a loading control. The protein band at 100 kDa corresponds to the PSMD2. **(B)** Summary data show the effect of KOA and EA on the protein level of the PSMD2 in PAG tissues. Data are expressed as means ± SEM (n = 4 mice in each group). ***$p < 0.001$.

CB1 receptor contributes to the RVD-hemopressin (α) effect on pain hypersensitivity in KOA mice. The AM251 reversed the RVD-hemopressin (α) effect on the tactile withdrawal thresholds ($p < 0.001$). As shown in Figure 5C, the time course curves (i.e., KOA, 5 nmol RVD-hemopressin (α), and AM251 + 5 nmol RVD-hemopressin (α) groups) were significantly different between treatments ($F_{(2, 182)} = 96.61$; $p < 0.0001$), across times ($F_{(6, 182)} = 1001.47$; $p < 0.0001$), and for their interactions ($F_{(12, 182)} = 15.28$; $p < 0.0001$). Further analyses showed that the mechanical thresholds in the AM251 + 5 nmol RVD-hemopressin (α) group were significantly less than those in the AM251 group from the 23rd to the 27th day after KOA induction ($p < 0.001$; Figure 5C). No significant difference was measured between the AM251 + 5 nmol RVD-hemopressin (α) group and the KOA group ($p > 0.05$; Figure 5C).

Similarly, the application of the AM251 into the vlPAG reversed the 5 nmol RVD-hemopressin (α) effect on the thermal withdrawal latency ($p < 0.001$). As shown in Figure 5D, the time course curves (i.e., KOA, 5 nmol RVD-hemopressin (α), and AM251 + 5 nmol RVD-hemopressin (α) groups) were significantly different between treatments ($F_{(2, 140)} = 47.80$; $p < 0.0001$), across times ($F_{(6, 140)} = 37.55$; $p < 0.0001$), and for their interactions ($F_{(12, 140)} = 9.409$; $p < 0.0001$). Further analyses showed that the withdrawal latency in the AM251 + 5 nmol RVD-hemopressin (α) group was significantly less than the AM251 group from the 23rd to the 27th day after KOA induction ($p < 0.05$; Figure 5D). No significant difference was measured between the AM251 + 5 nmol RVD-hemopressin (α) group and the KOA group from the 25th to the 27th day after KOA induction ($p > 0.05$; Figure 5D). The withdrawal latency in the AM251 + 5 nmol RVD-hemopressin (α) group was also significantly higher than in the KOA group on the 23rd day after KOA induction ($p < 0.05$; Figure 5D).

3.8 EA increased the 26S proteasome expression in the PAG of KOA mice

Studies have reported hemoglobin degradation by proteasome activity after ubiquitination or oxidation in erythrocytes (Pacifici et al., 1993; Wenzel and Baumeister, 1993). Moreover, the 26S proteasome is known to generate peptides ranging from 3 to 22 amino acids (Kisselev et al., 1999) and is consistent with the size of VD-hemopressin (α) and RVD-hemopressin (α). Thus, we used Western blotting to evaluate the effect of EA on the 26S proteasome protein level. The 26S proteasome protein bands were presented in the PAG tissues (Figure 6A). Compared with the control group, the 26S proteasome protein level was significantly reduced in the PAG of KOA mice ($p < 0.001$; Figure 6B). EA significantly increased the 26S proteasome level compared to the KOA group ($p < 0.001$; Figure 6B).

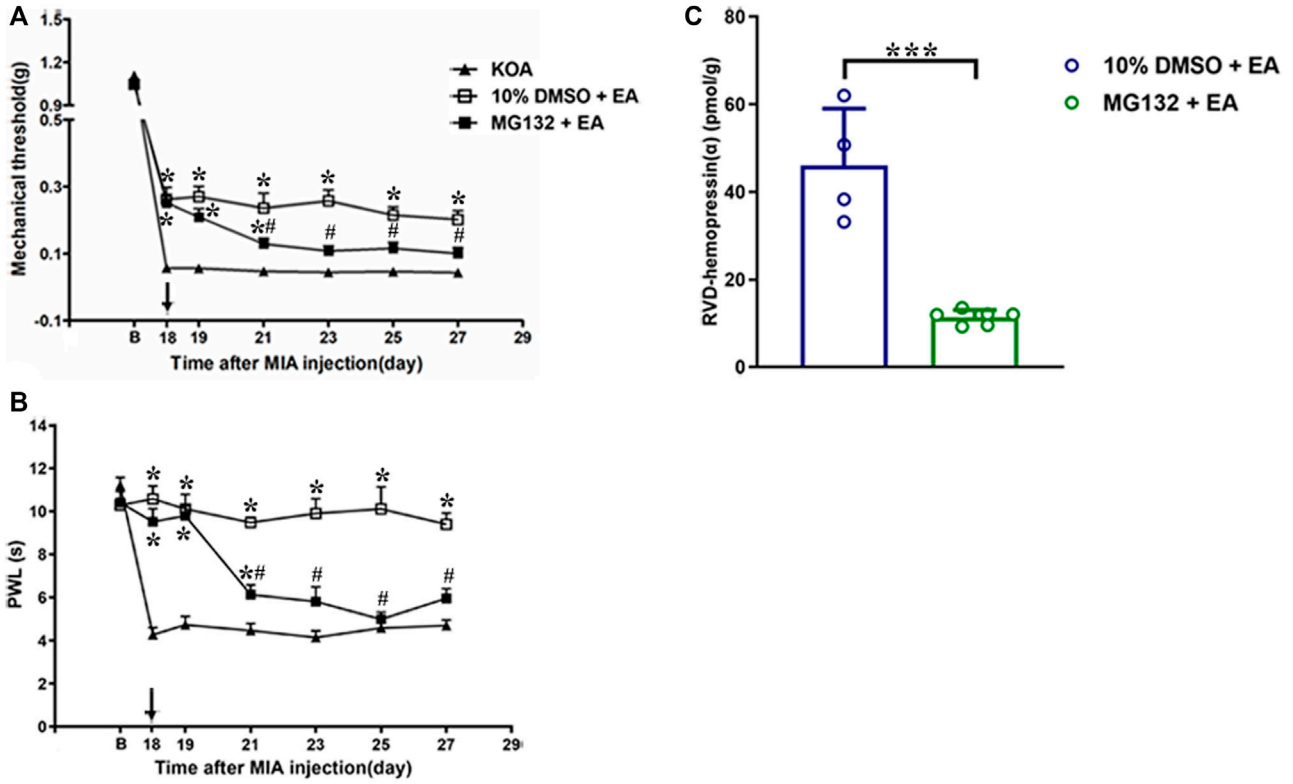

FIGURE 7
Effects of the 26S proteasome inhibitor MG132 on EA analgesia and RVD-hemopressin (α) concentration in the PAG. **(A, B)** Time course of the effect of the 26S proteasome inhibitor MG132 on tactile and thermal withdrawal thresholds of EA mice. EA was administered for 30 min, once every other day for 4 weeks, starting from 2 days after the MIA injection. The 26S proteasome inhibitor MG132 (4 μg) was microinjected into the vlPAG 30 min before EA starting from 18 days after MIA injection, once every other day for five times, as indicated by the black arrow. Data are expressed as means ± SEM (n = 8–11 mice in each group). *$p < 0.05$, compared with the KOA group; #$p < 0.05$, compared with the 10% DMSO + EA group. **(C)** Summary data show the concentration of RVD-hemopressin (α) in the PAG. Data are expressed as means ± SEM (n = 4–6 mice in each group). *$p < 0.001$.

3.9 vlPAG microinjection of the 26S proteasome inhibitor MG132 reversed the EA effects on pain hypersensitivity and upregulated the concentration of RVD-hemopressin (α)

To explore whether the 26S proteasome was involved in the degradation of hemoglobin, the 26S proteasome inhibitor MG132 (0.4 μg/0.5 μL) was administered 30 min before EA starting from the 18th day after KOA induction, once every other day for five times (Yang et al., 2008). The MG132 reversed the EA effect on the tactile withdrawal thresholds ($p < 0.001$). As shown in Figure 7A, the time course curves (i.e., KOA, MG132 + EA, and 10% DMSO + EA groups) were significantly different between treatments ($F_{(2, 189)} = 93.17$; $p < 0.0001$) across times ($F_{(6, 189)} = 843.88$; $p < 0.0001$), and for their interactions ($F_{(12, 189)} = 7.39$; $p < 0.0001$). Further analyses showed that the mechanical thresholds in the MG132 + EA group were significantly less than those in the 10% DMSO + EA group from the 21st to the 27th day after KOA induction ($p < 0.05$; Figure 7A). No significant difference was measured between the MG132 + EA and KOA groups from the 23rd to the 27th day after KOA induction ($p > 0.05$; Figure 7A).

Similarly, the MG132 reversed the EA effect on the thermal withdrawal latency ($p < 0.001$). As shown in Figure 7B, the time course curves (i.e., KOA, MG132 + EA, and 10% DMSO + EA groups) were significantly different between treatments ($F_{(2, 189)} = 145.56$; $p < 0.0001$) across times ($F_{(6, 189)} = 28.87$; $p < 0.0001$), and for their interactions ($F_{(12, 189)} = 11.04$; $p < 0.0001$). Further analyses showed that the withdrawal latency in the MG132 + EA group was significantly less than in the 10% DMSO + EA group from the 21st to the 27th day after KOA induction ($p < 0.05$; Figure 7B). No significant difference was measured between the MG132 + EA group and the KOA group from the 23rd to the 27th day after KOA induction ($p > 0.05$; Figure 7B). These results signify that MG132 reversed the ameliorating effect of EA on pain hypersensitivity.

We further examined the concentration of VD-hemopressin (α) and RVD-hemopressin (α). The result showed that microinjection of MG132 before EA prevented the effect of EA upregulation of the concentration of RVD-hemopressin (α) in the PAG ($p < 0.001$; Figure 7C), but VD-hemopressin (α) could not be detected in the MG132 + EA group.

3.10 vlPAG microinjection of the 26S proteasome inhibitor MG132 increased the expression of hemoglobin α-chain

Because VD-hemopressin (α) and RVD-hemopressin (α) peptides are derived from the hemoglobin α chain, we also

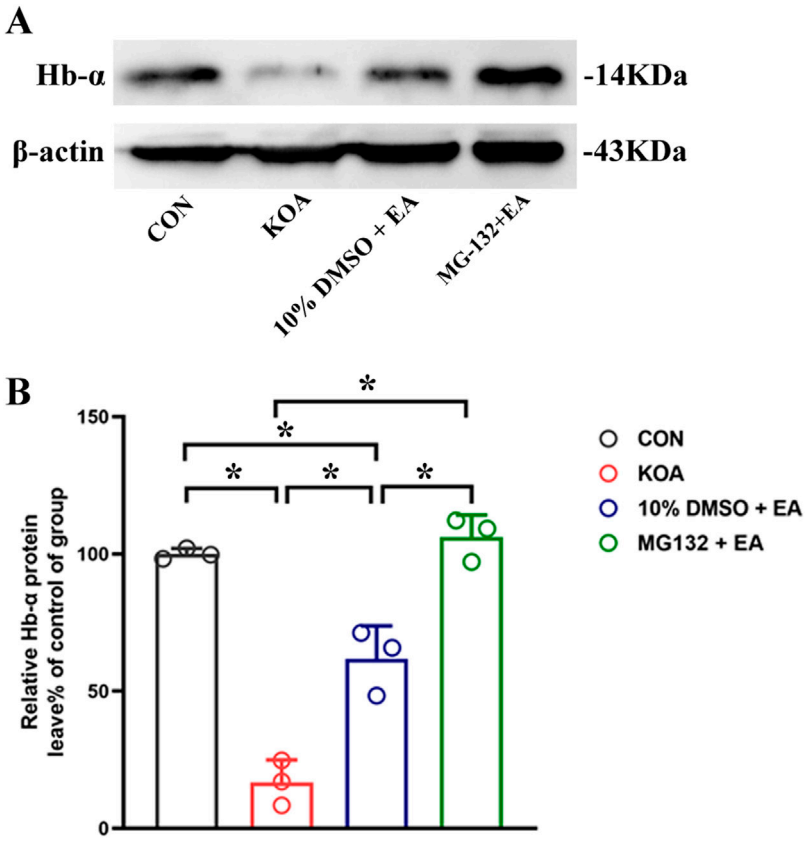

FIGURE 8
Effects of the 26S proteasome inhibitor MG132 on hemoglobin α-chain expression in the PAG. **(A)** The representative gel image shows the protein level of hemoglobin α-chain in PAG tissues obtained from CON, KOA, 10% DMSO + EA, and MG132 + EA groups. β-actin was used as a loading control. The protein band at 14 kDa corresponds to the hemoglobin α-chain. **(B)** Summary data show the effect of 26S proteasome inhibitor MG132 on the protein level of the hemoglobin α-chain in PAG tissues. EA was administered for 30 min, once every other day for 4 weeks, starting from 2 days after MIA injection. The 26S proteasome inhibitor MG132 (4 μg) was microinjected into the vlPAG 30 min before EA starting from 18 days after MIA injection, once every other day for five times. Data are expressed as means ± SEM (n = 3 mice in each group). *$p < 0.05$.

investigated detecting the expression of the hemoglobin α chain in the PAG. The result showed that compared with the 10% DMSO + EA group, the PSMD2 protein level was significantly increased in the MG132 + EA group ($p < 0.05$; Figures 8A, B). These results indicated that EA might produce VD-hemopressin (α) and RVD-hemopressin (α) by promoting 26S proteasome to degrade the hemoglobin α chain, thereby exerting an analgesic effect.

4 Discussion

The present study utilized RNA-seq to evaluate the involvement of differentially expressed genes *Hba-a1* and *Hba-a2*, which encode the hemoglobin α chain, in EA-induced analgesia. It was demonstrated that EA treatment of 2 Hz + 1 mA significantly increased the levels of hemoglobin α chain and its active-derived peptides VD-hemopressin (α) and RVD-hemopressin(α) in KOA mice. Microinjection of VD-hemopressin (α) and RVD-hemopressin (α) into the vlPAG mimicked the analgesic effect of EA, while microinjection of AM251 reversed this effect. Additionally, EA significantly increased the expression of 26S proteasome in the PAG, and microinjection of 26S proteasome inhibitor MG132 reversed the EA effects on pain hypersensitivity and upregulated the concentration of RVD-hemopressin (α). Meanwhile, we found that microinjection of MG132 before EA upregulated the expression of the hemoglobin α chain, indicating that it inhibited the degradation of the hemoglobin α chain. Our study provided evidence that EA upregulated the concentration of VD-hemopressin (α) and RVD-hemopressin (α) through the promotion of hemoglobin α chain degradation by 26S proteasome and activation of CB1 receptor, thereby exerting chronic pain inhibition in a mouse model of KOA.

EA has been widely used for alleviating diverse pains under morbid conditions (Chen et al., 2022; Li et al., 2019; Liao and Lin, 2021). However, the central mechanism by which EA modifies nociception is still a conundrum. In the present study, RNA-seq was used to obtain transcriptome data from control, KOA, and EA groups to explore EA-induced analgesia-related DEGs and their central regulatory mechanisms. Clustering analysis of DEGs showed that 10 genes were downregulated in the KOA group while upregulated in the EA group, and 12 genes were upregulated in the KOA group while downregulated in the EA group. Among these DEG data, two genes, Hba-a1 and Hba-a2, were selected to be explored because the gene *Hba-a2* has the largest fold change, and *Hba-a1* has more than three times change compared with the control group. The *Hba-a1* and *Hba-a2* encode for hemoglobin α

chain, which, upon degradation, yields cannabinopeptide ligands. We have been considering the role of the endocannabinoid system in EA analgesia. Therefore, we used RT-qPCR to explore it further for verification in this study. Interestingly, it was found that the expressions of *Hba-a1* and *Hba-a2* in the PAGs of KOA mice were significantly downregulated compared with the control group, and EA significantly increased the expression of *Hba-a1* and *Hba-a2*, which was consistent with the results of RNA-seq. Note that *Hba-a1* expression was notably more downregulated than *Hba-a2* in the KOA group. This may be caused by the different expression levels of *Hba-a1* and *Hba-a2* in the mice. These data indicate the involvement of *Hba-a1* and *Hba-a2* genes in EA-mediated analgesia.

It is established that *Hba-a1* and *Hba-a2* encode the hemoglobin α chain. As commonly understood, the hemoglobin α chain is an important component of hemoglobin, and it has long been thought that hemoglobin expression is restricted to erythrocytes and precursor cells of the erythroid lineage (Russo et al., 2013). However, recent studies have discovered that hemoglobin α also expressed in neurons of the midbrain and cortex, cerebellum, hippocampus, and striatum (Biagioli et al., 2009; Richter et al., 2009; Russo et al., 2013; Schelshorn et al., 2009). Similarly, the present study has found a significant increase in the protein level of the hemoglobin α chain in the PAG following repeated EA treatments. We further analyzed the correlation between the expression of *Hba-a1* and *Hba-a2* and hemoglobin α chain protein expression and observed a good correlation between them ($r_{Hba\text{-}a1}$ = 0.9169, $P_{Hba\text{-}a1}$ = 0.0005; $r_{Hba\text{-}a2}$ = 0.8451, $P_{Hba\text{-}a2}$ = 0.0041, Supplementary Figure S1). Thus, these data indicate that the hemoglobin α chain is involved in EA analgesia, but its mechanism remains unclear.

It has been demonstrated that VD-hemopressin (α) and RVD-hemopressin (α) peptides are derived from the hemoglobin α chain in mouse brains (Gomes et al., 2009). In this study, we have shown that the levels of VD-hemopressin (α) and RVD-hemopressin (α) were significantly increased after EA treatments. Further studies have shown that the CB1 receptor mediated the analgesic effect of VD-hemopressin (α), but whether RVD-hemopressin (α) has an analgesic effect is unclear (Gomes et al., 2009; Han et al., 2014; Zheng et al., 2017). To investigate this question, 10 nmol of VD-hemopressin (α) and various doses of RVD-hemopressin (α) were microinjected into the vlPAG, and a similar effect was observed mimicking EA treatment-induced analgesia. Moreover, the CB1 receptor selective antagonist AM251 reversed the analgesic effect of VD-hemopressin (α) and RVD-hemopressin (α). These results indicate that EA upregulated the concentration of VD-hemopressin (α) and RVD-hemopressin (α) in the PAG and activated the CB1 receptor to inhibit chronic pain in a mouse model of KOA.

It will be interesting to explore the mechanisms involved in generating VD-hemopressin (α) and RVD-hemopressin (α). Previous studies have demonstrated that the 26S proteasome is known to generate peptides ranging from 3 to 22 amino acids long (Kisselev et al., 1999; Yuan T. et al., 2018). Furthermore, the VD-hemopressin (α) and RVD-hemopressin (α) are within the appropriate size range for 26S proteasome products. Therefore, one possibility is that VD-hemopressin (α) and RVD-hemopressin (α) may be produced through 26S proteasome degradation of the hemoglobin α chain in neurons.

The present study further revealed that EA significantly increased the expression of 26S proteasome in the PAG. Moreover, microinjection of 26S proteasome inhibitor MG132 into the vlPAG before EA reversed both the anti-allodynic effect and upregulation of the concentration of RVD-hemopressin (α) by EA treatment, but VD-hemopressin (α) was not detected. It was earlier documented that RVD-hemopressin (α) is the most frequently detected α-hemoglobin-derived peptide by many folds, making it the most abundant neuropeptide (Gomes et al., 2009). Cleavage of hemopressin at the D-P bond would give rise to the shorter peptides. Therefore, it is reasonable to suggest that VD-hemopressin (α) could not be detected after microinjection of 26S proteasome inhibitor MG132 before EA because VD-hemopressin (α) degradation most likely produced other shorter peptides. Microinjection of the 26S proteasome inhibitor MG132 into the vlPAG before EA also significantly increased the expression of the hemoglobin α chain. These results provide support to the hypothesis that VD-hemopressin (α) and RVD-hemopressin (α) are produced through 26S proteasome degradation of the hemoglobin α chain.

5 Conclusion

Taken together, the present study demonstrated that the hemoglobin α chain in the PAG is involved in EA analgesia. A possible mechanism underlying this effect is that EA enhances the concentration of VD-hemopressin (α) and RVD-hemopressin (α) via the promotion of the hemoglobin α chain degradation by the 26S proteasome and activates the CB1 receptor, which brings about chronic pain inhibition in a mouse model of KOA.

Data availability statement

The data presented in this study are deposited in the Sequence Read Archive (SRA) repository (https://www.ncbi.nlm.nih.gov/sra/), accession numbers: SRR30787944, SRR30787945, SRR30787946, SRR30787947, SRR30787948, SRR30787949, SRR30787950, SRR30787951, SRR30787952.

Ethics statement

The animal study was approved by the Animal Ethics Committee of the Xi'an Jiaotong University Health Science Center. The study was conducted in accordance with the local legislation and institutional requirements.

Author contributions

XY: conceptualization, data curation, formal analysis, funding acquisition, investigation, validation, writing–original draft, and writing–review and editing. YG: methodology and writing–review and editing. HY: investigation and writing–review and editing. XH: investigation and writing–review and editing. YZ: data curation and writing–review and editing. YW: data curation and writing–review and editing. HJ: writing–review and editing. SB: writing–original draft and writing–review and editing. ML: project administration, supervision, and writing–review and editing. FH: conceptualization, funding acquisition, project administration, and writing–review and editing.

Funding

The author(s) declare that financial support was received for the research, authorship, and/or publication of this article. This work was supported by grants from the National Natural Science Foundation of China (Nos 81904288 and 81870886), the Natural Science Basic Research Program of Shaanxi Province (No. 2024JC-YBMS-668), and the Basic research expenses of Xi'an Jiaotong University (No. xzy012024093).

Conflict of interest

The authors declare that the research was conducted in the absence of any commercial or financial relationships that could be construed as a potential conflict of interest.

Publisher's note

Supplementary material

The Supplementary Material for this article can be found online at: https://www.frontiersin.org/articles/10.3389/fphar.2024.1439448/full#supplementary-material

References

Bauer, M., Chicca, A., Tamborrini, M., Eisen, D., Lerner, R., Lutz, B., et al. (2012). Identification and quantification of a new family of peptide endocannabinoids (Pepcans) showing negative allosteric modulation at CB1 receptors. *J. Biol. Chem.* 287 (44), 36944–36967. doi:10.1074/jbc.M112.382481

Biagioli, M., Pinto, M., Cesselli, D., Zaninello, M., Lazarevic, D., Roncaglia, P., et al. (2009). Unexpected expression of alpha- and beta-globin in mesencephalic dopaminergic neurons and glial cells. *Proc. Natl. Acad. Sci. U. S. A.* 106 (36), 15454–15459. doi:10.1073/pnas.0813216106

Chaplan, S. R., Bach, F. W., Pogrel, J. W., Chung, J. M., and Yaksh, T. L. (1994). Quantitative assessment of tactile allodynia in the rat paw. *J. Neurosci. Methods* 53 (1), 55–63. doi:10.1016/0165-0270(94)90144-9

Chen, L., Zhang, J., Li, F., Qiu, Y., Wang, L., Li, Y. H., et al. (2009). Endogenous anandamide and cannabinoid receptor-2 contribute to electroacupuncture analgesia in rats. *J. Pain* 10 (7), 732–739. doi:10.1016/j.jpain.2008.12.012

Chen, Y., Zhou, Y., Li, X. C., Ma, X., Mi, W. L., Chu, Y. X., et al. (2022). Neuronal GRK2 regulates microglial activation and contributes to electroacupuncture analgesia on inflammatory pain in mice. *Biol. Res.* 55 (1), 5. doi:10.1186/s40659-022-00374-6

de Hoon, M. J., Imoto, S., Nolan, J., and Miyano, S. (2004). Open source clustering software. *Bioinformatics* 20 (9), 1453–1454. doi:10.1093/bioinformatics/bth078

Eisen, M. B., Spellman, P. T., Brown, P. O., and Botstein, D. (1998). Cluster analysis and display of genome-wide expression patterns. *Proc. Natl. Acad. Sci. U. S. A.* 95 (25), 14863–14868. doi:10.1073/pnas.95.25.14863

Fernihough, J., Gentry, C., Malcangio, M., Fox, A., Rediske, J., Pellas, T., et al. (2004). Pain related behaviour in two models of osteoarthritis in the rat knee. *Pain* 112 (1-2), 83–93. doi:10.1016/j.pain.2004.08.004

Gelman, J. S., and Fricker, L. D. (2010). Hemopressin and other bioactive peptides from cytosolic proteins: are these non-classical neuropeptides? *AAPS J.* 12 (3), 279–289. doi:10.1208/s12248-010-9186-0

Gomes, I., Grushko, J. S., Golebiewska, U., Hoogendoorn, S., Gupta, A., Heimann, A. S., et al. (2009). Novel endogenous peptide agonists of cannabinoid receptors. *FASEB J.* 23 (9), 3020–3029. doi:10.1096/fj.09-132142

Han, Z. L., Fang, Q., Wang, Z. L., Li, X. H., Li, N., Chang, X. M., et al. (2014). Antinociceptive effects of central administration of the endogenous cannabinoid receptor type 1 agonist VDPVNFKLLSH-OH [(m)VD-hemopressin(α)], an N-terminally extended hemopressin peptide. *J. Pharmacol. Exp. Ther.* 348 (2), 316–323. doi:10.1124/jpet.113.209866

Harvey, V. L., and Dickenson, A. H. (2009). Behavioural and electrophysiological characterisation of experimentally induced osteoarthritis and neuropathy in C57Bl/6 mice. *Mol. Pain* 5, 18. doi:10.1186/1744-8069-5-18

Jiang, Z., Li, Y., Wang, Q., Fang, Z., Deng, J., Zhang, X., et al. (2022). Combined-acupoint electroacupuncture induces better analgesia via activating the endocannabinoid system in the spinal cord. *Neural Plast.* 2022, 7670629. doi:10.1155/2022/7670629

Kisselev, A. F., Akopian, T. N., Woo, K. M., and Goldberg, A. L. (1999). The sizes of peptides generated from protein by mammalian 26 and 20 S proteasomes. Implications for understanding the degradative mechanism and antigen presentation. *J. Biol. Chem.* 274 (6), 3363–3371. doi:10.1074/jbc.274.6.3363

La Porta, C., Bura, S. A., Aracil-Fernandez, A., Manzanares, J., and Maldonado, R. (2013). Role of CB1 and CB2 cannabinoid receptors in the development of joint pain induced by monosodium iodoacetate. *Pain* 154 (1), 160–174. doi:10.1016/j.pain.2012.10.009

Leone, S., Ferrante, C., Recinella, L., Chiavaroli, A., Mollica, A., Tomboly, C., et al. (2018). Effects of RVD-hemopressin (α) on feeding and body weight after standard or cafeteria diet in rats. *Neuropeptides* 72, 38–46. doi:10.1016/j.npep.2018.10.002

Li, Y., Yin, C., Li, X., Liu, B., Wang, J., Zheng, X., et al. (2019). Electroacupuncture alleviates paclitaxel-induced peripheral neuropathic pain in rats via suppressing TLR4 signaling and TRPV1 upregulation in sensory neurons. *Int. J. Mol. Sci.* 20 (23), 5917. doi:10.3390/ijms20235917

Liao, H. Y., and Lin, Y. W. (2021). Electroacupuncture attenuates chronic inflammatory pain and depression comorbidity through transient receptor potential V1 in the brain. *Am. J. Chin. Med.* 49 (6), 1417–1435. doi:10.1142/S0192415X2150066X

Luan, L., Bousie, J., Pranata, A., Adams, R., and Han, J. (2021). Stationary cycling exercise for knee osteoarthritis: a systematic review and meta-analysis. *Clin. Rehabil.* 35 (4), 522–533. doi:10.1177/0269215520971795

Lv, Z. T., Shen, L. L., Zhu, B., Zhang, Z. Q., Ma, C. Y., Huang, G. F., et al. (2019). Effects of intensity of electroacupuncture on chronic pain in patients with knee osteoarthritis: a randomized controlled trial. *Arthritis Res. Ther.* 21 (1), 120. doi:10.1186/s13075-019-1899-6

Ng, M. M., Leung, M. C., and Poon, D. M. (2003). The effects of electro-acupuncture and transcutaneous electrical nerve stimulation on patients with painful osteoarthritic knees: a randomized controlled trial with follow-up evaluation. *J. Altern. Complement. Med.* 9 (5), 641–649. doi:10.1089/107555303322524490

Pacifici, R. E., Kono, Y., and Davies, K. J. (1993). Hydrophobicity as the signal for selective degradation of hydroxyl radical-modified hemoglobin by the multicatalytic proteinase complex, proteasome. *J. Biol. Chem.* 268 (21), 15405–15411. doi:10.1016/s0021-9258(18)82272-4

Richter, F., Meurers, B. H., Zhu, C., Medvedeva, V. P., and Chesselet, M. F. (2009). Neurons express hemoglobin alpha- and beta-chains in rat and human brains. *J. Comp. Neurol.* 515 (5), 538–547. doi:10.1002/cne.22062

Russo, R., Zucchelli, S., Codrich, M., Marcuzzi, F., Verde, C., and Gustincich, S. (2013). Hemoglobin is present as a canonical α2β2 tetramer in dopaminergic neurons. *Biochim. Biophys. Acta* 1834 (9), 1939–1943. doi:10.1016/j.bbapap.2013.05.005

Saldanha, A. J. (2004). Java Treeview--extensible visualization of microarray data. *Bioinformatics* 20 (17), 3246–3248. doi:10.1093/bioinformatics/bth349

Schelshorn, D. W., Schneider, A., Kuschinsky, W., Weber, D., Kruger, C., Dittgen, T., et al. (2009). Expression of hemoglobin in rodent neurons. *J. Cereb. Blood Flow. Metab.* 29 (3), 585–595. doi:10.1038/jcbfm.2008.152

Selfe, T. K., and Taylor, A. G. (2008). Acupuncture and osteoarthritis of the knee: a review of randomized, controlled trials. *Fam. Community Health* 31 (3), 247–254. doi:10.1097/01.FCH.0000324482.78577.0f

Tai, H. C., and Schuman, E. M. (2008). Ubiquitin, the proteasome and protein degradation in neuronal function and dysfunction. *Nat. Rev. Neurosci.* 9 (11), 826–838. doi:10.1038/nrn2499

Wenzel, T., and Baumeister, W. (1993). Thermoplasma acidophilum proteasomes degrade partially unfolded and ubiquitin-associated proteins. *FEBS Lett.* 326 (1-3), 215–218. doi:10.1016/0014-5793(93)81793-y

Yang, L., Wang, S., Lim, G., Sung, B., Zeng, Q., and Mao, J. (2008). Inhibition of the ubiquitin-proteasome activity prevents glutamate transporter degradation and morphine tolerance. *Pain* 140 (3), 472–478. doi:10.1016/j.pain.2008.09.028

Yuan, T., Yan, F., Ying, M., Cao, J., He, Q., Zhu, H., et al. (2018a). Inhibition of ubiquitin-specific proteases as a novel anticancer therapeutic strategy. *Front. Pharmacol.* 9, 1080. doi:10.3389/fphar.2018.01080

Yuan, X. C., Wang, Q., Su, W., Li, H. P., Wu, C. H., Gao, F., et al. (2018b). Electroacupuncture potentiates peripheral CB2 receptor-inhibited chronic pain in a mouse model of knee osteoarthritis. *J. Pain Res.* 11, 2797–2808. doi:10.2147/JPR.S171664

Yuan, X. C., Wang, Y. Y., Tian, L. X., Yan, X. J., Guo, Y. X., Zhao, Y. L., et al. (2022). Spinal 5-HT(2A) receptor is involved in electroacupuncture inhibition of chronic pain. *Mol. Pain* 18, 17448069221087583. doi:10.1177/17448069221087583

Yuan, X. C., Yan, X. J., Tian, L. X., Guo, Y. X., Zhao, Y. L., Baba, S. S., et al. (2021). 5-HT(7) receptor is involved in electroacupuncture inhibition of chronic pain in the spinal cord. *Front. Neurosci.* 15, 733779. doi:10.3389/fnins.2021.733779

Yuan, X. C., Zhu, B., Jing, X. H., Xiong, L. Z., Wu, C. H., Gao, F., et al. (2018c). Electroacupuncture potentiates cannabinoid receptor-mediated descending inhibitory control in a mouse model of knee osteoarthritis. *Front. Mol. Neurosci.* 11, 112. doi:10.3389/fnmol.2018.00112

Zhang, R. S., He, Z., Jin, W. D., and Wang, R. (2016). Effects of the cannabinoid 1 receptor peptide ligands hemopressin, (m)RVD-hemopressin(α) and (m)VD-hemopressin(α) on memory in novel object and object location recognition tasks in normal young and Aβ1-42-treated mice (m)RVD-hemopressin(alpha) and (m)VD-hemopressin(alpha) on memory in novel object and object location recognition tasks in normal young and Abeta1-42-treated mice. *Neurobiol. Learn Mem.* 134 Pt B, 264–274. doi:10.1016/j.nlm.2016.07.030

Zheng, T., Zhang, R., Zhang, T., Zhang, M. N., Xu, B., Song, J. J., et al. (2018). CB1 cannabinoid receptor agonist mouse VD-hemopressin(α) produced supraspinal analgesic activity in the preclinical models of pain. *Brain Res.* 1680, 155–164. doi:10.1016/j.brainres.2017.12.013

Zheng, T., Zhang, T., Zhang, R., Wang, Z. L., Han, Z. L., Li, N., et al. (2017). Pharmacological characterization of rat VD-hemopressin(α), an α-hemoglobin-derived peptide exhibiting cannabinoid agonist-like effects in mice. *Neuropeptides* 63, 83–90. doi:10.1016/j.npep.2016.12.006

Zimmermann, M. (1983). Ethical guidelines for investigations of experimental pain in conscious animals. *Pain* 16 (2), 109–110. doi:10.1016/0304-3959(83)90201-4

frontiers | Frontiers in Molecular Neuroscience

TYPE Systematic Review
PUBLISHED 16 October 2024
DOI 10.3389/fnmol.2024.1412855

OPEN ACCESS

EDITED BY
Álvaro Llorente-Berzal,
Autonomous University of Madrid, Spain

REVIEWED BY
Fabio Turco,
Cannabiscientia SA, Switzerland
Inga Dammann,
University of Heidelberg, Germany

*CORRESPONDENCE
Iván Echeverria
✉ gomechiva@alumnos.uchceu.es;
✉ iecheverria@mgh.harvard.edu

‡These authors have contributed equally to this work and share first authorship

RECEIVED 05 April 2024
ACCEPTED 18 September 2024
PUBLISHED 16 October 2024

CITATION
Peraire M, Gimeno-Vergara R, Pick-Martin J, Boscá M and Echeverria I (2024) Ziconotide and psychosis: from a case report to a scoping review.
Front. Mol. Neurosci. 17:1412855.
doi: 10.3389/fnmol.2024.1412855

Ziconotide and psychosis: from a case report to a scoping review

Marc Peraire[1,2‡], Rita Gimeno-Vergara[1,2‡], Jennifer Pick-Martin[1,2], Mireia Boscá[1,2] and Iván Echeverria[1,2,3*]

[1]TXP Research Group, Universidad Cardenal Herrera-CEU, CEU Universities, Castellón de la Plana, Spain, [2]Department of Mental Health, Consorcio Hospitalario Provincial de Castellón, Castellón de la Plana, Spain, [3]Department of Psychiatry, Laboratory for Neuropsychiatry and Neuromodulation, Massachusetts General Hospital, Harvard Medical School, Boston, MA, United States

Ziconotide is a non-opioid analgesic that acts on N-type voltage-gated calcium channels. Despite its proven effectiveness in pain treatment, it can induce neuropsychiatric symptoms. The aim of this article is to present a case of psychosis secondary to ziconotide and to explore the variety of neuropsychiatric symptoms it produces, exploring the relationship between these symptoms and the mechanism of action of ziconotide. For this purpose, a clinical case is presented as well as a scoping review of other cases published in the scientific literature. A search on Web of Science, Pubmed and Embase databases was performed on December 11, 2023, following the criteria of the PRISMA-ScR Statement. The clinical case presented shows the variety of neuropsychiatric symptomatology that ziconotide can cause in the same patient. On the other hand, 13 papers were retrieved from the scoping review (9 case reports, 4 case series), which included 21 cases of patients treated with ziconotide who presented adverse effects ranging from psychotic symptoms to delirium. In conclusion, the variety of neuropsychiatric symptoms derived from ziconotide could be related to the blockade of N-type voltage-gated calcium channels in glutamatergic and GABAergic neurons, in turn affecting dopaminergic pathways.

KEYWORDS

ziconotide, psychosis, Cav2.2, GABA, glutamate, dopamine, scoping review, neuropsychiatric symptoms

1 Introduction

Ziconotide is a non-opioid analgesic that has contributed to a paradigm shift in pain treatment. It is a synthetic derivative of ω-Conotoxin MVIIA found in the venom of the marine snail Conus magus. The molecule consists of 25 amino acids containing 6 cysteine residues linked by three disulfide bridges that fold the structure and produce the characteristic 3D structure that is critical for its mechanism of action based on the selective blockade of N-type voltage-gated calcium channels (Cav2.2) (Brookes et al., 2017). These channels play a crucial role in the release of neurotransmitters, such as glutamate and substance P, responsible for pain transmission (Zamponi et al., 2015; Moore and McCrory, 2017).

Several cases of ziconotide-treated patients experiencing adverse effects, particularly neuropsychiatric symptoms, have been reported in the literature, including confusion, disorientation, decreased alertness, somnolence, drowsiness, hallucinations or other changes in perception and mood. These symptoms were already known from early clinical trials, and can last for as long as ziconotide is administered and for up to 2 weeks after discontinuation, although in some cases they may persist (Smith and Deer, 2009).

Indeed, there are some patient profiles that are more prone to experience these side effects, such as those with pre-existing psychiatric disorders (Smith and Deer, 2009). However, since this drug is usually prescribed by non-mental healthcare professionals, psychiatric symptoms are described briefly and vaguely as 'hallucinations' or 'confusion.' Thus, such a non-specific symptoms could be compatible with diagnoses as diverse as delirium or psychosis.

Despite the knowledge of the mechanism of action of the ziconotide and its association with neuropsychiatric adverse effects, there is a gap in the literature regarding the underlying physiological mechanisms. Although some hypotheses suggest that psychotic symptoms may be favored by the blockade of Cav2.2 in the prefrontal cortex and its relationship with dopaminergic neurotransmission (Burdge et al., 2018), no work has explored a specific pathway that may be involved in the appearance of these symptoms.

Therefore, our aim is to describe, from a novel psychiatric perspective, a ziconotide-induced psychotic episode with a wide range of neuropsychiatric symptoms. At the same time, this case report allowed a scoping review to analyze the clinical diversity of other published cases and to hypothesize about possible specific pathways associated with these adverse symptoms.

2 Methods

This case report was selected and described by the same mental health professionals that attended the patient. For this purpose, consent was requested from the patient herself and her relatives to obtain data from the clinical history.

Subsequently, a scoping review was conducted following the criteria of the PRISMA-ScR Statement, which was registered in the Open Science Framework (doi: 10.17605/OSF.IO/7C8RQ). A systematic review was completed on December 11, 2023, in the Web of Science, Pubmed and Embase databases. This combination was used because it ensured a recall of almost 96% of the papers (Bramer et al., 2017).

The terms chosen for the search were: ziconotide AND (psycho* OR delirium OR hallucination OR delusion). No filter was added, but the field code /exp was added to these terms in Embase to search for the related narrower or child terms. The references obtained (Figure 1) were entered into the systematic review management software COVIDENCE. The PICOS (participants, intervention, context, outcomes, and study design) framework was used to establish eligibility criteria. Two reviewers analyzed independently the results obtained according to the inclusion and exclusion criteria, and the resulting discrepancies were resolved by a third reviewer.

As inclusion criteria, case reports or case series were considered, whether in the form of an article, posters or oral communication, which included patients treated with ziconotide and who had presented psychosis, hallucinations, delusions or delirium. As exclusion criteria, we rejected those studies in which the psychopathology could not be clearly attributed to ziconotide, considering that the use of opioids can lead to confusional or even psychotic symptoms; studies that only provide the prevalence of neuropsychiatric adverse effects, but do not examine in depth the course of the disease itself; those cases in which there was a history of psychiatric disorders; and those studies whose language was not English or Spanish. The results of the studies obtained were grouped according to the clinical presentation and/or reported symptomatology (hallucinations, delirium, psychosis or delirium).

3 Results

3.1 Case presentation

The patient was a 54-year-old woman who was admitted to the psychiatric emergency room for auditory verbal hallucinations that began a few weeks earlier. Concretely, she felt that her son and his partner were talking about her and insulting her through speakers.

Her medical history included hypothyroidism and a thoracic sarcomatoid mesothelioma diagnosed in November 2010, with multiple recurrences in the following 12 years and secondary chronic refractory pain since 2011. At the time of her consultation in the psychiatric emergency room (2023), the patient was suffering from radicular syndrome under palliative treatment with intrathecal pump of morphine 2% (19 mL) and ziconotide 100 μg/day, she had fentanyl 100 μg rescues every 72 h. The rest of her usual treatment included lormetazepam 2 mg at night, lacosamide 200 mg every 12 h, levothyroxine 50 μg every morning and metamizole 575 mg on demand.

Regarding her psychiatric history, she has suffered from dysthymia since 2006 and had been treated with escitalopram 10 mg and alprazolam 0.5 mg until 2013, when she discontinued them.

On initial psychiatric evaluation, the patient was conscious but disoriented as to time, place, and person. Her appearance was cachectic, and her attitude was suspicious and distressed. Slow thinking was noted as well as incoherent and derailed speech evidencing delusions of prejudice toward his son and his partner. The patient also described self-references, being spied on through electronic devices, and false recognition phenomena. Moreover, she admitted to having complex visual hallucinations (human figures), gustatory (dysgeusia) and olfactory (parosmia). The patient also had a long history of depressed mood in response to the prolonged oncologic process, with passive suicidal ideation, hyporexia, and insomnia.

Complementary tests, brain CT and chest X-ray showed no significant findings of oncologic progression. Toxicological analysis was positive for morphine and benzodiazepines, compatible with her usual medication. Family members reported that the only significant change prior to her current situation was the adjustment of analgesic medication 8 days before due to inadequate pain control, increasing ziconotide from 0.2 μg/day to a total dose of 7.5 μg/day.

The patient was admitted to the psychiatric ward, where she presented gait instability, tremor, and fluctuation of temporal and spatial orientation during the first days of admission. She maintained a certain level of uneasiness and suspicion with her relatives and healthcare professionals, introducing them to her delusions of harm, and having episodes of hostility that required the administration of intramuscular haloperidol and five-point mechanical restraint to ensure her own safety. Olanzapine (15 mg/day) was initiated, but the patient continued with delusional, hallucinatory, false recognitions and mumbling speech.

Considering the complex clinical picture, the possibility of organic psychosis or psychosis induced by some of her usual treatments was suggested, as this picture was compatible with the adverse effects of ziconotide. Given the clinical suspicion, a progressive reduction of intrathecal ziconotide was agreed with the Pain Management Unit until discontinuation.

As the dose of ziconotide was reduced, the psychotic symptoms disappeared, until they completely resolved 48 hours after drug withdrawal. After 12 days of hospitalization, the condition was

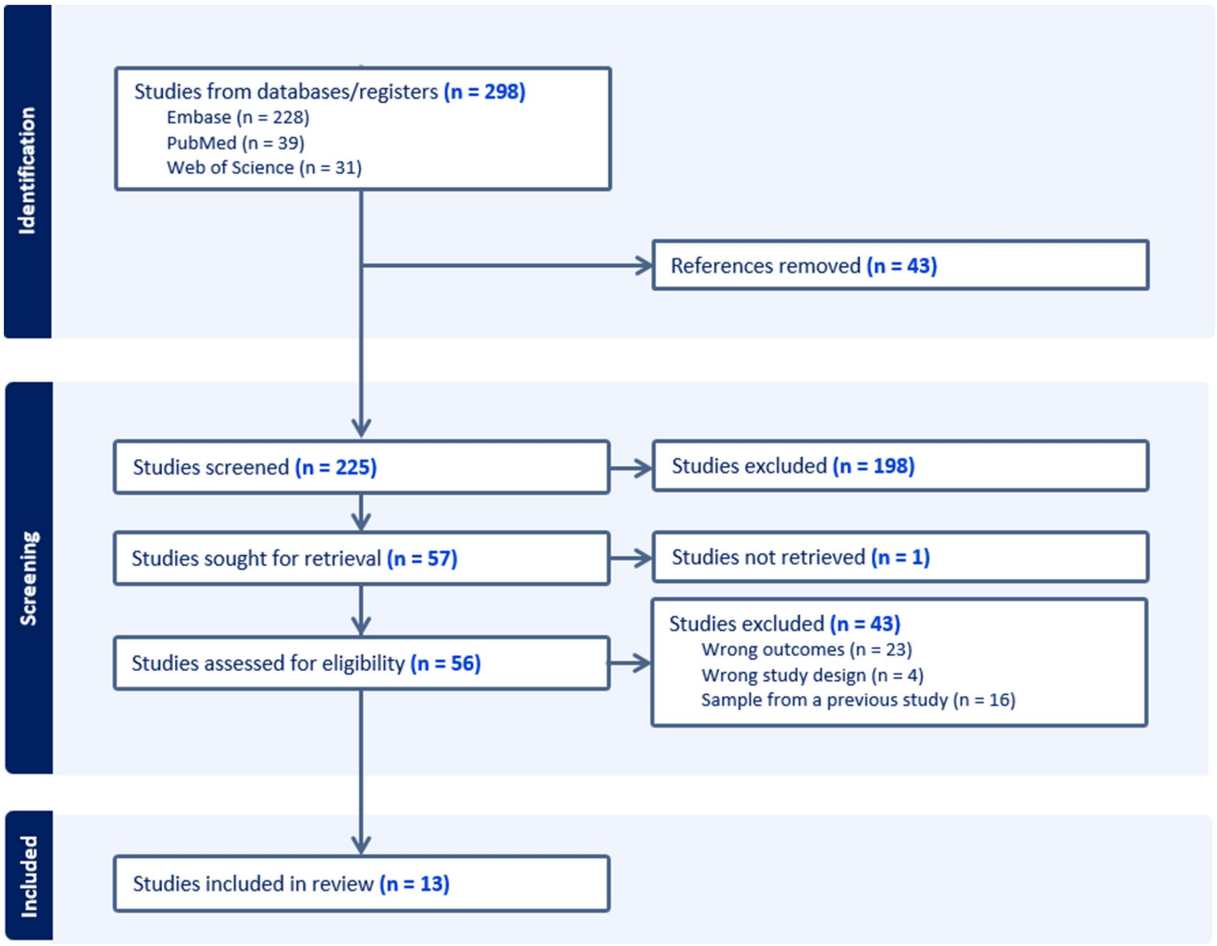

FIGURE 1
PRISMA flow diagram of study selection.

classified as a ziconotide-induced psychotic episode. The dose of olanzapine was reduced to 5 mg and the patient was referred to the Pain Unit for pain control, where the antipsychotic was eventually discontinued without recurrence of delusional symptoms.

3.2 Scoping review

A total of 13 papers (9 case reports, 4 case series) were included in this scoping review (Burdge et al., 2018; Su et al., 2021; Phan and Waldfogel, 2015; Whitlow et al., 2015; Abdelsayed et al., 2022; Stewart and Sarria, 2014; Kapural et al., 2009; Ayuga-Loro et al., 2011; Obafemi and Roth, 2013; Grajny et al., 2020; de la Calle Gil et al., 2015; Levin et al., 2002; Penn and Paice, 2000). They included 30 cases of patients with ziconotide who presented adverse effects, 21 of which consisted of neuropsychiatric symptoms (Table 1).

Considering the data in the table, it can be seen that most of the studies are from the United States. There is a male predominance in the occurrence of adverse effects (13 men vs. 8 women). Among the studies that recorded psychiatric antecedents (Burdge et al., 2018; Su et al., 2021; Phan and Waldfogel, 2015; Whitlow et al., 2015; Abdelsayed et al., 2022; Ayuga-Loro et al., 2011; Obafemi and Roth, 2013; Grajny et al., 2020), half of the patients had them (Phan and Waldfogel, 2015; Whitlow et al., 2015; Ayuga-Loro et al., 2011; Grajny et al., 2020) and the other half did not (Burdge et al., 2018; Bramer et al., 2017; Abdelsayed et al., 2022; Obafemi and Roth, 2013). On the other hand, the doses at which the adverse effects occurred were highly variable, ranging from a minimum of 0.6 mcg/d (Levin et al., 2002) to a maximum of 127.2 mcg/d (Webster, 2015).

In 7 patients the presentation was described as a "psychosis" (Burdge et al., 2018; Su et al., 2021; Phan and Waldfogel, 2015; Whitlow et al., 2015; Abdelsayed et al., 2022; Stewart and Sarria, 2014; Kapural et al., 2009), with auditory hallucinations and paranoid delusions in 5 of them (Burdge et al., 2018; Su et al., 2021; Phan and Waldfogel, 2015; Whitlow et al., 2015; Abdelsayed et al., 2022), and visual hallucinations in 3 cases (Su et al., 2021; Whitlow et al., 2015; Abdelsayed et al., 2022). However, in Stewart and Sarria (2014) the symptoms of the psychotic episode were not specified and in Kapural et al. (2009) they spoke of "psychotic delusions and hallucinations." In addition to the above, one case had psychotic (delusions of persecution, suspiciousness) and mania-like symptoms (verbosity, disinhibition) (Ayuga-Loro et al., 2011). Continuing with hallucinations, these also occurred in isolation, with one case describing auditory hallucinations, another visual hallucinations, and yet another unspecified hallucinations (Kapural et al., 2009).

Additionally, 4 patients presented delirium, either with auditory and visual hallucinatory symptoms (Obafemi and Roth, 2013), auditory only (Grajny et al., 2020), or without any psychiatric

TABLE 1 Summary table of ziconotide case report characteristics.

Author (year)	Country	Patient characteristics	Ziconotide peak dose /adverse effect dose	Neuropsychiatric symptoms	Management and treatment
Burdge et al. (2018)	United States	Male, 49 yo Chronic back pain after motor vehicle accident (spinal fusion surgeries) No previous neuropsychiatric history	14 mcg/d	Paranoia, auditory hallucinations, racing thoughts, pressure speech, labile affect and agitation	Ziconotide was reduced to 7 mcg/day, discontinued after 5 days, and risperidone 1 mg was added. After 10 days, the patient was discharged with risperidone 1 mg at bedtime
Su et al. (2021)	United States	Male, 60 yo Chronic back pain following a fall (L4 and L5 laminectomy) No previous neuropsychiatric history	7.37 mcg/d	Paranoid delusions, irrational beliefs of infestation, auditory, tactile and visual hallucinations, soliloquies, intermittently unintelligible speech and overvaluation of abilities	Ziconotide was reduced to 1.2 mcg/d and risperidone 0.5 mg/12 h was started. After 8 days, ziconotide was reduced to 0.158 mcg/d and risperidone was increased to 2 mg/12 h. The patient's psychiatric adverse effects improved and he was discharged with risperidone 2 mg/12 h
Phan and Waldfogel (2015)	United States	Female, 49 yo Complex regional pain syndrome related to a previous spinal injury (cervical fusion, spinal cord stimulation implantation) History of anxiety and depression	4.9 mcg/d	Paranoia, harm delusions, psychotic fear and hallucinations	Ziconotide was discontinued and risperidone 0.5 mg was started, with resolution of hallucinations and delusions in the first few hours
Whitlow et al. (2015)	United States	Female, 55 yo Stage IV endometrial cancer being treated with oral chemotherapy History of anxiety and depression	2.53 mcg/d	Fear (due to suspected poisoning), auditory and visual hallucinations, overestimation of abilities, recent memory impairment and agitation	Paliperidone 6 mg was started. After 7 days, a monthly injection of 234 mg paliperidone was started. Symptoms persisted over the next few weeks as there were no professionals available to handle the intrathecal pump
Abdelsayed et al. (2022)	United States	Male, 60 yo Refractory back pain No history of psychosis	7.32 mcg/d	Paranoia, auditory and visual hallucinations	Ziconotide was reduced daily and neuropsychiatric side effects disappeared
Stewart and Sarria (2014)	United States	Female, 37 yo Spinocerebellar ataxia and peripheral neuropathy	10.08 mcg/d	Psychosis	Ziconotide was discontinued and symptoms resolved. After 2 months, it was reintroduced due to failure of pain control, using a flexible dosing schedule and reaching a final dose of 11,437 mcg/d. No neuropsychiatric adverse effects returned

(Continued)

10.3389/fnmol.2024.1412855

TABLE 1 (Continued)

Author (year)	Country	Patient characteristics	Ziconotide peak dose /adverse effect dose	Neuropsychiatric symptoms	Management and treatment
Kapural et al. (2009)	United States	Case 3: Female, 16 yo Complex regional pain syndrome (CRPS) type I	3.5 mcg/d	Auditory hallucinations	Ziconotide was reduced to 2.5 mcg/d
		Case 4: Male, 35 yo Complex regional pain syndrome (CRPS) type I	6.48 mcg/d	Hallucinations and difficulty thinking	Ziconotide was reduced to 5.9 mcg/d and adverse effects resolved within 48 h
		Case 5: Female, 44 yo Complex regional pain syndrome (CRPS) type I	10.8 mcg/d	Visual hallucinations and cognitive impairment	Ziconotide was temporarily discontinued and the adverse effects resolved in 3 days. The pump was restarted 13 days later (5.4 mcg/d), causing panic attacks, so the dose was reduced to 4.2 mcg/d. Benzodiazepines and antipsychotics were added
		Case 6: Male, 34 yo Complex regional pain syndrome (CRPS) type I	13.44 mcg/d	Psychotic delusions, hallucinations, lack of concentration, speech difficulties, memory loss	Ziconotide was withdrawn and haloperidol and risperidone were started. Symptoms resolved in 9 days
		Case 7: Male, 52 yo Complex regional pain syndrome (CRPS) type I	11.78 mcg/d	Olfactory hallucinations, anxiety, and agitation	Ziconotide was reduced to 8.5 mcg/d
Ayuga-Loro et al. (2011)	Spain	Female, 66 yo Spinal cord injury at T12 secondary to disc prolapse after decompressive laminectomy for canal stenosis. History of depression	2.14 mcg/d	Delusional ideas of suspicion and persecution, accelerated speech and disinhibition	Ziconotide was withdrawn. Olanzapine was introduced
Obafemi and Roth (2013)	United States	Male, 37 yo Idiopathic small fiber peripheral neuropathy No history of psychosis	1.5 mcg/d	Hallucination and confusion	Ziconotide was reduced to 0.0353 mcg/day and adverse effects resolved
Grajny et al. (2020)	United States	Case 1: Female, 64 yo Spinal hemangioblastoma (resected)	6 mcg/d	Auditory hallucinations and delirium	Ziconotide was reduced to 0.25 mcg/day. Adverse effects improved but did not resolve completely
		Case 3: Male, 70 yo Cervical spondylosis History of depression	3.6 mcg/d	Hallucinations and disorientation	Ziconotide was reduced with improvement in symptoms, but was discontinued after recurrent hallucinations
de la Calle Gil et al. (2015)	Spain	Case 4: Female, 58 yo Metastatic rectal cancer and neuropathic pain	0.6 mcg/d	Neuropsychiatric disturbance	Ziconotide was withdrawn
		Case 5: Male, 63 yo Advanced colon cancer and neuropathic pain	5 mcg/d	Confusion and delirium	Ziconotide was discontinued. Due to lack of pain control, it was reintroduced, reaching a final dose of 4 mcg/day with no adverse effects
Levin et al. (2002)	United States	Male, 38 yo Painful glove-and-stocking peripheral neuropathy of unknown etiology	15.6 mcg/d	Agitated delirium	Ziconotide was withdrawn, haloperidol was started at up to 25 mg/h iv, and valproate was added. Electroconvulsive therapy was required for complete resolution of symptoms

(Continued)

10.3389/fnmol.2024.1412855

10.3389/fnmol.2024.1412855

TABLE 1 (Continued)

Author (year)	Country	Patient characteristics	Ziconotide peak dose /adverse effect dose	Neuropsychiatric symptoms	Management and treatment
Penn and Paice (2000)	United States	Case 1: Male, 47 yo Bladder cancer	14.4 mcg/d	Auditory and visual hallucinations and confusion	Ziconotide was withdrawn and reintroduced after 24 h due to lack of pain control. After several reductions and persistence of pain and non-neuropsychiatric adverse effects, the patient decided to discontinue ziconotide
		Case 2: Male, 62 yo Multiple sclerosis	127.2 mcg/d	Paranoid hallucinations, mild confusion, disorientation, episodes of unresponsiveness and severe agitation	Ziconotide was discontinued. Due to agitation persisting for 3 weeks after withdrawal, haloperidol 3 mg/day was added with good results
		Case 3: Male, 45 yo 10 back surgeries, spondylolisthesis, and arachnoiditis	16.8 mcg/d	Confusion, extremely talkative, nervous, and agitation	Ziconotide was increased to 18 mcg/day due to failure of pain control. Eight days later, the patient experienced syncope with nonspecific ECG changes. Ziconotide was discontinued and haloperidol was added, with gradual improvement

symptoms (de la Calle Gil et al., 2015; Levin et al., 2002). Although not named as such in the cases, 5 patients presented symptoms suggestive of delirium (agitation and disorientation alternating with unresponsiveness, confusion…), either with visual and auditory hallucinations (Penn and Paice, 2000), olfactory hallucinations (Kapural et al., 2009), or unspecified hallucinations (Grajny et al., 2020), or without them (Penn and Paice, 2000).

The most important strategies for the management of neuropsychiatric symptoms have been the reduction and discontinuation of ziconotide. In turn, several studies have added the use of antipsychotics, the most common being risperidone (Burdge et al., 2018; Su et al., 2021; Phan and Waldfogel, 2015; Kapural et al., 2009) and haloperidol (Kapural et al., 2009; Levin et al., 2002; Penn and Paice, 2000). Finally, electroconvulsive therapy has been used as a strategy (Levin et al., 2002).

4 Discussion

The case report presented is of particular interest because it shows almost the totality of the adverse effects produced by ziconotide, providing an opportunity to reflect on its action on Cav2.2, the distribution of these channels and the relationship of all this with the aforementioned adverse effects.

Previous studies have estimated that 12% of patients treated with ziconotide have hallucinations, 3% have paranoid reactions, and 1–2% have psychosis. In addition, it has also been shown to increase the incidence of suicidality, suicide attempts, and suicidal ideations. From a neurological point of view, up to 33% may present confusion and 2% delirium (Webster, 2015). As in our case report, most of the published cases present auditory hallucinations and paranoid delusions, being generally classified as psychosis. However, the clinical overlap with delirium is striking. In this sense, a larger number of cases may not have been classified as psychosis because they are not usually described by psychiatrists, leaving psychopathology and diagnostic judgment in the background. Thus, our case report presents a psychiatric perspective that enriches the debate on the adverse neuropsychiatric effects of ziconotide.

On the other hand, the non-specificity and variety of symptoms may be due to the mechanism of action of ziconotide, which would be involved in the pathophysiological pathways responsible for symptoms of psychosis and delirium. This possibility is supported by the fact that individuals with a history of psychiatric disorders are more susceptible to ziconotide-induced adverse effects (Poli and Ciaramella, 2011), as it happens in our case report, where the patient presents dysthymia of years of evolution. That common susceptibility would be in line with the Research Domain Criteria (RDoC) approach (Cuthbert and Insel, 2013).

It has been observed that cannabinoid receptor 1 (CB1R) mediated inhibition of Cav2.2 presynaptic channels is able to suppress GABA release (a phenomenon known as depolarization-induced suppression of inhibition) (Lozovaya et al., 2009; Borgan et al., 2021). As a consequence, there is an augmentation in presynaptic dopamine in areas with an increased presence of CB1R in GABAergic neurons, such as in the cortex or striatum (Borgan et al., 2021; Szabó et al., 2014), which has been associated with the presence of positive symptoms (Borgan et al., 2021) and schizophrenia itself (Fusar-Poli and Meyer-Lindenberg, 2013). In fact, partial agonism of CB1R has

been shown to be capable of producing positive, negative psychotic symptoms and cognitive deficits in healthy volunteers (Borgan et al., 2021). This suggests that inhibition of Cav2.2 channels, which is the mechanism of action of ziconotide, could play a central role in the generation of psychotic symptoms. In support of this, the CACNA1B gene, which codes for Cav2.2 channels, has been shown to be associated with schizophrenia (Andrade et al., 2019). On the other hand, the CB1R-Cav2.2 binomial is also able to suppress glutamate release in the hippocampus and anterior cingulate cortex through a similar mechanism of action (depolarization-induced suppression of excitation phenomenon) (Borgan et al., 2021), which has been associated with the occurrence of delusions and hallucinations (Egerton and Stone, 2012) and the presence of depression (Moriguchi et al., 2019; Duman et al., 2019). In fact, the Cav2.2 receptor has been directly linked to the appearance of depressive symptomatology in mice (Caminski et al., 2022). Regarding suicidal ideation, it has been hypothesized to be due to the inhibition of neurotransmitter release in areas of the brain associated with mood and cognition (e.g., prefrontal and cerebral cortex) (Webster, 2015). Likewise, CACNA1B gene has also been linked to major depressive disorder and suicide (Andrade et al., 2019) and even to bipolar disorder.

Dysregulation of neurotransmitters such as dopamine, GABA and glutamate in the prefrontal cortex has also been proposed as a causal hypothesis for delirium (Webster, 2015; Maldonado, 2013), being compatible with the pathophysiological mechanism of Cav2.2. In addition, the role of glutamate in the neuropsychiatric symptomatology present in anti-NMDA encephalitis has been demonstrated (Kayser and Dalmau, 2016) and it is speculated that both GABA and glutamate may be involved in the psychotic and affective symptomatology of Kleine-Levin syndrome (Ortega-Albás et al., 2021; Hédou et al., 2022). Finally, similar psychomimetic effects have been observed with analgesic treatments such as ketamine, which is a NMDA receptor antagonist (Corlett et al., 2016; Cheng et al., 2018).

Regarding the limitations of the study, only clinical cases were included. At the same time, not all cases explained whether there was a psychiatric history, nor did they give an accurate description of the neuropsychiatric symptomatology. Moreover, in those that did, this information was not described by mental health professionals. These facts limit the ability to infer causality, to analyze in depth the elements involved in the occurrence of these adverse effects, and thus to generalize the results. Nevertheless, the control of confounding factors such as the use of opioids and the temporal coincidence between the introduction of ziconotide and the appearance of adverse effects invite further studies to elucidate the physiopathological mechanisms responsible, which could be of interest in the study of psychosis and schizophrenia.

5 Conclusion

Chronic pain is a subjective symptom which is difficult to measure and has an impact on people's quality of life. At the same time, it has traditionally been underdiagnosed and undertreated. Opioids are drugs of first choice in these conditions, although they are not always effective or adequately tolerated. Moreover, the U.S. opioid crisis has highlighted the need for alternatives to opioids because of their high addictive risk. For this reason, other analgesics have been developed to solve this problem. Ziconotide is one of them, characterized by its peculiar origin and for being the first Cav2.2 channel antagonist used for severe chronic pain via intrathecal route. However, the mechanism of action could be related in processes other than analgesia, involving neurotransmitters such as dopamine, GABA and glutamate in brain areas related to the onset of neuropsychiatric symptoms.

Although these adverse effects are not common, their appearance in patients without a psychiatric history and the risk of decompensation in those with a mental disorder suggest that certain precautions should be taken when administering this drug. In this sense, clinicians should carefully evaluate individuals with pre-existing psychiatric disorders before prescribing ziconotide. Slow titration is advisable, and clinical response as well as the occurrence of adverse effects should be closely monitored (Smith and Deer, 2009). In the event of adverse symptoms, an early and individualized approach must be taken, considering discontinuation of ziconotide or combining antipsychotics (Webster, 2015).

Therefore, it is not only necessary to investigate the mechanism of action of Cav2.2 channels in the appearance of these symptoms, but also to expand the registry of cases presenting these undesired effects in order to better understand their heterogeneity and phenomenology.

Data availability statement

The raw data supporting the conclusions of this article will be made available by the authors, without undue reservation.

Author contributions

MP: Conceptualization, Supervision, Writing – original draft, Writing – review & editing. RG-V: Conceptualization, Writing – original draft, Writing – review & editing. JP-M: Writing – original draft, Writing – review & editing. MB: Writing – original draft, Writing – review & editing. IE: Conceptualization, Supervision, Writing – original draft, Writing – review & editing.

Funding

The author(s) declare financial support was received for the research, authorship, and/or publication of this article. This study received funding from Fundación de Investigación del Hospital Provincial de Castellón (CAFI 24–J02). The funders were not involved in the study design, data collection, analysis, interpretation of data, the writing of this article, or the decision to submit it for publication.

Acknowledgments

The authors would like to thank Professor Gonzalo Haro for his valuable diagnostic approach to the clinical case, which made it possible to publish this manuscript.

Conflict of interest

The authors declare that the research was conducted in the absence of any commercial or financial relationships that could be construed as a potential conflict of interest.

Publisher's note

References

Abdelsayed, N., Whitlow, B., Harned, M., Craig, J., and Grider, J. (2022). A case of prolonged psychosis with intrathecal ziconotide. *Neuromodulation Technol. Neural Interface* 25:S16. doi: 10.1016/j.neurom.2022.02.146

Andrade, A., Brennecke, A., Mallat, S., Brown, J., Gomez-Rivadeneira, J., Czepiel, N., et al. (2019). Genetic associations between voltage-gated calcium channels and psychiatric disorders. *Int. J. Mol. Sci.* 20:3537. doi: 10.3390/ijms20143537

Ayuga-Loro, F., Brocalero-Camacho, A., Quintas-López, M. V., and Cabrera-Feria, J. R. (2011). Efectos adversos neuropsiquiátricos del ziconotide intratecal. *Rev. Neurol.* 52, 61–63. doi: 10.33588/rn.5201.2010475

Borgan, F., Kokkinou, M., and Howes, O. (2021). The cannabinoid CB1 receptor in schizophrenia. *Biol. Psychiatry Cogn. Neurosci Neuroimaging* 6, 646–659. doi: 10.1016/j.bpsc.2020.06.018

Bramer, W. M., Rethlefsen, M. L., Kleijnen, J., and Franco, O. H. (2017). Optimal database combinations for literature searches in systematic reviews: a prospective exploratory study. *Syst. Rev.* 6:245. doi: 10.1186/s13643-017-0644-y

Brookes, M. E., Eldabe, S., and Batterham, A. (2017). Ziconotide monotherapy: a systematic review of randomised controlled trials. *Curr. Neuropharmacol.* 15, 217–231. doi: 10.2174/1570159x14666160210142056

Burdge, G., Leach, H., and Walsh, K. (2018). Ziconotide-induced psychosis: a case report and literature review. *Mental Health Clin.* 8, 242–246. doi: 10.9740/mhc.2018.09.242

Caminski, E. S., Antunes, F. T. T., Souza, I. A., Dallegrave, E., and Zamponi, G. W. (2022). Regulation of N-type calcium channels by nociceptin receptors and its possible role in neurological disorders. *Mol. Brain* 15:95. doi: 10.1186/s13041-022-00982-z

Cheng, W. J., Chen, C. H., Chen, C. K., Huang, M. C., Pietrzak, R. H., Krystal, J. H., et al. (2018). Similar psychotic and cognitive profile between ketamine dependence with persistent psychosis and schizophrenia. *Schizophr. Res.* 199, 313–318. doi: 10.1016/j.schres.2018.02.049

Corlett, P. R., Honey, G. D., and Fletcher, P. C. (2016). Prediction error, ketamine and psychosis: an updated model. *J. Psychopharmacol.* 30, 1145–1155. doi: 10.1177/0269881116650087

Cuthbert, B. N., and Insel, T. R. (2013). Toward the future of psychiatric diagnosis: the seven pillars of RDoC. *BMC Med.* 11:126. doi: 10.1186/1741-7015-11-126

de la Calle Gil, A. B., Peña Vergara, I., Cormane Bornacelly, M. A., and Pajuelo Gallego, A. (2015). Intrathecal ziconotide and morphine for pain relief: a case series of eight patients with refractory cancer pain, including five cases of neuropathic pain. *Neurol. Therapy* 4, 159–168. doi: 10.1007/s40120-015-0035-z

Duman, R. S., Sanacora, G., and Krystal, J. H. (2019). Altered connectivity in depression: GABA and glutamate neurotransmitter deficits and reversal by novel treatments. *Neuron* 102, 75–90. doi: 10.1016/j.neuron.2019.03.013

Egerton, A., and Stone, J. M. (2012). The glutamate hypothesis of schizophrenia: neuroimaging and drug development. *Curr. Pharm. Biotechnol.* 13, 1500–1512. doi: 10.2174/138920112800784961

Fusar-Poli, P., and Meyer-Lindenberg, A. (2013). Striatal presynaptic dopamine in schizophrenia, part II: meta-analysis of [(18)F/(11)C]-DOPA PET studies. *Schizophr. Bull.* 39, 33–42. doi: 10.1093/schbul/sbr180

Grajny, K., Durphy, J., Adam, O., Azher, S., Gupta, M., and Molho, E. (2020). Ziconotide-induced Oro-lingual dyskinesia: 3 cases. *Tremor Other Hyperkinetic Mov.* 10:37. doi: 10.5334/tohm.431

Hédou, J., Cederberg, K. L., Ambati, A., Lin, L., Farber, N., Dauvilliers, Y., et al. (2022). Proteomic biomarkers of Kleine-Levin syndrome. *Sleep* 45:097. doi: 10.1093/sleep/zsac097

Kapural, L., Lokey, K., Leong, M. S., Fiekowsky, S., Stanton-Hicks, M., Sapienza-Crawford, A. J., et al. (2009). Intrathecal ziconotide for complex regional pain syndrome: seven case reports. *Pain Practice* 9, 296–303. doi: 10.1111/j.1533-2500.2009.00289.x

Kayser, M. S., and Dalmau, J. (2016). Anti-NMDA receptor encephalitis, autoimmunity, and psychosis. *Schizophr. Res.* 176, 36–40. doi: 10.1016/j.schres.2014.10.007

Levin, T., Petrides, G., Weiner, J., Saravay, S., Multz, A. S., and Bailine, S. (2002). Intractable delirium associated with ziconotide successfully treated with electroconvulsive therapy. *Psychosomatics* 43, 63–66. doi: 10.1176/appi.psy.43.1.63

Lozovaya, N., Min, R., Tsintsadze, V., and Burnashev, N. (2009). Dual modulation of CNS voltage-gated calcium channels by cannabinoids: focus on CB1 receptor-independent effects. *Cell Calcium* 46, 154–162. doi: 10.1016/j.ceca.2009.07.007

Maldonado, J. R. (2013). Neuropathogenesis of delirium: review of current etiologic theories and common pathways. *Am. J. Geriatr. Psychiatry* 21, 1190–1222. doi: 10.1016/j.jagp.2013.09.005

Moore, D. M., and McCrory, C. (2017). The proteomics of intrathecal analgesic agents for chronic pain. *Curr. Neuropharmacol.* 15, 198–205. doi: 10.2174/1570159x14666160224124446

Moriguchi, S., Takamiya, A., Noda, Y., Horita, N., Wada, M., Tsugawa, S., et al. (2019). Glutamatergic neurometabolite levels in major depressive disorder: a systematic review and meta-analysis of proton magnetic resonance spectroscopy studies. *Mol. Psychiatry* 24, 952–964. doi: 10.1038/s41380-018-0252-9

Obafemi, A., and Roth, B. (2013). Prolonged delirium with psychotic features from omega conotoxin toxicity. *Pain Med.* 14, 447–448. doi: 10.1111/pme.12005

Ortega-Albás, J. J., López, R., Martínez, A., Carratalá, S., Echeverria, I., and Ortega, P. (2021). Kleine-Levin syndrome, GABA, and glutamate. *J. Clin. Sleep Med.* 17, 609–610. doi: 10.5664/jcsm.9058

Penn, R. D., and Paice, J. A. (2000). Adverse effects associated with the intrathecal administration of ziconotide. *Pain* 85, 291–296. doi: 10.1016/s0304-3959(99)00254-7

Phan, S. V., and Waldfogel, J. M. (2015). Ziconotide-induced psychosis: a case report. *Gen. Hosp. Psychiatry* 37, 97.e11–97.e12. doi: 10.1016/j.genhosppsych.2014.10.001

Poli, P., and Ciaramella, A. (2011). Psychiatric predisposition to autonomic and abnormal perception side-effects of ziconotide: a case series study. *Neuromodulation* 14, 219–224. doi: 10.1111/j.1525-1403.2011.00334.x

Smith, H. S., and Deer, T. R. (2009). Safety and efficacy of intrathecal ziconotide in the management of severe chronic pain. *Ther. Clin. Risk Manag.* 5, 521–534. doi: 10.2147/tcrm.s4438

Stewart, B., and Sarria, J. (2014). Analgesia and psychosis: intrathecal ziconotide in a young hospice patient with spinocerebellar ataxia and painful peripheral neuropathy. *J. Pain* 15:S72. doi: 10.1016/j.jpain.2014.01.297

Su, A., Johnson, H., Taylor, C., and Oros, S. (2021). Ziconotide-induced psychosis in patient without previous psychiatric history: a case report. *Pers. Med. Psychiatry* 29-30:100086. doi: 10.1016/j.pmip.2021.100086

Szabó, G. G., Lenkey, N., Holderith, N., Andrási, T., Nusser, Z., and Hájos, N. (2014). Presynaptic calcium channel inhibition underlies CB_1 cannabinoid receptor-mediated suppression of GABA release. *J. Neurosci.* 34, 7958–7963. doi: 10.1523/JNEUROSCI.0247-14.2014

Webster, L. R. (2015). The relationship between the mechanisms of action and safety profiles of intrathecal morphine and ziconotide: a review of the literature. *Pain Med.* 16, 1265–1277. doi: 10.1111/pme.12666

Whitlow, J., Mu, K., Coverdale, J. H., and Shah, A. A. (2015). Ziconotide-associated psychosis treated with invega. *Psychiatr. Ann.* 45, 64–66. doi: 10.3928/00485713-20150212-02

Zamponi, G. W., Striessnig, J., Koschak, A., and Dolphin, A. C. (2015). The physiology, pathology, and pharmacology of voltage-gated calcium channels and their future therapeutic potential. *Pharmacol. Rev.* 67, 821–870. doi: 10.1124/pr.114.009654

frontiers | Frontiers in Pharmacology

TYPE Original Research
PUBLISHED 17 October 2024
DOI 10.3389/fphar.2024.1480546

OPEN ACCESS

EDITED BY
Francesca Guida,
University of Campania Luigi Vanvitelli, Italy

REVIEWED BY
Kristen Willeumier,
Independent Researcher, Beverly Hills, United States
Rafal Roman Jaeschke,
Jagiellonian University Medical College, Poland

*CORRESPONDENCE
Miwako Takahashi,
takahashi.miwako@qst.go.jp
Satoshi Kasahara,
namahagenator@gmail.com

†These authors have contributed equally to this work and share first authorship

RECEIVED 14 August 2024
ACCEPTED 04 October 2024
PUBLISHED 17 October 2024

CITATION
Takahashi M, Kasahara S, Soma T, Morita T, Sato N, Matsudaira K, Niwa S-I and Momose T (2024) Precuneal hyperperfusion in patients with attention-deficit/hyperactivity disorder-comorbid nociplastic pain.
Front. Pharmacol. 15:1480546.
doi: 10.3389/fphar.2024.1480546

Precuneal hyperperfusion in patients with attention-deficit/hyperactivity disorder-comorbid nociplastic pain

Miwako Takahashi[1*†], Satoshi Kasahara[2,3*†], Tsutomu Soma[4], Taito Morita[2], Naoko Sato[5], Ko Matsudaira[3], Shin-Ichi Niwa[6] and Toshimitsu Momose[7]

[1]Department of Molecular Imaging and Theranostics, Institute for Quantum Medical Science, National Institutes for Quantum Science and Technology, Chiba, Japan, [2]Department of Anesthesiology and Pain Relief Center, The University of Tokyo Hospital, Tokyo, Japan, [3]Department of Pain Medicine, Fukushima Medical University School of Medicine, Fukushima, Japan, [4]Software Development Department, PDRadiopharma Inc., Tokyo, Japan, [5]Nursing Department, The University of Tokyo Hospital, Tokyo, Japan, [6]Department of Psychiatry, Aizu Medical Center, Fukushima Medical University, Fukushima, Japan, [7]Institute of Engineering Innovation, School of Engineering, The University of Tokyo, Tokyo, Japan

Introduction: Nociplastic pain (NP), a third category of chronic pain, offers a framework for elucidating its pathophysiology and treatment strategies. One of the characteristics of NP is comorbidity of symptoms other than pain, such as psychological and cognitive problems; therefore, these can be clues to understanding NP. Recently, we reported several cases with comorbid symptoms of attention-deficit/hyperactivity disorder (ADHD). Notably, ADHD medications, including methylphenidate (MP) and atomoxetine, improved chronic pain as well as the symptoms of ADHD. However, in clinical settings, identifying comorbid ADHD in patients with chronic pain is challenging, and underlying mechanisms have not been elucidated. To explore the common characteristics of brain function in patients with ADHD-comorbid NP, we identified brain regions where cerebral blood flow (CBF) distributions changed between pre- and post-treatment using single-photon emission computed tomography (SPECT). Additionally, we examined brain regions where CBF values correlated with clinical scores.

Methods: We retrospectively studied 65 patients (mean age 53 ± 14 years; 30 males and 35 females) with ADHD-comorbid NP who underwent CBF-SPECT before and after ADHD medication initiation. Clinical scores included the clinical global impression severity (CGI-S), pain numerical rating scale, hospital anxiety and depression scale, pain catastrophizing scale, and Conners' adult ADHD rating scale-self report scores. Voxel-based statistical methods were

Abbreviations: NP, nociplastic pain; ADHD, attention-deficit/hyperactivity disorder; CBF, cerebral blood flow; SPECT, single-photon emission computed tomography; CGI-S, clinical global impression severity; MP, methylphenidate; ATX, atomoxetine; NRS, numerical rating scale; HADS, hospital anxiety and depression scale; PCS, pain catastrophizing scale; CAARS-S, Conners' adult ADHD rating scale self-report; IRB, institutional review board; CGI-I, clinical global impression improvement; MCID, minimum clinically important difference; HADS-A, HADS-anxiety; HADS-D, HADS-depression; APZ, aripiprazole; CL, clonidine; ECD, ethyl cysteinate dimer; FWHM, full-width at half-maximum; DMN, default mode network; CEN, central executive network; GABA, γ-aminobutyric acid; ACG, anterior cingulate gyrus.

used to compare pre- and post-treatment CBF-SPECT images to identify significant differences and investigate brain regions correlated with clinical scores.

Results: The CBF was higher in the precuneus, insular gyrus, and thalamus before treatment than after treatment (paired t-test, cluster-definition $p < 0.001$, cluster-extent threshold $p < 0.05$, with family-wise error [FWE] correction). The hyperperfusion in the precuneus was positively correlated with the CGI-S score and significantly reduced after treatment with MP (paired t-test, cluster-definition $p < 0.005$, cluster-extent threshold $p < 0.05$, with FWE correction).

Conclusion: The finding of precuneal hyperperfusion may provide insight into the mechanisms of NP and help identify patients who would benefit most from ADHD medications.

KEYWORDS

nociplastic pain, attention-deficit/hyperactivity disorder, methylphenidate, cerebral blood flow, single-photon emission computed tomography

1 Introduction

Nociplastic pain (NP) has been proposed as a third category of pain, distinct from nociceptive or neuropathic pain. This is because the mechanisms of NP are remained to be eludicated and may overlap those of nociceptive or neuropathic pain but cannot be explained by these two mechanisms alone (Kosek et al., 2016; Fitzcharles et al., 2021; Kosek et al., 2021). Although the symptoms of NP are diverse, it is characterized by comorbidities with various neurological symptoms other than pain, such as sleep disturbances, fatigue, and cognitive dysfunction, including attention and memory impairments (Kosek et al., 2021). Identifying the presence of comorbidities may be helpful in diagnosing and treating patients with NP, especially when effective pharmacotherapy for these comorbidities is available.

Among the various co-existing psychological issues or cognitive impairments, symptoms of attention-deficit/hyperactivity disorder (ADHD) are frequently identified in patients with fibromyalgia (van Rensburg et al., 2018; Kasahara et al., 2021a; Pallanti et al., 2021), chronic low back pain (Kasahara et al., 2021b; Ibrahim and Hefny, 2022; Kasahara et al., 2022a; Kasahara et al. 2023a; Kasahara et al. 2023c), and idiopathic orofacial pain (Kasahara et al., 2022b; Kasahara et al. 2023b; Kasahara et al. 2023c), which are representative diseases associated NP. Moreover, 72.5% of patients with NP were shown to have comorbid ADHD (Kasahara et al., 2020). Although ADHD is characterized by inattention and/or hyperactivity-impulsivity (American psychiatric Association, 2013), predominantly observed in childhood, the symptoms persist into adulthood in approximately 40%–70% of cases (Biederman et al., 2010; Ebejer et al., 2012). ADHD medications typically include dopamine stimulants, such as methylphenidate (MP), and noradrenaline transporter inhibitors, such as atomoxetine (ATX), suggesting that dopaminergic and noradrenergic nervous system dysfunctions underpin ADHD (Stahl, 2021).

Under physiological conditions, dopamine and noradrenaline are also crucial for pain modulation, contributing to endogenous analgesia via brain networks and descending pathways (Wood, 2008; Suto et al., 2023). A mouse model with ADHD induced by selective dopaminergic neuron impairment exhibited lower pain thresholds and reduced spinal descending analgesia (Bouchatta et al., 2022; Meseguer-Beltrán et al., 2023; Sifeddine et al., 2023). In an epidemiological study of the general population, an increase in ADHD symptoms was significantly associated with a higher risk of pain, indicating a common underlying mechanism between ADHD and chronic pain (Stickley et al., 2016). In addition to ADHD, individuals with NP frequently present with other psychiatric disorders, such as autism, insomnia, depression, and anxiety, all of which can significantly impact the quality of life (Wiwe Lipsker et al., 2021). Notably, ADHD medications have been shown to improve symptoms, including chronic pain (Vorobeychik and Acquadro, 2008; Kasahara et al., 2017; Wiwe Lipsker et al., 2018; Kasahara et al., 2020; Kasahara et al. 2022b; Kasahara et al. 2023c; Kasahara et al. 2023a; Kasahara et al. 2023d; Kasahara et al. 2023e; Kasahara et al. 2023b; Zain et al., 2023; Kasahara et al., 2024). Therefore, detecting ADHD comorbidity in patients with NP could be crucial for effective treatment, especially in those who are refractory to other treatments.

We previously reported in case studies that changes in cerebral blood flow (CBF) using single-photon emission computed tomography (SPECT) after treatment occurred in patients with ADHD-comorbid NP who showed improvements with ADHD medication use (Kasahara et al., 2023c; Kasahara et al. 2023a; Kasahara et al. 2023e; Kasahara et al., 2024). Before treatment, there was a relative CBF increase in the posterior cingulate gyrus, precuneus, and insular gyrus, which was alleviated after treatment, and hypoperfusion in the frontal lobe was improved. These changes may reflect the pathophysiological basis of ADHD-comorbid NP.

In this study, we aimed to 1) identify brain regions of statistically significant CBF changes in a large number of patients who improved with ADHD medication use and 2) identify brain regions that correlate with clinical scores, such as ADHD severity and pain intensity scores. Using CBF-SPECT to assess brain function, we provided objective insights into the mechanisms underlying ADHD-comorbid NP, which may be useful for diagnosing and treating patients with NP.

2 Materials and methods

2.1 Participants

We retrospectively identified consecutive patients who were referred to a psychiatrist (S.K.) from 2016 to 2023, where they

were routinely evaluated using the numerical rating scale (NRS) (Jensen and Karoly, 2011), hospital anxiety and depression scale (HADS) (Zigmond and Snaith, 1983), pain catastrophizing scale (PCS) (Sullivan et al., 1995), and Conners' adult ADHD rating scale self-report (CAARS-S) (Conners et al., 1999) at treatment initiation and during CBF-SPECT sessions. The inclusion criteria were as follows: 1) a diagnosis of chronic pain considered to be ADHD-comorbid NP, 2) at least two CBF-SPECT sessions including CBF-SPECT performed before ADHD medication use, 3) no history of brain surgery, 4) the absence of other neurological disorders or psychosis, and 5) age ≥18 years at the first visit.

This retrospective study was conducted in accordance with the Helsinki Declaration and its later amendments and approved by our institutional review board (IRB) (approval number 20–011). The IRB waived informed consent because of the retrospective nature of the study. However, the participants were informed through our institute websites of the possibility to withdraw from or refuse to participate in the study. Patient data were anonymized to protect their privacy.

2.2 Assessment of NP severity and post-treatment improvement

NP severity and NP improvement with ADHD medication use were determined using the clinical global impression severity (CGI-S) and clinical global impression improvement (CGI-I) scores, respectively (Busner and Targum, 2007). The CGI-S and CGI-I scores were determined by evaluating the degree of interference with daily life due to NP and cognitive impairments, such as anxiety, depression, insomnia, attention impairment, and sensory sensitivity; the degree of improvement in these scores was also evaluated. The CGI-S score ranges from 1 to 7, where 1 = normal, 2 = borderline illness, 3 = mildly ill, 4 = moderately ill, 5 = markedly ill, 6 = severely ill, and 7 = extremely ill. The CGI-I score was used to assess NP relative to the baseline condition as follows: 1 = very much improved, 2 = much improved, 3 = minimally improved, 4 = no change, 5 = minimally worse, 6 = much worse, and 7 = very much worse.

2.3 Clinical scores

Subjective pain was evaluated using the NRS, an 11-point pain rating scale, with 0 indicating no pain and 10 indicating the highest pain. The minimum, maximum, and mean NRS scores were assessed (Jensen and Karoly, 2011). The minimum clinically important difference (MCID) in the NRS score for chronic pain is 1 point, and a decrease of 2 points or more is considered "much better" (Salaffi et al., 2004).

Anxiety and depression were assessed using the HADS-anxiety (HADS-A) and HADS-depression (HADS-D) scores (Zigmond and Snaith, 1983). A HADS score ≥11 is rated as clinically significant for adjustment disorder or major depressive disorder (Kugaya et al., 1998), with 1.5 being the MCID (Puhan et al., 2008).

Pain-related catastrophizing thoughts were assessed using the PCS (Sullivan et al., 1995). A PCS score of ≥30 represents clinically relevant levels and corresponds to the 75th percentile or higher in the distribution of patients with chronic pain (Sullivan, 2009); the MCID score is 6.48 (Suzuki et al., 2020). Catastrophizing thoughts reflect the psychological condition of patients with chronic pain, which further heightens pain and disability (Sullivan et al., 2001).

Subjective ADHD symptoms were assessed using the long version of CAARS-S (Conners et al., 1999). The long version of CAARS consists of 66 questions, and its key feature is that it allows the severity of a patient's ADHD symptoms to be quantified as a T-score, indicating where they fall within the population distribution for their age group. CAARS is the most widely used self-administered adult ADHD rating scale in controlled clinical studies. The ADHD index, which is the most important overall subscale score among the eight subscale scores of CAARS-S, indicates the degree to which the symptoms of patients with ADHD require treatment. Therefore, we used the ADHD index as a representative score for statistical comparisons. ADHD was diagnosed according to the Diagnostic and Statistical Manual of Mental Disorders, fifth edition, using a structured diagnostic interview for ADHD in adults (Kooij et al., 2019) and considering information about patient symptoms from all family members.

2.4 Medication algorithm

Treatments were administered according to the medication algorithm proposed by S.K. (Figure 1) (Kasahara et al., 2023d). Briefly, MP was used as the drug of choice in patients without contraindications (Stahl, 2021). MP is started at 18 mg/day, and the dosage is adjusted to the appropriate level for the patient in seven increments: 27 mg/day, 36 mg/day, 45 mg/day, 54 mg/day, 63 mg/day, and 72 mg/day, while monitoring for side effects such as headaches and loss of appetite. In case of insufficient MP efficacy or intolerable side effects, the medication was changed to a combination of MP and ATX or ATX alone. ATX is started at 40 mg/day and gradually increased to the standard dosage of 80–120 mg/day, adjusting to the appropriate dose for the patient while monitoring for side effects such as constipation and loss of appetite. Similarly, based on the efficacy and side effects, the medications were combined or changed successively to aripiprazole (APZ) and clonidine (CL). APZ, a partial dopamine D2 receptor agonist, is referred to as a dopamine system stabilizer because it acts as an inhibitor or activator when dopamine neurotransmission is excessive or low, respectively. APZ is started at 3 mg/day and gradually increased up to a maximum of 30 mg/day, adjusting to the appropriate dose for the patient while monitoring for extrapyramidal symptoms as a potential side effect. APZ ameliorates symptoms of chronic pain (Kasahara et al., 2011), idiopathic orofacial pain (Tu et al., 2019; Watanabe et al., 2022; Kasahara et al., 2023d), and ADHD (Ghanizadeh, 2013). CL, a noradrenaline alpha 2 receptor agonist, is effective in ADHD treatment (Stahl, 2021). CL is started at 150 μg/day and gradually increased up to a maximum of 450 μg/day, adjusting to the appropriate dose for the patient while monitoring for dry mouth and low blood pressure. For patients with severe depression accompanied by psychomotor retardation, antidepressants were used, and for those with bipolar disorder, anticonvulsants/mood stabilizers were administered. Sleep medications were also used for

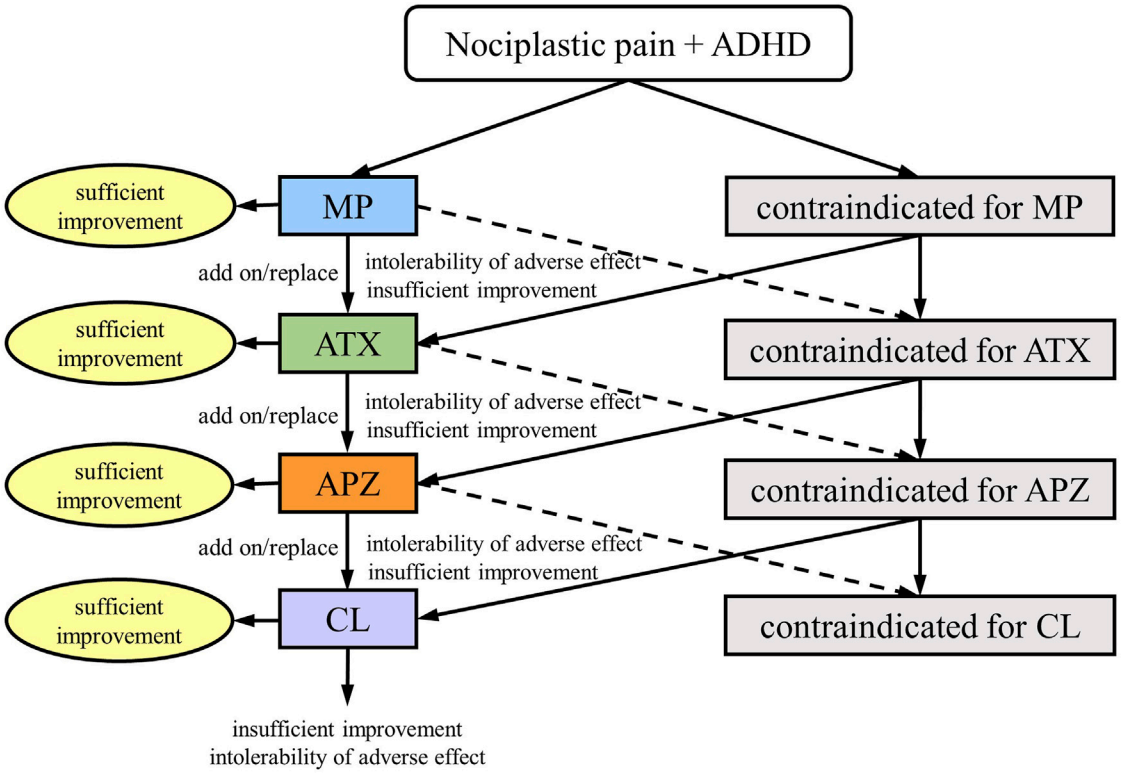

FIGURE 1
Medication algorithm for nociplastic pain in patients with attention-deficit/hyperactivity disorder (ADHD); MP, methylphenidate; ATX, atomoxetine; APZ, aripiprazole; CL, clonidine. (This figure is a modified excerpt from the original paper by Kasahara et al. (Kasahara S, Takahashi K, Matsudaira K, Sato N, Fukuda KI, Toyofuku A, Yoshikawa T, Kato Y, Niwa SI, Uchida K. Diagnosis and treatment of intractable idiopathic orofacial pain with attention-deficit/hyperactivity disorder. Sci Rep 2023; 13:1,678. DOI: 10.1038/s41598-023-28931-3, CC BY 4.0).

insomnia. Other than that, no medications outside of the treatment algorithm in Figure 1 were used. After adjusting the dose to enhance efficacy and confirming the absence of severe side effects for at least 2 months, the overall treatment effect was evaluated using the NRS, HADS, PCS, and CGI-C scores.

2.5 CBF-SPECT acquisition

Commercially available ^{99m}Tc-labeled ethyl cysteinate dimer (ECD; PDRadiopharma Inc. Chuo-ku, Japan) was used for CBF-SPECT imaging. Patients rested in the supine position with their eyes closed in a quiet SPECT room. A 740-MBq (20 mCi) dose of ECD was injected intravenously; approximately 5 min later, a 30-min scan was performed using a triple-head SPECT system (GCA-9300R; Cannon Medical Systems, Otawara, Japan) equipped with a high-resolution fan-beam collimator, which permitted a spatial resolution of 7.2 mm full-width at half-maximum (FWHM). The SPECT images were reconstructed using filtered backprojection with Butterworth and Ramp filters. Data were collected in a 128 × 128 × 89 matrix with a voxel size of 1.72 × 1.72 × 3.44 mm.

The images were prepared for axial, coronal, and sagittal views with a rainbow color after co-registration between the pre- and post-treatment CBF-SPECT images. All CBF-SPECT images were visually reviewed by two nuclear medicine experts (M.T. and T.M.), and characteristic findings were investigated.

2.6 Statistical analysis

2.6.1 CBF-SPECT voxel-based statistical analysis

First, the pre- and post-treatment SPECT images were realigned and averaged for each patient. The averaged images were anatomically standardized using a segmentation-based spatial normalization method implemented in Statistical Parametric Mapping 12 (Wellcome Institute for Cognitive Neurology, London, United Kingdom; RRID:SCR_002592). Subsequently, the realignment and spatial normalization parameters obtained through the abovementioned image processes were applied to the individual images to transform them into the Montreal Neurological Institute coordinate system. Finally, the transformed images were smoothed using a three-dimensional isotropic Gaussian kernel with a FWHM of 10 mm.

The voxel values of the CBF-SPECT images were standardized by dividing them by the mean number of counts per voxel in the cerebellum. To clarify the changes in regional CBF between pre- and post-treatment, a paired *t*-test was conducted for patients with post-treatment CGI-I scores of 1–3. Additionally, we focused on psychostimulant-induced CBF changes and performed a paired *t*-test for patients who showed improvement with MP use. Brain regions where CBF values were associated with clinical scores, such as CGI-S, pain NRS, ADHD index, HADS, and PCS scores, were investigated using regression analysis. Statistically related regions were detected using the cluster-extent-based thresholding method

(Woo et al., 2014), which comprised two steps. First, clusters were defined by contiguous voxels above a cluster-definition threshold *p*-value. In this study, we set the cluster-definition *p*-value to <0.001 and <0.005 for the paired *t*-test and regression analysis, respectively. Second, the cluster size (number of voxels) was statistically tested under the null hypothesis. We set a cluster-extent threshold *p*-value of <0.05 with family-wise error correction.

2.6.2 Clinical score statistical analysis

Clinical scores, including CGI-S scores as well as the maximum, mean, and minimum scores of NRS, HADS-A, HADS-D, PCS, and ADHD index, were compared before and after treatment using paired *t*-tests and Wilcoxon signed-rank tests for parametric and non-parametric numerical data, respectively. The *p*-value was initially calculated without correction for multiple comparisons, and then the significance threshold was set at $p < 0.00625$, specifically 0.05 divided by 8 (Bonferroni correction for a total of eight comparisons). Statistical analyses were performed using IBM SPSS Statistics for Windows, version 26 (IBM Corp., Armonk, NY, United States). Summary statistics were expressed as mean (standard deviation) for continuous variables and frequency (percentage) for categorical variables.

3 Results

Overall, 65 patients (mean age, 53 ± 14 years; 30 males and 35 females) were included in this study. The chief complaints in these patients were pain in three or more sites (n = 19, 29%), low back pain (n = 16, 25%), orofacial pain (n = 14, 22%), and pain in other areas (lower limb pain [n = 4]; abdominal pain [n = 3]; anal, perineal, and genital pain [n = 3]; shoulder and upper limb pain [n = 2]; pelvic pain [n = 2]; cervical pain [n = 1]; and thoracic pain [n = 1]). After treatment, 61 patients had CGI-I scores ranging from 1 to 3. The mean dose for patients receiving MP alone (n = 17) was 57.2 ± 20.6 mg/day. For patients receiving MP in combination with ATX or APZ (n = 20), the mean doses were as follows: 60.9 ± 20.2 mg/day (MP) and 101.9 ± 25.1 mg/day (ATX); 61.2 ± 11.7 mg/day (MP) and 5.3 ± 7.2 mg/day (APZ). For patients receiving ATX alone (n = 15), the mean dose was 72.7 ± 44.8 mg/day. For patients receiving ATX in combination with APZ or CL (n = 4), the mean doses were as follows: 75.0 ± 63.6 mg/day (ATX) and 2.5 ± 0.7 mg/day (APZ); 120.0 mg/day (ATX) and 375 ± 100 μg/day (CL). The mean dose was 6.0 ± 3.5 mg/day in patients receiving APZ alone (n = 2). After treatment, the number of patients with clinically significant HADS-A, HADS-D, and PCS scores decreased from 24 (37%) to 15 (23%), 31 (48%) to 17 (26%), and 39 (60%) to 21 (32%), respectively. The number of patients with ADHD index T-score ≥65 decreased from 20 (31%) to 12 (18%) after treatment.

The CGI-S score, as well as the maximum and mean NRS, HADS-A, HADS-D, and PCS scores, significantly decreased after treatment. The mean ADHD index T-score decreased from 61.7 to 56.9, although this change was not statistically significant. Based on CAARS, T-scores of ≥65, 60–65, and ≤60 are clinically significant, borderline, and within the normal range, respectively. Thus, this study suggests that after treatment, the mean T-scores fell within the normal range. Details of the clinical scores are presented in Table 1, and the number of patients at each stage of CGI-S is shown in Table 2. Compared to pre-treatment, post-treatment results showed a shift in the number of patients toward less severe stages, indicating an overall improvement in the severity.

The duration of pre- and post-treatment CBF-SPECT was 32 ± 18 months, ranging from 7 to 74 months. Regarding the comparison of CBF-SPECT images before and after treatment in 61 patients with CGI-I scores of 1–3, the CBF was significantly higher in the precuneus, insular gyrus, and medial thalamus in pre-treatment CBF-SPECT images (Figure 2). No brain region showed significantly lower CBF in pre-treatment CBF-SPECT images and higher or lower CBF in post-treatment images.

In this study, 37 patients were treated with MP or a combination of MP and other drug(s), and 36 of them had CGI-C scores of 1–3 after treatment. Before and after comparisons of CBF-SPECT images in these 36 MP-treated patients showed significantly higher precuneal perfusion in pre-treatment CBF-SPECT images (Figure 3).

Regarding the correlation analysis of regional CBF values with clinical scores, CBF was positively correlated with the CGI-S score in the precuneus (Figure 4A). Furthermore, CBF was positively correlated with the ADHD index in the isthmus of the posterior cingulate gyrus, anterior and middle cingulate gyri, medial thalamus, and caudate head (Figure 4B). A negative correlation was observed between CBF and minimum NRS score in regions along the corpus callosum in the cingulate gyrus (Figure 4C). No other clinical scores were significantly correlated with regional CBF values.

Cases with representative CBF-SPECT findings are shown in Figures 5–7. A patient in his 50s complained of low back pain before treatment and had relatively decreased frontal lobe CBF on CBF-SPECT images (Figures 5A–C). One year after ATX treatment, his symptoms improved, and CBF in the frontal lobe increased (Figures 5D–F). Figure 6 shows CBF-SPECT images of a patient in her 40s who presented with headache and orofacial pain before treatment. Pre-treatment CBF-SPECT (Figures 6A–C) showed that the CBF values in the subgenual anterior cingulate and precuneus were relatively higher than those in the surrounding frontal and parietal cortices. Two years after treatment with a dopamine system stabilizer, the symptoms improved, and the CBF in these regions decreased (Figures 6D–F). Figure 7 shows the CBF-SPECT images of a patient in her 50s with shoulder and upper limb pain before treatment. Her symptoms improved after ATX treatment, and her clinical condition remained stable 5 years later. Pre-treatment CBF-SPECT images showed relatively higher CBF in the insular gyrus (Figure 7A), which decreased in post-treatment images (Figure 7B).

4 Discussion

This study revealed two main findings. First, in patients with ADHD-comorbid NP, pre-treatment CBF was relatively higher in the precuneus, insular gyrus, medial thalamus, and caudate head than in other brain regions. Furthermore, in selected patients with post-MP treatment improvements, precuneal CBF was higher before treatment. Interestingly, precuneal CBF values positively correlated with CGI-S scores, reflecting NP severity. Second, regarding the

TABLE 1 Details of the clinical scores and statistical comparisons.

	Pre-treatment	Post-treatment	p-value
CGI-S	5.2 ± 1.0	3.6 ± 1.1	p < 0.001*
Pain NRS			
Maximum	5.9 ± 2.4	4.6 ± 2.8	p < 0.001*
Average	4.9 ± 2.2	3.6 ± 2.7	p < 0.001*
Minimum	2.7 ± 2.4	2.3 ± 2.7	p = 0.028
HADS			
Anxiety	9.8 ± 5.2	6.9 ± 5.5	p = 0.005*
Depression	9.8 ± 5.4	8.0 ± 5.8	p = 0.005*
PCS	30.7 ± 13.2	22.7 ± 15.0	p < 0.001*
ADHD Index (CAARS-S subscale)			
T-score	61.7 ± 12.3	56.9 ± 14.0	p = 0.007

CGI-S, clinical global impression severity; NRS, numerical rating scale for pain; HADS, hospital anxiety and depression scale; PCS, pain catastrophizing scale.
* Significance level was set at $p < 0.00625$ after Bonferroni correction for multiple comparisons, with a total of eight comparisons.

TABLE 2 The number of patients at each stage of clinical global impression severity.

CGI-S stage	1	2	3	4	5	6	7
Pre-treatment	0	0	3	14	18	28	2
Post-treatment	2	3	27	20	10	3	0

CGI, clinical global impression severity. The scores were determined by evaluating the degree of interference with daily life due to NP and cognitive impairments, ranging from 1 to 7, where 1 = normal, 2 = borderline illness, 3 = mildly ill, 4 = moderately ill, 5 = markedly ill, 6 = severely ill, and 7 = extremely ill.

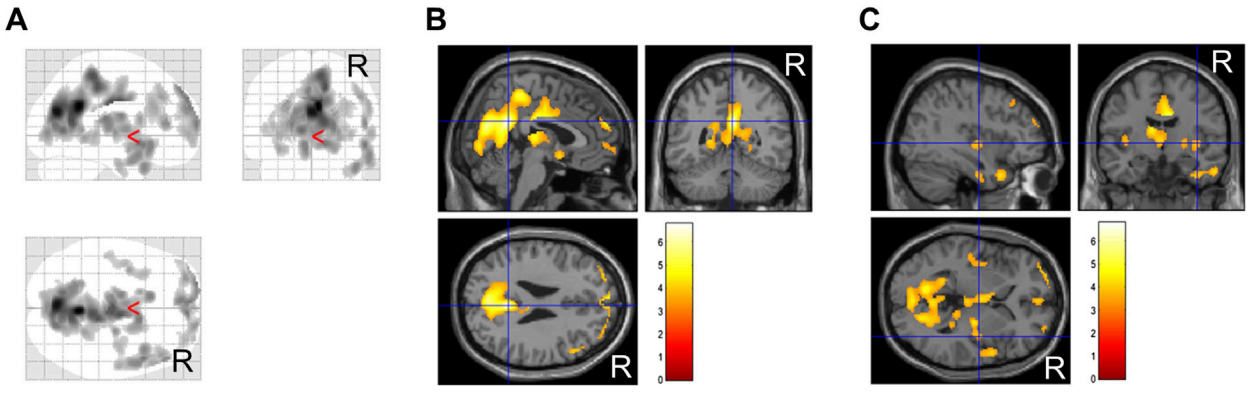

FIGURE 2
Significantly higher cerebral blood flow regions in pre-treatment images than in post-treatment images. The regions with significant changes are projected in three directions in gray **(A)** and colored (t-value) scales with cross-bars indicating the precuneus **(B)** and right insular cortex **(C)**. The medial thalamus is also identified as a higher cerebral blood flow region **(C)**. Cluster-extent $p < 0.05$ with family-wise error correction. R, patients' right side.

relationship between regional CBF values and other clinical scores, ADHD symptoms were positively correlated with CBF in the anterior and middle cingulate gyri, medial thalamus, and caudate head, and the minimum NRS score was negatively correlated with CBF in the narrow region along the corpus callosum in the cingulate gyrus.

Several reports have suggested that pain perception and regulation are performed in multiple brain regions through networks. Processes from the perception of physical pain stimuli to higher-order cognition are conceptualized as being performed by different levels of cortical networks (Garcia-Larrea and Peyron, 2013). In the first-order network, painful

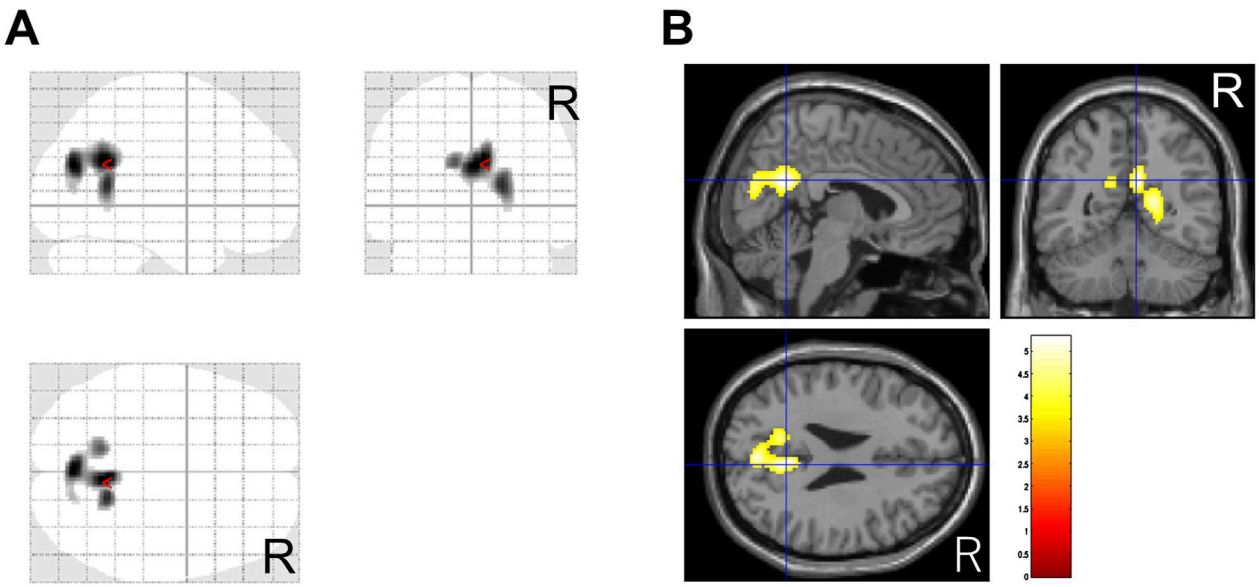

FIGURE 3
Significantly higher cerebral blood flow regions before methylphenidate treatment than after treatment. The significant regions are projected in three directions in gray **(A)** and colored (t-value) scales with a cross-bar indicating the precuneus **(B)**. Cluster-extent $p < 0.05$ with family-wise error correction. R, patients' right side.

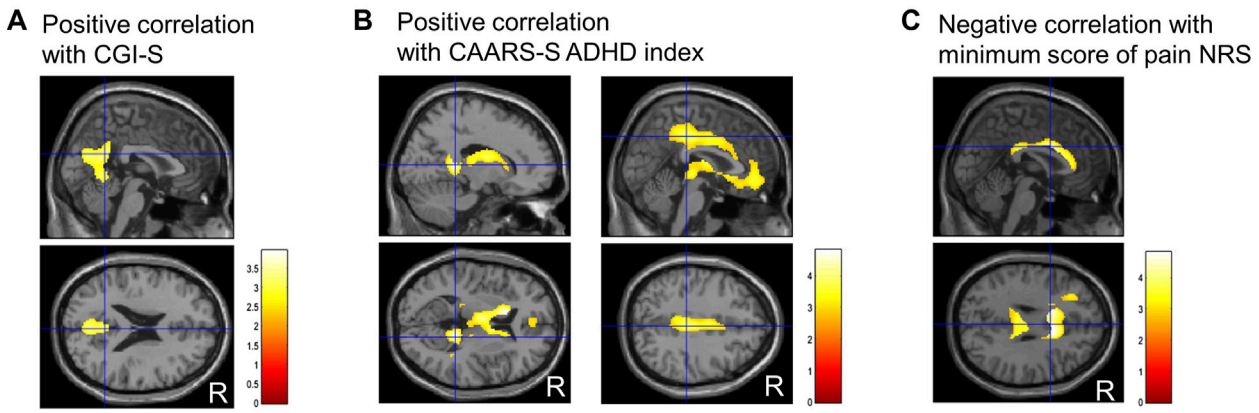

FIGURE 4
Representative images of significantly correlated regions with clinical scores. Clinical global impressions severity (CGI-S) score positively correlates with the precuneus **(A)**. ADHD index, a subscale of Conners' adult ADHD rating scale self-report (CAARS-S), positively correlates with the isthmus of the posterior cingulate gyrus, anterior and middle cingulate gyrus, medial thalamus, and caudate head **(B)**. The minimum numerical rating scale (NRS) score for pain negatively correlates with the narrow region along the corpus callosum in the cingulate gyrus **(C)**. Cluster-extent p < 0.05 with family-wise error correction. R, patients' right side; ADHD, attention-deficit/hyperactivity disorder.

stimuli generated by nociception are transmitted from the dorsal horn of the spinal cord to the thalamus through spinothalamic projections. In the second-order network, pain is transmitted from the thalamus to the anterior cingulate and insular gyri where it is perceived as an unpleasant sensation. These brain regions of the second-order network constitute the so-called pain matrix, part of which was identified as having higher CBF in this study; these findings were consistent with those of previous studies showing high perfusion or metabolism in the insular gyrus in response to unpleasant pain stimuli (Schreckenberger et al., 2005; Boly et al., 2008). Furthermore, pain-related information is relayed through the insular gyrus to higher cortical areas, such as the frontal and parietal lobes. Physical pain stimuli are emotionally recognized as discomfort caused by the pain matrix (Borsook et al., 2016). However, integrating this perception of unpleasant pain stimuli with individual knowledge and experience requires a higher level of networking, which enables it to be perceived as a personal experience. This can be considered a third-order network,

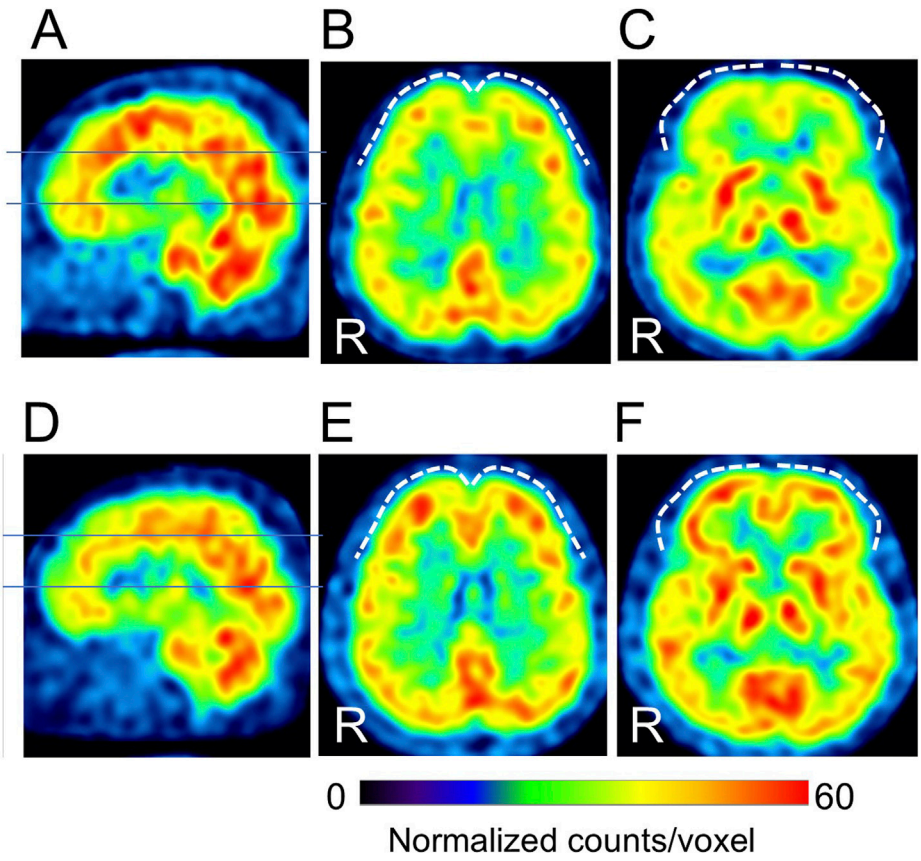

FIGURE 5
A typical example of our cases with hypofrontal perfusion (dashed curves) in cerebral blood flow single-photon emission computed tomographic images (SPECT) before treatment **(A–C)**, which is improved after treatment **(D–F)** (patient # 8). The lines in A and D indicate the axial levels of images **(B, C, E, F)**. The voxel values are normalized by the mean number of counts per voxel in the cerebellum being 50; the color ranges from 0 to 60. R, patients' right side. This case had no psychiatric comorbidities based on the Diagnostic and Statistical Manual of Mental Disorders, fifth edition. At the time of the pre-treatment SPECT, the patient was taking 100 mg/day of tramadol hydrochloride, and at the time of the post-treatment SPECT, the medications were 25 mg/day of atomoxetine, 10 mg/day of nitrazepam, and 0.25 mg/day of triazolam.

although specific findings and patterns have not yet been elucidated (Garcia-Larrea and Peyron, 2013).

The increased precuneal CBF observed in this study may constitute part of the third-order network in ADHD-comorbid NP. The precuneus, which is the posterior part of the default mode network (DMN), is responsible for maintaining awareness and attention to the environment via DMN activation at rest (Fiset et al., 1999; Laureys et al., 1999; Raichle et al., 2001). Conversely, the brain regions responsible for the performance of cognitive tasks primarily comprise the prefrontal cortex, known as the central executive network (CEN), which is inactive at rest. Persistent DMN activity during task performance may interfere with CEN activity; therefore, switching DMN and CEN activities is crucial for task execution (Sridharan et al., 2008). Functional magnetic resonance imaging studies have also suggested that psychostimulant use suppresses DMN activity in children with ADHD, restoring brain activity patterns similar to those of typically developing children and improving behavioral performance (Peterson et al., 2009; Querne et al., 2017). Our finding that pre-treatment precuneal hyperperfusion was associated with pain severity and was suppressed after ADHD medication use, resulting in the improvement of pain and ADHD symptoms, was consistent with the abovementioned previous study findings. Usui et al. reported hyperperfusion in the posterior cingulate gyrus and precuneus in patients with fibromyalgia, a representative NP-associated disorder. Notably, the gabapentin (an analog of the neurotransmitter γ-aminobutyric acid [GABA]) treatment-resistant group had higher CBF values in these regions than the treatment-responsive group (Usui et al., 2010), suggesting that a different nervous system than the GABAergic system was involved in these gabapentin treatment-refractory patients. Both previous and present study results suggest that the hyperactive status of the precuneus contributes to ADHD-comorbid NP and effectively responds to ADHD medications.

We also found a positive correlation between ADHD symptoms and a relative increase in CBF in the cingulate gyrus, which is consistent with the findings of previous studies showing that ADHD is associated with hyperactivity of the cingulate gyrus (Vieira de Melo et al., 2018). A study using a mouse model with ADHD induced by dopaminergic nerve damage demonstrated that hyperactivity of the anterior cingulate gyrus (ACG) results in electrical hyperactivity of the spinal dorsal horn nerve via ACG-

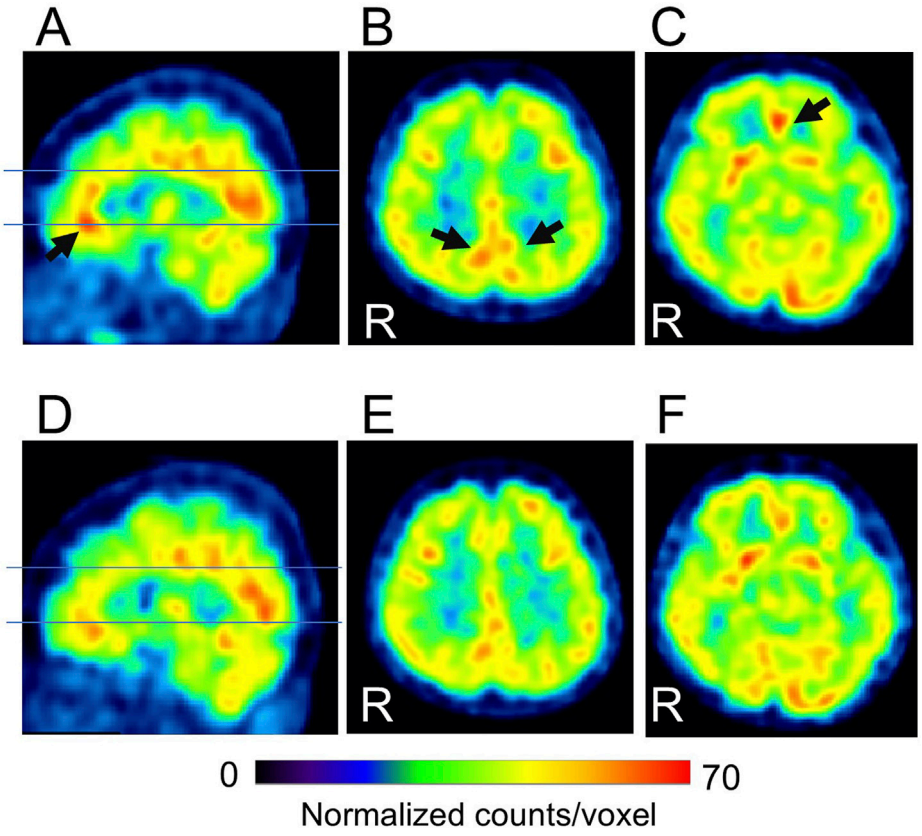

FIGURE 6
Representative images of cerebral blood flow single-photon emission tomography (SPECT) with typical findings that the subgenual anterior cingulate arrow in **(A, C)** and precuneus arrows in **(B)** show relative hyperperfusion before treatment **(A–C)**, which decreases after treatment **(D–F)** (patient # 45). The lines in A and D indicate the axial levels of images **(B, C, E, F)**. The voxel values are normalized by the mean number of counts per voxel in the cerebellum being 50; the color ranges from 0 to 70. R, patients' right side. This case had no psychiatric comorbidities based on the Diagnostic and Statistical Manual of Mental Disorders, fifth edition. At the time of the pre-treatment SPECT, the patient was not taking any medications. At the time of the post-treatment SPECT, the medications were 10 mg/day of atomoxetine, 225 mg/day of venlafaxine, and 5 mg/day of zolpidem tartrate.

insular gyrus fiber communication, resulting in hyperalgesia (Bouchatta et al., 2022). Another study using a spontaneously hypertensive rat model of ADHD showed that decreased pain threshold was associated with high noradrenaline levels in the dorsal horn of the spinal cord and low alpha2-adrenoceptor levels in postsynaptic sites (Suto et al., 2023). This study showed ACG hyperactivity in the resting state, which may contribute to the descending analgesic dysfunction and ADHD symptoms. Another significant area was found in the narrow region along the corpus callosum in the cingulate gyrus that correlated negatively with the minimum NRS. This region is known to have a high density of receptors, as observed in a diprenorphine receptor PET (Vogt et al., 1995), and may be associated with pain suppression. However, there are insufficient previous studies or basic data reports on pain regulation in the cingulate gyrus.

To the best of our knowledge, this is the first study to identify brain regions associated with both pain and ADHD symptom improvements following ADHD medication use. The regions with significant improvements were the precuneus, insular gyrus, and cingulate gyrus. Notably, the precuneal CBF was correlated with NP severity and showed significant changes after MP treatment. The insular and cingulate gyri are parts of the pain matrix, whereas the precuneus is a crucial component of the DMN; therefore, it is likely related to ADHD symptoms. Considering that more than 80% of ADHD symptoms are missed in general psychiatric practice (Ginsberg et al., 2014) and that patients with NP usually consult anesthesiologists or orthopedic surgeons, the CBF-SPECT findings would enhance the suspicion of ADHD underlying chronic pain and the need to consult to a pain management specialist.

This study had some limitations. First, we did not use a non-ADHD group in this study; thus, we could not separately investigate whether ADHD medication use altered CBF in ADHD- or pain-related regions. Second, this study evaluated and compared the pre-treatment characteristics of CBF-SPECT images with those of post-treatment CBF-SPECT images as a reference. Therefore, future studies should clarify these characteristics and enhance their clinical applicability by comparing them with those of patients with NP without ADHD or normal individuals.

In conclusion, this study demonstrated a positive correlation between regional precuneal CBF and NP severity, and the CBF reduced after ADHD medication use, with pain improvement. Therefore, our study proposes the CBF findings as clues for identifying patients who would benefit from ADHD medications.

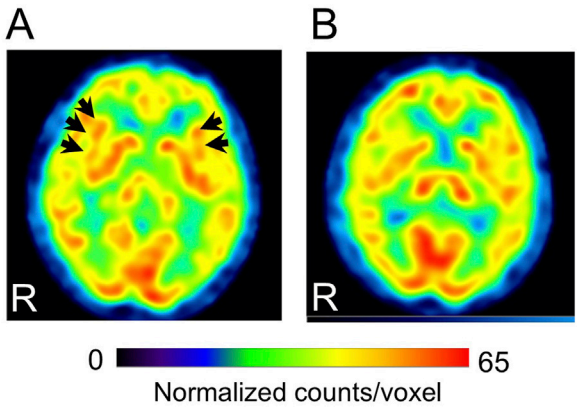

FIGURE 7
Representative images of cerebral blood flow single-photon emission computed tomography (SPECT) with a typical finding that the insular gyri show relative hyperperfusion before treatment **(A)**, which decreases after treatment **(B)** (patient # 32). Arrows in A indicate the bilateral insular gyri. The voxel values are normalized by the mean number of counts per voxel in the cerebellum being 50; the color ranges from 0 to 65. R, patients' right side. This case had bipolar disorder as a psychiatric comorbidity based on the Diagnostic and Statistical Manual of Mental Disorders, fifth edition. At the time of the pre-treatment SPECT, the medications were 3 mg/day of etizolam, 1 mg/day of flunitrazepam, and 5 mg of zolpidem tartrate. At the time of the post-treatment SPECT, the medications were 120 mg/day of atomoxetine, 800 mg/day of sodium valproate, 25 mg/day of lamotrigine, 50 mg/day of trazodone, and 1 mg/day of flunitrazepam.

Data availability statement

The authors may provide anonymized data in compliance with the ethical guidelines and privacy regulations. A data transfer agreement must be executed and approved by the Institutional Review Board (IRB) of our institution before data can be provided. Requests for access, including clear research purposes, should be directed to the corresponding author. Data will be shared in accordance with the approval conditions set by the IRB.

Ethics statement

The studies involving humans were approved by National Institutes for Quantum Science and Technology, Certified Review Board. The studies were conducted in accordance with the local legislation and institutional requirements. The ethics committee/institutional review board waived the requirement of written informed consent for participation from the participants or the participants' legal guardians/next of kin owing to the retrospective nature of the study.

Author contributions

MT: Conceptualization, Formal Analysis, Writing–original draft, Writing–review and editing. SK: Conceptualization, Data curation, Investigation, Resources, Writing–review and editing, Writing–original draft. TS: Software, Writing–review and editing. TaM: Investigation, Resources, Writing–review and editing. NS: Investigation, Writing–review and editing. KM: Funding acquisition, Writing–review and editing. S-IN: Supervision, Writing–review and editing. ToM: Supervision, Writing–review and editing.

Funding

The author(s) declare that financial support was received for the research, authorship, and/or publication of this article. This study was supported by a Grant-in-Aid for Scientific Research (C) from the Japan Society for the Promotion of Science [Grant number 24K13083, 20K07755].

Acknowledgments

We would like to thank Editage (www.edita ge.com) for English language editing.

Conflict of interest

One of our co-authors, TS, was employed by PDRadiopharma Inc., the supplier of the 99mTc-labeled ethyl cysteinate dimer used in this study. TS is an expert in Statistical Parametric Mapping (Wellcome Institute for Cognitive Neurology, London, United Kingdom) and was responsible for normalizing single-photon emission computed tomography data using SPM12.

The remaining authors declare that the research was conducted in the absence of any commercial or financial relationships that could be construed as a potential conflict of interest.

Publisher's note

References

American Psychiatric Association (2013). *Diagnostic and statistical manual of mental disorders*. 5th ed. Arlington, VA: American Psychiatric Publishing.

Biederman, J., Petty, C. R., Evans, M., Small, J., and Faraone, S. V. (2010). How persistent is ADHD? A controlled 10-year follow-up study of boys with ADHD. *Psychiatry Res.* 177, 299–304. doi:10.1016/j.psychres.2009.12.010

Boly, M., Faymonville, M. E., Schnakers, C., Peigneux, P., Lambermont, B., Phillips, C., et al. (2008). Perception of pain in the minimally conscious state with PET activation: an observational study. *Lancet Neurol.* 7, 1013–1020. doi:10.1016/S1474-4422(08)70219-9

Borsook, D., Veggeberg, R., Erpelding, N., Borra, R., Linnman, C., Burstein, R., et al. (2016). The insula: a "hub of activity" in migraine. *Neuroscientist* 22, 632–652. doi:10.1177/1073858415601369

Bouchatta, O., Aby, F., Sifeddine, W., Bouali-Benazzouz, R., Brochoire, L., Manouze, H., et al. (2022). Pain hypersensitivity in a pharmacological mouse model of attention-deficit/hyperactivity disorder. *Proc. Natl. Acad. Sci. U. S. A.* 119, e2114094119. doi:10.1073/pnas.2114094119

Busner, J., and Targum, S. D. (2007). The clinical global impressions scale: applying a research tool in clinical practice. *Psychiatry (Edgmont).* 4, 28–37.

Conners, C. K., Erhardt, D., and Sparrow, D. E. (1999). *Conners' adult ADHD rating scales (CAARS) technical manual*. North Tonawanda, NY: Multi-Health Systems Inc.

Ebejer, J. L., Medland, S. E., van der Werf, J., Gondro, C., Henders, A. K., Lynskey, M., et al. (2012). Attention deficit hyperactivity disorder in Australian adults: prevalence, persistence, conduct problems and disadvantage. *PLOS ONE* 7, e47404. doi:10.1371/journal.pone.0047404

Fiset, P., Paus, T., Daloze, T., Plourde, G., Meuret, P., Bonhomme, V., et al. (1999). Brain mechanisms of propofol-induced loss of consciousness in humans: a positron emission tomographic study. *J. Neurosci.* 19, 5506–5513. doi:10.1523/JNEUROSCI.19-13-05506.1999

Fitzcharles, M. A., Cohen, S. P., Clauw, D. J., Littlejohn, G., Usui, C., and Häuser, W. (2021). Nociplastic pain: towards an understanding of prevalent pain conditions. *Lancet*. 397, 2098–2110. doi:10.1016/S0140-6736(21)00392-5

Garcia-Larrea, L., and Peyron, R. (2013). Pain matrices and neuropathic pain matrices: a review. *Pain* 154 (Suppl. 1), S29–S43. doi:10.1016/j.pain.2013.09.001

Ghanizadeh, A. (2013). Systematic review of clinical trials of aripiprazole for treating attention deficit hyperactivity disorder. *Neurosci. (Riyadh)* 18, 323–329.

Ginsberg, Y., Quintero, J., Anand, E., Casillas, M., and Upadhyaya, H. P. (2014). Underdiagnosis of attention-deficit/hyperactivity disorder in adult patients: a review of the literature. *Prim. Care Companion CNS Disord.* 16, 13r01600. doi:10.4088/PCC.13r01600

Ibrahim, M. E., and Hefny, M. A. (2022). Central sensitization and adult attention deficit hyperactivity disorder in medical students with chronic back pain: a cross-sectional study. *Rheumatol. Rehabil.* 49, 24. doi:10.1186/s43166-022-00124-2

Jensen, M. P., and Karoly, P. (2011). "Self-report scales and procedures for assessing pain in adults," in *Handbook of pain assessment* Editors D. C. Turk and R. Melzack 3rd ed. 3 (USA: The Guilford Press), 19–44.

Kasahara, S., Kanda, S., Takahashi, M., Fujioka, M., Morita, T., Matsudaira, K., et al. (2023a). Case Report: guanfacine and methylphenidate improved chronic lower back pain in autosomal dominant polycystic kidney disease with comorbid attention deficit hyperactivity disorder and autism spectrum disorder. *Front. Pediatr.* 11, 1283823. doi:10.3389/fped.2023.1283823

Kasahara, S., Kato, Y., Takahashi, K., Matsudaira, K., Sato, N., Fukuda, K. I., et al. (2023b). Improvement in persistent idiopathic facial pain with comorbid ADHD using the combination of a dopamine system stabilizer and psychostimulant: a case report. *Clin. Case Rep.* 11, e7552. doi:10.1002/ccr3.7552

Kasahara, S., Kato, Y., Takahashi, M., Matsudaira, K., Sato, N., Niwa, S. I., et al. (2023c). Case report: remission of chronic low back pain and oral dysesthesia comorbid with attention deficit/hyperactivity disorder by treatment with atomoxetine and pramipexole. *Front. Pain Res. (Lausanne).* 4, 1159134. doi:10.3389/fpain.2023.1159134

Kasahara, S., Kunii, Y., Mashiko, H., Otani, K., Konno, S. I., and Niwa, S. I. (2011). Four cases of chronic pain that improved dramatically following low-dose aripiprazole administration. *Prim. Care Companion CNS Disord.* 13, 10l01078. doi:10.4088/PCC.10l01078

Kasahara, S., Matsudaira, K., Sato, N., and Niwa, S. I. (2021a). Pain and attention-deficit/hyperactivity disorder: the case of Margaret Mitchell. *Psychosom. Med.* 83, 492–493. doi:10.1097/PSY.0000000000000947

Kasahara, S., Matsudaira, K., Sato, N., and Niwa, S. I. (2022a). Attention-Deficit/hyperactivity disorder and centralized pain: a review of the case of John F. Kennedy. *Kennedy. Clin. Case Rep.* 10, e6422. doi:10.1002/ccr3.6422

Kasahara, S., Niwa, S. I., Matsudaira, K., Sato, N., Oka, H., Fujii, T., et al. (2021b). High attention-deficit/hyperactivity disorder scale scores among patients with persistent chronic nonspecific low back pain. *Pain Phys.* 24, E299–E307. doi:10.36076/ppj.2021/24/E299

Kasahara, S., Niwa, S. I., Matsudaira, K., Sato, N., Oka, H., and Yamada, Y. (2020). Attention-deficit/hyperactivity disorder and chronic pain. *Psychosom. Med.* 82, 346–347. doi:10.1097/PSY.0000000000000789

Kasahara, S., Okamura, Y., Matsudaira, K., Oka, H., Suzuki, Y., Murakami, Y., et al. (2017). Diagnosis and treatment of attention-deficit hyperactivity disorder in patients with chronic pain. *Open J. Psychiatry.* 7, 261–275. doi:10.4236/ojpsych.2017.74023

Kasahara, S., Takahashi, K., Matsudaira, K., Sato, N., Fukuda, K. I., Toyofuku, A., et al. (2023d). Diagnosis and treatment of intractable idiopathic orofacial pain with attention-deficit/hyperactivity disorder. *Sci. Rep.* 13, 1678. doi:10.1038/s41598-023-28931-3

Kasahara, S., Takahashi, M., Morita, T., Matsudaira, K., Sato, N., Momose, T., et al. (2023e). Case report: atomoxetine improves chronic pain with comorbid post-traumatic stress disorder and attention deficit hyperactivity disorder. *Front. Psychiatry.* 14, 1221694. doi:10.3389/fpsyt.2023.1221694

Kasahara, S., Takahashi, M., Takahashi, K., Morita, T., Matsudaira, K., Sato, N., et al. (2024). Case Report: methylphenidate and venlafaxine improved abdominal nociplastic pain in an adult patient with attention deficit hyperactivity disorder, autism spectrum disorder, and comorbid major depression. *Pain Res. (Lausanne).* 5, 1394131. doi:10.3389/fpain.2024.1394131

Kasahara, S., Takao, C., Matsudaira, K., Sato, N., Tu, T. T. H., Niwa, S. I., et al. (2022b). Case report: treatment of persistent atypical odontalgia with attention deficit hyperactivity disorder and autism spectrum disorder with risperidone and atomoxetine. *Front. Pain Res. (Lausanne).* 3, 926946. doi:10.3389/fpain.2022.926946

Kooij, J. J. S., Francken, M. H., and Bron, T. I. (2019). *Diagnostic interview for ADHD in adults*. 3rd ed. DIVA-5) (DIVA Foundation).

Kosek, E., Clauw, D., Nijs, J., Baron, R., Gilron, I., Harris, R. E., et al. (2021). Chronic nociplastic pain affecting the musculoskeletal system: clinical criteria and grading system. *Pain* 162, 2629–2634. doi:10.1097/j.pain.0000000000002324

Kosek, E., Cohen, M., Baron, R., Gebhart, G. F., Mico, J. A., Rice, A. S. C., et al. (2016). Do we need a third mechanistic descriptor for chronic pain states? *Pain* 157, 1382–1386. doi:10.1097/j.pain.0000000000000507

Kugaya, A., Akechi, T., Okuyama, T., Okamura, H., and Uchitomi, Y. (1998). Screening for psychological distress in Japanese cancer patients. *Jpn. J. Clin. Oncol.* 28, 333–338. doi:10.1093/jjco/28.5.333

Laureys, S., Lemaire, C., Maquet, P., Phillips, C., and Franck, G. (1999). Cerebral metabolism during vegetative state and after recovery to consciousness. *J. Neurol. Neurosurg. Psychiatry.* 67, 121. doi:10.1136/jnnp.67.1.121

Meseguer-Beltrán, M., Sánchez-Sarasúa, S., Landry, M., Kerekes, N., and Sánchez-Pérez, A. M. (2023). Targeting neuroinflammation with abscisic acid reduces pain sensitivity in females and hyperactivity in males of an ADHD mice model. *Cells* 12, 465. doi:10.3390/cells12030465

Pallanti, S., Porta, F., and Salerno, L. (2021). Adult attention deficit hyperactivity disorder in patients with fibromyalgia syndrome: assessment and disabilities. *J. Psychiatr. Res.* 136, 537–542. doi:10.1016/j.jpsychires.2020.10.027

Peterson, B. S., Potenza, M. N., Wang, Z., Zhu, H., Martin, A., Marsh, R., et al. (2009). An FMRI study of the effects of psychostimulants on default-mode processing during Stroop task performance in youths with ADHD. *Am. J. Psychiatry.* 166, 1286–1294. doi:10.1176/appi.ajp.2009.08050724

Puhan, M. A., Frey, M., Büchi, S., and Schünemann, H. J. (2008). The minimal important difference of the hospital anxiety and depression scale in patients with chronic obstructive pulmonary disease. *Health Qual. Life Outcomes* 6, 46. doi:10.1186/1477-7525-6-46

Querne, L., Fall, S., Le Moing, A. G., Bourel-Ponchel, E., Delignières, A., Simonnot, A., et al. (2017). Effects of methylphenidate on default-mode network/task-positive network synchronization in children with ADHD. *J. Atten. Disord.* 21, 1208–1220. doi:10.1177/1087054713517542

Raichle, M. E., MacLeod, A. M., Snyder, A. Z., Powers, W. J., Gusnard, D. A., and Shulman, G. L. (2001). A default mode of brain function. *Proc. Natl. Acad. Sci. U. S. A.* 98, 676–682. doi:10.1073/pnas.98.2.676

Salaffi, F., Stancati, A., Silvestri, C. A., Ciapetti, A., and Grassi, W. (2004). Minimal clinically important changes in chronic musculoskeletal pain intensity measured on a numerical rating scale. *Eur. J. Pain.* 8, 283–291. doi:10.1016/j.ejpain.2003.09.004

Schreckenberger, M., Siessmeier, T., Viertmann, A., Landvogt, C., Buchholz, H. G., Rolke, R., et al. (2005). The unpleasantness of tonic pain is encoded by the insular cortex. *Neurology* 64, 1175–1183. doi:10.1212/01.WNL.0000156353.17305.52

Sifeddine, W., Ba-M'hamed, S., Landry, M., and Bennis, M. (2023). Effect of atomoxetine on ADHD-pain hypersensitization comorbidity in 6-OHDA lesioned mice. *Pharmacol. Rep.* 75, 342–357. doi:10.1007/s43440-023-00459-3

Sridharan, D., Levitin, D. J., and Menon, V. (2008). A critical role for the right fronto-insular cortex in switching between central-executive and default-mode networks. *Proc. Natl. Acad. Sci. U. S. A.* 105, 12569–12574. doi:10.1073/pnas.0800005105

Stahl, S. M. (2021). *Neuroscientific basis and practical applications. Stahl's Essent. Psychopharmacol. Camb*. 5th ed. OXford: Univ. Press, 449–485.

Stickley, A., Koyanagi, A., Takahashi, H., and Kamio, Y. (2016). ADHD symptoms and pain among adults in England. *Psychiatry Res.* 246, 326–331. doi:10.1016/j.psychres.2016.10.004

Sullivan, M. J. (2009). The pain catastrophizing scale: user manual. Available at: https://aspecthealth.ca/wp-content/uploads/2017/03/PCSManual_English1.pdf (Accessed October 13, 2024).

Sullivan, M. J., Thorn, B., Haythornthwaite, J. A., Keefe, F., Martin, M., Bradley, L. A., et al. (2001). Theoretical perspectives on the relation between catastrophizing and pain. *Clin. J. Pain.* 17, 52–64. doi:10.1097/00002508-200103000-00008

Sullivan, M. J. L., Bishop, S. R., and Pivik, J. (1995). The pain catastrophizing scale: development and validation. *Psychol. Assess.* 7, 524–532. doi:10.1037/1040-3590.7.4.524

Suto, T., Kato, D., Koibuchi, I., Arai, Y., Ohta, J., Hiroki, T., et al. (2023). Rat model of attention-deficit hyperactivity disorder exhibits delayed recovery from acute incisional pain due to impaired descending noradrenergic inhibition. *Sci. Rep.* 13, 5526. doi:10.1038/s41598-023-32512-9

Suzuki, H., Aono, S., Inoue, S., Imajo, Y., Nishida, N., Funaba, M., et al. (2020). Clinically significant changes in pain along the Pain Intensity Numerical Rating Scale in patients with chronic low back pain. *PLOS ONE* 15, e0229228. doi:10.1371/journal.pone.0229228

Tu, T. T. H., Miura, A., Shinohara, Y., Mikuzuki, L., Kawasaki, K., Sugawara, S., et al. (2019). Pharmacotherapeutic outcomes in atypical odontalgia: determinants of pain relief. *J. Pain Res.* 12, 831–839. doi:10.2147/JPR.S188362

Usui, C., Hatta, K., Doi, N., Nakanishi, A., Nakamura, H., Nishioka, K., et al. (2010). Brain perfusion in fibromyalgia patients and its differences between responders and poor responders to gabapentin. *Arthritis Res. Ther.* 12, R64. doi:10.1186/ar2980

van Rensburg, R., Meyer, H. P., Hitchcock, S. A., and Schuler, C. E. (2018). Screening for adult ADHD in patients with fibromyalgia syndrome. *Pain Med.* 19, 1825–1831. doi:10.1093/pm/pnx275

Vieira de Melo, B. B., Trigueiro, M. J., and Rodrigues, P. P. (2018). Systematic overview of neuroanatomical differences in ADHD: definitive evidence. *Dev. Neuropsychol.* 43, 52–68. doi:10.1080/87565641.2017.1414821

Vogt, B. A., Watanabe, H., Grootoonk, S., and Jones, A. K. P. (1995). Topography of diprenorphine binding in human cingulate gyrus and adjacent cortex derived from coregistered PET and MR images. *Hum. Brain Mapp.* 3, 1–12. doi:10.1002/hbm.460030102

Vorobeychik, Y., and Acquadro, M. A. (2008). Use of atomoxetine in a patient with fibromyalgia syndrome and attention-deficit hyperactivity disorder. *J. Musculoskelet. Pain* 16, 189–192. doi:10.1080/10582450802161960

Watanabe, M., Takao, C., Liu, Z., Nayanar, G., Suga, T., Hong, C., et al. (2022). The effectiveness and adverse events of amitriptyline and aripiprazole in very elderly patients with BMS. *Front. Pain Res. (Lausanne).* 3, 809207. doi:10.3389/fpain.2022.809207

Wiwe Lipsker, C., Hirvikoski, T., Balter, L. J. T., Bölte, S., Lekander, M., Holmström, L., et al. (2021). Autistic traits and attention-deficit hyperactivity disorder symptoms associated with greater pain interference and depression, and reduced health-related quality of life in children with chronic pain. *Front. Neurosci.* 15, 716887. doi:10.3389/fnins.2021.716887

Wiwe Lipsker, C., von Heijne, M., Bölte, S., and Wicksell, R. K. (2018). A case report and literature review of autism and attention deficit hyperactivity disorder in paediatric chronic pain. *Acta Paediatr.* 107, 753–758. doi:10.1111/apa.14220

Woo, C. W., Krishnan, A., and Wager, T. D. (2014). Cluster-extent based thresholding in fMRI analyses: pitfalls and recommendations. *Neuroimage.* 91, 412–419. doi:10.1016/j.neuroimage.2013.12.058

Wood, P. B. (2008). Role of central dopamine in pain and analgesia. *Expert Rev. Neurother.* 8, 781–797. doi:10.1586/14737175.8.5.781

Zain, E., Sugimoto, A., Egawa, J., and Someya, T. (2023). Case report: methylphenidate improved chronic pain in an adult patient with attention deficit hyperactivity disorder. *Front. Psychiatry.* 14, 1091399. doi:10.3389/fpsyt.2023.1091399

Zigmond, A. S., and Snaith, R. P. (1983). The hospital anxiety and depression scale. *Acta Psychiatr. Scand.* 67, 361–370. doi:10.1111/j.1600-0447.1983.tb09716.x

frontiers | Frontiers in Pharmacology

TYPE Review
PUBLISHED 22 November 2024
DOI 10.3389/fphar.2024.1491570

OPEN ACCESS

EDITED BY
Álvaro Llorente-Berzal,
Autonomous University of Madrid, Spain

REVIEWED BY
Yasuhito Uezono,
Jikei University School of Medicine, Japan
Mitsuo Tanabe,
Kitasato University, Japan

*CORRESPONDENCE
Shengyuan Yu,
yusy1963@126.com

RECEIVED 05 September 2024
ACCEPTED 06 November 2024
PUBLISHED 22 November 2024

CITATION
Yang F, Wang Y, Zhang M and Yu S (2024) Mirogabalin as a novel calcium channel $\alpha_2\delta$ ligand for the treatment of neuropathic pain: a review of clinical update.
Front. Pharmacol. 15:1491570.
doi: 10.3389/fphar.2024.1491570

Mirogabalin as a novel calcium channel $\alpha_2\delta$ ligand for the treatment of neuropathic pain: a review of clinical update

Fei Yang, Yan Wang, Mingjie Zhang and Shengyuan Yu*

Department of Neurology, The First Medical Center, Chinese PLA General Hospital, Beijing, China

Neuropathic pain (NP) is often caused by diabetic neuropathy, chemotherapy, or spinal cord lesions and is associated with significant economic burden and poor quality of life. Sophisticated etiology and pathology recognized different pharmacologic interventions, and hitherto, the reported analgesic efficacy and safety of guideline-recommended drugs are not satisfactory. Overall, this article reviews the mechanism of $\alpha_2\delta$ ligand, the clinical pharmacokinetics, efficacy, safety and cost-effectiveness of mirogabalin for the treatment of NP, offering clinical perspectives into potential benefits of NP-related syndrome or comorbidities. Mirogabalin, a novel voltage-gated Ca^{2+} channel (VGCC) $\alpha_2\delta$ ligand with selective binding affinities to $\alpha_2\delta$-1 than $\alpha_2\delta$-2 subunit, exhibited a wider safety margin and a relatively lower incidence of adverse events compared with other gabapentinoids. Randomized-controlled trials and open-label studies have demonstrated the efficacy and long-term safety of mirogabalin in Asian patients with diabetic peripheral neuropathic pain (DPNP), postherpetic neuralgia (PHN), and central NP. Analgesic effects of mirogabalin for the single or add-on treatment on chemotherapy-induced peripheral neuropathy and orthopedic disease/postoperation-related NP were also evidenced. To date, mirogabalin is approved for the general indication of NP in Japan, PNP in South Korea, and DPNP in the Chinese Mainland and DPNP, PHN in Taiwan (China). In summary, mirogabalin emerges as a promising option for NP; further research is warranted to refine wider treatment strategies, flexible dosing in real-world setting.

KEYWORDS

central neuropathic pain, mechanism of action, mirogabalin, peripheral neuropathic pain, pharmacokinetics, voltage-gated Ca^{2+} channel

1 Introduction

Neuropathic pain (NP) is a condition characterized by lesions or diseases in the nervous system and may lead to loss of function, persist continuously or manifest as recurrent episodes (Scholz et al., 2019). NP can be classified as peripheral neuropathic pain (PNP), which is induced by herpes zoster (HZ), diabetes mellitus (DM), cauda equina compression, radiculopathy, chemotherapy, and central neuropathic pain (CNP), associated with spinal cord injury (SCI), poststroke pain, and multiple sclerosis. NP is a major contributor to the global disease burden and has a worldwide prevalence of 6.9%–10% in the general population (Van Hecke et al., 2014). Globally, there were approximately 206 million people with DM in 2021, of which China has 140 million (IDF Diabetes Atlas, 2021). Among Chinese patients with type 2 diabetes mellitus (T2DM), the prevalence of diabetic

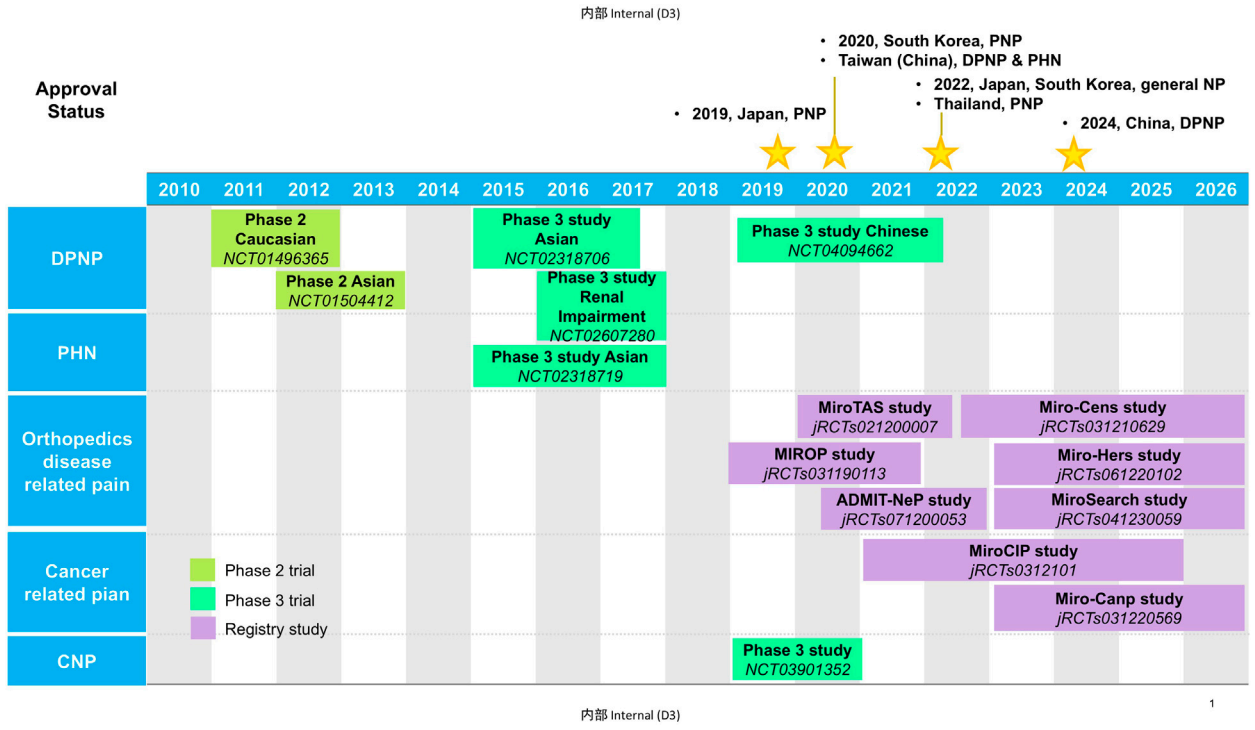

FIGURE 1
Clinical study milestones and approval status of Mirogabalin.

peripheral neuropathy (DPN) was as high as 57.2% (Li et al., 2023a). The overall incidence of HZ was 5.80 per 1,000 person-years in the United States and 6.64 per 1,000 person-years in China; about 7.3%–12.8% of patients with HZ had postherpetic neuralgia (PHN) (Sun et al., 2021; Thompson et al., 2021). The sophisticated etiology and pathology recognized different mechanisms and pain phenotypes for each diagnosis, as well as the difficulty of individualized treatment algorithms under particular physiology (Finnerup et al., 2021). In China, although there is a considerable amount of population meeting the criteria for the use of analgesics, clinical management of NP is relatively inadequate because of economic burden and other reasons (Lian et al., 2022).

The European Federation of Neurological Societies (EFNS), Canadian Pain Society, and Neuropathic Pain Special Interest Group (NeuPSIG) recommended tricyclic antidepressants (TCAs), serotonin norepinephrine reuptake inhibitors (SNRIs), and gabapentinoids including gamma-aminobutyric acid (GABA) analogs as the first line of treatment for various NP conditions (Attal et al., 2010; Dworkin et al., 2013; Moulin et al., 2014). However, available first-line pharmacological interventions have been reported to exert moderately effective or insufficient responses and the required numbers to treat (NNT) was 6–7 to achieve symptomatic pain relief of 50% (Dworkin et al., 2013; Finnerup et al., 2015). In Chinese patients with diabetic peripheral neuropathic pain (DPNP), gabapentinoids including gabapentin and pregabalin were recommended as the first-line treatment, and the most common analgesics. However, indications to use pregabalin for the management of DPNP have not yet been approved for marketing in China (Chen et al., 2023). Only 28% of patients reportedly believed that the analgesics had significantly reduced their pain, whereas 42% of patients believed that the side effects were affecting their daily life routine (Lian et al., 2022). Hence, there was a substantial and unmet need for effective and safe treatment for patients with NP, which has led researchers to develop new pharmacological therapies.

Mirogabalin besylate (herein called mirogabalin) is a novel ligand for $\alpha_2\delta$ subunit of voltage-gated Ca^{2+} channel (VGCC) developed by Daiichi Sankyo. Mirogabalin as a third member of gabapentinoids was first approved in Japan in January 2019 for the treatment of PNP and as general indication for NP including CNP in 2022. It was approved in South Korea for PNP in 2020, and then NP in 2022. In 2020, mirogabalin also got its approval for DPNP and PHN in Taiwan (China). In 2022, mirogabalin was approved for PNP in Thailand. In June 2024, based on the active observations from a phase 3 study on Chinese patients with DPNP, the Center for Drug Evaluation (CDE) of the National Medical Products Administration (NMPA) approved mirogabalin for the indication of DPNP in China (Center for Drug Evaluation of NMPA, 2023) (Figure 1). Currently, there are plenty of extensive investigations on mirogabalin for DPNP, PHN, postoperative NP, chemotherapy-induced peripheral neuropathy (CIPN), and CNP in Asian countries. In this review, we summarized the pharmacology, clinical pharmacokinetics, efficacy, and safety of mirogabalin to bridge the knowledge gap in the clinical care of NP.

2 General information and drug market

Mirogabalin was launched in the market with the brand name of Tarlige®. The chemical name of mirogabalin is [(1*R*,5*S*,6*S*)-6-

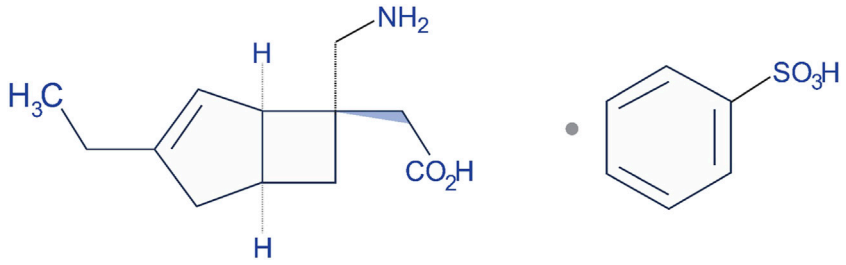

FIGURE 2
Chemical structure of mirogabalin.

(Aminomethyl)-3-ethylbicyclo [3.2.0]hept-3-en-6-yl]acetic acid monobenzenesulfonate (Figure 2). It is packaged in 2.5, 5, 10, and 15 mg tablets. The recommended initial dose for adult patients is 5 mg twice daily (BID) with at least a weekly increase of 5 mg per dose, up to a maximum dose of 15 mg BID (TABLETS, 2023). Based on creatinine clearance (CrCl) levels as exposure to the drug increases with worsening renal function, the dosage and administration interval of mirogabalin needs to be adjusted in those patients recommended 15 mg BID for mild renal impairment, 7.5 mg BID for moderate impairment, and 7.5 mg once daily (QD) for severe impairment (Baba et al., 2020c; Kimura et al., 2021).

Mirogabalin has been approved in Japan for the treatment of NP based on the effectiveness and safety in phase 3 study including Asian patients with DPNP or PHN, CNP, and subsequently in Korea and Taiwan (Deeks, 2019; TABLETS, 2023). Consistent with international guidelines and consensuses, the use of pregabalin, gabapentin, duloxetine, and other antidepressants or anticonvulsants was recommended in patients with DPNP, PHN, CIPN, multiple sclerosis–related pain, and central poststroke pain by Chinese Medical Association. In China, pregabalin and duloxetine has no approved indication for DPNP, as patients could claim using them to relieve pain according to the Food and Drug Administration (FDA) label. The indication of DPNP got its approval by NMPA in China in June 2024. Moreover, the European Patent Office and United States Patent and Trademark Office have issued patents for mirogabalin in September 2013 and May 2011, respectively (European Patent Ofce, 2008; United States Patent and Trademark Office, 2011).

3 Mechanism of action

3.1 Binding profile to the calcium channel

The mechanism of analgesia by gabapentinoids is largely related to the reduction of dorsal horn sensitivity via binding to the $\alpha_2\delta$ subunit of VGCC (Chincholkar, 2018). VGCCs consist of a pore-forming α_1 subunit and auxiliary subunits, including $\alpha_2\delta$ subunit ($\alpha_2\delta$-1 and $\alpha_2\delta$-2) (Dolphin, 2016). The $\alpha_2\delta$-1 subunit is expressed in skeletal, cardiac, and smooth muscles, along with many neuronal cell types and the dorsal root ganglia (DRG), and reported to be essential for behavioral sensitivity and mechanical hypersensitivity after partial sciatic nerve ligation (PSNL) in $\alpha_2\delta$-1 knockout mice (Patel et al., 2013). The $\alpha_2\delta$-2 subunit is mainly identified in the brain; such as the Purkinje cells in the cerebellum, medulla, hippocampus, and striatum; and $\alpha_2\delta$-2 gene deletion in mice will develop ataxia, paroxysmal dyskinesia, and absence epilepsy (Brill et al., 2004; Dolphin, 2016). *In vitro*, disassociation kinetic assay performed by radioactivity detection of ^{3}H-labeled compounds using stable $\alpha_2\delta$ expressing 293A cell line showed higher binding affinity to $\alpha_2\delta$-1 and $\alpha_2\delta$-2 subunits [equilibrium dissociation constant (K_d) = 13.5 nmol/L and 22.7 nmol/L] on mirogabalin than pregabalin (K_d = 62.5 nmol/L and 125.0 nmol/L) (Domon et al., 2018). Although with no significant subtype selectivity from K_d, the dissociation half-life ($t_{1/2}$) of mirogabalin is longer for $\alpha_2\delta$-1 (11.1 h) compared with $\alpha_2\delta$-2 subunit (2.4 h). Hence, mirogabalin exhibits a comparatively slower dissociation from $\alpha_2\delta$-1 (dissociation rate constant [K_{off}] = 0.0627 h^{-1}) than $\alpha_2\delta$-2 (K_{off} = 0.2837 h^{-1}). In contrast, pregabalin showed equal dissociation $t_{1/2}$ from both $\alpha_2\delta$-1 and $\alpha_2\delta$-2 subunits (1.4 h). The selective and unique binding characteristics of mirogabalin with $\alpha_2\delta$-1 and $\alpha_2\delta$-2 and its slower dissociation rate are considered to contribute to sustained analgesic effects and potential wider safety margin for the CNS side effects when compared with pregabalin that dissociates rapidly from $\alpha_2\delta$ subunits (Domon et al., 2018).

In in vitro cultured rat DRG neurons, mirogabalin (50 μmol/L), and pregabalin (200 μmol/L) inhibited the N-type calcium channel currents (Kitano et al., 2019). Similar to gabapentin and pregabalin, mirogabalin exerts analgesic effects through a multitude of actions, including inhibiting trafficking of $\alpha_2\delta$-1 from the dorsal root ganglion, recycling from endosomal compartments, thrombospondin-mediated processes, and stimulating glutamate uptake by excitatory amino acid transporters (Chincholkar, 2018). In a study conducted by Oyama et al. (2021), mirogabalin has shown both supraspinal and spinal actions on thermal and mechanical hypersensitivity to ameliorate NP after partial sciatic nerve ligation. The supraspinal analgesic effects of mirogabalin involves recruitment of the descending noradrenergic pain inhibitory system by spinal activation of α_2-adrenergic receptors. In R217A mutant mice, which substitute arginine with alanine at position 217 to significantly reduce the binding affinity to $\alpha_2\delta$-1 protein, mirogabalin lost its supraspinal analgesic effects, indicating that binding to $\alpha_2\delta$-1 subunit drives the efficacy of pain relief (Field et al., 2006). Furthermore, mirogabalin was also found to effectively inhibit the transient ($I_{Na(T)}$) and late ($I_{Na(L)}$) components of the voltage-gated Na^+ current (I_{Na}) in a concentration-dependent way in pituitary tumor (GH_3) cells, indicating the action on excitable

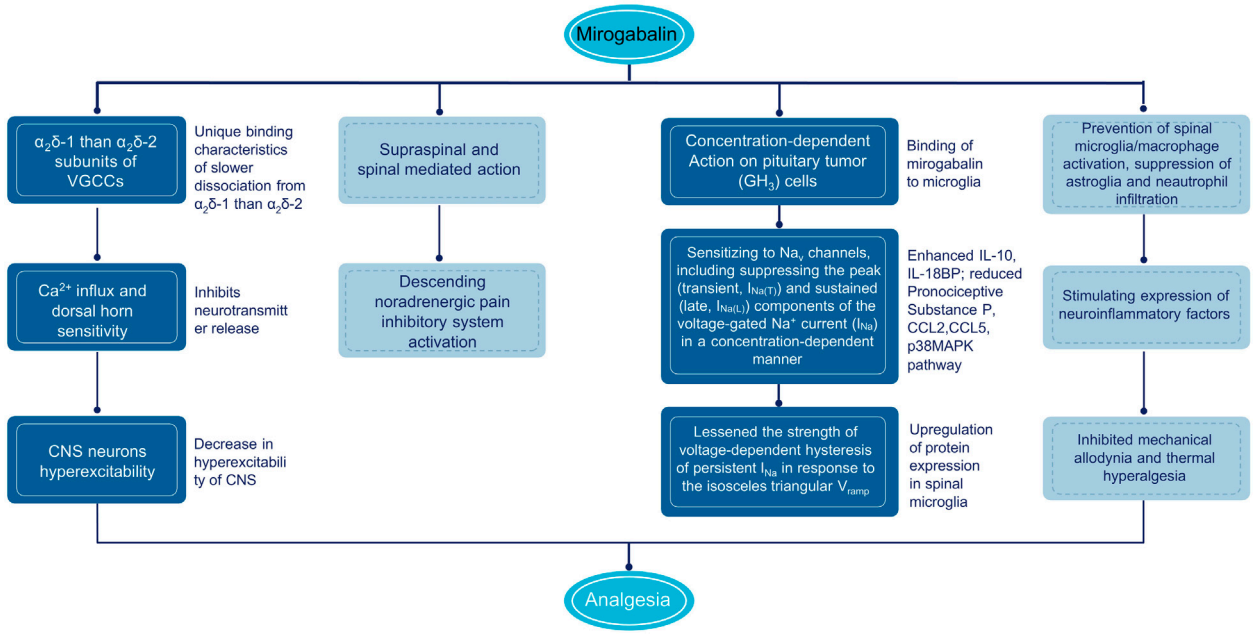

FIGURE 3
Mechanism of action of mirogabalin. CNS, central nervous system; IL, interleukin; TNF, tumor necrosis factor; VGCC, voltage gated calcium channels.

membranes also noticeably conferred the susceptibility to perturbations of Na_V channels (Figure 3) (Wu et al., 2022).

3.2 Inhibition of inflammation and neurotransmitters

Another possible mechanism of pain relief by mirogabalin may be indirectly caused by anti-inflammatory effects and stimulation of downstream signal inhibition. Currently, pain is considered a neuroimmune disorder, and microglia activation releases interleukin (IL)-6, IL-10, IL-4, IL-1β, tumor necrosis factor (TNF)-α, and brain-derived neurotrophic factor (BDNF), resulting in spinal dorsal horn neurons sensitization (Kawasaki et al., 2008; Wu et al., 2018). In rat model of spinal nerve ligation (SNL), intrathecal injection of gabapentin, pregabalin, and mirogabalin dose-dependently inhibited mechanical allodynia and thermal hyperalgesia (ED_{50}: 30.3, 6.2, and 1.5 μg) (Ahmad et al., 2021). The mRNA and protein expression of IL-10 and β-endorphin were upregulated in both SNL rats and primary spinal microglial, illustrating the alleviation of NP by gabapentinoids through stimulating expression of spinal microglial neuroinflammatory factors. It was also reported by Zajaczkowska that in the chronic constriction injury (CCI) mice model, after intraperitoneal (i.p.) administrations of mirogabalin, a decrease in tactile and thermal hypersensitivity and enhanced mRNA of IL-10 and IL-18BP and reduced pronociceptive substance P in the spinal cord were observed (Zajączkowska et al., 2022). In addition, the antinociceptive effects of morphine, buprenorphine, oxycodone, and ketamine were potentiated when administered with mirogabalin in CCI mice, indicating the promising clinical use of mirogabalin based on opioid and ketamine analgesia of NP. Recently, Zajaczkowska added a new mechanism for the anti-inflammatory effects of mirogabalin (i.p.), revealing the prevention of spinal microglia/macrophage activation and suppression of astroglia and neutrophil infiltration, with reducing levels of pronociceptive chemokines CCL2 and CCL5, and downstream p38MAPK pathway in CCI model (Zajączkowska et al., 2023).

3.3 Attenuation hyperexcitability in the spinal cord

The analgesic effects of mirogabalin were assessed in a rat model of SCI at the T6/7 level with a microvascular clip for CNP. The results showed that single oral administration of mirogabalin (2.5, 5, or 10 mg/kg) significantly increased the paw withdrawal threshold with long-lasting effects (Domon et al., 2018).

4 Clinical pharmacokinetics

4.1 Pharmacokinetics in Caucasian, Asian, and Chinese

The first randomized, double-blind, placebo-controlled, phase 1 studies investigated pharmacokinetic parameters by oral administration of single (3, 5, 10, 30, 50, or 75 mg) and multiple ascending dose (5, 10, 15, and 20 mg BID or 25 mg QD to BID) of mirogabalin (Brown et al., 2018). The results revealed that mirogabalin is quickly absorbed, with a mean time to maximum plasma concentration (T_{max}) of 1 h after both single and multiple ascending doses; the peak plasma concentration (C_{max} 49–1,060 and 97–426 ng/mL) and concentration-time curve ($AUC_{0\text{-inf}}$

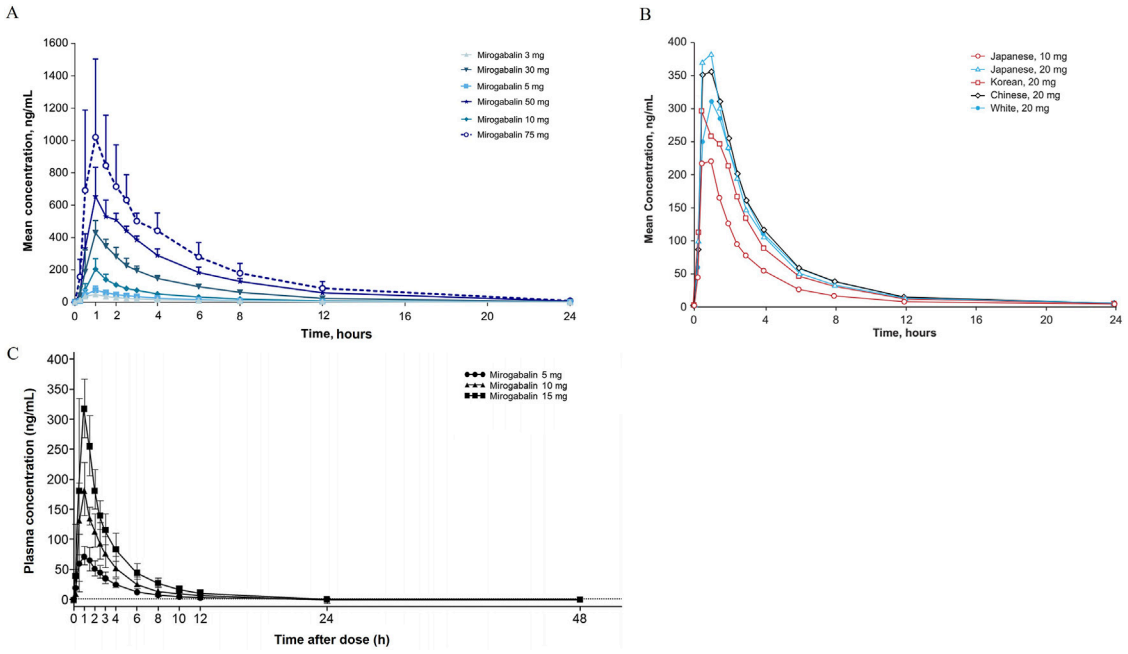

FIGURE 4
Mean concentration-time profiles after single dose administration of mirogabalin on **(A)** Caucasian, **(B)** Asian and **(C)** Chinese adults.

184–4,896 and $AUC_{0\text{-}\tau}$ 406–1,070 ng·h/mL) increased in a dose-dependent manner, respectively. In healthy subjects well tolerated at a daily dose of ≤30 mg, the mean half-life ranged from 2.96 to 3.37 h in a single ascending dose or 3.58–4.55 h in multiple ascending doses.

In a cohort of Asian subjects (Japanese, Korean, and Chinese) and an exclusively Chinese population, PK parameters of single- (5, 10, and 15 mg for the Chinese cohort; 10 and 20 mg for the Asian cohort) and multi-dose (up to 15 mg BID) mirogabalin were consistent with Caucasian participants, including T_{max} (approximately 1 h for both), $t_{1/2}$ (2.3–9 h and 2.57–3.86 h), and CL/F (16.1–19.1 L/h and 15.9–17.6 L/h), showing no difference between ethnicities (Figure 4) (Jansen et al., 2018b; Li et al., 2023b).

4.2 Special considerations in renal and hepatic impairment

Mirogabalin is eliminated mainly unchanged (61%–72%) via renal excretion by filtration and active secretion, suggesting >85% oral bioavailability, whereas 13%–20% of a small fraction is metabolized by hepatic uridine 5′-diphospho-glucuronosyltransferase (UGT) isoforms (Brown et al., 2018). The radioactive study of single oral administration of [^{14}C] mirogabalin at a dose of 30 mg to healthy subjects showed that the main metabolites were A200-0700 (a free form of mirogabalin) *N*-glucuronide, glucuronide of oxidized A204-4455 (lactam form) (Yamamura et al., 2021).

An open-label, parallel-group study included subjects with various degrees of renal function and revealed that the CL/F of mirogabalin was decreased by 25%, 54%, and 76% in those with mild (CrCl 50–80 mL/min/1.73 m^2), moderate (30–50 mL/min/1.73 m^2), and severe renal impairment (<30 mL/min/1.73 m^2); compared with 15 mg QD or BID dose with normal/mild renal impairment, similar AUC_{ss} values, but 37%–43% or 28%–32% lower $C_{max,ss}$, were observed in subjects receiving 50% or 75% reduced dose with moderate or severe renal impairment (Yin et al., 2016). Another open-label phase 1 study confirmed that mild hepatic impairment resulted in lower concentration of A200-700 and A204-4455, and moderate hepatic impairment did not affect that of A200-700, with only a marginal decrease in plasma protein binding (approximately 22.1%), indicating mild to moderate hepatic impairment had no significant effect on mirogabalin exposure (Duchin et al., 2018). Hence, adjustment by reducing 50% or 75% of the recommended dosage is suggested in patients with moderate or severe renal impairment, but no necessity in mild renal impairment or hepatic impairment.

4.3 Food effect and drug-drug interaction (DDI)

Mirogabalin can be taken without food restrictions. In an open-label, crossover, phase 1 study conducted in fasted and fed healthy subjects administrated 15 mg mirogabalin, PK parameters of C_{max} were reduced approximately 18% and T_{max} delayed by 0.5 h under fed versus fasting conditions, with similar total exposure (geometric least squares mean [LSM] of $AUC_{0\text{-}inf}$ = 94.16%; 90% CI: 91.08%–97.34%) and unaffected $t_{1/2}$, V_z/F, and CL/F (Brown et al., 2018).

A phase 1, open-label, crossover study assessed the DDI of inhibitor of metabolic and renal elimination on the exposure of mirogabalin as organic anion transporters 1 and 3 (OAT1/3), organic cation transporter 2 (OCT2), and multidrug and toxin extrusion (MATE) transporter (Tachibana et al., 2018). The

TABLE 1 Efficacy/effectiveness of mirogabalin clinical studies on neuropathic pain.

Author & Year	Study Design	Eligible patients	Dose of mirogabalin	Treatment period	Comparator	Endpoints	Key findings	Other results
Diabetic peripheral neuropathic pain								
Baba et al. (2019)	Phase 3, double-blind, multisite, placebo-controlled study (NCT02318706)	834 Asian patients aged ≥ 20 years with T1DM or T2DM and DPNP; painful distal symmetric polyneuropathy ≥ 6 months; VAS of the SF-MPQ ≥ 40 mm; ADPS ≥ 4	15 mg/d, 20 mg/d (10 mg BID), 30 mg/d (15 mg BID) fixed dose	Observation: 1 week; treatment (titration: 1–2 weeks; fixed-dose: 12–13 weeks); follow-up: 1 week	Placebo (2:1:1: 1 randomized)	Primary: Change in ADPS from baseline at week 14 Secondary: responder rate (≥50% in ADPS), VAS in SF-MPQ, ADSIS, PGIC	LSM vs placebo of 15, 20, 30 mg/d mirogablin: −0.03, −0.15, −0.50 (p = 0.0027 for 30 mg OD); [LSM −1.31, −1.34, −1.47 and −1.81 for placebo and mirogabalin 15, 20 and 30 mg/d]	Significantly greater response rate for 30 mg/d (p = 0.0048); Significant reduction in VAS (LSM vs placebo −5.9, p = 0.0018) and ADSIS (−0.60, p = 0.0001) for 30 mg/d; Significantly more with 30 mg/d reported PGIC of 'minimally improved or better (score≤ 3)' (p = 0.0129), 'much improved or better (score≤ 2)' (p = 0.0016)
Baba et al. (2020b)	Open-label extension of phase 3 study (NCT02318706)	214 Asian patients with DPNP who completed 14 weeks of administration of mirogabalin in phase 3 study	5, 10, 15 mg BID flexible dose	Treatment (titration: 4 weeks; flexible-dosage: 48 weeks, 5 mg BID first 2 weeks, 10 mg BID second 2 weeks, 15 mg BID from week 5); follow-up: 1 week	—	SF-MPQ subscales change from baseline at week 52	The VAS [−9.8 (SD 14.06)], and other subscales of SF-MPQ generally decreased over time from baseline to week 52	—
Guo et al. (2024)	Phase 3, multicenter, randomized, double-blind, placebo-controlled trial (NCT04094662)	393 Chinese patients aged ≥18 years with T1DM or T2DM; painful distal symmetric polyneuropathy ≥6 months; VAS of the SF-MPQ ≥40 mm	15 mg BID fixed dose	Observation: 2 weeks; treatment (titration: 2 weeks, fixed dose: 12 weeks); follow-up: 1 week	Placebo (1: 1 randomized)	Primary: change in ADPS from baseline at week 14 Secondary: ADPS responder rate, VAS in SF-MPQ, PGIC, ADSIS, EQ-5D-5L index and VAS	ADPS: LSM vs placebo: −0.39 (95% CI −0.74, −0.04, p=0.0301); [LSM −2.19 vs −1.81]	Significantly improved ADSIS: LSM vs. placebo −0.45, p = 0.0073), EQ-5D-5L index (LSM 0.0291, p=0.0107); Significantly higher PGIC of ≤ 3 (OR = 1.80, p = 0.0341), ≤ 2 (OR = 2.37, p < 0.0001)
Baba et al. (2020c)	Phase 3, multicenter, open-label study (NCT02607280)	35 Japanese patients aged ≥ 20 years with DPNP as T1DM or T2DM or PHN; CrCL15–59 mL/min; VAS of the SF-MPQ ≥ 40 mm to < 90 mm; ADPS ≥4	7.5 mg BID (CrCL30–59 mL/min), 7.5 mg QD (CrCL15–29 mL/min) fixed dose	Observation: 1 week; treatment (titration: 2 weeks, fixed dose: 12 weeks); follow-up: 1 week	—	Primary: TEAEs Secondary: change in ADPS from baseline at week 14; ADPS responder rate,	LSM change for total population: −1.9 (95% CI −2.8, −1.0); moderate renal impairment: −1.8 (−2.5, −1.1); severe renal impairment: −2.1 (−3.8, −0.4)	ADPS response rate ≥30%: 42.9%, ≥50%: 28.7%; For moderate and severe renal impairment, VAS in SF-MPQ: −20.8, −26.0, ADSIS: −1.4, −0.5, PGIC of ≤ 3: 76.7%, ≤ 2: 36.7%

(Continued on following page)

10.3389/fphar.2024.1491570

TABLE 1 (*Continued*) Efficacy/effectiveness of mirogabalin clinical studies on neuropathic pain.

Author & Year	Study Design	Eligible patients	Dose of mirogabalin	Treatment period	Comparator	Endpoints	Key findings	Other results
						SF-MPQ, ADSIS, PGIC		
Vinik et al. (2014) and Merante et al. (2017)	Phase 2, randomized, double-blind, placebo- and active comparator-controlled trial (NCT01496365)	452 American patients aged ≥ 18 years with T1DM or T2DM, HbA1c ≤ 10%; painful distal symmetric polyneuropathy ≥ 6 months; VAS of the SF-MPQ ≥ 40 mm; ADPS ≥4	5, 10, 15 mg/d, 20 mg/d (10 mg BID), 30 mg/d (15 mg BID) fixed dose	Screening: 3 weeks, treatment: 5 weeks (titration for mirogabalin 30 mg/d and pregabalin 300 mg/d: 1 week, fix dose: 4 weeks), follow-up: 1 week	Placebo, pregabalin 300 mg/d (150 mg BID) (2:1:1:1:1:1: 1 randomized)	Primary: change in ADPS from baseline at week 5 Secondary: ADPS responder rate, PGIC, modified BPI, ADSIS	LSM for mirogablin 5, 10, 15, 20, 30 mg/d, pregabalin vs. placebo: −0.22, −0.53, −0.94, −0.88, −1.01 ($p < 0.05$ for 15, 20, 30 mg/d), −0.05; [LSM −1.9, −2.0, −2.3, −2.7, −2.6, −2.8, −1.8 for placebo, mirogabalin, pregabalin]	LSM for mirogablin vs. pregabalin: −0.17, −0.47, −0.89, −0.83, −0.96 ($p < 0.05$ for 15, 30 mg/d); ADPS response rate ≥30%: 56%–67%, ≥50%: 39%–44%; Significant reductions in ADSIS: mirogabalin 15 ($p < 0.01$), 20, and 30 mg/d vs. placebo ($p < 0.05$); Significantly greater PGIC of ≤ 2: mirogabalin 5, 10, 15, 20, and 30 mg/d vs placebo ($p < 0.05$)
Baba et al. (2020a)	Phase 2, randomized, double-blind, controlled study (NCT01504412)	450 Asian patients age ≥ 20 years; T1DM or T2DM; painful distal symmetric polyneuropathy ≥ 6 months; VAS of the SF-MPQ ≥ 40 mm; ADPS ≥4 (excluded HbA1c > 9.0%)	10 mg/d (5 mg BID), 20 mg/d (10 mg BID), 30 mg/d (15 mg BID) fixed dose	Observation: 1 week; treatment: 7 weeks (titration: 1 week, fix dose: 6 weeks); follow-up: 1 week	Placebo, pregabalin 300 mg/d (150 mg BID) (1:1:1: 1 randomized)	Primary: change in ADPS from baseline at week 7 Secondary: ADPS responder rates, SF-MPQ, PGIC, ADSIS	LSM placebo adjusted difference for mirogabalin 10, 20, 30 mg/d, pregabalin vs. placebo: −0.4, −0.4, −0.3, 0.0 (all $p > 0.05$); [LSM −1.5, −1.9, −1.8, −1.7, −1.4, −1.5 for placebo, mirogabalin, pregabalin]	Significant reduction in total score (LSM vs placebo −1.9, $p = 0.0313$) and VAS of SF-MPQ for 30 mg/d (LSM vs placebo −7.4, $p = 0.0093$), ADSIS (−0.9, $p = 0.0002$); Significantly greater PGIC of ≤ 3 for 10 mg/d: 13.9%, $p = 0.0356$
Postherpetic neuralgia								
Kato et al. (2019)	Phase 3, randomized, double-blind, placebo-controlled trial (NCT02318719)	765 Asian patients aged >20 years with PHN; ADPS: >4; VAS of the SF-MPQ: ≥ 40 mm	15, 20, 30 mg/d	Observation: 1 week, titration: 2 weeks, fixed dose: 12 weeks	Placebo	Primary: weekly change in ADPS at week 14, secondary: responder rate; pain on the VAS of SF-MPQ; and ADSIS	LSM vs. placebo: −0.41, −0.47, and −0.77 for mirogabalin 15, 20, and 30 mg/d groups, respectively, ($p < 0.05$ for all)	Responder rate: 35.0%, 45.4%, 45.1%, and 49.7% for placebo, mirogabalin 15, 20, and 30 mg/d groups, respectively; LSM change from baseline to week 14 in VAS of the SF-MPQ and the ADSIS was significantly greater in all mirogabalin groups compared with placebo
Kato et al. (2020)	Open-label, 52-week, extension study (NCT02318719)	239 Asian patients who completed 14 weeks of double-blind study	15, 20, 30 mg/d	Titration: 4 weeks, dose adjustment: 48 weeks, follow-up: 1 week	—	TEAEs; pain on the VAS, SF-MPQ subscales	VAS mean (SD) change from baseline: −12.4 (16.1)	—
Neuropathic pain due to orthopedic disease/ Post operation NP								
Miyazaki et al. (2024)	Multicenter, randomized, open-		2.5, 5, 7.5, 10 mg BID	CrCL ≥ 60 mL/min: 5 mg BID in	NSAID and/or acetaminophen	Primary: Change in VAS	VAS from baseline to week 8: −51.3 mm in mirogabalin vs. −47.7 in NSAID ($p = 0.161$)	S-LANSS score ≥12: 50% at baseline to 20% at week 8 (p =

(Continued on following page)

10.3389/fphar.2024.1491570

TABLE 1 (*Continued*) Efficacy/effectiveness of mirogabalin clinical studies on neuropathic pain.

Author & Year	Study Design	Eligible patients	Dose of mirogabalin	Treatment period	Comparator	Endpoints	Key findings	Other results
	label, parallel-group study (jRCTs071200053)	128 patients who had undergone lung resection with peripheral NP		week 1, 10 mg BID in week 2, 10 or 15 mg BID from week 3; CrCL 30 to < 60 mL/min: 2.5 mg in week 1, 5 mg BID in week 2, 5 or 7.5 mg BID from week 3		from baseline to week 8; Secondary: S-LANSS score ≥12 at week 2, 4 and 8, PDAS, ADL EQ-5D-5L and QOL		0.003); 41.5% at baseline to 30.2% at week 8 in NSAID group (p = 0.134). Mirogabalin vs. NSAID - PDAS score: −24.1 ± 14.1 vs.−14.4 ± 14.8, $p < 0.001$; EQ-5D-5L score, 0.3363 ± 0.2127 vs. 0.1798 ± 0.1922, $p <$ 0.001
Nikaido et al. (2022)	Randomized, open-label, parallel group, interventional study (jRCTs021200007)	220 patients with leg pain due to radicular type of LSS	5, 7.5, 10, 15 mg BID	CrCL ≥ 60 mL/min: 5 mg BID in weeks 1–2, 10 mg BID in weeks 3–4, and 15 or 10 mg BID after Week 5; CrCL 30 to < 60 mL/min, 2.5 mg BID weeks 1–2, 5 mg BID weeks 3–4, and 7.5 or 5 mg BID after week 5	NSAIDs	Primary: change in VAS leg pain score from baseline, secondary: EQ-5D-5L, PGIC	LSM change in VAS score: 24.1 mm (mirogabalin and NSAIDs) and −14.2 mm (NSAIDs), both $p <$ 0.0001 vs. baseline. The difference in LSM: −9.9 [95% CI, −18.0, −1.8], p = 0.0174	EQ-5D-5L score in mirogabalin and NSAIDs vs. NSAIDs: mean difference, 0.0529 [0.0036, 0.1022], p = 0.0357. Proportions of patients with PGIC scores ≤ 3 and ≤ 2 in mirogabalin and NSAIDs vs. the NSAIDs group: 76.2% vs. 50.0%, p = 0.0006, and 47.6% vs. 32.4%, p = 0.0523
Kim et al. (2021b)	Retrospective study	52 patients treated with mirogabalin for lower extremity radiculopathy due to LSS or LDH	10 mg/d	8 weeks	—	NRS for leg symptoms and sleep disturbance, the NRS and RDQ scores for LBP, and QOL score	NRS for leg symptoms after 8 weeks: 1.8 ± 1.4 ($p < 0.05$); mean RDQ score: 2.4 ± 3.0	—
Chemotherapy-induced peripheral neuropathy								
Sugimoto et al. (2021)	Retrospective study	163 pancreatic cancer patients who underwent FOFIRINOX or GnP therapy and diagnosed with chemotherapy induced NP	5 or 10 or 15 or 20 or 30 mg/d	2, 4, 6 weeks	Pregabalin	Improvement in chemotherapy induced NP at 2, 4, or 6 weeks after treatment	Rate of pain improvement in mirogablin vs. pregabalin: 2 weeks 84.6% (11/13) vs. 33.3% (7/21), p = 0.005; 4 weeks, 6 weeks: 92.3% (12/13) vs. 33.3% (7/21), p = 0.001	—
Misawa et al. (2023)	Exploratory, interventional, open-label, single-arm study (jRCTs031210101)	58 patients experiencing moderate to severe CIPN while undergoing oxaliplatin- or taxane-containing chemotherapy for colorectal, gastric, non-small-cell lung, or breast cancer	5 and 15 mg BID	12 weeks	—	Primary: change in NRS pain score from baseline to week 12 Secondary: Changes from	NRS pain score from baseline to week 12: Mean change = −1.5 [−2.3, −0.8], $p < 0.001$ NRS score for tingling Mean change = −1.2 [−1.9, −0.4], p = 0.003 NRS score for sleep disturbance Mean change = −0.2 in from baseline to week 12 [−0.8, 0.4], p = 0.534	Patients with baseline NRS of ≥ 6 experienced a 44.0% reduction in score from baseline to week 12 (LOCF): mean change:− 3.3 [− 5.0, − 1.5], p = 0.002

(Continued on following page)

10.3389/fphar.2024.1491570

TABLE 1 (*Continued*) Efficacy/effectiveness of mirogabalin clinical studies on neuropathic pain.

Author & Year	Study Design	Eligible patients	Dose of mirogabalin	Treatment period	Comparator	Endpoints	Key findings	Other results
						baseline to weeks 4 and 12 in NRS scores in the last 7 days for tingling and sleep disturbance		
Saito et al. (2022)	Case report	Breast cancer patient with chemotherapy induced NP	5 or 10 mg BID	6 weeks	—	NRS for numbness and pain	NRS reduced from 5/10 to 3/10 for numbness and from 8/10 to 5/10 for pain	—
Central neuropathic pain								
Ushida et al. (2022)	Phase 3 randomized, double-blind, placebo-controlled study (NCT03901352)	300 patients with traumatic SCI; C4 to T12 SCI identified by MRI; stable CNP after SCI for ≥3 months before screening SFMPQ: ≥40 mm	5 mg BID for 1 week, 10 mg BID for 1 week, and 10 or 15 mg BID for 12 weeks	Observation: 1 week, titration: 2 weeks, maintenance: 12 weeks	Placebo (1: 1 randomized)	Primary: change from baseline in the weekly ADPS at week 14, Secondary: ADPS responder rate, VAS, PGIC, NPSI, ADSIS, EQ-5D-5L	LSM difference vs placebo −0.71 [−1.08, −0.34], p = 0.0001	Responder rates [odds ratio 1.91 (1.11, 3.27) for the ≥30%; 2.52 (1.11, 5.71) for the ≥50%]. LSM difference vs placebo for SF-MPQ: −2.4 [−3.8, −1.1], ADSIS −0.71 [−1.04, −0.38], and NPSI −7.7 [−11.1, −4.4] scores
Ushida et al. (2023)	Open-label extension of phase 3 study (NCT03901352)	210 patients: 106 patients CNP-SCI complete 14-week phase 3 period, newly recruited 94 CNP-SP and 10 CNP-PD	10 or 15 mg BID	Treatment (titration: 5 mg BID first 2 weeks, 10 mg BID second 2 weeks; maintenance: 10 or 15 mg BID 47 weeks; taper: 10 or 15 mg QD 1 week); follow-up: 1 week	—	Primary: TEAEs Secondary: SF-MPQ subscales, VAS in SF-MPQ	SF-MPQ VAS mean (SD) change from baseline to week 52 CNP-SCI: − 2.3 (21.13) mm CNP-CP: − 17.0 (24.99) mm CNP-PD: − 17.1 (35.32) mm	All other SF-MPQ subscales (sensory score, affective score, total score, and present pain intensity) decreased at week 52

ADPS, average daily pain score; ADSIS, average daily sleep interference score; BID, twice daily; BPI, brief pain inventory; CNP, central neuropathic pain; CNP-SCI, central neuropathic pain from spinal cord injury; CI, confidence interval; d, day; EQ-5D-5L, EuroQol five-dimensional descriptive system; FOLFORINOX, 5-fuorouracil, oxaliplatin, irinotecan, and leucovorin; GnP, gemcitabine plus nab-paclitaxel; LBP, low back pain; LDH, lumbar disc herniation; LOCF, last observation carried forward; LSM, least square mean; LSS, lumbar spine stenosis; MRI, magnetic resonance imaging; NP, neuropathic pain; NPSI, neuropathic pain symptom inventory; NRS, numerical rating scale; PGIC, patient global impression of change; PHN, postherpetic neuralgia; QOL, quality of life; RDQ, Roland–Morris Disability Questionnaire; SCI, spinal cord injury; SF-MPQ: Short-form McGill Pain questionnaire; TEAEs, treatment-emergent adverse events.

10.3389/fphar.2024.1491570

results demonstrated that C_{max} and AUC_{last} increased by 28.7% and 76.1% when coadministered with probenecid (OAT1/3, UGT inhibitor) and 17.1% and 43.7% with cimetidine (OCT2, MATE inhibitor); renal clearance was greatly slower after coadministration of probenecid (6.67 h^{-1}) and cimetidine (7.17 h^{-1}) in contrast to sole mirogabalin (11.3 h^{-1}), but these changes are not clinically significant. According to four randomized, double-blind, placebo-controlled studies, no clinically relevant PK interactions were observed between mirogabalin and lorazepam, zolpidem, tramadol, or ethanol after single-dose coadministration, in which only C_{max} decreased by 28% with tramadol and increased by 20% with ethanol (Jansen et al., 2018a). Concomitant administration of mirogabalin with lorazepam and ethanol increased the impairment of postural balance and attention. Therefore, its use in patients should be performed with caution, and suggestions from the physicians should be taken when mirogabalin is coadministered with lorazepam or ethanol (Tachibana et al., 2018; Yamamura et al., 2022).

5 Clinical efficacy

The efficacy of mirogabalin has been established in multiple studies for different types of NP. The summary of the available evidence in the treatment of PNP and CNP is presented in Table 1.

5.1 Peripheral neuropathic pain

5.1.1 Diabetic peripheral neuropathic pain

5.1.1.1 Phase 3 placebo-controlled study involving Asian patients

In a double-blind, multisite, placebo-controlled, phase 3 study (NCT02318706) reported by Baba et al. (2019), mirogabalin has a balanced efficacy and safety in Asian patients [Japan, Korea, Taiwan (China), and Malaysia] with dose-dependent pain relief results. A total of 834 patients aged ≥20 years with type 1 diabetes mellitus (T1DM) or type 2 diabetes mellitus (T2DM) and diagnosed DPNP at least 6 months were randomized to receive mirogabalin 15 mg/d (15 mg once daily; n = 164), 20 mg/d (10 mg BID; n = 165), and 30 mg/d (15 mg BID; n = 165) including 1–2 weeks step-wise dose titration and placebo (n = 330). At week 14, the primary end point average daily pain score (ADPS) from baseline was −1.34, −1.47 and −1.81 for mirogabalin 15, 20 and 30 mg/d, respectively, and −1.31 for placebo. The LSM change in ADPS of mirogabalin over placebo was −0.03, −0.15 and −0.50, respectively, in which a dosage of 30 mg/d demonstrated statistically significant benefit ($p = 0.0027$). The decrease in APDS started from week 1 in all mirogabalin treatment groups, significantly greater for 30 mg/d compared with placebo. Mirogabalin 30 mg/d showed a significantly higher responder rate of ≥50% improvement in APDS vs placebo ($p = 0.0048$).

There was a significantly better change from baseline to week 14 of the visual analog scale (VAS) of the short-form McGill pain questionnaire (SF-MPQ) and average daily sleep interference score (ADSIS) rated by patients in mirogabalin 30 mg/d dose ($p = 0.0018$ and 0.0001). In the patient global impression of change (PGIC), >30 mg/d recorded "minimally improved or better" (score ≤3: 70.3% vs 58.8%, $p = 0.0129$) or "much improved or better" (score ≤2: 40.0% vs 26.1%, $p = 0.0016$). The results indicated improvement in the QOL with patient satisfaction.

5.1.1.2 Phase 3 open-label, long-term study involving Asian patients

In an open-label, extension study of phase 3 study (NCT02318706), 214 patients from Japan, Korea, and Taiwan (China) received mirogabalin for 52 weeks (4-week titration with 5 mg BID, followed by a 48-week flexible dose of 10 or 15 mg BID) (Baba et al., 2020b). The VAS (mean change: −9.8) and the other subscales of SF-MPQ (sensory score: −1.2; affective score: −0.3; total score: −1.5; present pain intensity: −0.2) were all decreased from baseline to week 52, demonstrating long-term analgesic effects of mirogabalin in patients with DPNP.

5.1.1.3 Phase 3 placebo-controlled study involving Chinese patients

Guo et al. (2024) conducted a phase 3, multicenter, randomized, double-blind study (NCT04094662) in Chinese patients aged ≥18 years with T1DM or T2DM and DPNP. A total of 393 patients were randomized to receive mirogabalin or placebo for a 2-week titration of 5 or 10 mg BID and a 12-week fixed 15 mg BID period. The change from baseline in weekly ADPS at week 14 was evaluated as the primary end point. Mirogabalin elicited significant improvement over placebo ($p = 0.0301$) with an LSM difference of −0.39 [95% CI (−0.74, −0.04), $p = 0.0301$]. The LSM change in ADPS from baseline was −2.19 for mirogabalin and −1.81 for placebo. The responder rate of ≥30% (54.1% vs 46.2%) and ≥50% (29.1% vs 26.4%) reduction in APDS from baseline to week 14 was numerically higher in the mirogabalin group in comparison with placebo, with no significance, which may be because of the high placebo response and high baseline scores in the placebo group (6.09 vs 5.60 in Asian patients) (Baba et al., 2019).

Patients receiving mirogabalin had improved VAS of SF-MPQ (LSM vs. placebo: −3.3, $p = 0.0929$). Notably, the percentage of PGIC as "minimally improved or better" (87.2% vs. 79.2%, $p = 0.0341$) and "much or very much improved" (63.8% vs. 42.6%, $p < 0.0001$) were both greater in those treated with mirogabalin than in those treated with placebo. Mirogabalin showed significant change from baseline to week 14 regarding ADSIS (LSM vs. placebo: −0.45, $p = 0.0073$), index value (0.0291, $p = 0.0107$), and VAS (2.8, $p = 0.0457$) of EuroQol 5 Dimensions 5 Levels (EQ-5D-5L). Therefore, mirogabalin was found to be safe and effective in Chinese patients with DPNP as in Asian patients from other countries/regions.

5.1.1.4 Phase 2, placebo, active-controlled study

In a phase 2, randomized, double-blind, placebo, active-controlled study (NCT01496365), 913 patients from the US at the age of ≥18 years with T1DM or T2DM (HbA_{1c} ≤10%) and DPNP for ≥ 6 months were randomized to mirogabalin 5 mg/d (5 mg once daily), 10 mg/d (10 mg once daily), 15 mg/d (15 mg once daily), 20 mg/d (10 mg BID) and 30 mg/d (15 mg BID) treatment group; pregabalin 300 mg/d treatment group; or placebo group (Vinik et al., 2014). At week 5, mean changes in ADPS from baseline were −2.0, −2.3, −2.7, −2.6 and −2.8 for the mirogabalin dose ascending, −1.8 for pregabalin, and −1.9 for placebo. The LSM

differences were statistically significant versus placebo for mirogabalin 15, 20, and 30 mg/d (−0.94, −0.88 and −1.01, $p < 0.05$) and versus pregabalin for mirogabalin 15 and 30 mg/d (−0.89 and −0.96, $p < 0.05$). Mirogabalin 15 and 20 mg/d showed a significantly higher percentage of ≥30% reduction in ADPS (66.7% and 60.7%) from baseline to week 5 versus both pregabalin (38.0%, $p < 0.05$) and placebo (41.7%, $p < 0.05$); more percentage of 15, 20 and 30 mg/d had significantly ≥50% reduction (39.2%, 42.9% and 43.9%) versus placebo (24.1%).

Moreover, significant reductions in ADSIS were observed in the mirogabalin 15, 20, and 30 mg/d groups (−2.97, −2.52 and −2.69) compared with placebo (−1.98, $p < 0.05$), in mirogabalin 15 mg/d versus pregabalin (−1.94, $p < 0.05$) (Merante et al., 2017). In modified brief pain inventory (BPI), the subscales of interference with daily function (−2.58 vs. −1.58), worst pain intensity (−2.96 vs. −1.93), least pain intensity (−1.95 vs. −1.19), and average pain intensity (−2.32 vs. −1.55) were improved better with mirogabalin 30 mg/d than with placebo. The significant improvement in the status of PGIC as "minimally improved or better" was observed in 5, 10 and 30 mg/d group and "much or very much improved" in all dose groups of mirogabalin than placebo ($p < 0.05$). The available evidence favors the use of high-dose mirogabalin over pregabalin to some point for the treatment of patients with DPNP.

A phase 2, double-blind, randomized, placebo-controlled study (NCT01504412) conducted in Japan, South Korea, and Taiwan (China) evaluated the effect of mirogabalin versus pregabalin for DPNP caused by ineffective treatments available at the time of the study. In this study, patients (N = 450) aged ≥20 years with T1DM or T2DM and DPNP were randomized to treat with mirogabalin 10, 20, or 30 mg/d; pregabalin 300 mg/d BID; or placebo for 7 weeks (1-week dose escalation) (Baba et al., 2020a). Although nonsignificant, LSM placebo-adjusted difference in change from baseline in ADPS at week 7 was −0.4 [−1.0, 0.2] in the 5 mg BID group, −0.4 [− 0.9, 0.2] in the 10 mg BID group, −0.3 [−0.9, 0.3] in the 15 mg BID group, and 0.0 [− 0.5, 0.5] in the pregabalin group. For secondary end points, mirogabalin 30 mg/d significantly improved the VAS [LSM: −7.4 (−13.0, −1.8), $p = 0.0093$] and total score of SF-MPQ [LSM: −1.9 (−1.3, −0.4), $p = 0.0002$] and ADSIS [LSM: −0.9 (−1.3, −0.4), $p = 0.0002$].

A meta-analysis study on the efficacy of mirogabalin treatment included three randomized controlled trials (RCTs) with 1,732 patients with DPNP (Alyoubi et al., 2021). Mirogabalin showed a significant superior reduction in ADPS for 3, 4, and 5 weeks and observed a significant increase in the patient's proportion with ≥30% and ≥50% reduction in ADPS when compared with pregabalin and placebo.

5.1.2 Postherpetic neuralgia

5.1.2.1 Phase 3, placebo-controlled study

The efficacy of mirogabalin in patients with PHN has been established in phase 3 studies (Kato et al., 2019; Kato et al., 2020). In 2019, Kato et al. (2019) reported a multicenter, double-blind, placebo-controlled phase 3 study (NCT02318719) involving Asian patients with PHN and assessed the efficacy of mirogabalin based on the change from baseline with ADPS. A total of 765 patients were randomized to receive mirogabalin 15 mg/d (15 mg once daily; n = 153), 20 mg/d (10 mg BID; n = 153), 30 mg/d (15 mg BID; n = 155), or placebo (n = 304). At week 14, 15–30 mg/d doses of mirogabalin were well tolerated, and a statistically significant improvement in pain was observed with mirogabalin in ADPS LSM versus placebo: −0.41 ($p = 0.0170$), −0.47 ($p = 0.0058$), and −0.77 ($p < 0.0001$). The LSM change from baseline in ADPS was −1.61, −1.68 and −1.97 for mirogabalin dose ascending and −1.20 for placebo. The proportion of patients reporting ≥30% reduction in ADPS was also significantly higher than placebo in all three dosing regimens of mirogabalin.

Moreover, the LSM change from baseline in VAS of the SF-MPQ (−5.1, −5.7 and −7.8 for 15, 20 and 30 mg/d) and ADSIS (−0.50, −0.48 and −0.76) was significantly greater for mirogabalin than placebo. Significant improvements observed in more patients in the 15 mg/d mirogabalin group as a PGIC score of "much improved or better" (36.2% vs 26.4%, $p = 0.0318$) and in 20 and 30 mg/d mirogabalin groups as "minimally improved or better" (69.3% and 69.0% vs 54.5%, $p = 0.0025$ and 0.0028) versus placebo, suggesting a possible improvement in activities of daily living and QOL (Kato et al., 2019).

5.1.2.2 Phase 3, open-label, long-term study

Furthermore, an open-label extension study of the phase 3 study (NCT02318719) established the efficacy of a long-term flexible dosing regimen of mirogabalin 10 or 15 mg BID for 52 weeks in PHN (Kato et al., 2020). A total of 239 patients who completed the week 14 period were eligible for this 52-week extension study. In terms of efficacy, improvements in SF-MPQ subscales at week 52 were observed (sensory score: −1.5; affective score: −0.3; total score: −1.8; present pain intensity: −0.3 and VAS: −12.4). The VAS score decreased gradually from baseline through the extension study and remained stable (Kato et al., 2020). Although limited, the evidence on the efficacy of mirogabalin in patients with PHN is stable in the long term, and further studies with mirogabalin for the treatment of PHN in non-Asians are warranted.

5.1.3 Postoperative NP

It is anticipated that mirogabalin treatment will provide pain relief in patients with NP after surgery. Miyazaki reported a multicenter, randomized, open-label, parallel-group, interventional trial (jRCTs071200053) that assessed the effectiveness of mirogabalin in postoperative NP after thoracic surgery (Miyazaki et al., 2024). Patients diagnosed with NP after lung resection and a VAS score of ≥40 mm will receive either the monotherapy with conventional pain-relieving agents (nonsteroidal anti-inflammatory drugs [NSAIDs] and/or acetaminophen) or mirogabalin add-on (10–15 mg BID for CrCl ≥60 mL/min and 5–7.5 mg BID for CrCl ≥30 and <60 mL/min) for 8 weeks. The LSM changes of VAS [difference: −3.6 (−8.7, 1.5), $p = 0.161$], ≥30% (98.0% vs. 92.5%, $p = 0.364$) and ≥50% (94.0% vs. 92.5%, $p = 1.000$) reduction in ADPS from baseline to week 8 in mirogabalin add-on group and conventional group were similar. Notably, in patients with self-administered Leeds Assessment of Neuropathic Symptoms and Signs (S-LANSS) score ≥12, mirogabalin add-on group had significantly reduced score (from 50% to 20%, $p = 0.003$) while conventional treatment group had no significant decreasing (from 41.5% to 30.2%, $p = 0.134$). Changes in the Pain Disability Assessment Scale (PDAS) score and EQ-5D-5L also showed significance with the involvement of mirogabalin.

5.1.4 NP caused by orthopedic disease

The MiroTAS is a multicenter, randomized, open-label study that evaluated the efficacy and safety of mirogabalin when given as an add-on therapy in 220 enrolled patients with lumbar spinal stenosis (LSS) taking NSAIDs (jRCTs021200007) (Nikaido et al., 2022). Patients randomly received mirogabalin plus NSAIDs (n = 110) or NSAIDs alone (n = 104) according to package inserts; mirogabalin dose was adjusted based on renal function (CrCl ≥60 mL/min: 15 or 10 mg BID; CrCl ≥30 and <60 mL/min: 7.5 or 5 mg BID). At week 12, the LSM change in VAS score from baseline was −24.1 in the combination group and −14.2 in the NSAID monotherapy group (difference: −9.9, p = 0.0174). A significantly greater improvement in the EQ-5D-5L score (mean difference: 0.0529, p = 0.0357) and a higher proportion of PGIC scores ≤3 (76.2% vs. 50.0%, p = 0.0006) and ≤2 (47.6% vs. 32.4%, p = 0.0523) were observed in those treated with mirogabalin and NSAIDs in comparison with NSAIDs.

A retrospective study has also validated the effect of mirogabalin on PNP caused by orthopedic disease (Kim et al., 2021b). This study included 60 patients who had lower extremity radiculopathy owing to LSS or lumbar disc herniation (LDH) and treated with mirogabalin (flexible dose maximum to 30 mg/d) for PNP caused by orthopedic disease were assessed to compare the pre- and post-administration for leg symptoms and sleep disturbance, the NRS and for low back pain (LBP), and the EQ-5D-5L data. After 8-week therapy, significantly better improvements in leg symptoms of numerical rating scale (NRS) 1.8 versus 6.4 in pre-treatment, low back pain (LBP) in NRS (3.2 vs. 5.2), and Roland–Morris Disability Questionnaire (RDQ, 2.4 vs. 7.5) were observed. Sleep disturbance of NRS (9.7 vs. 5.9) was also improved, and the QOL was higher as EQ-5D-5L score (0.75 vs. 0.54, all p < 0.05). There are several studies ongoing in Japan (jRCTs061220102, jRCTs041230059, and UMIN000037150) that investigated the efficacy of mirogabalin in patients with PNP caused by orthopedic diseases.

5.1.5 Chemotherapy-induced peripheral neuropathy

Although limited evidence is available, studies have shown the effectiveness of mirogabalin in relieving CIPN (Sugimoto et al., 2021; Saito et al., 2022). An earlier study by Sugimoto et al. (2021) retrospectively analyzed the efficacy of mirogabalin and pregabalin in the treatment of CIPN. Patients with pancreatic cancer received chemotherapy regimens FOLFIRINOX (combination of 5-fluorouracil, oxaliplatin, irinotecan, and leucovorin) or GnP (gemcitabine plus nab-paclitaxel) and diagnosed CIPN during the treatment course were included in the study (n = 34; mirogabalin group: n = 13; pregabalin group: n = 21). Both mirogabalin and pregabalin reported effectiveness in improving CIPN but a significantly higher rate of improvement was observed with mirogabalin (2 weeks: 84.6% vs. 33.3%, p = 0.005; 4 and 6 weeks: 92.3% vs. 33.3%, p = 0.001). The discontinuation rate of mirogabalin was 15.4% and that of pregabalin was 52.4%. Hence, mirogabalin might be the first choice for CIPN in patients with pancreatic cancer. In a prospective, single-arm study (MiroCIP), patients with cancer prescribed with mirogabalin (5–15 mg BID) for moderate to severe CIPN while undergoing oxaliplatin- or taxane-containing chemotherapy showed a 30.9% decrease [mean change: −1.7 (−2.4, −1.0), p < 0.001] in the NRS pain score. Meanwhile, a 44% reduction [mean change: −3.3 (−5.0, −1.5), p = 0.002] in pain score from baseline to week 12 was observed in patients with a baseline NRS of ≥6, which shows the effectiveness of mirogabalin in chemotherapy-treated patients with cancer and moderate-to-severe CIPN (Misawa et al., 2023). Mirogabalin (5 mg BID increased to 22.5 mg/d) attenuated pain and numbness because of a reduction in NRS (from 8 to 5 and from 5 to 3), and duloxetine further decreased NRS value to 1 for both, suggesting the synergistic effect of this combination. In a case report of a 53-year-old patient with breast cancer, grade 2 CIPN and grade 1 symptoms were observed during adjuvant docetaxel and cyclophosphamide therapy, and both worsened when receiving eribulin (Sugimoto et al., 2021). Further evidence on the efficacy of mirogabalin for CIPN in patients with different types of tumors (UMIN000041467), primary breast cancer (jRCTs031220001), gastrointestinal cancer (UMIN000049555), or in gemcitabine plus nab-paclitaxel therapy (UMIN000038742) is worth expecting.

5.2 Central neuropathic pain

5.2.1 Placebo-controlled study

Ushida et al. (2022) first evaluated the efficacy and safety of mirogabalin in adult patients with CNP from Japan, Korea, and Taiwan (China) in a randomized, double-blind, placebo-controlled, phase 3 study (NCT03901352). Patients aged ≥20 years who experienced traumatic SCI for ≥6 months and stable CNP for ≥3 months, with VAS ≥40 mm, were enrolled. A total of 300 patients were randomized 1:1 to receive mirogabalin or placebo for 14 weeks (titrated dose for 2 weeks and fixed dose for 12 weeks: 10 or 15 mg BID for CrCl ≥60 mL/min and 5 or 7.5 mg BID for CrCl 30–60 mL/min). At week 14, a statistically significant improvement was observed with mirogabalin in the change from baseline in the weekly ADPS when compared with placebo [LSM difference: −0.71 (−1.08, −0.34), p = 0.0001]. Mirogabalin also showed higher responder rates of ≥30% [OR: 1.91 (1.11, 3.27)] and ≥50% [OR: 2.52 (1.11, 5.71)] for weekly ADPS than placebo. Moreover, more significant improvements in SF-MPQ [LSM: −2.4 (−3.8, −1.1)], ADSIS [LSM: −0.71 (−1.04, −0.38)], and neuropathic pain symptom inventory [NPSI: −7.7 (−11.1, −4.4)] scores were observed in the mirogabalin group versus the placebo group.

5.2.2 Open-label, long-term study

A recently published, open-label, extension study demonstrated the long-term efficacy of mirogabalin in treating CNP in Asian patients (Ushida et al., 2023). Patients with CNP (n = 210) caused by SCI (n = 106), Parkinson's disease (PD, n = 94), and central poststroke pain (CPSP; n = 10) received mirogabalin for 52 weeks, including 5 or 10 mg BID for 4-week titration, 10 or 15 mg BID for 47-week maintenance, and 10 or 15 mg/d for 1-week tapering. The mean VAS in SF-MPQ from baseline to week 52 was reduced gradually for patients with SCI (−2.3) and CPSP (−17.0) and rapidly at weeks 12 and 16 for those with PD (−17.1). Patients with CNP caused by CPSP or PD had a decrease in all SF-MPQ subscales, and patients with SCI who were included in the previous 14-week trial had no significant change. This indicates the sustained efficacy in long-term treatment.

TABLE 2 Most frequent TEAEs (≥5%) with mirogabalin for the treatment of neuropathic pain.

TEAEs	DPNP, N (%)					PHN, N (%)		CIPN, N (%)		NP related to lumbar disease, N (%)		CNP, N (%)	
	Asian patients (n = 165), mirogabalin 30 mg OD*(Baba et al., 2019)	Asian patients with long-term treatment (n = 214), mirogabalin 10 or 15 BID (Baba et al., 2020b)	Chinese patients (n = 196), mirogabalin 15 mg BID	Non-Asian patients (n = 57), mirogabalin 30 mg OD (Vinik et al., 2014)	Patients with renal impairment (n = 35), mirogabalin (7.5 mg BID for moderate, 7.5 mg OD for severe impairment) (Baba et al., 2020c)	Short-term treatment (n = 155), mirogabalin 30 mg OD*(Kato et al., 2019)	Long-term treatment (n = 237), mirogabalin 10 or 15 mg BID (Kato et al., 2020)	CIPN patients (n = 52), mirogabalin 5–15 mg BID (Misawa et al., 2023)	CIPN in patients with pancreatic cancer (n = 13), mirogabalin 5, 10, 15, 20 mg OD (Sugimoto et al., 2021)	Add-on to NSAIDs (n = 110), mirogabalin 10 or 15 mg BID (Nikaido et al., 2022)	Switching from pregabalin (n = 80), mirogabalin 10–30 mg OD (Akazawa et al., 2021)	Asian patients (n = 151), mirogabalin 10 or 15 mg BID (Ushida et al., 2022)	Long-term treatment (n = 210), mirogabalin 10 or 15 mg BID (Ushida et al., 2023)
Somnolence	24 (14.5)	20 (9.3)	12 (6.1)	9 (15.8)	4 (11.4)	37 (23.9)	36 (15.2)	7 (13.5)	—	33 (30.0)	6 (7.3)	45 (29.8)	35 (16.7)
Dizziness	18 (10.9)	16 (7.5)	13 (6.6)	6 (11.3)	2 (5.7)	24 (15.5)	26 (11.0)	5 (9.6)	1 (7.7)	28 (25.5)	4 (4.9)	13 (8.6)	16 (7.6)
Edema	—	13 (6.1)	—	—	—	11 (7.1)	14 (5.9)	—	1 (7.7)	—	—	—	24 (11.4)
Diarrhea	—	18 (8.4)	—	0 (0.0)	2 (5.7)	—	—	—	—	—	1 (1.2)	—	—
Weight gain	11 (6.7)	17 (7.9)	11 (5.6)	1 (1.8)	—	8 (5.2)	22 (9.3)	—	—	—	—	11 (7.3)	15 (7.1)
Back pain	—	11 (5.1)	—	—	—	—	9 (3.8)	—	—	—	—	—	11 (5.2)
Nasopharyngitis	27 (16.4)	58 (27.1)	—	—	8 (22.9)	20 (12.9)	39 (16.5)	—	—	—	—	12 (7.9)	23 (11.0)
Diabetic retinopathy	—	25 (11.7)	—	—	—	—	—	—	—	—	—	—	—
Peripheral Edema	14 (8.5)	24 (11.2)	10 (5.1)	2 (3.5)	3 (8.6)	—	11 (4.6)	2 (3.8)	—	6 (5.5)	—	9 (6.0)	26 (12.4)
Diabetes mellitus	—	12 (5.6)	—	—	—	—	—	—	—	—	—	—	11 (5.2)
Hypoglycemia	—	12 (5.6)	—	—	—	—	—	—	—	—	—	—	—
Constipation	—	12 (5.6)	—	3 (5.3)	—	—	11 (4.6)	—	—	—	—	9 (6.0)	13 (6.2)
Contusion	9 (5.5)	—	—	—	—	—	—	—	—	—	—	—	—
Nausea	—	—	—	1 (1.8)	2 (5.7)	—	8 (3.4)	—	—	—	—	—	—
Sensory disturbance	—	—	—	—	2 (5.7)	—	—	—	—	—	—	—	—
Hyperuricemia	—	—	25 (12.8)	—	—	—	—	—	—	—	—	—	—
UTI	—	—	21 (10.7)	0 (0.0)	—	—	—	—	—	—	—	—	—
Hyperlipidemia	—	—	21 (10.7)	—	—	—	—	—	—	—	—	—	—
Upper respiratory tract infection	—	—	13 (6.6)	—	—	—	—	—	—	—	—	—	12 (5.7)

(Continued on following page)

10.3389/fphar.2024.1491570

TABLE 2 (*Continued*) Most frequent TEAEs (≥5%) with mirogabalin for the treatment of neuropathic pain.

TEAEs	DPNP, N (%)					PHN, N (%)		CIPN, N (%)		NP related to lumbar disease, N (%)		CNP, N (%)	
	Asian patients (n = 165), mirogabalin 30 mg OD*(Baba et al., 2019)	Asian patients with long-term treatment (n = 214), mirogabalin 10 or 15 BID (Baba et al., 2020b)	Chinese patients (n = 196), mirogabalin 15 mg BID	Non-Asian patients (n = 57), mirogabalin 30 mg OD (Vinik et al., 2014)	Patients with renal impairment (n = 35), mirogabalin (7.5 mg BID for moderate, 7.5 mg OD for severe impairment) (Baba et al., 2020c)	Short-term treatment (n = 155), mirogabalin 30 mg OD*(Kato et al., 2019)	Long-term treatment (n = 237), mirogabalin 10 or 15 mg BID (Kato et al., 2020)	CIPN patients (n = 52), mirogabalin 5–15 mg BID (Misawa et al., 2023)	CIPN in patients with pancreatic cancer (n = 13), mirogabalin 5, 10, 15, 20 mg OD (Sugimoto et al., 2021)	Add-on to NSAIDs (n = 110), mirogabalin 10 or 15 mg BID (Nikaido et al., 2022)	Switching from pregabalin (n = 80), mirogabalin 10–30 mg OD (Akazawa et al., 2021)	Asian patients (n = 151), mirogabalin 10 or 15 mg BID (Ushida et al., 2022)	Long-term treatment (n = 210), mirogabalin 10 or 15 mg BID (Ushida et al., 2023)
Increase in blood creatine phosphokinase	—	—	10 (5.1)	—	—	—	—	—	—	—	—	—	—
Insomnia	—	—	—	—	—	—	8 (3.4)	—	—	—	—	—	—
Pharyngitis	—	—	—	—	—	—	8 (3.4)	—	—	—	—	—	—
Eczema	—	—	—	—	—	—	8 (3.4)	—	—	—	—	—	—
Headache	—	—	—	1 (1.8)	—	—	5 (2.1)	—	—	—	—	—	—
Hepatic function abnormal								1 (1.9)					—
Loss of consciousness								1 (1.9)					—

BID, twice daily; CNP, central neuropathic pain; DPNP, diabetic peripheral neuropathic pain; OD, once daily; NP, neuropathic pain; PHN, post-herpetic neuralgia; TEAEs, treatment-emergent adverse events; UTI, urinary tract infection.

10.3389/fphar.2024.1491570

6 Safety and tolerability

6.1 Safety data in clinical trials

Several phase 1 studies involving healthy volunteers have shown a tolerable safety profile of mirogabalin at doses ≤30 mg/d when administered with fed and fasting state (Brown et al., 2018). The most common adverse events leading to treatment discontinuation were somnolence and dizziness, which were dose dependent. In a randomized, sequential, ascending-dose study on single (10–40 mg) and repeated (10 and 15 mg BID) doses of mirogabalin in Korean, Chinese, and White subjects, the results showed an acceptable safety and tolerability profile and the most common treatment-emergent adverse events (TEAEs) were consistent with previous reports and known mechanism (Jansen et al., 2018b). As mirogabalin dissociates rapidly from $\alpha_2\delta$ subunits, it has lesser frequency of CNS adverse effects compared with other $\alpha_2\delta$ ligands (Kim et al., 2021a). In a meta-analysis reported by Lian including two, nine, and three RCTs for patients with DPNP treated on mirogabalin, pregabalin, and duloxetine, the percentage of total cases of somnolence were 9.7% (75/771), 10.1% (121/201), dizziness were 8.6% (66/771), 9.9% (119/1,201) with mirogabalin, pregabalin, respectively; rates of nasopharyngitis were 14.7% (73/494), 14.0% (24/171) of mirogabalin, duloxetine (Jingxuan et al., 2021).

A phase 3 study confirmed the tolerable safety profile of mirogabalin (Baba et al., 2019). Details of TEAEs are presented in Table 2. When mirogabalin was administered to patients with DPNP, the most frequent TEAEs were nasopharyngitis, somnolence, dizziness, peripheral edema, and weight gain. TEAEs leading to treatment discontinuation occurred in 13 (3.9%), 4 (2.4%), 7 (4.2%), and 16 (9.7%) patients in the placebo, mirogabalin 15, 20, and 30 mg/d groups, respectively, and were mild to moderate, mostly resolved without treatment. In the placebo and mirogabalin dose ascending groups, 11 (3.3%), 4 (2.4%), 8 (4.8%), and 11 (6.7%) patients reported serious TEAEs, which were not of particular concern. An open-label extension study revealed the long-term safety of mirogabalin (flexible to 10 or 15 mg BID) in patients with DPNP, with 13.1% of TEAEs leading to discontinuation (Baba et al., 2020b).

Mirogabalin has also been shown to be tolerable in patients with PHN with no new TEAEs reported (Kato et al., 2019). At week 14, 12 patients (4.0%) in the placebo group, 8 (5.3%) in the 15 mg/d group, 16 (10.5%) in the 20 mg/d group, and 12 (7.7%) in the 30 mg/d group reported one or more TEAE resulting in discontinuation. Serious TEAEs were reported in five, two, three, and five patients in the 15, 20, 30 mg/d, and placebo groups, respectively. No serious TEAE was reported by more than one patient in any treatment group. The discontinuation rate of mirogabalin because of TEAEs was 8.4% for patients with PHN in the long-term extension study (Kato et al., 2020).

Mirogabalin, when used in combination with NSAIDs in the treatment of LSS, had higher incidence of TEAEs than NSAIDs monotherapy (60.9% vs. 14.2%) (Nikaido et al., 2022). However, the observed events were mild to moderate and did not cause any safety concerns. The most common TEAEs were somnolence (30.0%) and dizziness (25.5%), and no serious TEAEs or deaths were reported. The proportion of patients who discontinued treatment because of TEAE was 8.2% in the combined group.

In patients with pancreatic cancer, mirogabalin showed better safety than pregabalin for chemotherapy-induced NP (TEAEs leading to discontinuation: 13 vs. 21) (Sugimoto et al., 2021). Treatment interruption because of mirogabalin was reported in two patients (15.4%) with one reported dizziness and in 11 patients (52.4%) receiving pregabalin with five reported AEs. Although nonsignificant, the incidence of adverse events was lower in the mirogabalin group than in the pregabalin group (15.4% vs 33.3%).

Safety data from a double-blind phase 3 study support the use of mirogabalin in patients with CNP (Ushida et al., 2022). The proportion of patients with at least one TEAE was 78.1% in the mirogabalin group and 55.4% in the placebo group. The most common TEAEs observed with mirogabalin were somnolence, dizziness, peripheral edema, nasopharyngitis, constipation, weight gain, and mild in severity. TEAEs leading to treatment discontinuation of mirogabalin were reported in 14 patients (9.3%) and serious TEAEs occurred in 9 patients (6.0%) treated with mirogabalin.

6.2 Safety of mirogabalin when switching from pregabalin

A prospective, single-arm, open-label study (MIROP) assessed the safety of mirogabalin in 152 patients with PNP (34.2% orthopedic diseases, 28.3% PHN, and 0.7% DPNP) switching from pregabalin (Kimura et al., 2021). The incidence of somnolence, dizziness, and peripheral edema was reported in 41.4%, 15.8%, and 2.6% of patients, and AEs were mild in severity in most of the patients. The discontinuation rate considered because of treatment was 13.8%, and no deaths were reported. Akazawa et al. (2021) reported a multicenter, retrospective study that included patients with PNP related to orthopedic disease who switched from pregabalin to mirogabalin (n = 82) because of AEs and lack of efficacy (AE incidence with pregabalin: 100% vs 11.1%). After switching, the AE incidence of mirogabalin did not have a significant difference between the two groups (23.5% vs 15.9%). The incidence of somnolence and dizziness was 12.2% and 14.6% with pregabalin, whereas a lower rate of 7.3% for somnolence and 4.9% for dizziness was observed with mirogabalin. In a short-term retrospective study conducted involving patients with PNP, AEs such as somnolence (28.8%), dizziness (14.8%), edema (2.1%), and weight gain (0.9%) led to a switch in therapy from pregabalin to mirogabalin (Tetsunaga et al., 2020). The study showed a tolerable safety profile for mirogabalin with no new safety concerns with somnolence (26.7%), dizziness (12.3%), edema (5.9%), and weight gain (0.5%) (Tetsunaga et al., 2020).

6.3 Mirogabalin for patients with renal or hepatic impairment

Mirogabalin was well tolerated by Japanese subjects with normal renal function, mild to severe renal impairment, and end-stage renal disease (ERSD) but a higher incidence of TEAEs, supporting dose adjustment (Kato et al., 2018). An open-label study enrolled patients with renal impairment aged ≥20 years diagnosed with DPNP or PHN and prescribed mirogabalin 7.5 mg BID for moderate renal impairment (CrCl: 30–59 mL/min) or 7.5 mg/d for severe renal impairment (CrCl 15–29 mL/min). The overall incidence of TEAEs was 82.9% (29/35) and most of them were mild or moderate, with the most common TEAE being nasopharyngitis (22.9%) and somnolence (11.4%). TEAEs leading

to discontinuation were reported by only four patients (11.4%) with moderate renal impairment (Baba et al., 2020c).

When mirogabalin was assessed in an open-label, single-dose study, only two patients with mild hepatic impairment treated with 15 mg mirogabalin daily reported mild somnolence and recovered rapidly (Duchin et al., 2018). No severe adverse events or discontinuation or death was observed in patients with mild to moderate hepatic impairment. More studies with a larger sample size on the safety of mirogabalin to determine whether dose adjustment or not for patients with hepatic impairment is warranted in the future.

7 Cost-effectiveness of mirogabalin

Currently, the evaluation of the cost-effectiveness of a drug is becoming an increasingly important criterion. Gray et al. (2021) analyzed the cost-effectiveness of mirogabalin 30 mg in the treatment of DPNP using a Markov model. The head-to-head base-case analysis demonstrated that mirogabalin 30 mg is a cost-effective treatment option compared with placebo with an incremental cost-effectiveness ratio (ICER) of US$15,658/quality-adjusted life years (QALY) in patients with DPNP in Taiwan (China), with an estimated QALY gain of 0.02 at an incremental cost of US$310 versus placebo. In addition, mirogabalin was cost-effective compared with pregabalin 300 mg (ICER: US$600/QALY). The cost-effectiveness of mirogabalin in Chinese patients with DPNP has also been established from the healthcare system perspective in the mainland China by a Markov model (He et al., 2023). The results showed that mirogabalin 30 mg is more cost-effective than pregabalin 300 mg, with an ICER of $6869.67/QALY [below the willingness-to-pay threshold in China ($11,339.43)].

The cost-effectiveness of mirogabalin in patients with PHN was also evaluated in Taiwan (China) (Ye et al., 2020). The cost-effectiveness of mirogabalin 30 mg with an incremental QALY gain of 0.041 was at an incremental cost of US$359 versus placebo (US$ 8786) resulting in an ICER of US$8766. Moreover, mirogabalin 30 mg was cost-effective compared with pregabalin 150 and 300 mg, with ICERs of US$16,720 and US$6535, respectively [below the WTP threshold in Taiwan (US$56,000)]. These results supported the good cost-effectiveness of using mirogabalin in Chinese patients.

8 Conclusion

Previously, the evidence on efficacy for the treatment for NP was insufficient with safety being a concern in the treated patients. Hence, a novel gabapentinoid, mirogabalin, which selectively binds to $\alpha_2\delta$ subunits with a unique mechanism of slower dissociation from $\alpha_2\delta$-1 than $\alpha_2\delta$-2, was developed, which emerges as a potential alternative for the treatment of NP. Several phase 3 studies have demonstrated the efficacy of mirogabalin in patients with DPNP and PHN, which ensured the clinical application in many Asian countries/regions. The post-authorization real-world studies will further evaluate the safety and effectiveness in plenty of clinical practice and may emphasize patient-tailored care for border NP. Although still in its infancy, mirogabalin has shown efficacy in palliating orthopedic disease, postoperative NP, and chemotherapy-induced NP. Furthermore, mirogabalin appears to offer superior analgesia for PNP than for CNP, and the clinical care in these patients is certainly promising. In the safety profile, patients with NP showed lower AEs after switching from pregabalin to mirogabalin, indicating a possible clinical action of switching between analgesics. In the MIROP study of patients with PNP, >70% patients were able to safely tolerate the step-wise dose titration of the effective doses of mirogabalin after switching from pregabalin to mirogabalin (Kimura et al., 2021). In patients with renal impairment, mirogabalin could be used in a dose-adjusted manner and was proved to be well tolerated, indicating its feasibility for its application on special groups, such as the elderly or patients with comorbidities, but a few studies did not show notable improvements. Hence, future research should focus on optimizing the efficacy and safety of mirogabalin in a large population for various chronic pain conditions thereby providing a wider array of therapeutic regimens for NP patients, especially in patients undergoing treatment for comorbidities. These research studies should primarily focus on examining flexible dosages in the effective range of 15–30 mg/d for mirogabalin fitting the clinical practice, with the hope of attaining better outcomes. In addition, comparative studies between mirogabalin and pregabalin, gabapentin, duloxetine, milnacipran, and amitriptyline would prove valuable in establishing the position of mirogabalin among the other analgesics for the treatment of NP.

In conclusion, the effectiveness and tolerability of mirogabalin in addressing NP signifies a valuable addition to the therapeutic options available.

Author contributions

FY: Conceptualization, Formal Analysis, Investigation, Methodology, Validation, Writing–original draft, Writing–review and editing. YW: Formal Analysis, Investigation, Methodology, Validation, Writing–original draft, Writing–review and editing. MZ: Formal Analysis, Investigation, Methodology, Validation, Writing–review and editing. SY: Formal Analysis, Investigation, Methodology, Validation, Writing–review and editing, Conceptualization, Supervision.

Funding

The author(s) declare that no financial support was received for the research, authorship, and/or publication of this article.

Acknowledgments

The authors would like to acknowledge Daiichi Sankyo (China) for providing academic support on the references of developing information, unpublished clinical trials, or ongoing trials of mirogabalin to the manuscript formation. The authors also would like to acknowledge Swathi Rajan, PhD, Natasha Aggarwal, PhD, and Roopa Subbaiah, PhD of Indegene Pvt. Ltd., Bangalore, India for manuscript modification and editorial support.

Conflict of interest

The authors declare that the research was conducted in the absence of any commercial or financial relationships that could be construed as a potential conflict of interest.

Publisher's note

References

Ahmad, K. A., Shoaib, R. M., Ahsan, M. Z., Deng, M.-Y., Ma, L., Apryani, E., et al. (2021). Microglial IL-10 and β-endorphin expression mediates gabapentinoids antineuropathic pain. *Brain Behav. Immun.* 95, 344–361. doi:10.1016/j.bbi.2021.04.007

Akazawa, T., Inoue, G., Tanaka, M., Umehara, T., Nagai, T., Oshita, Y., et al. (2021). Somnolence and dizziness during mirogabalin treatment in patients with neuropathic pain related to lumbar disease who switched from pregabalin: a retrospective study. *Glob. Spine J.* 13, 1319–1324. doi:10.1177/21925682211031185

Alyoubi, R. A., Alshareef, A. A., Aldughaither, S. M., Aljaroudi, A. M., Alabdulwahed, A., Alduraibi, F. M., et al. (2021). Efficacy and safety of mirogabalin treatment in patients with diabetic peripheral neuropathic pain: a systematic review and meta-analysis of randomised controlled trials. *Int. J. Clin. Pract.* 75, e13744. doi:10.1111/ijcp.13744

Attal, N., Cruccu, G., Baron, R., Haanpää, M., Hansson, P., Jensen, T. S., et al. (2010). EFNS guidelines on the pharmacological treatment of neuropathic pain: 2010 revision. *Euro J Neurology* 17, 1113–e88. doi:10.1111/j.1468-1331.2010.02999.x

Baba, M., Kuroha, M., Ohwada, S., Murayama, E., and Matsui, N. (2020a). Results of mirogabalin treatment for diabetic peripheral neuropathic pain in asian subjects: a phase 2, double-blind, randomized, placebo-controlled, study. *Pain Ther.* 9, 261–278. doi:10.1007/s40122-020-00156-6

Baba, M., Matsui, N., Kuroha, M., Wasaki, Y., and Ohwada, S. (2019). Mirogabalin for the treatment of diabetic peripheral neuropathic pain: a randomized, double-blind, placebo-controlled phase III study in Asian patients. *J. Diabetes Investig.* 10, 1299–1306. doi:10.1111/jdi.13013

Baba, M., Matsui, N., Kuroha, M., Wasaki, Y., and Ohwada, S. (2020b). Long-term safety and efficacy of mirogabalin in Asian patients with diabetic peripheral neuropathic pain. *J. Diabetes Investig.* 11, 693–698. doi:10.1111/jdi.13178

Baba, M., Takatsuna, H., Matsui, N., and Ohwada, S. (2020c). Mirogabalin in Japanese patients with renal impairment and pain associated with diabetic peripheral neuropathy or post-herpetic neuralgia: a phase III, open-label, 14-week study. *J. Pain Res.* 13, 1811–1821. doi:10.2147/JPR.S255345

Brill, J., Klocke, R., Paul, D., Boison, D., Gouder, N., Klugbauer, N., et al. (2004). entla, a novel epileptic and ataxic Cacna2d2 mutant of the mouse. *J. Biol. Chem.* 279, 7322–7330. doi:10.1074/jbc.M308778200

Brown, K., Mendell, J., Ohwada, S., Hsu, C., He, L., Warren, V., et al. (2018). Tolerability, pharmacokinetics, and pharmacodynamics of mirogabalin in healthy subjects: results from phase 1 studies. *Pharmacol. Res. Perspect.* 6, e00418. doi:10.1002/prp2.418

Center for Drug Evaluation of NMPA (2023). Mirogabalin besylate for listing in China. Available at: https://english.nmpa.gov.cn/2019-07/19/c_389169.htm (Accessed September 3, 2024).

Chen, Q., Wu, Q., Song, R., Wang, Y., Zhang, M., Li, F., et al. (2023). A phase I study to evaluate the safety, tolerability, and pharmacokinetics of a novel, potent GABA analog HSK16149 in healthy Chinese subjects. *Front. Pharmacol.* 14, 1296672. doi:10.3389/fphar.2023.1296672

Chincholkar, M. (2018). Analgesic mechanisms of gabapentinoids and effects in experimental pain models: a narrative review. *Br. J. Anaesth.* 120, 1315–1334. doi:10.1016/j.bja.2018.02.066

Deeks, E. D. (2019). Mirogabalin: first global approval. *Drugs* 79, 463–468. doi:10.1007/s40265-019-01070-8

Dolphin, A. C. (2016). Voltage-gated calcium channels and their auxiliary subunits: physiology and pathophysiology and pharmacology. *J. Physiol.* 594, 5369–5390. doi:10.1113/JP272262

Domon, Y., Arakawa, N., Inoue, T., Matsuda, F., Takahashi, M., Yamamura, N., et al. (2018). Binding characteristics and analgesic effects of mirogabalin, a novel ligand for the α2δ subunit of voltage-gated calcium channels. *J. Pharmacol. Exp. Ther.* 365, 573–582. doi:10.1124/jpet.117.247551

Duchin, K., Senaldi, G., Warren, V., Marbury, T., Lasseter, K., and Zahir, H. (2018). Open-label single-dose study to assess the effect of mild and moderate hepatic impairment on the pharmacokinetics of mirogabalin. *Clin. Drug Investig.* 38, 1001–1009. doi:10.1007/s40261-018-0692-7

Dworkin, R. H., O'Connor, A. B., Kent, J., Mackey, S. C., Raja, S. N., Stacey, B. R., et al. (2013). Interventional management of neuropathic pain: NeuPSIG recommendations. *Pain* 154, 2249–2261. doi:10.1016/j.pain.2013.06.004

European Patent Ofce (2008). European patent specifcation. Application number: 08833399. Available at: https://patentimages.storage.googleapis.com/fb/8b/48/462137eb934a5d/EP2192109B1.pdf.2

Field, M. J., Cox, P. J., Stott, E., Melrose, H., Offord, J., Su, T.-Z., et al. (2006). Identification of the alpha2-delta-1 subunit of voltage-dependent calcium channels as a molecular target for pain mediating the analgesic actions of pregabalin. *Proc. Natl. Acad. Sci. U. S. A.* 103, 17537–17542. doi:10.1073/pnas.0409066103

Finnerup, N. B., Attal, N., Haroutounian, S., McNicol, E., Baron, R., Dworkin, R. H., et al. (2015). Pharmacotherapy for neuropathic pain in adults: a systematic review and meta-analysis. *Lancet Neurology* 14, 162–173. doi:10.1016/S1474-4422(14)70251-0

Finnerup, N. B., Kuner, R., and Jensen, T. S. (2021). Neuropathic pain: from mechanisms to treatment. *Physiol. Rev.* 101, 259–301. doi:10.1152/physrev.00045.2019

Gray, E., Ye, X., Wang, Y.-F., and Wang, S.-J. (2021). Cost-effectiveness of mirogabalin for the treatment of diabetic peripheral neuropathic pain in taiwan. *Value Health Reg. Issues* 24, 148–156. doi:10.1016/j.vhri.2020.10.003

Guo, X., Yu, Y., Zhang, Y., Sun, L., Li, Y., Song, B., et al. (2024). A phase 3, multicenter, randomized, double-blind, placebo-controlled 14-week study of mirogabalin in Chinese patients with diabetic peripheral neuropathic pain. *Pain Ther.* 13, 937–952. doi:10.1007/s40122-024-00617-2

He, Y., Dai, D., Vashi, R., Xu, H., Jin, M., and Feng, Y. (2023). Cost-effectiveness of mirogabalin in treatment of diabetic peripheral neuropathic pain in mainland China. Available at: https://www.ispor.org/conferences-education/conferences/past-conferences/ispor-2023/program/program/session/intl2023-3668/124766 (Accessed August 12, 2024).

IDF Diabetes Atlas (2021). IDF diabetes Atlas 2021. Available at: https://diabetesatlas.org/atlas/tenth-edition/ (Accessed August 12, 2024).

Jansen, M., Mendell, J., Currie, A., Dow, J., He, L., Merante, D., et al. (2018a). Pharmacokinetics, pharmacodynamics, safety, and tolerability of mirogabalin when coadministered with lorazepam, zolpidem, tramadol, or ethanol: results from drug-drug interaction studies in healthy subjects. *Clin. Pharmacol. Drug Dev.* 7, 597–612. doi:10.1002/cpdd.582

Jansen, M., Warrington, S., Dishy, V., Ohwada, S., Johnson, L., Brown, K., et al. (2018b). A randomized, placebo-controlled, double-blind study of the safety, tolerability, pharmacokinetics, and pharmacodynamics of single and repeated doses of mirogabalin in healthy asian volunteers. *Clin. Pharmacol. Drug Dev.* 7, 661–669. doi:10.1002/cpdd.448

Jingxuan, L., Litian, M., and Jianfang, F. (2021). Different drugs for the treatment of painful diabetic peripheral neuropathy: a meta-analysis. *Front. Neurol.* 12, 682244. doi:10.3389/fneur.2021.682244

Kato, J., Matsui, N., Kakehi, Y., Murayama, E., and Ohwada, S. (2020). Long-term safety and efficacy of mirogabalin in Asian patients with postherpetic neuralgia: results from an open-label extension of a multicenter randomized, double-blind, placebo-controlled trial. *Med. Baltim.* 99, e21976. doi:10.1097/MD.0000000000021976

Kato, J., Matsui, N., Kakehi, Y., Murayama, E., Ohwada, S., and Sugihara, M. (2019). Mirogabalin for the management of postherpetic neuralgia: a randomized, double-blind, placebo-controlled phase 3 study in Asian patients. *Pain* 160, 1175–1185. doi:10.1097/j.pain.0000000000001501

Kato, M., Tajima, N., Shimizu, T., Sugihara, M., Furihata, K., Harada, K., et al. (2018). Pharmacokinetics and safety of a single oral dose of mirogabalin in Japanese subjects with varying degrees of renal impairment. *J. Clin. Pharmacol.* 58, 57–63. doi:10.1002/jcph.974

Kawasaki, Y., Zhang, L., Cheng, J.-K., and Ji, R.-R. (2008). Cytokine mechanisms of central sensitization: distinct and overlapping role of interleukin-1beta, interleukin-6, and tumor necrosis factor-alpha in regulating synaptic and neuronal activity in the superficial spinal cord. *J. Neurosci.* 28, 5189–5194. doi:10.1523/JNEUROSCI.3338-07.2008

Kim, J.-Y., Abdi, S., Huh, B., and Kim, K.-H. (2021a). Mirogabalin: could it be the next generation gabapentin or pregabalin? *Korean J. Pain* 34, 4–18. doi:10.3344/kjp.2021.34.1.4

Kim, K., Isu, T., Kokubo, R., Iwamoto, N., Morimoto, D., Kawauchi, M., et al. (2021b). Therapeutic effect of mirogabalin on peripheral neuropathic pain due to lumbar spine disease. *Asian Spine J.* 15, 349–356. doi:10.31616/asj.2020.0136

Kimura, Y., Yamaguchi, S., Suzuki, T., Kato, J., Chiba, S., Hirakawa, N., et al. (2021). Switching from pregabalin to mirogabalin in patients with peripheral neuropathic pain: a multi-center, prospective, single-arm, open-label study (MIROP study). *Pain Ther.* 10, 711–727. doi:10.1007/s40122-021-00255-y

Kitano, Y., Wakimoto, S., Tamura, S., Kubota, K., Domon, Y., Arakawa, N., et al. (2019). Effects of mirogabalin, a novel ligand for the α2δ subunit of voltage-gated calcium channels, on N-type calcium channel currents of rat dorsal root ganglion culture neurons. *Pharmazie* 74, 147–149. doi:10.1691/ph.2019.8833

Li, C., Wang, W., Ji, Q., Ran, X., Kuang, H., Yu, X., et al. (2023a). Prevalence of painful diabetic peripheral neuropathy in type 2 diabetes mellitus and diabetic peripheral neuropathy: a nationwide cross-sectional study in mainland China. *Diabetes Res. Clin. Pract.* 198, 110602. doi:10.1016/j.diabres.2023.110602

Li, Y., Toyama, K., Nakatsu, T., Ishizuka, H., Wu, H., Cao, G., et al. (2023b). Safety, tolerability and pharmacokinetics of single and multiple doses of mirogabalin in healthy Chinese participants: a randomized, double-blind, placebo-controlled study. *Adv. Ther.* 40, 1628–1643. doi:10.1007/s12325-022-02424-7

Lian, J., Wang, H., Cui, R., Zhang, C., and Fu, J. (2022). Status of analgesic drugs and quality of life results for diabetic peripheral neuropathy in China. *Front. Endocrinol.* 12, 813210. doi:10.3389/fendo.2021.813210

Merante, D., Rosenstock, J., Sharma, U., Feins, K., Hsu, C., Vinik, A., et al. (2017). Efficacy of mirogabalin (DS-5565) on patient-reported pain and sleep interference in patients with diabetic neuropathic pain: secondary outcomes of a phase II proof-of-concept study. *Pain Med.* 18, 2198–2207. doi:10.1093/pm/pnw342

Misawa, S., Denda, T., Kodama, S., Suzuki, T., Naito, Y., Kogawa, T., et al. (2023). Efficacy and safety of mirogabalin for chemotherapy-induced peripheral neuropathy: a prospective single-arm trial (MiroCIP study). *BMC Cancer* 23, 1098. doi:10.1186/s12885-023-11560-4

Miyazaki, T., Matsumoto, K., Sato, T., Sano, I., Furukawa, K., Shimoyama, K., et al. (2024). Efficacy and safety of add-on mirogabalin to conventional therapy for the treatment of peripheral neuropathic pain after thoracic surgery: the multicenter, randomized, open-label ADMIT-NeP study. *BMC Cancer* 24, 80. doi:10.1186/s12885-023-11708-2

Moulin, D., Boulanger, A., Clark, A., Clarke, H., Dao, T., Finley, G., et al. (2014). Pharmacological management of chronic neuropathic pain: revised consensus statement from the Canadian pain society. *Pain Res. Manag.* 19, 328–335. doi:10.1155/2014/754693

Nikaido, T., Takatsuna, H., Tabata, S., Shiosakai, K., Nakatani, T., and Konno, S. (2022). Efficacy and safety of add-on mirogabalin to NSAIDs in lumbar spinal stenosis with peripheral neuropathic pain: a randomized, open-label study. *Pain Ther.* 11, 1195–1214. doi:10.1007/s40122-022-00410-z

Oyama, M., Watanabe, S., Iwai, T., and Tanabe, M. (2021). Mirogabalin activates the descending noradrenergic system by binding to the α2δ-1 subunit of voltage-gated Ca2+ channels to generate analgesic effects. *J. Pharmacol. Sci.* 146, 33–39. doi:10.1016/j.jphs.2021.01.002

Patel, R., Bauer, C. S., Nieto-Rostro, M., Margas, W., Ferron, L., Chaggar, K., et al. (2013). α2δ-1 gene deletion affects somatosensory neuron function and delays mechanical hypersensitivity in response to peripheral nerve damage. *J. Neurosci.* 33, 16412–16426. doi:10.1523/JNEUROSCI.1026-13.2013

Saito, Y., Takekuma, Y., Oshino, T., and Sugawara, M. (2022). Combination of mirogabalin and duloxetine attenuates peripheral neuropathy by eribulin: a novel case report. *Case Rep. Oncol.* 15, 606–610. doi:10.1159/000525059

Scholz, J., Finnerup, N. B., Attal, N., Aziz, Q., Baron, R., Bennett, M. I., et al. (2019). The IASP classification of chronic pain for ICD-11: chronic neuropathic pain. *Pain* 160, 53–59. doi:10.1097/j.pain.0000000000001365

Sugimoto, M., Takagi, T., Suzuki, R., Konno, N., Asama, H., Sato, Y., et al. (2021). Mirogabalin vs pregabalin for chemotherapy-induced peripheral neuropathy in pancreatic cancer patients. *BMC Cancer* 21, 1319. doi:10.1186/s12885-021-09069-9

Sun, X., Wei, Z., Lin, H., Jit, M., Li, Z., and Fu, C. (2021). Incidence and disease burden of herpes zoster in the population aged ≥50 years in China: data from an integrated health care network. *J. Infect.* 82, 253–260. doi:10.1016/j.jinf.2020.12.013

Tachibana, M., Yamamura, N., Atiee, G. J., Hsu, C., Warren, V., He, L., et al. (2018). Coadministration of probenecid and cimetidine with mirogabalin in healthy subjects: a phase 1, randomized, open-label, drug-drug interaction study. *Br. J. Clin. Pharmacol.* 84, 2317–2324. doi:10.1111/bcp.13674

TARLIGE® TABLETS (2023). OD TABLETS. Available at: https://www.pmda.go.jp/PmdaSearch/iyakuDetail/ResultDataSetPDF/430574_1190026F1028_1_11 (Accessed August 12, 2024).

Tetsunaga, T., Tetsunaga, T., Nishida, K., Misawa, H., Takigawa, T., Yamane, K., et al. (2020). Short-term outcomes of mirogabalin in patients with peripheral neuropathic pain: a retrospective study. *J. Orthop. Surg. Res.* 15, 191. doi:10.1186/s13018-020-01709-3

Thompson, R. R., Kong, C. L., Porco, T. C., Kim, E., Ebert, C. D., and Acharya, N. R. (2021). Herpes zoster and postherpetic neuralgia: changing incidence rates from 1994 to 2018 in the United States. *Clin. Infect. Dis.* 73, e3210–e3217. doi:10.1093/cid/ciaa1185

United States Patent and Trademark Office (2011). Patent No.: US 7, 738 B2. Alexandria, VA, 947. Available at: https://patentimages.storage.googleapis.com/c3/f8/b9/191405f3ffb709/US7947738.pdf.

Ushida, T., Katayama, Y., Hiasa, Y., Nishihara, M., Tajima, F., Katoh, S., et al. (2022). Mirogabalin for central neuropathic pain after spinal cord injury: a randomized, double-blind, placebo-controlled, phase 3 study in asia. *Neurology*, 100, e1193, e1206. doi:10.1212/WNL.0000000000201709

Ushida, T., Katayama, Y., Hiasa, Y., Nishihara, M., Tajima, F., Katoh, S., et al. (2023). Long-term safety and efficacy of mirogabalin for central neuropathic pain: a multinational, phase 3, 52-week, open-label study in asia. *Pain Ther.* 12, 963–978. doi:10.1007/s40122-023-00513-1

Van Hecke, O., Austin, S. K., Khan, R. A., Smith, B. H., and Torrance, N. (2014). Neuropathic pain in the general population: a systematic review of epidemiological studies. *Pain* 155, 654–662. doi:10.1016/j.pain.2013.11.013

Vinik, A., Rosenstock, J., Sharma, U., Feins, K., Hsu, C., Merante, D., et al. (2014). Efficacy and safety of mirogabalin (DS-5565) for the treatment of diabetic peripheral neuropathic pain: a randomized, double-blind, placebo- and active comparator-controlled, adaptive proof-of-concept phase 2 study. *Diabetes Care* 37, 3253–3261. doi:10.2337/dc14-1044

Wu, C.-L., Chuang, C.-W., Cho, H.-Y., Chuang, T.-H., and Wu, S.-N. (2022). The evidence for effective inhibition of INa produced by mirogabalin ((1R,5S,6S)-6-(aminomethyl)-3-ethyl-bicyclo [3.2.0] hept-3-ene-6-acetic acid), a known blocker of CaV channels. *Int. J. Mol. Sci.* 23, 3845. doi:10.3390/ijms23073845

Wu, H.-Y., Mao, X.-F., Tang, X.-Q., Ali, U., Apryani, E., Liu, H., et al. (2018). Spinal interleukin-10 produces antinociception in neuropathy through microglial β-endorphin expression, separated from antineuroinflammation. *Brain Behav. Immun.* 73, 504–519. doi:10.1016/j.bbi.2018.06.015

Yamamura, N., Mendel-Harary, J., Brown, K., Uchiyama, M., Urasaki, Y., Takahashi, M., et al. (2021). Metabolism, excretion, and pharmacokinetics of [14C]mirogabalin, a novel α2δ ligand, in healthy volunteers following oral administration. *Xenobiotica* 51, 549–563. doi:10.1080/00498254.2021.1879408

Yamamura, N., Mikkaichi, T., Itokawa, K.-I., Hoshi, M., Damme, K., Geigner, S., et al. (2022). Mirogabalin, a novel α2δ ligand, is not a substrate of LAT1, but of PEPT1, PEPT2, OAT1, OAT3, OCT2, MATE1 and MATE2-K. *Xenobiotica* 52, 997–1009. doi:10.1080/00498254.2022.2129517

Ye, X., Gray, E., Wang, Y.-F., and Wang, S.-J. (2020). Cost-effectiveness of mirogabalin for the treatment of post-herpetic neuralgia in Taiwan. *J. Med. Econ.* 23, 529–536. doi:10.1080/13696998.2020.1720694

Yin, O. Q. P., Merante, D., Truitt, K., and Miller, R. (2016). Population pharmacokinetic modeling and simulation for assessing renal impairment effect on the pharmacokinetics of mirogabalin. *J. Clin. Pharmacol.* 56, 203–212. doi:10.1002/jcph.584

Zajączkowska, R., Pawlik, K., Ciapała, K., Piotrowska, A., Ciechanowska, A., Rojewska, E., et al. (2023). Mirogabalin decreases pain-like behaviors by inhibiting the microglial/macrophage activation, p38MAPK signaling, and pronociceptive CCL2 and CCL5 release in a mouse model of neuropathic pain. *Pharmaceuticals* 16, 1023. doi:10.3390/ph16071023

Zajączkowska, R., Rojewska, E., Ciechanowska, A., Pawlik, K., Ciapała, K., Kocot-Kępska, M., et al. (2022). Mirogabalin decreases pain-like behaviours and improves opioid and ketamine antinociception in a mouse model of neuropathic pain. *Pharm. (Basel)* 15, 88. doi:10.3390/ph15010088

frontiers | Frontiers in Neuroscience

TYPE Original Research
PUBLISHED 11 December 2024
DOI 10.3389/fnins.2024.1464477

OPEN ACCESS

EDITED BY
Fabio Turco,
Cannabiscientia SA, Switzerland

REVIEWED BY
Huadong Ni,
First Hospital of Jiaxing, China
Harsh Goel,
All India Institute of Medical Sciences, India

*CORRESPONDENCE
Lingyan Chen
✉ 125505219qq.com
Long Wang
✉ wanglongsdu1226@163.com
Peng Chen
✉ 740466982@qq.com

†These authors have contributed equally to this work and share first authorship

RECEIVED 14 July 2024
ACCEPTED 19 November 2024
PUBLISHED 11 December 2024

CITATION
Qu J, Gong Q, He S, Peng J, Chen L, Wang L and Chen P (2024) Analgesic effect of Dahuang Fuzi Decoction in neuropathic pain through inhibiting TNF-α and PI3K-AKT signaling. *Front. Neurosci.* 18:1464477. doi: 10.3389/fnins.2024.1464477

Analgesic effect of Dahuang Fuzi Decoction in neuropathic pain through inhibiting TNF-α and PI3K-AKT signaling

Jinglian Qu[1†], Qian Gong[2†], Siyu He[3†], Jiuyan Peng[2], Lingyan Chen[4*], Long Wang[3*] and Peng Chen[1*]

[1]Basic Medical School, Guizhou University of Traditional Chinese Medicine, Guiyang, Guizhou, China, [2]First Clinical Medical School, Guangzhou University of Chinese Medicine, Guangzhou, Guangdong, China, [3]School of Pharmacy, Southwest Medical University, Luzhou, Sichuan, China, [4]Department of Rehabilitation, The First Affiliated Hospital of Guangzhou Medical University, Guangzhou, China

Background: Neuropathic pain (NeP) presents considerable challenges in terms of effective management and significantly impacts the quality of life for affected patients. The current treatment options for NeP are limited, highlighting the need for alternative therapeutic approaches. Dahuang Fuzi Decoction (DF), a formula from traditional Chinese medicine, has shown potential in relieving pain symptoms associated with various types of NeP. However, the mechanisms through which DF exerts its effects remain largely unknown.

Methods: In this study, we employed ultra-high-performance liquid chromatography coupled with high-resolution mass spectrometry (UHPLC-HRMS) to analyze the chemical composition of DF. A chronic sciatic nerve compression injury (CCI) rat mode was used to assess the analgesic efficacy of DF for NeP. Network pharmacology analysis was performed to identify the potential signaling pathways affected by DF.

Results: DF treatment significantly increased the mechanical withdrawal threshold (MWT) and thermal withdrawal latency (TWL) in CCI rats, indicating its analgesic effect. Network pharmacology analysis suggested that DF potentially modulated TNF-α and PI3K-AKT signaling pathways. Furthermore, DF treatment decreased the levels of pro-inflammatory cytokines (IL-1β, IL-6, and TNF-α) in spinal cord tissues of CCI rats, suggesting an anti-inflammatory effect. Western blot analysis revealed that DF treatment reduced the expression of TNF-α, TNFR1, and phosphorylated forms of PI3K, AKT, IKKα/β, IKBα, and NF-κB in the spinal cord of CCI rats. Immunofluorescence analysis confirmed significant reductions in TNF-α and TNFR1 expression, as well as in AKT and NF-κB phosphorylation within astrocytes following DF administration.

Conclusion: Our findings characterize the chemical constituents of DF and elucidate its underlying mechanism for relieving NeP. The analgesic effect of DF involves the inhibition of TNF-α and PI3K-AKT signaling pathways, providing a potential therapeutic approach for NeP management.

KEYWORDS

Dahuang Fuzi Decoction, neuropathic pain, TNF signaling pathway, network pharmacology, PI3K-AKT signaling

1 Introduction

Neuropathic pain (NeP) is a form of chronic pain arising from injury or disease affecting the somatosensory nervous system, which may be caused by factors such as surgical incisions, nerve compression, autoimmune disorders, or channelopathies. NeP affects ~7–10% of the population and imposes a substantial burden on patients

(Racine et al., 2016). Current first-line treatments for NeP consist of tricyclic antidepressants (TCAs), serotonin-noradrenaline reuptake inhibitors, pregabalin, and gabapentin (Dosenovic et al., 2017). Although these medications target different mechanisms involved in NeP progression, their effectiveness is often limited, and they can be associated with severe side effects (Finnerup et al., 2015, 2021). Therefore, it is crucial to develop new therapeutic approaches to better manage NeP.

The spinal cord serves as the central hub for integrating and transmitting nociceptive signals (Wang et al., 2017). Central sensitization, marked by increased neuronal and circuit activity within the spinal cord, plays a crucial role in the development and maintenance of NeP (Latremoliere and Woolf, 2009; Lutolf et al., 2022). Microglia, the resident immune cells of the central nervous system, are key contributors to this process, with microglia-mediated neuroinflammation being a significant factor driving central sensitization in NeP (Inoue and Tsuda, 2018; Ji et al., 2018). Following nerve damage, microglia become rapidly activated, undergoing morphological changes, microgliosis, and increased transcriptional activity (Inoue and Tsuda, 2018). The activated cells subsequently release proinflammatory mediators such as tumor necrosis factor-α (TNF-α), IL-1β, and brain-derived neuropathic pain (BDNF), which influence synaptic activity across spinal segments, promoting central sensitization (Popiolek-Barczyk and Mika, 2016; Zhao et al., 2017; Ji and Xu, 2021). Consequently, targeting microglia-induced inflammation represents a promising therapeutic strategy for managing NeP (Fiore et al., 2023; Wang et al., 2023).

Recent studies have demonstrated the notable analgesic effects of traditional Chinese medicine (TCM) in managing NeP, both in clinical settings and animal models (Liu et al., 2021, 2022). Dahuang Fuzi Decoction (DF), a classical TCM formulation first documented in the *Synopsis of Prescriptions of the Golden Chamber*, comprises Rhubarb, Radix Aconiti Lateralis, and Asarum heterotropoides. It is commonly used to treat inflammatory conditions, neurological disorders, and headaches (Tai et al., 2021; Gu et al., 2022). Clinically, we have observed that DF can effectively alleviate pain symptoms in patients with various NeP conditions, such as sciatica and post-herpetic neuralgia. Despite these promising effects, the mechanisms underlying DF's analgesic properties in NeP remain poorly understood. This study aims to investigate the effects of DF in a chronic constriction injury (CCI) model and explore its mechanisms of action through network pharmacology and experimental validation.

2 Materials and methods

2.1 Preparation of DF

DF herbal granules, consisting of Rhubarb (Batch No. A2092591), Radix Aconiti Lateralis (Batch No. A2071291), and Asarum heterotropoides (Batch No. A209A882), were sourced from the Guangdong Yifang Chinese Herbal Medicine Department in a 3:4:1 ratio.

2.2 Fingerprint analysis of DF

Fingerprint analysis of DF was perfomed using a Thermo Vanquish Flex Ultra Performance Liquid chromatography system coupled with a Thermo Fisher QE high-resolution mass spectrometer (ThermoFisher, USA). Separation of the DF constituents was achieved with a Thermo Scientific HyPURITY C18 column (150 × 2.1 mm, 1.6 μm). The mobile phase consisted of methanol (solvent A) and 0.1% (v/v) phosphoric acid (solvent B), with the following elution gradient: 0–5 min, 3–21% A; 5–20 min, 21–36% A; 20–32 min, 36–50% A; 32–42 min, 50–62% A; 42–50 min, 62–85% A; 50–60 min, 85–95% A. The injection volume was 1 μL, and the column temperature was maintained at 30°C. Detection was carried out at 260 nm with a flow rate of 0.2 mL/min.

2.3 Network pharmacology analysis

2.3.1 Identification of potential targets of DF

The ingredients of DF identified through high-resolution mass spectrometry were screened for oral bioavailability (OB) ≥30% and drug-likeness (DL) ≥0.18 to qualify as active compounds. The targets associated with these active compounds were then obtained from the SwissTargetPrediction database (http://www.swisstargetprediction.ch/). Subsequently, all identified targets were cross-referenced with the UniProt database (https://www.uniprot.org/) to obtain annotated and reviewed gene symbols. Duplicate entries and non-standard targets were excluded to establish the final list of potential DF targets (Shi et al., 2019; Zhang J. Y. et al., 2019; Zhang J. et al., 2019).

2.3.2 Target prediction of DF for treating NeP

NeP-related targets were retrieved from the GeneCards database (http://www.genecards.org/), considering only genes with a relevance score of ≥1. Related targets associated with neuropathic pain were further compiled by integrating data from multiple databases, including DisGeNET (https://www.disgenet.org/) and DrugBank (http://www.drugbank.ca/), among others. By comparing the predicted targets of the active ingredients in DF with the NeP-related targets obtained, overlapping targets were identified as relevant to DF's treatment of NeP. The interactions between compounds and targets were visualized using a bioinformatics platform (www.bioinformatics.com.cn).

2.3.3 Network construction

The targets were processed by Cytoscape 3.7.2 software to construct a representation of the "drug disease–active ingredients–intersection targets." For protein-protein interaction (PPI) data visualization, the String database (https://string-db.org/) was employed, with the species parameter set to "Homo sapiens." During this process, only interactions with a P-value < 0.05 were retained. The significant potential targets of DF, along with those related to NeP treatment, were subsequently uploaded to Cytoscape 3.7.2 for further analysis.

2.3.4 Enrichment analysis of targets of DF against NeP

The Metascape database (https://metascape.org/) was utilized for conducting Gene Ontology (GO) analysis and Kyoto Encyclopedia of Genes and Genomes (KEGG) pathway enrichment analysis. Initially, the targets of DF against NeP were inputted into the Metascape database, which automatically annotated the gene IDs. Subsequently, the species option was set as "Homo sapiens." A significance threshold of $P \leq 0.05$ was chosen as the default option. Finally, the results of the GO analysis and KEGG pathway enrichment analysis were obtained.

2.4 Animals

Thirty-six-week-old male Sprague-Dawley (SD) rats (200 ± 20 g) were sourced from Guangdong Medical Laboratory Animal Center (Certificate NO. SCXK[Guangdong]2022-0002, Guangzhou, China). The temperature and relative humidity were maintained at 26°C and 60–70%, respectively, under a 12 h dark-light cycle. The animals were randomly divided into six groups ($n = 6$ per group): sham group, CCI group, low-dose DF group (DF-L), medium-dose DF group (DF-M), high-dose DF group (DF-H), and pregabalin group (PGB). The study adhered to the ethical guidelines and regulations approved by the Animal Experimentation Ethics Committee at The First Affiliated Hospital of Guangzhou University of Chinese Medicine (License No. GZTCMF1-2021100).

2.5 CCI surgery and DF treatment

The CCI model was established according to previously published protocols after inducing anesthesia with an intraperitoneal injection of pentobarbital sodium (Chen et al., 2023a,b). The left sciatic nerve was carefully exposed and ligated with four silk ligatures (4-0) at an average interval of 1–2 mm. The incision was closed in layers postoperatively. In the sham group, the sciatic nerve was exposed but not ligated. Rats in the DF-L (2.4 g/kg), DF-M (4.8 g/kg), and DF-H (9.6 g/kg) groups received DF solution via oral gavage once daily for 15 days, starting on the first postoperative day. The positive control group received pregabalin solution (15 mg/kg, Batch No. J20160021, Pfizer).

2.6 Behavioral test

2.6.1 Mechanical withdrawal threshold

The mechanical withdrawal threshold (MWT) was assessed using an electronic von Frey anesthesiometer (IITC Life Science Instruments, Woodland Hills, CA, USA; Chen et al., 2023a,b). Rats were placed in a clear Plexiglas chamber for 30 min prior to testing. The anesthesiometer tip was applied to stimulate the ipsilateral mid-plantar area of each rat three times, with a 5-min interval between stimuli. The onset of paw lifting or licking was recorded, and the average value was calculated to determine the MWT.

2.6.2 Thermal withdrawal latency

Thermal withdrawal latency (TWL) was measured using a thermal radiation stimulator (IITC Life Science Instruments, Woodland Hills, CA, USA; Chen et al., 2023a,b). Prior to the test, rats were acclimated in a transparent Plexiglas box for 30 min. The radiant heat source was applied to the ipsilateral mid-plantar area three times, with a 10-min interval between exposures. The appearance of paw lifting or licking was noted, and the average TWL was calculated.

2.7 Enzyme-linked immunosorbent assay analysis

After the behavioral tests on day 15 post-surgery, rats were deeply anesthetized with an intraperitoneal injection of pentobarbital (40 mg/kg). Spinal cord tissues were harvested and homogenized using a tissue homogenizer. Levels of inflammatory cytokines (IL-1β, IL-6, and TNF-α) in the spinal cord were quantified using ELISA kits (Meimian, Jiangsu, China) following the manufacturer's instructions.

2.8 Western blot analysis

Western blotting was performed to assess the protein expressions of TNF-α, TNFR1, PI3K, AKT, IKKα/β, IKBα, NF-κB, p-PI3K, p-AKT, p-IKKα/β, p-IKBα, and p-NF-κB. Briefly, spinal cord tissues were lysed in RIPA buffer (Meilunbio, Dalian, China) and centrifuged at 12,000 × *g* for 5 min at 4°C. The supernatant was collected after dilution and denaturation. Protein samples of 40 μg were then subjected to sodium dodecyl sulfate-polyacrylamide gel electrophoresis (SDS-PAGE) for separation. Following electrophoresis, proteins were transferred to a polyvinylidene difluoride membrane. After blocking with TBST containing 5% skim milk powder or 1% bovine serum albumin (for phosphorylated proteins) for 2 h, membranes were incubated overnight at 4°C with primary antibodies. The membranes were then incubated with a secondary antibody (IRDye 800CW Goat anti-Rabbit, Boster, Wuhan, China). The primary antibodies used included anti-TNFα (Beyotime, Shanghai, China), anti-TNFR1 (Abclonal, Wuhan, China), anti-PI3K (Affinity, Jiangsu, China), anti-AKT (Affinity, Jiangsu, China), anti-IKKα/β (Affinity, Jiangsu, China), anti-IKBα (Affinity, Jiangsu, China), anti-NF-κB (Affinity, Jiangsu, China), anti-p-PI3K (Affinity, Jiangsu, China), anti-p-AKT (Affinity, Jiangsu, China), anti-p-IKKα/β (Affinity, Jiangsu, China), anti-p-IκBα (Affinity, Jiangsu, China), anti-p-NF-κB (Affinity, Jiangsu, China), and anti-GAPDH (Goodhere, Hangzhou, China). Bands were quantified using Image-Pro Plus 6.0.

2.9 Immunofluorescence

Immunofluorescence assays were conducted following established protocols. Briefly, spinal cord tissues were dehydrated with increasing concentrations of alcohol and subsequently cleared with xylene. The cleared tissues were embedded in paraffin, and

sections were prepared using a microtome. Paraffin was removed from the sections, and antigen retrieval was performed with an electric heat-retrieval device. Normal serum was applied around the sections for blocking. Diluted primary antibodies were added and incubated overnight. Following washes, sections were treated with Cy3-labeled goat anti-rabbit IgG secondary antibody (Boster, Wuhan, China). Nuclear staining was achieved using DAPI. Excess liquid was removed, and sections were mounted and visualized under a fluorescence microscope. The primary antibodies utilized included anti-TNFR1 (Abclonal, Wuhan, China), anti-TNF-α (Beyotime, Shanghai, China), and anti-p-NF-κB (Affinity, Jiangsu, China).

2.10 Molecular docking

For molecular docking, the three-dimensional structure of the target protein was retrieved from the Protein Data Bank (PDB). The protein was then optimized using specialized software such as PyMOL or Chimera. During optimization, water molecules were removed, missing hydrogen atoms were added, and any non-standard residues were corrected to ensure a reliable protein structure. The three-dimensional structure of the ligand was obtained from a relevant database like PubChem, and the ligand was optimized using molecular editing software such as Open Babel or Avogadro. This optimization involved adding hydrogen atoms, adjusting charge states, and generating Gasteiger-Marsili type charges for accurate ligand representation. Finally, the prepared protein and ligand structure files were imported into Autodock Vina for docking simulations.

2.11 Statistical analysis

Experimental data are presented as means ± standard deviations and analyzed using one-way analysis of variance (ANOVA) in IBM SPSS Statistics 26.0. A p-value of < 0.05 was considered statistically significant.

3 Results

3.1 Characterization of ingredients of DF

The ingredients of DF were identified using ultra-high-performance liquid chromatography coupled with high-resolution mass spectrometry (UHPLC-HRMS). Figures 1A, B illustrate the total ion current chromatograms, while Table 1 lists the identified components. A total of 24 ingredients were tentatively characterized, with their structural formulas presented in Figure 1C.

3.2 Effects of DF on the behavior of CCI rats

To assess the analgesic effect of DF, MWT and TWL were measured before and at 3, 7, 11, and 15 days post-CCI surgery (Figures 2A, B). There were no significant differences in MWT and TWL values across the groups prior to surgery ($P > 0.05$). From the third day after operation, y the third postoperative day, MWT and TWL values in the CCI group significantly declined and remained low compared to the sham group ($P < 0.01$). Starting from day 7 post-drug administration, both the DF-M and pregabalin groups exhibited a significant increase in MWT and TWL compared to the CCI group ($P < 0.05$). The DF-L and DF-H groups also demonstrated varying improvements in these values during the treatment period. These findings indicate that DF has a notable analgesic effect in CCI rats.

3.3 Identification of targets of DF against NeP

Network pharmacology was utilized to predict the targets of DF against NeP. The 24 compounds of DF identified by UHPLC-HRMS served as input for the analysis. This approach yielded 843 targets linked to the 24 DF ingredients and 1,321 targets associated with NeP (Figure 3A). Among them, 229 targets were identified as common targets between DF and NeP (Figure 3A). A drug-disease-ingredients-targets network was constructed, as shown in Figure 3B. To explore the interactions among DF's targets in relation to NeP, a protein-protein interaction (PPI) network was created using STRING. This network included 228 nodes and 3,047 edges, with an average degree of 26.7 (Figure 3C). Each node represented a target, with node size reflecting degree value and connection strength. Topological analysis of the PPI network was performed to identify core targets, revealing 51 targets with values exceeding the 2-fold median (Figure 3C). Further analysis in STRING, using the 2-fold median as the criterion, identified the top 14 targets, which included TNF, MTOR, MAPK3, SRC, ALB, CASP3, AKT1, APP, MAPK1, GRIN2B, PRKCA, NOS3, HSP90A1, and IL6 (Figure 3C). These 14 targets were considered the core targets of DF in the treatment of NeP.

3.4 GO and KEGG pathway enrichment analysis of the targets of DF against NeP

GO and KEGG enrichment analyses were conducted using the Metascape database for the 51 targets of DF against NeP. GO enrichment indicated that these targets are involved in processes such as modulation of chemical synaptic transmission, neuron death and positive regulation of synaptic transmission in biological process (BP); asymmetric synapse, neuron spine and synaptic membrane in cellular component (CC); and neurotransmitter receptor activity, phosphoprotein binding and protein serine/threonine/tyrosine kinase activity in molecular function (MF; Figures 4A–C). KEGG analysis revealed that the 51 targets were primarily associated with pathways such as the PI3K-AKT signaling pathway, TNF signaling pathway, calcium signaling pathway, glutamatergic synapse, inflammatory mediator regulation of TRP channels and pathways of neurodegeneration-multiple diseases (Figure 4D), all of which were closely related to NeP. Notably, the PI3K-AKT and TNF signaling pathways showed the most significant enrichment (Figure 4D), suggesting their potential central roles in DF's mechanisms of action.

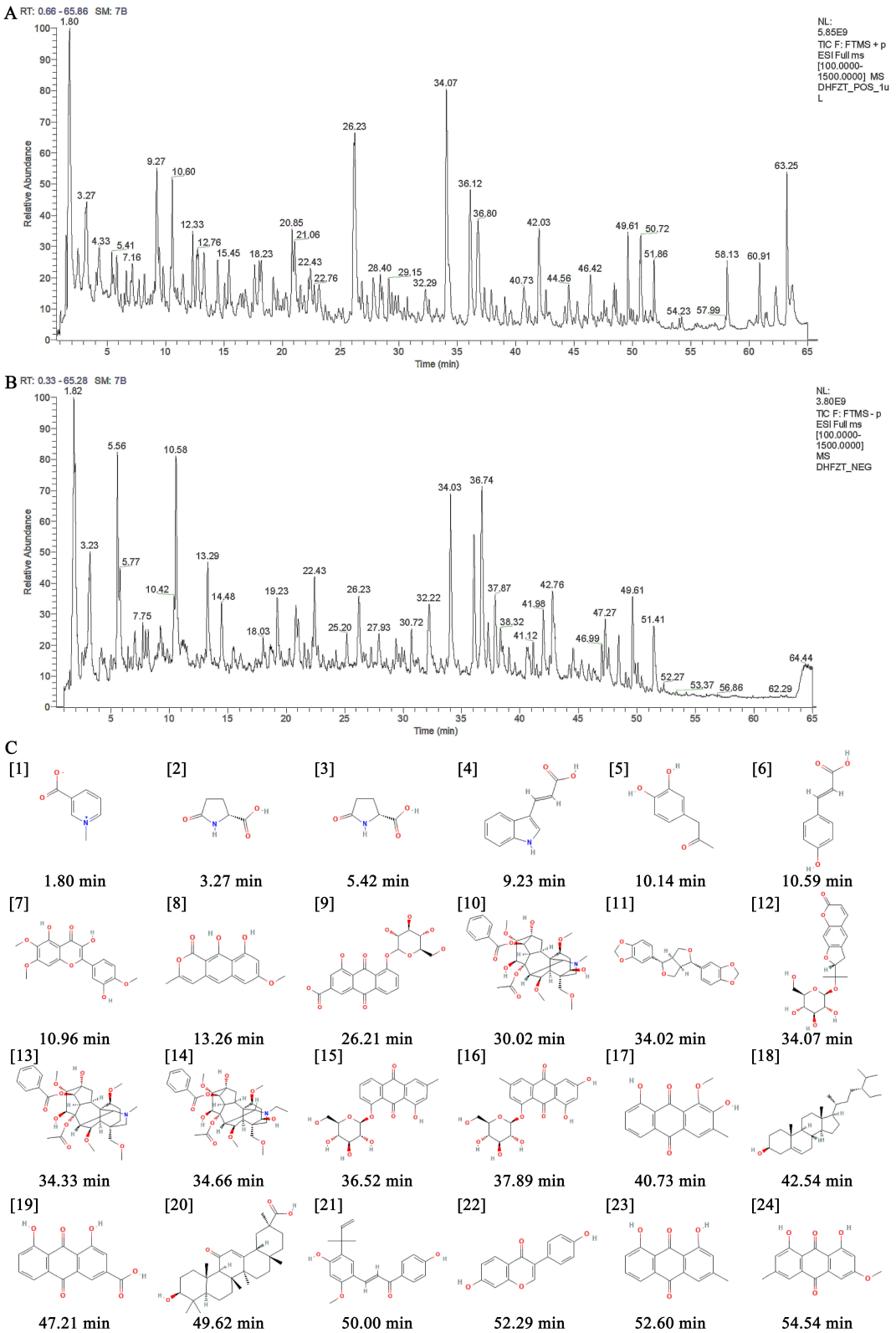

FIGURE 1
Identification of ingredients of DF using UHPLC-HRMS. **(A)** The total ion current chromatogram of DF under the positive mode. **(B)** The total ion current chromatogram of DF under the negative mode. **(C)** Chemical structures of identified compounds present in DF.

TABLE 1 The compounds of aqueous extracts of DF.

No.	Identity	Mode	Molecular formula	RT (min)	[M+H]+ (m/z)
1	Trigonelline	Pos	$C_7H_7NO_2$	1.80	138.05487
2	D-Pyroglutamic acid	Pos	$C_5H_7NO_3$	3.27	130.04991
3	Adenosine	Pos	$C_{10}H_{13}N_5O_4$	5.42	268.10385
4	Trans-3-Indoleacrylic acid	Pos	$C_{11}H_9NO_2$	9.23	188.07047
5	3′,4′-Dihydroxyphenylacetone	Pos	$C_9H_{10}O_3$	10.14	167.07033
6	4-Coumaricacid	Pos	$C_9H_8O_3$	10.59	165.05456
7	Eupatin	Pos	$C_{13}H_{12}O_3$	10.96	217.08688
8	Toralactone	Pos	$C_{15}H_{12}O_5$	13.26	273.07541
9	Rhein-8-o-beta-o-glucoside	Neg	$C_{21}H_{18}O_{11}$	26.21	445.07440
10	Mesaconitine	Pos	$C_{33}H_{45}NO_{11}$	30.02	632.30652
11	Sesamin	Pos	$C_{20}H_{18}O_6$	34.02	355.11758
12	Nodakenin	Pos	$C_{20}H_{24}O_9$	34.07	431.13037
13	Hypaconitine	Pos	$C_{33}H_{45}NO_{10}$	34.33	616.31067
14	Aconitine	Pos	$C_{34}H_{47}NO_{11}$	34.66	646.32214
15	Chrysophanol-1-O-β-D-glucoside	Neg	$C_{21}H_{20}O_9$	36.52	415.10300
16	Emodin-1-O-β-D-glucopyranoside	Pos	$C_{21}H_{20}O_{10}$	37.89	455.09467
17	Obtusifolin	Neg	$C_{16}H_{12}O_5$	40.73	285.07526
18	Beta-sitosterol	Pos	$C_{29}H_{50}O$	42.54	415.13406
19	Rhein	Pos	$C_{15}H_8O_6$	47.21	283.06080
20	Glycyrrhetinic acid	Neg	$C_{30}H_{46}O_4$	49.62	453.33557
21	Licochalcone A	Pos	$C_{21}H_{22}O_4$	50.00	361.14142
22	Daidzein	Pos	$C_{15}H_{10}O_4$	52.29	255.06484
23	Chrysophanol	Neg	$C_{15}H_{10}O_4$	52.60	253.05070
24	Physcion	Neg	$C_{16}H_{12}O_5$	54.54	283.06080

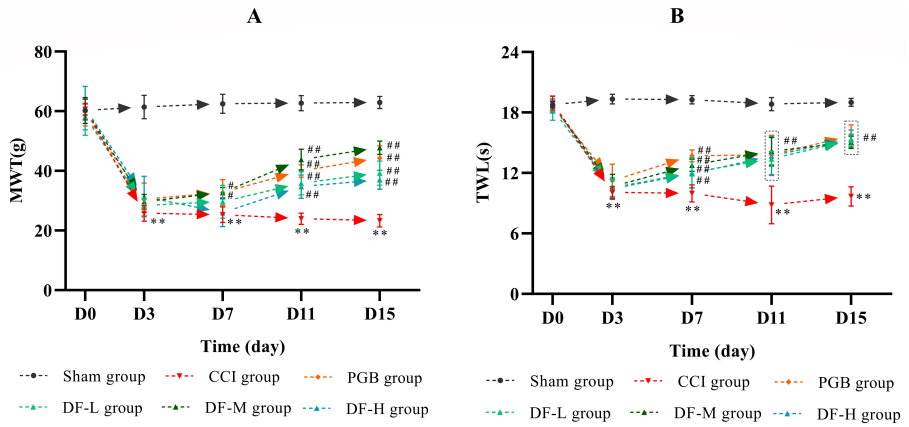

FIGURE 2
The effects of DF on the behavior in the CCI rats. **(A, B)** The MWT and TWL values among the sham, CCI, DF-L, DF-M, DF-H, and PGB groups before and 3, 7, 11, and 15 days after CCI surgery ($n = 6$ in each group). $^{**}P < 0.01$ compared with the sham group; $^{\#}P < 0.05$ and $^{\#\#}P < 0.01$ compared with the CCI group.

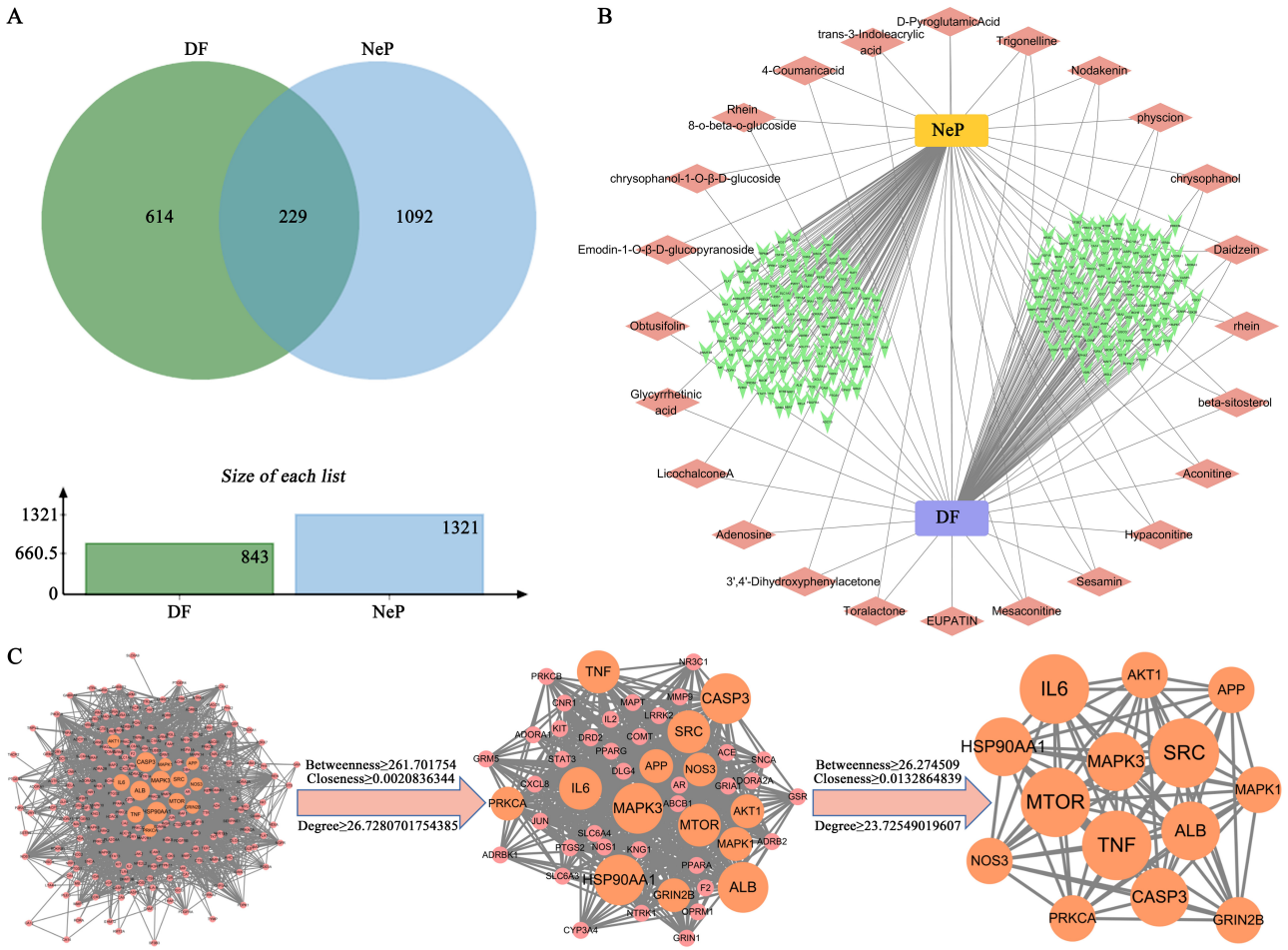

FIGURE 3
Prediction of the targets of DF against NeP by network pharmacology. **(A)** The Venn diagram of the common targets of DF and NeP. **(B)** Drug-disease-ingredients-targets network. **(C)** PPI network of targets of DF against NeP.

3.5 DF treatment reduced inflammatory cytokines levels in CCI model spinal cords

To investigate the anti-inflammatory effects of DF, levels of IL-1β, IL-6, and TNF-α in the spinal cord were assessed using ELISA. The medium-dose DF granules were selected due to their significant impact on hyperalgesia following CCI surgery. Results indicated that DF significantly reduced the elevated levels of IL-1β, IL-6, and TNF-α in the spinal cord caused by CCI surgery ($P < 0.01$), highlighting DF's inhibitory effects on neuroinflammation in NeP (Figures 5A–C).

3.6 DF treatment suppressed TNF-α and PI3K-AKT signaling pathways in in CCI model spinal cords

Based on KEGG enrichment analysis and inflammatory cytokine measurements, it was clear that the TNF-α and PI3K-AKT signaling pathways played crucial roles in DF's mechanism for treating NeP. To further examine this, the expression levels of key molecules involved in these pathway were evaluated in the spinal cord tissue. Results showed elevated levels of TNF-α, TNFR1, and phosphorylated PI3K, AKT, IKKα/β, IKBα, and NF-κB in the model group compared to the sham group ($P < 0.01$, Figure 6). In contrast, the DF-M group exhibited lower levels of TNF-α, TNFR1, and phosphorylated proteins compared to the model group ($P < 0.01$, Figure 6). These findings suggested that DF effectively suppressed the TNF-α and PI3K-AKT signaling pathway in CCI rat spinal cords. Additionally, immunofluorescence results indicated that expressions of the astrocyte marker GFAP, the microglia marker IBA, TNF-α, TNFR1, and phosphorylated AKT and NF-κB were significantly elevated in the model group relative to the sham group, while levels in the DF-M group were markedly reduced compared to the model group (Figure 7). Collectively, these results demonstrate that DF mediates its analgesic effects through the inhibition of the TNF-α and PI3K-AKT signaling pathways.

3.7 The molecular docking verification

To further investigate the direct interactions between DF ingredients and TNF-α, PI3K, and AKT, molecular docking was performed to predict their binding affinities. The results indicated

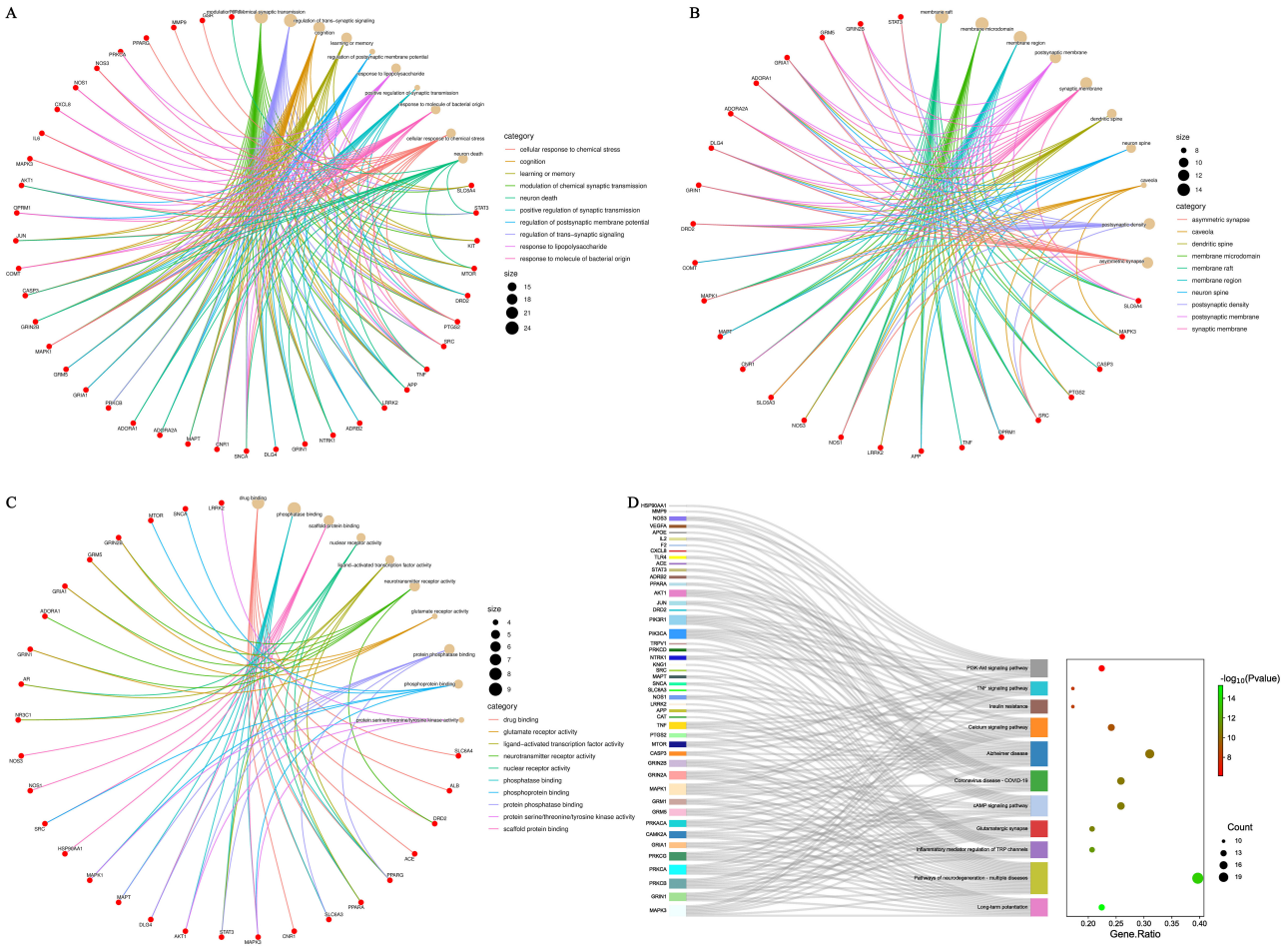

FIGURE 4
GO and KEGG enrichment analysis of the core targets of DF against NeP. **(A)** GO enrichment analysis of BP. **(B)** GO enrichment analysis of CC. **(C)** GO enrichment analysis of MF. **(D)** KEGG enrichment analysis.

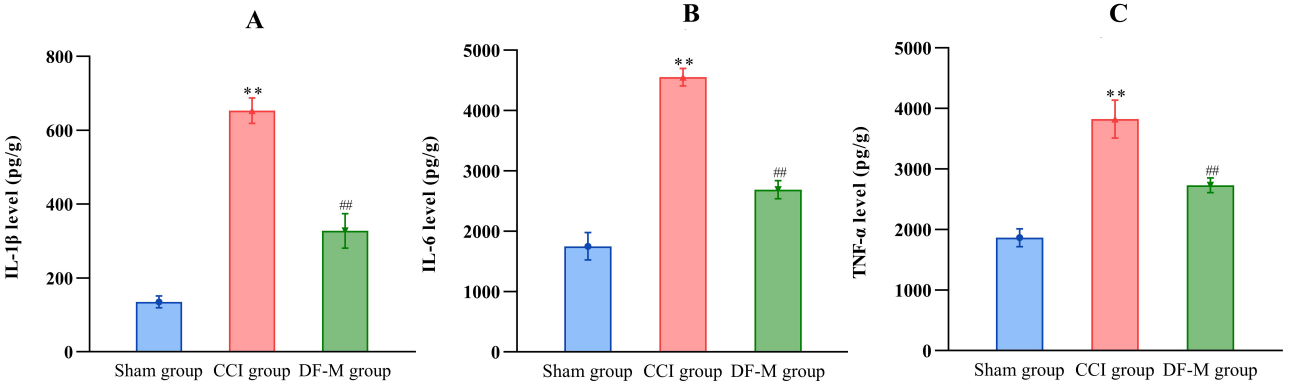

FIGURE 5
The effects of DF on the levels of inflammatory cytokines in the spinal cord of the CCI rats. **(A–C)** The levels of IL-1β, IL-6, and TNF-α in the spinal cord of the sham, CCI and DF-M group ($n = 3$ in each group). $^{**}P < 0.01$ compared with the sham group; $^{\#\#}P < 0.01$ compared with the CCI group.

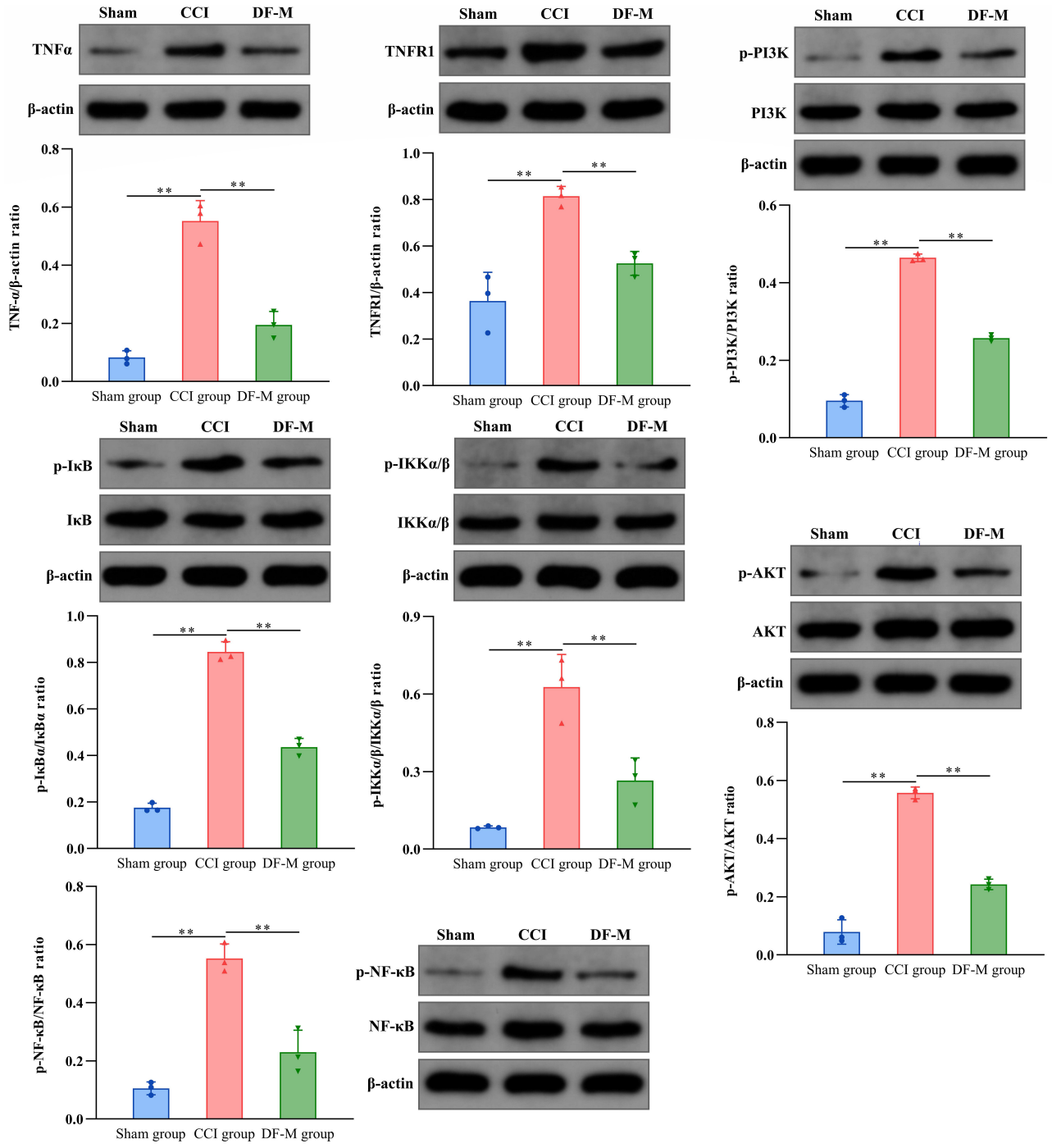

FIGURE 6
Effects of DF on the expressions of TNF-α and TNFR1, as well as the phosphorylation of PI3K, AKT, IKKα/β, IKBα, and NF-κB in the spinal cord of the sham group, CCI group, and DF-M group. Data are expressed as the mean ± SD ($n = 3$). **$p < 0.01$ compared to the CCI group.

that aconitine, chrysophanol, rhein, sesamin, and toralactone exhibited strong binding capabilities with both TNF-α and PI3K (Figure 8). Nodakenin, daidzein, and physcion showed significant binding affinity with TNF-α, while daidzein, obtusifolin, and beta-sitosterol demonstrated good binding potential with PI3K (Figure 8). These findings suggest that the diverse ingredients of DF can directly interact with specific targets, indicating that individual DF components may engage multiple targets associated with NeP.

4 Discussion

NeP is marked by a variety of clinical manifestations and a complex pathogenesis, significantly affecting patients' quality of life and imposing considerable economic, physical, and psychological burdens (Blyth, 2018). Therefore, it is crucial to urgently explore effective and safe treatments that address the underlying mechanisms of NeP. Recently, several TCM

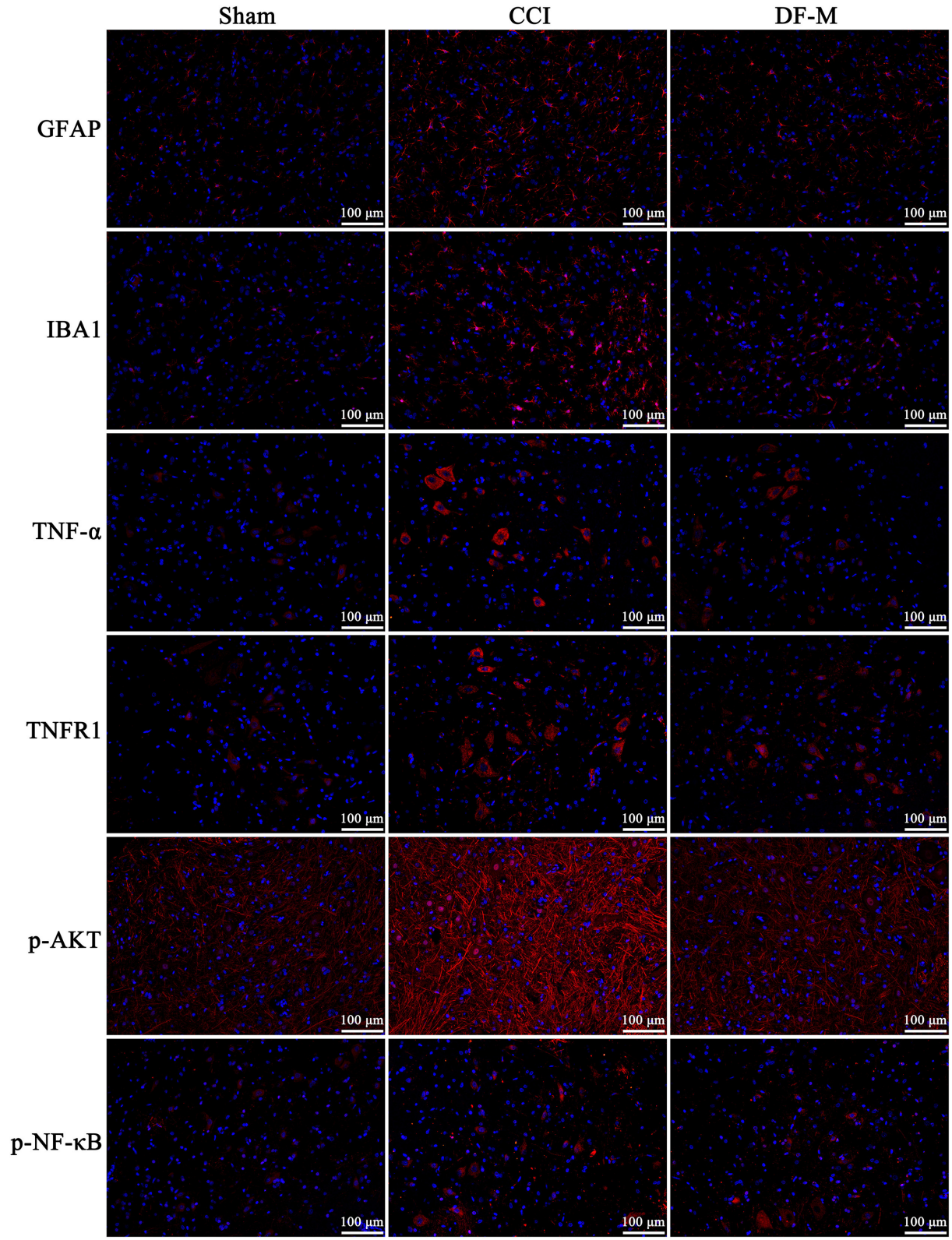

FIGURE 7
Immunofluorescence detection of the expressions of GFAP, IBA1, TNF-α, and TNFR1, as well as the phosphorylation of AKT and NF-κB in the spinal cord of the sham group, CCI group, and DF-M group. Spinal cord sections were stained with DAPI to visualize the nuclei (blue), while antibodies targeting the specific proteins were used for immunostaining (red).

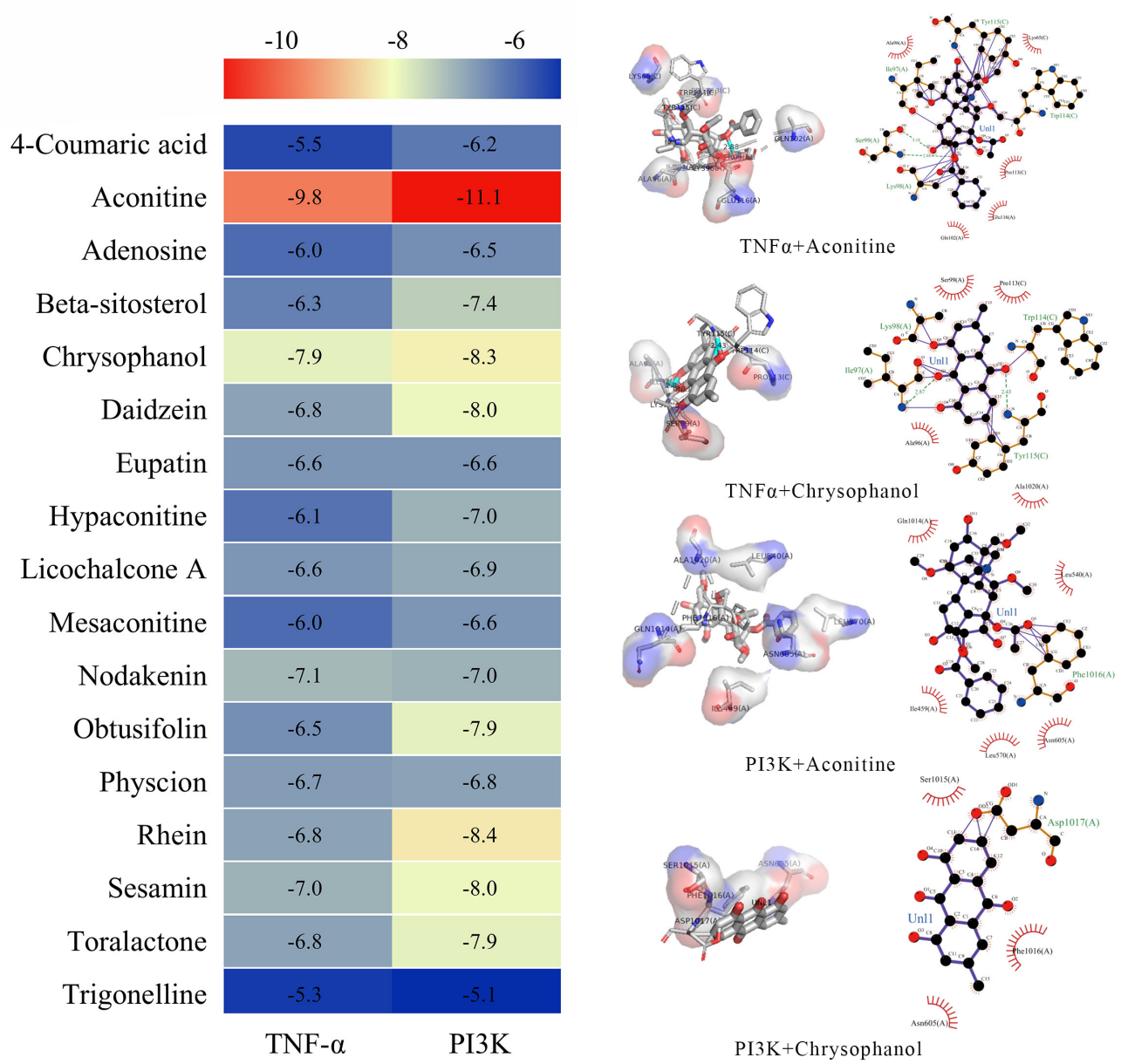

FIGURE 8
Molecular docking analysis of the binding affinity between the ingredients of DF and PI3K and TNF-α.

formulations have shown promise in alleviating NeP through multi-target strategies (Zhang et al., 2014, 2021). DF is a notable analgesic candidate due to its warming and pain-relieving properties, along with its ability to suppress inflammatory responses (Tu et al., 2014; Guo et al., 2022). Central sensitization is a key mechanism underlying the development and maintenance of neuropathic pain, significantly amplifying pain signaling within the nervous system. The spinal cord is the primary site where this process occurs, integrating and modulating nociceptive input, making it a crucial focus for understanding the persistence of neuropathic pain.

This study aims to elucidate, for the first time, the pharmacological mechanisms responsible for the analgesic effects of DF by integrating network pharmacology with experimental validation.

In our study, we first identified the components of DF using UHPLC-HRMS, successfully detecting a total of 24 distinct ingredients. Several of these compounds have been reported to possess anti-inflammatory, analgesic, and neuroprotective properties. Notably, aconitine, daidzein, licochalcone A, mesaconitine, and obtusifolin have demonstrated significant analgesic effects in various acute and chronic pain models. These effects are mediated through the regulation of transient receptor potential (TRP) channels, inhibition of microglial activation and neuroinflammation, as well as the suppression of neuronal apoptosis (He et al., 2014; Sun et al., 2020; Cankal et al., 2021; Deng

et al., 2021; Jin et al., 2023; Zafar et al., 2023). Additionally, sesamin has been shown to provide significant pain relief in patients with rheumatoid arthritis and to improve pain-related behaviors in rat models by reducing inflammatory mediators and inhibiting ROS-induced apoptosis (Deng et al., 2018; Helli et al., 2019). Furthermore, trigonelline, eupatin, and physcion have exhibited neuroprotective effects across various neurological disorders (Xunli et al., 2019; Chou et al., 2020; Liang et al., 2023).

We found that DF exhibited a significant analgesic effect in CCI rats and reduced inflammatory cytokine levels in the spinal cord. Neuroinflammation, defined as localized inflammation within the nervous system, is a key factor in the development of NeP. This condition is characterized by increased vascular permeability, the migration of inflammatory cells, activation of glial cells, and heightened secretion of inflammatory mediators (Teixeira-Santos et al., 2020). The interaction between microglia and astrocytes plays a crucial role in neuroinflammation associated with NeP. In our study, DF treatment resulted in significantly lower levels of IL-1β, IL-6, and TNF-α in the spinal cord compared to the CCI models, suggesting that DF effectively inhibits the CCI-induced inflammatory response. Additionally, we observed a marked reduction in the abnormal elevation of ionized calcium-binding adaptor molecule 1 (IBA1) and glial fibrillary acidic protein (GFAP) in response to DF treatment. These proteins are widely recognized markers for reactive microglia and astrocytes in the central nervous system (Chen et al., 2022; Hiraga et al., 2022).

To explore the mechanism by which DF alleviates neuroinflammation in the treatment of NeP, we performed network pharmacology analysis. The findings indicated that DF targets were primarily enriched in inflammation-related pathways, including the TNF-α signaling pathway, PI3K-AKT signaling pathway, and NF-κB signaling pathway. TNF-α, a key pro-inflammatory cytokine released from activated microglia, initiates a cytokine storm and activates pain-related pathways through TNF receptors, thus influencing central sensitization (Zhao et al., 2017; Chen et al., 2018). Numerous studies have shown that inhibiting TNF-α or genetically knocking out TNFR1 prevents NeP-induced hyperalgesia and aberrant synaptic plasticity changes (Liu et al., 2017; Lamacchia et al., 2019; Son et al., 2022). The transcription factor nuclear factor κB (NF-κB), a downstream effector of the TNF-α signaling pathway, acts as a master regulator of inflammation and other pathological processes in NeP (Niederberger and Geisslinger, 2008; Han et al., 2023). When TNF-α binds to TNFR1, the IκB kinase (IKK) complex, comprising IKKα, IKKβ, and the regulatory subunit IKKγ, is recruited and activated. This activated IKK phosphorylates NF-κB inhibitor-α (IκBα), resulting in its polyubiquitination and subsequent proteasomal degradation (Varfolomeev and Vucic, 2018). Consequently, NF-κB is released and translocates to the nucleus, where it activates various target genes and stimulates the production and release of inflammatory cytokines (Ding and Chen, 2023). Several studies have reported elevated expression of NF-κB in the spinal cords of various NeP animal models, and inhibiting NF-κB activity significantly reduces both the inflammatory response and neuronal excitability (Miao et al., 2020; Chen et al., 2023a,b; Khan et al., 2023). In our study, DF-M treatment significantly reduced the expression of TNF-α and TNFR1, as well as the phosphorylation levels of IKKα/β, IκBα, and NF-κB in the spinal cord of CCI rats. Thus, we conclude that the inhibition of TNF-α signaling is a critical mechanism underlying the analgesic effects of DF.

PI3K, a lipid kinase, plays a crucial role in several key intracellular signaling processes and regulates major cellular functions through its downstream target, AKT (He et al., 2022). Previous research has shown that the PI3K-AKT signaling pathway is involved in various pathological mechanisms associated with the onset and persistence of NeP by phosphorylating multiple critical downstream molecules, including NF-κB (Chen et al., 2017; Liu et al., 2018; Ji and Xu, 2021). In our study, we noted a significant reduction in the phosphorylation levels of PI3K and AKT in the spinal cords of rats treated with DF-M compared to CCI rats. These results indicate that DF may exert its analgesic effects in NeP by inhibiting the PI3K-AKT signaling pathway. However, we acknowledge that the mechanisms of action of DF are complex and may involve multiple signaling pathways. In future studies, we will employ multi-omics analysis and other methods to conduct in-depth investigations into other enriched signaling pathways, aiming to comprehensively elucidate the mechanisms of action of DF against NeP.

5 Conclusion

In conclusion, our findings indicate that DF effectively reduces CCI-induced mechanical and thermal hyperalgesia by inhibiting neuroinflammation in the spinal cord, primarily mediated through the TNF-α and PI3K-AKT signaling pathways. These results offer a new perspective for research aimed at developing analgesic drugs that target neuroinflammation.

Data availability statement

The raw data supporting the conclusions of this article will be made available by the authors, without undue reservation.

Ethics statement

The animal study was approved by the First Affiliated Hospital of Guangzhou University of Chinese Medicine (License No. GZTCMF1). The study was conducted in accordance with the local legislation and institutional requirements.

Author contributions

JQ: Conceptualization, Project administration, Writing – original draft. QG: Project administration, Writing – original draft. SH: Writing – original draft, Software. JP: Project administration, Writing – original draft. LC: Writing – review & editing, Validation. LW: Conceptualization, Supervision, Writing – review & editing.

PC: Conceptualization, Funding acquisition, Methodology, Writing – review & editing.

Funding

The author(s) declare that financial support was received for the research, authorship, and/or publication of this article. This work was supported by Grants from Guizhou Science and Technology Foundation [[ZK 2021] General 544], National Natural Science Foundation of China (82104658 and 82360894), Guangdong Administration of Traditional Chinese Medicine Research Project (20221239), and Guangzhou Chinese Medicine and Integrated Traditional Chinese and Western Medicine Science and Technology project (20222A011014).

Acknowledgments

We thank Shuai Ye of Fudan University for help with our study.

Conflict of interest

The authors declare that the research was conducted in the absence of any commercial or financial relationships that could be construed as a potential conflict of interest.

Publisher's note

Supplementary material

The Supplementary Material for this article can be found online at: https://www.frontiersin.org/articles/10.3389/fnins.2024.1464477/full#supplementary-material

References

Blyth, F. M. (2018). Global burden of neuropathic pain. *Pain* 159, 614–617. doi: 10.1097/j.pain.0000000000001127

Cankal, D., Akkol, E. K., Kilinc, Y., Ilhan, M., and Capasso, R. (2021). An effective phytoconstituent aconitine: a realistic approach for the treatment of trigeminal neuralgia. *Mediat. Inflamm.* 2021:6676063. doi: 10.1155/2021/6676063

Chen, G., Zhang, Y. Q., Qadri, Y. J., Serhan, C. N., and Ji, R. R. (2018). Microglia in pain: detrimental and protective roles in pathogenesis and resolution of pain. *Neuron* 100, 1292–1311. doi: 10.1016/j.neuron.2018.11.009

Chen, P., Huang, N. Y., Pang, B., Ye, Z. J., Luo, R. X., and Liu, C., et al. (2023a). Proteomic and metabolomic approaches elucidate the molecular mechanism of emodin against neuropathic pain through modulating the gamma-aminobutyric acid (GABA)-ergic pathway and PI3K/AKT/NF-kappaB pathway. *Phytother. Res.* 37, 1883–1899. doi: 10.1002/ptr.7704

Chen, P., Wang, C., Gong, Q., Chai, Y., Chen, Y., and Song, C., et al. (2023b). Alterations of endogenous pain-modulatory system of the cerebral cortex in the neuropathic pain. *iScience* 26:106668. doi: 10.1016/j.isci.2023.106668

Chen, S. P., Zhou, Y. Q., Liu, D. Q., Zhang, W., Manyande, A., and Guan, X. H., et al. (2017). PI3K/Akt pathway: a potential therapeutic target for chronic pain. *Curr. Pharm. Des.* 23, 1860–1868. doi: 10.2174/1381612823666170210150147

Chen, Y. L., Feng, X. L., Cheung, C. W., and Liu, J. A. (2022). Mode of action of astrocytes in pain: from the spinal cord to the brain. *Prog. Neurobiol.* 219:102365. doi: 10.1016/j.pneurobio.2022.102365

Chou, C. H., Hsu, K. C., Lin, T. E., and Yang, C. R. (2020). Anti-inflammatory and tau phosphorylation-inhibitory effects of eupatin. *Molecules* 25:5625. doi: 10.3390/molecules25235652

Deng, J., Han, J., Chen, J., Zhang, Y., Huang, Q., and Wang, Y., et al. (2021). Comparison of analgesic activities of aconitine in different mice pain models. *PLoS ONE* 16:e0249276. doi: 10.1371/journal.pone.0249276

Deng, S., Zhou, J. L., Fang, H. S., Nie, Z. G., Chen, S., and Peng, H. (2018). Sesamin protects the femoral head from osteonecrosis by inhibiting ROS-induced osteoblast apoptosis in rat model. *Front. Physiol.* 9:1787. doi: 10.3389/fphys.2018.01787

Ding, Y., and Chen, Q. (2023). The NF-kappaB pathway: a focus on inflammatory responses in spinal cord injury. *Mol. Neurobiol.* 60, 5292–5308. doi: 10.1007/s12035-023-03411-x

Dosenovic, S., Jelicic, K. A., Miljanovic, M., Biocic, M., Boric, K., and Cavar, M., et al. (2017). Interventions for neuropathic pain: an overview of systematic reviews. *Anesth. Analg.* 125, 643–652. doi: 10.1213/ANE.0000000000001998

Finnerup, N. B., Attal, N., Haroutounian, S., Mcnicol, E., Baron, R., and Dworkin, R. H., et al. (2015). Pharmacotherapy for neuropathic pain in adults: a systematic review and meta-analysis. *Lancet Neurol.* 14, 162–173. doi: 10.1016/S1474-4422(14)70251-0

Finnerup, N. B., Kuner, R., and Jensen, T. S. (2021). Neuropathic pain: from mechanisms to treatment. *Physiol. Rev.* 101, 259–301. doi: 10.1152/physrev.00045.2019

Fiore, N. T., Debs, S. R., Hayes, J. P., Duffy, S. S., and Moalem-Taylor, G. (2023). Pain-resolving immune mechanisms in neuropathic pain. *Nat. Rev. Neurol.* 19, 199–220. doi: 10.1038/s41582-023-00777-3

Gu, M., Ying, P., Miao, Z., Yu, X., Bao, R., and Xiao, J., et al. (2022). Treatment of modified dahuang fuzi decoction on cognitive impairment induced by chronic kidney disease through regulating AhR/NF-kappaB/JNK signal pathway. *Evid. Bas. Complement Altern. Med.* 2022:8489699. doi: 10.1155/2022/8489699

Guo, J. F., Zhao, Y. T., Du, Q. Y., Ren, Y., Wang, Y., and Wang, Z. X., et al. (2022). The network pharmacology study of dahuang fuzi decoction for treating incomplete intestinal obstruction. *Biomed. Res. Int.* 2022:2775434. doi: 10.1155/2022/2775434

Han, G., Li, X., Wen, C. H., Wu, S., He, L., and Tan, C., et al. (2023). FUS contributes to nerve injury-induced nociceptive hypersensitivity by activating NF-kappaB pathway in primary sensory neurons. *J. Neurosci.* 43, 1267–1278. doi: 10.1523/JNEUROSCI.2082-22.2022

He, X., Li, Y., Deng, B., Lin, A., Zhang, G., and Ma, M., et al. (2022). The PI3K/AKT signalling pathway in inflammation, cell death and glial scar formation after traumatic spinal cord injury: mechanisms and therapeutic opportunities. *Cell Prolif.* 55:e13275. doi: 10.1111/cpr.13275

He, Z. W., Wei, W., Li, S. P., Ling, Q., Liao, K. J., and Wang, X. (2014). Anti-allodynic effects of obtusifolin and gluco-obtusifolin against inflammatory and neuropathic pain. *Biol. Pharm. Bull.* 37, 1606–1616. doi: 10.1248/bpb.c14-00307

Helli, B., Shahi, M. M., Mowla, K., Jalali, M. T., and Haghighian, H. K. (2019). A randomized, triple-blind, placebo-controlled clinical trial, evaluating the sesamin supplement effects on proteolytic enzymes, inflammatory markers, and clinical indices in women with rheumatoid arthritis. *Phytother. Res.* 33, 2421–2428. doi: 10.1002/ptr.6433

Hiraga, S. I., Itokazu, T., Nishibe, M., and Yamashita, T. (2022). Neuroplasticity related to chronic pain and its modulation by microglia. *Inflamm. Regen.* 42:15. doi: 10.1186/s41232-022-00199-6

Inoue, K., and Tsuda, M. (2018). Microglia in neuropathic pain: cellular and molecular mechanisms and therapeutic potential. *Nat. Rev. Neurosci.* 19, 138–152. doi: 10.1038/nrn.2018.2

Ji, A., and Xu, J. (2021). Neuropathic pain: biomolecular intervention and imaging via targeting microglia activation. *Biomolecules* 11:1343. doi: 10.3390/biom11091343

Ji, R. R., Nackley, A., Huh, Y., Terrando, N., and Maixner, W. (2018). Neuroinflammation and central sensitization in chronic and widespread pain. *Anesthesiology* 129, 343–366. doi: 10.1097/ALN.0000000000002130

Jin, X., Cheng, J., Zhang, Q., Ji, H., Zhu, C., and Yang, Y., et al. (2023). Aconitine—a promising candidate for treating cold and mechanical allodynia in cancer induced bone pain. *Biomed. Pharmacother*. 161:114284. doi: 10.1016/j.biopha.2023.114284

Khan, A., Shal, B., Ullah, K. A., Ullah, S. K., Saniya, Z. S., and Ul, H. I., et al. (2023). Neuroprotective mechanism of Ajugarin-I against Vincristine-Induced neuropathic pain via regulation of Nrf2/NF-kappaB and Bcl2 signalling. *Int. Immunopharmacol*. 118:110046. doi: 10.1016/j.intimp.2023.110046

Lamacchia, Z. M., Spengler, R. N., Jaffari, M., Abidi, A. H., Ahmed, T., and Singh, N., et al. (2019). Perispinal injection of a TNF blocker directed to the brain of rats alleviates the sensory and affective components of chronic constriction injury-induced neuropathic pain. *Brain. Behav. Immun*. 82, 93–105. doi: 10.1016/j.bbi.2019.07.036

Latremoliere, A., and Woolf, C. J. (2009). Central sensitization: a generator of pain hypersensitivity by central neural plasticity. *J. Pain* 10, 895–926. doi: 10.1016/j.jpain.2009.06.012

Liang, Y., Dai, X., Cao, Y., Wang, X., Lu, J., and Xie, L., et al. (2023). The neuroprotective and antidiabetic effects of trigonelline: a review of signaling pathways and molecular mechanisms. *Biochimie* 206, 93–104. doi: 10.1016/j.biochi.2022.10.009

Liu, T., Li, T., Chen, X., Zhang, K., Li, M., and Yao, W., et al. (2021). A network-based analysis and experimental validation of traditional Chinese medicine Yuanhu Zhitong Formula in treating neuropathic pain. *J. Ethnopharmacol*. 274:114037. doi: 10.1016/j.jep.2021.114037

Liu, W., Lv, Y., and Ren, F. (2018). PI3K/Akt pathway is required for spinal central sensitization in neuropathic pain. *Cell. Mol. Neurobiol*. 38, 747–755. doi: 10.1007/s10571-017-0541-x

Liu, Y., Zhou, L. J., Wang, J., Li, D., Ren, W. J., and Peng, J., et al. (2017). TNF-alpha differentially regulates synaptic plasticity in the hippocampus and spinal cord by microglia-dependent mechanisms after peripheral nerve injury. *J. Neurosci*. 37, 871–881. doi: 10.1523/JNEUROSCI.2235-16.2016

Liu, Y. W., Chen, Y. J., Chen, Y. H., and Tsai, M. Y. (2022). Therapeutic efficacy of traditional Chinese medicine syndrome-based formulae to neuropathic pain caused by chemotherapy. *Integr. Cancer Ther*. 21:1553436231. doi: 10.1177/15347354221121095

Lutolf, R., Rosner, J., Curt, A., and Hubli, M. (2022). Indicators of central sensitization in chronic neuropathic pain after spinal cord injury. *Eur. J. Pain* 26, 2162–2175. doi: 10.1002/ejp.2028

Miao, J., Zhou, X., Ji, T., and Chen, G. (2020). NF-kappaB p65-dependent transcriptional regulation of histone deacetylase 2 contributes to the chronic constriction injury-induced neuropathic pain via the microRNA-183/TXNIP/NLRP3 axis. *J. Neuroinflam.* 17:225. doi: 10.1186/s12974-020-01901-6

Niederberger, E., and Geisslinger, G. (2008). The IKK-NF-kappaB pathway: a source for novel molecular drug targets in pain therapy? *FASEB. J.* 22, 3432–3442. doi: 10.1096/fj.08-109355

Popiolek-Barczyk, K., and Mika, J. (2016). Targeting the microglial signaling pathways: new insights in the modulation of neuropathic pain. *Curr. Med. Chem*. 23, 2908–2928. doi: 10.2174/0929867323666160607120124

Racine, M., Moulin, D. E., Nielson, W. R., Morley-Forster, P. K., Lynch, M., and Clark, A. J., et al. (2016). The reciprocal associations between catastrophizing and pain outcomes in patients being treated for neuropathic pain: a cross-lagged panel analysis study. *Pain* 157, 1946–1953. doi: 10.1097/j.pain.0000000000000594

Shi, X. Q., Yue, S. J., Tang, Y. P., Chen, Y. Y., Zhou, G. S., and Zhang, J., et al. (2019). A network pharmacology approach to investigate the blood enriching mechanism of Danggui buxue Decoction. *J. Ethnopharmacol*. 235, 227–242. doi: 10.1016/j.jep.2019.01.027

Son, J. Y., Ju, J. S., Kim, Y. M., and Ahn, D. K. (2022). TNF-alpha-mediated RIPK1 pathway participates in the development of trigeminal neuropathic pain in rats. *Int. J. Mol. Sci*. 23:506. doi: 10.3390/ijms23010506

Sun, Z., Yang, L., Zhao, L., Cui, R., and Yang, W. (2020). Neuropharmacological effects of mesaconitine: evidence from molecular and cellular basis of neural circuit. *Neural Plast*. 2020:8814531. doi: 10.1155/2020/8814531

Tai, C. J., El-Shazly, M., Tsai, Y. H., Csupor, D., Hohmann, J., and Wu, Y. C., et al. (2021). Uncovering modern clinical applications of fuzi and fuzi-based formulas: a nationwide descriptive study with market basket analysis. *Front. Pharmacol*. 12:641530. doi: 10.3389/fphar.2021.641530

Teixeira-Santos, L., Albino-Teixeira, A., and Pinho, D. (2020). Neuroinflammation, oxidative stress and their interplay in neuropathic pain: focus on specialized pro-resolving mediators and NADPH oxidase inhibitors as potential therapeutic strategies. *Pharmacol. Res*. 162:105280. doi: 10.1016/j.phrs.2020.105280

Tu, Y., Sun, W., Wan, Y. G., Gao, K., Liu, H., and Yu, B. Y., et al. (2014). Dahuang Fuzi Decoction ameliorates tubular epithelial apoptosis and renal damage via inhibiting TGF-beta1-JNK signaling pathway activation *in vivo*. *J. Ethnopharmacol*. 156, 115–124. doi: 10.1016/j.jep.2014.08.035

Varfolomeev, E., and Vucic, D. (2018). Intracellular regulation of TNF activity in health and disease. *Cytokine* 101, 26–32. doi: 10.1016/j.cyto.2016.08.035

Wang, K., Wang, F., Bao, J. P., Xie, Z. Y., Chen, L., and Zhou, B. Y., et al. (2017). Tumor necrosis factor alpha modulates sodium-activated potassium channel SLICK in rat dorsal horn neurons via p38 MAPK activation pathway. *J. Pain Res*. 10, 1265–1271. doi: 10.2147/JPR.S132185

Wang, X., Lin, C., Jin, S., Wang, Y., Peng, Y., and Wang, X. (2023). Cannabidiol alleviates neuroinflammation and attenuates neuropathic pain via targeting FKBP5. *Brain. Behav. Immun*. 111, 365–375. doi: 10.1016/j.bbi.2023.05.008

Xunli, L.iu, Y., Chu, S., Yang, S., Peng, Y., and Ren, S., et al. (2019). Physcion and physcion 8-O-beta-glucopyranoside: a review of their pharmacology, toxicities and pharmacokinetics. *Chem. Biol. Interact*. 310:108722. doi: 10.1016/j.cbi.2019.06.035

Zafar, S., Luo, Y., Zhang, L., Li, C. H., Khan, A., and Khan, M. I., et al. (2023). Daidzein attenuated paclitaxel-induced neuropathic pain via the down-regulation of TRPV1/P2Y and up-regulation of Nrf2/HO-1 signaling. *Inflammopharmacology* 23:1225. doi: 10.1007/s10787-023-01225-w

Zhang, J., Liang, R., Wang, L., and Yang, B. (2019). Effects and mechanisms of Danshen-Shanzha herb-pair for atherosclerosis treatment using network pharmacology and experimental pharmacology. *J. Ethnopharmacol*. 229, 104–114. doi: 10.1016/j.jep.2018.10.004

Zhang, J. Y., Hong, C. L., Chen, H. S., Zhou, X. J., Zhang, Y. J., and Efferth, T., et al. (2019). Target identification of active constituents of Shen Qi Wan to treat kidney yang deficiency using computational target fishing and network pharmacology. *Front. Pharmacol*. 10:650. doi: 10.3389/fphar.2019.00650

Zhang, X., Wang, Y., Zhang, K., Sheng, H., Wu, Y., and Wu, H., et al. (2021). Discovery of tetrahydropalmatine and protopine regulate the expression of dopamine receptor D2 to alleviate migraine from Yuanhu Zhitong formula. *Phytomedicine* 91:153702. doi: 10.1016/j.phymed.2021.153702

Zhang, Y., Wang, C., Wang, L., Parks, G. S., Zhang, X., and Guo, Z., et al. (2014). A novel analgesic isolated from a traditional Chinese medicine. *Curr. Biol*. 24, 117–123. doi: 10.1016/j.cub.2013.11.039

Zhao, H., Alam, A., Chen, Q., A, E. M., Pal, A., and Eguchi, S., et al. (2017). The role of microglia in the pathobiology of neuropathic pain development: what do we know? *Br. J. Anaesth*. 118, 504–516. doi: 10.1093/bja/aex006

frontiers | Frontiers in Pharmacology

TYPE Brief Research Report
PUBLISHED 18 December 2024
DOI 10.3389/fphar.2024.1459735

OPEN ACCESS

EDITED BY
Álvaro Llorente-Berzal,
Autonomous University of Madrid, Spain

REVIEWED BY
Isabella Salzer,
Medical University of Vienna, Austria
Ivan Ezquerra Romano,
Helmholtz Association of German Research Centers (HZ), Germany

*CORRESPONDENCE
Ruirui Lu,
Lu@em.uni-frankfurt.de

RECEIVED 04 July 2024
ACCEPTED 26 November 2024
PUBLISHED 18 December 2024

CITATION
Engel P, Zhou F, Tran BTT, Schmidtko A and Lu R (2024) Slick potassium channels limit TRPM3-mediated activation of sensory neurons. *Front. Pharmacol.* 15:1459735. doi: 10.3389/fphar.2024.1459735

Slick potassium channels limit TRPM3-mediated activation of sensory neurons

Patrick Engel, Fangyuan Zhou, Bang Tam Thi Tran, Achim Schmidtko and Ruirui Lu*

Institute of Pharmacology and Clinical Pharmacy, Goethe University Frankfurt, Frankfurt, Germany

Heat sensation is mediated by specialized heat-sensitive neurons in the somatosensory system that innervates the skin. Previous studies revealed that noxious heat sensation is controlled by the sodium (Na^+)-activated potassium (K^+) channel Slick (Kcnt2), which is highly expressed in nociceptive Aδ-fibers. However, the mechanism by which Slick modulates heat sensation is poorly understood. Here, we generated mice lacking Slick conditionally in sensory neurons expressing Nav1.8 (SNS-Slick$^{-/-}$ mice). In SNS-Slick$^{-/-}$ mice, the latency to express any nocifensive behavior was reduced in the hot plate and tail immersion tests. *In situ* hybridization experiments revealed Slick was highly co-expressed with the essential heat sensor, transient receptor potential (TRP) melastatin (TRPM) 3, but not with TRP vanilloid 1, TRP ankyrin 1, or TRPM2 in sensory neurons. Notably, SNS-Slick$^{-/-}$ mice exhibited increased nocifensive behaviors following intraplantar injection of the TRPM3 activator pregnenolone sulfate. Patch-clamp recordings detected increased Na^+-dependent outward K^+ current (I_K) after TRPM3 activation in sensory neurons, which showed no prominent I_K after the replacement of NaCl with choline chloride. Thus, our study suggests that Slick limits TRPM3-mediated activation of sensory neurons, thereby inhibiting noxious heat sensing.

KEYWORDS

heat nociception, TRPM3, Slick, sensory neurons, potassium current

1 Introduction

Potassium (K^+) ion channels are a diverse group of ion channels that selectively enable the rapid diffusive flow of K^+ across the plasma membrane, thereby shaping the neuron response. They play key roles in controlling neuronal activity and signal propagation throughout the nervous system (Ocana et al., 2004; Tsantoulas and McMahon, 2014). Slick (also known as $K_{Na}1.2$ or Slo2.1; *Kcnt2* gene), a Na^+-activated K^+ (K_{Na}) channel, is highly expressed in the nervous system and is involved in various physiological and pathological functions (Kaczmarek, 2013; Kaczmarek et al., 2017). Various studies, including ours, showed that mice lacking Slick globally (Slick$^{-/-}$) exhibit increased nocifensive responses to noxious heat (Tomasello et al., 2017; Flauaus et al., 2022). However, the specific roles of Slick in noxious heat sensation remains unclear.

Noxious heat is detected by various heat-sensitive ion channels in the plasma membranes of sensory neurons with cell bodies located in the dorsal root ganglia (DRGs) and trigeminal ganglia. Several heat-sensitive members of the transient receptor potential (TRP) ion channels superfamily, including TRP vanilloid 1 (TRPV1), TRP ankyrin 1 (TRPA1), TRP melastatin (TRPM) 3 (TRPM3) and TRPM2, have been identified (Vandewauw et al., 2018; Vriens and

Voets, 2018; Vilar et al., 2020). Deletion of TRPV1, TRPA1 and TRPM3 in mice alters the behavioral sensation of heat at noxious temperatures >45°C (Vandewauw et al., 2018). TRPM2 is activated at 30°C–40°C *in vivo* (Tan and McNaughton, 2016; Vilar et al., 2020). After these channels are activated by noxious heat, rapid influx of calcium (Ca^{2+}) and sodium (Na^{+}) causes depolarization of the membrane potential, leading to action potential firing in response to painful stimuli (Vangeel and Voets, 2019; Zhang et al., 2023). We hypothesized that Slick in sensory neurons can be functionally coupled to any of these essential heat sensors. To test this hypothesis, we generated tissue-specific knockout mice lacking Slick in sensory neurons and performed behavioral, electrophysiological, and tissue-staining experiments in this study. Our data suggest that Slick is functionally coupled to TRPM3 in sensory neurons.

2 Materials and methods

2.1 Animals

Slick$^{-/-}$ and wild-type mice with C57BL/6 background were generated as previously described (Flauaus et al., 2022). To ablate Slick selectively in sensory neurons, floxed Slick (Slick$^{fl/fl}$) mice (B6(129S4)-Kcnt2$^{tm1.1Clin}$/J, JAX stock No. 028419; The Jackson Laboratory, United States) were crossed with SNS-Cre mice, which express the Nav1.8-driven Cre recombinase in nearly all primary nociceptive neurons (Agarwal et al., 2004), to obtain homozygous conditional Slick knockout mice (SNS-Slick$^{-/-}$). Littermate Slick$^{fl/fl}$ mice were used as controls. The mice were provided free access to food and water, and group-housed under a 12:12 light/dark cycle with controlled temperature (22°C ± 2°C) and humidity (55% ± 10%). Experiments were performed with 8- to 16-week-old animals. Littermate mice of both sexes were used in the behavioral studies. All experiments adhered to the Animal Research: Reporting on *In Vivo* Experiments guidelines and Replacement, Reduction, and Refinement principles, and were approved by our local Ethics Committee for Animal Research (Regierungspräsidium Darmstadt, Germany).

2.2 Real-time reverse transcription (RT)-polymerase chain reaction (PCR)

Mice were euthanized via carbon dioxide (CO_2) inhalation, and lumbar (L4–L5) DRGs, lumbar (L4–L5) spinal cord, and prefrontal cortex were rapidly dissected, snap frozen in liquid nitrogen and stored at −80°C until use. Total RNA was isolated using the innuPREP Micro RNA Kit (#C-6134; Analytik Jena, Berlin, Germany) following the manufacturer's instructions. Isolated RNA was quantified with a NanoDrop 2000 (Thermo Fisher Scientific, Dreieich, Germany), and cDNA was synthesized from 200 ng RNA using the first-strand cDNA synthesis kit (#10774691; Thermo Fisher Scientific) with random hexamer primers. qRT-PCR was performed with the CFX96 Touch Real-Time System (Bio-Rad, Hercules, Germany) using the iTaq Universal SYBR Green SuperMix (#1725120; Bio-Rad) and primer pairs (Biomers, Ulm, Germany) for Slick, TRPA1, TRPV1, TRPM3, and glyceraldehyde 3-phosphate dehydrogenase. All primer sequences used are listed in Table 1. Reactions were performed in duplicate by incubating for 2 min at 50°C and 10 min at 95°C, followed by 40 cycles of 15 s at 95°C and 60 s at 60°C. Water was used as a control to ensure specificity. Relative expression of the target gene levels was determined using the comparative $2^{-\Delta\Delta CT}$ method and normalized to that of glyceraldehyde 3-phosphate dehydrogenase.

TABLE 1 List of primers, antibodies and *in situ* hybridization probes used.

List of RT-qPCR primers used	
Slick	fwd: 5′-gaaagcaccatgagtgcaga-3′; rev: 5′-gttttgaaagcgcgagagag-3′
Slack	fwd 5′-ctgctgtgcctggtcttca-3′, rev 5′-aaggaggtcagcaggttcaa-3′
TRPA1	fwd 5′-ggaaataccccactgcattgt-3′, rev 5′-cagctatgtgaaggggtgaca-3′
TRPV1	fwd 5′-actcttaccacacagcagcc-3′, rev 5′-gcccaatttgcaaccagcta-3′
TRPM3	fwd 5′-ggtgtggcttcaggagtact-3′, rev 5′-ccagatacttgttcacgccg-3′
TRPM2	fwd 5′-ctgcgcctagcgatgagatg-3′, rev 5′-catcctggacatactggtctgc-3′
GAPDH	fwd 5′-caatgtgtccgtcgtggatct-3′, rev 5′-gtcctcagtgtagcccaagatg-3′

List of antibodies used	
mouse anti-neurofilament 200	NF200, 1:2000, #N0142, Sigma-Aldrich
rabbit anti-calcitonin gene-related peptide	CGRP; 1:800, #PC205L, Sigma-Aldrich
rabbit anti-vesicular glutamate transporter 3	VGLUT3, 1:100, #135203, Synaptic Systems
mouse anti-Slick	1:500, clone N11/33, #75-055, antibodiesinc
goat anti-mouse AF555	1:1000, #A21127. Thermo Fisher Scientific
goat anti-rabbit AF488	1:1000, #A11008. Thermo Fisher Scientific
Alexa Fluor 488-conjugated IB4	3.3 µg/ml, #121411, Thermo Fisher Scientific
Alexa Fluor 488-conjugated anti-tubulin β3	1:1000, #801203, BioLegend

List of *in situ* hybridization probes used (Thermo Fisher Scientific)	
type-1 probe for mouse Slick	1:40; #VB1-17744
type-1 probe for mouse scramble control	1:40; #VF1-17155
type-6 probe for mouse TRPA1	1:20; #VB6-18246
type-6 probe for mouse TRPV1	1:80; #VB6-16610
type-6 probe for mouse TRPM3	1:40; #VB6-3216456-VT
type-6 probe for mouse TRPM2	1:20; #VB6-3197141-01
type-6 probe for mouse scramble control	1:40; #VF6-18580

2.3 Immunohistochemistry and *in situ* hybridization

Mice were euthanized via CO_2 inhalation and intracardially perfused with 0.9% saline, followed by 1% or 4% paraformaldehyde

in phosphate-buffered saline (PBS) at pH 7.4. Lumbar (L4–L5) DRGs, sciatic nerves and lumbar (L4–L5) spinal cord were dissected, cryoprotected with 30% sucrose overnight, frozen in a tissue freezing medium (Tissue-Tek O.C.T. Compound; #4583; Sakura, Torrance, CA, United States) on dry ice, cut into 14- or 20-µm sections with a cryostat (CRYOSTAR NX50; Thermo Fisher Scientific) placed directly onto the adhesion microscope slide (#J1800AMNZ; Epredia, Breda, Netherlands), and stored at −80°C.

Immunohistochemistry was performed as previously described (Flauaus et al., 2022). The following primary antibodies were used: mouse anti-neurofilament 200 (NF200), rabbit anti-calcitonin gene-related peptide (CGRP), rabbit anti-vesicular glutamate transporter 3 (VGLUT3), and mouse anti-Slick. All antibodies used are listed in Table 1. After incubation with the primay antibodies, the sections were washed in PBS and incubated with the AlexaFluor-conjugated secondary antibodies (Thermo Fisher Scientific) diluted 1:1000. For *Griffonia simplicifolia* isolectin B4 (IB4) staining, the sections were incubated with Alexa Fluor 488-conjugated IB4 (3.3 µg/mL in PBS buffer containing 1 mM $CaCl_2{\cdot}2H_2O$, 1 mM $MgCl_2$, 1 mM $MnCl_2$ and 0.2% Trion X-100, pH = 7.4) for 2 h at 4°C. For βIII-tubulin (TUBB3) staining, the sections were incubated with Alexa Fluor 488-conjugated anti-tubulin β3 antibody diluted in PBS for 2 h at 4°C. After immunostaining, the slides were washed with PBS, and cover-slipped with Fluoromount-G (No. 00–4958-02; Thermo Fisher Scientific). All antibodies used are listed in Table 1.

For *in situ* hybridization, the QuantiGene View-RNA tissue assay (Affymetrix, Thermo Fisher Scientific) was performed as previously described (Flauaus et al., 2022). Type-1 probe sets for mouse Slick, mouse scramble control, and type-6 probe sets for mouse TRPA1, TRPV1, TRPM3, TRPM2, and mouse scramble control were used. All probe sets used are listed in Table 1. In double *in situ* hybridization experiments, type-1 and type-6 labeled probes were simultaneously incubated. Finally, the sections were mounted using Fluoromount G.

Images were captured using the Eclipse Ni-U microscope (Nikon Europe B.V., Amsterdam, Netherlands) equipped with a monochrome DS-Qi2 camera (Nikon Europe B.V.). Specificity controls included omitting the first and/or the second primary antibodies, incubating type-1 and type-6 scramble probes, and incubating tissues of $Slick^{-/-}$ mice.

For quantification of marker-positive neuron subpopulations in DRGs, serial sections of DRGs from SNS-$Slick^{-/-}$ and control mice were cut, and 3–4 sections, at least 100 µm apart, per animal were counted. Only cells exhibiting clear staining above specificity control were included. The percentage of marker-positive DRG neurons is expressed as the ratio of marker-positive cells to number of pan-neuronal marker βIII-tubulin.

To quantify the intensity of Slick immunoreactivity in lamina I and outer lamina II of the dorsal horn, spinal cord sections of SNS-$Slick^{-/-}$ and control mice were double-stained with antibodies to Slick and CGRP, and images were taken using the Eclipse Ni-U microscope. Grey value images were analyzed using ImageJ software (National institution Health, MD, United States). The area of CGRP-immunoreactivity was manually selected by the polygon selection tool and considered as the region of interest. The same region of interest was evaluated in the corresponding Slick image. With the analysis function, the mean gray value was measured in the defined region of interest.

2.4 Behavioral assays

All mice were acclimatized to the experimental environment for at least 2 days before the testing and were investigated by an observer blinded to the mouse genotype. All experiments were performed between 8:00 a.m. and 5:00 p.m.

2.4.1 Rotarod test

The mice were tested for overall motor coordination and balance using a rotarod apparatus (Ugo Basile, Comerio, Italy) programmed gradually and uniformly to accelerate from 4 to 40 revolutions per minute for 300 s. The latency to fall off from the rotarod was recorded up to 300 s using a stopwatch. After the mice were trained for 3 consecutive days, three consecutive falls were recorded on the experiment day (Harada et al., 2017; Vandewauw et al., 2018).

2.4.2 Hot plate test

Mice were individually confined to a Plexiglas cylinder on a heated metal surface (Hot/Cold Plate; Ugo Basile). The time interval between placement and observation of nocifensive behaviors (shaking or licking of the hindpaw, jumping) was recorded, and the mice were removed from the plate immediately after a notable response. To prevent tissue damage, temperatures of 47, 48, 49 and 50°C were applied with cut-off times of 90, 80, 70, and 60 s, respectively, as previously reported (Flauaus et al., 2022).

2.4.3 Tail immersion test

Mice were immobilized in aluminum foil to allow free tail movement. For accommodation, the tip of the tail (approximately one-third of the tail length) was first immersed in a water bath (Sunlab D-8810; NeoLab, Germany) at 32°C for 20 s and then immersed in another water bath at 45, 47, 49, or 50°C, with cutoff times of 120, 60, 30, or 20 s, respectively. Then, the latency time to a tail withdrawal reflex was recorded. To prevent tissue damage, the tail was removed from the bath immediately after a notable response or upon reaching the cut-off time using a stopwatch (Vandewauw et al., 2018).

2.4.4 Cold plate test

Mice were individually placed on a cold metal surface (Hot/Cold Plate; Ugo Basile) maintained at 10 or 5°C, and the total time the mouse spent lifting one or both forepaws over 60 s was recorded using a stopwatch (Luiz et al., 2019). Only one test per animal per day was performed at every indicated temperature.

2.4.5 Von frey test

Mechanical thresholds were determined using von Frey filaments and the up-down method. The mice were individually placed in a chamber with a wire-mesh floor and acclimatized for 30 min before testing. Calibrated von Frey filaments (0.2–19.6 mN; 0.02–2.0 g; Ugo Basile) were applied to the plantar surface of the hindpaw, and measurements were started with the 0.6 g filament. Clear paw withdrawal, shaking, or licking during or immediately after the stimulus (up to 3 s after the filament was bowed) was defined as a nociceptive response. The 50% withdrawal thresholds were calculated using the online tool, "Up-down method for von Frey experiments" (https://bioapps.shinyapps.io/von_frey_app/) (Christensen et al., 2020).

2.4.6 Pregnenolone sulfate (PS)-, capsaicin-, and allyl isothiocyanate (AITC)-induced nocifensive behavior

PS (5 nmol; #P162; Sigma-Aldrich, Darmstadt, Germany), capsaicin (5 μg; BML-EI125-0200; Enzo, Farmingdale, NY, United States), and AITC (10 mM; #36682; Sigma-Aldrich) in 20 μL 0.9% NaCl containing 0.5% dimethyl sulfoxide (DMSO) were injected into the plantar surface of the hind paw. After the injection, the behaviors of the mice were recorded using a video camera for 5 min in the absence of any observer. The video recordings were subsequently replayed, and the time spent licking, biting or lifting the injected paw was determined using a stopwatch by an observer blinded to the genotype.

2.5 Calcium imaging

Mice were euthanized with CO_2, and lumbar (L1–L5) DRGs were quickly dissected and transferred to Hank's Balanced Salt Solution without $CaCl_2$ and $MgCl_2$ (#14170088; Thermo Fisher Scientific) on ice. Primary cell cultures of lumbar DRG neurons for Ca^{2+} imaging were prepared as previously described (Zhou et al., 2022). Then, 20–26 h after primary cell culture preparation, the cells were loaded with 5 μM Fura-2-AM-ester (#50033; Biotium, Fremont, CA, United States) in Neurobasal A Medium (Thermo Fisher Scientific) for 45 min at 37°C. After loading, the coverslips were transferred to a perfusion chamber and continuously superfused with a physiological bath solution (145 mM NaCl, 5 mM KCl, 1.25 mM $CaCl_2$, 1 mM $MgCl_2$, 10 mM glucose, and 10 mM HEPES; adjusted to pH 7.4 with NaOH) at a flow rate of 1–2 mL/min. A Nikon Eclipse Ts2R inverse microscope equipped with a complete illumination system (DG4; Sutter Instruments, Novato, CA, United States), a Hamamatsu digital camera (ORCA-05G; Hamamatsu, Shizuoka Prefecture, Japan), Fura-2 filters, and a motorized microscope stage (Märzhäuser Wetzlar, Wetzlar, Germany) were used for calcium imaging. Images were taken every 2 s at two wavelengths (340 and 380 nm) and were processed using the NIS-Elements software (Nikon). Baseline measurements were performed in Ringer solution at a flow rate of 1–2 mL/min for 3 min.

For a functionality test of TRPM3, TRPA1, and TPPV1, the TRPM3 activator PS (100 μM), the TRPA1 agonist AITC (200 μM) and the TRPV1 activator capsaicin (100 nM) were dissolved in the bath solution from a 1,000 × stock solution in DMSO, and applied by bath perfusion for 20 s. At the end of each measurement, viable neurons were identified by the application of 75 mM KCl for 20 s. A Ca^{2+} response was defined as a simultaneous increase at 340 nm and a decrease at 380 nm, when the fluorescence ratio of 340 nm divided by 380 nm (F340/F380) normalized to baseline exceeded 20% of the baseline level. All experiments were performed at room temperature. Acquired images were displayed as the ratio of F340/F380.

2.6 Patch-clamp recording

Mice were euthanized with CO_2, lumbar (L1–L5) DRGs were quickly dissected and transferred to dulbecco´s modified eagle´s medium containing 50 μg/mL gentamicin (Sigma-Aldllrich). After incubation with 500 U/mL collagenase IV and 2.5 U/mL dispase II for 30 min (both from Sigma-Aldrich), and 0.05% Trypsin/ethylenediaminetetraacetic acid (Thermo Fisher Scientific) for 10 min at 37°C, cells were washed twice with neurobasal medium supplemented with L-glutamine (2 mM) and 10% fetal calf serum. The cells were then mechanically dissociated using a pipette, seeded onto coverslips coated with poly-D-lysine-coated (200 μg/mL, Sigma-Aldrich) and cultured in TNB 100 medium supplemented with TNB 100 lipid protein complex, 100 μg/mL streptomycin, and penicillin (all from biochrom, Berlin, Germany) at 37°C and 5% CO_2. To avoid neurite outgrowth, which could cause variations in expressed types and amounts of current, and to circumvent space clamp problems, the DRG neurons were studied within 28 h after plating.

To record the total outward K^+ current (I_K), the cultured coverslips were transferred to a recording chamber (RC-26G; Warner Instruments, Holliston, MA, United States) fitted to the stage of an up-right microscope (Axiovert 200; Zeiss, Oberkochen, Germany) and superfused with the extracellular solution. Physiological extracellular buffer contained 140 mM NaCl, 5 mM KCl, 2 mM $CaCl_2$, 2 mM $MgCl_2$ and 10 mM HEPES, adjusted to pH 7.4 with NaOH. For the Na^+ free extracellular buffer, NaCl was replaced with 140 mM choline chloride, and adjusted to pH 7.4 with KOH. The pipette solution contained 140 mM KCl, 2 mM $MgCl_2$, 5 mM EGTA, and 10 mM HEPES, adjusted to pH 7.4 with KOH (Lu et al., 2015; Lu et al., 2021). Recordings were conducted at room temperature with an EPC 9 patch-clamp amplifier combined with the Patchmaster software (HEKA Electronics, Lambrecht, Germany), and data were analyzed using the Fitmaster software (version 2 × 73.5, HEKA Electronics) and plotted using the GraphPad Prism software (version 10.0) for Windows (GraphPad, San Diego, CA, United States). The currents were filtered at 5 kHz and sampled at 20 kHz. The holding potential was −70 mV, and I_K was evoked by 500 ms voltage steps ranging from −120 to +120 mV in 20 mV increments. Patch micro-electrodes were fabricated with a Flaming/Brown micropipette puller (Sutter Instruments), and had a pipette resistance of 5–7 MΩ. Shortly before a coverslip was mounted for recordings, it was dipped in extracellular solution containing 3.3 μg/mL Alexa Fluor 488-conjugated Griffonia simplicifolia IB4 for 10 min, and only IB4-negative small-sized DRG neurons, larger than the IB4-positive DRG neurons were recorded. PS stock solution (100 μL, 500 μM in 20% DMSO) was added with a pipette to the bath chamber to reach a final concentration of 50 μM (Zhao and MacKinnon, 2023), and recordings were started 180 s thereafter. Afterwards, Na^+ free extracellular buffer was infused into the bath chamber at a flow rate of 1–2 mL/min for 5 min and a recording was performed. All recordings were taken after stopping the superfusion system. PS-responsive neurons with reduced I_K after a 5-min washout with Na^+ free extracellular buffer were used for analysis.

2.7 Statistical analysis

All statistical analyses were performed with the GraphPad Prism software (version 10.0; GraphPad Software). A probability value of

10.3389/fphar.2024.1459735

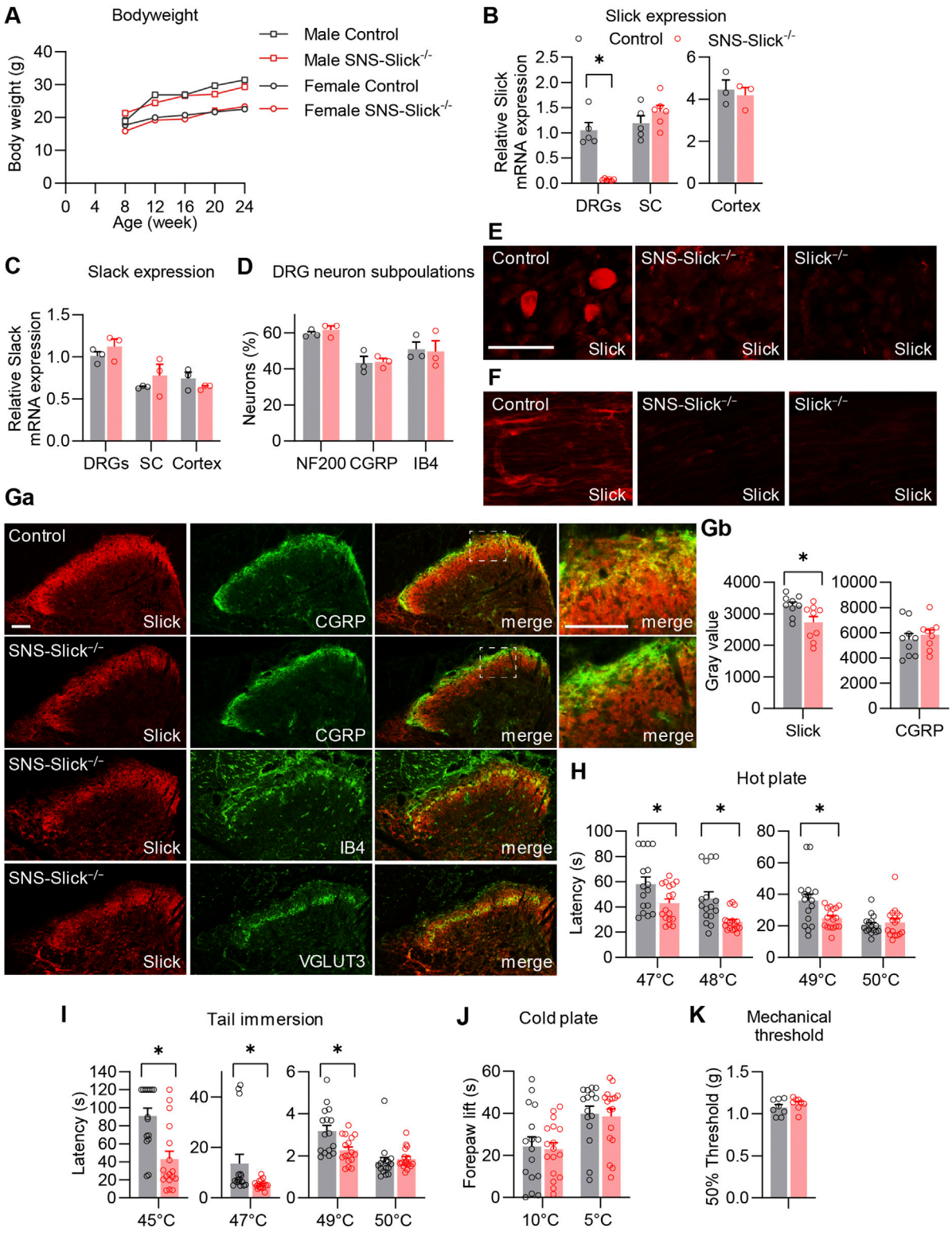

FIGURE 1
Tissue-specific deletion of Slick in sensory neurons affects heat sensation. **(A)** Body weight of SNS-Slick$^{-/-}$ and control mice disaggregated by sex and age [SNS-Slick$^{-/-}$: n = 14 (6 females and 8 males); control: n = 13 (6 females and 7 males)]. **(B)** Quantitative reverse transcription-polymerase chain reaction (qRT-PCR) analyses revealed that Slick mRNA levels were considerably reduced in the dorsal root ganglia [DRGs; $p = 0.008$; SNS-Slick$^{-/-}$: n = 6 (3 females and 3 males); control: n = 5 (3 females and 2 males)], but unaltered in the spinal cord [SC; $p = 0.454$; SNS-Slick$^{-/-}$: n = 6 (3 females and 3 males); control: n = 5 (3 females and 2 males)] and prefrontal cortex [$p = 0.670$; SNS-Slick$^{-/-}$: n = 3 (2 females and 1 male); control: n = 3 (2 females and 1 male)] of SNS-Slick$^{-/-}$ mice. **(C)** Slack mRNA levels in DRGs ($p = 0.352$), SC ($p = 0.401$) and prefrontal cortex ($p = 0.299$) are similar in SNS-Slick$^{-/-}$ and littermate control mice [SNS-Slick$^{-/-}$: n = 3 (2 females and 1 male); control: n = 3 (2 females and 1 male)]. **(D)** Percentages of sensory neurons immunoreactive to neurofilament 200 (NF200; $p = 0.451$) or calcitonin gene-related peptide (CGRP; $p = 0.903$), and binding isolectin B4 (IB4; $p = 0.873$),
(*Continued*)

FIGURE 1 (Continued)
were similar in SNS-Slick$^{-/-}$ mice [n = 3 (2 females and 1 male)] and littermate controls (n = 4 females). **(E, F)** Slick immunostaining of DRGs **(E)** and sciatic nerves **(F)** of control, SNS-Slick$^{-/-}$, and Slick$^{-/-}$ mice revealed specific Slick immunoreactivity in the tissues of control mice. **(G) (Ga)** Double-staining of Slick and markers [CGRP, IB4, and vesicular glutamate transporter 3 (VGLUT3)] in the spinal dorsal horn of control and SNS-Slick$^{-/-}$ mice. Areas marked by white boxes are shown at higher magnification on the right. **(Gb)** Mean grey values of Slick and CGRP immunofluorescence in lamina I and outer lamina II of the spinal dorsal horn [$p = 0.023$; n = 9 section per group from 5 (4 females and 1 male) SNS-Slick$^{-/-}$ mice and 8 (3 females and 5 males) control mice]. These data revealed that Slick immunoreactivity in lamina I and outer lamina II (marked by CGRP staining) was reduced in SNS-Slick$^{-/-}$ mice compared to that in control mice. **(H)** Hot plate tests revealed significantly reduced latencies in SNS-Slick$^{-/-}$ mice at 47°C ($p = 0.043$), 48°C ($p = 0.002$), and 49°C ($p = 0.023$) but not at 50°C [$p = 0.950$; SNS-Slick$^{-/-}$: n = 17 (7 females and 10 males); control: n = 16 (8 females and 8 males)]. **(I)** Tail immersion tests showed significantly reduced latencies in SNS-Slick$^{-/-}$ mice at 45°C ($p < 0.001$), 47°C ($p = 0.006$), and 49°C ($p = 0.007$) but not at 50°C [$p = 0.176$; SNS-Slick$^{-/-}$: n = 17 (6 females and 11 males); control: n = 16 (7 females and 9 males)]. **(J)** In cold plate tests, SNS-Slick$^{-/-}$ and control mice exhibited similar forepaw lift times at temperatures of 10°C ($p = 0.812$) and 5°C [$p = 0.809$; SNS-Slick$^{-/-}$: n = 17 (6 females and 11 males); control: n = 16 (7 females and 9 males)]. Unpaired *t*-test. **(K)** In the von Frey test, SNS-Slick$^{-/-}$ and control mice exhibited normal mechanical thresholds [$p = 0.231$; SNS-Slick$^{-/-}$: n = 8 (5 females and 3 males); control: n = 11 (6 females and 5 males)]. Unpaired *t*-test. Scale bars: 50 μm **(E, F)** and 25 μm **(G)**. *$p < 0.05$. In **(A)** two-way repeated-measures analysis of variance with Sidak's multiple comparison test was used. In **(B–D, H–J)**, multiple unpaired *t*-test was used. In **(K)**, unpaired t-test was used. All data are presented as means ± standard errors of the mean.

$p < 0.05$ was considered statistically significant. No statistical power calculation or sample size calculation was performed before the study, however, the sample sizes employed are similar to those used in the field (Held et al., 2015; Lu et al., 2015; Flauaus et al., 2022; Zhou et al., 2022). The statistical test, statistical results, and group sizes are indicated in the figure legends or the main text. The results of the rotarod test are presented as median with interquartile range. All other data are shown as mean ± standard errors of the mean.

3 Results

3.1 Slick in sensory neurons inhibits the noxious heat sensing

To investigate the functional role of Slick in the peripheral nervous system in pain processing *in vivo*, we generated mice that specifically lack Slick in nociceptive sensory neurons. For this purpose, we crossed mice carrying the floxed *Kcnt2* gene (Martinez-Espinosa et al., 2015) with SNS-Cre mice expressing Cre under the control of Scn10a ($Na_V1.8$) promoter (Agarwal et al., 2004). The resulting conditional knockout mice (SNS-Slick$^{-/-}$ mice) were viable and fertile, with no gross physical or behavioral defects compared to the littermate controls. No difference in body weight was observed between SNS-Slick$^{-/-}$ and control mice (Figure 1A). To confirm the selective ablation of Slick in the DRGs of SNS-Slick$^{-/-}$ mice, we analyzed Slick expression levels in lumbar DRGs, lumbar spinal cord, and prefrontal cortex via qRT-PCR. Indeed, *Slick* mRNA levels were significantly reduced in the DRGs of SNS-Slick$^{-/-}$ mice compared to those in the DRGs of control mice (Figure 1B), but similar in the spinal cord and prefrontal cortex (Figure 1B) of both genotypes, confirming the specific deletion of *Slick* in sensory neurons. The expression of Slack (Kcnt1), which encodes the $K_{Na}1.1$ subunits that are homologous to Slick, was not compensatorily regulated in the lumbar DRGs, lumbar spinal cord, and prefrontal cortex of SNS-Slick$^{-/-}$ mice (Figure 1C). Furthermore, *Slick* deletion in sensory neurons did not affect the general structural properties of sensory neurons as the overall frequencies of DRG neuron populations positive for standard markers (NF200, CGRP, and IB4) were similar between the genotypes (Figure 1D).

Immunostaining using a specific anti-Slick antibody showed clear Slick immunoreactivity in the DRG neurons and the sciatic nerves of control mice, but not of SNS-Slick$^{-/-}$ and Slick$^{-/-}$ mice (Figures 1E, F). These data not only confirmed the specific deletion of Slick in the sensory neurons of SNS-Slick$^{-/-}$ mice (Figure 1E), but also indicate that Slick protein is present in the sciatic nerve (Figure 1F). We also detected Slick protein in the spinal cord of SNS-Slick$^{-/-}$ and control mice (Figure 1Ga). With the deletion of *Slick* in the central terminals of sensory neurons in the superficial dorsal horn, Slick immunoreactivity was significantly reduced in lamina I and outer lamina II of the spinal dorsal horn (indicated by CGRP staining; Figure 1Gb) but not in the dorsal region of inner lamina II (indicated by IB4 staining), and ventral region of inner lamina II (indicated by vesicular glutamate transporter-3 staining). Slick immunoreactivity observed in the spinal cord of SNS-Slick$^{-/-}$ mice (Figure 1G) most likely represents dorsal horn neurons that express Slick (Flauaus et al., 2022). Together, these data indicate that *Slick* is specifically deleted in sensory neurons of SNS-Slick$^{-/-}$ mice.

As a prerequisite for behavioral testing, we investigated the motor function of SNS-Slick$^{-/-}$ mice and control mice using an accelerating rotarod test. SNS-Slick$^{-/-}$ mice demonstrated intact motor coordination and balance as compared to the control mice (median fall-off latencies: SNS-Slick$^{-/-}$, 300 s [interquartile range: 272.0–300.0 s]; control, 296 s [interquartile range: 254.0–300.0 s]; $p = 0.253$; Mann-Whitney U test; n = 16–17 mice/group), indicating that SNS-Slick$^{-/-}$ mice are suitable for behavioral profiling of animal pain models. Next, we tested heat sensation in SNS-Slick$^{-/-}$ and control mice using the hot plate test. Compared to the littermate control mice, SNS-Slick$^{-/-}$ mice demonstrated significantly shorter latency times to noxious heat on the plate at 47, 48, and 49°C, but a normal latency time at 50°C (Figure 1H). Similarly, in the tail immersion test, SNS-Slick$^{-/-}$ mice demonstrated shorter latency times at 45, 47, and 49°C (Figure 1I), but normal latency time at 50°C (Figure 1I). In contrast, SNS-Slick$^{-/-}$ mice showed normal responses in the cold plate test at 10°C and 5°C (Figure 1J) and normal mechanical thresholds (Figure 1K). We analyzed female and male mice in the behavior tests including hot plate and tail immersion tests; the data disaggregated by sex are presented in Supplementary Figures S1A, B. However, we did not analyze the effect of sex as we were not powered to detect sex differences. Our finding suggest that specific ablation of Slick in sensory neurons enhances responses to noxious heat.

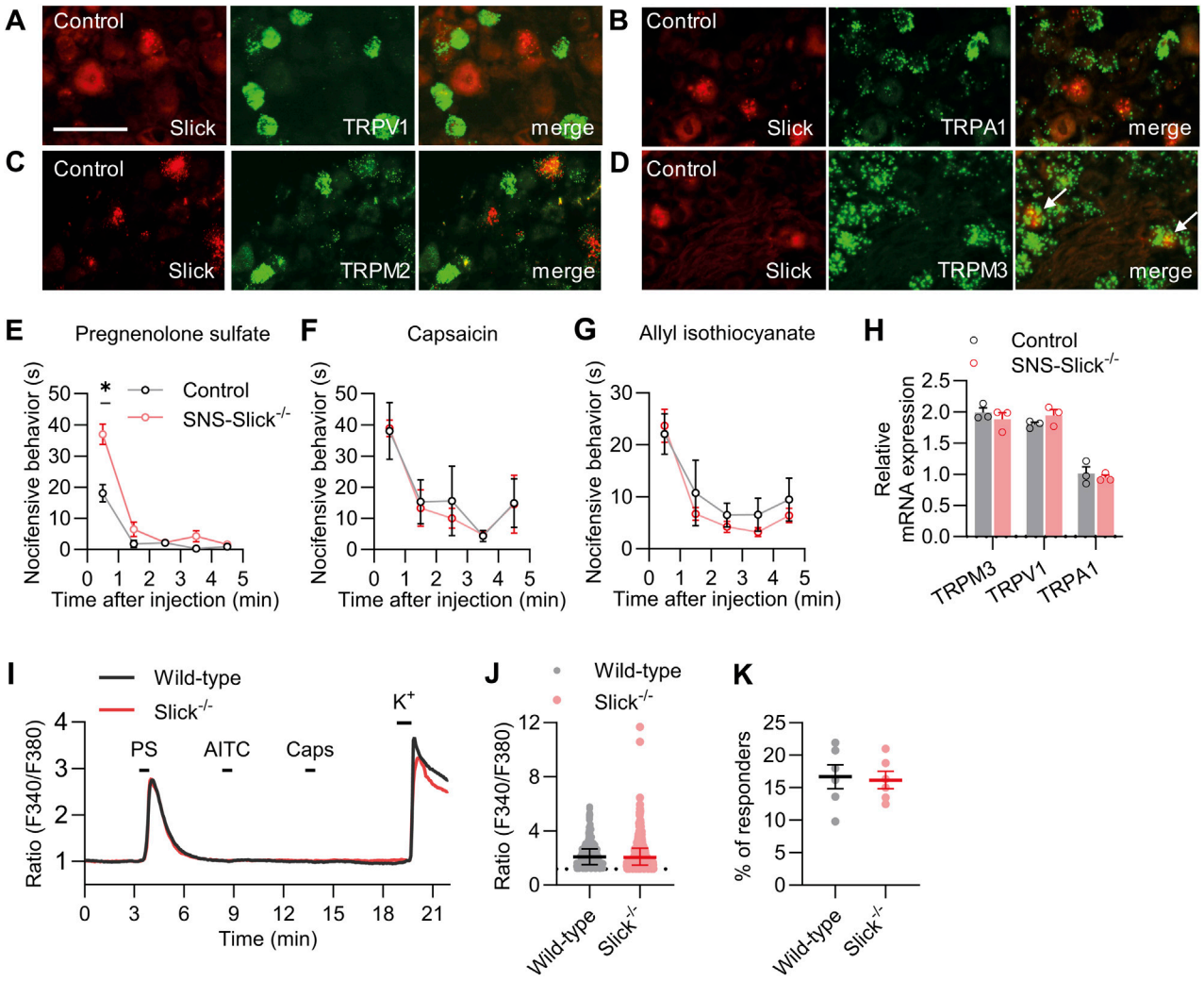

FIGURE 2
Slick is involved in transient receptor potential melastatin 3 (TRPM3) activation-induced nocifensive behavior. **(A–D)** Double *in situ* hybridization of *Slick* and *TRPV1* **(A)**, *TRPA1* **(B)**, *TRPM2* **(C)**, and *TRPM3* **(D)** mRNAs in the DRGs of control mice. Colocalization of Slick and TRPM3 is indicated by the white arrows. **(E)** SNS-Slick$^{-/-}$ mice showed enhanced nocifensive behaviors in the first minute after the intraplantar injection of pregnenolone sulfate [PS; p = 0.004; SNS-Slick$^{-/-}$: n = 8 (4 females and 4 males); control: n = 8 (4 females and 4 males)]. **(F, G)** Nocifensive behaviors of SNS-Slick$^{-/-}$ mice were unaltered after the intraplantar injection of capsaicin (F; SNS-Slick$^{-/-}$: n = 5 [2 females and 3 males]; control: n = 5 [2 females and 3 males]) or allyl isothiocyanate (G; AITC; SNS-Slick$^{-/-}$: n = 8 [5 females and 3 males]; control: n = 8 [5 females and 3 males]). **(H)** qRT-PCR analyses revealed that *TRPM3* (p = 0.458), *TRPV1* (p = 0.250), and *TRPA1* mRNA (p = 0.610) levels are similar in the DRGs of SNS-Slick$^{-/-}$ (n = 3 [2 females and 1 male]) and littermate control (n = 3 [2 females and 1 male]) mice. **(I)** Representative examples of Fura-2-ratiometric calcium traces in sensory neurons of wild-type and Slick$^{-/-}$ mice that reacted to a stimulation with PS and KCl, but not with capsaicin or AITC. **(J)** Ratio of the calcium response to PS stimulation in sensory neurons from wild-type (n = 495 neurons in 6 mice [3 females and 3 males]) and Slick$^{-/-}$ mice (n = 460 neurons in 6 mice [3 females and 3 males]). p = 0.505. **(K)** Percentage of sensory neurons from wild-type and Slick$^{-/-}$ mice that responded to the PS stimulation, but not to the AITC or capsaicin stimulation (n = 6 mice [Slick$^{-/-}$: 3 females and 3 males; WT: 3 females and 3 males]). p = 0.821. Scale bar: 50 µm *$p < 0.05$. In **(E–G)**, two-way repeated-measures analysis of variance with Sidak's multiple comparison test was used. In **(H)**, multiple unpaired t-test was used. In **(J, K)**, unpaired t-test was used. Data are presented as means ± standard errors of the mean.

3.2 Slick in sensory neurons inhibits TRPM3 activation-induced nocifensive behavior

Next, we explored whether the increased heat sensitivity of SNS-Slick$^{-/-}$ mice is related to the functional coupling with essential heat detectors in sensory neurons. Acute noxious heat sensing in mice depends on a triad of TRP ion channels: TRPV1, TRPA1, and TRPM3 (Vandewauw et al., 2018). In addition to these channels, TRPM2 is a thermally activated ion channel in the peripheral sensory neurons (Tan and McNaughton, 2016; Vilar et al., 2020). To estimate the possible interaction of Slick with these TRP channels, we performed double *in situ* hybridization experiments using lumbar DRG sections. These experiments showed that Slick did not colocalize with TRPV1, TRPA1, and TRPM2 in sensory neurons (Figures 2A–C). However, Slick was expressed in a subset of TRPM3-expressing sensory neurons (89.1% ± 4.4% of Slick-positive neurons expressed TRPM3, whereas 35.0% ± 6.2% of TRPM3-positive neurons expressed Slick; Figure 2D). These data support our hypothesis that Slick might be functionally coupled to TRPM3 in sensory neurons.

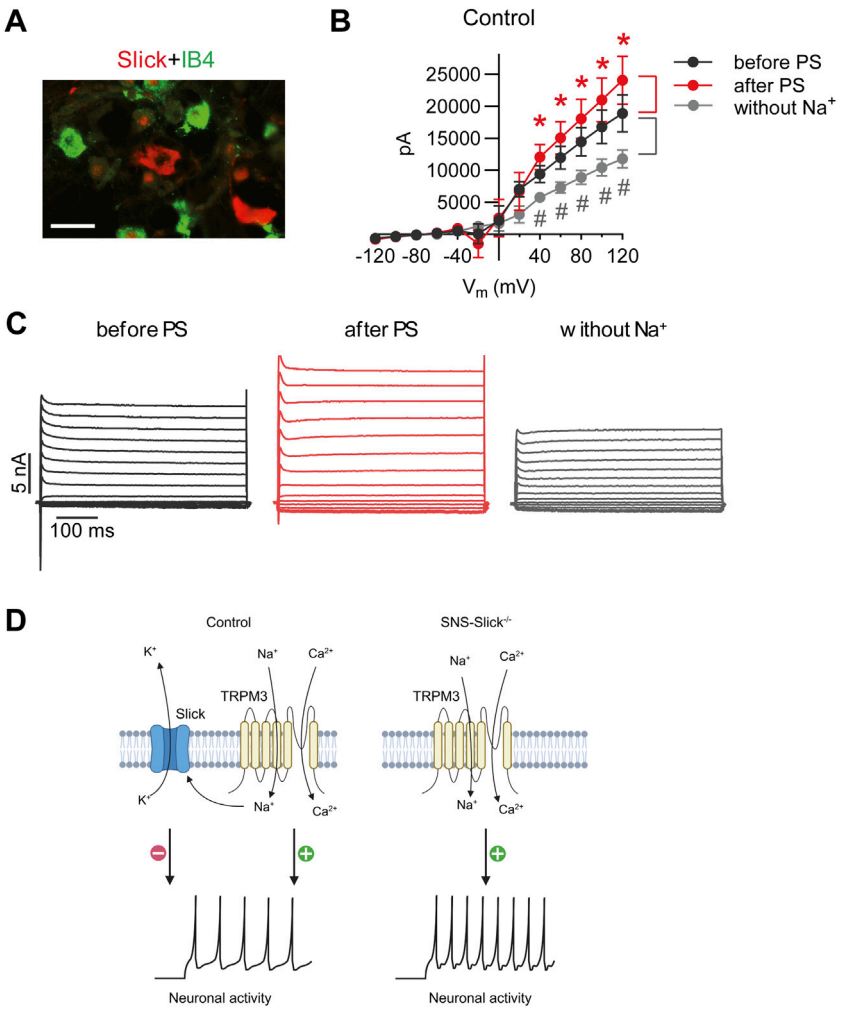

FIGURE 3
PS-mediated modulation of potassium currents in the isolectin B4 (IB4)-negative sensory neurons of control mice. **(A)** Double immunostaining of Slick and IB4 in the lumbar DRGs of wild-type mice revealed that Slick is expressed in IB4-negative small-diameter DRG neurons. **(B)** IV relations of outward potassium currents (I_K) determined in whole-cell patch-clamp recordings on DRG neurons of twelve wild-type mice at baseline, after PS (50 μM) application in the physiological extracellular buffer, and after 5 min washout using an extracellular buffer without Na^+. In total, 56 DRG neurons from twelve mice were analyzed. Shown are the recordings of the cells (n = 7) that exhibited increased I_K after PS application (indicating that the cell was TRPM3-positive) and decreased I_K in the Na^+-free buffer (indicating that the cell was Slick-positive). $^*p < 0.05$ indicates significantly increased I_K after PS application (after PS). $^\#p < 0.05$ indicates significantly decreased I_K after Na^+ replacement (without Na^+) compared to that before PS application (before PS). **(C)** Representative I_K traces before and after PS application in the physiological extracellular buffer and after washout with the Na^+-free buffer. **(D)** Schematic diagram demonstrating the functional coupling of Slick and TRPM3 in IB4-negative small-diameter sensory neurons. TRPM3 activation by heat or PS leads to an influx of Na^+ and Ca^{2+} into sensory neurons to activate neuronal activity. Increased Na^+ influx activates Slick, which results in K^+ efflux and thus inhibits neuronal activity. **(D)** is created with BioRender.com/z68j113. Scale bar: 100 μm. In **(B)**, multiple paired *t*-test was used. Data are presented as means ± standard errors of the mean.

In addition to its role in heat sensation, TRPM3 acts as a nociceptor sensitive to various physical and chemical stimuli, most notably the endogenous neurosteroid PS (Wagner et al., 2008; Bamps et al., 2021). To explore whether TRPM3 is functionally coupled to Slick in sensory neurons, we tested the nocifensive behavior of SNS-Slick$^{-/-}$ and control mice following the intraplantar injection of PS (Vriens et al., 2011). Interestingly, nocifensive behavior induced by PS injection was significantly enhanced in SNS-Slick$^{-/-}$ mice compared to that in control mice in the first minute after injection, suggesting that Slick limits the nocifensive behavior induced by activation of TRPM3 in sensory neurons (Figure 2E). We analyzed female and male mice in the PS test and present the data disaggregated by sex in Supplementary Figure S1C. As control experiments, we intraplantarly injected TRPV1 activator capsaicin and TRPA1 activator AITC in SNS-Slick$^{-/-}$ and control mice. Unlike the TRPM3-mediated nocifensive behavior, the nocifensive responses to capsaicin and AITC were unaltered in SNS-Slick$^{-/-}$ mice (Figures 2F, G). Further control experiments using qRT-PCR revealed that the mRNA levels of *TRPM3*, *TRPV1*, and *TRPA1* were similar in DRGs of SNS-Slick$^{-/-}$ and control mice (Figure 2H). These results indicate that Slick in sensory neurons is functionally coupled to TRPM3 but not TRPV1 and TRPA1.

We then investigated whether the enhanced PS-induced nocifensive behavior in SNS-Slick$^{-/-}$ mice is related to altered TRPM3-dependent Ca^{2+} influx into sensory neurons. We compared the PS-induced changes in intracellular Ca^{2+} in cultured DRG neurons of wild-type and Slick$^{-/-}$ mice via Ca^{2+} imaging. As TRPM3, TRPV1, and TRPA1 exhibit largely overlapping expression profiles (Vriens et al., 2011; Vandewauw et al., 2018) and Slick is only expressed in a subpopulation of TRPM3-positive sensory neurons (Figure 2D) but not in the TRPV1- or TRPA1-expressing sensory neurons (Figures 2A,B), we consecutively stimulated the cultured DRG neurons with 100 μM PS, 200 μM AITC, and 100 nM capsaicin (each for 20 s) and analyzed only those neurons that reacted to PS, but not to AITC and capsaicin (Figure 2I). Notably, average value to peak amplitudes induced by PS stimulation (Figure 2J) and percentage of neurons only responsive to PS (Figure 2K) were indistinguishable between the wild-type and Slick$^{-/-}$ mice. Therefore, TRPM3-dependent Ca^{2+} transients were not modulated by Slick in sensory neurons.

3.3 TRPM3 activation alters Slick-mediated potassium currents in sensory neurons

Next, we performed patch-clamp recordings of sensory neurons to explore the interaction between Slick and TRPM3. We previously reported that the cellular distribution of Slick in DRGs is restricted to neurons not binding to IB4 but positive for both NF200 and CGRP (Flauaus et al., 2022). As shown in Figure 3A, Slick-positive DRG neurons did not overlap with the IB4-positive neurons. Therefore, we performed whole-cell patch-clamp recordings of IB4-negative small-diameter DRG neurons of control mice to analyze the I_K currents. For each neuron, three consecutive recordings were performed: (1) at the baseline, (2) after adding PS to the bath chamber, and (3) after 5-min washout and replacement of NaCl with choline chloride (to obtain an Na^+-free solution) in the extracellular buffer in order to detect I_K currents driven by the Na^+-activated K^+ channel. To identify the Slick-positive cells, we calculated the ratio of I_K current at the baseline (before PS) and after the replacement of NaCl with choline chloride (without Na^+) at +80 mV. Neurons with a prominent reduction in I_K current by more than 20% after the removal of extracellular Na^+ were defined as Slick-positive cells. We patched 56 sensory neurons from twelve control mice and identified seven neurons responding to PS and with reduced I_K after Na^+ replacement. In these seven neurons, a prominent reduction in I_K peak amplitude with a linear I–V relationship at positive potentials ranging from +40 to +120 mV was detected (Figure 3B), suggesting the presence of a large Na^+-activated K^+ current. Notably, the amplitude of I_K significantly increased after the addition of PS, with a linear I–V relationship at positive potentials ranging from +40 to +120 mV as compared to the amplitude of I_K before PS (Figure 3B). Representative examples of I_K currents evoked by PS and NaCl replacement are shown in Figure 3C. Together, these data suggest that TRPM3 activation by PS in sensory neurons leads to Na^+ influx, thereby activating Slick to limit further neuronal activation (Figure 3D).

4 Discussion

This study demonstrated that Slick in sensory neurons plays a functional role in heat sensation. Our *in situ* hybridization experiments revealed that most of Slick-positive sensory neurons expressed the essential heat sensor, TRPM3. At the behavioral level, SNS-Slick$^{-/-}$ mice showed reduced latency time to express any nocifensive behavior in the hot plate and tail immersion tests, and greater nocifensive responses after the intraplantar injection of a TRPM3 activator. At the cellular level, activation of TRPM3 increased the Na^+-dependent I_K currents in sensory neurons, which are driven by Slick in TRPM3-positive cells. These findings suggest that Slick exerts specific inhibitory effects upon TRPM3 activation in sensory neurons. The main findings from this study are highlighted in a schematic diagram in Figure 3D.

TRPM3 is highly expressed in a proportion of small-diameter DRG neurons, which have a size distribution similar to that of capsaicin-sensitive neurons (Vriens et al., 2011). Despite the limited expression of Slick in DRG neurons (only approximately 9% of total DRG neurons express Slick) and its enrichment in CGRP; NF200-positive Aδ-fiber nociceptors (Flauaus et al., 2022), Slick was almost exclusively expressed in the TRPM3-positive neurons, but not in the TRPV1-, TRPA1-, and TRPM2-positive neurons. TRPM3 expressed in sensory neurons facilitates noxious heat sensation and plays key roles in inflammatory hyperalgesia and neuropathic pain (Thiel et al., 2017; Behrendt, 2019; Aloi et al., 2023). Therefore, TRPM3 is a promising novel target for pain treatment. Using another Slick$^{-/-}$ mouse line, Tomasello et al. reported that Slick$^{-/-}$ mice exhibited increased thermal hyperalgesia during chronic inflammatory pain and neuropathic pain (Tomasello et al., 2017). However, Slick is highly expressed in spinal dorsal horn neurons (Flauaus et al., 2022), possibly contributing to chronic pain. Therefore, further studies are necessary to elucidate the functional roles of Slick in sensory and dorsal horn neurons in chronic pain.

Heterologous expression of the Slick channel indicates that it is predominantly activated by intracellular Na^+ and Cl^- (Bhattacharjee et al., 2003). TRPM3 is a non-selective cation channel that is permeable for Ca^{2+}, Mg^{2+}, and Zn^{2+} via the central pore (Oberwinkler et al., 2005; Wagner et al., 2010). In addition to the central pore, an alternative ion permeation pathway has been identified in TRPM3. This alternative pathway allows massive Na^+ influx at negative voltages, thereby enhancing neuronal excitation and exacerbating TRPM3-dependent pain (Vriens et al., 2014; Vriens and Voets, 2018). Because Slick is a K_{Na} channel, the opening of Slick can lead to action potential repolarization in an intracellular Na^+ dependent manner (Gao et al., 2008). Despite the well-established existence of the Slick channel, the circumstances under which cytosolic Na^+ elevation arising from physiological stimuli is sufficient to produce Slick activation remain unclear. Therefore, we can only speculate that TRPM3 activation-induced Na^+ influx may be responsible for Slick activation and subsequent inhibition of the processing of noxious thermal stimuli <50°C. In our patch-clamp experiments, TRPM3 was stimulated by PS applied to the extracellular buffer, because PS is membrane-impermeant and the PS-interacting domain is located at the extracellular side (Wagner et al., 2008; Held et al., 2015). Notably, TRPM3 has an unusually large number of splice variants (Oberwinkler et al., 2005), and PS activates

TRPM3α2 to produce both outward and inward current (Vriens et al., 2011; Held et al., 2015; Van Hoeymissen et al., 2020; Hossain Saad et al., 2021). Unfortunately, our experimental setup does not allow us to distinguish between PS-induced outward and inward currents. Therefore, the increased I_K current after PS possibly includes the TRPM3 currents. However, the proportions of Slick- and TRPM3-mediated currents remain unclear, warranting further investigation.

The ion channel modulation by noxious heat has been addressed in several reviews (Palkar et al., 2015; Vriens and Voets, 2018; Lamas et al., 2019; Kashio and Tominaga, 2022). In addition to the channels tested in this study, Ca^{2+}-activated Cl^- channel anoctamin 1 (ANO1) also acts as a heat sensor in DRG neurons (Cho et al., 2012; Lee et al., 2014). ANO1 activation in DRG neurons causes depolarization, thus firing the action potential (Liu et al., 2010; Cho et al., 2012; Lee et al., 2014). Mice lacking ANO1 in DRG neurons exhibit significantly increased withdrawal latencies in the tail immersion test at 50°C–54°C (Cho et al., 2012). Notably, ANO1 is barely expressed in peptidergic nociceptors (Usoskin et al., 2015). Here, SNS-Slick$^{-/-}$ mice exhibited short latencies in the tail immersion test at temperatures <50°C; therefore, an interaction between Slick and ANO1 seems unlikely. Recently, a novel sensor of noxious heat, the transmembrane channel-like (TMC) 6 has been identified. Mice selectively lacking TMC6 in the sensory neurons exhibited longer latencies to noxious heat on the hot plate at 48°C–56°C. However, TMC6-mediated noxious heat-elicited Ca^{2+} response and action potential firing, but did not affect Na^+ current (Zhang et al., 2024). Therefore, it is less likely that Slick modulates heat sensation via TMC6. These findings suggest that Slick specifically limits TRPM3-mediated activation of sensory neurons upon noxious heat stimulation.

In conclusion, our observations indicate that Slick in sensory neurons exerts a critical inhibitory function in the processing of noxious heat sensing.

Data availability statement

The raw data supporting the conclusions of this article will be made available by the authors, without undue reservation.

Ethics statement

The animal study was approved by Regierungspräsidium Darmstadt, Germany. The study was conducted in accordance with the local legislation and institutional requirements.

Author contributions

PE: Data curation, Investigation, Methodology, Validation, Formal Analysis, Writing–original draft. FZ: Investigation, Writing–original draft. BT: Investigation, Writing–original draft. AS: Conceptualization, Writing–review and editing, Writing–original draft. RL: Conceptualization, Data curation, Formal Analysis, Funding acquisition, Investigation, Methodology, Project administration, Supervision, Validation, Visualization, Writing–original draft, Writing–review and editing.

Funding

The author(s) declare that financial support was received for the research, authorship, and/or publication of this article. This work was funded by the Deutsche Forschungsgemeinschaft (DFG, German Research Foundation) – projects 440899966 and 546368299 (to Lu).

Acknowledgments

The authors thank Prof. Rohini Kuner (Institute of Pharmacology, Heidelberg University, Heidelberg, Germany) for providing SNS-Cre mice and Sylvia Oßwald, Cyntia Schäfer, and Sabina Hassan (Institute of Pharmacology and Clinical Pharmacy, Goethe University Frankfurt, Frankfurt am Main, Germany) for their excellent technical assistance.

Conflict of interest

The authors declare that the research was conducted in the absence of any commercial or financial relationships that could be construed as a potential conflict of interest.

Publisher's note

Supplementary material

The Supplementary Material for this article can be found online at: https://www.frontiersin.org/articles/10.3389/fphar.2024.1459735/full#supplementary-material

SUPPLEMENTARY FIGURE S1
Data of key behavior experiments disaggregated by sex. Data correspond to those presented in Figures 1H, 1I, and 2E, but are separated in male and female cohorts. Behavioral responses of SNS-Slick$^{-/-}$ mice in the hot plate test **(A)**, in the tail immersion test **(B)** and pregnenolon sulfate **(C)**. *$P < 0.05$. In Figure 1A, B multiple unpaired *t*-test was used. In Figure 1C two-way repeated-measures analysis of variance with Sidak's multiple comparison test was used. Data are presented as means ± standard errors of the mean.

References

Agarwal, N., Offermanns, S., and Kuner, R. (2004). Conditional gene deletion in primary nociceptive neurons of trigeminal ganglia and dorsal root ganglia. *Genesis* 38, 122–129. doi:10.1002/gene.20010

Aloi, V. D., Pinto, S., Van Bree, R., Luyten, K., Voets, T., and Vriens, J. (2023). TRPM3 as a novel target to alleviate acute oxaliplatin-induced peripheral neuropathic pain. *Pain* 164, 2060–2069. doi:10.1097/j.pain.0000000000002906

Bamps, D., Vriens, J., De Hoon, J., and Voets, T. (2021). TRP channel cooperation for nociception: therapeutic opportunities. *Annu. Rev. Pharmacol. Toxicol.* 61, 655–677. doi:10.1146/annurev-pharmtox-010919-023238

Behrendt, M. (2019). Transient receptor potential channels in the context of nociception and pain - recent insights into TRPM3 properties and function. *Biol. Chem.* 400, 917–926. doi:10.1515/hsz-2018-0455

Bhattacharjee, A., Joiner, W. J., Wu, M., Yang, Y., Sigworth, F. J., and Kaczmarek, L. K. (2003). Slick (Slo2.1), a rapidly-gating sodium-activated potassium channel inhibited by ATP. *J. Neurosci.* 23, 11681–11691. doi:10.1523/JNEUROSCI.23-37-11681.2003

Cho, H., Yang, Y. D., Lee, J., Lee, B., Kim, T., Jang, Y., et al. (2012). The calcium-activated chloride channel anoctamin 1 acts as a heat sensor in nociceptive neurons. *Nat. Neurosci.* 15, 1015–1021. doi:10.1038/nn.3111

Christensen, S. L., Hansen, R. B., Storm, M. A., Olesen, J., Hansen, T. F., Ossipov, M., et al. (2020). Von Frey testing revisited: provision of an online algorithm for improved accuracy of 50% thresholds. *Eur. J. Pain* 24, 783–790. doi:10.1002/ejp.1528

Flauaus, C., Engel, P., Zhou, F., Petersen, J., Ruth, P., Lukowski, R., et al. (2022). Slick potassium channels control pain and itch in distinct populations of sensory and spinal neurons in mice. *Anesthesiology* 136, 802–822. doi:10.1097/ALN.0000000000004163

Gao, S. B., Wu, Y., Lu, C. X., Guo, Z. H., Li, C. H., and Ding, J. P. (2008). Slack and Slick KNa channels are required for the depolarizing afterpotential of acutely isolated, medium diameter rat dorsal root ganglion neurons. *Acta Pharmacol. Sin.* 29, 899–905. doi:10.1111/j.1745-7254.2008.00842.x

Harada, A., Suzuki, K., and Kimura, H. (2017). TAK-063, a novel phosphodiesterase 10A inhibitor, protects from striatal neurodegeneration and ameliorates behavioral deficits in the R6/2 mouse model of huntington's disease. *J. Pharmacol. Exp. Ther.* 360, 75–83. doi:10.1124/jpet.116.237388

Held, K., Kichko, T., De Clercq, K., Klaassen, H., Van Bree, R., Vanherck, J. C., et al. (2015). Activation of TRPM3 by a potent synthetic ligand reveals a role in peptide release. *Proc. Natl. Acad. Sci. U. S. A.* 112, E1363–E1372. doi:10.1073/pnas.1419845112

Hossain Saad, M. Z., Xiang, L., Liao, Y. S., Reznikov, L. R., and Du, J. (2021). The underlying mechanism of modulation of transient receptor potential melastatin 3 by protons. *Front. Pharmacol.* 12, 632711. doi:10.3389/fphar.2021.632711

Kaczmarek, L. K. (2013). Slack, Slick and sodium-activated potassium channels. *ISRN Neurosci.* 2013, 354262. doi:10.1155/2013/354262

Kaczmarek, L. K., Aldrich, R. W., Chandy, K. G., Grissmer, S., Wei, A. D., and Wulff, H. (2017). International union of basic and clinical Pharmacology. C. Nomenclature and properties of calcium-activated and sodium-activated potassium channels. *Pharmacol. Rev.* 69, 1–11. doi:10.1124/pr.116.012864

Kashio, M., and Tominaga, M. (2022). TRP channels in thermosensation. *Curr. Opin. Neurobiol.* 75, 102591. doi:10.1016/j.conb.2022.102591

Lamas, J. A., Rueda-Ruzafa, L., and Herrera-Perez, S. (2019). Ion channels and thermosensitivity: TRP, TREK, or both? *Int. J. Mol. Sci.* 20, 2371. doi:10.3390/ijms20102371

Lee, B., Cho, H., Jung, J., Yang, Y. D., Yang, D. J., and Oh, U. (2014). Anoctamin 1 contributes to inflammatory and nerve-injury induced hypersensitivity. *Mol. Pain* 10, 5. doi:10.1186/1744-8069-10-5

Liu, B., Linley, J. E., Du, X., Zhang, X., Ooi, L., Zhang, H., et al. (2010). The acute nociceptive signals induced by bradykinin in rat sensory neurons are mediated by inhibition of M-type K+ channels and activation of Ca2+-activated Cl- channels. *J. Clin. Invest* 120, 1240–1252. doi:10.1172/JCI41084

Lu, R., Bausch, A. E., Kallenborn-Gerhardt, W., Stoetzer, C., Debruin, N., Ruth, P., et al. (2015). Slack channels expressed in sensory neurons control neuropathic pain in mice. *J. Neurosci.* 35, 1125–1135. doi:10.1523/JNEUROSCI.2423-14.2015

Lu, R., Metzner, K., Zhou, F., Flauaus, C., Balzulat, A., Engel, P., et al. (2021). Functional coupling of Slack channels and P2X3 receptors contributes to neuropathic pain processing. *Int. J. Mol. Sci.* 22, 405. doi:10.3390/ijms22010405

Luiz, A. P., Macdonald, D. I., Santana-Varela, S., Millet, Q., Sikandar, S., Wood, J. N., et al. (2019). Cold sensing by NaV1.8-positive and NaV1.8-negative sensory neurons. *Proc. Natl. Acad. Sci. U. S. A.* 116, 3811–3816. doi:10.1073/pnas.1814545116

Martinez-Espinosa, P. L., Wu, J., Yang, C., Gonzalez-Perez, V., Zhou, H., Liang, H., et al. (2015). Knockout of Slo2.2 enhances itch, abolishes KNa current, and increases action potential firing frequency in DRG neurons. *Elife* 4, e10013. doi:10.7554/eLife.10013

Oberwinkler, J., Lis, A., Giehl, K. M., Flockerzi, V., and Philipp, S. E. (2005). Alternative splicing switches the divalent cation selectivity of TRPM3 channels. *J. Biol. Chem.* 280, 22540–22548. doi:10.1074/jbc.M503092200

Ocana, M., Cendan, C. M., Cobos, E. J., Entrena, J. M., and Baeyens, J. M. (2004). Potassium channels and pain: present realities and future opportunities. *Eur. J. Pharmacol.* 500, 203–219. doi:10.1016/j.ejphar.2004.07.026

Palkar, R., Lippoldt, E. K., and Mckemy, D. D. (2015). The molecular and cellular basis of thermosensation in mammals. *Curr. Opin. Neurobiol.* 34, 14–19. doi:10.1016/j.conb.2015.01.010

Tan, C. H., and Mcnaughton, P. A. (2016). The TRPM2 ion channel is required for sensitivity to warmth. *Nature* 536, 460–463. doi:10.1038/nature19074

Thiel, G., Rubil, S., Lesch, A., Guethlein, L. A., and Rossler, O. G. (2017). Transient receptor potential TRPM3 channels: Pharmacology, signaling, and biological functions. *Pharmacol. Res.* 124, 92–99. doi:10.1016/j.phrs.2017.07.014

Tomasello, D. L., Hurley, E., Wrabetz, L., and Bhattacharjee, A. (2017). Slick (Kcnt2) sodium-activated potassium channels limit peptidergic nociceptor excitability and hyperalgesia. *J. Exp. Neurosci.* 11, 1179069517726996. doi:10.1177/1179069517726996

Tsantoulas, C., and Mcmahon, S. B. (2014). Opening paths to novel analgesics: the role of potassium channels in chronic pain. *Trends Neurosci.* 37, 146–158. doi:10.1016/j.tins.2013.12.002

Usoskin, D., Furlan, A., Islam, S., Abdo, H., Lonnerberg, P., Lou, D., et al. (2015). Unbiased classification of sensory neuron types by large-scale single-cell RNA sequencing. *Nat. Neurosci.* 18, 145–153. doi:10.1038/nn.3881

Vandewauw, I., De Clercq, K., Mulier, M., Held, K., Pinto, S., Van Ranst, N., et al. (2018). A TRP channel trio mediates acute noxious heat sensing. *Nature* 555, 662–666. doi:10.1038/nature26137

Vangeel, L., and Voets, T. (2019). Transient receptor potential channels and calcium signaling. *Cold Spring Harb. Perspect. Biol.* 11, a035048. doi:10.1101/cshperspect.a035048

Van Hoeymissen, E., Held, K., Nogueira Freitas, A. C., Janssens, A., Voets, T., and Vriens, J. (2020). Gain of channel function and modified gating properties in TRPM3 mutants causing intellectual disability and epilepsy. *Elife* 9, e57190. doi:10.7554/eLife.57190

Vilar, B., Tan, C. H., and Mcnaughton, P. A. (2020). Heat detection by the TRPM2 ion channel. *Nature* 584, E5–E12. doi:10.1038/s41586-020-2510-7

Vriens, J., Held, K., Janssens, A., Toth, B. I., Kerselaers, S., Nilius, B., et al. (2014). Opening of an alternative ion permeation pathway in a nociceptor TRP channel. *Nat. Chem. Biol.* 10, 188–195. doi:10.1038/nchembio.1428

Vriens, J., Owsianik, G., Hofmann, T., Philipp, S. E., Stab, J., Chen, X., et al. (2011). TRPM3 is a nociceptor channel involved in the detection of noxious heat. *Neuron* 70, 482–494. doi:10.1016/j.neuron.2011.02.051

Vriens, J., and Voets, T. (2018). Sensing the heat with TRPM3. *Pflugers Arch.* 470, 799–807. doi:10.1007/s00424-017-2100-1

Wagner, T. F., Drews, A., Loch, S., Mohr, F., Philipp, S. E., Lambert, S., et al. (2010). TRPM3 channels provide a regulated influx pathway for zinc in pancreatic beta cells. *Pflugers Arch.* 460, 755–765. doi:10.1007/s00424-010-0838-9

Wagner, T. F., Loch, S., Lambert, S., Straub, I., Mannebach, S., Mathar, I., et al. (2008). Transient receptor potential M3 channels are ionotropic steroid receptors in pancreatic beta cells. *Nat. Cell Biol.* 10, 1421–1430. doi:10.1038/ncb1801

Zhang, C., Tong, F., Zhou, B., He, M., Liu, S., Zhou, X., et al. (2024). TMC6 functions as a GPCR-like receptor to sense noxious heat via Gαq signaling. *Cell Discov.* 10, 66. doi:10.1038/s41421-024-00678-9

Zhang, M., Ma, Y., Ye, X., Zhang, N., Pan, L., and Wang, B. (2023). TRP (transient receptor potential) ion channel family: structures, biological functions and therapeutic interventions for diseases. *Signal Transduct. Target Ther.* 8, 261. doi:10.1038/s41392-023-01464-x

Zhao, C., and Mackinnon, R. (2023). Structural and functional analyses of a GPCR-inhibited ion channel TRPM3. *Neuron* 111, 81–91.e7. doi:10.1016/j.neuron.2022.10.002

Zhou, F., Metzner, K., Engel, P., Balzulat, A., Sisignano, M., Ruth, P., et al. (2022). Slack potassium channels modulate TRPA1-mediated nociception in sensory neurons. *Cells* 11, 1693. doi:10.3390/cells11101693

frontiers | Frontiers in Pharmacology

TYPE Original Research
PUBLISHED 03 January 2025
DOI 10.3389/fphar.2024.1505980

OPEN ACCESS

EDITED BY
Francisco R. Nieto,
University of Granada, Spain

REVIEWED BY
Caroline A. Browne,
Munster Technological University, Ireland
Neil M. Fournier,
Trent University, Canada

*CORRESPONDENCE
David P. Finn,
david.finn@universityofgalway.ie

RECEIVED 04 October 2024
ACCEPTED 29 November 2024
PUBLISHED 03 January 2025

CITATION
Di Marino C, Llorente-Berzal Á, Diego AM, Bella A, Boullon L, Berrocoso E, Roche M and Finn DP (2025) Characterisation of the effects of the chemotherapeutic agent paclitaxel on neuropathic pain-related behaviour, anxiodepressive behaviour, cognition, and the endocannabinoid system in male and female rats.
Front. Pharmacol. 15:1505980.
doi: 10.3389/fphar.2024.1505980

Characterisation of the effects of the chemotherapeutic agent paclitaxel on neuropathic pain-related behaviour, anxiodepressive behaviour, cognition, and the endocannabinoid system in male and female rats

Chiara Di Marino[1,2,3,4], Álvaro Llorente-Berzal[1,2,3], Alba M. Diego[1,2,3], Ariadni Bella[2,3,5], Laura Boullon[1,2,3], Esther Berrocoso[4,6,7], Michelle Roche[2,3,5] and David P. Finn[1,2,3]*

[1]Pharmacology and Therapeutics, School of Medicine, University of Galway, Galway, Ireland, [2]Galway Neuroscience Centre, University of Galway, Galway, Ireland, [3]Centre for Pain Research, University of Galway, Galway, Ireland, [4]Department of Neuroscience, Neuropsychopharmacology and Psychobiology Research Group, University of Cádiz, Cádiz, Spain, [5]Physiology, School of Medicine, University of Galway, Galway, Ireland, [6]Instituto de Investigación e Innovación Biomédica de Cádiz (INiBICA), Hospital Universitario Puerta del Mar, Cádiz, Spain, [7]Centro de Investigación Biomédica en Red de Salud Mental (CIBERSAM), Instituto de Salud Carlos III, Madrid, Spain

Paclitaxel (PTX) is a commonly used chemotherapeutic drug, however, one of its major adverse effects is chronic neuropathic pain, with the incidence being higher in women than in men. The neurobiological mechanisms behind this sex difference are still largely unclear, and the endocannabinoid system, which exhibits sexual dimorphism and plays a key role in pain regulation, is a promising area for further studies. The present study aimed to characterise pain-, cognition-, anxiety-, and depression-related behaviours in male and female rats following PTX administration, and associated alterations in the endocannabinoid system. After the induction of the model, pain-related behaviours were assessed using von Frey, Acetone Drop and Hargreaves' tests, Novel Object Recognition and T-Maze Spontaneous Alternation tests were used for cognition-related behaviours, Elevated Plus Maze, Open Field, and Light Dark Box tests were used to assess anxiety-related behaviours, and Sucrose Preference, Sucrose Splash, and Forced Swim tests for depression-related behaviours. At each time point analysed, animals treated with PTX exhibited mechanical and cold hypersensitivity, with females displaying lower hind paw withdrawal thresholds to mechanical stimulation than males. No PTX-induced alterations in the other behavioural tests were detected. *Post-mortem* measurement of endocannabinoid and related *N*-acylethanolamine levels in spinal cord and discrete brain regions revealed a PTX-induced increase of 2-Arachidonoyl Glycerol (2-AG), *N*-Palmitoylethanolamine (PEA) and *N*-Oleoylethanolamine (OEA) levels in the amygdala of male and female animals, but not in the other areas. Collectively, these results suggest that PTX

causes similar long-lasting hypersensitivity to mechanical and cold stimuli, but not heat, in rats of both sexes, effects accompanied by increases in amygdalar levels of endocannabinoids and *N*-acylethanolamines.

KEYWORDS

paclitaxel, chemotherapy, neuropathic pain, endocannabinoids, behaviour

1 Introduction

Paclitaxel (PTX) is a chemotherapeutic agent first extracted in 1971 from the bark of the Pacific yew tree (*Taxus brevifolia)* (Picard and Castells, 2015). It belongs to the class of antineoplastic drugs known as taxanes, which interfere with the normal cycle of microtubule de- and re-polymerisation (Alqahtani et al., 2019). Specifically, PTX interacts with β-tubulin through the microtubule lattice, increasing microtubule stability and polymerisation, with consequent cell death (Klein and Lehmann, 2021).

Between 1992 and 1994, the US Food and Drug Administration approved PTX for several cancer types, including ovarian, breast, non-small cell lung, prostate cancer, Kaposi sarcoma, gastric cancer, oesophageal cancer, bladder cancer, and other carcinomas (Tkaczuk and Yared, 2012), either as a monotherapy or in combination with other chemotherapeutic compounds (Armstrong et al., 2006; Loesch et al., 2010). It is mostly prescribed to female patients, primarily due to its use in treating many female-specific cancers. However, a significant limit to PTX usage is its dose-limiting adverse side effects. These adverse effects include alopecia, nausea, vomiting, and general hypersensitivity (i.e., dyspnoea, urticaria, hypotension, and fever), in addition to peripheral neuropathy which is considered one of the primary adverse effects in patients treated with this drug (Walker, 1993). In fact, PTX induces peripheral neuropathy in up to 97% of all treated patients, and 60% of patients subsequently develop chronic neuropathy (Tanabe et al., 2013), with symptoms that normally include weakness, numbness, and pain, typically in the hands and feet.

Cognitive impairment, often referred as “chemo brain”, is another adverse effect that patients experience even after 6 months following cessation of chemotherapy (Ibrahim et al., 2021). Common symptoms of chemo brain include learning problems, selective attention and memory impairment (Lindner et al., 2014). There can also be a higher prevalence of depression or anxiety in patients receiving chemotherapy, including taxanes (Ibrahim et al., 2021).

Despite the progress made to characterise the molecular mechanisms and the effects of chemotherapeutic drugs, the role of biological sex is often ignored. Women who receive chemotherapy experience more severe side effects when compared to men (Choi et al., 2024; Yamamoto et al., 2008), and in this context, preclinical models can be useful to further elucidate the mechanisms underlying the adverse effects induced by these compounds. However, most of the studies published so far in chemotherapy-induced peripheral neuropathy (CIPN) models have used only male rodents (Currie et al., 2019), overlooking sex as a variable and potentially missing important factors for advancing personalised treatment.

First line treatments for CIPN (typically include antidepressants, such as serotonin and norepinephrine reuptake inhibitors, and anticonvulsants, like gabapentinoids (Quintão et al., 2019). However, both classes of drugs have exhibited a limited effectiveness for this purpose. For instance, patients treated with duloxetine appeared comparable to those treated with placebo in several clinical trials (Chow et al., 2023). Similarly, gabapentin demonstrated a lack of efficacy in alleviating CIPN symptoms associated with increased pain scores in paediatric patients (Anghelescu et al., 2020).

Cannabis-based medicines, including nabiximols (Sativex®) or cannabidiol, have been shown to reduce chemotherapy-evoked neuropathic pain (Lynch et al., 2014; Weiss et al., 2023). Further evidence is provided by studies performed with the aid of preclinical models: AM1710, a cannabilactone CB_2 agonist, induces antinociception in both cisplatin- and PTX-induced neuropathic pain models in rats (Deng et al., 2012). JZL184 and URB597, both compounds able to increase the levels of endocannabinoids through catabolic enzyme inhibition, reversed PTX-induced mechanical hypersensitivity in mice (Curry et al., 2018; Slivicki et al., 2019). These findings suggest a role for the endocannabinoid system in CIPN that requires further evaluation.

The endocannabinoid system is a complex neuromodulatory system that comprises the cannabinoid receptors 1 and 2 (respectively, CB_1 and CB_2), which are $G_{i/o}$-coupled receptors (GPCRs) negatively coupled to adenylate cyclase (Howlett, 2002; Munro et al., 1993), as well as their endogenous ligands, known as endocannabinoids, and the enzymes that either synthesise or degrade them. Other receptor targets for endocannabinoids include transient receptor potential vanilloid 1 (TRPV1), and peroxisome proliferator-activated receptors (PPAR) (Lago-Fernandez et al., 2021). CB_1 is expressed in both the peripheral and central nervous system, where it is widely distributed in neocortex, cerebellum, basal ganglia and limbic regions on the axon terminals and pre-terminal axon segments (Herkenham et al., 1991). Conversely, CB_2 is mainly expressed in the cells and tissues of the immune system and in activated microglia in the brain (Klegeris et al., 2003; Galiègue et al., 1995). The two best-characterised endocannabinoids are anandamide (AEA) (Devane et al., 1992) and 2-arachidonoyl glycerol (2-AG) (Sugiura et al., 1995). The *N*-acylethanolamines, *N*-Palmitoylethanolamine (PEA) and *N*-Oleoylethanolamine (OEA), are also substrates for the AEA-catabolising enzyme fatty acid amide hydrolase (FAAH) and can alter levels of AEA via substrate competition at FAAH (Cravatt et al., 1996). On the other hand, 2-AG is degraded into arachidonic acid and glycerol by the presynaptic enzyme monoacylglycerol lipase (MGL) (Dinh et al., 2002). Interestingly, numerous lines of evidence indicate that the endocannabinoid system exhibits sexual dimorphism in levels of endocannabinoids and related *N*-acylethanolamines or expression of endocannabinoid system

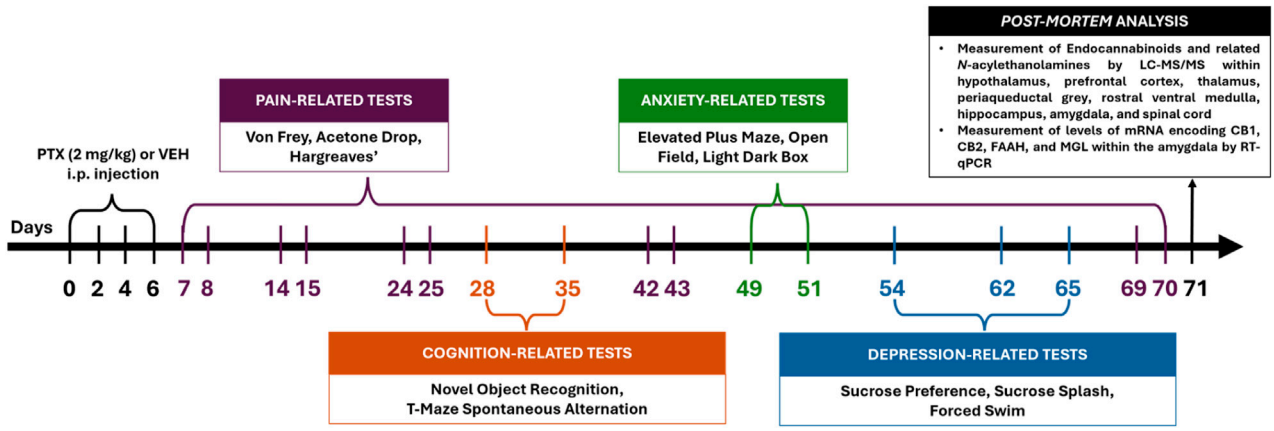

FIGURE 1
Schematic timeline of the experimental procedures (intraperitoneal injection indicated as i.p.).

components (Bradshaw et al., 2006; Rubino and Parolaro, 2011; Blanton et al., 2021). This is particularly interesting considering the observed sex differences in humans treated with chemotherapeutic compounds, highlighting the need for further investigation to clarify its role and clinical potential.

Therefore, the aim of the present study was to characterise the effects of PTX on neuropathic pain-related behaviour, anxiodepressive behaviour, and cognition in rats of both sexes, and to define associated biochemical and molecular changes induced in the endocannabinoid system.

2 Materials and methods

2.1 Animals

Forty adult Sprague-Dawley (SD) rats (Males 280–300 g, Females 200–220 g, 9–10 weeks of age) were purchased from Charles River UK (United Kingdom). Animals were pair-housed in cages (males together and females together) with water and food (14% Harlan Teklad 2014 Maintenance Diet, Envigo, Huntingdon, Cambridgeshire, United Kingdom) available *ad libitum*, and all animals housed in the same holding room. The holding room was at a constant temperature of 21°C ± 2°C under standard light conditions (12:12 h light: dark, lights on from 07.00 to 19.00 h). Every procedure was performed during the light phase by a female researcher.

The experimental procedures were approved by the Animal Care and Research Ethics Committee (ACREC), University of Galway, in accordance with the ARRIVE guidelines, under licence from the Health Products Regulatory Authority in the Republic of Ireland (HPRA) and in accordance with EU Directive 2010/63.

2.2 Establishment of PTX-induced neuropathic pain model

Paclitaxel (PTX; Taxol–Tocris by Biotechne, United Kingdom) was dissolved in ethanol (Sigma-Aldrich, Ireland):Kolliphore (Sigma-Aldrich, Ireland):saline (1:1:18) to a concentration of 2 mg/mL. PTX (2 mg/kg/day) or its vehicle (VEH) was administrated via intraperitoneal injections (1 mL/kg injection volume) on four alternative days (day 0, 2, 4, 6), with the first injection occurring 28 days after arrival of the rats into the animal facility. Male and female rats were pseudorandomly allocated to either the PTX or VEH (n = 10 rats per group) groups following baseline pain-related behaviour testing to ensure no significant between-group differences in baseline behaviour.

2.3 Behavioural procedures

All behavioural testing (Figure 1) was carried out by an experimenter blinded to PTX/VEH treatment.

2.3.1 Pain-related behaviour

2.3.1.1 Von Frey test

To measure mechanical hypersensitivity, the animals were placed on an elevated metal wire mesh, divided into six individual plexiglass compartments (14 × 20 × 25 cm) in which the light levels were set at 45 lux. They were left to habituate for 15 min before the assessment of mechanical sensitivity threshold using Electronic von Frey (BioSeb/Canada), able to determine the threshold based on the pressure applied on the surface by the experimenter (Martinov et al., 2013). The plastic tip was pressed against the centre of the hind paw until the withdrawal response for a total of three trials per hind paw (right and left). The test was performed 2 days before PTX or VEH administration, and on days 7, 14, 24, 42 and 69 after the first PTX injection (from now on indicated as "post-PTX").

2.3.1.2 Acetone Drop test

To measure cold hypersensitivity, the test was performed according to (Yoon et al., 1994), i.e., three applications of a cold drop of acetone were made on the centre surface of the hind paws using a 1 mL syringe. Test was performed after von Frey, so on days 7, 14, 24, 42 and 69 post-PTX, on both the left and right hind paws, using the same light conditions (45 lux). Latency to the first paw

withdrawal after the drop application and number of responses were recorded within the first 60 s.

2.3.1.3 Hargreaves' test

As previously described (Ferdousi et al., 2023), to measure heat hypersensitivity, the animals were placed in the apparatus (IITC Life Sci Inc., United States) comprised of a six-chambered acrylic arena (11 × 20 × 15 cm per compartment) positioned on a glass panel to habituate for 15 min with the same light conditions used for the other pain-related tests (45 lux). After the acclimatisation, a radiant light source (active intensity of 30% corresponding to 53°C) was applied from below to the centre surface of the hind paw for up to 20 s or until a hind paw withdrawal, lick or flinch response occurred. The latency to these responses was recorded. The test was performed 1 day before the PTX or VEH administration and on days 8, 15, 25, 43, and 70 post-PTX, on both the left and right hind paws.

2.3.2 Cognition-related behaviour

2.3.2.1 Novel object recognition test

The test was performed on day 28 post-PTX as previously described (Llorente-Berzal et al., 2012) to assess the presence of cognitive impairment. The animals were placed in a circular arena (75 cm diameter, with an aluminium reflective wall 40 cm high) for 5 min for 4 consecutive days with light levels set at 100 lux. On the fifth day, the animals were exposed first to two identical objects (called familiar objects from now on) with which they had to interact for a minimum period of 30 s or a maximum of 4 min. Animals that do not exhibit the minimum interaction time required are excluded from the test. At the end of this phase, they were put back in their home cages. After 4 h, they were re-exposed to one of the familiar objects and a novel object for 3 min. Total time, first 30 and 60 s spent exploring each object were recorded with an overhead camera and analysed with the aid of EthoVision XT software (Noldus Information Technology, Wageningen, Netherlands) and the Discrimination Ratio (DR) was calculated as follows with T being the time spent exploring objects

$$DR = \frac{T_{(novel)} - T_{(familiar)}}{T_{(total)}}$$

2.3.2.2 T-Maze Spontaneous Alternation test

The test was performed on days 35 and 36 post-PTX according to (Deacon and Rawlins, 2006) with some minor changes to better assess the presence of any spatial memory impairment in the model used. The animals were placed into a black-painted T-shaped arena (50 cm in length and 10 cm in width) with 18 lux level. During the first phase (sample phase), animals were placed in the arena with a central partition and left free to choose one of the two arms of the apparatus. After making their choice, a guillotine door slid down, and the animals were kept there for 30 s. In the following phase (choice phase), animals were placed in the arena without the central partition and left free to choose one of the arms for a maximum of 90 s. The test was carried out over 2 days with five exposures per day, and a total number of ten exposures per animal. The percentage of alternation, error in alternation, error of missed choice were analysed for each animal.

2.3.3 Anxiety-related behaviour

2.3.3.1 Elevated Plus Maze test

The test was performed to assess changes in the natural tendency of rodents to avoid open spaces (Kraeuter et al., 2019) on day 49 post-PTX. The arena in which animals were placed was elevated 50 cm above the floor of the testing room, and it consisted of a maze with two arms closed by walls (30 cm high, 50 × 10 cm), two open arms (50 × 10 cm), and a central area that connected the arms (10 × 10 cm). The light levels were at 45 lux in the open arms and 15 lux in the closed arms. Animals were placed in the central platform facing one of the open arms for 5 min, while the time spent in, and the frequency of entries into, the central area of the arena and the open and closed arms were recorded with an overhead camera and analysed with the aid of EthoVision XT software (Noldus Information Technology, Wageningen, Netherlands).

2.3.3.2 Open Field test

Immediately after the Elevated Plus Maze test on day 49 post-PTX, animals were placed in a square arena (43 × 43 × 43 cm) for 5 min to monitor the exploration of different areas of a novel brightly lit apparatus and locomotor activity (Gould et al., 2009). The light levels were at 200 lux. The locomotor activity and time spent in the inner and outer zones were recorded with an overhead camera and analysed with the aid of EthoVision XT software (Noldus Information Technology, Wageningen, Netherlands).

2.3.3.3 Light Dark Box test

The test was performed on day 51 post-PTX (Crawley, 1985). The two-chambered arena was comprised of a light area (30 × 30 cm) illuminated at 150 lux, and a dark area of the same size at 0 lux at the corner of the compartment was defined as the illuminated light chamber at 150 lux. The other compartment was designated as the dark chamber illuminated at 0 lux at the corners and 5 lux at the passage entrance connecting both chambers. Animals were placed in the bright area and left free to explore the apparatus for 20 min. The frequency of entries and time spent in each chamber were recorded with an overhead camera and analysed with the aid of EthoVision XT software (Noldus Information Technology, Wageningen, Netherlands).

2.3.4 Depression-related behaviour

2.3.4.1 Sucrose Preference test

To measure the natural inclination of animals to consume a palatable liquid, deficits in which are considered a measure of depression-related behaviours (Willner et al., 1987), the test was carried out as described in (Boullon et al., 2021) starting on day 54 post-PTX. Briefly, for 4 days the pair-housed animals were trained to drink from a bottle placed on either side of the home cage (right or left), where the light levels were set at 30 lux. On days 1 and 2, the bottle was filled with a solution of 0.5% sucrose, while on days 3 and 4 the bottle was filled with water. The position of the bottle changed from the right to the left every 24 h. On day 5, the animals were provided with a bottle of sucrose 0.5% placed on the right side, and a bottle of water placed on the left. The bottle positions were swapped after 12 h and the test ended after an additional 12 h. At any stage of this test, the bottles were weighed. The preference for sucrose solution was calculated as:

$$\%\,Sucrose\,Preference = \frac{Sucrose\,Intake}{Total\,Intake} mL \times 100$$

Additionally, the sucrose intake was expressed as a percentage of 0.5% sucrose consumed per body weight (Hestehave et al., 2020), calculated as:

$$Percentage\,of\,0.5\%\,sucrose\,per\,body\,weight = \frac{Sucrose\,Intake\,(mL)}{Body\,weight\,(g)} \times 100$$

The body weight and the sucrose intake used were the average value between the weights and the consumption of the two animals in the cage, as they were pair-housed.

2.3.4.2 Sucrose splash test

Considering the importance of self-grooming behaviour in rats (Kalueff et al., 2016), this behaviour may be considered a measure of self-care and was analysed using the Sucrose Splash test. The test was carried out on day 62 post-PTX by placing the animals in a Plexiglass box (30 × 30 × 40 cm^3) at 30 lux for a habituation period of 10 min. After this time, the dorsum of the animals was sprayed with a 10% sucrose solution and the self-grooming behaviour was recorded for 10 min with a camera placed underneath the arena and analysed with the aid of EthoVision XT software (Noldus Information Technology, Wageningen, Netherlands).

2.3.4.3 Forced Swim test

The test was carried out on day 65 post-PTX with the first exposure, and on day 66 post-PTX for the second exposure, according to (Detke et al., 1995), considering immobility as a passive coping strategy that rats adopt after a period of active escape-oriented behaviour. Essentially, the animals were forced to swim for 15 min in Plexiglass cylinders (45 cm height, 20 cm diameter) containing water at 25°C; the light level in the room was set a 30 lux. After 24 h, rats were re-exposed to this environment for 5 min. The exposures were recorded with a camera, and the time spent immobile (absence of movements), climbing (vertical movements), and swimming (horizontal movements) were scored with the aid of EthoVision software XT (Noldus Information Technology, Wageningen, Netherlands).

2.4 Tissue collection

Animals were euthanised at day 71 post-PTX by live decapitation. The hypothalamus, prefrontal cortex, amygdala, hippocampus, periaqueductal grey, thalamus, rostral ventral medulla, and dorsal lumbar area of the spinal cord were gross-dissected, snap-frozen on dry ice and stored at −80°C prior to measurement of endocannabinoids and related *N*-acylethanolamines (Figure 1). Lateralised regions were harvested separately as left and right.

2.5 Measurement of endocannabinoids and related *N*-acylethanolamines by liquid chromatography coupled to tandem mass spectrometry (LC-MS/MS)

Levels of endocannabinoids (AEA, 2-AG) and related *N*-acylethanolamines (PEA, OEA) were measured according to (Boullon et al., 2021; Corcoran et al., 2020; Kerr et al., 2012) in the spinal cord, prefrontal cortex, hypothalamus, amygdala, hippocampus, periaqueductal grey, thalamus, and rostral ventral medulla.

A solution composed of 200 µL of 100% acetonitrile containing deuterated internal standards (2.5 ng d8-AEA, 50 ng d8-2-AG, 2.5 ng d4-PEA, 2.5 ng d4-OEA; Cayman Chemicals, Cambridge Biosciences, UK) was added to each sample, and 75 µL of 100% acetonitrile only. The samples were then homogenised using a sonicator (Sonifier, Branson, Ireland) for ~5 s and then centrifuged at 14,000 × g for 15 min at 4°C (Hettich® centrifuge Mikro 22R, Hettich, Germany). To calculate the unknown analyte concentration, a 10-point standard curve was made by adding 75 µL of acetonitrile 100% to the higher standard (10), composed of 25 µL of acetonitrile 100% and non-deuterated 25 ng AEA, PEA, OEA and 250 ng 2-AG; the sample was vortexed, and 25 µL of this mixture was removed and placed into the next tube, with serial dilution from the highest to the lower standard (1), discarding the last 25 µL to ensure the same volume in each tube. Once completed, the solution composed of 200 µL of 100% acetonitrile with deuterated internal standard were added to each standard tube. A total amount of 40 µL was removed from sample and standard tubes and transferred to HPLC vials.

A solution comprised of HPLC grade water with 0.1% formic acid, and a solution comprised of 100% acetonitrile with 0.1% formic acid for 3 min were used with a flow rate of 0.2 mL/min using a Waters Atlantis T3 column (3 µm particles, 100 mm length, 2.1 mm diameter; Waters, UK). The elution was carried out using in reverse-phase gradient, starting with 2% acetonitrile for 3 min, followed by an increase to 65% acetonitrile at 3.1 min for 1 min, and then a linear ramp to 100% by 8 min, where it was maintained until 16 min. The initial conditions were then restored at 16.1 min for 12 min to re-equilibrate the column before the next injection.

Detection of analytes was performed using electrospray-positive ionization mode on an Agilent 1100 HPLC system, which was connected to a triple quadrupole 6,460 mass spectrometer (Agilent Technologies, Cork, Ireland). Quantification was achieved ratiometrically with the Agilent Mass-Hunter Quantitative Analysis Software (Agilent Technologies, Cork, Ireland). The analyte concentrations in unknown samples were determined by calculating the peak area response ratio of the analyte to the internal standard.

2.6 Measurement of levels of mRNA encoding CB_1, CB_2, FAAH, and MGL within the amygdala by real time-quantitative polymerase chain reaction

The total RNA was extracted from pellets following the preparation for LC-MS/MS using a Macherey-Nagel NucleoSpin RNA (Mini Kit for RNA purification, Fisher Scientific, Ireland), as per manufacturer instructions. RNA concentration, integrity, and purity were assessed using a Nanodrop spectrophotometer (ND-1000; Nanodrop, Labtech International, UK). Purity was assessed by the absorbance ratio at 260/280, with values ~2 considered acceptable, while the 260/230 ratio, with an acceptable range of 2.0–2.2, was used to indirectly assess integrity. The samples were

TABLE 1 Summary table of the results of behavioural assays performed relative to the days post-PTX.

		Days post-PTX																
Behaviour	Assay	7	8	14	15	24	25	28	35	42	43	49	51	54	62	65	69	70
Pain-related	Von Frey	+		+		+				+							+	
	Acetone Drop	+		+		+				+							+	
	Hargreaves'		–		–		–				–							–
Cognition-related	Novel Object Recognition							–										
	T-Maze Spontaneous Alternation								–									
Anxiety-related	Elevated Plus Maze											–						
	Open Field											–						
	Light Dark Box												–					
Depression-related	Sucrose Preference													–				
	Sucrose Splash														–			
	Forced Swim															–		

(+) indicates a significant effect of PTX; (–) indicates absence of effect; empty cell indicates that the test was not performed at that time point.

normalised to a concentration of 88 ng/μL. The transcription of the RNA to cDNA was done using a High-Capacity cDNA Reverse Transcription Kit (ThermoFisher Scientific, Ireland). TaqMan gene expression assay was carried out using an Applied Biosystems "StepOne Plus" instrument (Bio-Sciences, Dun Laoghaire, Ireland) using TaqMan Universal PCR Master Mix, no AmpErase UNG (ThermoFisher Scientific, Ireland), and different FAM-labelled probes to quantify the genes of interest (*cnr1* gene for CB_1, assay ID: Rn00562880_m1; *cnr2* gene for CB_2, assay ID: Rn03993699_s1; *faah* gene for FAAH, assay ID: Rn00577086_m1; *mgll* gene for MGL, assay ID: Rn00593297_m1) and a VIC-labelled ACTB for beta-actin as housekeeping gene (Assay ID: Rn00667869_m1).

2.7 Statistical analysis

IBM SPSS Statistics 27.0 statistical software (Chicago, United States) was used to perform the statistical analysis and GraphPad Prism 10.2.3 (GraphPad Software, Boston, Massachusetts United States) for graph design. Normality and homogeneity were assessed by Shapiro-Wilk test and Levene's test, respectively. When parametric assumptions were met, datasets were analysed either with a standard two-way Analysis of Variance (ANOVA) (factors: Sex, Treatment) followed by Tukey HSD (Honest Significant Difference) *post hoc* test for multiple comparisons or a two-way repeated measures ANOVA followed by Tukey's HSD. Three-way ANOVA (Factor: Sex, Treatment, Side) was used to analyse levels of endocannabinoids and *N*-acylethanolamines in lateralised regions (spinal cord, hippocampus, and amygdala). When parametric assumptions were not met, datasets were analysed by Friedman's two-way ANOVA by ranks followed by Mann–Whitney U *post hoc* with Bonferroni-Holm correction to assess differences between groups at each specific time point. If significant main effects of PTX or sex were observed, or their interaction, then *a priori post-hoc* pairwise group comparisons were carried out. Parametric data are expressed as group means ± standard error of the mean (±SEM) and non-parametric data as medians with interquartile range, and for all the significance level was set at $p < 0.05$.

3 Results

Tables 1, 2 summarise the results of the behavioural assays performed relative to the days post-PTX and the results of the *post-mortem* analysis, respectively. Data on body weight throughout the study are presented in Supplementary Figure S1.

3.1 PTX induced long-term mechanical hypersensitivity in SD rats of both sexes

There were no significant between-group differences in hind paw withdrawal thresholds (PWT) to mechanical stimulation (electronic von Frey) at baseline. Significant differences between groups in mechanical hypersensitivity, measured as paw withdrawal thresholds (PWT), were observed at every post-PTX time point analysed for both hind paws (Figures 2A, B). Two-way ANOVA with repeated measures with sex and treatment as factors for both paws revealed a significant effect of time (Left: $F_{(3.58,128.74)} = 3.791$; $p = 0.008$. Right: $F_{(3.71,133.52)} = 8.591$; $p < 0.001$), a significant effect of the interaction Time × Treatment (Left paw: $F_{(3.58,128.74)} = 3.791$; $p < 0.001$ Right paw: $F_{(3.71,133.52)} = 18.670$; $p < 0.001$), and a significant effect of Sex (Left: $F_{(1,36)} = 18.886$; $p < 0.001$. Right: $F_{(1,36)} = 18.047$; $p < 0.001$) and Treatment (Left: $F_{(1,36)} = 160.148$; $p < 0.001$. Right: $F_{(1,36)} = 134.784$; $p < 0.001$).

Post hoc analysis revealed that PTX induced a decrease in PWT in the left (Figure 2A) and right (Figure 2B) hind paws in both sexes at each time point analysed, compared with VEH-treated controls.

10.3389/fphar.2024.1505980

TABLE 2 Summary table of the results of *post-mortem* analysis performed.

		Targets							
Analysis	Region	AEA	PEA	OEA	2-AG	CB_1	CB_2	MAGL	FAAH
LC-MS/MS	Hypothalamus	–	–	–	–				
	Prefrontal Cortex	–	–	–	–				
	Thalamus	–	–	–	–				
	Periaqueductal grey	–	–	–	–				
	Rostral ventral medulla	–	–	–	–				
	Hippocampus	–	–	–	–				
	Amygdala	–	+	+	+				
	Spinal Cord	–	–	–	–				
RT-qPCR	Amygdala					–	–	–	–

(+) indicates a significant effect of PTX; (–) indicates absence of effect; empty cell indicates that the test was not performed.

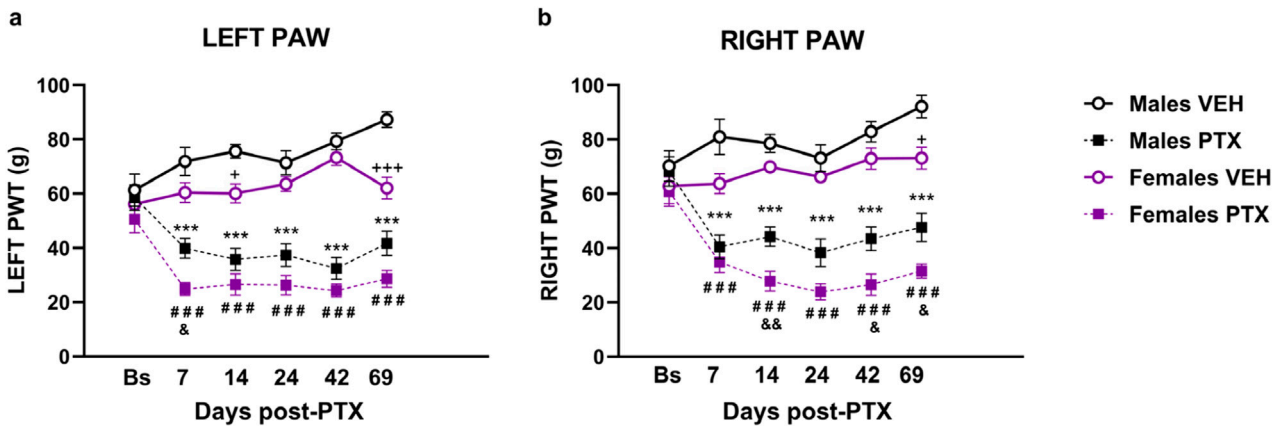

FIGURE 2
Von Frey test. Investigation of mechanical hypersensitivity in male and female rats following Paclitaxel (PTX) or vehicle (VEH) intraperitoneal injections from Baseline (Bs) to day 69. Paw withdrawal threshold (PWT): left paw **(A)** and right paw **(B)**. Two-way repeated measures ANOVA followed by Tukey HSD (Honest Significant Difference) *post hoc*. Data expressed as mean ± S.E.M (n = 10 per group) *$p < 0.05$, **$p < 0.01$, ***$p < 0.001$ Males PTX vs. Males VEH, #$p < 0.05$, ##$p < 0.01$, ###$p < 0.001$ Females PTX vs. Females VEH, and $p < 0.05$, and $p < 0.01$ Females PTX vs. Males PTX, + $p < 0.05$, +++ $p < 0.001$ Females VEH vs. Males VEH.

Females treated with PTX exhibited significantly lower left hind paw PWT on day 7, and significantly lower right hind paw PWT on days 14, 42 and 69, compared with male counterparts. However, females treated with VEH also exhibited significantly lower left hind paw PWT on days 14 and 69, and significantly lower right hind paw PWT on day 69, compared with male counterparts.

3.2 PTX-induced cold hypersensitivity long-term in SD rats of both sexes

Friedman's test revealed significant differences between groups in cold hypersensitivity, measured as latency to the first response in seconds, in both hind paws (Left Paw Latency: χ^2 (5) = 52.693, $p < 0.001$, Figure 3A; Right Paw Latency: χ^2 (5) = 35.315, $p < 0.001$, Figure 3B). *Post hoc* analysis revealed that PTX induced a decrease in the latency to the first response in the left (Figure 3A) and right (Figure 3B) hind paw in both sexes at each time point analysed, compared to VEH-treated controls and compared with baseline. No significant differences were observed between the other groups.

Furthermore, significant differences between groups were found when measuring cold hypersensitivity as the number of responses within 60 s, at every time point analysed in left (χ^2 (5) = 46.803, $p < 0.001$, Figure 3C) and right (χ^2 (5) = 37.675, $p < 0.001$, Figure 3D) hind paws. *Post hoc* analysis revealed that PTX induced an increase in the number of responses within 60 s on the left (Figure 3C) and right (Figure 3D) hind paws in both sexes at each time point analysed, compared to VEH-treated controls and compared with baseline. No significant differences were observed in the other groups.

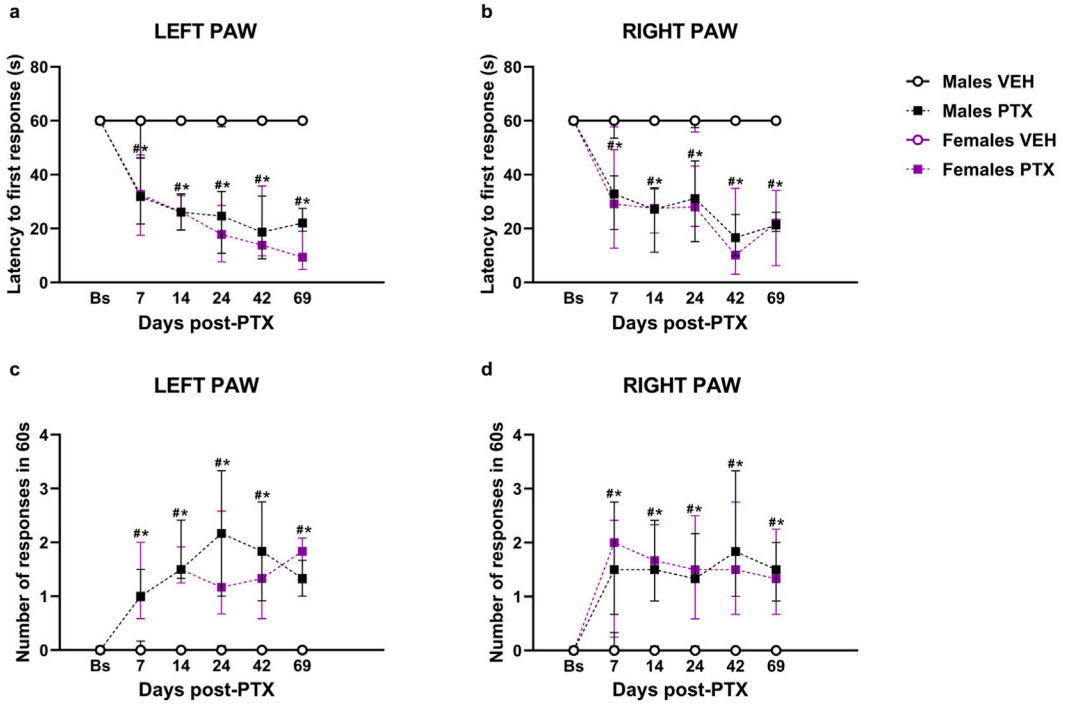

FIGURE 3
Acetone Drop test. Investigation of cold hypersensitivity in male and female rats following PTX or VEH intraperitoneal injections. Left **(A)** and right **(B)** paw latency to the first response after acetone stimulation and left **(C)** and right paw **(D)** number of responses after acetone stimulation. Data expressed as Median with IQR (n = 10 per group). Friedman's two-way ANOVA by ranks followed by Mann–Whitney U *post hoc* with Bonferroni-Holm correction, *$p < 0.05$ Males PTX vs. Males VEH, #$p < 0.05$ Females PTX vs. Females VEH, and $p < 0.05$ Females PTX vs. Males PTX.

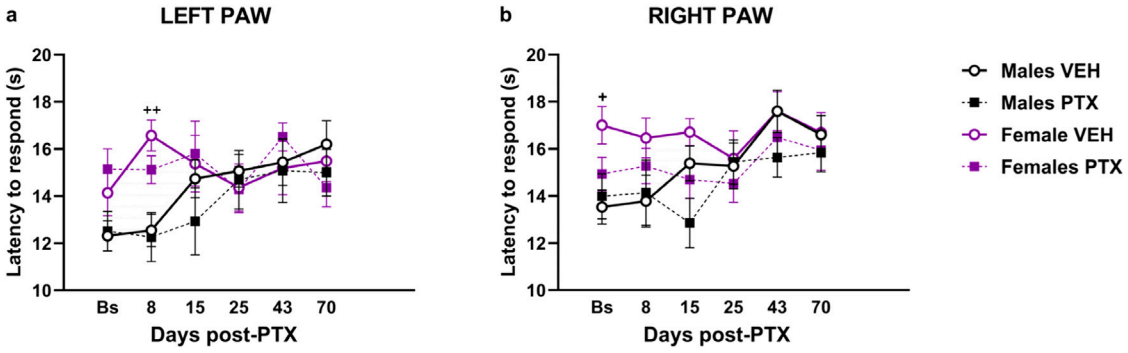

FIGURE 4
Hargreaves' test. Investigation of heat hypersensitivity in male and female rats following Paclitaxel (PTX) or vehicle (VEH) intraperitoneal injections from Baseline (Bs) to day 70. Left **(A)** and right **(B)** latency to the first response after heat stimulation. Two-way repeated measure ANOVA followed by Tukey HSD (Honest Significant Difference) *post hoc*. Data expressed as mean ± S.E.M (n = 10 per group) + $p < 0.05$, ++ $p < 0.01$ Females VEH vs. Males VEH.

3.3 PTX did not induce heat hypersensitivity in SD rats of both sexes

Significant differences between groups were found in heat sensitivity, measured as latency to the first response within 20 s at different time points analysed in both paws (Figures 4A, B). Two-way ANOVA with repeated measures with sex and treatment as factors revealed a significant effect of time for both paws (Left: $F_{(3.58,128.74)} = 3.791$; $p = 0.008$. Right: $F_{(3.71,133.52)} = 8.591$; $p < 0.001$) and a significant effect of the interaction of Time × Treatment for both paws (Left paw: $F_{(5,180)} = 3.509$; $p = 0.005$. Right paw: $F_{(5,180)} = 5.152$; $p < 0.001$). *Post hoc* analysis revealed that PTX did not induce any changes in the latency to the first response in the left (Figure 4A) and right (Figure 4B) in both sexes at each time point analysed, compared with VEH-treated controls or compared with baseline. However, females treated with VEH showed a significant increase in paw latency compared to their male counterparts, on the left paw latency on day 8, and on the right paw latency at the Baseline.

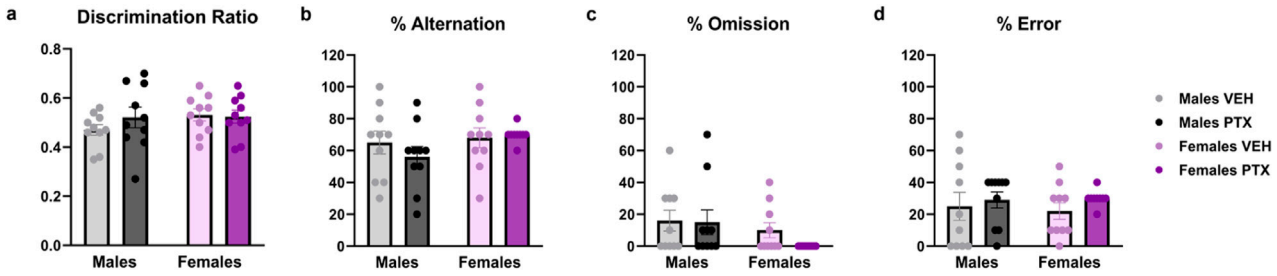

FIGURE 5
Novel Object Recognition and T-Maze Spontaneous Alternation tests. Investigation of cognition-related behaviour in male and female rats on days 28 (Novel Object Recognition test) and 35 (Alternated T-Maze test) following PTX or VEH intraperitoneal injections. The ratio **(A)** was calculated as Discrimination Ratio = (Time spent exploring the novel object - Time spent exploring the familiar object)/Total time spent exploring the objects. The percentage of alternation **(B)**, omission **(C)**, and error **(D)** in the T-Maze Spontaneous Alternation test. Data expressed as mean ± SEM (n = 10 per group).

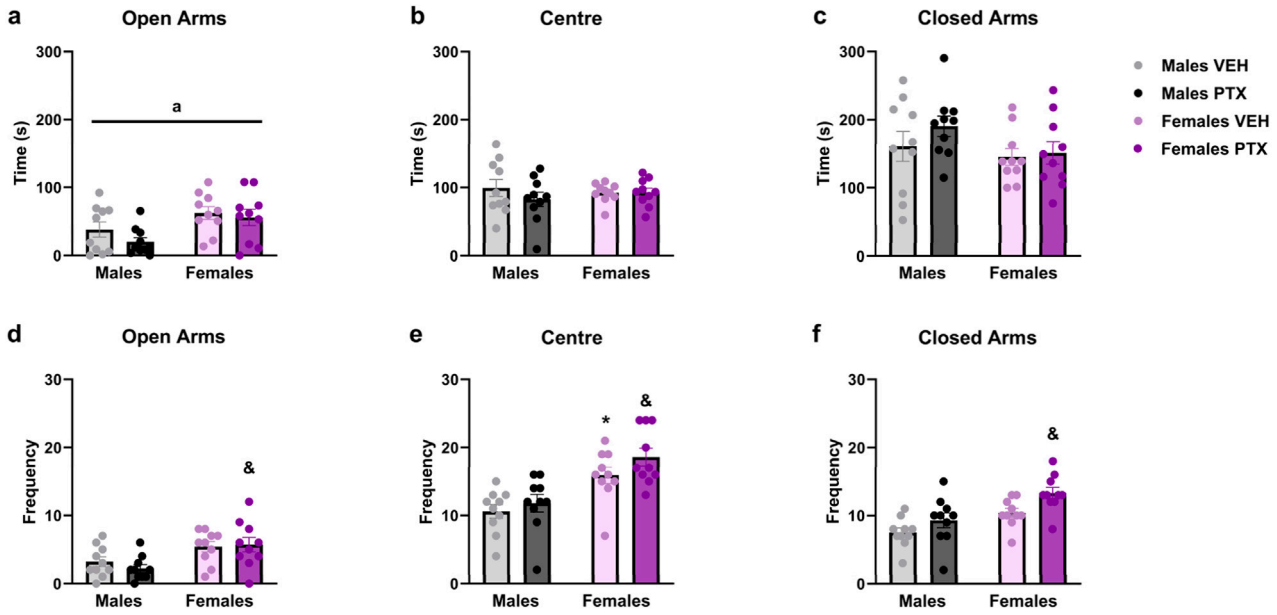

FIGURE 6
Elevated Plus Maze test. Investigation of anxiety-related behaviour in male and female rats on day 49 following PTX or VEH intraperitoneal injections. Time spent in open arms **(A)**, central area of the apparatus **(B)**, and closed arms **(C)**. Frequency of entries in open arms **(D)**, central area of the apparatus **(E)**, and closed arms **(F)**. Two-way ANOVA followed by Tukey HSD (Honest Significant Difference) *post hoc*. Data expressed as mean ± S.E.M (n = 10 per group). *$p < 0.05$ Males PTX vs. Males VEH, and $p < 0.05$ Females PTX vs. Males PTX, a = significant effect of sex in ANOVA.

3.4 PTX did not alter cognition-related behaviour in SD rats of both sexes

No significant differences between groups were found in Novel Object Recognition test (Figure 5A; Supplementary Figures S2A–S2C) or T-Maze Spontaneous Alternation test (Figures 5B–D).

3.5 PTX did not alter anxiety-related behaviour in SD rats of both sexes

PTX had no significant effects on behaviour in the Elevated Plus Maze (Figure 6A–F). However, a significant ANOVA effect for the factor sex emerged in the time spent in the open arms (Figure 6A), with an increase for females treated either with PTX or VEH (Time spent in the open arms: $F_{(1,36)} = 9.204$; $p = 0.004$). Regarding the frequency of entries into the different areas of the apparatus: there was a significant increase in: entries in open arms displayed by females treated with PTX when compared to their male counterparts (Figure 6D) (Frequency of entries into open arms: $F_{(1,36)} = 12.842$; $p = 0.001$); entries in the central area of the apparatus where females treated either with PTX or VEH showed a significant increase when compared to their male counterparts (Figure 6E) (Frequency of entries into the central area: $F_{(1,36)} = 24.989$; $p < 0.0010$); entries in the closed arms where females treated with PTX showed a significant increase

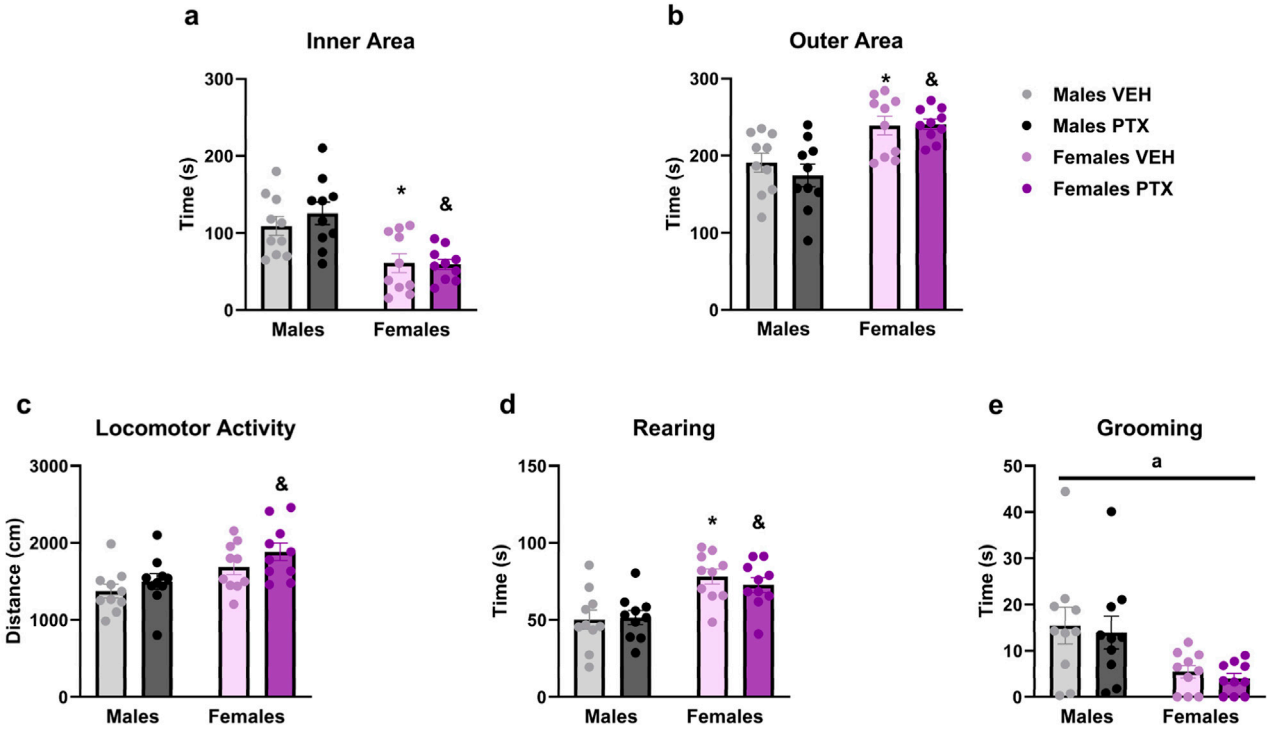

FIGURE 7
Open field test. Investigation of anxiety-related behaviour in male and female rats on day 49 following PTX or VEH intraperitoneal injections. Time spent in the inner area of the apparatus **(A)**, outer area **(B)**, locomotor activity **(C)**, rearing **(D)**, and grooming **(E)**. Two-way ANOVA followed by Tukey HSD (Honest Significant Difference) *post hoc*. Data expressed as mean ± S.E.M (n = 10 per group). *$p < 0.05$ Males PTX vs. Males VEH, and $p < 0.05$ Females PTX vs. Males PTX, a = significant effect of sex in ANOVA.

when compared to their male counterparts (Figure 6F) (Frequency of entries in the closed arms: $F_{(1,36)} = 7.855$; $p = 0.008$).

PTX had no significant effects on behaviour in the Open field test. However, there were significant main effects of sex on time spent in the inner area of the apparatus (Figure 7A) ($F_{(1,36)} = 23.717$; $p < 0.001$), time spent in the outer area of the apparatus (Figure 7B) ($F_{(1,36)} = 23.707$; $p < 0.001$), distance moved (Figure 7C) ($F_{(1,36)} = 11.937$; $p = 0.001$), time spent rearing (Figure 7D) ($F_{(1,36)} = 22.836$; $p < 0.001$) and time spent grooming (Figure 7E) ($F_{(1,36)} = 12.566$; $p = 0.001$). Further *post hoc* analysis confirmed that females treated either with VEH or PTX displayed increased time in the inner area, outer area, rearing and grooming, compared to their male counterparts. Females treated with PTX exhibited an increase in distance moved compared to their male counterparts.

No significant differences between groups were observed in Light Dark Box test (Figures 8A–D).

3.6 PTX had no effects on depression-related behaviour in SD rats of both sexes

No significant differences between groups were found in the Sucrose Preference (Figures 9A, B), Sucrose Splash (Figures 9C, D), or Forced Swim (Figures 10A–C; Supplementary Figures S3A–S3C) tests.

3.7 PTX induced an increase in PEA, OEA, and 2-AG in the amygdala but not in the other regions in SD rats of both sexes

The measurement of endocannabinoids and related *N*-acylethanolamines in various brain regions and spinal cord revealed a main effect of PTX on 2-AG ($F_{(1,72)} = 6.108$; $p = 0.016$), PEA ($F_{(1,72)} = 12.842$; $p = 0.001$), and OEA ($F_{(1,72)} = 4.158$; $p = 0.005$) in the amygdala, in which also an effect of side was found for AEA ($F_{(1,72)} = 10.271$; $p = 0.002$) and OEA ($F_{(1,72)} = 8.257$; $p = 0.005$) (Figures 11A–D). Further *post hoc* analyses did not reveal any significant pairwise between-group differences. No significant differences between groups were found in the other brain regions analysed (hypothalamus (Figures 12A–D), prefrontal cortex (Figures 12E–H), hippocampus (Figures 11E–H), thalamus (Figures 12I–L), periaqueductal grey (Figures 12M–P), rostral ventral medulla (Figures 12Q–T) or spinal cord (Figures 13A–D)).

RT-qPCR on the amygdala tissue revealed a main effect of sex with females showing an increased expression of *cnr2* ($F_{(1,72)} = 9.491$; $p = 0.003$) and *faah* ($F_{(1,72)} = 7.283$; $p = 0.009$). However, the *post hoc* analysis did not reveal any significant pairwise between-group differences (Figures 14A–D).

4 Discussion

There is a paucity of published studies investigating sex differences in animal models of CIPN (Currie et al., 2019). Such

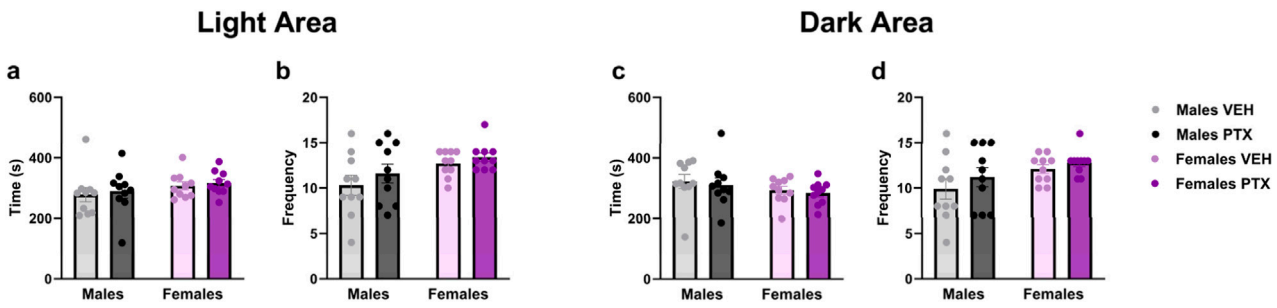

FIGURE 8
Light Dark Box. Investigation of anxiety-related behaviour in male and female rats on day 51 following PTX or VEH intraperitoneal injections. Time **(A)** and frequency **(B)** in the light area, and time **(C)** and frequency **(D)** in the dark area. Data expressed as mean ± S.E.M (n = 10 per group).

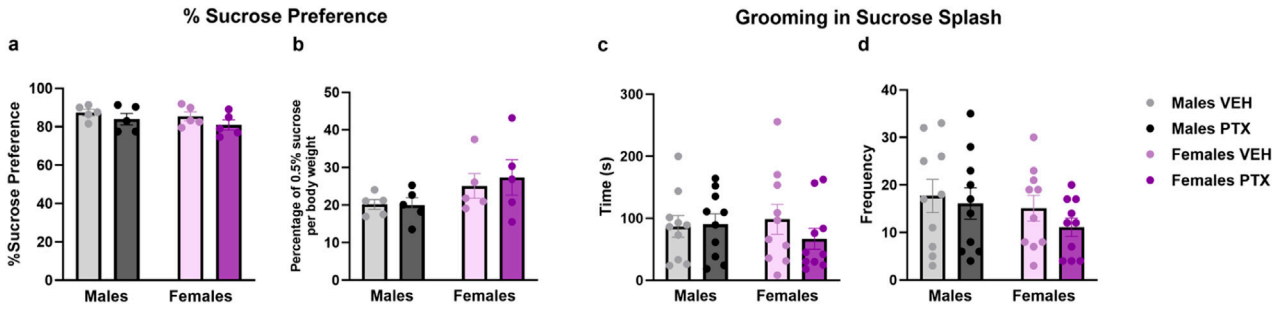

FIGURE 9
Sucrose preference and Sucrose Splash. Investigation of depression-related behaviour in male and female rats respectively on day 54 and 62 following PTX or VEH intraperitoneal injections. Percentage of Sucrose preference calculated as (Sucrose Intake/Total Intake) × 100 **(A)**, and Percentage of 0.5% sucrose per body weight calculated as (Sucrose Intake)/(Body weight) × 100 **(B)**. Data expressed as mean ± S.E.M (n = 5 per group). Time spent grooming **(C)**, and frequency **(D)** in sucrose splash. Data expressed as mean ± S.E.M (n = 10 per group).

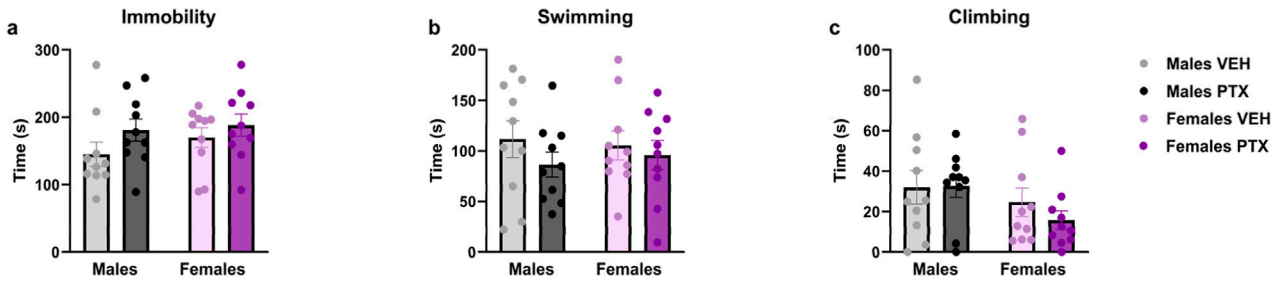

FIGURE 10
Forced Swim test. Investigation of learned helplessness or behavioural despair in male and female rats on day 65 following PTX or VEH intraperitoneal injections. Time spent immobile **(A)**, swimming **(B)**, and climbing **(C)**. Data expressed as mean ± S.E.M (n = 10 per group).

studies are required to advance the understanding and personalised treatment of this condition. Here, we show that PTX administration induced a robust and sustained neuropathic pain-related phenotype in both male and female Sprague-Dawley rats. PTX-treated animals of both sexes exhibited mechanical and cold hypersensitivity over 70 days post-PTX. Paw withdrawal thresholds to mechanical stimulation were lower in PTX-treated female rats than in male counterparts, however, VEH-treated females also exhibited lower withdrawal thresholds than VEH-treated males at discrete time points. The tendency for female rats to exhibit lower paw withdrawal thresholds than males to mechanical stimulation has been already published (Hendrich et al., 2012), consistent with the findings in this study. In addition, it has been reported that hypersensitivity induced by PTX can be more robust in female versus male mice (Ward et al., 2011). While few studies to date have analysed sex differences in the PTX model or in any other CIPN model, the data obtained from male animals in this study is consistent with the majority of studies to date in the PTX-

10.3389/fphar.2024.1505980

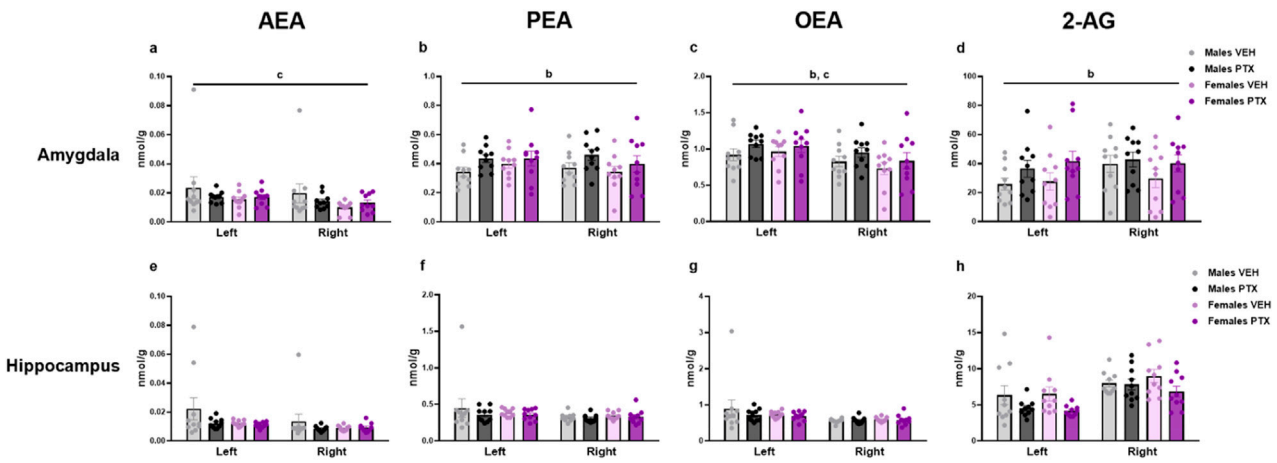

FIGURE 11
Investigation of levels of endocannabinoids and related *N*-acylethanolamines (nmol/g of tissue) in male and female rats following intraperitoneal injection of VEH or PTX in the amygdala **(A–D)**, and hippocampus **(E–H)**. Three-way ANOVA (factors: sex, treatment, side). Data expressed as mean ± S.E.M (n = 10 per group). b = significant effect of treatment; c = significant effect of side in ANOVA.

induced neuropathic pain model (Toma et al., 2017) and in other CIPN models such as oxaliplatin (Noya-Riobó et al., 2023). On the other hand, they highlight the need for inclusion of both sexes in future studies to increase the understanding of sex differences in neuropathic pain.

PTX had no effect on sensitivity to noxious heat assessed with the Hargreaves' test, as previously reported in other publications in which the same strain has been used (Griffiths et al., 2018; Huynh et al., 2019). This is also in line with findings for the same model in mouse, where the same cumulative dose of this study was used (Smith et al., 2004), and it may be related to the absence of neurodegeneration observed with this regimen (Flatters and Bennett, 2006).

Between days 28 and 35 post-PTX, cognition-related behaviour was tested with the Novel Object Recognition and T-Maze Spontaneous Alternation tests, and the animals did not exhibit any PTX-induced alterations in cognitive performance in these tests. However, the VEH-treated groups did not show the expected degree of preference for the novel object under the conditions employed in this study, making it very difficult to draw any firm conclusions relating to the effects of PTX on object recognition memory in this study. The protocol used has previously been used successfully in Wistar rats (Llorente-Berzal et al., 2012), however Sprague-Dawley rats were used in the present study and this strain has previously exhibited lower novel object recognition performance compared to other strains (Gökçek-Saraç et al., 2015). Regardless, the absence of cognitive impairment has been seen in another CIPN model: animals treated with oxaliplatin did not display any treatment effect in the Novel Object Recognition test (Fardell et al., 2015). Moreover, in Sprague-Dawley, PTX has been shown to impair reversal learning without affecting prior learning, new learning, and episodic memory (Panoz-Brown et al., 2017), suggesting that the mechanism underlying this impairment may be both distinctive and highly specific.

The battery of anxiety-related tests was performed between days 49 and 51 post-PTX, and PTX treatment did not alter anxiety-related behaviour in any of the tests performed. However, a sex difference was observed in both the Elevated Plus Maze and the Open Field tests, with females being more active and spending more time in the open arms and central areas compared to males, which is corroborating previous work (Börchers et al., 2022). No between-group differences were detected in the Light Dark Box test; however, animals did not exhibit the expected preference for the dark area of the apparatus versus the light area. It is possible that light levels, which were set at 150 lux in the light chamber, may not have been sufficiently aversive in the Sprague-Dawley strain (Campos-Cardoso et al., 2023). Nevertheless, these affective behaviours seem more evident in mice rather than in rats, where animals showed anxiety-like behaviours in the Elevated Plus Maze, Open Field and Light Dark Box tests (Toma et al., 2017; Liu et al., 2022).

The battery of depression-related tests was conducted between days 54 and 65 post-PTX, and PTX had no effects in any of the tests carried out. To our knowledge, data on these behaviours in the PTX-induced neuropathic pain model in rats have not been documented in the existing literature to date. Effects induced by PTX have been reported in mice for anhedonia and learned helplessness or behavioural despair, respectively after one and 2 weeks from the induction of the model, with animals exhibiting higher time spent immobile in the Forced Swim test and a marked preference for the sucrose solution in the Sucrose preference (Toma et al., 2017). However, an absence of PTX-induced changes within the same tests, strain and species has also been reported (Huehnchen et al., 2017).

Taken together, these results indicate that it is difficult to draw any firm conclusions on anxiety- and depression-related behaviour considering the paucity of studies published so far. More research is needed to fully determine conclusively whether impairments are present in different species, sexes and at different time points. In fact, it is possible that alterations in these behaviours are not present at the time points used in this study but may be found at other time points relative to PTX injection.

On the other hand, the pain behaviour post-PTX appeared to be robust and sustained over time. The underlying mechanisms may involve the endocannabinoid system due to its key role in

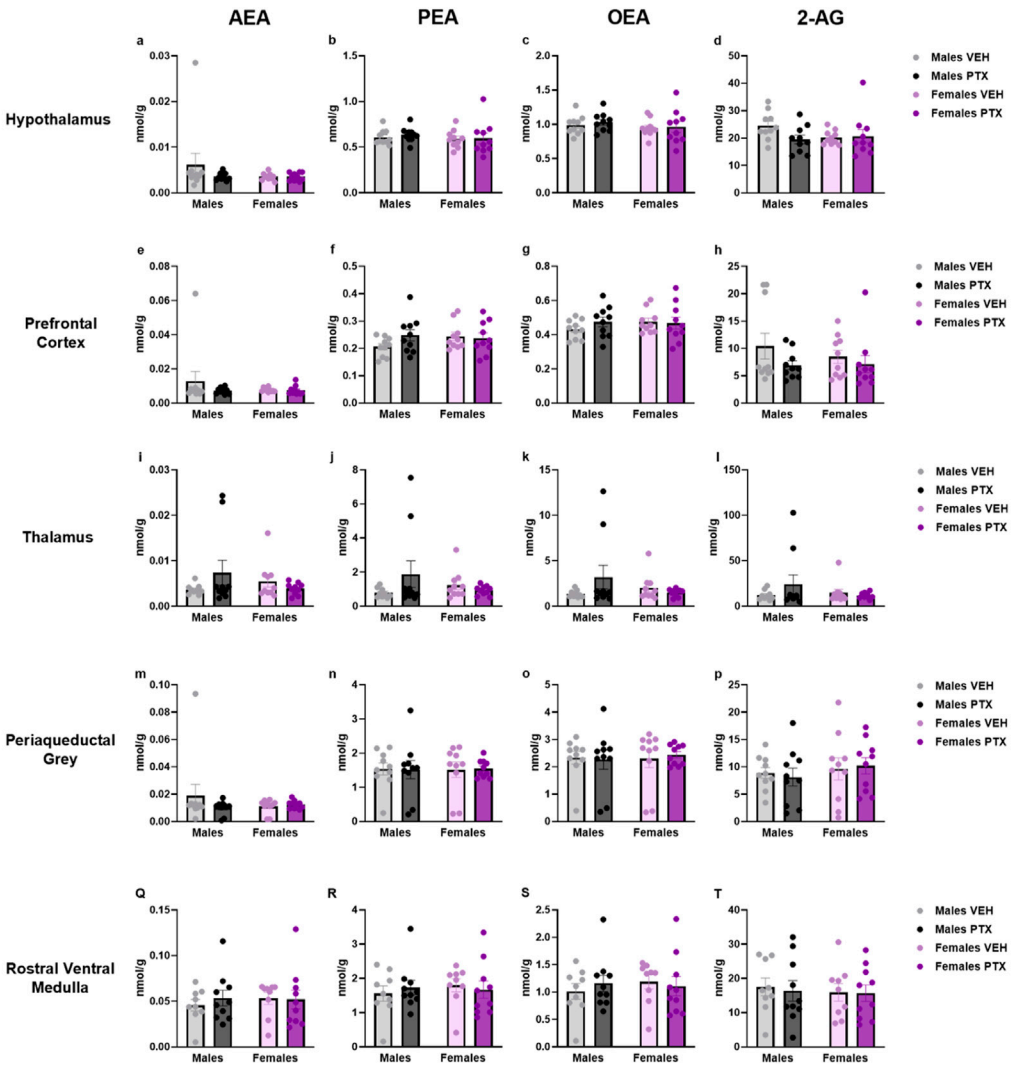

FIGURE 12
Investigation of endocannabinoid ligands and related *N*-acylethanolamine levels (nmol/g of tissue) in male and female rats following VEH or PTX intraperitoneal injections in the hypothalamus **(A–D)**, prefrontal cortex **(E–H)**, thalamus **(I–L)**, periaqueductal grey **(M–P)**, rostral ventral medulla **(Q–T)**. Data expressed as mean ± S.E.M (n = 10 per group).

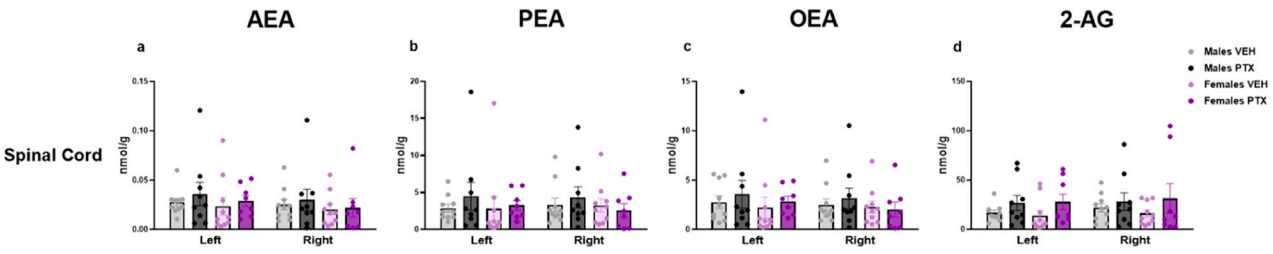

FIGURE 13
Investigation of endocannabinoid ligands **(A–D)** and related N-acylethanolamine levels **(B,C)** (nmol/g of tissue) in male and female rats following VEH or PTX intraperitoneal injections in the spinal cord. Data expressed as mean ± S.E.M (n = 10 per group).

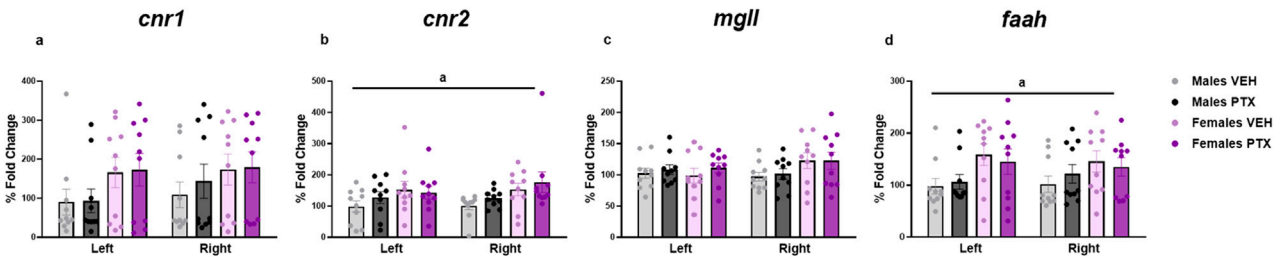

FIGURE 14
Levels of mRNA for *cnr1* **(A)**, *cnr2* **(B)**, *mgll* **(C)**, *and faah* **(D)**, respectively coding for CB_1, CB_2, MGL, and FAAH, in male and female in the amygdala of rats following intraperitoneal injection of VEH or PTX. Three-way ANOVA (factors: sex, treatment, side). Data expressed as mean ± S.E.M (n = 10 per group). a = significant effect of sex in ANOVA.

modulating pain through the descending pain pathway, which includes the periaqueductal grey, rostral ventromedial medulla, and spinal cord. In those areas, CB_1 receptors are widely expressed and their activation modulates the nociceptive transmission (Hendrich et al., 2012). In the context of CIPN, the potential of the endocannabinoid system as a therapeutic target is well-documented (Deng et al., 2012; Curry et al., 2018), but the role of the endocannabinoid system, specifically in PTX-induced neuropathic pain and associated sexual dimorphism, requires further study.

Our findings indicate that at the time points and conditions employed herein, there were very few effects of PTX on levels of endocannabinoids and related *N*-acylethanolamines in the regions investigated. The only significant change occurred in the amygdala, where we observed a PTX-induced increase in levels of PEA, OEA, and 2-AG. As seen in the spinal nerve ligation model of neuropathic pain, the increase in the endocannabinoid and *N*-acylethanolamine levels may be a response to the pain condition (Mitrirattanakul et al., 2006). Alterations in the endocannabinoid system have been already reported in CIPN models induced by cisplatin, in which 2-AG and AEA levels increased in the lumbar spinal cord (Guindon et al., 2013; Khasabova et al., 2014), but not in the brain (Khasabova et al., 2014).

Regardless, while changes in the endocannabinoid system within the amygdala have been observed in this model, the gross dissection method used in this study limits our ability to draw conclusions on this matter. This procedure does not allow us to determine whether the changes were restricted to one or more amygdalar subdivisions, and further investigation is warranted.

Within the whole amygdala, the analysis of the expression of mRNA for the endocannabinoid system components (receptors and enzymes that catabolise endocannabinoids and *N*-acylethanolamines) was performed, but PTX did not elicit any changes. Nevertheless, it must be noted that there was an effect of sex on the expression of the genes encoding CB_2 and FAAH; in fact, females exhibited a higher expression of mRNA for these genes when compared to males. To date, investigation of sex differences in the endocannabinoid system has been focused mostly on CB_1 receptors, with greater expression of mRNA in males compared to females in several regions, including the amygdala (Castelli et al., 2014). There are fewer studies of CB_2 expression in the brain, however, sexual dimorphism in CB_2 may mediate a sex difference in glial cell genesis during amygdalar development (Krebs-Kraft et al., 2010). Data provided in this study not only help to fill the existing gap in knowledge, but also provide further evidence of sexual dimorphism in the endocannabinoid system.

In conclusion, this study represents a comprehensive behavioural characterisation of the PTX model of CIPN in adult Sprague-Dawley rats of both sexes. The data indicate long-lasting PTX-induced mechanical and cold hypersensitivity in female and male rats and extend the characterisation of the effects of PTX alone, in the absence of a tumour. Furthermore, the results advance our understanding of sex as a variable in behavioural outcomes and the role of the endocannabinoid system in this model.

Data availability statement

The raw data supporting the conclusions of this article will be made available by the authors, without undue reservation.

Ethics statement

The animal study was approved by University of Galway's Animal Care and Research Ethics Committee. The study was conducted in accordance with the local legislation and institutional requirements.

Author contributions

CDM: Conceptualization, Data curation, Formal Analysis, Investigation, Methodology, Writing–original draft, Writing–review and editing. ÁL-B: Conceptualization, Writing–review and editing. AD: Investigation, Methodology, Writing–review and editing. AB: Investigation, Methodology, Writing–review and editing. LB: Investigation, Methodology, Writing–review and editing. EB: Funding acquisition, Project administration, Resources, Supervision, Writing–review and editing. MR: Conceptualization, Funding acquisition, Project administration, Resources, Supervision, Writing–review and editing. DF: Conceptualization, Funding acquisition, Project administration, Resources, Supervision, Writing–review and editing.

Funding

The author(s) declare that financial support was received for the research, authorship, and/or publication of this article. This research was supported by the European Union's Horizon 2020 research and innovation programme under the Marie Skłodowska-Curie grant agreement number 955684.

Acknowledgments

The authors thank Daniel M. Kerr, and Brendan Harhen for technical assistance.

Conflict of interest

The authors declare that the research was conducted in the absence of any commercial or financial relationships that could be construed as a potential conflict of interest.

Generative AI statement

The author(s) declare that no Generative AI was used in the creation of this manuscript.

Publisher's note

All claims expressed in this article are solely those of the authors and do not necessarily represent those of their affiliated organizations, or those of the publisher, the editors and the reviewers. Any product that may be evaluated in this article, or claim that may be made by its manufacturer, is not guaranteed or endorsed by the publisher.

Supplementary material

The Supplementary Material for this article can be found online at: https://www.frontiersin.org/articles/10.3389/fphar.2024.1505980/full#supplementary-material

References

Alqahtani, F. Y., Aleanizy, F. S., EL Tahir, E., Alkahtani, H. M., and Alquadeib, B. T. (2019). Paclitaxel. *Pro. Dr. Subst. Excip. Relat. Methodol.* 44, 205–238. doi:10.1016/bs.podrm.2018.11.001

Anghelescu, D. L., Tesney, J. M., Jeha, S., Wright, B. B., Trujillo, L., Sandlund, J. T., et al. (2020). Prospective randomized trial of interventions for vincristine-related neuropathic pain. *Pediatr. Blood and Cancer* 67, e28539. doi:10.1002/pbc.28539

Armstrong, D. K., Bundy, B., Wenzel, L., Huang, H. Q., Baergen, R., Lele, S., et al. (2006). Intraperitoneal cisplatin and paclitaxel in ovarian cancer. *N. Engl. J. Med.* 354, 34–43. doi:10.1056/NEJMoa052985

Blanton, H. L., Barnes, R. C., Mchann, M. C., Bilbrey, J. A., Wilkerson, J. L., and Guindon, J. (2021). Sex differences and the endocannabinoid system in pain. *Pharmacol. Biochem. Behav.* 202, 173107. doi:10.1016/j.pbb.2021.173107

Börchers, S., Krieger, J.-P., Asker, M., Maric, I., and Skibicka, K. P. (2022). Commonly-used rodent tests of anxiety-like behavior lack predictive validity for human sex differences. *Psychoneuroendocrinology* 141, 105733. doi:10.1016/j.psyneuen.2022.105733

Boullon, L., Finn, D. P., and Llorente-Berzal, Á. (2021). Sex differences in a rat model of peripheral neuropathic pain and associated levels of endogenous cannabinoid ligands. *Front. Pain Res.* 2, 673638. doi:10.3389/fpain.2021.673638

Bradshaw, H. B., Rimmerman, N., Krey, J. F., and Walker, J. M. (2006). Sex and hormonal cycle differences in rat brain levels of pain-related cannabimimetic lipid mediators. *Am. J. Physiology-Regulatory, Integr. Comp. Physiology* 291, R349–R358. doi:10.1152/ajpregu.00933.2005

Campos-Cardoso, R., Godoy, L. D., Lazarini-Lopes, W., Novaes, L. S., Dos Santos, N. B., Perfetti, J. G., et al. (2023). Exploring the light/dark box test: protocols and implications for neuroscience research. *J. Neurosci. Methods* 384, 109748. doi:10.1016/j.jneumeth.2022.109748

Castelli, M., Fadda, P., Casu, A., Spano, M., Casti, A., Fratta, W., et al. (2014). Male and female rats differ in brain cannabinoid CB1 receptor density and function and in behavioural traits predisposing to drug addiction: effect of ovarian hormones. *Curr. Pharm. Des.* 20, 2100–2113. doi:10.2174/13816128113199990430

Choi, S., Seo, S., Lee, J. H., Suh, K. J., Kim, J.-W., Kim, J. W., et al. (2024). Impact of patient sex on adverse events and unscheduled utilization of medical services in cancer patients undergoing adjuvant chemotherapy: a multicenter retrospective cohort study. *Cancer Res. Treat.* 56, 404–413. doi:10.4143/crt.2023.784

Chow, R., Novosel, M., So, O. W., Bellampalli, S., Xiang, J., Boldt, G., et al. (2023). Duloxetine for prevention and treatment of chemotherapy-induced peripheral neuropathy (CIPN): systematic review and meta-analysis. *BMJ Support. and Palliat. Care* 13, 27–34. doi:10.1136/spcare-2022-003815

Corcoran, L., Mattimoe, D., Roche, M., and Finn, D. P. (2020). Attenuation of fear-conditioned analgesia in rats by monoacylglycerol lipase inhibition in the anterior cingulate cortex: potential role for CB_2 receptors. *Br. J. Pharmacol.* 177, 2240–2255. doi:10.1111/bph.14976

Cravatt, B. F., Giang, D. K., Mayfield, S. P., Boger, D. L., Lerner, R. A., and Gilula, N. B. (1996). Molecular characterization of an enzyme that degrades neuromodulatory fatty-acid amides. *Nature* 384, 83–87. doi:10.1038/384083a0

Crawley, J. N. (1985). Exploratory behavior models of anxiety in mice. *Neurosci. and Biobehav. Rev.* 9, 37–44. doi:10.1016/0149-7634(85)90030-2

Currie, G. L., Angel-Scott, H. N., Colvin, L., Cramond, F., Hair, K., Khandoker, L., et al. (2019). Animal models of chemotherapy-induced peripheral neuropathy: a machine-assisted systematic review and meta-analysis. *PLOS Biol.* 17, e3000243. doi:10.1371/journal.pbio.3000243

Curry, Z. A., Wilkerson, J. L., Bagdas, D., Kyte, S. L., Patel, N., Donvito, G., et al. (2018). Monoacylglycerol lipase inhibitors reverse paclitaxel-induced nociceptive behavior and proinflammatory markers in a mouse model of chemotherapy-induced neuropathy. *J. Pharmacol. Exp. Ther.* 366, 169–183. doi:10.1124/jpet.117.245704

Deacon, R. M. J., and Rawlins, J. N. P. (2006). T-maze alternation in the rodent. *Nat. Protoc.* 1, 7–12. doi:10.1038/nprot.2006.2

Deng, L., Guindon, J., Vemuri, V. K., Thakur, G. A., White, F. A., Makriyannis, A., et al. (2012). The maintenance of cisplatin- and paclitaxel-induced mechanical and cold allodynia is suppressed by cannabinoid CB_2 receptor activation and independent of CXCR4 signaling in models of chemotherapy-induced peripheral neuropathy. *Mol. Pain* 8, 1744–8069. doi:10.1186/1744-8069-8-71

Detke, M. J., Rickels, M., and Lucki, I. (1995). Active behaviors in the rat forced swimming test differentially produced by serotonergic and noradrenergic antidepressants. *Psychopharmacology* 121, 66–72. doi:10.1007/BF02245592

Devane, W. A., Hanuš, L., Breuer, A., Pertwee, R. G., Stevenson, L. A., Griffin, G., et al. (1992). Isolation and structure of a brain constituent that binds to the cannabinoid receptor. *Science* 258, 1946–1949. doi:10.1126/science.1470919

Dinh, T. P., Carpenter, D., Leslie, F. M., Freund, T. F., Katona, I., Sensi, S. L., et al. (2002). Brain monoglyceride lipase participating in endocannabinoid inactivation. *Proc. Natl. Acad. Sci.* 99, 10819–10824. doi:10.1073/pnas.152334899

Fardell, J. E., Vardy, J., Monds, L. A., and Johnston, I. N. (2015). The long-term impact of oxaliplatin chemotherapy on rodent cognition and peripheral neuropathy. *Behav. Brain Res.* 291, 80–88. doi:10.1016/j.bbr.2015.04.038

Ferdousi, M. I., Calcagno, P., Sanchez, C., Smith, K. L., Kelly, J. P., Roche, M., et al. (2023). Characterization of pain-anxiety-and cognition-related behaviors in the complete Freund's adjuvant model of chronic inflammatory pain in Wistar–Kyoto rats. *Front. Pain Res.* 4, 1131069. doi:10.3389/fpain.2023.1131069

Flatters, S. J. L., and Bennett, G. J. (2006). Studies of peripheral sensory nerves in paclitaxel-induced painful peripheral neuropathy: evidence for mitochondrial dysfunction. *Pain* 122, 245–257. doi:10.1016/j.pain.2006.01.037

Galiègue, S., Mary, S., Marchand, J., Dussossoy, D., Carrière, D., Carayon, P., et al. (1995). Expression of central and peripheral cannabinoid receptors in human immune tissues and leukocyte subpopulations. *Eur. J. Biochem.* 232, 54–61. doi:10.1111/j.1432-1033.1995.tb20780.x

Gökçek-Saraç, Ç., Wesierska, M., and Jakubowska-Doğru, E. (2015). Comparison of spatial learning in the partially baited radial-arm maze task between commonly used rat strains: Wistar, Spargue-Dawley, Long-Evans, and outcrossed Wistar/Sprague-Dawley. *Learn. and Behav.* 43, 83–94. doi:10.3758/s13420-014-0163-9

Gould, T. D., Dao, D. T., and Kovacsics, C. E. (2009). *The open field test*. Humana Press. Available at: https://link.springer.com/protocol/10.1007/978-1-60761-303-9_1.

Griffiths, L. A., Duggett, N. A., Pitcher, A. L., and Flatters, S. J. L. (2018). Evoked and ongoing pain-like behaviours in a rat model of paclitaxel-induced peripheral neuropathy. *Pain Res. Manag.* 2018, 1–11. doi:10.1155/2018/8217613

Guindon, J., Lai, Y., Takacs, S. M., Bradshaw, H. B., and Hohmann, A. G. (2013). Alterations in endocannabinoid tone following chemotherapy-induced peripheral neuropathy: effects of endocannabinoid deactivation inhibitors targeting fatty-acid amide hydrolase and monoacylglycerol lipase in comparison to reference analgesics following cisplatin treatment. *Pharmacol. Res.* 67, 94–109. doi:10.1016/j.phrs.2012.10.013

Hendrich, J., Alvarez, P., Joseph, E. K., Ferrari, L. F., Chen, X., and Levine, J. D. (2012). *In vivo* and *in vitro* comparison of female and male nociceptors. *J. Pain* 13, 1224–1231. doi:10.1016/j.jpain.2012.09.009

Herkenham, M., Lynn, A., Johnson, M., Melvin, L., DE Costa, B., and Rice, K. (1991). Characterization and localization of cannabinoid receptors in rat brain: a quantitative *in vitro* autoradiographic study. *J. Neurosci.* 11, 563–583. doi:10.1523/JNEUROSCI.11-02-00563.1991

Hestehave, S., Abelson, K. S. P., Brønnum Pedersen, T., Finn, D. P., Andersson, D. R., and Munro, G. (2020). The influence of rat strain on the development of neuropathic pain and comorbid anxio-depressive behaviour after nerve injury. *Sci. Rep.* 10, 20981. doi:10.1038/s41598-020-77640-8

Howlett, A. C., Barth, F., Bonner, T. I., Cabral, G., Casellas, P., Devane, W. A., et al. (2002). International union of Pharmacology. XXVII. Classification of cannabinoid receptors. *Pharmacol. Rev.* 54, 161–202. doi:10.1124/pr.54.2.161

Huehnchen, P., Boehmerle, W., Springer, A., Freyer, D., and Endres, M. (2017). A novel preventive therapy for paclitaxel-induced cognitive deficits: preclinical evidence from C57BL/6 mice. *Transl. Psychiatry* 7, e1185. doi:10.1038/tp.2017.149

Huynh, P. N., Giuvelis, D., Christensen, S., Tucker, K. L., and Mcintosh, J. M. (2019). RgIA4 accelerates recovery from paclitaxel-induced neuropathic pain in rats. *Mar. Drugs* 18, 12. doi:10.3390/md18010012

Ibrahim, E. Y., Domenicano, I., Nyhan, K., Elfil, M., Mougalian, S. S., Cartmel, B., et al. (2021). Cognitive effects and depression associated with taxane-based chemotherapy in breast cancer survivors: a meta-analysis. *Front. Oncol.* 11, 642382. doi:10.3389/fonc.2021.642382

Kalueff, A. V., Stewart, A. M., Song, C., Berridge, K. C., Graybiel, A. M., and Fentress, J. C. (2016). Neurobiology of rodent self-grooming and its value for translational neuroscience. *Nat. Rev. Neurosci.* 17, 45–59. doi:10.1038/nrn.2015.8

Kerr, D. M., Burke, N. N., Ford, G. K., Connor, T. J., Harhen, B., Egan, L. J., et al. (2012). Pharmacological inhibition of endocannabinoid degradation modulates the expression of inflammatory mediators in the hypothalamus following an immunological stressor. *Neuroscience* 204, 53–63. doi:10.1016/j.neuroscience.2011.09.032

Khasabova, I. A., Yao, X., Paz, J., Lewandowski, C. T., Lindberg, A. E., Coicou, L., et al. (2014). JZL184 is anti-hyperalgesic in a murine model of cisplatin-induced peripheral neuropathy. *Pharmacol. Res.* 90, 67–75. doi:10.1016/j.phrs.2014.09.008

Klegeris, A., Bissonnette, C. J., and Mcgeer, P. L. (2003). Reduction of human monocytic cell neurotoxicity and cytokine secretion by ligands of the cannabinoid-type CB2 receptor. *Br. J. Pharmacol.* 139, 775–786. doi:10.1038/sj.bjp.0705304

Klein, I., and Lehmann, H. (2021). Pathomechanisms of paclitaxel-induced peripheral neuropathy. *Toxics* 9, 229. doi:10.3390/toxics9100229

Kraeuter, A.-K., Guest, P. C., and Sarnyai, Z. (2019). *The elevated Plus maze test for measuring anxiety-like behavior in rodents*. New York: Springer.

Krebs-Kraft, D. L., Hill, M. N., Hillard, C. J., and Mccarthy, M. M. (2010). Sex difference in cell proliferation in developing rat amygdala mediated by endocannabinoids has implications for social behavior. *Proc. Natl. Acad. Sci.* 107, 20535–20540. doi:10.1073/pnas.1005003107

Lago-Fernandez, A., Zarzo-Arias, S., Jagerovic, N., and Morales, P. (2021). Relevance of peroxisome proliferator activated receptors in multitarget paradigm associated with the endocannabinoid system. *Int. J. Mol. Sci.* 22, 1001. doi:10.3390/ijms22031001

Lindner, O. C., Phillips, B., Mccabe, M. G., Mayes, A., Wearden, A., Varese, F., et al. (2014). A meta-analysis of cognitive impairment following adult cancer chemotherapy. *Neuropsychology* 28, 726–740. doi:10.1037/neu0000064

Liu, J., Li, D., Huang, J., Cao, J., Cai, G., Guo, Y., et al. (2022). Glutamatergic neurons in the amygdala are involved in paclitaxel-induced pain and anxiety. *Front. Psychiatry* 13, 869544. doi:10.3389/fpsyt.2022.869544

Llorente-Berzal, A., Mela, V., Borcel, E., Valero, M., López-Gallardo, M., Viveros, M.-P., et al. (2012). Neurobehavioral and metabolic long-term consequences of neonatal maternal deprivation stress and adolescent olanzapine treatment in male and female rats. *Neuropharmacology* 62, 1332–1341. doi:10.1016/j.neuropharm.2011.07.031

Loesch, D., Greco, F. A., Senzer, N. N., Burris, H. A., Hainsworth, J. D., Jones, S., et al. (2010). Phase III multicenter trial of doxorubicin Plus cyclophosphamide followed by paclitaxel compared with doxorubicin Plus paclitaxel followed by weekly paclitaxel as adjuvant therapy for women with high-risk breast cancer. *J. Clin. Oncol.* 28, 2958–2965. doi:10.1200/JCO.2009.24.1000

Lynch, M. E., Cesar-Rittenberg, P., and Hohmann, A. G. (2014). A double-blind, placebo-controlled, crossover pilot trial with extension using an oral mucosal cannabinoid extract for treatment of chemotherapy-induced neuropathic pain. *J. Pain Symptom Manag.* 47, 166–173. doi:10.1016/j.jpainsymman.2013.02.018

Martinov, T., Mack, M., Sykes, A., and Chatterjea, D. (2013). Measuring Changes in Tactile Sensitivity in the Hind Paw of Mice Using an Electronic von Frey Apparatus. *J. Vis. Exp.*, e51212. doi:10.3791/51212

Mitrirattanakul, S., Ramakul, N., Guerrero, A. V., Matsuka, Y., Ono, T., Iwase, H., et al. (2006). Site-specific increases in peripheral cannabinoid receptors and their endogenous ligands in a model of neuropathic pain. *Pain* 126, 102–114. doi:10.1016/j.pain.2006.06.016

Munro, S., Thomas, K. L., and Abu-Shaar, M. (1993). Molecular characterization of a peripheral receptor for cannabinoids. *Nature* 365, 61–65. doi:10.1038/365061a0

Noya-Riobó, M. V., Miguel, C. Á., Soriano, D. B., Brumovsky, P. R., Villar, M. J., and Coronel, M. F. (2023). Changes in the expression of endocannabinoid system components in an experimental model of chemotherapy-induced peripheral neuropathic pain: evaluation of sex-related differences. *Exp. Neurol.* 359, 114232. doi:10.1016/j.expneurol.2022.114232

Panoz-Brown, D., Carey, L. M., Smith, A. E., Gentry, M., Sluka, C. M., Corbin, H. E., et al. (2017). The chemotherapeutic agent paclitaxel selectively impairs reversal learning while sparing prior learning, new learning and episodic memory. *Neurobiol. Learn. Mem.* 144, 259–270. doi:10.1016/j.nlm.2017.08.001

Picard, M., and Castells, M. C. (2015). Re-Visiting hypersensitivity reactions to taxanes: a comprehensive review. *Clin. Rev. Allergy and Immunol.* 49, 177–191. doi:10.1007/s12016-014-8416-0

Quintão, N. L. M., Santin, J. R., Stoeberl, L. C., Corrêa, T. P., Melato, J., and Costa, R. (2019). Pharmacological treatment of chemotherapy-induced neuropathic pain: PPARγ agonists as a promising tool. *Front. Neurosci.* 13, 907. doi:10.3389/fnins.2019.00907

Rubino, T., and Parolaro, D. (2011). Sexually dimorphic effects of cannabinoid compounds on emotion and cognition. *Front. Behav. Neurosci.* 5, 64. doi:10.3389/fnbeh.2011.00064

Slivicki, R. A., Xu, Z., Mali, S. S., and Hohmann, A. G. (2019). Brain permeant and impermeant inhibitors of fatty-acid amide hydrolase suppress the development and maintenance of paclitaxel-induced neuropathic pain without producing tolerance or physical dependence *in vivo* and synergize with paclitaxel to reduce tumor cell line viability *in vitro*. *Pharmacol. Res.* 142, 267–282. doi:10.1016/j.phrs.2019.02.002

Smith, S. B., Crager, S. E., and Mogil, J. S. (2004). Paclitaxel-induced neuropathic hypersensitivity in mice: responses in 10 inbred mouse strains. *Life Sci.* 74, 2593–2604. doi:10.1016/j.lfs.2004.01.002

Sugiura, T., Kondo, S., Sukagawa, A., Nakane, S., Shinoda, A., Itoh, K., et al. (1995). 2-Arachidonoylglycerol: a possible endogenous cannabinoid receptor ligand in brain. *Biochem. Biophysical Res. Commun.* 215, 89–97. doi:10.1006/bbrc.1995.2437

Tanabe, Y., Hashimoto, K., Shimizu, C., Hirakawa, A., Harano, K., Yunokawa, M., et al. (2013). Paclitaxel-induced peripheral neuropathy in patients receiving adjuvant chemotherapy for breast cancer. *Int. J. Clin. Oncol.* 18, 132–138. doi:10.1007/s10147-011-0352-x

Tkaczuk, K., and Yared, J. (2012). Update on taxane development: new analogs and new formulations. *Drug Des. Dev. Ther.* 371, 371. doi:10.2147/dddt.s28997

Toma, W., Kyte, S. L., Bagdas, D., Alkhlaif, Y., Alsharari, S. D., Lichtman, A. H., et al. (2017). Effects of paclitaxel on the development of neuropathy and affective behaviors in the mouse. *Neuropharmacology* 117, 305–315. doi:10.1016/j.neuropharm.2017.02.020

Walker, F. E. (1993). Paclitaxel (TAXOL): side effects and patient education issues. *Seminars Oncol. Nurs.* 9, 6–10. doi:10.1016/s0749-2081(16)30036-5

Ward, S. J., Ramirez, M. D., Neelakantan, H., and Walker, E. A. (2011). Cannabidiol prevents the development of cold and mechanical allodynia in paclitaxel-treated female C57Bl6 mice. *Anesth. and Analgesia* 113, 947–950. doi:10.1213/ANE.0b013e3182283486

Weiss, M. C., Giaddui, M., Kjelstrom, S., Erebor, E., Meske, S., Saeed, L., et al. (2023). Safety and efficacy of cannabidiol in the management of chemotherapy-induced peripheral neuropathy. *J. Clin. Oncol.* 41, 12020. doi:10.1200/jco.2023.41.16_suppl.12020

Willner, P., Towell, A., Sampson, D., Sophokleous, S., and Muscat, R. (1987). Reduction of sucrose preference by chronic unpredictable mild stress, and its restoration by a tricyclic antidepressant. *Psychopharmacology* 93, 358–364. doi:10.1007/BF00187257

Yamamoto, H., Sekine, I., Yamada, K., Nokihara, H., Yamamoto, N., Kunitoh, H., et al. (2008). Gender differences in treatment outcomes among patients with non-small cell lung cancer given a combination of carboplatin and paclitaxel. *Oncology* 75, 169–174. doi:10.1159/000159268

Yoon, C., Wook, Y. Y., Sik, N. H., Ho, K. S., and Mo, C. J. (1994). Behavioral signs of ongoing pain and cold allodynia in a rat model of neuropathic pain. *Pain* 59, 369–376. doi:10.1016/0304-3959(94)90023-x

frontiers | Frontiers in Pharmacology

TYPE Mini Review
PUBLISHED 26 February 2025
DOI 10.3389/fphar.2025.1500313

OPEN ACCESS

EDITED BY
Fabio Turco,
Cannabiscientia SA, Switzerland

REVIEWED BY
Rosmara Infantino,
University of Galway, Ireland
Kristen Willeumier,
Independent Researcher, Beverly Hills, United States

*CORRESPONDENCE
Satoshi Kasahara,
namahagenator@gmail.com

RECEIVED 23 September 2024
ACCEPTED 07 February 2025
PUBLISHED 26 February 2025

CITATION
Kasahara S, Takahashi M, Suto T, Morita T, Obata H and Niwa S-I (2025) Innovative therapeutic strategies using ADHD medications tailored to the behavioral characteristics of patients with chronic pain.
Front. Pharmacol. 16:1500313.
doi: 10.3389/fphar.2025.1500313

Innovative therapeutic strategies using ADHD medications tailored to the behavioral characteristics of patients with chronic pain

Satoshi Kasahara[1,2]*, Miwako Takahashi[3], Takashi Suto[4], Taito Morita[1], Hideaki Obata[5] and Shin-Ichi Niwa[6]

[1]Department of Anesthesiology and Pain Relief Center, The University of Tokyo Hospital, Tokyo, Japan, [2]Department of Pain Medicine, Fukushima Medical University School of Medicine, Fukushima, Japan, [3]Institute for Quantum Medical Science, National Institutes for Quantum Science and Technology, Chiba, Japan, [4]Department of Anesthesiology, Gunma University Graduate School of Medicine, Gunma, Japan, [5]Department of Anesthesiology, Saitama Medical Center, Saitama Medical University, Saitama, Japan, [6]Department of Psychiatry, Aizu Medical Center, Fukushima Medical University, Fukushima, Japan

Chronic pain affects a significant portion of adults and is linked to psychosocial issues, cognitive dysfunction, and psychiatric disorders, complicating treatment. Attention deficit hyperactivity disorder (ADHD) is increasingly recognized as a contributing factor to chronic pain, particularly nociplastic pain, with a notable prevalence of comorbidity between ADHD and conditions like fibromyalgia and chronic low back pain. ADHD behaviors such as impulsivity and overactivity can exacerbate pain by leading patients to seek risky treatments or discontinue care prematurely. ADHD medications are expected to alleviate pain severity by improving associated cognitive dysfunction and addressing central sensitization, a fundamental mechanism in chronic pain. Brain abnormalities in ADHD contribute to increased spontaneous activity in the anterior cingulate cortex-posterior insular pathway due to neuroinflammation, alterations in action potential firing, and changes in transmission pathways in the spinal dorsal horn. Additionally, increased norepinephrine synthesis and reduced transmission efficiency amplify nociceptive information from the periphery and facilitate central sensitization in ADHD. Beyond typical ADHD medications like central stimulants, norepinephrine reuptake inhibitors, and alpha-2 receptor agonists, various antidepressants, mood stabilizers, antipsychotics, Parkinson's disease medications, and antidementia medications have proven effective in alleviating ADHD symptoms. These medications, effective for ADHD, may offer innovative solutions for managing chronic pain by targeting both the cognitive/behavioral dysfunction and central sensitization observed in chronic pain comorbid with

Abbreviations: NP, nociplastic pain; 6-OHDA, 6-hydroxydopamine; SHR, spontaneously hypertensive rats; NSIA, noxious stimulus-induced analgesia; NE, norepinephrine; ACC, anterior cingulate cortex; PI, posterior insula; ACC-PI pathway, anterior cingulate cortex posterior insula; DA, dopamine; NRI, norepinephrine reuptake inhibitor.

ADHD. Further research into these mechanisms could lead to new, more effective pharmacological treatments for chronic pain with comorbid ADHD, a condition that is often overlooked.

KEYWORDS

nociplastic pain, central sensitization, attention deficit hyperactivity disorder, ADHD medication, dopamine, norepinephrine, pain matrix, ergomania

1 Introduction

Chronic pain affects 13%–50% of adults (Mills et al., 2019) and is associated with psychosocial factors, cognitive dysfunction, and psychiatric disorders. Moreover, inadequate management of pain and the underlying physical conditions that cause it can also lead to cognitive impairment and psychiatric disorders. This complexity makes assessing and treating chronic pain particularly challenging and imposes an extremely high economic burden (Sarria-Santamera et al., 2022). Consequently, elucidating the pathophysiological mechanisms of chronic pain is vital for discovering new pharmacological targets.

Understanding the cognitive and behavioral characteristics of patients with chronic pain, both clinically and in daily life, alongside psychiatric disorders, is crucial for implementing effective pharmacological strategies targeting these mechanisms.

Patients with chronic pain resistant to multidisciplinary treatment often experience repeated accidents (Swanson et al., 1977), which has been linked to attention deficit hyperactivity disorder (ADHD), a neurodevelopmental disorder (Kaplan and Kaplan, 2006). Chronic pain patients frequently display three behavioral traits (Flor and Turk, 2015): (1) overconcentration on pain and susceptibility to distraction, (2) overactivity exceeding personal limits (traditionally called "ergomania") (Vlaeyen and Morley, 2004), and (3) persistent, intense anger—features also characteristic of ADHD (American Psychiatric Association, 2013). Due to impulsivity and impatience, ADHD patients often pursue invasive, high-risk treatments (e.g., surgery, tooth extraction, opioids) for rapid relief or abandon treatments prematurely if results are not immediate, leading to "doctor shopping" (Kasahara et al., 2023d). Notably, 72.5% of chronic pain patients have comorbid ADHD, and ADHD medications can reduce the pain NRS score by 3.5 points (61.5%), indicating that ADHD comorbidity may drive cognitive and behavioral dysfunction in chronic pain (Kasahara et al., 2020).

Over 80% of adult ADHD cases go undiagnosed, especially in psychiatric settings (Ginsberg et al., 2014). Because most chronic pain patients receive care from orthopedic surgeons, rheumatologists, and pain specialists with limited ADHD expertise, comorbid ADHD often remains overlooked. Recognizing this gap could provide a breakthrough for new, behaviorally tailored pharmacotherapies.

Herein, we review clinical and basic research on the relationship between chronic pain and ADHD and explore the potential pathophysiological mechanisms involved. We also examine effective ADHD medications for chronic pain, offering insights into novel pharmacotherapeutic approaches.

2 Findings from clinical studies

An epidemiological study revealed an association between ADHD symptoms and work-related pain (Stickley et al., 2016). In 2017, chronic pain—previously categorized as psychogenic or somatoform—was redefined as nociplastic pain (NP), recognized alongside nociceptive and neuropathic pain (Kosek et al., 2016; Aydede and Shriver, 2018). NP is believed to result from central sensitization, involving plastic changes in central nervous system circuits that amplify nociceptive signals (Kosek et al., 2021; Treede et al., 2019; Nijs et al., 2021). NP rarely appears in isolation, instead presenting with hyperalgesia, fatigue, sensory hypersensitivity, sleep disturbances, mood disorders, or cognitive dysfunction in concentration and memory (Kosek et al., 2021), which—combined with psychosocial factors—makes treatment particularly challenging.

Recent findings indicate ADHD, a developmental disorder, frequently coexists with representative NP-related conditions such as fibromyalgia (Pallanti et al., 2021), chronic low back pain (Kasahara et al., 2021b), idiopathic orofacial pain (Kasahara et al., 2023b), chronic chest pain (Zain et al., 2023), and chronic abdominal pain (Asztély et al., 2019; Kasahara et al., 2024). ADHD may contribute to central sensitization and cognitive impairments in NP, including attention deficits and sensory hypersensitivity (Ibrahim and Hefny, 2022). Historical figures with NP, such as John F. Kennedy, who suffered from chronic low back pain (Kasahara et al., 2022a), and Margaret Mitchell, the author of *Gone with the Wind*, who struggled with fibromyalgia and experienced multiple car accidents (Kasahara et al., 2021a), were also speculated to have had comorbid ADHD.

The coexistence of ADHD and chronic pain is thought to stem from dual impairments in cognitive-emotional factors and motor control associated with ADHD. ADHD exacerbates pain, and pain, in turn, worsens ADHD, with central nervous system inflammation potentially perpetuating this relationship (Battison et al., 2023) (Figure 1). Individuals with ADHD have been shown to exhibit considerably more motor control issues and increased muscle tension than those without ADHD, which are also associated with widespread and severe pain (Stray et al., 2013).

Furthermore, when ADHD accompanies NP, ADHD medications have been reported to improve pain and the associated cognitive dysfunctions. (Kasahara et al., 2017; Kasahara et al., 2022b; Kasahara et al., 2023a; Kasahara et al., 2023b; Kasahara et al., 2023c; Kasahara et al., 2023d; Kasahara et al., 2023e; Zain et al., 2023; Kasahara et al., 2024). ADHD medications administered to patients with NP have also been shown to regulate blood flow in the prefrontal cortex, precuneus, anterior cingulate cortex, and insular cortex—regions involved in the core pain matrix and related emotional processing areas (Garcia-

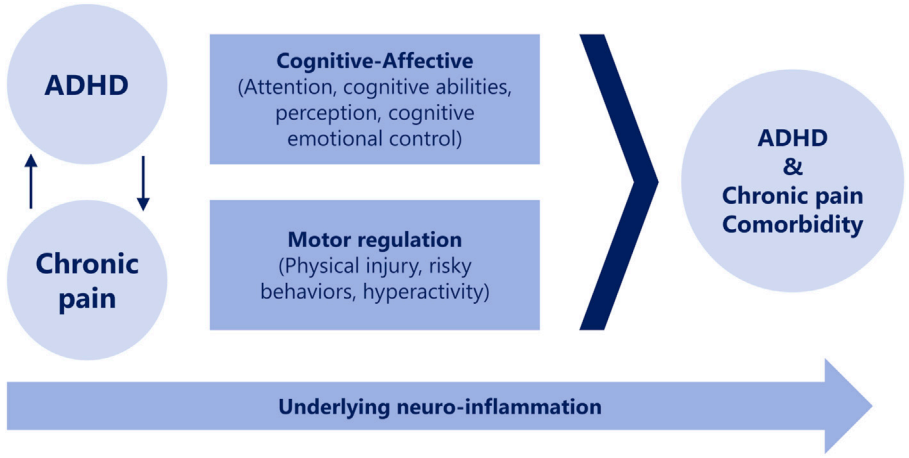

FIGURE 1
Potential associations between chronic pain and ADHD over time. (Battison et al., 2023). ADHD, attention-deficit hyperactivity disorder.

Larrea and Peyron, 2013; Kasahara et al., 2023a; Kasahara et al., 2023c; Kasahara et al., 2023e; Kasahara et al., 2024). Notably, increased blood flow in the precuneus showed a positive correlation with NP severity scores. In the group that responded to methylphenidate, the precuneus was identified as a region of significantly elevated blood flow before treatment compared to that of after treatment. In typical cases, a decrease in precuneus hyperperfusion was accompanied by an increase in blood flow in the prefrontal cortex (Takahashi et al., 2024). Moreover, methylphenidate has been shown to alleviate motor control issues and high muscle tension in individuals with ADHD (Stray et al., 2009. See Additional Video Files 1–4.). Additionally, ADHD medications have been found to improve family relationships, which are significant psychosocial factors contributing to the maintenance and exacerbation of chronic pain (Kasahara et al., 2024). Therefore, ADHD medications are gaining attention as a new approach for treating NP, which is often difficult to manage.

However, as previously mentioned, many chronic pain patients are treated by non-psychiatric specialists such as orthopedic surgeons, rheumatologists, or pain specialists. For these physicians, diagnosing ADHD or prescribing ADHD medications is not straightforward. Therefore, when clinical behavioral characteristics of ADHD are observed, it is practical to use self-administered questionnaires such as the Adult ADHD Self-Report Scale (Kessler et al., 2005) or the Conners' Adult ADHD Rating Scale (Conners et al., 1999) for screening and to consult with a psychiatric specialist. Both scales have also been utilized in clinical research on chronic pain (Stickley et al., 2016; Kasahara et al., 2021b). Patients with coexisting ADHD often exhibit the following behavioral characteristics (Kooij and Francken, 2010): difficulty maintaining attention and concentration, which leads to omissions when responding to questionnaires; a tendency to become bored easily and frequently change jobs; procrastination on tasks requiring effort, such as returning to work or completing administrative procedures; reliance on family members for difficult tasks; disorganized speech, resulting in scattered conversations; tardiness or forgetting appointment dates; organizational difficulties, leading to overfilled bags; fidgeting with hands or feet even while seated; hyperactivity, resulting in involvement in numerous activities and subsequent exhaustion; excessive talking; impatience and impulsive pursuit of high-risk treatments, with demands such as 'take the pain away immediately; ' inability to control anger; over-involvement with others; and a dislike of waiting, resulting in a preference for the earliest possible appointment slots."

3 Findings from basic studies

NP is associated with central sensitization (Kosek et al., 2021). Recently, basic research suggests that ADHD is more likely to cause central sensitization. At least 21 types of rodent ADHD model animals have been reported in basic research, with eight frequently cited models being identified as the most notable (Kantak K. M., 2022; Table 1).

In spontaneously hypertensive rats (SHR), an animal model for ADHD, noxious stimulus-induced analgesia (NSIA) (Tambeli et al., 2009) was weaker compared to the control group. Additionally, *in vivo* studies have shown that the concentration of norepinephrine (NE) in the dorsal horn of the spinal cord, which increases in response to nociceptive stimuli, decreases in SHR (Suto et al., 2023). This decrease suggests a weakened endogenous analgesia, including the descending inhibitory system, in ADHD.

In spinal cord slices, SHR exhibited a larger immunostaining area for NE-synthesizing enzymes in the dorsal horn than that of the control group, alongside higher extracellular NE concentrations than those of the control group. This suggests more active NE synthesis under pain-free conditions (Suto et al., 2023). Conversely, SHR exhibited a larger staining area for the norepinephrine transporter (NET) but a smaller staining area for the α2A receptor, the target receptor for NE, compared to the control group. This pattern indicates that excessive NE production in a pain-free state leads to NET overexpression and α2A receptor downregulation, resulting in diminished NE activity during NSIA and weakened descending inhibition.

Similarly, 6-hydroxydopamine (6-OHDA) mice, another ADHD model, showed shorter latency and a lower threshold

TABLE 1 Rodent models of ADHD.

Rat models	ADHD features		
	Hyperactivity	Impulsivity	Inattention
Neonatal 6-OHDA	+	+	+
Spontaneously Hypertensive Rat	+	+	+
Poor performance in a 5-choice serial reaction time task		+	+
Naples High-Excitability Rat	+		+
Polychlorinated Biphenyl Exposure	+		+
Congenic Wiggling Rat	+	+	
Prenatal Alcohol Exposure	+	+	+
Prenatal Nicotine Exposure	+	+	+
Lphn3 Knockout	+	+	
Mouse models	**Hyperactivity**	**Impulsivity**	**Inattention**
Coloboma Mutant	+		
Thyroid Receptor β Mutant	+	+	+
DAT Knockout	+	+	
DAT Knockdown	+	+	
NK1 Receptor Knockout	+	+	
Prenatal Nicotine Exposure	+	+	+
CdK5 Dysregulation	+	+	
Git1 Knockout	+		
Lphn3 Knockout	+	+	
High Active Line	+	+	
DAT Val559 Knockin	+	+	
Neonatal 6-OHDA	+	+	+

The major models with more than 10 references are highlighted in bold. Cdk5, cyclin-dependent kinase 5; DAT, dopamine transporter; NK1, neurokinin-1; 6-OHDA, 6-hydroxydopamine (Kantak 2022).

for licking hind limbs in response to thermal or mechanical stimuli than those shown by controls, indicating heightened baseline nociceptive sensitivity (Bouchatta et al., 2022). In these mice, inhibitory synaptic connections in the spinal dorsal horn lamina II were similar to controls, but excitatory connections were significantly increased (Bouchatta et al., 2022). This suggests that ADHD-related anatomical changes, including increased excitatory pathways in the dorsal horn, may promote pain sensitization.

Central sensitization mechanisms have also been studied by examining the pathway from the anterior cingulate cortex (ACC) to the posterior insula (PI), known as the ACC-PI pathway (Bouchatta et al., 2022). In 6-OHDA-induced ADHD, spontaneous activity in this pathway was higher than that in controls, and ACC activity evoked by mechanical stimulation of the contralateral hind limb was stronger than that evoked in controls. This intensified activity boosted firing in second-order nociceptive neurons in the spinal dorsal horn, further lowering the pain threshold. Conversely, inhibiting the ACC-PI pathway in 6-OHDA mice more effectively suppressed dorsal horn action potentials and raised the pain threshold. Hence, ADHD-driven ACC-PI activity can both increase and reduce pain sensitivity, potentially triggering overactivity (ergomania).

Regarding the cause of elevated spontaneous ACC-PI activity, a sex-specific neuroinflammatory response to dopamine (DA) neuronal depletion in 6-OHDA mice has been reported (Meseguer-Beltrán et al., 2023). In males, DA depletion triggered inflammation only in the ACC, resulting in hyperactivity but no hyperalgesia. In females, inflammation occurred in the ACC-PI pathway, leading to hyperalgesia but not hyperactivity; reducing this inflammation alleviated hyperalgesia. These findings may explain why females experience higher rates of conditions like fibromyalgia (Queiroz, 2013) or burning mouth syndrome (Khawaja et al., 2023), as DA dysfunction in females may manifest primarily as hyperalgesia rather than hyperactivity.

TABLE 2 Medications effective for ADHD.

Compounds	Medicinal classification	Main indications	Dosage
Methylphenidate	Psychostimulant	ADHD	20–60 mg/day
Lisdexamfetamine	Psychostimulant	ADHD	30–70 mg/day
Amphetamine	Psychostimulant	ADHD/Narcolepsy	5–40 mg/day
Modafinil	Psychostimulant	Narcolepsy	200 mg/day
Pemoline	Psychostimulant	Narcolepsy	56.25–75 mg/day
Atomoxetine	NRI	ADHD	40–100 mg/day
Reboxetine	NRI	Depression	8–10 mg/day
Guanfacine	α2 agonist	ADHD	1–6 mg/day
Clonidine	α2 agonist	Hypertension	0.2–0.6 mg/day
Bupropion	NDRI	Depression	150–450 mg/day
Duloxetine	SNRI	Depression	30–120 mg/day
Venlafaxine	SNRI	Depression	37.5–300 mg/day
Paroxetine	SSRI	Depression	20–60 mg/day
Desipramine	TCA	Depression	100–200 mg/day
Nortriptyline	TCA	Depression	75–150 mg/day
Amitriptyline	TCA	Depression	50–150 mg/day
Lithium	mood stabilizer	Bipolar Disorder	600–1200 mg/day
Lamotrigine	mood stabilizer	Bipolar Disorder	100–200 mg/day
Haloperidol	Antipsychotic	Schizophrenia	1–40 mg/day
Chlorpromazine	Antipsychotic	Schizophrenia	200–800 mg/day
Risperidone	Antipsychotic	Schizophrenia	2–8 mg/day
Aripiprazole	Antipsychotic	Schizophrenia/Bipolar disorder	2–30 mg/day
Pramipexole	Antiparkinsonism	Parkinson's disease	1.5–4.5 mg/day
Selegiline	Antiparkinsonism	Parkinson's disease	5–10 mg/day
Donepezil	Antidementia	Dementia	5–10 mg/day
Galantamine	Antidementia	Dementia	16–24 mg/day
Memantine	Antidementia	Dementia	20 mg/day

ADHD, attention deficit hyperactivity disorder; NDRI, norepinephrine-dopamine reuptake inhibitor; NRI, norepinephrine reuptake inhibitor; SNRI, serotonin norepinephrine reuptake inhibitor; SSRI, selective serotonin reuptake inhibitor; TCA, tricyclic antidepressant.

In summary, in SHR and 6-OHDA mice, which have been reported to demonstrate a relationship between pain and ADHD, brain abnormalities in ADHD are thought to increase the spontaneous activity of the ACC-PI pathway owing to neuroinflammation, changes in the firing of action potentials and transmission pathways in the spinal dorsal horn, increased NE synthesis, and reduced transmission efficiency. These factors may amplify peripheral nociceptive information, increasing susceptibility to central sensitization. Furthermore, it has been shown that in SHR and 6-OHDA mice, hyperalgesia caused by central sensitization and ADHD symptoms, such as hyperactivity and inattention, can be improved by atomoxetine—a selective norepinephrine reuptake inhibitor (NRI) used as an ADHD medication (Sifeddine et al., 2023; Suto et al., 2023).

However, among the ADHD models listed in Table 1, only the SHR and 6-OHDA mice have been reported to show a relationship between pain and ADHD, while such investigations have not been conducted for other ADHD model animals. Therefore, there is room to explore the relationship between pain and ADHD in these other models as well. Additionally, ADHD is believed to result from gene-environment interactions, highlighting the need to develop models that integrate both genetic and environmental factors. This integration remains a challenge for ADHD models as a whole (Regan et al., 2022). Furthermore, since all rodent ADHD models exhibit hyperactivity or impulsivity, developing a model that specifically represents inattentive-type ADHD without hyperactivity or impulsivity remains an important task.

4 Discussion

Medications that are effective for treating ADHD may also be effective in treating chronic pain and its associated cognitive dysfunction mediated by central sensitization. Here, we briefly introduce the representative drug candidates (Table 2).

The main ADHD medications include the central stimulant methylphenidate, the selective NRI atomoxetine, the α2 receptor agonist guanfacine, and the central stimulant lisdexamfetamine (Stahl, 2021). There have been reports that the first three of these drugs have shown improvements in chronic pain and its associated cognitive dysfunction (Kasahara et al., 2023a; Kasahara et al., 2023e; Zain et al., 2023). However, even with these so-called ADHD medications approved by the Food and Drug Administration, more than 33% of children and over 50% of adults discontinue treatment within a year due to suboptimal efficacy or tolerance issues (Childress A., 2024). Therefore, alternative ADHD treatments that have proven effective for ADHD, as discussed below, are also considered pertinent (Buoli et al., 2016).

Other central stimulants such as amphetamines, modafinil, and pemoline are also considered effective for ADHD (Stahl, 2020). It has been suggested that the amphetamine, which John F. Kennedy used to treat back pain, may have also inadvertently improved ADHD symptoms (Kasahara et al., 2022a).

Additionally, antidepressants, such as duloxetine and venlafaxine, which are norepinephrine-serotonin reuptake inhibitors, have been reported to improve ADHD symptoms (Buoli et al., 2016) and NP (Kasahara et al., 2024). Traditional tricyclic antidepressants (TCAs), used to treat chronic pain (Feinmann and Harris, 1984), also improve ADHD (Banaschewski et al., 2004). TCAs inhibit norepinephrine reuptake. Dopamine reuptake occurs via norepinephrine transporters in the prefrontal cortex. Consequently, TCAs enhance both norepinephrine and dopamine levels in this region. Among TCAs, desipramine is considered the most effective for ADHD, whereas imipramine, nortriptyline, and amitriptyline are slightly less effective. On the other hand, clomipramine and protriptyline are deemed less effective and generally unsuitable due to intolerable side effects. The effects of TCAs on ADHD primarily affect behavioral symptoms rather than cognitive symptoms. Furthermore, it has been suggested that their effectiveness in treating chronic pain may have been due to the improvement of undiagnosed coexisting ADHD (Kasahara et al., 2023d). Other antidepressants, such as the selective serotonin reuptake inhibitor paroxetine, the NE-DA reuptake inhibitor bupropion, and the selective NRI reboxetine, are also considered effective for ADHD (Buoli et al., 2016). Regarding the role of serotonin in ADHD treatment, studies report that hyperactivity caused by high extracellular dopamine levels in 6-OHDA mice is regulated and improved by enhancing serotonergic tone (Regan et al., 2022). Furthermore, mood stabilizers such as lithium and lamotrigine are also considered effective for ADHD (Buoli et al., 2016; Sablaban and Sivananthan, 2022). These agents have been shown to improve ADHD symptoms associated with addictive behaviors, intense anger, and comorbid bipolar disorder (Buoli et al., 2016). Notably, the effectiveness of lithium in treating ADHD has been reported to be comparable to that of methylphenidate (Dorrego et al., 2002).

Haloperidol, chlorpromazine (Stahl, 2020), risperidone, and aripiprazole (Ghanizadeh, 2013; Lamberti et al., 2016) are effective treatments for ADHD. There have also been reports that risperidone (Kasahara et al., 2022b) and aripiprazole (Kasahara et al., 2011; Kasahara et al., 2023d) have improved chronic pain. Haloperidol and chlorpromazine are considered useful for managing hyperactivity and aggression in ADHD (Stahl, 2020). Risperidone and aripiprazole have been found beneficial for ADHD patients experiencing anxiety, irritability, depression, anger, or self-injurious behavior (Alsayouf, 2024). Antipsychotics are thought to ameliorate ADHD by addressing these cognitive-emotional factors. Notably, the effectiveness of risperidone in treating ADHD symptoms has been reported to be comparable to that of methylphenidate (Arabgol et al., 2015).

Additionally, although antipsychotics block dopamine D2 receptors and may initially seem counterproductive for ADHD, which is typically characterized by low dopamine levels, the "Complex DA Model" has been proposed to explain this phenomenon (Yanofski, 2010). According to this model, ADHD involves low tonic dopamine levels and high DA bursts. Stimulants act presynaptically to increase tonic dopamine, suppress DA bursts, and downregulate postsynaptic receptors. Conversely, antipsychotics like risperidone and aripiprazole function postsynaptically to increase tonic dopamine, suppress DA bursts, and upregulate postsynaptic receptors. Therefore, while stimulants and antipsychotics are each effective for ADHD when used alone, their combination proves particularly effective. This combined approach acts on both pre- and postsynaptic mechanisms, increasing tonic dopamine, suppressing DA bursts, and stabilizing postsynaptic receptor regulation. Consequently, this strategy is believed to prevent tolerance to treatment, minimize side effects due to receptor upregulation, and allow for low medication dosages.

DA agonists such as pramipexole (Kurlan et al., 2012) and the selective monoamine oxidase B inhibitor selegiline (Buoli et al., 2016; Akhondzadeh et al., 2003), commonly used to treat Parkinson's disease, have also been found to be effective for ADHD by enhancing DA neurotransmission at the synapse. Pramipexole improves chronic low back pain (Kasahara et al., 2023c) and fibromyalgia (Holman and Myers, 2005). Clonidine, an α2 agonist like guanfacine and an antihypertensive, is considered effective for ADHD (Stahl, 2020) and has shown efficacy in treating chronic pain (Guay, 2001). Additionally, cholinesterase inhibitors such as donepezil (Doyle et al., 2006) and galantamine (Buoli et al., 2016), along with the N-methyl-D-aspartate receptor antagonist memantine (Surman et al., 2013), typically used as anti-dementia drugs, are known to activate dopamine neurotransmission and have been reported to be effective against ADHD. These medications may also potentially improve chronic pain.

The contents of this mini-review can be summarized as follows: The cognitive-emotional and motor control issues associated with ADHD mutually amplify and exacerbate both ADHD and pain. Neuroinflammation and alterations in neurotransmission within the ADHD brain contribute to central sensitization, amplifying nociceptive input and promoting pain chronicity. ADHD medications can correct the increased blood flow in the precuneus and decreased blood flow in the prefrontal cortex, thereby improving cognitive-emotional factors such as anxiety, depression, anger, and aggression, as well as motor control issues

like increased muscle tension. These treatments have the potential to alleviate not only chronic pain itself but also its associated psychosocial issues. However, it is assumed that the ADHD phenotype encompasses multiple models, each responding differently to medication. Therefore, instead of limiting treatment to a single medication, it is pertinent to implement a treatment algorithm composed of multiple medications with different mechanisms of action, as discussed in this review (e.g., Kasahara et al., 2023d).

In the future, to develop innovative pharmacological treatments for chronic pain, it is considered important to discover approaches that utilize ADHD medications targeting the clinical features of ADHD coexisting with chronic pain and the pathophysiological mechanisms of central sensitization.

Author contributions

SK: Writing–original draft, Writing–review and editing. MT: Writing–original draft, Writing–review and editing. TS: Writing–original draft, Writing–review and editing. TM: Writing–original draft, Writing–review and editing. HO: Writing–original draft, Writing–review and editing. S-IN: Writing–original draft, Writing–review and editing.

Funding

The author(s) declare that financial support was received for the research, authorship, and/or publication of this article. This paper was supported by a Grant-in-Aid for Scientific Research (C) from the Japan Society for the Promotion of Science [Grant numbers: 20K07755, 24K13083].

Acknowledgments

We would like to thank Editage (www.editage.com) for English language editing.

Conflict of interest

The authors declare that the research was conducted in the absence of any commercial or financial relationships that could be construed as a potential conflict of interest.

Generative AI statement

The author(s) declare that no Generative AI was used in the creation of this manuscript.

Publisher's note

References

Akhondzadeh, S., Tavakolian, R., Davari-Ashtiani, R., Arabgol, F., and Amini, H. (2003). Selegiline in the treatment of attention deficit hyperactivity disorder in children: a double blind and randomized trial. *Prog. Neuropsychopharmacol. Biol. Psychiatry* 27, 841–845. doi:10.1016/S0278-5846(03)00117-9

Alsayouf, H. A. (2024). Growing evidence of pharmacotherapy effectiveness in managing attention-deficit/hyperactivity disorder in young children with or without autism spectrum disorder: a minireview. *Front. Psychiatry* 15, 1408876. doi:10.3389/fpsyt.2024.1408876

American Psychiatric Association (2013). *Diagnostic and Statistical Manual of Mental Disorders, DSM-5*. Washington, DC: American Psychiatric Association.

Arabgol, F., Panaghi, L., and Nikzad, V. (2015). Risperidone versus methylphenidate in treatment of preschool children with attention-Deficit Hyperactivity Disorder. *Iran. J. Pediatr.* 25, e265. doi:10.5812/ijp.265

Asztély, K., Kopp, S., Gillberg, C., Waern, M., and Bergman, S. (2019). Chronic pain and health-related quality of life in women with autism and/or ADHD: A prospective longitudinal study. *J. Pain Res.* 12, 2925–2932. doi:10.2147/jpr.s212422

Aydede, M., and Shriver, A. (2018). Recently introduced definition of "nociplastic pain" by the International Association for the Study of Pain needs better formulation. *Pain* 159, 1176–1177. doi:10.1097/j.pain.0000000000001184

Banaschewski, T., Roessner, V., Dittmann, R. W., Janardhanan Santosh, P., and Rothenberger, A. (2004). Non?stimulant medications in the treatment of ADHD. *Eur. Child Adolesc. Psychiatry* 13, I102–I116. doi:10.1007/s00787-004-1010-x

Battison, E. A. J., Brown, P. C. M., Holley, A. L., and Wilson, A. C. (2023). Associations between chronic pain and Attention-Deficit Hyperactivity Disorder (ADHD) in youth: A scoping review. *Child. (Basel)* 10, 142. doi:10.3390/children10010142

Bouchatta, O., Aby, F., Sifeddine, W., Bouali-Benazzouz, R., Brochoire, L., Manouze, H., et al. (2022). Pain hypersensitivity in a pharmacological mouse model of attention-deficit/hyperactivity disorder. *Proc. Natl. Acad. Sci. U. S. A.* 119, e2114094119. doi:10.1073/pnas.2114094119

Buoli, M., Serati, M., and Cahn, W. (2016). Alternative pharmacological strategies for adult ADHD treatment: a systematic review. *Expert Rev. Neurother.* 16, 131–144. doi:10.1586/14737175.2016.1135735

Childress, A. (2024). Recent advances in pharmacological management of attention-deficit/hyperactivity disorder: moving beyond stimulants. *Expert Opin. Pharmacother.* 25, 853–866. doi:10.1080/14656566.2024.2358987

Conners, C. K., Erhardt, D., and Sparrow, E. P. (1999). *Conners' Adult ADHD Rating Scales (CAARS): Technical Manual*. North Tonawanda, NY: Multi-Health Systems Inc.

Dorrego, M. F., Canevaro, L., Kuzis, G., Sabe, L., and Starkstein, S. E. (2002). A randomized, double-blind, crossover study of methylphenidate and lithium in adults with attention-deficit/hyperactivity disorder: preliminary findings. *J. Neuropsychiatry Clin. Neurosci.* 14, 289–295. doi:10.1176/jnp.14.3.289

Doyle, R. L., Frazier, J., Spencer, T. J., Geller, D., Biederman, J., and Wilens, T. (2006). Donepezil in the treatment of ADHD-like symptoms in youths with pervasive developmental disorder: a case series. *J. Atten. Disord.* 9, 543–549. doi:10.1177/1087054705284091

Feinmann, C., and Harris, M. (1984). Psychogenic facial pain. Part 2: Management and prognosis. *Br. Dent. J.* 156, 205–208. doi:10.1038/sj.bdj.4805304

Flor, H., and Turk, D. C. (2015). *Chronic Pain: An Integrated Biobehavioral Approach*. Philadelphia, PA: Lippincott Williams and Wilkins.

Garcia-Larrea, L., and Peyron, R. (2013). Pain matrices and neuropathic pain matrices: a review. *Pain* 154 (Suppl. 1), S29–S43. doi:10.1016/j.pain.2013.09.001

Ghanizadeh, A. (2013). Systematic review of clinical trials of aripiprazole for treating attention deficit hyperactivity disorder. *Neurosci. (Riyadh)* 18, 323–329.

Ginsberg, Y., Quintero, J., Anand, E., Casillas, M., and Upadhyaya, H. P. (2014). Underdiagnosis of attention-deficit/hyperactivity disorder in adult patients: A review of the literature. *Prim. Care Companion CNS Disord* 16. doi:10.4088/pcc.13r01600

Guay, D. R. P. (2001). Adjunctive agents in the management of chronic pain. *Pharmacotherapy* 21, 1070–1081. doi:10.1592/phco.21.13.1070.34622

Holman, A. J., and Myers, R. R. (2005). A randomized, double-blind, placebo-controlled trial of pramipexole, a dopamine agonist, in patients with fibromyalgia receiving concomitant medications. *Arthritis Rheum.* 52, 2495–2505. doi:10.1002/art.21191

Ibrahim, M. E., and Hefny, M. A. (2022). Central sensitization and adult attention deficit hyperactivity disorder in medical students with chronic back pain: a cross-sectional study. *Egypt. Rheumatol. Rehabil* 49, 24. doi:10.1186/s43166-022-00124-2

Kantak, K. M. (2022). Rodent models of attention-deficit hyperactivity disorder: An updated framework for model validation and therapeutic drug discovery. *Pharmacol. Biochem. Behav.* 216, 173378. doi:10.1016/j.pbb.2022.173378

Kaplan, M. S., and Kaplan, L. R. (2006). Why do chronic pain patients have multiple accidents? *Pain Med* 7, 466.1–466. doi:10.1111/j.1526-4637.2006.00208_1.x

Kasahara, S., Kanda, S., Takahashi, M., Fujioka, M., Morita, T., Matsudaira, K., et al. (2023a). Case Report: Guanfacine and methylphenidate improved chronic lower back pain in autosomal dominant polycystic kidney disease with comorbid attention deficit hyperactivity disorder and autism spectrum disorder. *Front. Pediatr.* 11, 1283823. doi:10.3389/fped.2023.1283823

Kasahara, S., Kato, Y., Takahashi, K., Matsudaira, K., Sato, N., Fukuda, K.-I., et al. (2023b). Improvement in persistent idiopathic facial pain with comorbid ADHD using the combination of a dopamine system stabilizer and psychostimulant: A case report. *Clin. Case Rep.* 11, e7552. doi:10.1002/ccr3.7552

Kasahara, S., Kato, Y., Takahashi, M., Matsudaira, K., Sato, N., Niwa, S.-I., et al. (2023c). Case report: Remission of chronic low back pain and oral dysesthesia comorbid with attention deficit/hyperactivity disorder by treatment with atomoxetine and pramipexole. *Front. Pain Res. (Lausanne)* 4, 1159134. doi:10.3389/fpain.2023.1159134

Kasahara, S., Kunii, Y., Mashiko, H., Otani, K., Konno, S.-I., and Niwa, S.-I. (2011). Four cases of chronic pain that improved dramatically following low-dose aripiprazole administration. *Prim. Care Companion CNS Disord* 13. doi:10.4088/pcc.10l01078

Kasahara, S., Matsudaira, K., Sato, N., and Niwa, S.-I. (2021a). Pain and attention-deficit/hyperactivity disorder: The case of Margaret Mitchell. *Psychosom. Med.* 83, 492–493. doi:10.1097/psy.0000000000000947

Kasahara, S., Matsudaira, K., Sato, N., and Niwa, S.-I. (2022a). Attention-Deficit/hyperactivity disorder and centralized pain: A review of the case of John F. Kennedy. *Clin. Case Rep.* 10, e6422. doi:10.1002/ccr3.6422

Kasahara, S., Niwa, S. I., Matsudaira, K., Sato, N., Oka, H., Fujii, T., et al. (2021b). High attention-deficit/hyperactivity disorder scale scores among patients with persistent chronic nonspecific low back pain. *Pain Physician* 24, E299–E307. doi:10.36076/ppj.2021/24/e299

Kasahara, S., Niwa, S.-I., Matsudaira, K., Sato, N., Oka, H., and Yamada, Y. (2020). Attention-deficit/hyperactivity disorder and chronic pain. *Psychosom. Med.* 82, 346–347. doi:10.1097/psy.0000000000000789

Kasahara, S., Okamura, Y., Matsudaira, K., Oka, H., Suzuki, Y., Murakami, Y., et al. (2017). Diagnosis and treatment of attention-deficit hyperactivity disorder in patients with chronic pain. *Open J. Psychiatr.* 07, 261–275. doi:10.4236/ojpsych.2017.74023

Kasahara, S., Takahashi, K., Matsudaira, K., Sato, N., Fukuda, K.-I., Toyofuku, A., et al. (2023d). Diagnosis and treatment of intractable idiopathic orofacial pain with attention-deficit/hyperactivity disorder. *Sci. Rep.* 13, 1678. doi:10.1038/s41598-023-28931-3

Kasahara, S., Takahashi, M., Morita, T., Matsudaira, K., Sato, N., Momose, T., et al. (2023e). Case report: Atomoxetine improves chronic pain with comorbid post-traumatic stress disorder and attention deficit hyperactivity disorder. *Front. Psychiatry* 14, 1221694. doi:10.3389/fpsyt.2023.1221694

Kasahara, S., Takahashi, M., Takahashi, K., Morita, T., Matsudaira, K., Sato, N., et al. (2024). Case Report: Methylphenidate and venlafaxine improved abdominal nociplastic pain in an adult patient with attention deficit hyperactivity disorder, autism spectrum disorder, and comorbid major depression. *Front. Pain Res. (Lausanne)* 5, 1394131. doi:10.3389/fpain.2024.1394131

Kasahara, S., Takao, C., Matsudaira, K., Sato, N., Tu, T. T. H., Niwa, S.-I., et al. (2022b). Case report: Treatment of persistent atypical odontalgia with attention deficit hyperactivity disorder and autism spectrum disorder with risperidone and atomoxetine. *Front. Pain Res. (Lausanne)* 3, 926946. doi:10.3389/fpain.2022.926946

Kessler, R. C., Adler, L., Ames, M., Demler, O., Faraone, S., Hiripi, E., et al. (2005). The World Health Organization Adult ADHD Self-Report Scale (ASRS): a short screening scale for use in the general population. *Psychol. Med.* 35, 245–256. doi:10.1017/s0033291704002892

Khawaja, S. N., Alaswaiti, O. F., and Scrivani, S. J. (2023). Burning mouth syndrome. *Dent. Clin. North Am.* 67, 49–60. doi:10.1016/j.cden.2022.07.004

Kooij, J. J., and Francken, M. H. (2010). *Diagnostic Interview for ADHD in adults 2.0 (DIVA 2.0)*. The Hague, Netherlands: DIVA Foundation.

Kosek, E., Clauw, D., Nijs, J., Baron, R., Gilron, I., Harris, R. E., et al. (2021). Chronic nociplastic pain affecting the musculoskeletal system: clinical criteria and grading system. *Pain* 162, 2629–2634. doi:10.1097/j.pain.0000000000002324

Kosek, E., Cohen, M., Baron, R., Gebhart, G. F., Mico, J.-A., Rice, A. S. C., et al. (2016). Do we need a third mechanistic descriptor for chronic pain states? *Pain* 157, 1382–1386. doi:10.1097/j.pain.0000000000000507

Kurlan, R., Crespi, G., Coffey, B., Mueller-Vahl, K., Koval, S., Wunderlich, G., et al. (2012). A multicenter randomized placebo-controlled clinical trial of pramipexole for Tourette's syndrome. *Mov. Disord.* 27, 775–778. doi:10.1002/mds.24919

Lamberti, M., Siracusano, R., Italiano, D., Alosi, N., Cucinotta, F., Di Rosa, G., et al. (2016). Head-to-head comparison of aripiprazole and risperidone in the treatment of ADHD symptoms in children with autistic spectrum disorder and ADHD: A pilot, open-label, randomized controlled study. *Paediatr. Drugs* 18, 319–329. doi:10.1007/s40272-016-0183-3

Meseguer-Beltrán, M., Sánchez-Sarasúa, S., Landry, M., Kerekes, N., and Sánchez-Pérez, A. M. (2023). Targeting neuroinflammation with abscisic acid reduces pain sensitivity in females and hyperactivity in males of an ADHD mice model. *Cells* 12, 465. doi:10.3390/cells12030465

Mills, S. E. E., Nicolson, K. P., and Smith, B. H. (2019). Chronic pain: a review of its epidemiology and associated factors in population-based studies. *Br. J. Anaesth.* 123, e273–e283. doi:10.1016/j.bja.2019.03.023

Nijs, J., George, S. Z., Clauw, D. J., Fernández-de-Las-Peñas, C., Kosek, E., Ickmans, K., et al. (2021). Central sensitisation in chronic pain conditions: latest discoveries and their potential for precision medicine. *Lancet Rheumatol* 3, e383–e392. doi:10.1016/S2665-9913(21)00032-1

Pallanti, S., Porta, F., and Salerno, L. (2021). Adult attention deficit hyperactivity disorder in patients with fibromyalgia syndrome: Assessment and disabilities. *J. Psychiatr. Res.* 136, 537–542. doi:10.1016/j.jpsychires.2020.10.027

Queiroz, L. P. (2013). Worldwide epidemiology of fibromyalgia. *Curr. Pain Headache Rep* 17, 356. doi:10.1007/s11916-013-0356-5

Regan, S. L., Williams, M. T., and Vorhees, C. V. (2022). Review of rodent models of attention deficit hyperactivity disorder. *Neurosci. Biobehav. Rev.* 132, 621–637. doi:10.1016/j.neubiorev.2021.11.041

Sablaban, I. M., and Sivananthan, M. (2022). Attention-deficit hyperactivity disorder–associated impulsive aggression treated with lamotrigine. *Am. J. Ther.* 29, e747–e748. doi:10.1097/mjt.0000000000001219

Sarria-Santamera, A., Kuntuganova, A., and Alonso, M. (2022). Economic costs of pain in the Spanish working population. *J. Occup. Environ. Med.* 64, e261–e266. doi:10.1097/jom.0000000000002497

Sifeddine, W., Ba-M'hamed, S., Landry, M., and Bennis, M. (2023). Effect of atomoxetine on ADHD-pain hypersensitization comorbidity in 6-OHDA lesioned mice. *Pharmacol. Rep.* 75, 342–357. doi:10.1007/s43440-023-00459-3

Stahl, S. M. (2020). *Prescriber Guide: Stahl's Essential Psychopharmacology*. Cambridge University Press.

Stahl, S. M. (2021). *Stahl's Essential Psychopharmacology: Neuroscientific Basis and Practical Applications*. Cambridge University Press.

Stickley, A., Koyanagi, A., Takahashi, H., and Kamio, Y. (2016). ADHD symptoms and pain among adults in England. *Psychiatry Res* 246, 326–331. doi:10.1016/j.psychres.2016.10.004

Stray, L. L., Kristensen, Ø., Lomeland, M., Skorstad, M., Stray, T., and Tønnessen, F. E. (2013). Motor regulation problems and pain in adults diagnosed with ADHD. *Behav. Brain Funct.* 9, 18. doi:10.1186/1744-9081-9-18

Stray, L. L., Stray, T., Iversen, S., Ruud, A., and Ellertsen, B. (2009). Methylphenidate improves motor functions in children diagnosed with Hyperkinetic Disorder. *Behav. Brain Funct.* 5, 21. doi:10.1186/1744-9081-5-21

Surman, C. B. H., Hammerness, P. G., Petty, C., Spencer, T., Doyle, R., Napolean, S., et al. (2013). A pilot open label prospective study of memantine monotherapy in adults with ADHD. *World J. Biol. Psychiatry* 14, 291–298. doi:10.3109/15622975.2011.623716

Suto, T., Kato, D., Koibuchi, I., Arai, Y., Ohta, J., Hiroki, T., et al. (2023). Rat model of attention-deficit hyperactivity disorder exhibits delayed recovery from acute incisional pain due to impaired descending noradrenergic inhibition. *Sci. Rep.* 13, 5526. doi:10.1038/s41598-023-32512-9

Swanson, D. W., Swenson, W. M., Maruta, T., and Floreen, A. C. (1977). The dissatisfied patient with chronic pain. *Pain* 4, 367–378. doi:10.1016/0304-3959(77)90147-6

Takahashi, M., Kasahara, S., Soma, T., Morita, T., Sato, N., Matsudaira, K., et al. (2024). Precuneal hyperperfusion in patients with attention-deficit/hyperactivity disorder-comorbid nociplastic pain. *Front. Pharmacol.* 15, 1480546. doi:10.3389/fphar.2024.1480546

Tambeli, C. H., Levine, J. D., and Gear, R. W. (2009). Centralization of noxious stimulus-induced analgesia (NSIA) is related to activity at inhibitory synapses in the spinal cord. *Pain* 143, 228–232. doi:10.1016/j.pain.2009.03.005

Treede, R.-D., Rief, W., Barke, A., Aziz, Q., Bennett, M. I., Benoliel, R., et al. (2019). Chronic pain as a symptom or a disease: the IASP classification of Chronic pain for the International Classification of diseases (ICD-11). *Pain* 160, 19–27. doi:10.1097/j.pain.0000000000001384

Vlaeyen, J. W. S., and Morley, S. (2004). Active despite pain: the putative role of stop-rules and current mood. *Pain* 110, 512–516. doi:10.1016/j.pain.2004.04.037

Yanofski, J. (2010). The dopamine dilemma: using stimulants and antipsychotics concurrently. *Psychiatry (Edgmont)* 7, 18–23.

Zain, E., Sugimoto, A., Egawa, J., and Someya, T. (2023). Case report: Methylphenidate improved chronic pain in an adult patient with attention deficit hyperactivity disorder. *Front. Psychiatry* 14, 1091399. doi:10.3389/fpsyt.2023.1091399

Frontiers in Pharmacology

Explores the interactions between chemicals and living beings

The most cited journal in its field, which advances access to pharmacological discoveries to prevent and treat human disease.

Discover the latest Research Topics

See more →

Frontiers

Avenue du Tribunal-Fédéral 34
1005 Lausanne, Switzerland
frontiersin.org

Contact us

+41 (0)21 510 17 00
frontiersin.org/about/contact